frontiers | Research Topics

Case reports in general cardiovascular medicine

2022, 2nd edition

Edited by
Leonardo Roever, Junjie Xiao and Pietro Enea Lazzerini

Published in
Frontiers in Cardiovascular Medicine

ISSN 1664-8714
ISBN 978-2-8325-5570-5
DOI 10.3389/978-2-8325-5570-5

About Frontiers

Frontiers is more than just an open access publisher of scholarly articles: it is a pioneering approach to the world of academia, radically improving the way scholarly research is managed. The grand vision of Frontiers is a world where all people have an equal opportunity to seek, share and generate knowledge. Frontiers provides immediate and permanent online open access to all its publications, but this alone is not enough to realize our grand goals.

Frontiers journal series

The Frontiers journal series is a multi-tier and interdisciplinary set of open-access, online journals, promising a paradigm shift from the current review, selection and dissemination processes in academic publishing. All Frontiers journals are driven by researchers for researchers; therefore, they constitute a service to the scholarly community. At the same time, the *Frontiers journal series* operates on a revolutionary invention, the tiered publishing system, initially addressing specific communities of scholars, and gradually climbing up to broader public understanding, thus serving the interests of the lay society, too.

Dedication to quality

Each Frontiers article is a landmark of the highest quality, thanks to genuinely collaborative interactions between authors and review editors, who include some of the world's best academicians. Research must be certified by peers before entering a stream of knowledge that may eventually reach the public - and shape society; therefore, Frontiers only applies the most rigorous and unbiased reviews. Frontiers revolutionizes research publishing by freely delivering the most outstanding research, evaluated with no bias from both the academic and social point of view. By applying the most advanced information technologies, Frontiers is catapulting scholarly publishing into a new generation.

What are Frontiers Research Topics?

Frontiers Research Topics are very popular trademarks of the *Frontiers journals series*: they are collections of at least ten articles, all centered on a particular subject. With their unique mix of varied contributions from Original Research to Review Articles, Frontiers Research Topics unify the most influential researchers, the latest key findings and historical advances in a hot research area.

Find out more on how to host your own Frontiers Research Topic or contribute to one as an author by contacting the Frontiers editorial office: frontiersin.org/about/contact

Case reports in general cardiovascular medicine: 2022, 2nd edition

Topic editors

Leonardo Roever — Federal University of Uberlandia, Brazil

Junjie Xiao — Shanghai University, China

Pietro Enea Lazzerini — University of Siena, Italy

Citation

Roever, L., Xiao, J., Lazzerini, P. E., eds. (2024). *Case reports in general cardiovascular medicine: 2022, 2nd edition*. Lausanne: Frontiers Media SA. doi: 10.3389/978-2-8325-5570-5

Publisher's note: This is a 2nd edition due to an article retraction.

Table of contents

frontiers | Frontiers in Cardiovascular Medicine

TYPE Editorial
PUBLISHED 23 August 2023
DOI 10.3389/fcvm.2023.1271412

OPEN ACCESS

EDITED BY
Xiaofeng Yang,
Temple University, United States

REVIEWED BY
Keman Xu,
Temple University, United States

*CORRESPONDENCE
Leonardo Roever
leonardoroever@hotmail.com
Pietro Enea Lazzerini
pietro.lazzerini@unisi.it
Junjie Xiao
junjiexiao@live.cn

RECEIVED 02 August 2023
ACCEPTED 15 August 2023
PUBLISHED 23 August 2023

CITATION
Wang L, Wan W, Roever L, Lazzerini PE and Xiao J (2023) Editorial: Case reports in general cardiovascular medicine: 2022.
Front. Cardiovasc. Med. 10:1271412.
doi: 10.3389/fcvm.2023.1271412

Editorial: Case reports in general cardiovascular medicine: 2022

Lijun Wang[1], Wensi Wan[1], Leonardo Roever[2,3]*, Pietro Enea Lazzerini[4]* and Junjie Xiao[1]*

[1]Cardiac Regeneration and Ageing Lab, Institute of Cardiovascular Sciences, Shanghai Engineering Research Center of Organ Repair, School of Life Science, Shanghai University, Shanghai, China, [2]Department of Clinical Research, Federal University of Uberlândia, Uberlândia, Brazil, [3]Gilbert and Rose-Marie Chagoury School of Medicine, Lebanese American University, Beirut, Lebanon, [4]Department of Medical Sciences, Surgery and Neurosciences, University of Siena, Siena, Italy

KEYWORDS

case reports, prognosis, diagnosis, treatment, general cardiovascular medicine section, 2022

Editorial on the Research Topic
Case reports in general cardiovascular medicine: 2022

In this 2022 Topic and Case Reports, an international collection of case reports is presented that aims to contribute to the advancement of understanding of personalized approaches to the prognosis, diagnosis, and treatment of cardiovascular disease. This editorial features the collection of Case reports published in Frontiers in Cardiovascular Medicine (General Cardiovascular Medicine Section) in 2022. In total 33 papers are published in this Research Topic. Case reports of the contributions in this special issue highlight unique cases that present with an unexpected diagnosis, treatment outcome, or clinical course. Hereby, reports on this issue can not only describe the cases' clinical presentation, diagnostic process, and treatment but also provide important experience and treatment strategies to manage patients with similar conditions. Following are the Case Reports that are published in the General Cardiovascular Medicine Section of the year 2022 (**Table 1**).

–*Amiodarone-Induced Multi-Systemic Toxicity Involving the Liver, Lungs, Thyroid, and Eyes: A Case Report* (You et al.).

Amiodarone is a widely used anti-arrhythmia drug despite its side effects on various organs. However, cases of simultaneous toxicity of different organs in one patient have been rarely reported. This report describes an original case that multi-systemic amiodarone organ toxicity occurred in high-risk patients. This study provides important information for the diagnosis and treatment of amiodarone toxicity that could be useful for both physicians and researchers, as well as guideline makers in amiodarone administration.

–*The Diagnostic Challenge of Eosinophilic Granulomatosis With Polyangiitis Presenting as Acute Eosinophilic Myocarditis: Case Report and Literature Review* (Yamamoto et al.).

Eosinophilic granulomatosis with polyangiitis (EGPA) is a rare disease that is typically associated with infection and drug factors. It commonly affects multiple organs in the body and manifests with various discomforting symptoms. EGPA-associated eosinophilic myocarditis is rare but can lead to death if left untreated. This report describes a case with this rare disease cured by timely treatment with systemic and oral corticosteroids. The description in this report provides critical clinical features and therapy strategies that can be useful for physicians to identify and treatment of this disease.

TABLE 1 Metrics (on July 7, 2023) of the articles published in case reports in general cardiovascular medicine: 2022.

Title	Authors	Views	Downloads
Amiodarone-Induced Multi-Systemic Toxicity Involving the Liver, Lungs, Thyroid, and Eyes: A Case Report	Hye-Su You, et al.	2,042	560
The Diagnostic Challenge of Eosinophilic Granulomatosis With Polyangiitis Presenting as Acute Eosinophilic Myocarditis: Case Report and Literature Review	Hiroyuki Yamamoto, et al.	3,044	541
Case Report: Intravascular Ultrasound-guided Intervention for Anastomosis Stenosis of the Left Main Coronary Artery Post-Cabrol Technique	Seok Oh, et al.	1,151	486
Aortic Coarctation Associated With Hypertrophic Cardiomyopathy in a Woman With Hypertension and Syncope: A Case Report With 8-Year Follow-Up	Hong Yang, et al.	1,094	444
Case report: Myocarditis following COVID-19 protein subunit vaccination	Yi-ming Dong, et al.	1,371	436
Case report: Aggressive progression of acute heart failure due to juvenile tuberculosis-associated Takayasu arteritis with aortic stenosis and thrombosis	Wenjie Xuan, et al.	496	430
Case report: Changes in the levels of stress hormones during Takotsubo syndrome	Pablo Ruiz, et al.	569	420
Inverted Takotsubo Syndrome With HELLP Syndrome: A Case Report	Paul Gabarre, et al.	1,162	419
Decisive diagnostic clue for infectious abdominal aortic aneurysm caused by Arthrobacter russicus in a diabetic elderly woman with renal dysfunction: A case report and literature review	Hiroyuki Yamamoto, et al.	1,838	401
Disrupting arrhythmia in a professional male wrestler athlete after rapid weight loss and high-intensity training—Case report	Aleksandra Milovančev, et al.	574	335
Myocardial infarction with non-obstructive coronary arteries in a patient double-seropositive for anti-glomerular basement membrane and anti-neutrophil cytoplasmic antibodies: A case report	Marcell Krall, et al.	1,121	312
Case Report: Danon Disease: Six Family Members and Literature Review	Yuanyuan Wang, et al.	957	310
Case report: Pulmonary arterial hypertension in ENG-related hereditary hemorrhagic telangiectasia	Dong Liu, et al.	803	283
Case Report: An Unusual Case of Pheochromocytoma	Ying Liao, et al.	881	276
Case Report: Family Curse: An SCN5A Mutation, c.611C>A, p.A204E Associated With a Family History of Dilated Cardiomyopathy and Arrhythmia	Wen Huang, et al.	1,252	270
Case report: From monkeypox pharyngitis to myopericarditis and atypical skin lesions	María Ascensión Sanromán Guerrero, et al.	639	266
Case report: Conquer a complex variant: Coronary-pulmonary artery fistulas, atrial septal defect and bicuspid pulmonary valve, under beating heart surgery	Ting Zhou, et al.	530	262
Case report: Coronavirus Disease 2019 (COVID-19) modified RNA vaccination-induced Adult-Onset Still's Disease with fulminant myocarditis as initial presentation	Mi Zhou, et al.	960	254
Case report: Sudden cardiorespiratory collapse in a healthy male after coronavirus disease 2019 vaccination at a vaccination center	Cze Ci Chan, et al.	1,118	247
Multisystem immune-related adverse events due to toripalimab: Two cases-based review	Yanran Chen, et al.	486	232
A case report and review of literature: Tuberculous pericarditis with pericardial effusion as the only clinical manifestation	Shipeng Wang, et al.	639	218
Case report: A novel surgical technique for rapid valve-in-ring implantation into the native aortic annulus during left ventricular assist device implantation	Yuriy Pya, et al.	512	215
Case report: Severe dry cough associated with superior vena cava syndrome—Caused recurrent chylothorax	Ziming Wan, et al.	760	212
Multimodal Imaging for Total Anomalous Systemic Venous Drainage Diagnosis and Preoperative Planning: A Case Report and Literature Review	Mingyan Ding, et al.	675	191
Massive pleural effusion following high-power and short-duration radiofrequency ablation for treatment of atrial fibrillation: A case report and review of the literature	Miaomiao He, et al.	1,012	179
Case report: Delayed cardiac rupture with congenital absence of pericardium after blunt trauma	Tuo Shen, et al.	333	164
Case report: Reducing the duration of positive-pressure ventilation for large mediastinal masses	Zaili Zhang, et al.	329	146
Case report: Metastatic myxoid liposarcoma arising from the right atrium extends as cardiac tamponade—A rare case of atrial oncology	Muralidharan Thoddi Ramamurthy, et al.	897	144
Right atrial cardiac lipoma with distinctive imaging characteristics. A rare case report and literature review	Qiqing Chen, et al.	492	142
Successful simultaneous stenting of a pulmonary artery and vein in pulmonary vascular stenosis due to silicosis. Case report and literature review	M. Westhoff, et al.	489	101
An adult female patient with single atrium and single ventricle undergoing appendectomy: A case report	Yu Wu, et al.	496	90
Acute myocardial infarction after inactivated COVID-19 vaccination: a case report and literature review	Weimei Ou, et al.	739	81
Case report: Aortoesophageal fistula—an extremely rare but life-threatening cardiovascular cause of hematemesis	Alexis Ching Wong, et al.	542	70

The order of appearance according to the number of downloads (on July 7, 2023).

–*Case Report: Intravascular Ultrasound-guided Intervention for Anastomosis Stenosis of the Left Main Coronary Artery Post-Cabrol Technique* (Oh et al.).

This study reports a case of acute myocardial infarction that is successfully treated with intravascular ultrasound (IVUS)-guided percutaneous coronary intervention (PCI). This is the first report that combined PVCI with virtual IVUS. The observations in this paper provide important information for physicians about how to evaluate plaque composition and conduct PCI in patients with chronic inflammatory diseases like Behçet's disease.

–*Aortic Coarctation Associated With Hypertrophic Cardiomyopathy in a Woman With Hypertension and Syncope: A Case Report With 8-Year Follow-Up* (Yang et al.).

Coarctation of the aorta (CoA) and hypertrophic cardiomyopathy (HCM) are two irrelevant cardiovascular diseases (1). This report describes a diagnosis, management, and

8-year follow-up in a patient with the co-existence of CoA and HCM. This is the first case that reports the concurrent presence of CoA and HCM in one patient. This report suggests that, albeit with low probability, CoA and HCM may co-exist in one patient, physicians should keep an eye on CoA in young hypertensive patients.

–*Case report: Myocarditis following COVID-19 protein subunit vaccination* (Dong et al.).

This study reports a case of myocarditis following ZF2001 vaccination in a female patient. This report describes the patient's clinical symptoms and immunohistochemical characteristics of heart sections. Though some patients with myocarditis following COVID-19 vaccination were vaccinated types of vaccines have been reported. Limited knowledge has been known about the association between vaccination and myocarditis in subunit vaccines against COVID-19. The report here suggests that physicians should consider the potential link between vaccination and myocarditis in clinical diagnosis. Also, investigating the specific mechanism underlying myocarditis after vaccination should be significant to guild the development of a new generation of subunit vaccines.

–*Case report: Aggressive progression of acute heart failure due to juvenile tuberculosis-associated Takayasu arteritis with aortic stenosis and thrombosis* (Xuan et al.).

Takayasu arteritis (TA) is a chronic granulomatous vasculitis of unknown pathophysiological mechanisms. The report describes a case of tuberculosis-associated TA who fail to survive after surgery. In this paper, the authors share their clinical experience in the diagnosis of TA and what they could learn from the case. The information provides in this paper can offer important knowledge for physicians to timely diagnose TA at an early stage with few typical features.

–*Case report: Changes in the levels of stress hormones during Takotsubo syndrome* (Ruiz et al.). *Inverted Takotsubo Syndrome With HELLP Syndrome: A Case Report* (Gabarre et al.).

Takotsubo syndrome is a sudden, transient, acute episode of left ventricular dysfunction, usually triggered by physical or emotional stress (2). These two reports describe an unusual case of Takotsubo syndrome which is accompanied by HELLP syndrome in a postpartum woman after spontaneous vaginal delivery. These studies provide indicative information for physicians that, in addition to non-invasive cardiac imaging, detecting circulating cortisol and cardiac biomarkers can be a useful complement strategy to diagnose Takotsubo syndrome. Further efforts are also warranted for researchers to identify more cardiac biomarkers in assisting the diagnosis of this disease.

–*Decisive diagnostic clue for infectious abdominal aortic aneurysm caused by Arthrobacter russicus in a diabetic elderly woman with renal dysfunction: A case report and literature review* (Yamamoto et al.).

Infectious aortic aneurysm (IAA) is a rare but serious infectious inflammatory disease of the aortic wall with high mortality. This report describes a case of IAA caused by *Arthrobacter russicus* that is successfully treated with a combination of surgery and long-term antimicrobial therapy. *Arthrobacter russicus* is identified as a potential causative microorganism by using 16S rRNA sequencing. This paper indicates that a molecular diagnosis is important for identifying the causative microorganism, in particular in cases of Gram staining and tissue culture-negative IAA.

–*Disrupting arrhythmia in a professional male wrestler athlete after rapid weight loss and high-intensity training—Case report* (Milovančev et al.).

It is well-known that physical exercise can induce physiological cardiac adaptions and benefit cardiovascular health (3, 4). However, in some cases, physiological heart adaptations may lead to increased susceptibility to arrhythmia in athletes. In this paper, the authors report a case of a wrestler athlete who developed disrupting arrhythmia during rapid weight loss and high-intensity training. This report provides useful information for athletes' physicians that precise intensive training prescriptions for individuals should be given by cardiovascular screening.

–*Myocardial infarction with non-obstructive coronary arteries in a patient double-seropositive for anti-glomerular basement membrane and anti-neutrophil cytoplasmic antibodies: A case report* (Krall et al.).

Anti-neutrophil cytoplasm antibody (ANCA)-associated vasculitides (AAV) and anti-glomerular basement membrane (GBM) disease are rare diseases with high mortality. This report describes a myocardial infarction with non-obstructive coronary arteries (MINOCA) patient with double seropositive for anti-ANCA and anti-GBM antibodies. Limited cases have been reported of anti-GBM disease patients with cardiovascular complications. These observations provide important information for physicians that endothelial injury or systemic inflammation patients with double-positive disease might be at higher risk to develop MINOCA. Further in-depth investigations to understand the clear causality and mechanism are required in the future.

–*Case Report: Danon Disease: Six Family Members and Literature Review* (Wang et al.).

Danon disease is a rare X-linked dominant genetic disorder characterized clinically by hypertrophic cardiomyopathy, skeletal muscle weakness, and intellectual disability (5). This report describes a case of Danon disease and his family members and reviews other relevant literature to discuss the clinical symptoms and possible strategies to treat Danon disease. This study offers critical information for the diagnosis and treatment of this disease.

–*Case report: Pulmonary arterial hypertension in ENG-related hereditary hemorrhagic telangiectasia* (Liu et al.).

The etiology of pulmonary arterial hypertension (PAH) can stem from various factors and is often multifactorial. It is crucial to implement standardized diagnostic procedures, investigate potential causes, and identify risk factors early on to enhance patient prognosis. In this paper, the authors report a case of hereditary hemorrhagic telangiectasia (HHT) combined with PAH. The clinical presentation, diagnostic process, and treatment of this rare case report provide useful information for physicians to diagnose HHT combined PAH patients. Further studies to better the pathogenesis of PAH in HHT should be of contribution to the timely and accurate diagnosis of this disease.

–*Case Report: An Unusual Case of Pheochromocytoma* (Liao et al.).

This report describes a female patient with acquired long QT syndrome, which is a rare complication of pheochromocytoma. Limited to the rarity and nonspecific clinical manifestations, diagnosis of pheochromocytoma is difficult. This study provides a successful diagnosis procedure of pheochromocytoma in this reported case and can offer important points for physicians to identify rare causes of common symptoms.

–*Case Report: Family Curse: An SCN5A Mutation, c.611C>A, p.A204E Associated With a Family History of Dilated Cardiomyopathy and Arrhythmia* (Huang et al.).

This study reports that *SCN5A* mutation with various dilated cardiomyopathy (DCM) associated gene mutations result in multiple phenotypes in a 3-generation family. By analyzing clinical data and genetic testing, this report suggests that a combination of *SCN5A* and PRKAG2 mutation can lead to DCM plus multifocal ectopic Purkinje-related premature contractions and PRKAG2 syndrome. This study discusses the possible causality between gene variants and observed clinical phenotype and indicates that gene diagnosis can offer early intervention to help physicians to improve diagnoses of DCM.

–*Case report: From monkeypox pharyngitis to myopericarditis and atypical skin lesions* (Guerrero et al.).

In this report, the authors describe a case of myopericarditis which is caused by human monkeypox, which is an endemic disease, infection followed by the onset of atypical skin lesions. This paper presents the clinical presentation, and diagnostic experience of this patient and provides antiviral treatment recommendations for physicians.

–*Case report: Conquer a complex variant: Coronary-pulmonary artery fistulas, atrial septal defect and bicuspid pulmonary valve, under beating heart surgery* (Zhon et al.).

This report describes a rare patient with two coronary artery to pulmonary artery fistula (CPAF) from two branches of the left anterior descending coronary to the main pulmonary artery, coexisting with a bicuspid pulmonary valve and atrial septal defect and treated by on-pump beating-heart surgery (OPBHS). This study discusses the potential origin and reason of this case as well as the clinical advantages of OPBHS. This report is a very complex case that has not yet been previously reported in the literature. This study offers important information for surgeries to treat CPAFs by OPBHS for patients with low surgical risk.

–*Case report: Coronavirus Disease 2019 (COVID-19) modified RNA vaccination-induced Adult-Onset Still's Disease with fulminant myocarditis as initial presentation* (Zhou et al.).

Several types of vaccines against the coronavirus disease 2019 (COVID-19). In this paper, the authors report a case of an elderly female who is diagnosed with post-vaccination about Adult-Onset Still's Disease after receiving a modified mRNA vaccine (BNT162b2). Adult-Onset Still's Disease is a rare autoinflammatory disease and potentially life-threatening. The report here describes the clinical presentation and diagnosis of this rare Adult-Onset Still's Disease following mRNA vaccines can provide important knowledge for physicians about this disease.

–*Case report: Sudden cardiorespiratory collapse in a healthy male after coronavirus disease 2019 vaccination at a vaccination center* (Chan et al.).

This paper reports a case of sudden cardiorespiratory collapse in a healthy young male after receiving the Oxford-AstraZeneca (ChAdOx1 nCoV-19) COVID-19 vaccination. This report addresses the importance of careful medical attention by healthcare providers to avoid possible severe adverse events following COVID-19 vaccination which could be certainly useful for healthcare policymakers, and physicians.

–*Multisystem immune-related adverse events due to toripalimab: Two cases-based review* (Chen et al.).

Immune checkpoint inhibitors (ICIs) significantly prolong survival in patients with advanced cancer. However, immune-mediated adverse events (irAEs) caused by ICIs pose a major threat to patients' lives. In this paper, the authors report 2 patients with advanced tumors suffering from severe multisystem irAEs following treated with toripalimab (anti-PD-1). This report also reviews the Case reports regarding multisystem irAEs based on myocarditis induced by PD-1 inhibitors. Early detection and diagnosis of multisystem inflammation are critical for the management of patients treated with ICIs. This study can provide important experience and critical information for physicians to manage patients undergoing ICIs treatment.

–*A case report and review of literature: Tuberculous pericarditis with pericardial effusion as the only clinical manifestation* (Wang et al.).

Tuberculosis (TB) remains a serious public health problem worldwide. In this paper, the authors report a case of a patient with Tuberculous pericarditis (TBP) who is admitted to the hospital with massive pericardial effusion. This patient is examined as negative with all routine laboratory tests for the pericardial effusion of unknown origin. This report provides experience and information for physicians to diagnose and treat percardial effuion patients, in particular to those demonstrated as non-TB causes negative.

–*Case report: A novel surgical technique for rapid valve-in-ring implantation into the native aortic annulus during left ventricular assist device implantation* (Pya et al.).

Left ventricular assist device (LVAD) implantation is an excellent option for treating end-stage heart failure patients (6). This report describes a novel and feasible surgical technique for performing transcatheter aortic valve replacement in valve-in-ring along with LVAD implantation for the treatment of a male patient suffering from refractory heart failure due to dilated cardiomyopathy and pure aortic insufficiency in need of a new aortic bioprosthesis. This study reports a novel surgical technique that can share treatment experience for cardiologists in aortic valve repair.

–*Case report: Severe dry cough associated with superior vena cava syndrome—Caused recurrent chylothorax* (Wan).

This case reports a patient with uremia who suffered from severe dry cough. This patient is finally diagnosed with superior vena cava and treated by percutaneous balloon dilatation. Chronic coughs, which may be caused by many diseases, are very common syndrome in the respiratory department outpatient clinic. This paper reports a severe dry cough case caused by superior vena cave occlusion-induced recurrent chylothorax can provide information for physicians to diagnose recurring severe cough patients.

–*Multimodal Imaging for Total Anomalous Systemic Venous Drainage Diagnosis and Preoperative Planning: A Case Report and Literature Review* (Ding et al.).

Total anomalous systemic venous drainage (TASVD) is a rare congenital heart disease (7). In this case report, the authors report a 40-year-old male patient with TASVD. As a rare heart disease, limited information can be obtained from a literature review about the description of TASVD except Case reports. Diagnosing TASVD would be a difficult task in the medical field, primarily because of the variations observed in individuals and the absence of specific laboratory tests. In general, echocardiography is the first-line examination for TASVD diagnosis. This report provides information for physicians that multimodal imaging (Transthoracic, transesophageal, 3D echocardiography, contrast echocardiography, and computed tomography angiography) can be performed to verify the diagnosis of TASVD.

–*Massive pleural effusion following high-power and short-duration radiofrequency ablation for treatment of atrial fibrillation: A case report and review of the literature* (He et al.).

Radiofrequency catheter ablation (RFCA) is a non-pharmacological treatment for drug-refractory atrial fibrillations. Postpericardial injury syndrome (PPIS) is defined as pericarditis or pericardial effusion during myocardial infarction or cardiac intervention. It is widely recognized as a common complication of cardiac surgery, with an incidence ranging from 3% to 30%. Different from previously reported PPIS which is most characterized by pericardial effusion, this report describes a case of PPIS that presents pleural effusion as a main feature after the operation. This case report also systematically reviews the clinical characteristics of PPIS. The study in this paper provides useful reference information for physicians to timely diagnose a patient with massive pleural effusion alone following RFCA.

–*Case report: Delayed cardiac rupture with congenital absence of pericardium after blunt trauma* (Shen et al.).

As a rare disease with no specific symptoms and signs, the clinical diagnosis of congenital absence of pericardium (CAP) is very difficult. In this paper, the authors report a case of a patient with CAP and present some atypical features which are different from previously reported literature. The clinical presentation and diagnostic process of this patient should be useful to physicians in the diagnosis and treatment of CAP.

–*Case report: Reducing the duration of positive-pressure ventilation for large mediastinal masses* (Zhang et al.).

This report describes two high-risk patients with large mediastinal tumors (MMs) during general anesthesia undergoing tumorectomy by thoracotomy. The perioperative management of patients with large MMs is challenging. This study suggests that patients with large MM should receive positive-pressure ventilation following muscle relaxants given, but that cardiothoracic surgeons should immediately transect the sternum to relieve compression. This study provides important information and experiences for physicians to manage patients with large MMs.

–*Case report: Metastatic myxoid liposarcoma arising from the right atrium extends as cardiac tamponade—A rare case of atrial oncology* (Ramamurthy et al.). *Right atrial cardiac lipoma with distinctive imaging characteristics. A rare case report and literature review* (Chen et al.).

Cardiac lipomas is rare primary cardiac tumors, many of them do not exhibit obvious features and are difficult to identify. These two reports describe patients presenting a lipomas in the right atrium. In these papers, the authors share their experimence in the diagnosis and treatment of cardiac lipomas can provide useful information for physicians.

–*Successful simultaneous stenting of a pulmonary artery and vein in pulmonary vascular stenosis due to silicosis. Case report and literature review* (Westhoff et al.).

This report describes a successful stenting of a pulmonary artery and vein in a silicosis-caused pulmonary vascular stenosis patient. In this paper, the authors provide interventional procedure recommendations for this pulmonary vascular stenosis for physicians *via* clinical symptom presentation and literature review.

–*An adult female patient with single atrium and single ventricle undergoing appendectomy: A case report* (Wu et al.).

This paper reports an adult female patient with a single atrium and single ventricle undergoing appendectomy. Single atrium and single ventricle is a rare heart disease with very few patients surviving into adulthood. This report describes their associated surgical findings and can share useful experiences for physicians to diagnose patients with similar conditions.

–*Acute myocardial infarction after inactivated COVID-19 vaccination: a case report and literature review* (Ou et al.).

Many types of vaccines have been developed to restrain the pandemic of COVID-19. This study reports an acute myocardial infarction case following post-COVID-19 vaccination and discusses the potential pathogenesis mechanisms. This study provides clinical experience and recommendations for physicians to manage patients with similar conditions.

–*Case report: Aortoesophageal fistula—an extremely rare but life-threatening cardiovascular cause of hematemesis* (Wong et al.).

In this paper, the authors report a hematemesis patient with underlying diagnosed esophageal cancer who presents typical aortoesophageal fistula (AEF) clinical features. This report highlights the clinical features and diagnosis process of this extremely rare but life-threatening disease. This paper also provides recommendations for physicians to timely diagnose AEF.

In conclusion, the high-quality clinical case contributions presented in this Research Topic have significantly boosted knowledge, diagnosis, and treatment of cardiovascular disease in complex cases.

Author contributions

LW: Writing – original draft, Writing – review & editing. WW: Writing – original draft, Writing – review & editing. LR: Writing – original draft, Writing – review & editing, Supervision. PL: Supervision, Writing – original draft, Writing – review & editing.

Funding

This work was supported by the grants from National Natural Science Foundation of China (82020108002 and 82225005 to JX and 82270291 to LW), Science and Technology Commission of Shanghai Municipality (23410750100, 20DZ2255400 and 21XD1421300 to JX) and Natural Science Foundation of Shanghai (23ZR1423000 to LW).

Conflict of interest

The authors declare that the research was conducted in the absence of any commercial or financial relationships that could be construed as a potential conflict of interest.

The author(s) declared that they were an editorial board member of Frontiers, at the time of submission. This had no impact on the peer review process and the final decision.

Publisher's note

All claims expressed in this article are solely those of the authors and do not necessarily represent those of their affiliated organizations, or those of the publisher, the editors and the reviewers. Any product that may be evaluated in this article, or claim that may be made by its manufacturer, is not guaranteed or endorsed by the publisher.

References

1. Hermida U, van Poppel MPM, Lloyd DFA, Steinweg JK, Vigneswaran TV, Simpson JM, et al. Learning the hidden signature of fetal arch anatomy: a three-dimensional shape analysis in suspected coarctation of the aorta. *J Cardiovasc Transl Res*. (2023) 16(3):738–47. doi: 10.1007/s12265-022-10335-9

2. Xiong T, Yang Y, Zuo B, Chen X, Wang D. Metabolic remodeling in takotsubo syndrome. *Front Cardiovasc Med*. (2022) 9:1060070. doi: 10.3389/fcvm.2022.1060070

3. Xiao J, Rosenzweig A. Exercise and cardiovascular protection: update and future. *J Sport Health Sci*. (2021) 10:607–8. doi: 10.1016/j.jshs.2021.11.001

4. Bei Y, Liang Q, Lin S, Liu S, Lu X, Shen Y, et al. Animal exercise studies in cardiovascular research: current knowledge and optimal design-A position paper of the committee on cardiac rehabilitation, Chinese medical Doctors' association. *J Sport Health Sci*. (2021) 10:660–74. doi: 10.1016/j.jshs.2021.08.002

5. Zhai Y, Miao J, Peng Y, Wang Y, Dong J, Zhao X. Clinical features of danon disease and insights gained from LAMP-2 deficiency models. *Trends Cardiovasc Med*. (2023) 33(2):81–9. doi: 10.1016/j.tcm.2021.10.012

6. Ben Gal T, Ben Avraham B, Milicic D, Crespo-Leiro MG, Coats AJS, Rosano G, et al. Guidance on the management of left ventricular assist device (LVAD) supported patients for the non-LVAD specialist healthcare provider: executive summary. *Eur J Heart Fail*. (2021) 23(10):1597–609. doi: 10.1002/ejhf.2327

7. Maddali MM, Al Kindi HN, Kandachar PS, Al Farqani A, Al Alawi KS, Al Kindi F, et al. Identifying anomalies of systemic venous drainage: systemic venous anomalies; atrial morphology. *World J Pediatr Congenit Heart Surg*. (2023) 14(4):490–6. doi: 10.1177/21501351231158539

frontiers in Cardiovascular Medicine

CASE REPORT
published: 25 January 2022
doi: 10.3389/fcvm.2021.818884

Aortic Coarctation Associated With Hypertrophic Cardiomyopathy in a Woman With Hypertension and Syncope: A Case Report With 8-Year Follow-Up

*Hong Yang†, Hong Wang†, Zongzhe Li, Jiangtao Yan, Yu-E Song, Hesong Zeng, Xingwei He, Rui Li and Dao Wen Wang**

Division of Cardiology and Department of Internal Medicine, Tongji Hospital, Tongji Medical College of Huazhong University of Science and Technology, Wuhan, China

OPEN ACCESS

Edited by:
Yan Zhang,
Peking University, China

Reviewed by:
Zhejun Cai,
Zhejiang University, China
Gong Wei,
Capital Medical University, China

***Correspondence:**
Dao Wen Wang
dwwang@tjh.tjmu.edu.cn

†These authors have contributed equally to this work and share first authorship

Specialty section:
This article was submitted to General Cardiovascular Medicine, a section of the journal Frontiers in Cardiovascular Medicine

Received: *20 November 2021*
Accepted: *21 December 2021*
Published: *25 January 2022*

Citation:
Yang H, Wang H, Li ZZ, Yan JT, Song Y-E, Zeng HS, He XW, Li R and Wang DW (2022) Aortic Coarctation Associated With Hypertrophic Cardiomyopathy in a Woman With Hypertension and Syncope: A Case Report With 8-Year Follow-Up. Front. Cardiovasc. Med. 8:818884. doi: 10.3389/fcvm.2021.818884

Background: Coarctation of the aorta (CoA) is a common congenital cardiovascular malformation with aortic narrowing in the region of the ligamentum arteriosum. Hypertrophic cardiomyopathy (HCM) is a primary cardiomyopathy that is characterized by left ventricular wall thickening and likely left ventricular outflow tract (LVOT) obstruction. They are two irrelevant diseases, and their coexistence has not been reported before. Here, we described a young female patient who concurrently has CoA and HCM.

Case Presentation: The patient has had hypertension since 18-years old and complained of chest discomfort on effort and fatigue thereafter. Initially, she was diagnosed as having hypertrophic cardiomyopathy and primary hypertension. The presence of CoA was not found until she was 35 years old when she had an onset of paroxysmal supraventricular tachycardia (PSVT) and presented with syncope. Failure of the ablation procedure *via* the femoral artery revealed the possibility of CoA and PDA that was confirmed by aortic CTA and angiography. CoA was then treated successfully with a covered stent, and the symptoms of the patient improved remarkably. Additionally, the patient had typical imaging features of HCM, and two novel HCM-causing heterozygous mutations were identified by genetic testing, DSP-encoding desmoplakin, and MYBPC3-encoding myosin-binding protein C. The HCM was suspected to be contributing to the clinical presentations of the patient and challenged the timely diagnosis of CoA. The 8-year follow-up on aortic CTA and angiography revealed no stent graft-related complications. Moreover, no changes in HCM-related imaging features were found in the follow-up echocardiography 8 years after the correction of aortic coarctation, which strengthened the diagnosis of HCM.

Conclusion: Here, we reported the diagnostic challenges, management, and 8-yeasr follow-up findings in a rare case of CoA combined with HCM. The case highlighted the importance for physicians to exclude CoA in young hypertensive patients, and proved the efficacy of stent repair in treating CoA in older patients.

Keywords: aortic aoarctation, hypertrophic cardiomyopathy, hypertension, genetic variant, stent repair

INTRODUCTION

Aortic aoarctation (CoA) represents a spectrum of aortic narrowing that varies from discrete narrowing of thoracic aorta to tubular hypoplasia. Hypertrophic cardiomyopathy (HCM) is defined by the presence of increased wall thickness (usually ≥ 15 mm) in one or more left ventricular myocardial segments and is considered primary cardiomyopathy after exclusion of other cardiac conditions or systemic diseases. In up to 60% of cases, HCM is an autosomal-dominant genetic trait caused by variants of cardiac sarcomere protein genes (1). CoA is a common congenital heart disease, and its prognosis is poor if untreated (2). Clinically, these two anomalies are irrelevant and rarely coexist.

Here, we described the diagnostic challenges, clinical course, imaging studies, management, and 8-year follow-up in an adult female patient who has concurrent presence of CoA and HCM. Patent ductus arteriosus (PDA) and paroxysmal supraventricular tachycardia (PSVT) were also present, which complicated further the clinical features of the patient. Exome sequencing was performed to investigate genetic involvement in the patient. As a result, two likely novel heterozygous HCM-causing mutations in DSP and MYBPC3 genes were identified.

CASE PRESENTATION

A 35-year-old woman presented to our hospital because of repeated episodes of transitory amaurosis and presyncope during the last 3 months. These episodes were often preceded by a short period of palpitation. She also complained of chest discomfort on effort, and she quitted her work as a warehouse manager because of marked fatigue. She had a 17-year history of hypertension and took long-acting nifedipine everyday. She had a 12-year history of mild chest discomfort, and she had been diagnosed as having hypertrophic cardiomyopathy in a local hospital. She also suffered from systemic lupus erythematosus and has been taking oral glucocorticoid for 7 years. She had no family history of hypertension, cardiovascular diseases, or sudden death. The patient had normal vital signs upon admission. Blood pressure (right upper arm) was 135/75 mmHg. There was a systolic murmur at the left sternal border and in second to third intercostal spaces. No other remarkable abnormalities were found during regular physical examination. EKG showed sinus rhythm with right bundle branch block (RBBB) and T wave inversion in precordial, I, and aVL leads.

Transthoracic echocardiography (TTE) demonstrated asymmetric left ventricular (LV) hypertrophy with abnormal systolic anterior motion (SAM) of the anterior mitral valve leaflet and obstruction of left ventricular outflow tract (LVOT) (**Figures 1A,B**). There was no critical valvular disease, and systolic function of the left ventricle was normal. Cardiac MRI showed a finding of asymmetric left ventricular hypertrophy as TTE (**Figures 1E,F**).

Abbreviations: CoA, coarctation of the aorta; CHD, congenital heart disease; HCM, hypertrophic cardiomyopathy; LV, left ventricle; PDA, patent ductus arteriosus; RBBB, right bundle branch block; TTE, transthoracic echocardiography; LVOT, left ventricular outflow tract.

On the second day of admission, the patient had an acute episode of palpitation associated with light-headedness. EKG showed supraventricular tachycardia with RBBB (**Figure 1G**). Electrophysiology study revealed atrioventricular reentrant tachycardia using the left-sided concealed accessory pathway. Catheter ablation procedure was then performed. Surprisingly, *via* the right femoral artery the ablation catheter was failed to access the left heart but the right ventricle, showing left bundle branch block in EKG by stimulation. The ablation procedure was discontinued, and aortic angiography was performed instead. Advancement of the angiographic catheter was blocked at the proximal end of descending aorta, while the wire could be delivered to the right ventricle. Angiography performed on the descending aorta could disclose pulmonary artery rather than aortic arch and ascending aorta.

Coarctation of the aorta (CoA) and PDA were suspected and then confirmed by CT angiography (CTA) of the aorta. The descending aorta was remarkably narrowed at the isthmus by approximately 2 cm past the left subclavian artery (**Figures 2A,B**). The innominate artery and the left subclavian artery were dilated with extensive collateral circulation arising from those arteries (**Figure 2B**). A small vessel, immediately distal to the aortic obstruction, was found to be connecting the descending aorta and the pulmonary artery (**Figure 2A**), confirming the presence of PDA. Blood pressure was measured again, and a pressure gradient of 50 mmHg was noted between the upper and lower extremities. Holter monitor results showed frequent premature ventricular beats (**Figure 1I**), non-sustained ventricular tachycardia and supraventricular tachycardia (**Figure 1H**) that had the same morphology as the one captured by 12-lead EKG (**Figure 1G**).

The catheter ablation procedure was performed again thereafter. An ablation catheter was delivered to the right atrium *via* the right femoral vein and advanced to the left side of the heart by trans-septal puncture. By this way, ablation was completed successfully.

After ablation, the patient had no episodes of presyncope and paroxysmal palpitation. However, she still felt chest discomfort on effort and marked fatigue, and could not go back to work. One month later, she was readmitted to our hospital, and balloon angioplasty with stenting was performed. A catheter was delivered to the root of the aorta *via* the right brachial artery. Angiography of the root of the aorta showed narrowing of the aortic isthmus (**Figure 2D**) and marked collateral circulation (**Figure 2E**). Pressure was 200/100 mmHg at the proximal end of the descending aorta to the obstruction and 124/90 mmHg at the distal end to the obstruction (**Figure 2H**). After balloon dilatation, the covered endovascular stent was placed at the aortic isthmus, and PDA was blocked by the stent concomitantly (**Figure 2F**). Aortic pressures were equalized at the proximal and distal ends of the descending aorta (**Figure 2I**). The symptoms of the patient of chest discomfort and fatigue were relieved remarkably after reconstruction. Her blood pressure was below 120/80 mmHg with metoprolol succinate (95 mg/day) that was given to treat premature ventricular beats and ventricular tachycardia and HCM. The patient went back to work one month later after successful repair of CoA. She remained normotensive

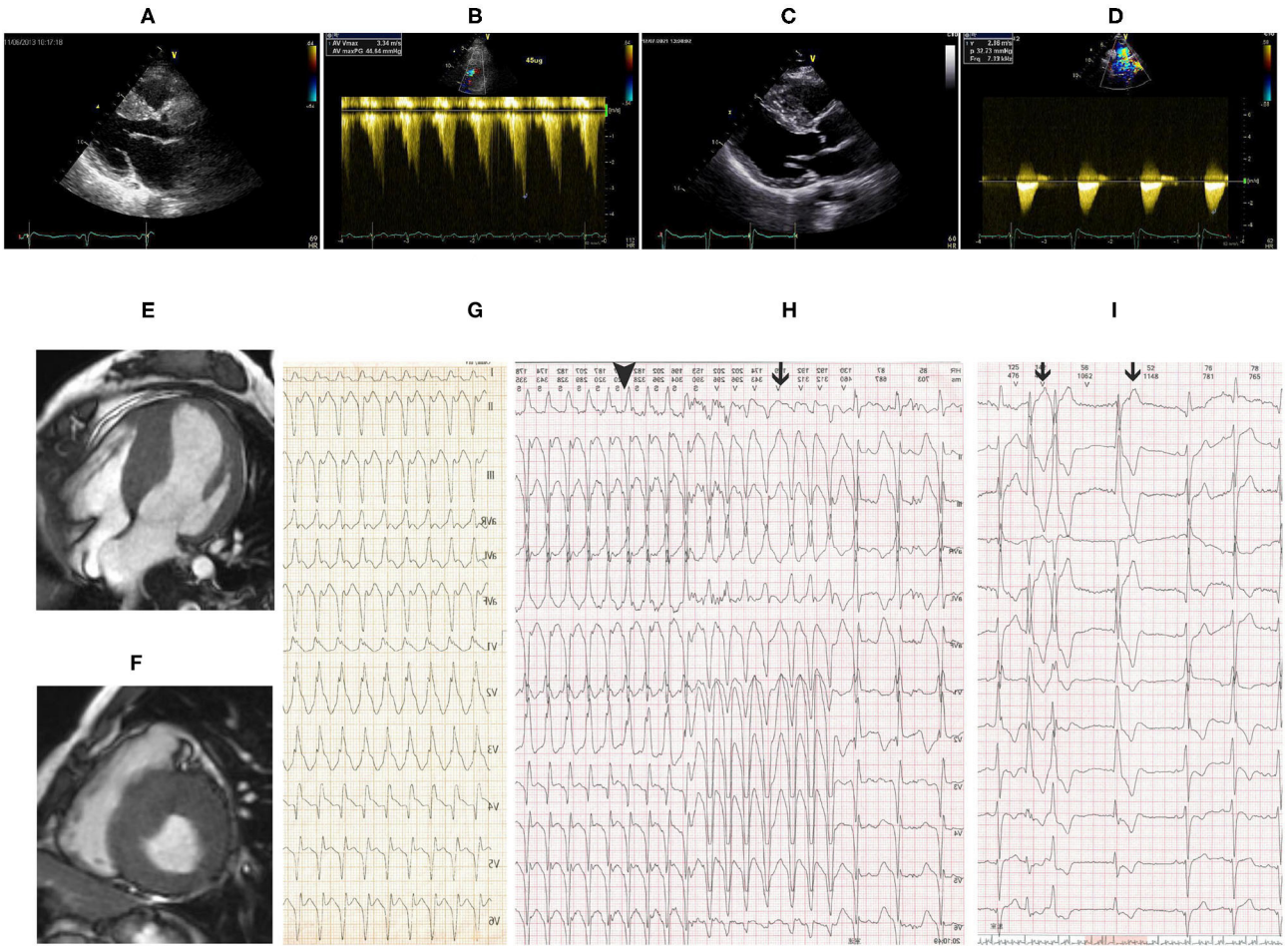

FIGURE 1 | (A) Transthoracic echocardiography (TTE) showed remarkably asymmetric left ventricular (LV) hypertrophy with 23-mm thickness of the interventricular septum and 10-mm thickness of the posterior wall. **(B)** Pressure gradient of the left ventricular outflow tract (LVOT) was 44 mmHg after dobutamine infusion at a speed of 45 ug/ml. Follow-up TTE 8 years after CoA correction showed similar LV hypertrophy as before intervention **(C)** and flow velocity at the descending aorta was 2.9 m/s **(D)**. Cardiac magnetic resonance imaging (MRI) showed asymmetric LV hypertrophy in **(E)** apical 4 chamber view and **(F)** short-axis view. **(G)** Twelve-lead echocardiogram (EKG) showed supraventricular tachycardia with right bundle branch block (RBBB) at a heart rate of 190 bpm. Holter monitor **(H,I)** revealed non-sustained ventricular tachycardia (black line in H), supraventricular tachycardia with RBBB (black triangle in H), and premature ventricular beats (black line in I).

and was doing well thereafter. On 8-year follow-up, aortic CTA and angiography were repeated, which showed patency of the covered stent (**Figures 2C,G**), and no pressure gradient was detected at the proximal and distal ends of the descending aorta (**Figure 2J**). Pressure was 177/90 mmHg at the proximal end and 174/92 mmHg at the distal end of the descending aorta, respectively (**Figure 2J**). Aortic CTA showed reduced collateral circulation and disappearance of PDA compared to before the stent treatment (**Figure 2C**). Moreover, repeated TTE on 8-year follow-up showed similar HCM-related imaging features as before the stent treatment, such as similarly thickened interventricular septum (**Figure 1C**), and flow velocity in the descending aorta was around 2.9 m/s (**Figure 1D**).

We performed whole exome sequencing with high depth (>100-fold coverage) by next-generation sequencing and then validation by Sanger sequencing to identify genetic involvement in the causation of the disease. After filtering intron variants, synonymous variants, and minor allele frequency >0.005 variants in the dbSNP database, variants in the ESP database, nonpathogenic variants in the ClinVar database, and *in silico* functional predicting, we identified two likely novel heterozygous HCM-causing mutations, DSP (p.Val520Met, c.1558G>A) (SIFT = 0.05; PolyPhen-2 = 1) and MYBPC3 (p.Tyr525Ser, c.1574A>C) (SIFT = 0; PolyPhen-2 = 0.976) (**Figure 3**) according to the guideline (3). Except for these mutations, we detected no other likely pathogenic mutation in all cardiomyopathy-related genes. Notably, these mutations are located in evolutionary highly conservative areas across multiple species (phylop = 2.6 and 1.94, respectively). Furthermore, the following Sanger sequencing demonstrated that they did not exist in the 500 unrelated ethnically matched healthy controls.

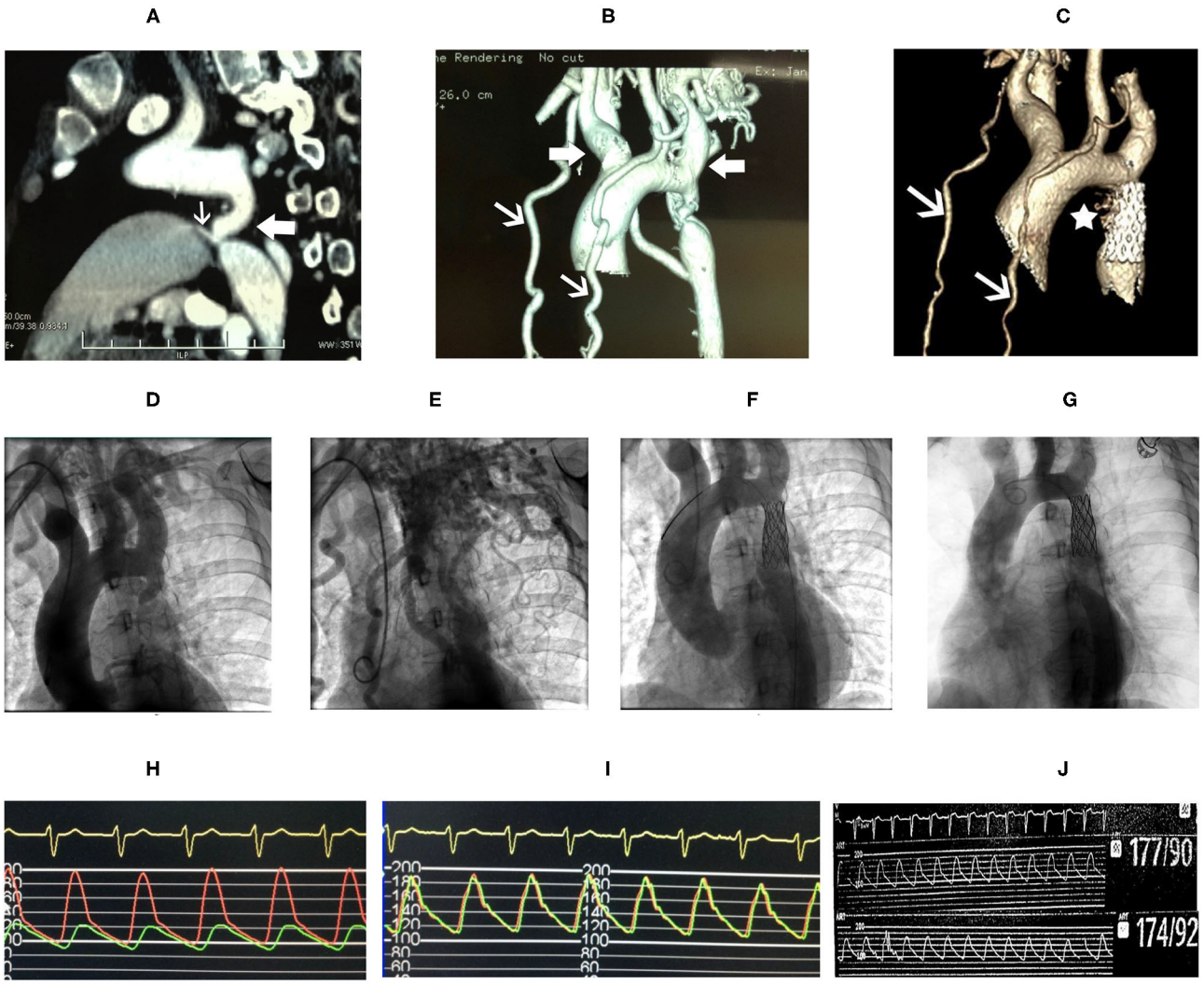

FIGURE 2 | CT angiography (CTA) of the aorta **(A)** showed marked narrowing in the isthmic region of the descending aorta **(white block arrow)** and patent ductus arteriosus (PDA) **(white arrow)** connecting the aorta and the pulmonary artery. Dilatation of the innominate artery and the left subclavian artery **(white block arrows)**, and extensive collateral circulation **(white arrows)** were shown in **(B)**. Follow-up CTA of the aorta 8 years after stent repair showed reduced collateral circulation **(C, white arrows)**, and the PDA is not shown **(C, asterisk)**. Aortic angiography showed remarkable isthmic coarctation of the aorta with dilated innominate artery and left subclavian artery **(D)** and exuberant collateral circulation **(E)**. Pressure gradient between the proximal and distal ends to the aortic obstruction was 74 mmHg **(H)**. The descending aorta, after placement of stent, was shown **(F)** with equalization of pressure at the proximal and distal ends of the descending aorta **(I)**. Repeated aortic angiography at 8-year follow-up showed patency of the covered stent and reduction in collateral circulation **(G)**, and no pressure gradient was found, 177/90 mmHg at the proximal vs. 174/92 mmHg at the distal end of descending aorta, respectively **(J)**.

DISCUSSION

Coarctation of the aorta (CoA) and HCM are two irrelevant cardiac malformations according to anatomy and pathophysiology. These anomalies have not been reported to concurrently exist in the same case. In this case, the clinical features of the patient were complex, and the diagnosis was challenging because of the concurrent presence of CoA and HCM. In addition, PDA and atrioventricular reentrant tachycardia by the accessory pathway were present in the same case, which further complicated the clinical manifestation of the patient. CoA is a common lesion in congenital heart diseases (CHDs), accounting for 6–8% of live births with CHD (4). It can be associated with other congenital defects, such as bicuspid aortic valve, subaortic stenosis, ventricular septal defect, and PDA (5). In this case, CoA was associated with PDA. CoA in adults usually comes to medical attention because of arterial hypertension. The 2008 ACC/AHA guidelines for adults with CHD recommended that every patient with hypertension should have the brachial and femoral pulses palpated to search for "brachial-femoral delay" of CoA, and that blood pressure should be measured in both bilateral arms and legs to search for pressure

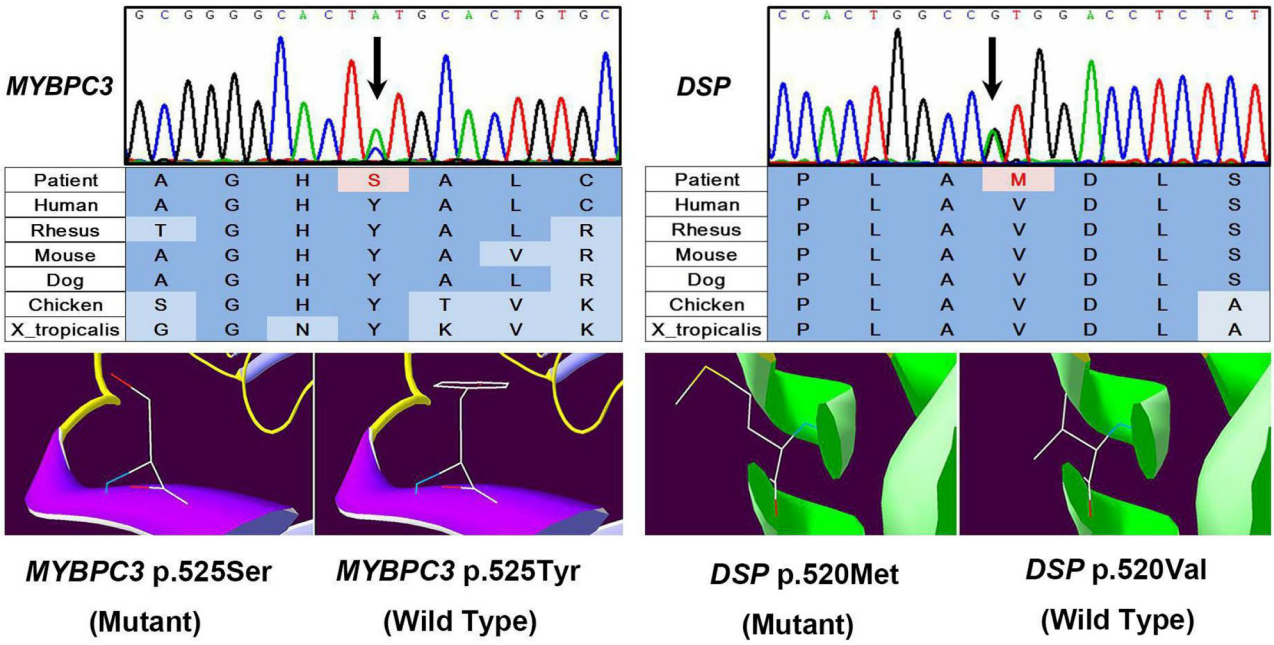

FIGURE 3 | Results of sequencing quality and mutation identification. Two likely novel heterozygous hypertrophic cardiomyopathy (HCM)-causing mutations were identified, DSP (p.Val520Met, c.1558G>A) (SIFT = 0.05; PolyPhen-2 = 1) and MYBPC3 (p.Tyr525Ser, c.1574A>C) (SIFT = 0; PolyPhen-2 = 0.976).

difference (5). Discrepant blood pressures or pulses between the upper- and lower-extremities are an important sign of CoA. In this case, HCM was diagnosed first by echo during early years of presentation, and the detection of CoA and PDA was delayed until the onset of PSVT. Failure of the ablation procedure for PSVT *via* the femoral artery made the suspicion of CoA and PDA accidently and the following aortic CTA confirmed the diagnosis. Reasons for the delayed diagnosis of CoA in this case include: (1) Presence of HCM complicated the clinical features of the patient, it could explain the patient's presentations as chest discomfort and the murmur on heart auscultation, and made the providers fail to search other possible etiologies; (2) The patient presented with hypertension in 18-years old, but etiology was not fully explored. Blood pressure was only measured in the arms but not in the ankles or legs. Pulse discrepancy between the arms and legs was also ignored; and (3) the initial echo did not include a suprasternal notch view that should reveal high-velocity flow in the descending aorta if done and provide diagnostic clues of CoA.

The prognosis of CoA was poor if untreated, with an average survival age of 35 years and 75% mortality at 46 years of age (2). Therefore, CoA should be diagnosed and treated early in life. Other than treating hypertension, intervention or correction of coarctation should be performed in selected patients. Indications for intervention in adult patients with CoA by the 2008 ACC/AHA guidelines are: (1) peak-to-peak coarctation gradient $\geq$ 20 mg; which is the difference in peak pressure proximal and beyond the narrowed segment; (2) peak-to-peak coarctation gradient <20 mg with imaging evidence of significant coarctation and radiologic evidence of significant collateral flow (5). So far, there has been no consensus on the choice of surgical repair or percutaneous interventions in older patients. A recent study showed that stent repair of coarctation of the aorta was a safe and feasible alternative to surgical correction (6). For this patient, angioplasty and stenting were performed. Adequate dilatation of the region was achieved, and a covered stent was placed with equalization of pressures in the proximal and distal descending aorta and closure of PDA. After the procedure, the patient was free of major symptoms during the 8-year follow-up and remained normotensive with 95 mg of metoprolol succinate per day. Repeated aortic CTA and angiography after 8 years confirmed persistent patency of the stent graft and revealed no stent-related complications. The clinical and imaging findings of long-term follow-up demonstrated the efficacy of stent repair in treating CoA in older patients.

Hypertrophic cardiomyopathy (HCM) is defined by unexplained cardiac hypertrophy and should be considered only after exclusion of other cardiac or systemic diseases. In this case, increased afterload by CoA and hypertension may also cause LV hypertrophy, and the diagnosis of HCM was questionable. However, in the follow-up, when the CoA of the patient was effectively corrected and her blood pressure was also maintained in the normal range for 8 years, repeated TTE still showed a similar significant LV hypertrophy as before the stent treatment. These follow-up imaging data provide strong evidence supporting the presence of HCM.

Genetic variants in genes that encode different components of cardiac sarcomere protein could explain HCM in up to 60% cases (1). We performed genetic testing in this case and identified a novel mutation in gene-encoding myosin-binding protein C

(MYBPC3). MYBPC3 and beta-myosin heavy chain (MYH7) are two large genes accounting for the majority of sarcomere protein gene mutations in HCM (7). Other than MYBPC3, we identified another novel mutation in the DSP gene. DSP makes a protein called desmoplakin that is a crucial component of desmosome structures in cardiac muscle cells. DSP gene mutations have been reported to play a role in arrhythmogenic right ventricular cardiomyopathy, dilated cardiomyopathy, and restrictive cardiomyopathy, but they can present with HCM and atrioventricular block (8, 9). We speculated that mutations in MYBP3 and DSP are contributory to HCM and likely arrhythmias in the patient.

CONCLUSION

Here, we reported a rare case of CoA combined with HCM in a 35-year-old woman and discussed the diagnostic challenge, management, and long-term (8 years) follow-up results. The case again highlights that CoA is a rare but important etiology in young hypertensive patients. Moreover, percutaneous interventions such as stent repair are effective treatments of CoA in older patients, as proved by the long-term follow-up aortic CTA and angiography in this case.

DATA AVAILABILITY STATEMENT

The original contributions presented in the study are included in the article/supplementary material, further inquiries can be directed to the corresponding author.

ETHICS STATEMENT

Written informed consent was obtained from the individual(s) for the publication of any potentially identifiable images or data included in this article.

AUTHOR CONTRIBUTIONS

DWW contributed to the conception of the report and critical revision of the report for important intellectual content. HY and HW drafted the manuscript, and were responsible for acquisition and interpretation of the data the searched the literature and revised the figures. ZZL performed genetic testing and analysis. HSZ, JTY, and XWH performed aortic angiography and stenting. Y-ES and RL reconstructed the images and drew the figures. All authors were involved in the treatment of the patient and made a substantial contribution to the preparation of the manuscript, read, and approved the final version of the manuscript.

ACKNOWLEDGMENTS

We thank Dr. Sishu Yuan who helped in the reconstruction and drawing of the images.

REFERENCES

1. Gersh BJ, Maron BJ, Bonow RO, Dearani JA, Fifer MA, Link MS, et al. 2011 Accf/Aha guideline for the diagnosis and treatment of hypertrophic cardiomyopathy: a report of the American College of Cardiology Foundation/American Heart Association Task Force on Practice Guidelines. *Circulation.* (2011) 124:e783–831. doi: 10.1161/CIR.0b013e318223e2bd
2. Jenkins NP, Ward C. Coarctation of the aorta: natural history and outcome after surgical treatment. *Qjm.* (1999) 92:365–71. doi: 10.1093/qjmed/92.7.365
3. Richards S, Aziz N, Bale S, Bick D, Das S, Gastier-Foster J, et al. Standards and guidelines for the interpretation of sequence variants: a joint consensus recommendation of the American College of Medical Genetics and Genomics and the Association for Molecular Pathology. *Genet Med.* (2015) 17:405–24. doi: 10.1038/gim.2015.30
4. Kenny D, Hijazi ZM. Coarctation of the aorta: from fetal life to adulthood. *Cardiol J.* (2011) 18:487–95. doi: 10.5603/CJ.2011.0003
5. Warnes CA, Williams RG, Bashore TM, Child JS, Connolly HM, Dearani JA, et al. Acc/Aha 2008 guidelines for the management of adults with congenital heart disease: a report of the American College of Cardiology/American Heart Association Task Force on Practice Guidelines (Writing Committee to Develop Guidelines on the Management of Adults with Congenital Heart Disease). *Circulation.* (2008) 118:e714–833. doi: 10.1161/CIRCULATIONAHA.108.190690
6. Suarez de. Lezo J, Romero M, Pan M, Suarez de Lezo J, Segura J, Ojeda S, et al. Stent repair for complex coarctation of aorta. *JACC Cardiovasc Interv.* (2015) 8:1368–79. doi: 10.1016/j.jcin.2015.05.018
7. Lopes LR, Zekavati A, Syrris P, Hubank M, Giambartolomei C, Dalageorgou C, et al. Genetic complexity in hypertrophic cardiomyopathy revealed by high-throughput sequencing. *J Med Genet.* (2013) 50:228–39. doi: 10.1136/jmedgenet-2012-101270
8. Norman M, Simpson M, Mogensen J, Shaw A, Hughes S, Syrris P, et al. Novel Mutation in desmoplakin causes arrhythmogenic left ventricular cardiomyopathy. *Circulation.* (2005) 112:636–42. doi: 10.1161/CIRCULATIONAHA.104.532234
9. Olive M, Goldfarb L, Moreno D, Laforet E, Dagvadorj A, Sambuughin N, et al. Desmin-related myopathy: clinical, electrophysiological, radiological, neuropathological and genetic studies. *J Neurol Sci.* (2004) 219:125–37. doi: 10.1016/j.jns.2004.01.007

Conflict of Interest: The authors declare that the research was conducted in the absence of any commercial or financial relationships that could be construed as a potential conflict of interest.

frontiers in Cardiovascular Medicine

CASE REPORT
published: 28 February 2022
doi: 10.3389/fcvm.2022.839441

Amiodarone-Induced Multi-Systemic Toxicity Involving the Liver, Lungs, Thyroid, and Eyes: A Case Report

Hye-Su You[1], Jae Hyun Yoon[1], Sung Bum Cho[2], Yoo-Duk Choi[3], Yung Hui Kim[4], Wonsuk Choi[5], Ho-Cheol Kang[5] and Sung Kyu Choi[1]*

[1] Department of Gastroenterology and Hepatology, Chonnam National University Hospital and Medical School, Gwangju, South Korea, [2] Department of Gastroenterology and Hepatology, Hwasun Chonnam National University Hospital and Medical School, Hwasun, South Korea, [3] Department of Pathology, Chonnam National University Hospital and Medical School, Gwangju, South Korea, [4] Department of Ophthalmology, Chonnam National University Hospital and Medical School, Gwangju, South Korea, [5] Department of Endocrinology, Hwasun Chonnam National University Hospital and Medical School, Hwasun, South Korea

Objectives: Amiodarone is widely used to treat arrhythmia. However, amiodarone is known for its severe toxicity to the liver, lungs, and thyroid. Amiodarone causes liver damage ranging from asymptomatic serum aminotransferase elevation to hepatic failure requiring liver transplantation. Although amiodarone toxicity has been reported, its simultaneous multi-organ toxicity is not well-known. Here, we introduce a novel case of multi-systemic amiodarone toxicity involving the liver, lungs, thyroid, and eyes.

Case Presentation: A 61-year-old woman visited the emergency room due to general weakness, nausea, visual disturbance, heat intolerance, and a non-productive cough. The patient had been using clopidogrel and amiodarone due to underlying atrial fibrillation. The total level of bilirubin was 0.71 mg/dL, aspartate aminotransferase was 358 U/L, alanine aminotransferase was 177 U/L, and prothrombin time was 27.1 s. Computed tomography showed diffuse increased liver intensity and scattered hyperattenuated nodular consolidations in both lungs. Transthoracic needle lung biopsy revealed fibrinoid interstitial inflammation with atypical change of type II pneumocytes and intra-alveolar foamy macrophages. In addition, the thyroid-stimulating hormone level was <0.008 μIU/mL, and free thyroxine was 4.67 ng/dL. The thyroid scan showed diffuse homogenous intake of technetium-99 m pertechnetate in both thyroid lobes. The ophthalmologic exam detected bilateral symmetrical corneal deposits in a vortex pattern. With these findings, we could diagnose amiodarone-induced hepatic, pulmonary, thyroid, and ophthalmologic toxicity. Liver function was restored after cessation of amiodarone, and thyroid function was normalized with methimazole administration. However, due to aggravated lung consolidations, systemic steroid treatment was administered, and improvement was seen 1 week after, at the follow-up exam. As her symptoms improved, she was discharged with a plan of steroid administration for 3 to 6 months.

Conclusions: This case implies the possibility of multi-systemic amiodarone toxicity. Thus, the toxicity of amiodarone to multiple organs must be monitored. Prompt cessation of the drug should be considered upon diagnosis.

Keywords: amiodarone, toxicity, liver, lung, thyroid

OPEN ACCESS

Edited by:
Gian Marco Rosa,
San Martino Hospital (IRCCS), Italy

Reviewed by:
Fausto Bogazzi,
University of Pisa, Italy
David Marti,
University of Alcalá, Spain

***Correspondence:**
Jae Hyun Yoon
zenmake14@gmail.com

Specialty section:
This article was submitted to General Cardiovascular Medicine, a section of the journal Frontiers in Cardiovascular Medicine

Received: *20 December 2021*
Accepted: *02 February 2022*
Published: *28 February 2022*

Citation:
You H-S, Yoon JH, Cho SB, Choi Y-D, Kim YH, Choi W, Kang H-C and Choi SK (2022) Amiodarone-Induced Multi-Systemic Toxicity Involving the Liver, Lungs, Thyroid, and Eyes: A Case Report. Front. Cardiovasc. Med. 9:839441. doi: 10.3389/fcvm.2022.839441

INTRODUCTION

Amiodarone is an iodine-containing benzofuran derivative classified as a class III antiarrhythmic drug. It is clinically used for the treatment of tachyarrhythmias, including atrial fibrillation and reentrant tachyarrhythmias (1), which is one of the most prevalent types of arrhythmia (2). However, with the increasing use of amiodarone, there have been reports of side effects to various organs, including the lungs, liver, heart, thyroid gland, eyes, skin, and the nervous system (3).

Overall incidence of adverse effects can range from 30 to 90%, and serious side effects can take place in 10 to 26% of patients (1). Pulmonary toxicity is one of the fatal adverse effects of amiodarone, with mortality estimated between 1 and 33% and incidence of approximately 10% shown in previous studies (4). Patients with amiodarone-induced pulmonary toxicity usually present with dyspnea, non-productive cough, malaise, fever, and pleuritic chest pain (5). The most fatal manifestation of pulmonary toxicity is a rapidly progressing diffuse pneumonitis with acute respiratory distress requiring mechanical ventilation with mortality as high as 50 to 100% (6).

About 24% of patients taking amiodarone showed asymptomatic elevations of serum aminotransferase levels (7). Less than 1% of patients in various studies reported developing significant drug-induced liver injury ranging from symptomatic hepatitis and micronodular liver cirrhosis to hepatic failure requiring liver transplantation (8–14).

In addition, about 14–18% of patients taking amiodarone for a long period showed thyroid dysfunction, including hypothyroidism and thyrotoxicosis (15). However, a third of Korean patients developed thyroid dysfunction, and most cases involved hypothyroidism (16). Patients with amiodarone-induced hypothyroidism usually present with fatigue, cold intolerance, and dry skin, similar to symptoms of classic hypothyroidism (17).

The most typical symptom of amiodarone-induced ocular toxicity is corneal microdeposits, 98% of which are found after 2 months of treatment (18). Asymptomatic corneal changes are observed in 50–60% of patients, and visual disturbance is rarely reported (19).

Although much is known about amiodarone toxicity, cases of simultaneous toxicity in various organs have rarely been reported. Here, we present a novel case of multi-systemic amiodarone toxicity, involving the liver, lungs, thyroid, and eyes.

CASE REPORT

A 61-year-old woman visited the emergency room due to general weakness, nausea, visual disturbance, heat intolerance, and a non-productive cough with dyspnea, which had persisted between 3 and 6 months. The patient had underlying ischemic heart disease and paroxysmal atrial fibrillation, for which she was being treated with clopidogrel, pitavastatin, valsartan, rivaroxaban, nicorandil, diltiazem, furosemide, and amiodarone. More specifically, amiodarone was prescribed for 34 months at an initial dose of 200 mg/day for 11 months, and then due to intermittent chest discomfort with palpitation, her cardiologist increased the maintenance dose to 400 mg/day for the next 23 months. The patient was not taking any other medications, including herbal agents, and did not have a history of alcohol consumption.

The laboratory workup showed that the level of the total bilirubin was 0.71 mg/dL (reference range, 0.22–1.3), the aspartate aminotransferase level was 358 U/L (reference range, 10–37), the alanine aminotransferase level was 177 U/L (reference range, 10–37), and the prothrombin time was 1.90 International Normalized Ratio (INR) (reference range, 0.8–1.2). Enhanced computed tomography (CT) showed diffusely increased liver intensity and scattered hyper attenuated nodular consolidations in the subpleural areas of both lungs (**Figures 1A,B**). To evaluate the possibility of malignancy, positron emission tomography–CT (PET–CT) was performed, and multiple hypermetabolic lesions (maximal standardized uptake values 7.3, **Figure 1C**) were examined. To confirm the diagnosis of the lung lesions, transthoracic needle biopsy was performed, and the pathologic examination showed fibrinoid interstitial inflammation with atypical change of type II pneumocytes and intra-alveolar foamy macrophages (**Figure 2**). Using both the CT and biopsy findings, we could diagnose the amiodarone-induced hepatic and pulmonary toxicity.

Further, to assess the possibility of amiodarone-induced thyroid dysfunction, we examined thyroid function tests. The thyroid-stimulating hormone level was less than 0.008 uIU/mL (reference range, 0.55–4.78), free thyroxine was 4.67 ng/dL (reference range, 0.89–1.76), triiodothyronine was 1.27 ng/mL (reference range, 0.6–1.81), thyroid binding inhibitor immunoglobulin (TBII) was 18.3 IU/L (reference range, 0–1.5), anti-microsome antibody was 139.0 U/mL (reference range, 0–60), and anti-thyroglobulin antibody was 125 U/L (reference range, 0–60). The PET–CT scan of the thyroid showed no metabolic lesion (**Figure 3A**). The thyroid scan (technetium-99 m pertechnetate scintigraphy) showed diffuse homogenous intake of technetium-99 m pertechnetate in both thyroid lobes (**Figure 3B**). Anti-microsomal antibody and anti-thyroglobulin antibody may be detected in Graves' disease (anti-microsomal antibody: 69.2%, anti-thyroglobulin antibody: 23–30%) (20); furthermore, with the results of TBII and the thyroid scan results, we diagnosed our patient as having type 1 amiodarone-induced thyrotoxicosis, a form of iodine-induced hyperthyroidism caused by excessive, uncontrolled biosynthesis of thyroid hormone by autonomously functioning thyroid tissue in response to iodine load, which typically develops in underlying latent Graves' disease (21). After consultation with the endocrinology department, methimazole (20 mg for 17 days followed by 5 mg/d) was used as treatment to manage excessive thyroid hormone synthesis.

The patient persistently complained of blurred vision, and the ophthalmologic exam detected bilateral symmetrical corneal deposits in a vortex pattern (**Figure 3C**), which was compatible with amiodarone-induced vortex keratopathy.

As amiodarone toxicity was considered as the possible cause of disease, amiodarone was discontinued from the first day of admission. As there was neither extensive lung involvement nor hypoxemia, steroid treatment was not immediately initiated. However, serial follow-up chest CT scans showed aggravation

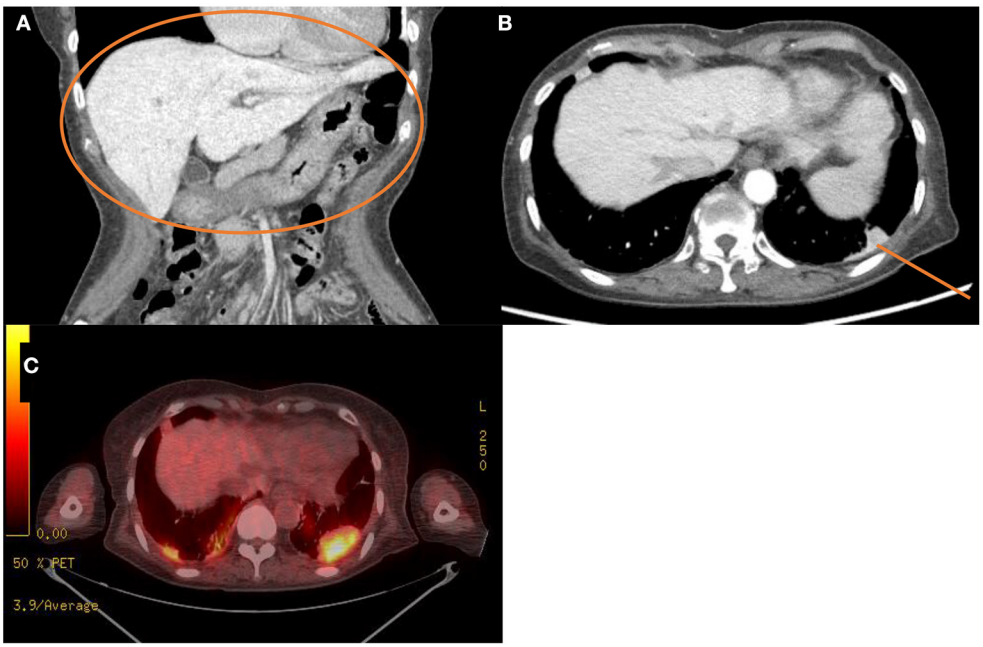

FIGURE 1 | Radiologic findings of the abdominal cavity and the chest. **(A,B)** Initial computed tomography scan of the abdominal cavity and the chest. This scan shows diffuse increased liver intensity [**(A)**, orange circle] and scattered hyperattenuation nodular consolidations in the subpleural areas of both lungs [**(B)**, orange line]. **(C)** Fluorodeoxyglucose positron emission tomography–computed tomography scan of the whole body showing about 4.8 cm hypermetabolic lesion in the left lung field (maximal standardized uptake, 7.3).

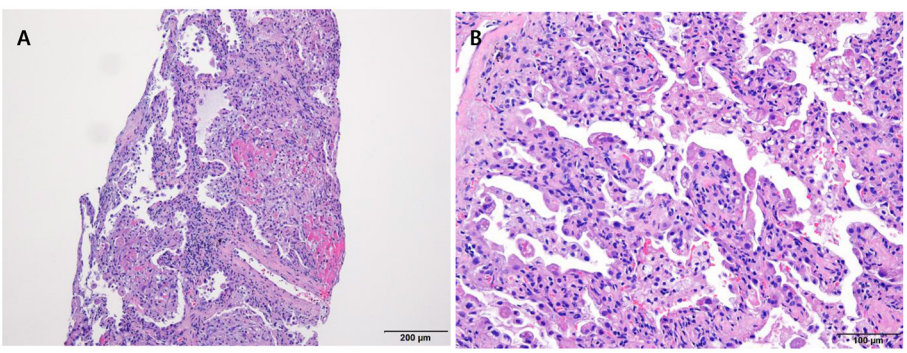

FIGURE 2 | Pathologic examination of the lung via trans-thoracic needle biopsy showing amiodarone-induced lung toxicity. **(A)** Chronic interstitial pneumonitis and interstitial fibrosis and focal fibrinoid necrosis. **(B)** Accumulation of foamy macrophages within alveolar spaces.

of previous lung lesions. After exclusion of lung malignancy via transthoracic needle biopsy, we decided on treatment with a systemic steroid regimen (methylprednisolone 40 mg) for pulmonary toxicity from day 29 of hospitalization. After 1 week of steroid medication, a follow-up CT showed an overall decreased extent of high attenuated subpleural mass-like consolidations and small nodules in both upper lung fields and the right middle lobe, suggesting an improved state of R/O amiodarone-induced pulmonary toxicity. After 4 months of steroid medication, a follow-up CT showed resolution of previous lung consolidations (**Figure 4A**). The laboratory examination showed that both aspartate aminotransferase and alanine aminotransferase levels were within the normal range after cessation of amiodarone for 1 month without any treatment (**Figure 4B**). Free thyroxine and thyroid-stimulating hormone were within the normal range after 6 weeks of methimazole medication (**Figure 4C**). The patient recovered from her general weakness, cough, and hand tremor 1 month after amiodarone cessation and was discharged after most of the symptoms were resolved.

DISCUSSION

To the best of our knowledge, this is the first report demonstrating multi-systemic toxicity, involving four vital organs, induced by amiodarone. Amiodarone

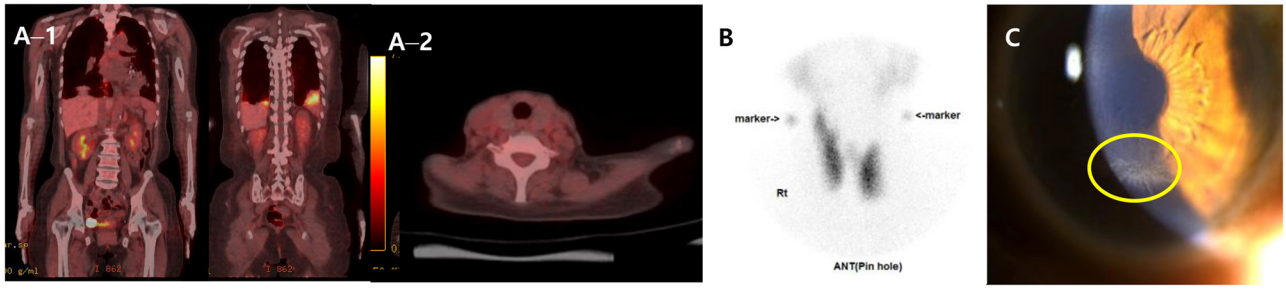

FIGURE 3 | FDG PET–CT, Thyroid scan and ophthalmologic exam. **(A)** FDG PET–CT scans of the whole body (A−1) and the thyroid (A−2) showing multiple hypermetabolic lesion in both lungs and no metabolic lesion in other organ including the thyroid. **(B)** Thyroid scan (technetium-99 m pertechnetate scintigraphy) presenting diffuse homogenous intake of technetium-99 m pertechnetate in both thyroid lobes. **(C)** Slit-lamp biomicroscopy showing numerous dense gray granular lines forming vortex patterns radiating from a median point at the junction of the middle and lower thirds of the cornea. FDG, fluorodeoxyglucose; PET–CT, positron emission tomography–computed tomography.

is a widely prescribed antiarrhythmic drug used to treat tachyarrhythmias, including atrial fibrillation and reentrant tachyarrhythmias of the accessory pathways. Amiodarone principally acts through multiple mechanisms, such as depressing the sinus and atrioventricular nodes and prolonging repolarization and refractoriness in the myocardium.

Amiodarone is a lipophilic drug, which accumulates mainly in adipose tissue and organs with high blood perfusion, such as the liver, lungs, and skin. Its long-term use leads to numerous adverse reactions, including photosensitivity, hypothyroidism, hyperthyroidism, hepatic dysfunction, bone marrow suppression, corneal microdeposits, and neuromotor defects (3). Due to its long biological half-life ranging up to 100 days, the drug activity may last more than 3 to 4 months after discontinuation (1).

Hepatotoxicity is a relatively uncommon adverse reaction to amiodarone. Amiodarone induces histological findings similar to alcohol-induced steatohepatitis, so differential diagnosis from alcoholic liver disease should be considered. Pathologic findings include macro- and microvesicular steatosis, Mallory bodies, polymorphonuclear leukocyte infiltration, ballooning degeneration of hepatocytes and phospholipidosis (22). The possible reason for hepatotoxicity is amiodarone, as its principal metabolite, desethylamidoarone induces production of reactive oxygen species and leads to hepatic triglyceride accumulation and microvesicular steatosis in hepatocytes (23). Pulmonary toxicity, an uncommon but serious adverse effect of amiodarone, reveals various patterns of lung involvement, including chronic interstitial pneumonia, bronchiolitis with or without organizing pneumonia, acute respiratory distress syndrome, diffuse alveolar hemorrhage, pleural effusion, and pulmonary nodules or masses. Especially, pulmonary mass and pulmonary nodules can mimic lung malignancy (24). The mechanism underlying the development of nodular pulmonary disease may be the inflammatory response to the accumulation of phospholipids in alveolar cells induced by the drug (25). Corticosteroid therapy should be considered in patients showing extensive lung involvement in imaging or those that develop hypoxemia, with a starting dose of 40 to 60 mg/day of prednisolone (26, 27). Due to the structural similarity between amiodarone and thyroid hormones, amiodarone causes thyroid dysfunction due to excessive iodine overload or due to its direct cytotoxicity to the thyroid gland (28). Amiodarone can induce both hypothyroidism and hyperthyroidism. The incidence of amiodarone-induced thyrotoxicosis is 2 to 10%, and it more commonly develops in areas of the world where iodine deficiency is common (29). The type of thyroid dysfunction caused by amiodarone treatment may depend on the presence of underlying thyroid disease or dietary iodine content (30). Moreover, amiodarone leads to drug-induced lipidosis, which leads to typical side-effects in the eyes, such as vortex keratopathy (31). Although the most common findings are corneal and lens opacities, optic neuropathy has also been reported (32). There have been reports of amiodarone toxicity to one or two vital organs. Cho et al. (33) reported a case of a 65-year-old man with amiodarone-induced hepatitis and hypothyroidism. Turk et al. (34) also reported a case of a 54-year-old female with amiodarone toxicity to the skin, thyroid, and eyes.

In this study, we observed multi-systemic amiodarone toxicity involving the liver, lungs, thyroid, and eyes. The main mechanism of amiodarone-induced toxicity is known as direct cytotoxicity and immunologic reaction. Patients who have received a daily dose of 400 mg or more for more than 2 months or a lower dose for more than 2 years are considered at high risk (26). Our patient can be considered as high-risk, as she was on 400 mg/day amiodarone for nearly 2 years. The long duration and high dosage of amiodarone were combined with treatment that may interact pharmacologically with amiodarone metabolism. First of all, she had been taking a statin concurrently with amiodarone for 3 years. Many studies have reported an interaction between statins and amiodarone as the potential cause of hepatotoxicity due to inhibition of the mitochondrial enzyme CYP3A4, which metabolizes statins, by amiodarone (35–38). Additionally, the patient in this study took diltiazem, a recognized CYP3A4 inhibitor that may have jeopardized amiodarone metabolism. Furthermore, our patient showed significant improvement of

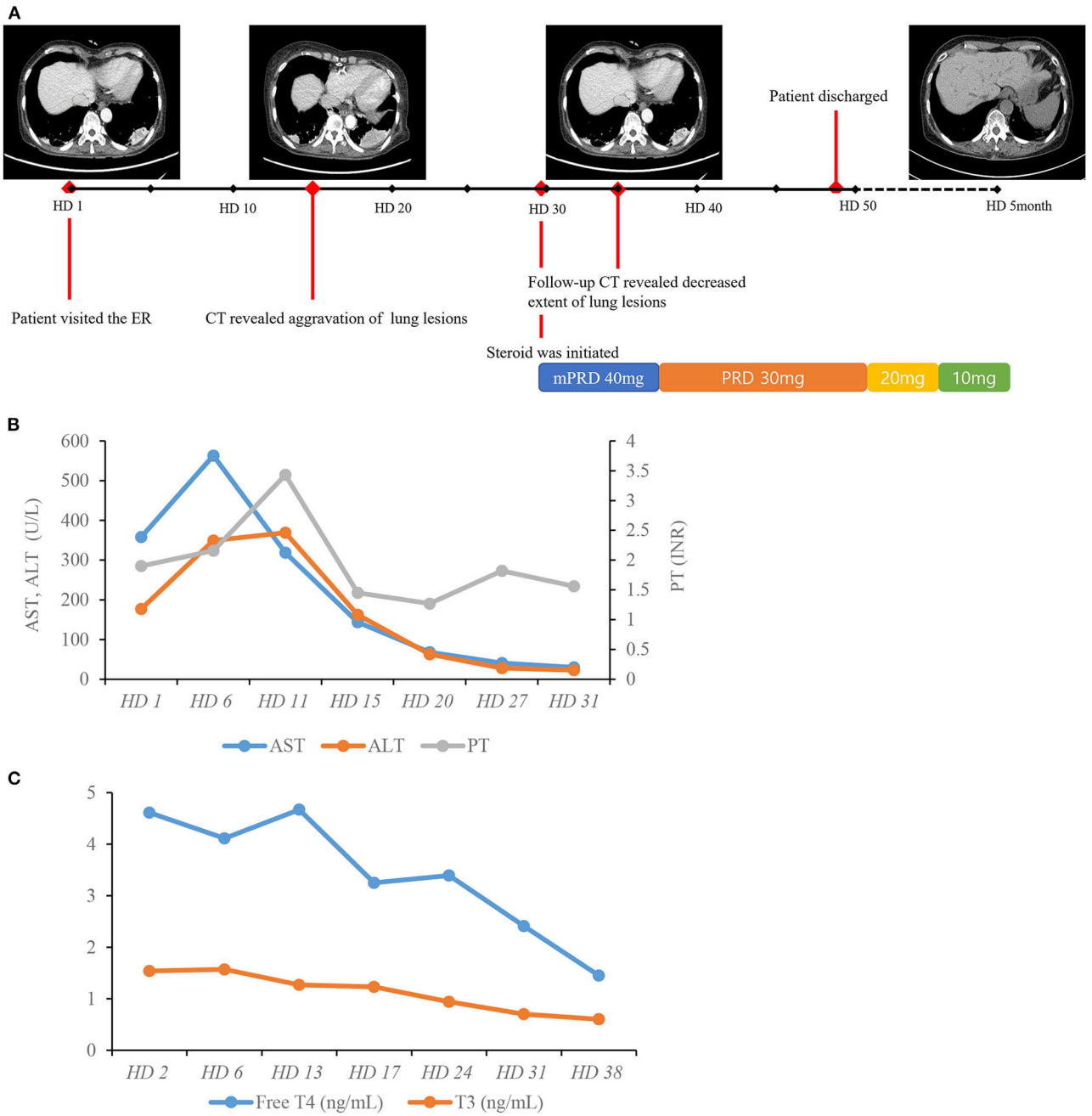

FIGURE 4 | Hospital course of the patient. **(A)** Timeline of chest CT scans and resolution of lung lesions with systemic steroid therapy. **(B)** Course of AST, ALT, and PT. **(C)** Course of free T4 and T3. AST, aspartate aminotransferase; ALT, alanine aminotransferase; HD, hospital day; INR, international normalized ratio; PT, prothrombin time; TSH, thyroid-stimulating hormone; T4, thyroxine; T3, triiodothyronine.

lung lesions with the use of systemic steroid therapy, suggesting the usefulness of corticosteroids in extensive lung involvement, as reported in previous studies (26, 27).

Our study has some limitations. First, although our report indicates multi-systemic amiodarone toxicity, the number of cases examined was very small. Second, the precise mechanism of amiodarone toxicity to multiple vital organs is not clearly verified. Lastly, the drug interactions associated with amiodarone metabolism, which may be the cause of amiodarone toxicity in our patient, had not been thoroughly examined. Further studies are warranted to elucidate the mechanism of multi-organ toxicity and classify high-risk patients to prevent amiodarone-induced toxicity.

In conclusion, this case indicates that multi-systemic amiodarone organ toxicity is a cause of concern in high-risk patients. Amiodarone toxicity should be considered in patients receiving amiodarone with any new symptoms, because this may involve various organs. A multisystem approach to amiodarone toxicity is important, because adverse events may occur in various organs simultaneously. Guidelines for monitoring adverse events in patients taking amiodarone for a long time must be established. Once diagnosis is determined, amiodarone must be discontinued promptly, and the use of systemic steroids needs to be assessed.

DATA AVAILABILITY STATEMENT

The original contributions presented in the study are included in the article/supplementary material, further inquiries can be directed to the corresponding author/s.

AUTHOR CONTRIBUTIONS

H-SY and JY conceived and designed the study, reviewed the literature, and contributed to manuscript drafting. SBC and SKC contributed to manuscript drafting. JY reviewed the case and edited the manuscript. Y-DC reviewed the pathologic findings. YK reviewed the ophthalmologic findings. WC and H-CK contributed to interpretation of data and reviewed of the case regarding amiodarone-induced thyrotoxicosis. All authors approved the final version to be submitted and approved the publication of the manuscript.

FUNDING

This study was supported by a grant from the Chonnam National University Hospital Biomedical Research Institute (BCRI21069) and National Research Foundation of Korea (2021R1F1A1061719).

REFERENCES

1. Mason JW. Amiodarone. *N Engl J Med.* (1987) 316:455–66. doi: 10.1056/NEJM198702193160807
2. Doyle JF, Ho KM. Benefits and risks of long-term amiodarone therapy for persistent atrial fibrillation: a meta-analysis. *Mayo Clin Proc.* (2009) 84, 234–42. doi: 10.4065/84.3.234
3. Park HS, Kim YN. Adverse effects of long-term amiodarone therapy. *Korean J Intern Med.* (2014) 29:571. doi: 10.3904/kjim.2014.29.5.571
4. Jackevicius CA, Tom A, Essebag V, Eisenberg MJ, Rahme E, Tu JV, et al. Population-level incidence and risk factors for pulmonary toxicity associated with amiodarone. *Am J Cardiol.* (2011) 108:705–10. doi: 10.1016/j.amjcard.2011.04.024
5. Dusman RE, Stanton MS, Miles WM, Klein LS, Zipes DP, Fineberg NS, et al. Clinical features of amiodarone-induced pulmonary toxicity. *Circulation.* (1990) 82:51–9. doi: 10.1161/01.CIR.82.1.51
6. Iskandar SB, Abi-Saleh B, Keith RL, Byrd RP Jr, Roy TM. Amiodarone-induced alveolar hemorrhage. *South Med J.* (2006) 99:383–8. doi: 10.1097/01.smj.0000208971.43461.bb
7. Lewis JH, Ranard RC, Caruso A, Jackson LK, Mullick F, Ishak KG, et al. Amiodarone hepatotoxicity: prevalence and clinicopathologic correlations among 104 patients. *Hepatology.* (1989) 9:679–85. doi: 10.1002/hep.1840090504
8. Harris L, McKenna WJ, Rowland E, Krikler DM. Side effects and possible contraindications of amiodarone use. *Am Heart J.* (1983) 106:916–23. doi: 10.1016/0002-8703(83)90016-9
9. Greene HL, Graham EL, Werner JA, Sears GK, Gross BW, Gorham JP, et al. Toxic and therapeutic effects of amiodarone in the treatment of cardiac arrhythmias. *J Am Coll Cardiol.* (1983) 2:1114–28. doi: 10.1016/S0735-1097(83)80338-6
10. Raeder EA, Podrid PJ, Lown B. Side effects and complications of amiodarone therapy. *Am Heart J.* (1985) 109:975–83. doi: 10.1016/0002-8703(85)90238-8
11. Smith WM, Lubbe WF, Whitlock RM, Mercer J, Rutherford JD, Roche AH. Long-term tolerance of amiodarone treatment for cardiac arrhythmias. *Am J Cardiol.* (1986) 57:1288–93. doi: 10.1016/0002-9149(86)90206-7
12. Heger JJ, Prystowsky EN, Jackman WM, Naccarelli GV, Warfel KA, Rinkenberger RL, et al. Amiodarone: clinical efficacy and electrophysiology during long-term therapy for recurrent ventricular tachycardia or ventricular fibrillation. *N Engl J Med.* (1981) 305:539–45. doi: 10.1056/NEJM198109033051002
13. Morady F, Sauve MJ, Malone P, Shen EN, Schwartz AB, Bhandari A, et al. Long-term efficacy and toxicity of high-dose amiodarone therapy for ventricular tachycardia or ventricular fibrillation. *Am J Cardiol.* (1983) 52:975–9. doi: 10.1016/0002-9149(83)90515-5
14. McGovern B, Garan H, Kelly E, Ruskin JN. Adverse reactions during treatment with amiodarone hydrochloride. *Br Med J.* (1983) 287:175–80. doi: 10.1136/bmj.287.6386.175
15. Tsang W, Houlden RL. Amiodarone-induced thyrotoxicosis: a review. *Can J Cardiol.* (2009) 25:421–4. doi: 10.1016/S0828-282X(09)70512-4
16. Jin SW, Yoon HJ, Lee JM, Oh YS, Lee MY, Rho TH, et al. Incidence of amiodarone-induced thyroid dysfunction in Korean. *Korean J Med.* (2003) 64:664–9.
17. Han T, Williams G, Vanderpump M. Benzofuran derivatives and the thyroid. *Clin Endocrinol.* (2009) 70:2–13. doi: 10.1111/j.1365-2265.2008.03350.x
18. Ingram D, Jaggarao N, Chamberlain D. Ocular changes resulting from therapy with amiodarone. *Br J Ophthalmol.* (1982) 66:676–9. doi: 10.1136/bjo.66.10.676
19. Mäntyjärvi M, Tuppurainen K, Ikäheimo K. Ocular side effects of amiodarone. *Surv Ophthalmol.* (1998) 42:360–6. doi: 10.1016/S0039-6257(97)00118-5
20. Dham S, Anand A, Dhananjayan G, Shetty K. Microsomal and thyroglobulin antibodies in thyroid disorders. *Med J Armed Forces India.* (1995) 51:247–50. doi: 10.1016/S0377-1237(17)30984-X
21. Bartalena L, Bogazzi F, Chiovato L, Hubalewska-Dydejczyk A, Links TP, Vanderpump M. 2018 European thyroid association (ETA) guidelines for the management of amiodarone-associated thyroid dysfunction. *Eur Thyroid J.* (2018) 7:55–66. doi: 10.1159/000486957
22. Raja K, Thung SN, Fiel MI, Chang C. Drug-induced steatohepatitis leading to cirrhosis: long-term toxicity of amiodarone use, seminars in liver disease. *Semin Liver Dis Case Rep.* (2009) 29:423–8. doi: 10.1055/s-0029-1240011
23. Fromenty B, Fisch C, Labbe G, Degott C, Deschamps D, Berson A, et al. Amiodarone inhibits the mitochondrial beta-oxidation of fatty acids and produces microvesicular steatosis of the liver in mice. *J Pharmacol Exp Ther.* (1990) 255:1371–6.
24. Rodriguez-Garcia JL, Garcia-Nieto JC, Ballesta F, Prieto E, Villanueva MA, Gallardo J. Pulmonary mass and multiple lung nodules mimicking a lung neoplasm as amiodarone-induced pulmonary toxicity. *Eur J Intern Med.* (2001) 12:372–6. doi: 10.1016/S0953-6205(01)00127-3
25. Piccione Jr W, Faber LP, Rosenberg MS. Amiodarone-induced pulmonary mass. *Ann Thorac Surg.* (1989) 47:918–9. doi: 10.1016/0003-4975(89)90037-4
26. Wolkove N, Baltzan M. Amiodarone pulmonary toxicity. *Can Respir J.* (2009) 16:43–8. doi: 10.1155/2009/282540

27. Schwaiblmair M, Berghaus T, Haeckel T, Wagner T, von Scheidt W. Amiodarone-induced pulmonary toxicity: an under-recognized and severe adverse effect? *Clin Res Cardiol.* (2010) 99:693–700. doi: 10.1007/s00392-010-0181-3
28. Martino E, Bartalena L, Bogazzi F, Braverman LE. The effects of amiodarone on the thyroid. *Endocr Rev.* (2001) 22:240–54. doi: 10.1210/edrv.22.2.0427
29. Bogazzi F, Bartalena L, Tomisti L, Rossi G, Brogioni S, Martino E. Continuation of amiodarone delays restoration of euthyroidism in patients with type 2 amiodarone-induced thyrotoxicosis treated with prednisone: a pilot study. *J Clin Endocrinol Metab.* (2011) 96:3374–80. doi: 10.1210/jc.2011-1678
30. Danzi S, Klein I. Amiodarone-induced thyroid dysfunction. *J Intensive Care Med.* (2015) 30:179–85. doi: 10.1177/0885066613503278
31. D'Amico DJ, Kenyon KR, Ruskin JN. Amiodarone keratopathy: drug-induced lipid storage disease. *Arch Ophthalmol.* (1981) 99:257–61. doi: 10.1001/archopht.1981.03930010259007
32. Flach AJ, Dolan BJ, Sudduth B, Weddell J. Amiodarone-induced lens opacities. *Arch Ophthalmol.* (1983) 101:1554–6. doi: 10.1001/archopht.1983.01040020556010
33. Cho YS, Han JH, Chae HB, Kim JS, Kang KM, Park SM, et al. A case of simultaneously occurred amiodarone-induced hepatitis and hypothyroidism. *Korean J Gastroenterol.* (2013) 62:59–63. doi: 10.4166/kjg.2013.62.1.59
34. Turk U, Turk BG, Yilmaz SG, Tuncer E, Alioglu E, Dereli T. Amiodarone-induced multiorgan toxicity with ocular findings on confocal microscopy. *Middle East Afr J Ophthalmol.* (2015) 22:258. doi: 10.4103/0974-9233.154411
35. McKelvie PA, Dennett X. Myopathy associated with HMG-CoA reductase inhibitors (statins): a series of 10 patients and review of the literature. *J Clin Neuromuscul Dis.* (2002) 3:143–8. doi: 10.1097/00131402-200206000-00002
36. Roten L, Schoenenberger RA, Krähenbühl S, Schlienger RG. Rhabdomyolysis in association with simvastatin and amiodarone. *Ann Pharmacother.* (2004) 38:978–81. doi: 10.1345/aph.1D498
37. Wratchford P, Ponte CD. High-dose simvastatin and rhabdomyolysis. *Am J Health Syst Pharm.* (2003) 60:698–700. doi: 10.1093/ajhp/60.7.698
38. Denus SD, Spinler SA. Amiodarone's role in simvastatin-associated rhabdomyolysis. *Am J Health Syst Pharm.* (2003) 60:1791–2. doi: 10.1093/ajhp/60.17.1791

Conflict of Interest: The authors declare that the research was conducted in the absence of any commercial or financial relationships that could be construed as a potential conflict of interest.

Publisher's Note: All claims expressed in this article are solely those of the authors and do not necessarily represent those of their affiliated organizations, or those of the publisher, the editors and the reviewers. Any product that may be evaluated in this article, or claim that may be made by its manufacturer, is not guaranteed or endorsed by the publisher.

frontiers in Cardiovascular Medicine

CASE REPORT
published: 02 March 2022
doi: 10.3389/fcvm.2022.778815

Case Report: Intravascular Ultrasound-guided Intervention for Anastomosis Stenosis of the Left Main Coronary Artery Post-Cabrol Technique

Seok Oh[1], Ju Han Kim[1,2], Dae Young Hyun[1], Kyung Hoon Cho[1], Min Chul Kim[1,2], Doo Sun Sim[1,2], Young Joon Hong[1,2], Youngkeun Ahn[1,2], Myung Ho Jeong[1,2] and Yochun Jung[3]*

[1] Department of Cardiology, Chonnam National University Hospital, Gwangju, South Korea, [2] Department of Cardiology, Chonnam National University Medical School, Gwangju, South Korea, [3] Department of Thoracic and Cardiovascular Surgery, Chonnam National University Hospital, Gwangju, South Korea

OPEN ACCESS

Edited by:
Tae-Hoon Kim,
CHA Univeristy, South Korea

Reviewed by:
Nicolas Amabile,
L'Institut Mutualiste Montsouris, France
Gary Mintz,
Cardiovascular Research Foundation, United States

***Correspondence:**
Ju Han Kim
kim@zuhan.com

Specialty section:
This article was submitted to General Cardiovascular Medicine, a section of the journal Frontiers in Cardiovascular Medicine

Received: 08 October 2021
Accepted: 08 February 2022
Published: 02 March 2022

Citation:
Oh S, Kim JH, Hyun DY, Cho KH, Kim MC, Sim DS, Hong YJ, Ahn Y, Jeong MH and Jung Y (2022) Case Report: Intravascular Ultrasound-guided Intervention for Anastomosis Stenosis of the Left Main Coronary Artery Post-Cabrol Technique. Front. Cardiovasc. Med. 9:778815. doi: 10.3389/fcvm.2022.778815

Introduction: Some cases of percutaneous coronary intervention (PCI) for the anastomotic site between the Cabrol-type conduit and the left main coronary artery (LMCA) have been reported. Nevertheless, the combination of PCI with a detailed description of lesion appearance using virtual histology-intravascular ultrasound (VH-IVUS) has never been reported. In this study, we present a case of acute myocardial infarction that was successfully treated with intravascular ultrasound (IVUS)-guided PCI for focal stenosis at the anastomotic site, and the plaque composition was studied in detail.

Case Presentation: A 35-year-old Korean male with Behçet's disease was diagnosed with acute myocardial infarction. He had previously undergone three cardiothoracic surgeries including two aortic replacements, followed by modified Bentall operation with a Cabrol-type aortocoronary anastomosis. Coronary angiogram (CAG) showed focal critical stenosis at the anastomosis site between the conduit and the LMCA, and VH-IVUS showed fibrotic plaque with mainly fibrous tissue but without a confluent necrotic core. PCI was performed using a drug-eluting stent (4.5 × 12 mm, Synergy™, Boston Scientific, Marlborough, MA, USA). Since a repeat CAG and IVUS post-surgery showed an under-expanded stent strut, post-dilation ballooning was additionally performed. Subsequently, the repeat IVUS revealed wellapposed and optimized deployment of the drug-eluting stent with full lesion coverage. Final CAG showed optimal angiographic results. After successful PCI, the patient's anginal symptoms improved dramatically, and he was successfully discharged from our hospital.

Conclusion: This study presents an IVUS-guided PCI case for an anastomotic site between the conduit and the LMCA. It is the first to investigate the characteristics of this lesion through VH-IVUS, which demonstrated the presence of fibrous plaques at the

anastomotic site. IVUS radiofrequency data allow for a detailed assessment of plaque composition and provide new insights into the histopathological nature of stenotic lesions at the anastomotic site, especially in patients with chronic inflammatory diseases like Behçet's disease.

Keywords: intravascular ultrasound, percutaneous coronary intervention, aortocoronary graft, acute myocardial infarction, Behçet's disease

INTRODUCTION

Several surgical techniques have been introduced for re-implantation of the native coronary arteries after aortic root replacement. Bentall and De Bono introduced a novel method of direct re-implantation of epicardial coronary arteries into the aortic graft in 1968 (1). However, this procedure has several limitations owing to postoperative complications including anastomotic bleeding or pseudoaneurysm formation. The Cabrol technique, introduced in 1981, includes interposition of an 8- to 10-mm-diameter Dacron graft between the aortic root and the native coronary artery (2). Because the interposed graft attenuates tension at the coronary–aorta anastomosis, the Cabrol technique is beneficial when a scar from any previous surgery inhibits coronary mobilization.

Whereas the Bentall operation has a very low incidence of coronary stenosis, there have been several reports of graft-coronary anastomosis in the Cabrol and Cabrol-related surgical techniques (3–6). In many cases, this complication is mainly treated through percutaneous coronary intervention (PCI). We found 11 reports about PCI of Cabrol conduit–left main coronary artery (LMCA) anastomosis. However, thus far, cases involving the combination of PCI and virtual histology-intravascular ultrasound (VH-IVUS), which provides a detailed description of lesion appearance, have never been reported. Herein, we describe an unusual case of acute myocardial infarction (AMI) that was successfully treated with IVUS-guided PCI for focal stenosis at the anastomotic site, with a detailed assessment of plaque composition.

CASE PRESENTATION

A 35-year-old Korean man visited our hospital with a chief complaint of chest pain (Canadian Cardiovascular Society Grade II). The patient had Behçet's disease and aortic regurgitation, which is one of its cardiovascular manifestations. For Behçet's disease, the patient had received anti-inflammatory medications–sulfasalazine (1,000 mg/day); prednisolone (5 mg/day); and colchicine (0.6 mg/day) with high adherence. In the outpatient clinic, laboratory blood parameters including inflammatory markers (erythrocyte sedimentation rate) were routinely checked, which is illustrated in **Figure 1**. He underwent three cardiothoracic surgeries: aortic valve (AoV) replacement (in 2006) with a 21-mm St. Jude Medical AoV prosthesis (St. Jude Medical, Inc., St. Paul, MN, USA), aortic root replacement (in 2007) with an Edwards Prima stentless porcine prosthesis (Edwards Lifesciences Corp., Irvine, CA, USA) for AoV detachment, and the modified Bentall procedure (on 7 March 2017, ∼4 years ago from the time of presentation) for prosthetic valve failure and moderate aortic regurgitation. During the last surgery, a Cabrol-type aortocoronary anastomosis was performed. Because his anginal symptoms gradually deteriorated, the patient visited our cardiovascular center for diagnosis and management.

His vital signs were as follows: temperature, 36.3°C; heart rate, 75 beats/min; respiratory rate, 20 breaths/min; and blood pressure, 110/80 mmHg. A 12-lead electrocardiogram showed normal sinus rhythm with a right bundle branch block. However, the electrocardiogram also revealed ST-segment elevation in aVR and V1, with ST-segment depression in lead I, II, and aVL and precordial leads V4–6, suggesting LMCA occlusion (**Supplementary Figure 1**). Chest radiography showed mild cardiomegaly and definite evidence of prior median sternotomy and valvular replacement (**Supplementary Figure 2**). Laboratory tests showed elevated levels of troponin I (0.887 ng/mL; reference: 0–0.050 ng/mL) and pro-brain natriuretic peptide (1,549 pg/mL; reference: 0–300 pg/mL). The patient was administered warfarin, therefore, the prothrombin time–international normalized ratio was estimated to be 1.90. A two-dimensional transthoracic echocardiogram revealed a well-functioning AoV with akinetic movement at the anterior and anteroseptal parts of the myocardium, and a left ventricular ejection fraction of 36.3%. We reviewed the findings of previous coronary computed tomography angiography to obtain detailed anatomical information about the focal stenosis at the anastomotic site between the LMCA and the aortocoronary graft (**Figures 2**, **3A**). Since the patient was diagnosed with non-ST-segment elevation acute coronary syndrome, PCI was performed.

Coronary angiography (CAG) was performed through the right femoral artery during cardiac catheterization. Critical stenosis was observed at the anastomotic site between the LMCA and the conduit (**Figure 4A**; **Supplementary Video 1**). Right-sided CAG showed no significant stenosis, with collateral flow toward the left coronary artery (**Figure 4B**; **Supplementary Video 2**). After a 6F Judkins guiding catheter was engaged at the ostium of the left Cabrol-type composite

Abbreviations: AMI, acute myocardial infarction; AoV, aortic valve; CAG, coronary angiography; IVUS, intravascular ultrasound; LMCA, left main coronary artery; PCI, percutaneous coronary intervention; VH-IVUS, virtual histology-intravascular ultrasound.

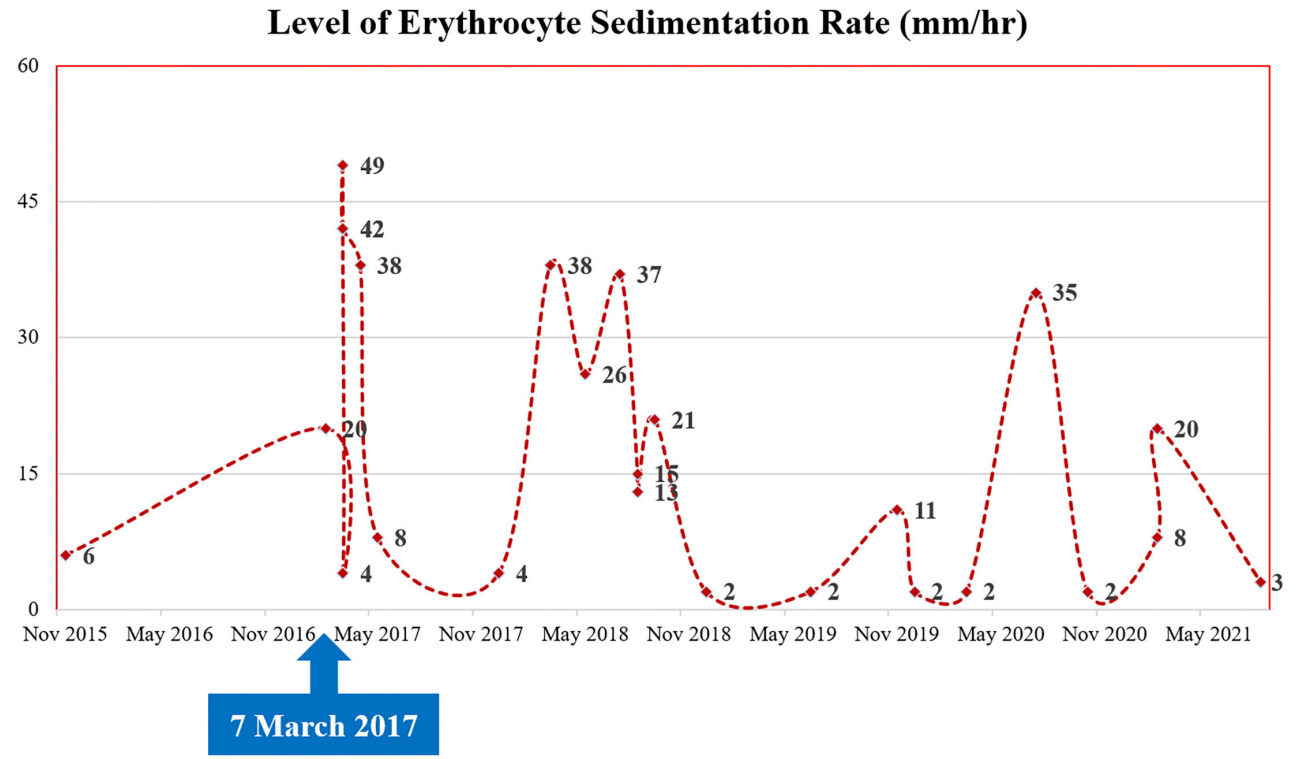

FIGURE 1 | Patient's clinical course: the change of inflammatory markers (levels of erythrocyte sedimentation rate).

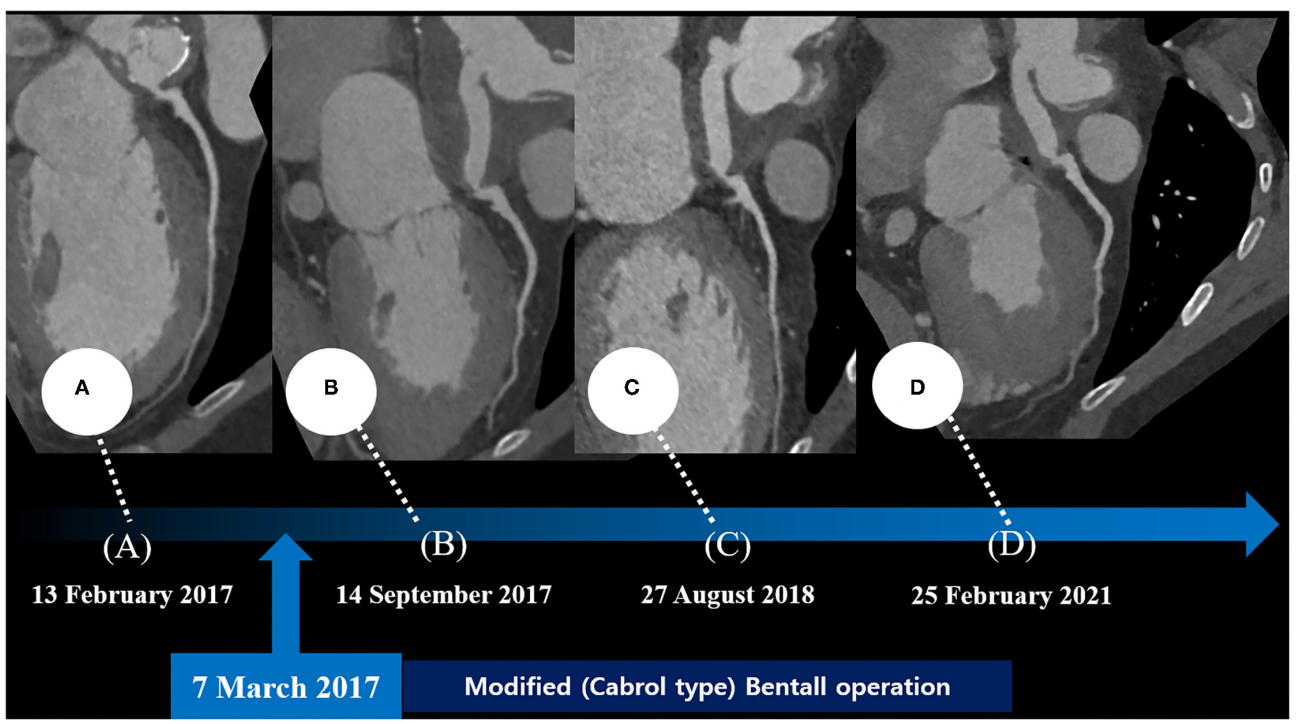

FIGURE 2 | Series of coronary computed tomography angiographies at the preoperative period **(A)** and the postoperative period **(B–D)**.

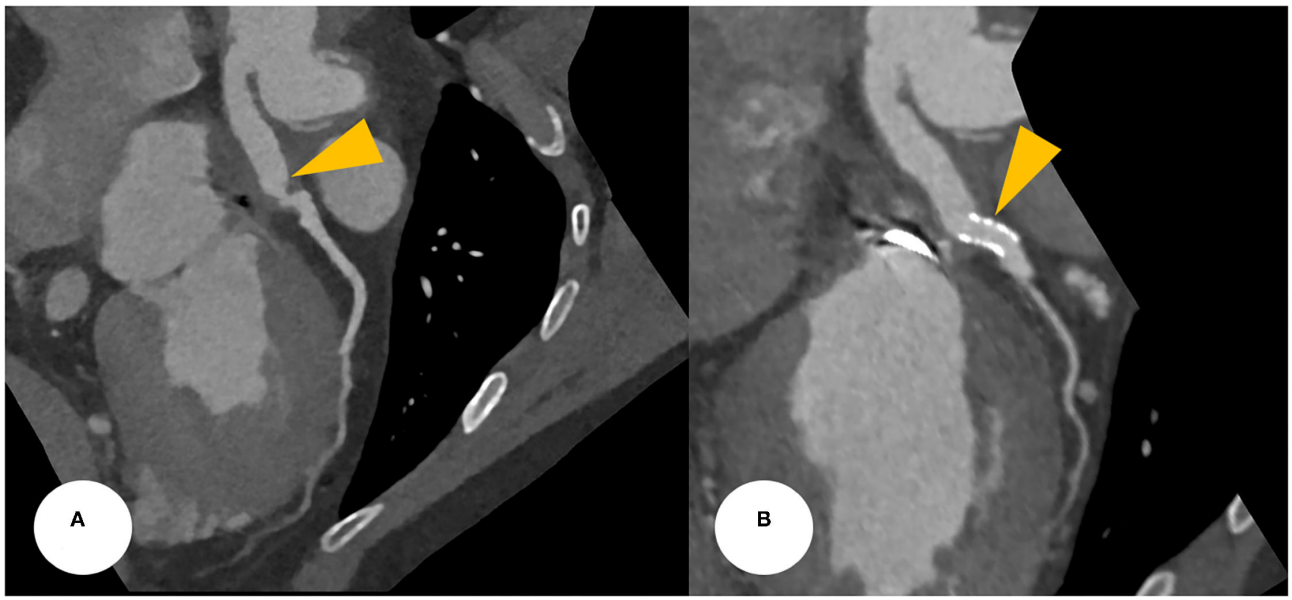

FIGURE 3 | (A) CCTA at the postoperative period found a focally narrowed and kinked lesion at the anastomotic site between the Cabrol-type graft and LMCA (a yellowish arrowhead). **(B)** After a successful PCI, CCTA was evaluated, revealing a stent deployment state between the conduit and LMCA with good patency (yellowish arrowheads). CCTA, coronary computed tomography angiography; LMCA, left main coronary artery; PCI, percutaneous coronary intervention.

graft, a 0.014-inch guidewire (Runthrough®, Terumo, Tokyo, Japan) was crossed through the LMCA to the left anterior descending coronary artery. Pre-PCI IVUS was performed using a guidance system (Eagle Eye® Platinum RX Digital IVUS Catheter, Volcano Corporation, Rancho Cordova, CA, USA), and a focally kinked and narrowed lesion with a minimum lumen area of 2.9 mm^2 was observed (**Figure 5A**; **Supplementary Video 3**). In the VH-IVUS, fibrotic plaque was seen with mainly fibrous tissue but without a confluent necrotic core (**Figure 5B**; **Supplementary Video 4**). Thereafter, PCI was performed using a drug-eluting stent (4.5 × 12 mm, Synergy™, Boston Scientific, Marlborough, MA, USA) (**Figure 4C**; **Supplementary Videos 5 and 6**). Immediately after the stent deployment, IVUS demonstrated an under-expanded stent strut with a minimum stent area of 18.4 mm^2 (**Figure 5C**). Repeated CAG showed improved stenosis but under-expanded stent strut (**Figure 4D**; **Supplementary Video 7**). For this reason, the lesion was post-dilated using a noncompliant balloon (5.5 × 8 mm, Raiden 3™, Kaneka Corporation, Osaka, Japan) to mitigate stent under-expansion (**Figure 4E**; **Supplementary Video 8**). A repeat IVUS revealed well-apposed and optimized deployment of the drug-eluting stent with full lesion coverage (**Figure 5D**; **Supplementary Video 9**). The final CAG also showed optimal angiographic results (**Figure 4F**; **Supplementary Video 10**).

After the PCI procedure, the patient received optimal medical therapy, including dual antiplatelet agents–aspirin (100 mg/day) and clopidogrel (75 mg/day), an oral anticoagulant–warfarin (1 mg/day), a high-intensity statin–rosuvastatin (20 mg/day), a beta-blocker–bisoprolol (2.5 mg/day), and an angiotensin II receptor blocker–valsartan (40 mg/day). The post-PCI coronary computed tomography angiography demonstrated a well-expanded and well-apposed stent strut at the anastomotic site (**Figure 3B**). His anginal symptoms dramatically improved, and he was successfully discharged from our hospital.

DISCUSSION AND CONCLUSION

Behçet's disease is a multi-systemic illness, mainly manifested as mucocutaneous lesions (oral ulceration, genital ulcer, and other skin lesions), joint symptoms and signs (arthritis and arthralgia), eye lesions, and systemic vasculitis (7, 8). In addition, it may involve a variety of organs including the cardiovascular system (9, 10). Although it is still unclear as to which factor contributed to the development of stenosis at an anastomotic site, we presume that this fibrotic change was due to an aggressive healing process after the surgery, and Behçet's disease particularly contributed to the acceleration of this inflammatory response. Although the patient had received anti-inflammatory agents with good adherence, there would have been existing recurrent inflammatory insults considering the fluctuating levels of inflammatory markers (erythrocyte sedimentation rate), as shown in **Figure 1**. In other words, repeated inflammatory response toward Behçet's disease would have resulted in the development of fibrous plaques while inhibiting the healing process of the anastomotic site. The present study describes a successful PCI procedure for focal stenosis at an anastomotic site in a patient with Behçet's disease who previously received an aortocoronary graft anastomosed to the LMCA. During the PCI procedure, we evaluated the stenotic characteristics, confirming this fibrous change using VH-IVUS.

In a PubMed search, we found 11 successful PCI cases of anastomotic stenosis or occlusion between the aortocoronary

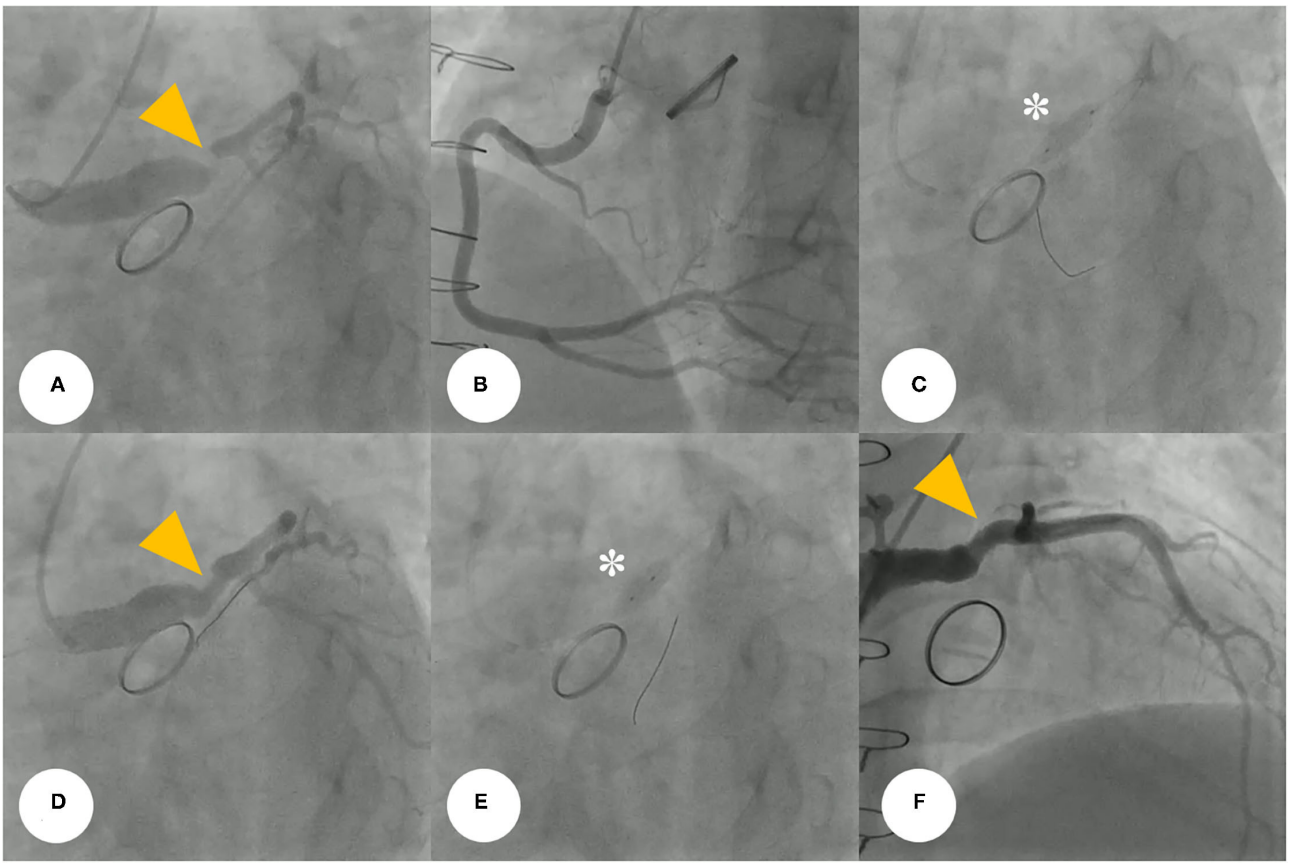

FIGURE 4 | (A) Coronary angiogram demonstrates severe post-anastomotic left main coronary artery stenosis (yellow arrowhead) in a patient with Behçet's disease after a previous modified Bentall procedure. **(B)** Right-selective coronary angiogram shows no significant stenosis. **(C)** For this stenotic lesion, we used a drug-eluting stent (asterisk) (4.5 × 12 mm, Synergy^{TM}, Boston Scientific, Marlborough, MA, USA). **(D,E)** The repeated coronary angiogram shows residual stent under-expansion (yellow arrowhead), hence, a non-compliant balloon (asterisk) (5.5 × 8 mm, Raiden 3^{TM}, Kaneka Corporation, Osaka, Japan) was post-dilated. **(F)** Final coronary angiogram showing an optimal angiographic result (yellow arrowhead).

conduit and the LMCA (3–5, 11–18). These results are summarized in **Supplementary Table 1**. In these studies, all patients were male and had underlying aortic conditions; 9 and 6 patients were diagnosed with AMI and cardiogenic shock, respectively and 9 patients survived. Thus, most cases presented as AMI, as seen in our case, and all patients had severe impairment of myocardial performance, leading to cardiogenic shock. To date, the present study describes an IVUS-guided PCI to the anastomotic site between the graft and the LMCA after a modified Bentall procedure. To our best knowledge, the present study is the first to investigate the characteristics of this lesion through VH-IVUS, which demonstrated the presence of a high content of fibrous plaques at the anastomotic site. Although VH-IVUS is considered an outdated analytic technique, and there are better methods to evaluate the plaque composition, including iMAP^{TM} IVUS, near-infrared spectroscopy, and optical coherence tomography, it is true that VH-IVUS provides accurate information about this lesion compared to IVUS alone. In this present case, it is particularly interesting to confirm the fibrous change caused by the inflammatory change through VH-IVUS in our patient with Behçet's disease.

The patient in the present case underwent PCI for anastomotic stenosis, instead of quadruple open-heart surgery owing to increased surgical risk associated with the latter. Despite many cardiothoracic surgeons having recently favored coronary artery bypass grafting as the treatment of choice (15), using autologous arterial grafts to artificial or vein grafts, it seems that a non-surgical intervention would have been a better treatment option in terms of patient safety. Furthermore, even after implantation of this stent, stenosis/occlusion at this anastomotic site could recur through the same inflammatory reaction. Although most published studies describe PCI or surgery as appropriate treatment strategies for the management of primary stenosis, little is known about an appropriate prevention strategy for its recurrence. However, regarding this case, it is hypothesized that both intensive medical treatment and active surveillance are needed to suppress the inflammatory reaction that can aggravate due to underlying Behçet's disease.

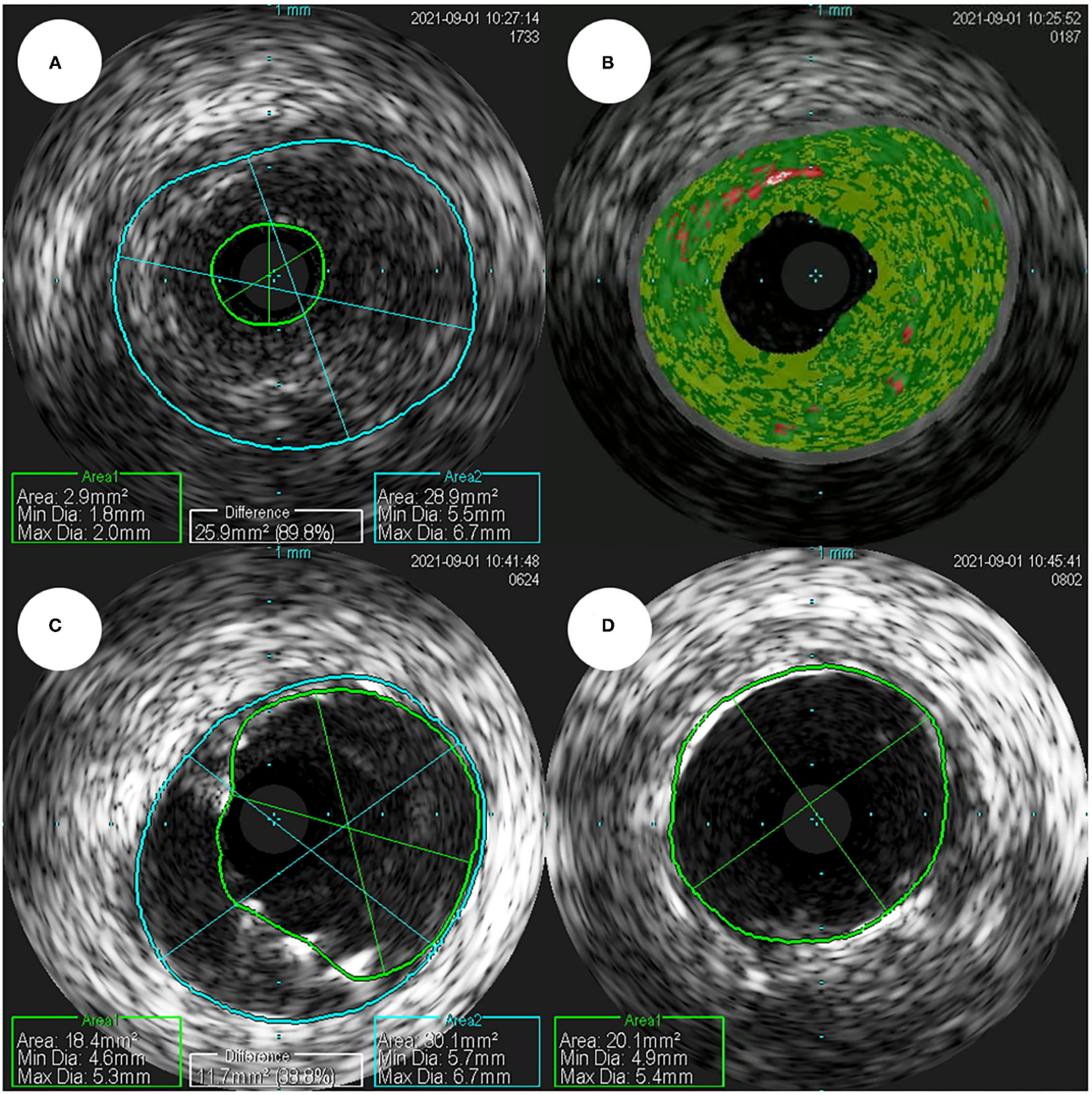

FIGURE 5 | (A) In a pre-percutaneous coronary intervention intravascular ultrasound, the smallest lumen area as seen, was estimated to be 2.9 mm^2 (plaque burden was estimated to be 89.8%). **(B)** In a virtual histology-intravascular ultrasound study, the fibrotic plaque shows mainly fibrous tissue, but no confluent necrotic core. **(C)** In a post-percutaneous coronary intervention intravascular ultrasound, the minimum stent area was estimated to be 18.4 mm^2. **(D)** The repeated intravascular ultrasound shows optimized deployment of a drug-eluting stent with the full lesion coverage.

In conclusion, the IVUS radiofrequency data allow for a detailed assessment of plaque composition *in vivo*, therefore, the present case will provide new insights into the histopathological nature of stenotic lesions at the anastomotic site, especially in patients with chronic inflammatory diseases like Behçet's disease.

DATA AVAILABILITY STATEMENT

The original contributions presented in the study are included in the article/**Supplementary Material**, further inquiries can be directed to the corresponding author/s.

ETHICS STATEMENT

The studies involving human participants were reviewed and approved by the Institutional Review Board of Chonnam National University Hospital (IRB No. CNUH-EXP-2022-027). Written informed consent for participation was not required for this study in accordance with the national legislation and the institutional requirements.

AUTHOR CONTRIBUTIONS

SO and JK drafted the manuscript. SO, DH, DS, and JK designed the study methodology. SO, DH, KC, DS, and JK collected the data. KC, MK, DS, YH, JK, YA, and MJ reviewed and edited the manuscript. All authors read and approved the final manuscript.

FUNDING

This study was supported by a Grant (BCRI21074) of Chonnam National University Hospital Biomedical Research Institute.

ACKNOWLEDGMENTS

We sincerely thank SO, DS, and JK for providing CAG and successful IVUS-guided PCI for this lesion.

SUPPLEMENTARY MATERIAL

The Supplementary Material for this article can be found online at: https://www.frontiersin.org/articles/10.3389/fcvm.2022.778815/full#supplementary-material

Supplementary Figure 1 | The electrocardiogram also revealed ST-segment elevation in aVR and V1, with ST-segment depression in lead I, II, and aVL and precordial leads V4–6, suggesting LMCA occlusion. LMCA, left main coronary artery.

Supplementary Figure 2 | Chest radiography showed mild cardiomegaly and definite evidence of prior median sternotomy and valvular replacement.

Supplementary Table 1 | Clinical characteristics of cases about successful PCI for aortocoronary graft-LMCA anastomosis in the literature review.

REFERENCES

1. Bentall H, De Bono A. A technique for complete replacement of the ascending aorta. *Thorax.* (1968) 23:338–9. doi: 10.1136/thx.23.4.338
2. Cabrol C, Pavie A, Gandjbakhch I, Villemot JP, Guiraudon G, Laughlin L, et al. Complete replacement of the ascending aorta with reimplantation of the coronary arteries: new surgical approach. *J Thorac Cardiovasc Surg.* (1981) 81:309–15. doi: 10.1016/S0022-5223(19)37641-X
3. Coram R, George Z, Breall JA. Percutaneous intervention through a Cabrol composite graft. *Catheter Cardiovasc Interv.* (2005) 66:356–9. doi: 10.1002/ccd.20496
4. Hoskins MH, Kacharava AG, Green TF, Mavromatis K, Veterans Affairs Medical Center Decatur GA. Percutaneous intervention of Cabrol graft-left main anastomosis during acute myocardial infarction. *Int J Cardiol.* (2010) 140:e27–9. doi: 10.1016/j.ijcard.2008.11.073
5. Wells TA, Kapoor A. Percutaneous coronary intervention through a Cabrol composite graft. *Int J Cardiol.* (2007) 116:e44–5. doi: 10.1016/j.ijcard.2006.08.101
6. Witzenbichler B, Schwimmbeck P, Schultheiss HP. Images in cardiovascular medicine. myocardial infarction caused by occlusion of cabrol conduit graft. *Circulation.* (2005) 112:e79–80. doi: 10.1161/CIRCULATIONAHA.104.500215
7. Ghate JV, Jorizzo JL. Behcet's disease and complex aphthosis. *J Am Acad Dermatol.* (1999) 40:1–18. doi: 10.1016/S0190-9622(99)70523-2
8. James DG, Spiteri MA. Behçet's disease. *Ophthalmology.* (1982) 89:1279–84. doi: 10.1016/S0161-6420(82)34644-8
9. Gurgun C, Ercan E, Ceyhan C, Yavuzgil O, Zoghi M, Aksu K, et al. Cardiovascular involvement in Behcet's disease. *Jpn Heart J.* (2002) 43:389–98. doi: 10.1536/jhj.43.389
10. Ozkan M, Emel O, Ozdemir M, Yurdakul S, Kocak H, Ozdogan H, et al. M-mode, 2-D and Doppler echocardiographic study in 65 patients with Behcet's syndrome. *Eur Heart J.* (1992) 13:638–41. doi: 10.1093/oxfordjournals.eurheartj.a060228
11. Hussain F, Ducas J, Gosal T. Emergent percutaneous intervention with a drug-eluting stent of a cabrol graft-to-left main anastomosis during a non-ST-elevation infarction in a patient with Marfan's syndrome. *J Invasive Cardiol.* (2006) 18:E250–2.
12. Ikenaga H, Kurisu S, Kihara Y. Percutaneous coronary intervention for interposed coronary graft stenosis after modified Bentall procedure in a teenaged boy with Takayasu arteritis. *Tex Heart Inst J.* (2019) 46:207–10. doi: 10.14503/THIJ-16-5824
13. Bozlar U, Ragosta M, Arora V, Hagspiel KD. Anastomotic leak after cabrol composite graft procedure: diagnosis by computed tomographic angiography and treatment by covered stent. *Tex Heart Inst J.* (2008) 35:214–5.
14. Siddiqui S, Ayzenberg S, Sabharwal N, Frankel R, Shani J. Protected percutaneous coronary intervention. (PCI) of Cabrol type anastomosis of saphenous vein graft. (SVG) to the left main coronary artery. (LMCA). *Cureus.* (2020) 12:e8829. doi: 10.7759/cureus.8829
15. Komatsu T, Miyazawa I, Abe N, Miyashita Y, Totsuka N, Yoshioka J. Percutaneous intervention for ostial stenosis of left main coronary artery after modified Bentall-Piehler procedure. *Cardiovasc Interv Ther.* (2019) 34:379–80. doi: 10.1007/s12928-018-0563-4
16. Uribe Gonzalez J, Pena Duque MA, Larraga M.P. Early stenosis in a Gore-Tex graft connected to the left main: an emergency transradial angioplasty for a complication in a Cabrol procedure. *J Invasive Cardiol.* (2012) 24:539–42.
17. Fukuda K. Percutaneous intervention for an occluded left Cabrol graft. *J Cardiol Cases.* (2019) 20:205–8. doi: 10.1016/j.jccase.2019.08.015
18. Karanfil M, Erdol M.A, Acar B, Arugaslan E, Ertem AG. Left main coronary artery stenosis treated with renal stents after Cabrol operation. *Turk Gogus Kalp Damar Cerrahisi Derg.* (2020) 28:531–5. doi: 10.5606/tgkdc.dergisi.2020.19151

Conflict of Interest: The authors declare that the research was conducted in the absence of any commercial or financial relationships that could be construed as a potential conflict of interest.

Publisher's Note: All claims expressed in this article are solely those of the authors and do not necessarily represent those of their affiliated organizations, or those of the publisher, the editors and the reviewers. Any product that may be evaluated in this article, or claim that may be made by its manufacturer, is not guaranteed or endorsed by the publisher.

frontiers in Cardiovascular Medicine

CASE REPORT
published: 31 March 2022
doi: 10.3389/fcvm.2022.832098

Inverted Takotsubo Syndrome With HELLP Syndrome: A Case Report

*Paul Gabarre[1†], Pablo Ruiz[2†], Camille Chenevier-Gobeaux[3], Etienne Charpentier[4], Laurie Soulat-Dufour[5,6], Ariel Cohen[5,6], Laurence Monnier-Cholley[7], Lotfi Chemali[2], Hélène François[1,8], Mathieu Kerneis[9], Guillaume Lefèvre[2] and Mathieu Boissan[2,10]**

[1] AP-HP, Hôpital Tenon, Soins Intensifs Néphrologiques et Rein Aigu (SINRA), Paris, France, [2] AP-HP, Hôpital Tenon, Laboratoire de Biochimie, Paris, France, [3] AP-HP-Centre Université de Paris, Hôpital Cochin, Department of Automated Biological Diagnostic, Paris, France, [4] AP-HP, Groupe Hospitalier Pitié Salpêtrière, Unité d'Imagerie Cardiovasculaire et Thoracique ICT, Institut de Cardiologie, Paris, France, [5] AP-HP, Hôpital Saint-Antoine-Tenon, Service de Cardiologie, Paris, France, [6] Sorbonne Université, Inserm, Unité de Recherche sur les Maladies Cardiovasculaires, le Métabolisme et la Nutrition, ICAN, Paris, France, [7] AP-HP, Hôpital Saint-Antoine, Département de Radiologie, Paris, France, [8] Sorbonne Université, Inserm, UMR_S1155, Paris, France, [9] Sorbonne Université, ACTION Study Group, INSERM UMRS_1166, Institut de Cardiologie (AP-HP), Paris, France, [10] Sorbonne Université, Inserm, Centre de Recherche Saint-Antoine, CRSA, Paris, France*

OPEN ACCESS

Edited by:
Francesco Santoro, University of Foggia, Italy

Reviewed by:
John David Horowitz, University of Adelaide, Australia
Giuseppe Sangiorgi, University of Rome Tor Vergata, Italy
Nicola Tarantino, Montefiore Medical Center, United States

***Correspondence:**
Mathieu Boissan
mathieu.boissan@inserm.fr

[†]These authors have contributed equally to this work

Specialty section:
This article was submitted to General Cardiovascular Medicine, a section of the journal Frontiers in Cardiovascular Medicine

Received: *09 December 2021*
Accepted: *03 February 2022*
Published: *31 March 2022*

Citation:
Gabarre P, Ruiz P, Chenevier-Gobeaux C, Charpentier E, Soulat-Dufour L, Cohen A, Monnier-Cholley L, Chemali L, François H, Kerneis M, Lefèvre G and Boissan M (2022) Inverted Takotsubo Syndrome With HELLP Syndrome: A Case Report. Front. Cardiovasc. Med. 9:832098. doi: 10.3389/fcvm.2022.832098

Background: Takotsubo syndrome is an acute cardiac condition involving sudden, transient apical ballooning of the left ventricle of the heart that may be triggered by emotional stress and some non-cardiac conditions. Its diagnosis is based on clinical presentation, electrocardiogram, cardiac imaging and biomarkers.

Case Summary: Here, we present a novel and original case report of a patient presenting very soon in the post-partum period with an unusual form of Takotsubo syndrome without clinical symptoms of cardiac disease and accompanied by HELLP syndrome. The overall dynamics of the changes in troponin I, troponin T and NT-proBNP levels after delivery were generally similar, but the amount of troponin I was much greater than that of troponin T and troponin I was already elevated before delivery. NT-proBNP levels peaked around the same time as the troponins and the peak concentration was within the same range as that of troponin I.

Discussion: Our findings indicate that assaying circulating cardiac biomarkers, especially troponin I and NT-proBNP, may be a useful complement to non-invasive cardiac imaging including transthoracic echocardiography and cardiovascular magnetic resonance imaging, in the diagnosis of Takotsubo syndrome. They illustrate the importance of cardiac biomarkers in assisting diagnosis of this disease.

Keywords: troponin T, troponin I, NT-proBNP, Takotsubo, HELLP syndrome, pregnancy, case report

INTRODUCTION

Takotsubo syndrome is a sudden, transient, and acute dysfunction of the left ventricle of the heart that can also involve the right ventricle. It is frequently preceded by physical or emotional stress. Takotsubo syndrome affects women more often than men and, commonly, 60–75-year-olds; thus, at onset, it can be mistaken for acute coronary syndrome. Although its exact pathophysiology is unknown, the main hypothesis is that it is due to exaggerated sympathetic stimulation, inducing a catecholamine excess, which seems to be more increased in Takotsubo syndrome than in acute myocardial infarction (1).

The effect of Takotsubo syndrome on circulating cardiac biomarkers is controversial. Two types of cardiac biomarker—natriuretic peptides and cardiac troponins—are used in the diagnosis of both Takotsubo syndrome and acute myocardial infarction (1, 2). In the International Takotsubo Diagnostic Criteria (InterTAK Diagnostic Criteria), levels of cardiac biomarkers, including troponin, are described as moderately elevated in most cases whereas levels of brain natriuretic peptide (BNP) are substantially elevated. Some exceptions have been reported, however (1, 3).

Here, we describe the clinical and biological features as well as non-invasive cardiac imaging of an unusual case of peri-partum HELLP (hemolysis, elevated liver enzymes, low platelet) syndrome complicated by an inverted Takotsubo syndrome. This patient was asymptomatic for cardiac disease, the twelve-derivation electrocardiogram demonstrated no pathological features, and the amount of troponin I was strongly increased to within the same concentration range as the N-terminal prohormone of BNP (NT-proBNP). Our interpretation of the biological test results illustrates the potential use of these cardiac biomarkers in assisting diagnosis of Takotsubo syndrome.

All patient-specific information was anonymized.

METHODS

Plasma levels of cardiac high-sensitivity troponin I (cTnIhs) and troponin T (cTnThs) in samples collected in lithium heparin were assayed by using the Architect *ci* 8200 (Abbott) and Cobas E801 (Roche Diagnostics) analyzers, respectively. Normal values of cTnIhs and cTnThs (women cTnIhs 99th percentile, cTnThs overall population) were <15.6 and <14 ng/L, respectively (manufacturer's data). Plasma levels of N-terminal prohormone of brain natriuretic peptide (NT-proBNP) were assayed by using the Cobas analyzer (women 97.5th percentile value <254 ng/L). Calculation of molar concentrations of cardiac biomarkers was based on the following estimated molecular masses: troponin T, 37 kDa; troponin I, 24 kDa; NT-proBNP, 8.5 kDa.

CASE PRESENTATION

A 38-year-old pregnant woman (gravida 2, para 0) was admitted at 40 weeks of gestation to our labor and delivery unit with regular contractions after an uncomplicated, regularly supervised pregnancy. She reported a history of mild asthma, endometriosis, and an early miscarriage. At admission, physical examination showed normal vital signs and a fully dilated cervix. Laboratory results were unremarkable. She had an uncomplicated spontaneous vaginal delivery with Apgar scores of 10 and 10. A blood pressure of 152/67 mmHg was noted once during labor.

The patient received extremely stressful news about her child just after delivery. Thirty hours after delivery, she reported a sudden and intense headache associated with epigastric pain. She had no chest pain or respiratory discomfort, such as dyspnea, and neurological examination found no abnormalities. Laboratory tests revealed cytolysis (ASAT, 414 U/L and ALAT, 399 U/L; LDH, 1,017 U/L), associated with a slightly low haptoglobin concentration (0.44 g/L). A whole blood count showed thrombocytopenia (84 G/L) but no evidence of disseminated intravascular coagulation. Slight signs of inflammation were present (white blood cells count, 12.9 G/L; CRP, 77 mg/L). The blood creatinine concentration was elevated (1.12 mg/dl or 85 μmol/L) and was associated with *de novo* proteinuria. The urinary protein profile demonstrated tubular and glomerular involvement (total proteinuria, 0.45 g/mmol creatininuria; albumin, 227 mg/mmol creatininuria; alpha-1-microglobulin, 9.03 mg/mmol creatininuria; alpha-2-macroglobulin, 2.27 mg/mmol creatininuria; IgG, 60.43 mg/mmol creatininuria; retinol-binding protein, 0.53 mg/mmol creatininuria; transferrin, 37.90 mg/mmol creatininuria). We diagnosed HELLP (hemolysis, elevated liver enzymes, low platelet) syndrome, a complication of pregnancy with a risk of kidney failure. The patient was admitted to the nephrology intensive care unit on day 2.

On admission to the nephrology intensive care unit, we found elevated levels of cTnIhs and cTnThs, indicating cardiac necrosis, as well as elevated levels of NT-proBNP. Retrospective assays of cTnIhs and cTnThs in stored plasma samples revealed that pathological concentrations of cTnIhs (i.e., above the 99th percentile threshold) were already present 1 h before delivery but not of cTnThs (**Figure 1**). Measurements of these cardiac biomarkers up to 6 days after delivery found distinct qualitative and quantitative differences. Qualitatively, whereas pathological levels of cTnIhs were already present before delivery, cTnThs began to increase 0.5 day later. Quantitatively, between admission and day 6, cTnIhs concentrations ranged from 115 to 6,264 ng/L whereas cTnThs concentrations were much lower, ranging from 10 to 273 ng/L; NT-proBNP concentrations ranged from 200 to 4,056 ng/L. Both cTnIhs and cTnThs reached a peak concentration at day 2 and decreased soon after. The peak concentration of cTnIhs, however, was much greater than that of cTnThs (median cTnIhs/cTnThs molar ratio = 20.9; 95% C.I., 14.9–36.6—see Methods Section). NT-proBNP levels peaked around the same time as those of the troponins but decreased only after day 3.

The twelve-derivation electrocardiogram was unremarkable. No coronary stenosis or dissection was found by coronary computed tomographic angiography. Transthoracic echocardiography performed at day 1 after transfer to the nephrology intensive care unit (i.e., at day 3 post-delivery) revealed hyperechogenicity, ballooning and akinesia of the basal and mid segments of the inferoseptal (**Supplementary Video 1**), inferior (**Supplementary Video 2**) and anteroseptal (**Supplementary Video 3**) walls, with mild impairment of left ventricular ejection function (LVEF, 45%), suggesting inverted Takotsubo syndrome, a rare variant of this disease that presents with basal ballooning instead of apical ballooning. Cardiac MRI performed at day 3 after transfer to the nephrology intensive care unit (i.e., at day 5 post-delivery) revealed a non-dilated, non-hypertrophied left ventricle, slightly altered global LVEF (51%) and characteristic wall motion abnormalities of inverted Takostubo syndrome including hypokinesia of the basal third predominating over the septum

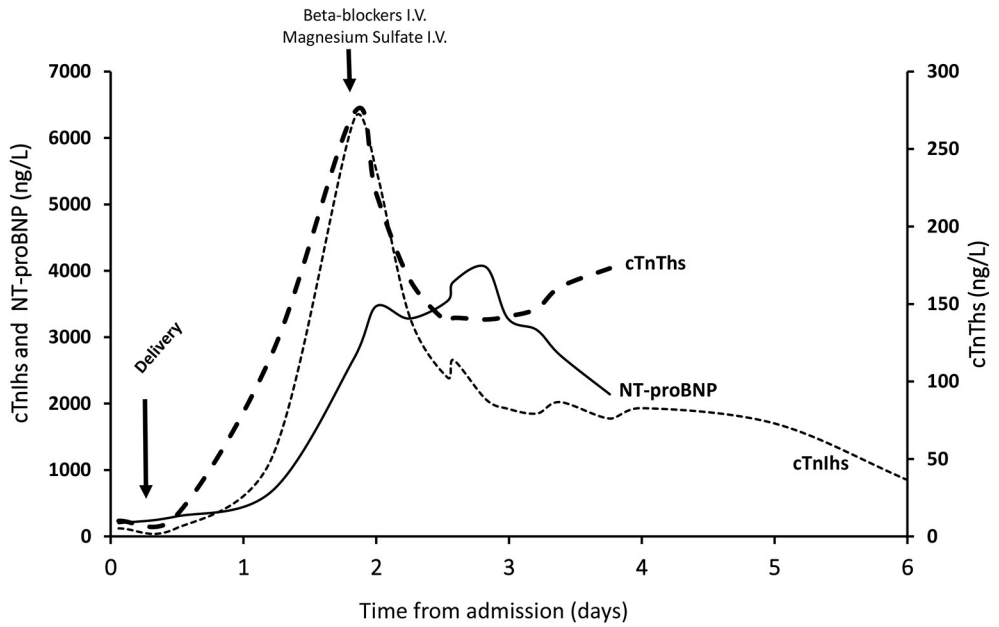

FIGURE 1 | Changes in the cardiac biomarkers cTnIhs, cTnThs, and NT-proBNP. Concentrations of circulating cardiac biomarkers were measured upon admission to hospital (day 0) and at intervals until to discharge (day 6). They are presented as ng/L. Delivery occurred between day 0 and 1 after admission. Intravenous (i.v.) magnesium sulfate and the beta-blocker labetalol were administered as indicated.

and apical hyperkinesia (**Supplementary Video 4**) associated with diffuse basal myocardial edema detected by T2 mapping sequence without late gadolinium enhancement (**Figures 2A–C**). Global T2 mapping values demonstrated a gradient from the base to the apex of the left ventricle: 56 ± 4 ms in the first third, 51 ± 7 ms in the second third, and 48 ± 3 ms at the apical level.

The patient was treated with an intravenous beta-blocker (labetalol) as soon as the diagnosis of HELLP syndrome was made and with intravenous magnesium sulfate until abolition of neurological signs. Her evolution was favorable, with a reversal of headache, hepatic cytolysis, acute renal failure and thrombocytopenia. In addition to the beta-blocker, an angiotensin-converting enzyme inhibitor (captopril) was used at day 3 to improve blood pressure control with no adverse events. cTnIhs levels slowly decreased to 849 ng/L on day 6 when she was discharged from the nephrology intensive care unit. One month after discharge, the patient was in complete remission of her post-partum inverted Takotsubo syndrome. A follow-up cardiac MRI demonstrated complete resolution of left ventricular dysfunction (LVEF, 60%) and regional left ventricular function recovery (**Supplementary Video 5**). Moreover, normalization of T2 mapping values indicated the disappearance of myocardial edema (in **Figure 2D**): 50 ± 5 ms in the first third, 46 ± 6 ms in the second third, and 46 ± 5 ms at the apical level. These findings from cardiac MRI were consistent with our diagnosis of inverted Takotsubo syndrome. Three months after discharge, medical examination found a normal blood pressure of 123/82 mmHg and blood analyses were normal. The main results of the case presentation were summarized in **Supplementary Figure 1**.

DISCUSSION

Here, we describe a case of Takotsubo syndrome in a 38-year-old woman, which occurred post-partum after spontaneous vaginal delivery. This case is novel and interesting, first, because it occurred very soon after childbirth, second, because of the unusual clinical features and, third, because it was accompanied by HELLP syndrome. Our measurements of elevated levels of circulating cardiac biomarkers illustrate the importance of these biomarkers in assisting diagnosis and treatment of this condition.

Although the definitive diagnosis of Takotsubo syndrome was made only several days post-partum, retrospective assays of circulating troponins revealed myocardial damage occurring at the same time as or prior to childbirth. Reports of changes in blood cardiac biomarker levels during pregnancy, delivery and post-partum in the literature are rare. According to one study, changes in cardiac morphology occur within 1 week post-partum, but not during pregnancy (4). Using the same assay for cTnIhs as that used in our study, that study found only slightly but statistically significant elevated levels of cTnIhs at the end of pregnancy (2 ng/L, i.e., 0.07-fold > normal threshold) when compared those observed during the first trimester. In our case, by contrast, the first cTnIhs measurement 1 h before delivery was already substantially increased (120 ng/L, i.e., 7.7-fold > normal threshold) probably due to early cardiac injury.

The case of our patient has unusual clinical features: she was asymptomatic for cardiac disease, the twelve-derivation electrocardiogram demonstrated no pathological features, and

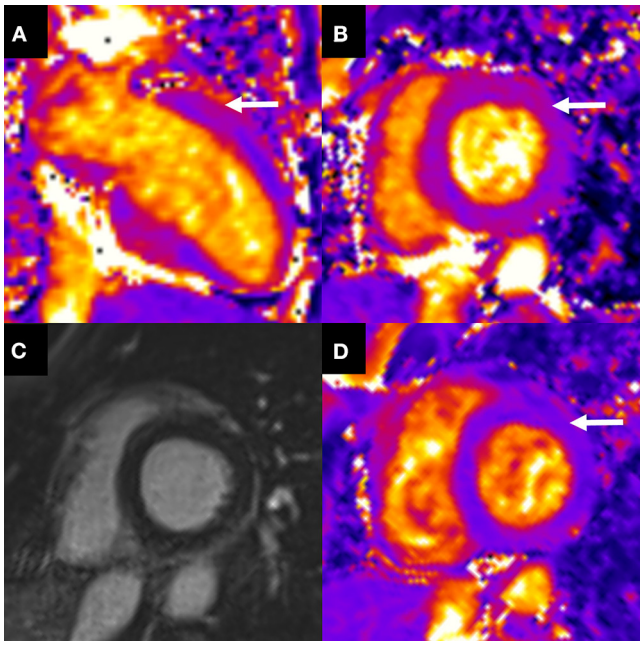

FIGURE 2 | Initial cardiac MRI and follow-up. Cardiac MRI at day 3 after transfer to the nephrology intensive care unit, showed **(A,B)** an elevation of basal T2 mapping value (60 ± 5 ms) related to myocardial edema (arrows) not involving the mid and apical left ventricle without late gadolinium enhancement **(C)**. **(D)** One month later, short axis T2 mapping showed regression of the myocardial edema with a normal T2 mapping value (49 ± 1 ms) (arrow).

the amount of cTnIhs was strongly increased to within the same concentration range as NT-proBNP. The findings from ultrasound and MRI imaging were characteristic of a rare form of the disease: inverted Takotsubo syndrome, in which there was severe basal hypokinesia and a moderate apical hyperkinesia. Takotsubo syndrome is a complex, acute cardiac condition that resembles acute coronary syndrome, usually occurring in the absence of obstructive coronary artery disease and leading to regional left ventricular wall motion abnormality and an impairment of left ventricular contractility (5). The area most often affected is the apical region of the left ventricle (6); in some cases, however, as in our case, the basal area of the left ventricle is affected (7).

In addition to Takotsubo syndrome, the patient presented with HELLP syndrome. The simultaneous occurrence of Takotsubo syndrome in patients with HELLP syndrome has been reported in only a few other cases (8). In a study of 10 cases of post-partum Takotsubo syndrome, two women (20%) presented with HELLP syndrome and five (50%) with preeclampsia (9).

Our understanding of the literature is that the precise pathophysiology of Takotsubo syndrome is unknown; several different pathophysiological mechanisms probably act, individually or synergistically, to cause Takotsubo syndrome. Moreover, it appears that it is often difficult to assess whether any observed modification of a signaling pathway is a cause or a consequence of the episode of Takotsubo syndrome. Sympathetic hyperstimulation is a crucial pathophysiological feature, and catecholamines and $G_i\alpha$ signaling pathways at the level of β2 adrenergic receptor have an important role, resulting in acute myocardial inflammation, myocardial lipotoxicity, low energy production, and NO synthesis, which are hallmarks of Takotsubo syndrome (10, 11). Other possible mechanisms include disruption of calcium regulation, generalized endothelial dysfunction, and oxidative stress (10, 11).

Although the exact pathophysiology of HELLP syndrome has not been clearly defined, we have identified several similarities between the documented mechanisms of HELLP and Takotsubo syndromes, including systemic endothelial dysfunction, strong involvement of oxidative stress, and a systemic inflammatory response (12). A possible link between these two diseases should be evaluated by future studies. One plausible hypothesis to explain the possible link between HELLP and Takotsubo syndrome is an interplay between endothelial abnormalities as recently discussed (13). In HELLP syndrome and during pre-eclampsia there is an imbalance of vasoconstriction and vasodilation mediators mainly at the placental level, and in Takotsubo syndrome dysfunctions in the microcirculation have been documented (14), suggesting that abnormal regulation of vasoconstriction/vasodilation in the microcirculation may underlie both syndromes.

The diagnosis of Takotsubo syndrome is based partly on clinical data, but some biological signs, such as cardiac biomarker changes, have been identified as diagnostic tools (15). No definitive specific or sensitive biomarker for the disease has been proposed, although several biomarkers such as copeptin, lipid profile, sLOX-1, ischemia-modified albumin, sST-2, and chromogranin-A have been proposed to distinguish it from acute coronary syndrome (16, 17). Little is known about cardiac biomarker changes during the acute and remission phases of Takotsubo syndrome (18).

The main cardiac biomarkers reported to be modified in Takotsubo syndrome are NT-proBNP and BNP (19). There is a significant and persistent elevation of NT-proBNP and BNP levels during the acute phase of the disease, which correlates with both the elevation of catecholamines and the severity of left ventricular systolic dysfunction (20). BNP levels ≥238 ng/L and the absence of calcium channel blocker use are independent risk factors for delayed recovery, whereas a leptosomic build (BMI $<$ 20 kg/m^2) is an independent predictor of rapid recovery (21). This increase in BNP levels is more substantial than that of cTnThs in Takotsubo syndrome patients (22). In our case, the increase of circulating troponin isoforms was unusual. The increase in cTnIhs was greater than the increase in cTnThs, as already reported (23), and was within the same range as NT-proBNP; however, whereas pathological levels of cTnIhs were already present before delivery, cTnThs began to increase later.

Some authors have reported similar changes in troponins during acute coronary syndrome and Takotsubo syndrome, which may result in a misdiagnosis (22). Acute coronary syndrome and Takotsubo syndrome overlap significantly in their clinical presentations and Takotsubo syndrome is often mistaken for acute anterior wall ST-segment elevation myocardial infarction (due to an occlusion of the proximal left anterior

descending artery). In our case, the ratio of NT-proBNP (ng/L) to cTnThs (μg/L) at peak was 9,798. This was greater than the threshold level of 5,000 indicating Takotsubo syndrome rather than acute anterior wall ST-segment elevation myocardial infarction (24).

Whereas, the dynamics of the changes in cTnIhs, cTnThs and NT-proBNP in the days following delivery were similar, the amount of cTnIhs was much greater than that of cTnThs (at peak, 400-fold > normal threshold for cTnIhs compared to 25-fold > normal threshold for cTnThs). One caveat to these measurements is that post-translational modifications of troponins upon cardiac necrosis may affect the quantification of circulating forms of the proteins (25); thus, our observations should be substantiated by quantification of all circulating forms of troponins throughout the duration of the disease. Although no definitive conclusion can be drawn at the moment about the comparative sensitivity of cTnIhs or cTnThs for optimal cardiac monitoring during Takotsubo syndrome, our findings suggest that monitoring cTnIhs and/or NT-proBNP would be more useful than monitoring cTnThs because cTnIhs levels increase sooner and much more than cTnThs levels.

In the case presented here, the onset of Takotsubo syndrome post-partum occurred soon after spontaneous vaginal delivery, whereas it generally occurs several days later (26). Takotsubo syndrome is much more common after cesarean section than after vaginal delivery because several risk factors are associated with it, including the psychological and physical stress associated with cesarean section, acute pain and bleeding causing increased catecholamine levels, and use of uterotonic or tocolytic treatments (26, 27). Takotsubo syndrome is often associated with a preceding stressful physical or emotional event (5); physical triggering factors are more prevalent than emotional triggers. The absence of triggering factors does not preclude the diagnosis of Takotsubo syndrome, however. Interestingly, our patient received extremely stressful news about her child just after delivery, which may have contributed to triggering Takotsubo syndrome. The patient received no exogenous drugs, notably, no catecholamines or sympathomimetic drugs that might have precipitated the episode of Takotsubo syndrome.

Because the pathophysiology of Takotsubo syndrome is not precisely understood, there are no well-established guidelines for treating and managing this condition. We treated our patient with angiotensin-converting enzyme (ACE) inhibitors to address the observed abnormal left ventricle wall motion and impaired LVEF, and with a beta-blocker to prevent the potential effects of an adrenergic surge. The use of angiotensin-converting enzyme inhibitors to treat Takotsubo syndrome is associated with improved survival and fewer recurrent events (5, 28). The effectiveness of beta-blockers, by contrast, is less clear. Whereas, observational studies and meta-analyses have found that short- and long-term treatment with beta-blockers is not beneficial in reducing mortality or preventing recurrence (5, 28–31), a recent state-of-the-art review (32) recommended treating patients with Takotsubo syndrome with both angiotensin-converting enzyme inhibitors and beta-blockers. Specifically, they recommended carvedilol, which is a non-cardioselective beta-blocker. In our case, we used labetalol, which is also a non-cardioselective beta-blocker, because our patient wished to breastfeed her baby. Beta-blockers in breast milk can cause hypotension, bradycardia, and hypoglycemia in the infant (33). According to the *Centre de Référence sur les Agents Tératogènes* in France, there are no data concerning the secretion of carvedilol into breast milk, but secretion of labetalol into breast milk is weak and it is estimated that the infant receives <1% of the maternal dose. Moreover, the half-life for elimination of labetalol is short (4 h), whereas that of carvedilol is substantially longer (7–10 h).

Takotsubo syndrome was originally thought not to be a life-threatening disease (34), however, more recent studies have found higher mortality rates in Takotsubo syndrome patients than expected due to long-term mortality, which surpasses that of patients with ST-segment elevation myocardial infarction (35). Moreover, there are reports that the initial presentation can be associated with fatal complications, including cardiogenic shock, congestive heart failure, and lethal arrhythmias, leading to an in-hospital mortality of 2.0–8.7% (5, 36). Thus, the prognosis of Takotsubo syndrome ranges from rapid recovery to poor early and long-term outcomes. A multicenter study of over 1,000 patients from the German and Italian Stress Cardiomyopathy (GEIST) registry yielded four variables as independent predictors of in-hospital complications: a history of neurologic disorders, right ventricular involvement, reduced LVEF, and male sex (36). Therefore, a GEIST prognostic score may be helpful in early risk stratification. Another analysis of the GEIST registry revealed dyspnea at admission as an independent risk factor for in-hospital complications and poor long-term outcomes (37). Also, in-hospital complication rates and long-term mortality were reported to be similar in typical and atypical types of Takotsubo syndrome (38). Our patient recovered full cardiac function 1 month after delivery with no cardiac complications. Consistent with this rapid recovery, she presented good prognostic factors: no neurologic disorder, no right ventricular involvement, only mild impairment of LVEF, and was a female presenting with no dyspnea at the onset of the episode of Takotsubo syndrome.

CONCLUSION

We describe an unusual case of Takotsubo syndrome in a post-partum woman after spontaneous vaginal delivery. This patient was asymptomatic for cardiac disease, the twelve-derivation electrocardiogram demonstrated no pathological features, and the Takotsubo syndrome was accompanied by HELLP syndrome. The overall dynamics of the changes in troponin I, troponin T and NT-proBNP levels after delivery were similar, but the amount of troponin I was much greater than that of troponin T and troponin I was already elevated before delivery. The magnitude of the increase of troponin I was similar to that of the increase of NT-proBNP. Our findings indicate that assaying

circulating cardiac biomarkers, especially troponin I and NT-proBNP, may be a useful complement to the diagnosis of Takotsubo syndrome by non-invasive cardiac imaging. They illustrate the importance of cardiac biomarkers in assisting diagnosis of this disease.

DATA AVAILABILITY STATEMENT

The original contributions presented in the study are included in the article/**Supplementary Material**, further inquiries can be directed to the corresponding author/s.

ETHICS STATEMENT

Written informed consent was obtained from the individual for the publication of any potentially identifiable images or data included in this article.

AUTHOR CONTRIBUTIONS

PG and HF performed physical examination. PR, CC-G, and LC performed biological analysis. EC, LS-D, AC, LM-C, and MK performed imaging. PG, PR, GL, and MB wrote the manuscript. All authors contributed to the article and approved the submitted version.

SUPPLEMENTARY MATERIAL

The Supplementary Material for this article can be found online at: https://www.frontiersin.org/articles/10.3389/fcvm.2022.832098/full#supplementary-material

Supplementary Video 1 | Transthoracic echocardiography, apical four-chamber view. Hyperechogenicity, ballooning and akinesia of the basal and mid segments of the inferoseptal wall.

Supplementary Video 2 | Transthoracic echocardiography, apical two-chamber view. Hyperechogenicity, ballooning and akinesia of the basal and mid segments of the inferior wall.

Supplementary Video 3 | Transthoracic echocardiography, apical three-chamber view. Hyperechogenicity, ballooning and akinesia of the basal and mid segments of the anteroseptal wall.

Supplementary Video 4 | Initial cardiac MRI performed at day 3 after transfer to the nephrology intensive care unit. Left ventricular long axis view showed severe basal hypokinesia sparing the mid and apical cavity, which are in moderate hyperkinesia. This aspect is highly suggestive of a basal type of Takotsubo syndrome.

Supplementary Video 5 | Cardiac MRI follow-up performed 1 month later showed complete resolution of wall motion abnormalities including complete recovery of the basal left ventricular wall motion.

Supplementary Figure 1 | Timeline. I.V, intravenous; HELLP, hemolysis elevated liver enzymes and low platelets count; TTE, transthoracic echocardiography; ACE, angiotensin conversion enzyme; LVEF, left ventricular ejection fraction; TKS, Takotsubo syndrome; MRI, magnetic resonance imaging; cTnThs, cardiac high-sensitivity troponin I; cTnIhs, cardiac high-sensitivity troponin I; NT-proBNP, N-terminal prohormone of brain natriuretic peptide.

REFERENCES

1. Kinno R, Ono K. Takotsubo syndrome: optimizing care with a multidisciplinary approach. *J Multidiscip Healthc.* (2021) 14:2487–99. doi: 10.2147/JMDH.S283667
2. Akashi YJ, Musha H, Nakazawa K, Miyake F. Plasma brain natriuretic peptide in takotsubo cardiomyopathy. *QJM.* (2004) 97:599–607. doi: 10.1093/qjmed/hch094
3. Doyen D, Moceri P, Chiche O, Schouver E, Cerboni P, Chaussade C, et al. Cardiac biomarkers in Takotsubo cardiomyopathy. *Int J Cardiol.* (2014) 174:798–801. doi: 10.1016/j.ijcard.2014.04.120
4. Umazume T, Yamada T, Yamada S, Ishikawa S, Furuta I, Iwano H, et al. Morphofunctional cardiac changes in pregnant women: associations with biomarkers. *Open Heart.* (2018) 5:e000850. doi: 10.1136/openhrt-2018-000850
5. Templin C, Ghadri JR, Diekmann J, Napp LC, Bataiosu DR, Jaguszewski M, et al. Clinical features and outcomes of takotsubo (stress) cardiomyopathy. *N Engl J Med.* (2015) 373:929–38. doi: 10.1056/NEJMoa1406761
6. Akashi YJ, Nef HM, Lyon AR. Epidemiology and pathophysiology of Takotsubo syndrome. *Nat Rev Cardiol.* (2015) 12:387–97. doi: 10.1038/nrcardio.2015.39
7. Awad HH, McNeal AR, Goyal H. Reverse Takotsubo cardiomyopathy: a comprehensive review. *Ann Transl Med.* (2018) 6:460. doi: 10.21037/atm.2018.11.08
8. Kalavakunta JK, Zoltowska DM, Agrawal Y, Gupta V. Regadenoson cardiac stress test-induced stress cardiomyopathy. *BMJ Case Rep.* (2017) 2017:bcr2017221217. doi: 10.1136/bcr-2017-221217
9. Kim DY, Kim SR, Park SJ, Seo JH, Kim EK, Yang JH, et al. Clinical characteristics and long-term outcomes of peripartum takotsubo cardiomyopathy and peripartum cardiomyopathy. *ESC Heart Fail.* (2020) 7:3644–52. doi: 10.1002/ehf2.12889
10. Ghadri JR, Wittstein IS, Prasad A, Sharkey S, Dote K, Akashi YJ, et al. international expert consensus document on takotsubo syndrome (part I): clinical characteristics, diagnostic criteria, and pathophysiology. *Eur Heart J.* (2018) 39:2032–46. doi: 10.1093/eurheartj/ehy076
11. Rawish E, Stiermaier T, Santoro F, Brunetti ND, Eitel I. Current knowledge and future challenges in takotsubo syndrome: part 1-pathophysiology and diagnosis. *J Clin Med.* (2021) 10:479. doi: 10.3390/jcm10030479
12. Benedetto C, Marozio L, Tancredi A, Picardo E, Nardolillo P, Tavella AM, et al. Biochemistry of HELLP syndrome. *Adv Clin Chem.* (2011) 53:85–104. doi: 10.1016/B978-0-12-385855-9.00004-7
13. Kornacki J, Gutaj P, Kalantarova A, Sibiak R, Jankowski M, Wender-Ozegowska E. Endothelial dysfunction in pregnancy complications. *Biomedicines.* (2021) 9:1756. doi: 10.3390/biomedicines9121756
14. Gopalakrishnan P, Zaidi R, Sardar MR. Takotsubo cardiomyopathy: pathophysiology and role of cardiac biomarkers in differential diagnosis. *World J Cardiol.* (2017) 9:723–30. doi: 10.4330/wjc.v9.i9.723
15. Goico A, Chandrasekaran M, Herrera CJ. Novel developments in stress cardiomyopathy: from pathophysiology to prognosis. *Int J Cardiol.* (2016) 223:1053–8. doi: 10.1016/j.ijcard.2016.08.241
16. Wu AH, Tabas JA, Vollert JO, Lauterbach T, Mockel M. Results of novel cardiac biomarkers in Tako-tsubo cardiomyopathy. *Int J Cardiol.* (2012) 159:53–5. doi: 10.1016/j.ijcard.2011.10.127
17. Tarantino N, Santoro F, Di Biase L, Di Terlizzi V, Vitale E, Barone R, et al. Chromogranin-A serum levels in patients with takotsubo syndrome and ST elevation acute myocardial infarction. *Int J Cardiol.* (2020) 320:12–7. doi: 10.1016/j.ijcard.2020.07.040
18. Dias A, Nunez Gil IJ, Santoro F, Madias JE, Pelliccia F, Brunetti ND, et al. Takotsubo syndrome: state-of-the-art review by an expert panel - Part 1. *Cardiovasc Revasc Med.* (2019) 20:70–9. doi: 10.1016/j.carrev.2018.11.015
19. Ueyama T. Emotional stress-induced Tako-tsubo cardiomyopathy: animal model and molecular mechanism. *Ann N Y Acad Sci.* (2004) 1018:437–44. doi: 10.1196/annals.1296.054
20. Nguyen TH, Neil CJ, Sverdlov AL, Mahadavan G, Chirkov YY, Kucia AM, et al. N-terminal pro-brain natriuretic protein levels in takotsubo cardiomyopathy. *Am J Cardiol.* (2011) 108:1316–21. doi: 10.1016/j.amjcard.2011.06.047

21. Shiomura R, Nakamura S, Takano H, Kato K, Inui K, Kubota Y, et al. Impact of brain natriuretic peptide, calcium channel blockers, and body mass index on recovery time from left ventricular systolic dysfunction in patients with takotsubo cardiomyopathy. *Am J Cardiol.* (2015) 116:515–9. doi: 10.1016/j.amjcard.2015.05.006
22. Madhavan M, Borlaug BA, Lerman A, Rihal CS, Prasad A. Stress hormone and circulating biomarker profile of apical ballooning syndrome (Takotsubo cardiomyopathy): insights into the clinical significance of B-type natriuretic peptide and troponin levels. *Heart.* (2009) 95:1436–41. doi: 10.1136/hrt.2009.170399
23. Ramaraj R, Sorrell VL, Movahed MR. Levels of troponin release can aid in the early exclusion of stress-induced (takotsubo) cardiomyopathy. *Exp Clin Cardiol.* (2009) 14:6–8.
24. Frohlich GM, Schoch B, Schmid F, Keller P, Sudano I, Luscher TF, et al. Takotsubo cardiomyopathy has a unique cardiac biomarker profile: NT-proBNP/myoglobin and NT-proBNP/troponin T ratios for the differential diagnosis of acute coronary syndromes and stress induced cardiomyopathy. *Int J Cardiol.* (2012) 154:328–32. doi: 10.1016/j.ijcard.2011.09.077
25. Katrukha IA, Katrukha AG. Myocardial injury and the release of troponins I and T in the blood of patients. *Clin Chem.* (2021) 67:124–30. doi: 10.1093/clinchem/hvaa281
26. Citro R, Giudice R, Mirra M, Petta R, Baldi C, Bossone E, et al. Is Tako-tsubo syndrome in the postpartum period a clinical entity different from peripartum cardiomyopathy? *J Cardiovasc Med.* (2013) 14:568–75. doi: 10.2459/JCM.0b013e32835f1a49
27. Kilian L, Haaf P, Pfister O, Vischer AS, Lapaire O, Burkard T. Reverse Takotsubo syndrome, a case report of a rare cause for postpartum heart failure. *Cardiogenetics.* (2018) 8:13–16. doi: 10.4081/cardiogenetics.2018.7671
28. Singh K, Carson K, Usmani Z, Sawhney G, Shah R, Horowitz J. Systematic review and meta-analysis of incidence and correlates of recurrence of takotsubo cardiomyopathy. *Int J Cardiol.* (2014) 174:696–701. doi: 10.1016/j.ijcard.2014.04.221
29. Isogai T, Matsui H, Tanaka H, Fushimi K, Yasunaga H. Early beta-blocker use and in-hospital mortality in patients with Takotsubo cardiomyopathy. *Heart.* (2016) 102:1029–35. doi: 10.1136/heartjnl-2015-308712
30. Dias A, Franco E, Koshkelashvili N, Bhalla V, Pressman GS, Hebert K, et al. Antiplatelet therapy in Takotsubo cardiomyopathy: does it improve cardiovascular outcomes during index event? *Heart Vessels.* (2016) 31:1285–90. doi: 10.1007/s00380-015-0729-2
31. Santoro F, Ieva R, Musaico F, Ferraretti A, Triggiani G, Tarantino N, et al. Lack of efficacy of drug therapy in preventing takotsubo cardiomyopathy recurrence: a meta-analysis. *Clin Cardiol.* (2014) 37:434–9. doi: 10.1002/clc.22280
32. Lyon AR, Citro R, Schneider B, Morel O, Ghadri JR, Templin C, et al. Pathophysiology of takotsubo syndrome: JACC state-of-the-art review. *J Am Coll Cardiol.* (2021) 77:902–21. doi: 10.1016/j.jacc.2020.10.060
33. Beardmore KS, Morris JM, Gallery ED. Excretion of antihypertensive medication into human breast milk: a systematic review. *Hypertens Pregn.* (2002) 21:85–95. doi: 10.1081/PRG-120002912
34. Elesber A, Lerman A, Bybee KA, Murphy JG, Barsness G, Singh M, et al. Myocardial perfusion in apical ballooning syndrome correlate of myocardial injury. *Am Heart J.* (2006) 152:469.e9–13. doi: 10.1016/j.ahj.2006.06.007
35. Stiermaier T, Moeller C, Oehler K, Desch S, Graf T, Eitel C, et al. Long-term excess mortality in takotsubo cardiomyopathy: predictors, causes and clinical consequences. *Eur J Heart Fail.* (2016) 18:650–6. doi: 10.1002/ejhf.494
36. Santoro F, Nunez Gil IJ, Stiermaier T, El-Battrawy I, Guerra F, Novo G, et al. Assessment of the german and italian stress cardiomyopathy score for risk stratification for in-hospital complications in patients with takotsubo syndrome. *JAMA Cardiol.* (2019) 4:892–9. doi: 10.1001/jamacardio.2019.2597
37. Arcari L, Musumeci MB, Stiermaier T, El-Battrawy I, Moller C, Guerra F, et al. Incidence, determinants and prognostic relevance of dyspnea at admission in patients with Takotsubo syndrome: results from the international multicenter GEIST registry. *Sci Rep.* (2020) 10:13603. doi: 10.1038/s41598-020-70445-9
38. Ghadri JR, Cammann VL, Napp LC, Jurisic S, Diekmann J, Bataiosu DR, et al. Differences in the clinical profile and outcomes of typical and atypical takotsubo syndrome: data from the international takotsubo registry. *JAMA Cardiol.* (2016) 1:335–40. doi: 10.1001/jamacardio.2016.0225

Conflict of Interest: The authors declare that the research was conducted in the absence of any commercial or financial relationships that could be construed as a potential conflict of interest.

Publisher's Note: All claims expressed in this article are solely those of the authors and do not necessarily represent those of their affiliated organizations, or those of the publisher, the editors and the reviewers. Any product that may be evaluated in this article, or claim that may be made by its manufacturer, is not guaranteed or endorsed by the publisher.

frontiers | Frontiers in Cardiovascular Medicine

CASE REPORT
published: 25 April 2022
doi: 10.3389/fcvm.2022.786278

Multimodal Imaging for Total Anomalous Systemic Venous Drainage Diagnosis and Preoperative Planning: A Case Report and Literature Review

*Mingyan Ding†, Huihui Zhang†, Dandan Sun, Qiang Li, Ni Jiao and Fang Zhu**

Department of Cardiovascular Function, People's Hospital of China Medical University, People's Hospital of Liaoning Province, Shenyang, China

Total anomalous systemic venous drainage (TASVD) is a rare congenital heart malformation. Here, we report a case of a 40-year-old male patient who had a total anomalous systemic venous drainage. It was diagnosed as the TASVD for the first time through multimodal imaging combined Transthoracic (TTE), transesophageal (TEE) and three-dimensional (3D-TTE) echocardiography, contrast echocardiography and computed tomography angiography (CTA). We review 15 published reports on TASVD and summarize the ultrasonographic characteristics. After intracardiac repair through ectopic venous drainage in cardiac surgery, the patient's cyanosis symptoms were alleviated greatly. Echocardiography was the first-line examination for TASVD. Multimodal imaging combined TTE, TEE, 3D TEE, contrast echocardiography and CTA was necessary for confirmed diagnosis of TASVCD.

Keywords: total anomalous systemic venous drainage, multimodal imaging, echocardiography, coronary sinus atrial septal defect, computed tomography angiography

OPEN ACCESS

Edited by:
Gian Marco Rosa, San Martino Hospital (IRCCS), Italy

Reviewed by:
Maruti Haranal, U. N. Mehta Institute of Cardiology and Research, India
Sara Seitun, San Martino Polyclinic Hospital IRCCS, Italy

***Correspondence:**
Fang Zhu
zfmoon@126.com

†These authors have contributed equally to this work

Specialty section:
This article was submitted to General Cardiovascular Medicine, a section of the journal Frontiers in Cardiovascular Medicine

Received: *01 October 2021*
Accepted: *11 March 2022*
Published: *25 April 2022*

Citation:
Ding M, Zhang H, Sun D, Li Q, Jiao N and Zhu F (2022) Multimodal Imaging for Total Anomalous Systemic Venous Drainage Diagnosis and Preoperative Planning: A Case Report and Literature Review. Front. Cardiovasc. Med. 9:786278. doi: 10.3389/fcvm.2022.786278

INTRODUCTION

Anomalous systemic venous drainage is a rare type of congenital heart malformation and has a 5% incidence rate among all congenital heart diseases (1). It is divided into partial systemic venous return anomalies and total anomalous systemic venous drainage (TASVD). The definition is that the drainage of all systemic veins (SVC, IVC, and the coronary sinus) to the LA. TASVD may also be part of heterotaxy syndrome (2). We report a case of TASVD diagnosed by multimodal imaging and was successfully corrected by surgery.

CASE REPORT

A 40-year-old male reporting "thirty years chest pain and palpitation after exercise, which got worsened for five days" was admitted to our hospital. Echocardiography revealed atrial septal defect in 2009, but it was untreated. Electrocardiogram revealed (1) sinus bradycardia, (2) high voltage in chest leads, and (3) flat T waves in leads I, III, and aVL. His physical examination revealed stunted growth, cyanosis of lips, 53.4 mmHg partial pressure of oxygen, and 88.6% blood oxygen saturation level. A loud, soft pan systolic murmur could be heard over the cardiac apex. His past medical

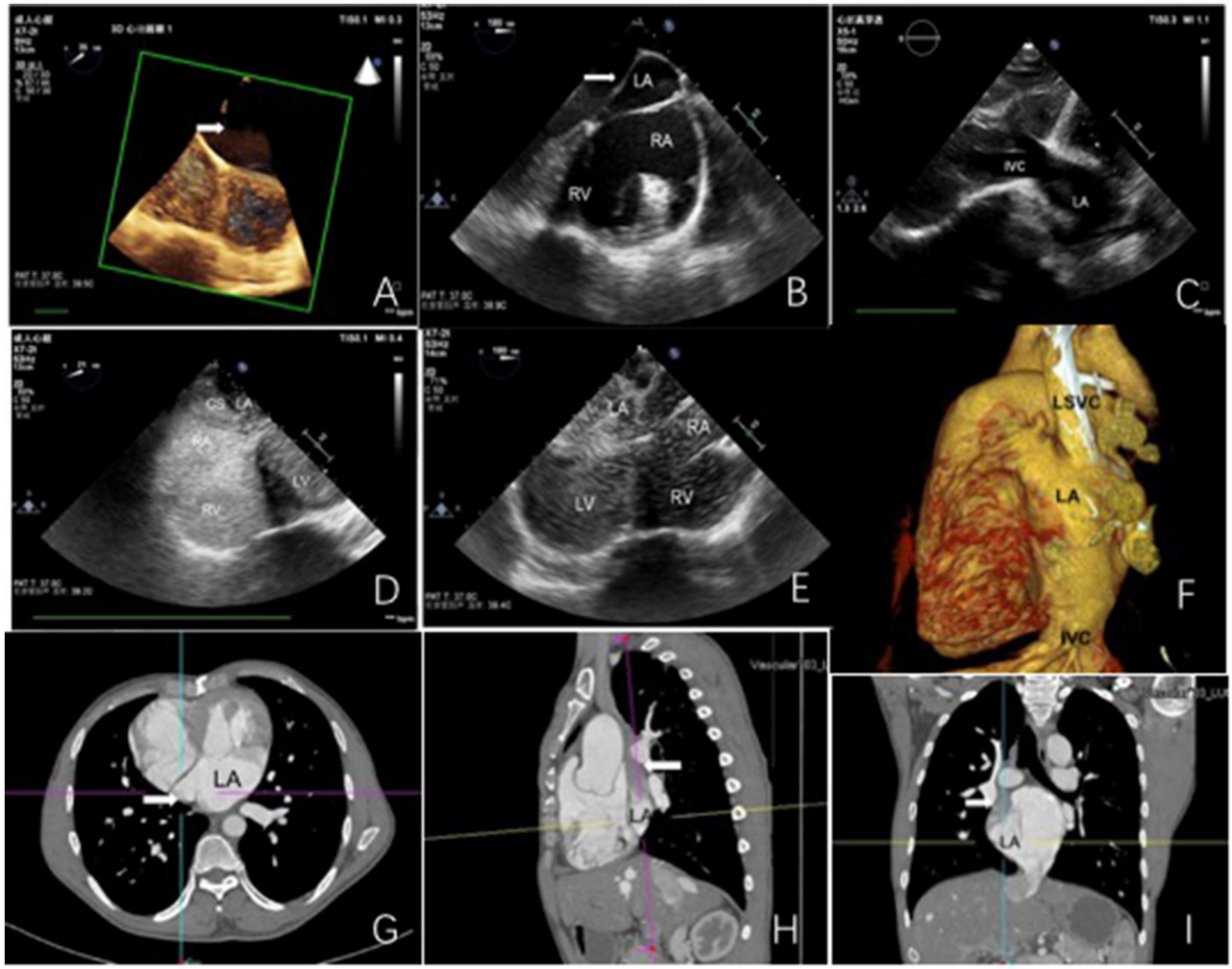

FIGURE 1 | Echocardiography and computed tomography angiography. **(A)** complete coronary sinus atrial septal defect (white arrowheads). **(B)** white arrowheads show an abnormal conduit. **(C)** A connection between the inferior vena cava and the left atrium. **(D)** saline microbubbles injected into the lower limb vein expressed first in the LA and left ventricle (LV), and then in the RA and RV. **(E)** saline microbubbles injected into the right elbow vein expressed almost simultaneously in the LA and RA. **(F)** CT shows the left superior vena cava and the inferior vena cava draining into the LA. **(G–I)** CT shows the superior vena cava (white arrowheads) draining into the.

history included cerebral infarction and migraine. 1 month before hospitalization, the patient had acute cerebellar infarction that improved after medical treatment. Biochemical parameters were within normal limits.

Transthoracic (TTE), transesophageal (TEE) and three-dimensional (3D-TTE) echocardiography revealed (1) coronary sinus dilatation and a complete coronary sinus atrial septal defect (ASD) (**Figure 1A**, **Supplementary Videos 1, 2**), (2) an anomalous conduit enters left atrium (LA) at its roof (**Figure 1B**), and (3) the inferior vena cava (IVC) opens into LA (**Figure 1C**) (4) the superior vena cava (SVC) is not connected with the right atrium (RA). Contrast echocardiography revealed (1) saline microbubbles injected to the left elbow vein expressed first in the LA and then in the RA and right ventricle (RV) (**Supplementary Video 3**); (2) saline microbubbles injected into the right elbow vein expressed almost simultaneously in the LA and RA (**Figure 1D**, **Supplementary Video 4**); (3) saline microbubbles injected into the lower limb vein expressed first in the LA and left ventricle (LV) and then in the RA and RV (**Figure 1E**, **Supplementary Videos 5, 6**). Arch was normal. Accordingly, these were diagnosed as complete coronary sinus ASD, persistent ectopic venous draining from the left SVC to the LA, ectopic venous draining from the IVC to the LA, and ectopic venous draining from the right SVC to the LA. Hepatic veins were draining into the IVC, and pulmonary veins were draining into the LA. ECG-gated computed tomography angiography (CTA) demonstrated complete coronary sinus ASD, persistent left SVC draining into the LA (**Figure 1F**), right SVC draining

Abbreviations: LA, left atrium; IVC, inferior vena cava; RA, right atrium; RV, right ventricle; LV, left ventricle; CS, coronary sinus; LSVC, left superior vena cava.

into the LA (**Figures 1G–I**), and IVC draining into the LA (**Figure 1F**). A contrast medium was injected in the left elbow vein. Finally, it was diagnosed as total anomalous systemic venous drainage (TASVD) through cardiac surgery, and was consistent with the multimodal imaging (TTE, TEE, 3D TEE, contrast echocardiography and CTA).

During the cardiac surgery, we saw a complete coronary sinus atrial septal defect, the right superior vena cava being slightly thinner and draining into the coronary sinus opening in the right atrium, persistent left superior vena cava draining into the left atrium, which opened between the left atrial appendage and the left superior pulmonary vein, and the inferior vena cava opening between the mitral valve and the right inferior pulmonary vein. Both atrial appendages were normal in morphology. Thus, we performed a repair of the atrial septal defect and an intracardiac repair through ectopic venous drainage.

After the operation, the patient recovered well: his face and lip color was normal; his partial pressure of oxygen was 97.7 mmHg, and his blood oxygen saturation level was 97.8%. 3 months after the operation, TTE revealed that his cardiac size returned to normal. At 1-year follow-up, the man was doing well and had normal oxygen saturation and unobstructed systemic venous drainage.

DISCUSSION

TASVD is a rare type of congenital heart malformation. TASVD drainage requires the presence of a left-to-right shunt (PDA, ASD, or VSD) to allow the systemic venous return to reach the pulmonary circulation (3). Functional drainage of systemic venous blood into the left atrium across an atrial septal defect has been described. The mechanisms is that TASVD probably results from the sinus venosus being incorporated into the LA (4) or that the right valve of the systemic venous sinus fails to regress (5). There are three subsets of TASVD based on the type of vena cava cannulation (2). In type I, the IVC is not interrupted and conventional cardiopulmonary bypass can be performed. In type II, the IVC is interrupted, and single cannulation of the SVC would suffice for venous drainage. In type III, the IVC drains to an accessory chamber like coronary sinus. According to the above classifications, our case belongs to type I. Electronic databases including Pubmed, Web of Science, and Medline were searched to identify TASVD, from inception to May 2021. We reviewed 13 published reports on TASVC and summarized the ultrasonographic characteristics in **Table 1**.

Because of individual differences and lack of specific laboratory tests, medical diagnosis of TASVD is usually challenging. Up to now, echocardiography is still the most common clinical examination. In this case, multimodal imaging was performed to diagnose TASVD. Echocardiography manifestations are as follows: (1) two-dimensional echocardiography shows that the LA is significantly enlarged and that the right heart system is relatively small; (2) communication between the SVC and the LA was not seen in the conventional ultrasound view of two-dimensional transthoracic

TABLE 1 | Ultrasonographic characteristics of the 15 cases of total anomalous systemic venous drainage.

Authors	Year	Age	Sex	Symptom	RSVC	Persisitent LSVC	IVC	Isomerism	ASD	VSD	Arch	PDA
Samaan (6)	2016	20y	M	shortness of breath,cyanosis	LA	LA	LA	Not committed	YES	-	Normal	-
Agarwal (7)	2014	12y	M	Asymptomatic	LA	-	interrupted	-	-	-	Normal	-
Simha (8)	2012	11y	F	cyanosis, fatigue, palpitations	LA	-	interrupted	left atrial isomerism	YES	-	Normal	-
Khandenahally (9)	2013	11y	F	fatigue, cyanosis	LA	-	interrupted	-	YES	-	Normal	-
Kao (10)	1983	4y	F	Cyanosis	LA	-	interrupted	-	YES	YES	Normal	-
Awasthy (2)	2014	5y	F	Cyanosis	LA	-	LA	left atrial isomerism	YES	YES	Right arch	-
		5y	F	Cyanosis	LA	-	interrupted	left atrial isomerism	YES	YES	Right arch	-
		2y	M	Cyanosis	LA	LA	interrupted	left atrial isomerism	YES	-	Normal	-
Yildirim (11)	2014	2d	M	Cyanosis	-	LA	interrupted	left atrial isomerism	YES	YES	Normal	-
Roberts (4)	1972	3y	F	Cyanosis	LA	LA	interrupted	-	YES	-	Normal	-
Vo (12)	2015	7y	F	dyspnea, cyanosis	LA	LA	interrupted	left atrial isomerism	-	YES	Normal	-
Vaidyanathan (13)	2016	9y	F	Dyspnea	LA	-	LA	-	YES	-	Normal	-
Zhang (14)	2009	33m	F	Cyanosis	LA	LA	LA	-	YES	YES	Normal	-
Devendran (15)	2013	27y	F	Cyanosis	LA	-	LA	-	YES	-	Normal	-
Lazzarin (16)	2009	1d	F	mild dyspnea, cyanosis	LA	-	LA	-	YES	-	Normal	YES

M, male; F, female; LA, left atrium; RSVC, right superior vena cava; IVC, inferior vena cava; ASD, atrial septal defect; VSD, ventricular septal defect; PDA, patent ductus arteriosus.

echocardiography; (3) two-dimensional transesophageal echocardiography clearly shows that the SVC and the IVC are not communicating with the RA; (4) right heart contrast echocardiography can help assess the connection between veins and atriums effectively, and the communication between the SVC, the IVC, and the LA; (5) three-dimensional transesophageal echocardiography can directly display the communication between the abnormal duct and the LA. TTE, TEE, and 3D TEE are considered useful approaches to help observe the hind and inside of heart structures. Contrast echocardiography can help assess the connection between veins and atriums effectively. CTA examination is an invasive and reliable way to examine congenital heart diseases and can provide more comprehensive and three-dimensional cardiovascular imaging. Through CTA examination, the connection between pericardia great vessel system and heart chambers can be assessed. The main advantage of CT is its high-resolution tridimensionality, and a 3D image could add an interesting view of the cardiac anomaly. This case was finally diagnosed and compressively expressed by multimodal imaging (TTE, TEE, 3D TEE, contrast echocardiography, and CTA). Noninvasive examinations such as MRI can be used to assess defects of cardiovascular walls or help observe flow signals from vein to the LA without using contrast media, especially in pediatric populations with congenital heart disease because of lack of ionizing radiation (17).

TASVD is a rare and usually hard to detect congenital heart malformation. As the first diagnostic examination, ultrasound examination has its unique advantages in TASVD diagnosis. In the face of cases of complex anomalous cardiac venous system connection, we need to perform multimodal imaging to confirm the diagnosis of TASVD.

DATA AVAILABILITY STATEMENT

The original contributions presented in the study are included in the article/**Supplementary Material**, further inquiries can be directed to the corresponding author/s.

ETHICS STATEMENT

Written informed consent was obtained from the individual(s) for the publication of any potentially identifiable images or data included in this article.

AUTHOR CONTRIBUTIONS

MD, HZ, NJ, and DS: study concept, acquisition of data and figures, and writing of the manuscript. QL and FZ: study concept and critical revision of the manuscript for intellectual content. All the authors cared for the patient and contributed to the writing of the report.

FUNDING

This study was supported by the Liaoning Province Xingliao Talents Plan Project (XLYC2005007) and Science and Technology Fund of Liaoning Province (20180530109).

ACKNOWLEDGMENTS

We thank the doctors of the Department of Cardiovascular Function and Cardiac Surgery.

SUPPLEMENTARY MATERIAL

The Supplementary Material for this article can be found online at: https://www.frontiersin.org/articles/10.3389/fcvm.2022.786278/full#supplementary-material

Supplementary Videos 1, 2 | Coronary sinus dilatation and complete coronary sinus atrial septal defect (ASD).

Supplementary Video 3 | Saline microbubbles injected to left elbow vein expressed first in LA, and then in RA and right ventricle.

Supplementary Video 4 | Saline microbubbles injected into right elbow vein expressed almost simultaneously in LA and RA.

Supplementary Videos 5, 6 | Saline microbubbles injected into lower limb vein expressed first in LA and left ventricle (LV), and then in RA and RV.

REFERENCES

1. Leval MRde, Ritter DG, McGoon DC, Danielson GK. Anomalous systemic venous connection. surgical considerations. *Mayo Clin Proc.* (1975) 50:599–610.
2. Awasthy N, Radhakrishnan S, Kaushal S, Sharma R. Total anomalous systemic venous drainage to the left atrium: an entity reviewed and investigated. *Ann Pediatr Cardiol.* (2014) 7:98–102. doi: 10.4103/0974-2069.132476
3. Maillis MS, Cheng TO, Meyer JF, Crawley IS, J. Lindsay Jr. Cyanosis in patients with atrial septal defect due to systemic venous drainage into the left atrium *Am J Cardiol.* (1974) 33:674–8. doi: 10.1016/0002-9149(74)90261-6
4. Roberts KD, Edwards JM, Astley R. Surgical correction of total anomalous systemic venous drainage. *J Thorac Cardiovasc Surg.* (1972) 64:803–10. doi: 10.1016/S0022-5223(19)40855-6
5. van Ledden-Klok M, Mol Ade, Backx A. Images in congenital heart disease. Symptomatic divided right atrium in a newborn. *Cardiol Young.* (2007) 17:110. doi: 10.1017/S1047951106001478
6. Samaan AA, Abdelsalam S. Total anomalous systemic venous drainage in an adult. *Eur Heart J Cardiovasc Imaging.* (2016) 17:1127. doi: 10.1093/ehjci/jew125
7. Agarwal, N. Agrawal, S. Patra, and C.N. Manjunath, Total anomalous systemic venous drainage to coronary sinus. *BMJ Case Rep*. 2014 (2014):1493. doi: 10.1136/bcr-2013-201493
8. Simha PP, Patel MD, Jagadeesh AM. Anesthetic implications of total anomalous systemic venous connection to left atrium with left isomerism. *Ann Card Anaesth.* (2012) 15:134–7. doi: 10.4103/0971-9784.95077
9. Khandenahally RS, Deora S, Math RS. Total anomalous systemic venous drainage in left heterotaxy syndrome. *Cardiol Young.* (2013) 23:284–6. doi: 10.1017/S1047951112000819
10. Kao CT, Ban T, Sakata R, Soeda K. Surgical correction of total anomalous systemic venous drainage with ventricular septal defect and pulmonary stenosis–report of a case. *Nihon Geka Hokan.* (1983) 52:256–62.
11. Yildirim A, Kosger P, Ozdemir G, Ucar B, Kilic Z. Total anomalous systemic venous drainage with heterotaxia syndrome: a rare case. *Case Rep Cardiol.* (2014) 2014:392841. doi: 10.1155/2014/392841

12. Vo AT, Cao KD, Le KM, Nguyen DH. Left isomerism syndrome with total anomalous systemic connection. *Asian Cardiovasc Thorac Ann.* (2017) 25:58–61. doi: 10.1177/0218492315618507
13. Vaidyanathan S, Kothandam S, Kumar R, Pradhan PM, Agarwal R. Unusual presentation of total anomalous systemic venous connection. *Asian Cardiovasc Thorac Ann.* (2017) 25:453–6. doi: 10.1177/0218492316644355
14. Zhang ZW, Duan QJ, Gao Z, Ru W, Ying LY. Total anomalous systemic venous drainage to the left atrium. *Ann Thorac Surg.* (2009) 87:1599–601. doi: 10.1016/j.athoracsur.2008.09.025
15. Devendran V, Varghese R, Gudeboyana K, Jessudian V. Isolated total anomalous systemic venous drainage in an adult: case report. *Pediatr Cardiol.* (2013) 34:1918–21. doi: 10.1007/s00246-012-0458-6
16. O. Lazzarin, RD, Rossl. Total anomalous systemic venous drainage. a case report surgical considerations. *Revista Argentina De Cardiologla.* (2009) (77):404–7.
17. Chaturvedi A, Dubinsky TJ, Maki JH. MR findings of a rare defect, coronary sinus ASD. *Int J Cardiovasc Imaging.* (2012) 28:429–30. doi: 10.1007/s10554-010-9670-8

Conflict of Interest: The authors declare that the research was conducted in the absence of any commercial or financial relationships that could be construed as a potential conflict of interest.

Publisher's Note: All claims expressed in this article are solely those of the authors and do not necessarily represent those of their affiliated organizations, or those of the publisher, the editors and the reviewers. Any product that may be evaluated in this article, or claim that may be made by its manufacturer, is not guaranteed or endorsed by the publisher.

frontiers | Frontiers in Cardiovascular Medicine

CASE REPORT
published: 06 May 2022
doi: 10.3389/fcvm.2022.822150

Case Report: Family Curse: An *SCN5A* Mutation, c.611C>A, p.A204E Associated With a Family History of Dilated Cardiomyopathy and Arrhythmia

Wen Huang[1,2], *Rui Xu*[2]*, *Ning Gao*[2], *Xia Wu*[2] *and Cong Wen*[3]

[1] Department of Medical Ultrasound, Shandong Provincial Qianfoshan Hospital, Shandong University, Jinan, China, [2] Department of Cardiology, The First Affiliated Hospital of Shandong First Medical University & Shandong Provincial Qianfoshan Hospital, Shandong Medicine and Health Key Laboratory of Cardiac Electrophysiology and Arrhythmia, Shandong University, Jinan, China, [3] Department of Cardiology, Shandong Provincial Qianfoshan Hospital, Weifang Medical University, Jinan, China

Objective: We report a 3-generation family with *SCN5A* c.611 C>A rare variant, whose clinical characteristics are dilated cardiomyopathy (DCM) combined with multifocal ectopic Purkinje-related premature contractions (MEPPC). We tried to explain why the same *SCN5A* variant carriers had different phenotypes.

Methods: We collected the clinical data from the family, and followed up this family members. Genetic testing was done for whom DNA samples could be collected.

Results: Information was collected from 15 people in this family, 8 of whom had genetic testing. The *SCN5A* variant was present in all patients of this family, whose clinical features showed DCM combined with MEPPC. The proband's children developed DCM and MEPPC in their childhood. They both carried a *SCN5A* p.A204E mutation from their mother and a mutation *PRKAG2* p.D372N from their father. The son did heart transplant and his heart was both dilated and thickened. The pathology confirmed the presence of glycogen accumulation in the myocardium, which were consistent with the diagnosis of *PAKAG2* syndrome.

Conclusion: SCN5A c.611 C>A variant was related to DCM combined with MEPPC. This case report is the first to demonstrate that a combination of *SCN5A* and *PRKAG2* mutations can cause DCM plus MEPPC and *PRKAG2* Syndrome.

Keywords: *SCN5A*, *PRKAG2*, dilated cardiomyopathy, sudden cardiac death, familial case report

OPEN ACCESS

Edited by:
Takeru Makiyama, Kyoto University, Japan

Reviewed by:
Koichi Kato, Shiga University of Medical Science, Japan
Oscar Campuzano, University of Girona, Spain

***Correspondence:**
Rui Xu
xuruicn@hotmail.com

Specialty section:
This article was submitted to General Cardiovascular Medicine, a section of the journal Frontiers in Cardiovascular Medicine

Received: *18 January 2022*
Accepted: *31 March 2022*
Published: *06 May 2022*

Citation:
Huang W, Xu R, Gao N, Wu X and Wen C (2022) Case Report: Family Curse: An SCN5A Mutation, c.611C>A, p.A204E Associated With a Family History of Dilated Cardiomyopathy and Arrhythmia. Front. Cardiovasc. Med. 9:822150. doi: 10.3389/fcvm.2022.822150

INTRODUCTION

Dilated cardiomyopathy (DCM) is the most common non-ischemic cardiomyopathy, with an incidence of about 1/2500, which can lead to severe heart failure. It is associated with arrhythmia and sudden death, and the incidence of sudden death within 5 years is 10–15% (1). The main pathogenic genes are related to cardiac structural proteins, sarcomereproteins, and nuclear membrane proteins. About 2% of patients with heart dilatation are caused by *SCN5A* gene mutation.

A family case of DCM with an *SCN5A* mutation, c.611C>A, p.A204E is reported as follows. The same mutation has been reported in one case in the literature, and no family report has been

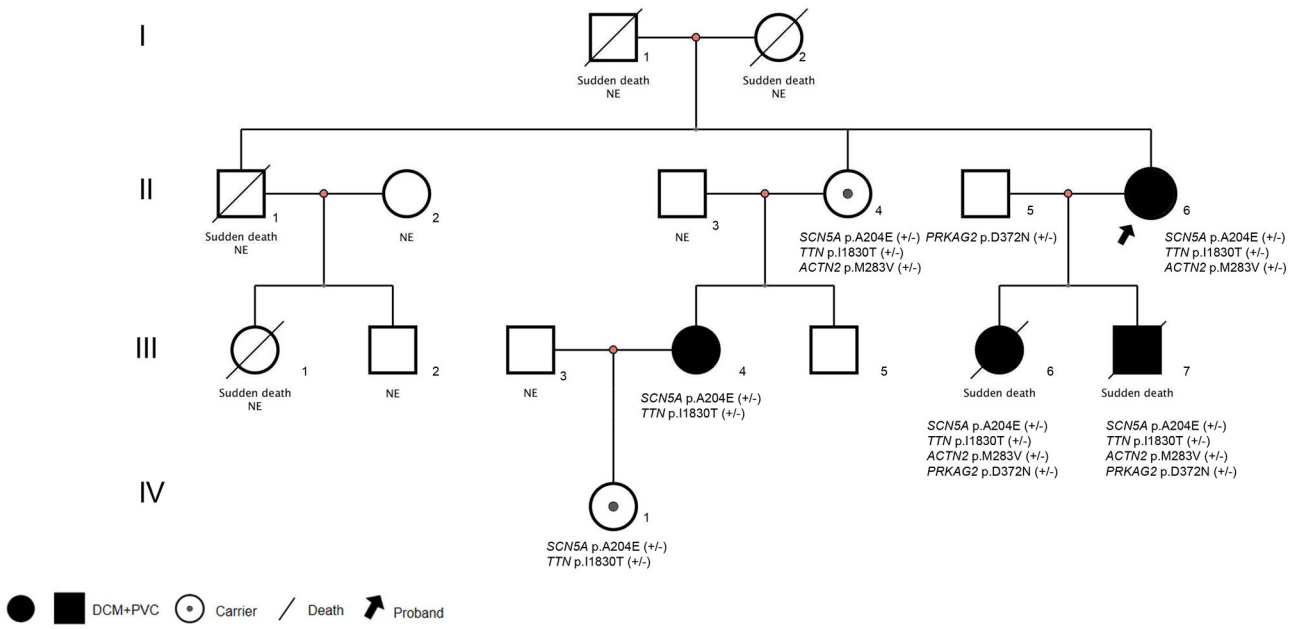

FIGURE 1 | Pedigrees and diagnosis of the families assessed. Squares indicate male family members, circles indicate female family members. NE:Genomic DNA was not examined. (+/-): Haplotype. DCM, Dilated cardiomyopathy; PVC, Premature ventricular contractions.

found (2). The variant is unique from, so far, reported typical *SCN5A* variants because of its characteristic phenotype expression: Purkinje-related premature contractions. We report a 3-generation family with this rare variant (**Figure 1**), where patients presented dilated cardiomyopathy (DCM) combined with premature ventricular contractions (PVC), and carriers manifested a variety of premature contractions.

CASE PRESENTATIONS

Case 1

The proband (**Figure 1**: II-6), a 49-year-old woman, was admitted to a hospital with a 14-year history of recurrent chest distress, aggravated by palpitations for 4 days. She had a family history of sudden death: her father (I-1) died of cerebrovascular disease at 50 years, her mother (I-2) died suddenly at 40 years, a brother (II-1) died suddenly at 33 years old, and his daughter (III-1) died suddenly at 19 years. All of the sudden deaths happened during sleep. The patient had a daughter (III-6) and a son (III-7), who were diagnosed with DCM at the age of 16 and 9 years, respectively. The patient developed chest tightness and dyspnea, accompanied by nausea and vomiting after catching a cold 14 years ago. At that time, she underwent cardiac color ultrasound and was diagnosed with DCM. Hospitalization, ventricular tachycardia, and ventricular fibrillation occurred several times. Twelve years ago, 1 month after having her second child, the proband was readmitted for chest tightness for about 3 weeks, aggravated by palpitations for 1 week. During her hospital stay, more than 50 episodes of ventricular tachycardia or ventricular fibrillation occurred; an implantable cardiac defibrillator was recommended, but the patient refused. After discharge, the patient took metoprolol and was followed regularly. A conventional echocardiogram showed a large left ventricular end-diastolic diameter (LVEDD) of 69 mm and an LV ejection fraction (LVEF) of 40% (**Figure 2**). Because of her family history, genomic DNA was extracted from the peripheral blood of eight family members [the proband and her husband (II-5), two children (III-6) (III-7), sister (II-4), the sister's two children (III-4) (III-5), and granddaughter (IV-1)], and a genomic library was constructed. The enriched target gene fragments were sequenced by Illumina sequencing (3). The proband carried 3 possible pathogenic mutation associated with DCM and PVC, including *SCN5A* p.A204E, *TTN* p.I1830T, and *ACTN2* p.M283V. The pathogenicity of the mutation was analyzed concerning the American College of Medical Genetics and Genomics(ACMG)guidelines (4). *SCN5A* p.A204E was considered "likely pathogenic." *TTN* p.I1830T and *ACTN2* p.M283V were considered "uncertain significance." **Figure 3** shows the *SCN5A* variant of the DNA analyses. The proband's parents, brother, and niece were not tested because they had all died before this time point. Her brother's ex-wife (II-2) and son (III-2) were not tested because the ex-wife took her son when she remarried and lost contact.

Case 2

At 16 years, the proband's daughter (III-6) was admitted to a hospital for "chest tightness and shortness of breath for 20 days." Twenty days after catching a cold, she developed fatigue, chest congestion, shortness of breath, and gradually decreased endurance. She became short of breath after walking for 5–6 min and could not lie supine at night. Twelve days later, an outpatient electrocardiogram (ECG) showed frequent atrial premature beats accompanied by differential transmission and interface escape. The echocardiogram showed a large LV, and the LVEF was 24%.

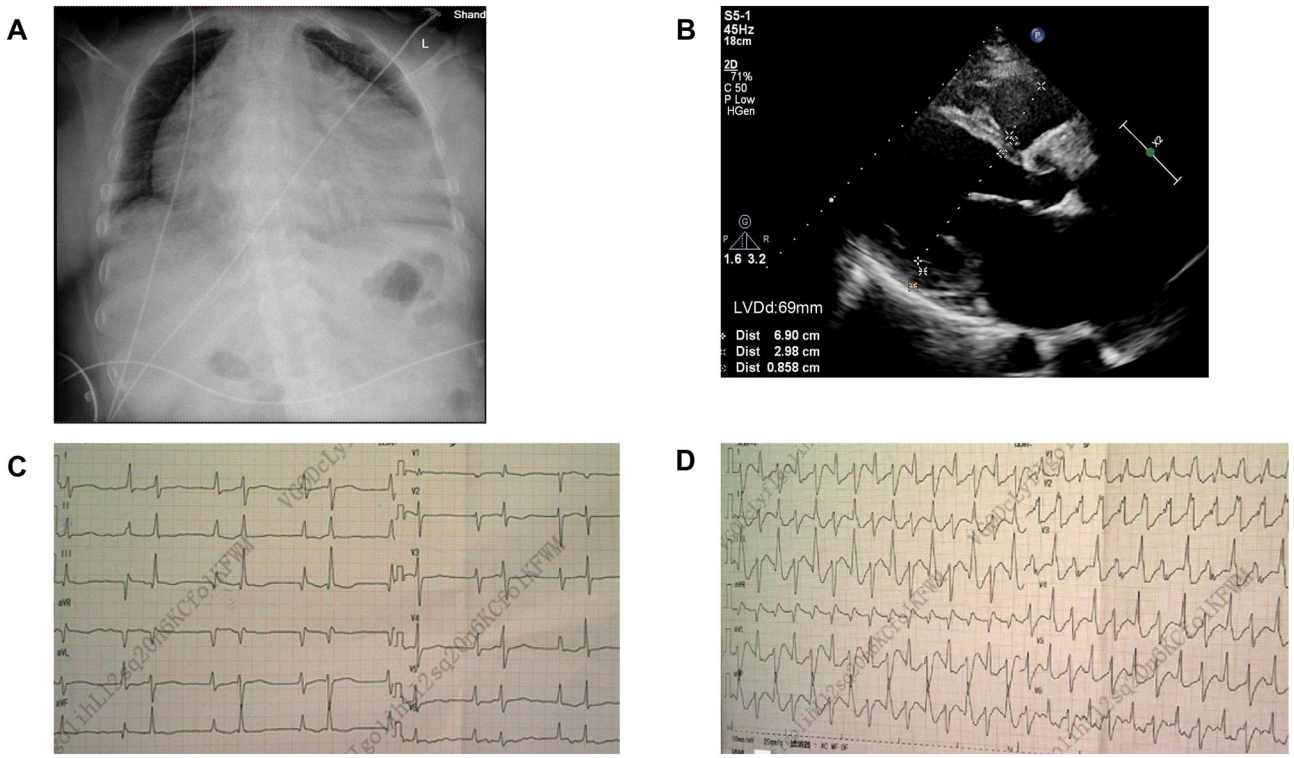

FIGURE 2 | Image of case 1 (**Figure 1**:II-6). **(A)** Chest X-ray showed congestion with a cardiothoracic ratio of 80%. **(B)** Echocardiogram revealed an enlarged left ventricle. LVDd, Left ventricular end-diastolic diameter. **(C,D)**: Electrocardiogram (ECG) comparison between the normal state and frequent premature ventricular contractions.

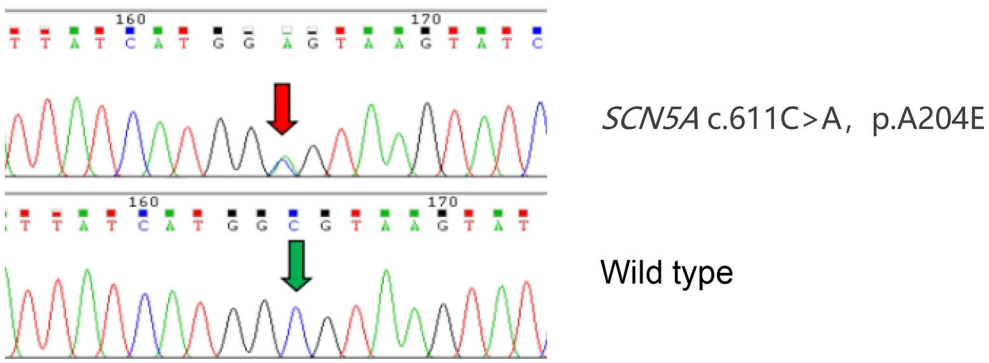

FIGURE 3 | Identification of the SCN5A variant. Sanger sequence SCN5A in a wild-type (WT) subject and proband confirms the presence of the A204E variation. The variant nucleotide residue is indicated by a red arrow. The same nucleotide residue of WT is indicated by a green arrow.

She had previously been healthy and had a normal ECG when she was 13. She died suddenly at the age of 19 years from "shock," following her brother's car accident. In addition to carrying the same three mutations as her mother, Case 2 carried the *PRKAG2* p.D372N variant from her father (II-5).

Case 3

The proband's son (III-7), her second child, was hospitalized with a fractured femur from a car accident at 6 years. At that time, echocardiography showed no abnormality. Three years later, he was hospitalized for nausea and vomiting for 4 days and chest distress for 2 days after catching a cold. An ECG showed multi-source ventricular-accelerated spontaneous rhythm, nodal beats, nodal tachycardia, atrial chaotic tachycardia, ventricular concurrent rhythm, a visible ventricular fusion wave, and ST-T changes. Echocardiography showed an enlarged heart, and the LVEF was 27%. The diagnosis was DCM, arrhythmic cardiomyopathy, and heart failure. A pediatrician diagnosed

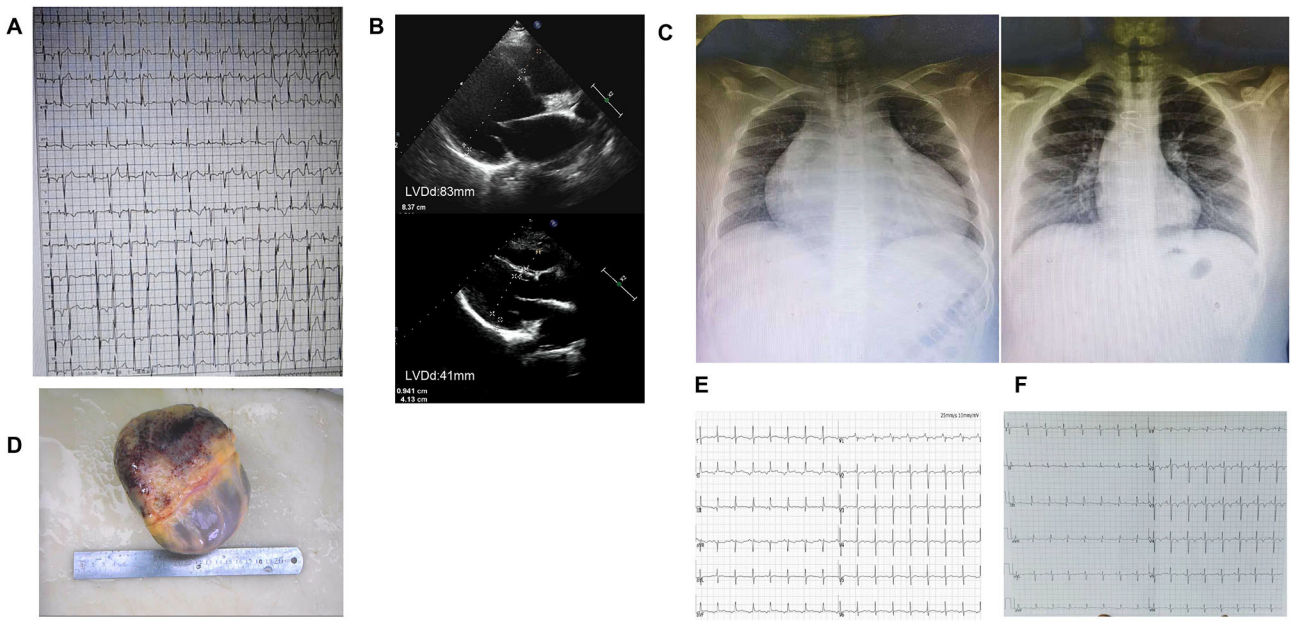

FIGURE 4 | Image of case 3 (III-7). **(A)** ECG before heart transplantation showed frequent ventricular premature contractions with narrow QRS. **(B)** Echocardiogram findings of changes in heart size before and after heart transplantation. **(C)** X-ray findings of changes in heart size before and after heart transplantation. **(D)** The enlarged specimen of the heart. **(E,F)** ECG in the first and second years after heart transplantation,T wave was inverted.

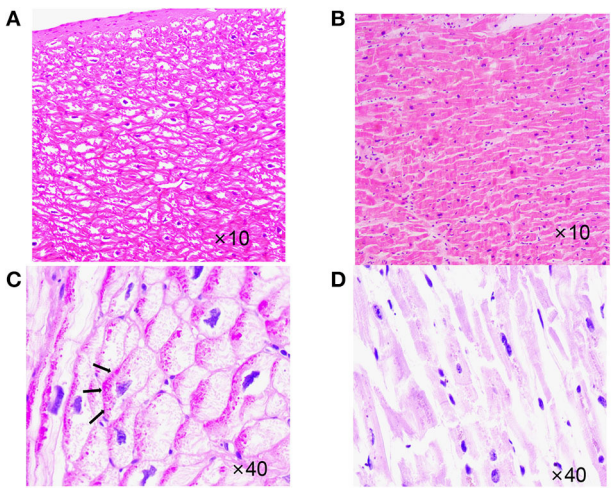

FIGURE 5 | Case 3 (III-7) vs. normal myocardial tissue. **(A)** Hematoxylin-eosin staining (HE staining),cardiomyocyte hypertrophy with large, malformed nuclei,some myocardial cells had vacuolated cytoplasm. **(B)** HE staining,Normal myocardial tissue. **(C)** Periodate-Scherff staining (PAS staining), red PAS staining-positive material in the cytoplasm of cardiomyocytes. Arrows indicate intracellular glycogen accumulation. **(D)** PAS staining, Normal myocardial tissue, red PAS staining-negative.

TABLE 1 | The change of echocardiogram index and BNP of case 3 (III-7).

AGE(year)	LVDd(mm)	IVST(mm)	PWT(mm)	LVEF(%)	BNP (pg/ml)
6	36	6	5	60	
9	54	7.5	6	27	9,930
9.5	83	7	6	24	1,380
10	84	7	6	23	2,040
Heart transplantation					
10	44	9	8	60	123
11	41	9	8	64	12.2
11.5	39	9	8.5	77	6.8

LVDd, Left ventricular end-diastolic diameter; IVST, Interventricular septum thickness; PWT, Posterior wall thickness; LVEF, Left ventricular ejection fraction; BNP, Brain natriuretic peptide.

the boy with end-stage heart failure, and heart transplantation was performed in our hospital when he was 10. His heart was significantly expanded before surgery, and a chest X-ray revealed slight congestion, with a cardiothoracic ratio of 80%. The LVEDD was 83 mm, and the LVEF was 24% (**Figure 4**). His heart was found to have increased marked dilatation of four chambers and thickened ventricular walls, interventricular septum thickness (IVST) 16 mm and posterior wall thickness (PWT) 20 mm. The changes we can see under the microscope are hypertrophy of cardiomyocytes with large and malformed nuclei. Some myocardial cells had vacuolated cytoplasm. The periodate-Scherff staining (PAS staining) found red PAS staining-positive material in the cytoplasm of cardiomyocytes (**Figure 5**).

Re-examination within 2 years after surgery showed a normal heart size; the LVEDD was 41 mm, and the LVEF was 74% (**Table 1**). Two and a half years after heart transplantation, he died suddenly at school, although nothing abnormal was found.

The boy did the gene test before the heart transplantation. He carried multiple mutations, including *SCN5A* p.A204E, *RMND1*

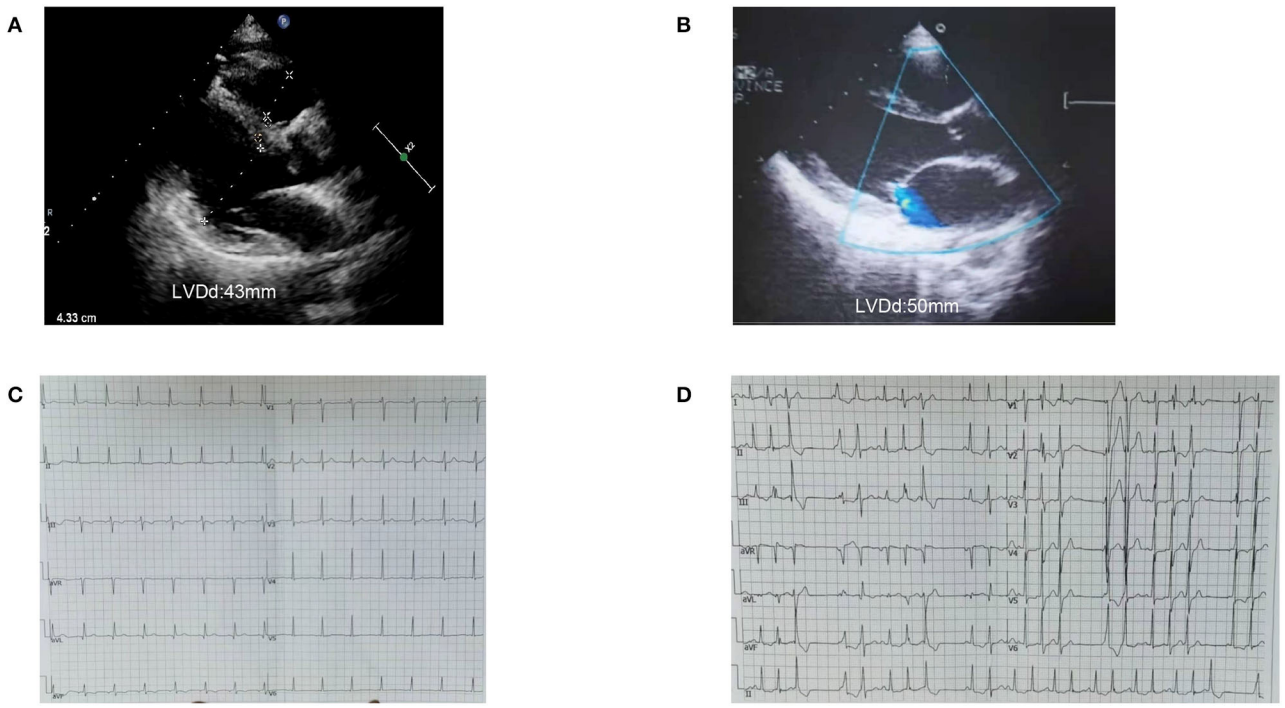

FIGURE 6 | Image of case 4 (II-4) and 5 (III-4). **(A,B)** Case 4 and Case 5 presented a normal left ventricle on echocardiogram. **(C)** ECG of case 4 (II-4) showed atrial rhythm, PR was shorter than 0.12s. **(D)** ECG of case 5 (III-4) showed frequent ventricular premature contractions with narrow QRS.

frame-shift mutation, *MLYCD* p.R412C, *POMT1* p.Y282C, *ACTN2* p.M283V, *TTN* p.I18305T, and *PRKAG2* p.D372N. Except for *SCN5A* p.A204E, the ACMG guidelines considered its pathogenicity to be "likely pathogenicity," and other variants were considered to be of "uncertain significance."

Case 4

The proband's sister (II-4) is an asymptomatic carrier of the *SCN5A* mutation, c.611C>A, p.A204E and is in good health now. Her ECG showed atrial rhythm; the PR was shorter than 0.12 s, and the echocardiogram showed LVEDD 43 mm and LVEF 63% (**Figure 6**). The proband and her sister carried the same three mutations, which were *SCN5A* p.A204E, *TTN* p.I1830T, and *ACTN2* p.M283V, but their clinical phenotypes differed completely.

Case 5

The proband's niece (III-4) had two mutations, which were *SCN5A* p.A204E and *TTN* p.I18305T. She had syncope and was found to have frequent ventricular premature beats with narrow QRS as a teenager. Her heart was borderline enlarged at that time. She took metoprolol for a few years and then stopped. She suffered syncope again when she was 20. The ECG showed a threshold heart rate and polymorphic premature ventricular contractions. Her current heart size is still in the normal range (LVEDD, 50 mm; LVEF, 55%). She is being followed and has good medical compliance. The niece's daughter (IV-1) carries the same gene mutation as her mother. She is still a toddler and has no obvious symptoms.

DISCUSSION AND CONCLUSIONS

Some studies have examined the association between genetic variants and DCM phenotypes (5) which may affect patient clinical prognosis differently. The genetic background of patients with DCM is complex: 7% have a single heterozygous mutation, more than 38% have a compound heterozygous or combined mutation, and 12.8% have three or more mutations (6, 7).

The proband and her sister carried the same three mutations, but her sister did not have heart disease. Various tests showed that her sister's heart function and rhythm were normal. The proband's children developed DCM in childhood. They had identical genetic variants, carrying the same four mutations, which were *SCN5A* p.A204E, *TTN* p.I1830T, *ACTN2* p.M283V, and *PRKAG2* p.D372N. The mutation *PRKAG2* p.D372N was from their father, and the others were from their mother. At the beginning, we thought the father had no family history of related diseases and considered that the variant had little to do with DCM. However, their clinical phenotype was more severe than their mother's, and they both carried *PRKAG2* p.D372N from their father, which might be a modified gene. The *PRKAG2* gene encodes the AMPK γ2 subunit in humans. The mutations of *PRKAG2* can cause *PRKAG2* syndrome. *PRKAG2* syndrome is a rare autosomal dominant disorder characterized by myocardial glycogen storage, myocardial hypertrophy, and ventricular preexcitation. Patients have a high risk of arrhythmias and sudden cardiac death (8). We reviewed the cardiac slides of Case 3 and did PAS staining. Cardiomyocyte hypertrophy and cytoplasmic vacuolization can be seen under the microscope. The vast cytoplasmic glycogen accumulation was confirmed by

a positive PAS stain. Although the ACMG guidelines considered the pathogenicity of the *PRKAG2* variant to be "uncertain significance," these findings further confirmed the *PRKAG2* syndrome. The early onset and severe disease of children might be due to a combination effect of the *SCN5A* p.A204E mutation from their mother and the *PRKAG2* p.D372N mutation from their father.

In the third case, the boy had a heart transplant at the age of 10 years and died suddenly at school 2.5 years postoperatively. No cause of the sudden death was confirmed. Although he had undergone a heart transplant, his paracardial microenvironment might have also been affected. Because the patient did not undergo an endomyocardial biopsy, it was impossible to determine whether he had a chronic rejection reaction. An ECG within 2 years after transplantation showed dynamic changes in T-wave inversion, suggesting ischemia. The underlying molecular genetic mechanisms of the child and environmental factors combined to cause the sudden death. Clinical studies indicate that sudden cardiac death (SCD) is common after heart transplantation. There is no anatomic cause of death in some patients. These deaths are assumed to be primary arrhythmic deaths (9).

It was previously thought that abnormalities in the *SCN5A* gene, which encodes the α subunit of the cardiomyocyte sodium channel, affect the release and utilization of calcium ions in cardiomyocytes *via* the sodium-calcium exchanger, leading to an increased risk for arrhythmias, but with no apparent effect on cardiac anatomy (10). Olson et al. (11) summarized a series of cases with enlarged hearts, pump failure, and a combination of arrhythmias as the main manifestations, and found that *SCN5A* not only caused abnormalities in the electrical activity of the heart but also caused heart enlargement and mechanical abnormalities, which lead to heart failure. The literature suggests that dimers are formed by interactions between the sodium channel α subunits.

Patients with DCM combined with *SCN5A* mutations are prone to ventricular tachycardia, atrioventricular block, and supraventricular tachycardia, and have a higher mortality rate, with life-threatening ventricular arrhythmias occurring at LVEF $< 35\%$, also known as arrhythmogenic DCM (AR-DCM) (12). Patients with AR-DCM should be evaluated carefully and systematically by monitoring for arrhythmia. A family history of ventricular arrhythmias often indicates a poor prognosis and an increased risk for SCD (13). The patients in this family had a variety of clinical presentations, but the ECG waveforms of their premature ventricular beats were very similar. The ECG showed bidirectional ventricular tachycardia, multiple sources of premature ventricular beats, and alternating right and left bundle branch blocks, suggesting that the location of the lesion originated from multiple sites in the Hippo lineage. The main manifestations in patients with the same *SCN5A* c.611C>A mutation (2) are multifocal ectopic Purkinje-related premature contractions (MEPPC) and non-sustained ventricular tachycardia. MEPPC syndrome is caused by mutations in the *SCN5A* gene, and patients with or without DCM are at significantly higher risk for SCD. When we found the *SCN5A* mutation in many family members, we performed analyses with the bio-information software SIFT (14), PolyPhen2 (15), and MutationTaster (16). All predicted that the mutation might be harmful, and the ClinVar database included the mutation as "likely pathogenic." Other mutations at the same amino acid (c.611C>T) are pathogenic and associated with Brugada syndrome, as reported in the Human Gene Mutation Database (17). The mutation was not included in The Genome Aggregation Database (gnomAD) and the genotype and disease co-segregation within the family. Electrophysiological studies showed that Nav1.5-A204E mutant channels exhibited a significant leftward shift of 8mV of the activation curve, leading to a larger hyperpolarized window current when compared to wild type. The ACMG guidelines considered its pathogenicity to be "likely pathogenic." We concluded that this mutation was the genetic basis for the family.

DCM families are characterized by DCM with conduction system abnormalities. The molecular genetic mechanism of DCM is being elucidated with the discovery of more pathogenic genes and their mutated loci. Cardiomyopathy in many families still cannot be explained by the identified pathogenic genes, which implies that there are unknown pathogenic genes in patients with DCM. A monistic etiology still needs to be considered when cardiomyopathy is combined or complicated with arrhythmias. Our current understanding of the genetic factors associated with DCM and their relationship with prognosis remains inadequate, given that genotype–phenotype interactions are the basis for the molecular mechanisms of disease and translational studies. Genetic testing of patients with DCM is important, and guidelines recommend the genetic testing of first-degree relatives of patients with DCM to facilitate earlier identification of potential patients with DCM and early intervention (18). However, available genetic tests for pathogenicity do not yet explain the pathogenesis in all cases, while clinical sequencing currently detects genetic variants in only 40% of patients with DCM (19), and pathogenic mutations that can be confirmed by genotype–phenotype co-segregation currently account for only about 20% of positive genetic results (20).

In conclusion, the *SCN5A* mutation with multiple DCM-related gene mutations caused a variety of phenotypes, including DCM, arrhythmia, and sudden death in this family. The clinical manifestations of the family with the same mutation are diverse. The early and severe onset in children may be the result of a combination of *SCN5A* and *PRKAG2* mutations. This report shows that a similar phenotype caused by the same variant in a different ethnic background is strong evidence of the variant's DCM and arrhythmic causality. In addition, it broadens the spectrum of mutations in the *SCN5A* and *PRKAG2* genes for possible combined pathogenesis. The dosage effect of the two mutations between the genotype and the phenotype needs further research. Gene diagnosis allows the early detection of patients with subclinical DCM and facilitates early interventions to improve a prognosis, which can be more helpful in the diagnosis and research of DCM.

DATA AVAILABILITY STATEMENT

The original contributions presented in the study are included in the article/supplementary material, further inquiries can be directed to the corresponding author.

ETHICS STATEMENT

Written informed consent was obtained from the individual(s), and minor(s)' legal guardian/next of kin, for the publication of any potentially identifiable images or data included in this article.

AUTHOR CONTRIBUTIONS

All authors listed have made a substantial, direct, and intellectual contribution to the work and approved it for publication.

ACKNOWLEDGMENTS

We would like to thank Prof. Dan Hu from Department of Cardiology, Renmin Hospital of Wuhan University, Wuhan, China for the suggestion to check the pathogenicity of the PRKAG2 mutation, Prof. Qiji Liu from Department of Genetics, Shandong University, Jinan, China for the genetic guidance, and Prof. Qing Sun and Min Yang from Department of Pathology, the First Affiliated Hospital of Shandong First Medical University and Shandong Provincial Qianfoshan Hospital, Jinan, China for the pathological diagnosis.

REFERENCES

1. Hershberger RE, Hedges DJ, Morales A. Dilated cardiomyopathy: the complexity of a diverse genetic architecture. *Nat Rev Cardiol.* (2013) 10:531–47. doi: 10.1038/nrcardio.2013.105
2. Doisne N, Waldmann V, Redheuil A, Waintraub X, Fressart V, Ader F, et al. A novel gain-of-function mutation in SCN5A responsible for multifocal ectopic Purkinje-related premature contractions. *Hum Mutat.* (2020) 41:850–9. doi: 10.1002/humu.23981
3. Ackerman MJ, Priori SG, Willems S, Berul C, Brugada R, Calkins H, et al. HRS/EHRA expert consensus statement on the state of genetic testing for the channelopathies and cardiomyopathies this document was developed as a partnership between the Heart Rhythm Society (HRS) and the European Heart Rhythm Association (EHRA). *Heart Rhythm.* (2011) 8:1308–39. doi: 10.1016/j.hrthm
4. Richards S, Aziz N, Bale S, Bick D, Das S, Gastier-Foster J, et al. ACMG Laboratory Quality Assurance Committee. Standards and guidelines for the interpretation of sequence variants: a joint consensus recommendation of the American College of medical genetics and genomics and the association for molecular pathology. *Genet Med.* (2015) 17:405–24. doi: 10.1038/gim.2015.30
5. Pinto YM, Elliott PM, Arbustini E, Adler Y, Anastasakis A, Böhm M, et al. Proposal for a revised definition of dilated cardiomyopathy, hypokinetic non-dilated cardiomyopathy, and its implications for clinical practice: a position statement of the ESC working group on myocardial and pericardial diseases. *Eur Heart J.* (2016) 37:1850–8. doi: 10.1093/eurheartj/ehv727
6. Akinrinade O, Ollila L, Vattulainen S, Tallila J, Gentile M, Salmenperä P, et al. Genetics and genotype-phenotype correlations in Finnish patients with dilated cardiomyopathy. *Eur Heart J.* (2015) 36:2327–37. doi: 10.1093/eurheartj/ehv253
7. Haas J, Frese KS, Peil B, Kloos W, Keller A, Nietsch R, et al. Atlas of the clinical genetics of human dilated cardiomyopathy. *Eur Heart J.* (2015) 36:1123–35a. doi: 10.1093/eurheartj/ehu301
8. Hu D, Hu D, Liu L, Barr D, Liu Y, Balderrabano-Saucedo N, et al. Identification, clinical manifestation and structural mechanisms of mutations in AMPK associated cardiac glycogen storage disease. *EBioMedicine.* (2020) 54:102723. doi: 10.1016/j.ebiom.2020.102723
9. Chantranuwat C, Blakey JD, Kobashigawa JA, Moriguchi JD, Laks H, Vassilakis ME, et al. Sudden, unexpected death in cardiac transplant recipients: an autopsy study. *J Heart Lung Transplant.* (2004) 23:683–9. doi: 10.1016/s1053-2498(03)00295-x
10. McNally EM, Mestroni L. Dilated cardiomyopathy: genetic determinants and mechanisms. *Circ Res.* (2017) 121:731–48. doi: 10.1161/CIRCRESAHA.116.309396
11. Olson TM, Michels VV, Ballew JD, Reyna SP, Karst ML, Herron KJ, et al. Sodium channel mutations and susceptibility to heart failure and atrial fibrillation. *JAMA.* (2005) 293:447–54. doi: 10.1001/jama.293.4.447
12. Towbin JA, McKenna WJ, Abrams DJ, Ackerman MJ, Calkins H, Darrieux FCC, et al. 2019 HRS expert consensus statement on evaluation, risk stratification, and management of arrhythmogenic cardiomyopathy. *Heart Rhythm.* (2019) 16:e301–72. doi: 10.1016/j.hrthm.2019.05.007
13. Japp AG, Gulati A, Cook SA, Cowie MR, Prasad SK. the diagnosis and evaluation of dilated cardiomyopathy. *J Am Coll Cardiol.* (2016) 67:2996–3010. doi: 10.1016/j.jacc.2016.03.590
14. Kumar P, Henikoff S, Ng PC. Predicting the effects of coding non-synonymous variants on protein function using the SIFT algorithm. *Nat Protoc.* (2009) 4:1073–81. doi: 10.1038/nprot.2009.86
15. Adzhubei IA, Schmidt S, Peshkin L, Ramensky VE, Gerasimova A, Bork P, et al. A method and server for predicting damaging missense mutations. *Nat Methods.* (2010) 7:248–9. doi: 10.1038/nmeth0410-248
16. Schwarz JM, Rödelsperger C, Schuelke M, Seelow D. Mutation taster evaluates disease-causing potential of sequence alterations. *Nat Methods.* (2010) 7:575–6. doi: 10.1038/nmeth0810-575
17. Kapplinger JD, Tester DJ, Alders M, Benito B, Berthet M, Brugada J, et al. An international compendium of mutations in the SCN5A-encoded cardiac sodium channel in patients referred for Brugada syndrome genetic testing. *Heart Rhythm.* (2010) 7:33–46. doi: 10.1016/j.hrthm.2009.09.069
18. Hershberger RE, Givertz MM, Ho CY, Judge DP, Kantor PF, McBride KL, et al. Genetic evaluation of cardiomyopathy-a heart failure society of America practice guideline. *J Card Fail.* (2018) 24:281–302. doi: 10.1016/j.cardfail.2018.03.004
19. Pugh TJ, Kelly MA, Gowrisankar S, Hynes E, Seidman MA, Baxter SM, et al. The landscape of genetic variation in dilated cardiomyopathy as surveyed by clinical DNA sequencing. *Genet Med.* (2014) 16:601–8. doi: 10.1038/gim.2013.204
20. Zimmerman RS, Cox S, Lakdawala NK, Cirino A, Mancini-DiNardo D, Clark E, et al. A novel custom resequencing array for dilated cardiomyopathy. *Genet Med.* (2010) 12:268–78. doi: 10.1097/GIM.0b013e3181d6f7c0

Conflict of Interest: The authors declare that the research was conducted in the absence of any commercial or financial relationships that could be construed as a potential conflict of interest.

frontiers | Frontiers in Cardiovascular Medicine

CASE REPORT
published: 20 May 2022
doi: 10.3389/fcvm.2022.842282

Case Report: Danon Disease: Six Family Members and Literature Review

*Yuanyuan Wang, Meixue Jia, Yingjie Guo, Ting Zhang and Bin Ning**

Department of Cardiology, People's Hospital of Fuyang, Fuyang, China

Danon disease is a rare X-linked dominant genetic disorder that manifests with a clinical triad of cardiomyopathy, skeletal myopathy, and intellectual disability. It is caused by mutations in the lysosome-associated membrane 2 (LAMP2) gene. We report one case of Danon disease and his family members, characterized by ventricular pre-excitation, ventricular hypertrophy, abnormal muscle enzymes, and aberrant liver function. All the patients were confirmed to have Danon disease through genetic screening. Relevant literature was reviewed as a reference for the diagnosis and treatment of the disease.

Keywords: case report, Danon disease, lysosome-associated membrane 2, ventricular hypertrophy, pre-excitation, liver injury

OPEN ACCESS

Edited by:
Dragos Cretoiu,
Carol Davila University of Medicine and Pharmacy, Romania

Reviewed by:
Mona Mostafa Rayan,
Ain Shams University, Egypt
Elena V. Zaklyazminskaya,
Russian National Research Center of Surgery Named After B. V. Petrovsky, Russia
Antonio Toscano,
University of Messina, Italy

***Correspondence:**
Bin Ning
muyi20180726@163.com

Specialty section:
This article was submitted to General Cardiovascular Medicine, a section of the journal Frontiers in Cardiovascular Medicine

Received: *23 December 2021*
Accepted: *08 April 2022*
Published: *20 May 2022*

Citation:
Wang Y, Jia M, Guo Y, Zhang T and Ning B (2022) Case Report: Danon Disease: Six Family Members and Literature Review. Front. Cardiovasc. Med. 9:842282. doi: 10.3389/fcvm.2022.842282

INTRODUCTION

Danon disease (DD; MIM#300257) refers to a rare lysosomal storage disease with various manifestations. Male patients display severe cardiomyopathy, skeletal myopathy, and developmental delay, while females show cardiac insufficiency and arrhythmia (1). Moreover, retinopathy in pigment epithelium, lens damage and unusual electroretinograms are also reported (2). DD was first described in 1981, in male members of a family who complained of limb weakness but were found with myocardial hypertrophy (3). The biopsy of skeletal muscle revealed vacuole bodies in the cytoplasm which contained autophagic material and glycogen. Nishino et al. (4) confirmed mutation of the lysosome-associated membrane 2 (LAMP2) gene (Xq24-q25) and the subsequent loss of LAMP-2 protein in these patients.

The pathology of DD includes vacuoles containing autophagic substances and the accumulation of massive glycogen in cardiomyocytes and skeletal muscle cells (1). Patients with DD display prominent ventricular hypertrophy and dilatation, with the former arising more in males. Female patients usually evince electrical conduction anomalies such as ventricular pre-excitation (5). Male patients with X-linked dominant inheritance pass the tendency to daughters, but not sons. Therefore, more females than males theoretically suffer from DD, although for the atypical symptoms, most cases are not identified in females. Mild cardiac disorders will develop swiftly into end-stage heart failure in the third decade of life unless the patient receives heart transplantation (6).

The present study reports one case of DD and his family members within three generations (see **Supplementary Figure 1** for the comprehensive pedigree). To provide a reference for clinical practice, we searched more than 15 years of medical history and relevant literature in PubMed to review the manifestations, causes, diagnosis, therapy, and prognosis of DD.

METHODS

The six patients were collected from 2003 to 2021 at Fuyang People's Hospital in the province of Anhui, China. All the medicines, medical procedures, and mechanotherapy conformed to the recommendation of the Chinese Guidelines for Diagnosis and Treatment of Heart Failure (2018) and Atrial Fibrillation: Current Understanding and Treatment Recommendations—2018 (7, 8).

REPORT ON THE CASE AND FAMILY MEMBERS

Case (III4)

The proband (Pt 1) was a male aged 16 years who was admitted to hospital for palpitation. The electrocardiogram (ECG) showed overt ventricular pre-excitation with 74 ms of PR interval, > 2.5 mV of R_{V5}, > 4.0 mV of $R_{V5} + S_{Vl}$, > 1.5 mV of R_I, > 1.2 mV of R_{aVL}, and > 2.0 mV of R_{aVF}, which suggested a hypertrophic remodeling of the left ventricle. Secondary ST-T changes were present in all leads and Delta-waves were detected in II and III leads. The narrow QRS tachycardia indicated atrioventricular reentrant tachycardia (**Figures 1A,B**). The serum concentrations of creatine kinase (1129.6 U/L), alanine transferase, and aspartate aminotransferase were higher than normal. Echocardiography detected hypertrophy in the ventricular septum and left ventricular wall (**Supplementary Figure 2**). A diffused thickness of the left ventricle and multiple patchy delayed enhancements were observed on the magnetic resonance imaging (MRI, **Supplementary Figure 3**). Pt 1 received radiofrequency ablation (RFA) of multiple atrioventricular accessories. After the treatment, the pre-excitations in the ECG disappeared and the PR interval was restored, but the hypertrophic remodeling of the left ventricle remained (**Figure 1C**). The patient has been taking metoprolol tartrate (25 mg/d) and benazepril (5 mg/d) orally. Motor function and muscle strength are normal. A genetic test revealed a hemizygous mutation in the LAMP2 gene (LAMP2: c.963G > A: **Figure 2**). Throughout the treatment period, the patient showed a quite good compliance and tolerance and was satisfied with the curative effect. During the subsequent 2 years of follow-up, echocardiography still indicated a hypertrophic wall of the left ventricle, and the serum creatine kinase remained abnormal (1,432 U/L, 2 months after the treatment). The patient reported average muscular strength, but low performance in primary school (not verified by professional tests). There was no indication of heart failure in the patient.

Family Member 1 (II4)

Pt 1's mother (Pt 2), aged 38 years, was repeatedly admitted to hospital due to palpitation, chest tightness, short of breath or low endurance to activity. Atrioventricular reentrant tachycardia and hypertrophic cardiomyopathy (HCM) was diagnosed. The electrophysiological examination suggested a concealed accessory pathway in the right anterior interventricular septum. Echocardiography and MRI revealed a thick interventricular septum and posterior wall in the left ventricle (**Table 1** and **Supplementary Figures 4, 5**). From 2003 to 2021, the patient's condition aggravated bit by bit, successively developing dilated cardiomyopathy, complete left bundle branch block (CLBBB), ventricular premature beats with a QRS wave width of 150 ms (**Figures 3A,B**), and paroxysmal atrial fibrillation (**Figure 3C**). The cardiac function attenuated to New York Heart Association (NYHA) functional classification III. Transesophageal echoaortography revealed left atrial appendage thrombosis. After 3 months of regular anticoagulation therapy, the patient received RFA (**Supplementary Figure 6**), which recovered sinus rhythm (**Figure 3D**) and improved the cardiac function to NYHA II. However, her condition worsened again soon after the procedure, with an enlarged heart, moderate pulmonary hypertension, right heart failure, and liver failure. The cardiac function was at NYHA III-IV, which improved to NYHA II after medication treatment, but this improvement also lasted for a short time. The patient was soon barely able to get out of bed and the ECG showed sinus tachycardia and CLBBB with a QRS wave width of 220 ms (**Figure 3E**). Multiple organ failure appeared. Standard medication treatment failed to alleviate the situation and the blood pressure of the patient fluctuated at 75–85/50–60 mmHg. Therefore, a cardiac resynchronization therapy defibrillator (CRT-D) was implanted (**Supplementary Figure 7**). The post-operative ECG showed sinus rhythm and biventricular pacing with 190 ms of QRS wave width (**Figure 3F**). The blood pressure stayed above 95/65 mmHg, with the clinical symptoms overtly improved. Electromyogram (EMG) revealed no abnormality all the way. The patient also received funduscopy examination which found normal cup to disk ratio and no hypopigmentation. The medication of the patient included oral metoprolol (23.75 mg/d), spironolactone (20 mg/d), furosemide (20 mg/d) and benazepril (5 mg/d), which was later replaced by valsartan (50 mg/d). At the same time, amiodarone (0.2 g/d) and rivaroxaban (15 mg/d) were given to manage arrhythmia and hypercoagulability, respectively. During the treatment, the patient consistently complained of fatigue, and she remains under follow-up as of this writing. The genetic testing unveiled a similar mutation in LAMP2, as in Pt 1 (**Figure 2**).

Family Member 2 (II2)

Pt 3 was the elder sister of Pt 2, aged 40 years, and was hospitalized twice for chest tightness. The coronary angiography showed coronary atherosclerosis and coronary myocardial bridge. The ECG indicated atrial premature contractions, ventricular premature contractions, and poor R wave progression. The echocardiography showed enlargement of both atriums, but normal ventricular wall thickness (**Supplementary Figure 8**). Heart MRI showed diffuse late gadolinium enhancement in the subendocardium and midmyocardium of the left ventricular wall (**Supplementary Figure 9**). The EMG was normal for this patient. The medication consisted of oral metoprolol (50 mg/d), furosemide (20 mg/d), spironolactone (20 mg/d), warfarin (2.5 mg/d) and valsartan (50 mg/d). The genetic test revealed the similar mutation of LAMP2 as in Pt 1. At present, Pt 3 performs normal daily activities competently. The most recent evaluation showed NYHA I cardiac function.

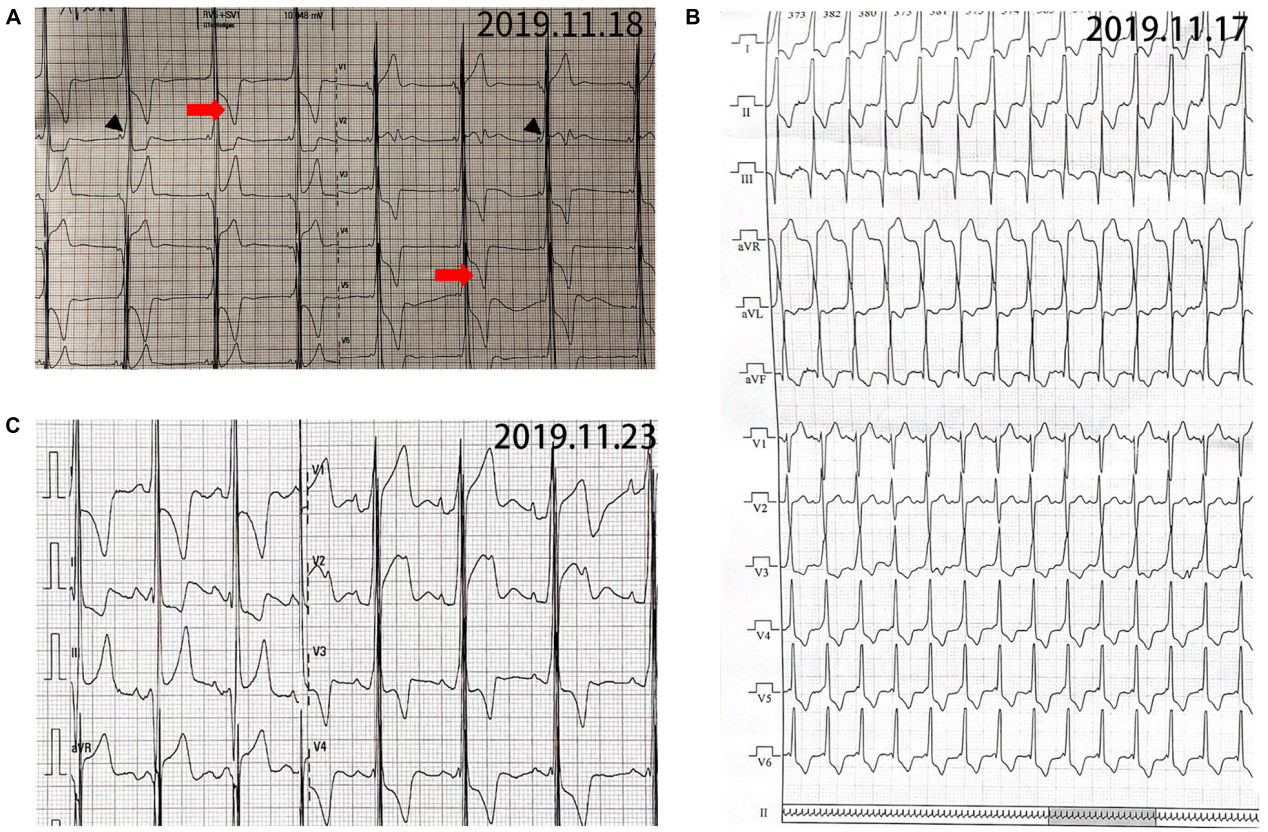

FIGURE 1 | Electrocardiogram (ECG) of patient 1. **(A)** ECG before operation showing sinus rhythm and 74 ms of PR interval. Delta-wave (black arrowhead) was present in II and III leads. RV_5 > 2.5 mV and RV_5 + SV_I > 4.0 mV in precordial leads. RI > 1.5 mv, RaVL > 1.2 mv, RaVF > 2.0 mv with secondary ST-T changes (red arrow). **(B)** Narrow QRS tachycardia indicating atrioventricular reentrant tachycardia (AVRT). **(C)** ECG after operation showing sinus rhythm and 144 ms of PR interval. No δwave presented, but the hypertrophic remodeling of left ventricle still existed.

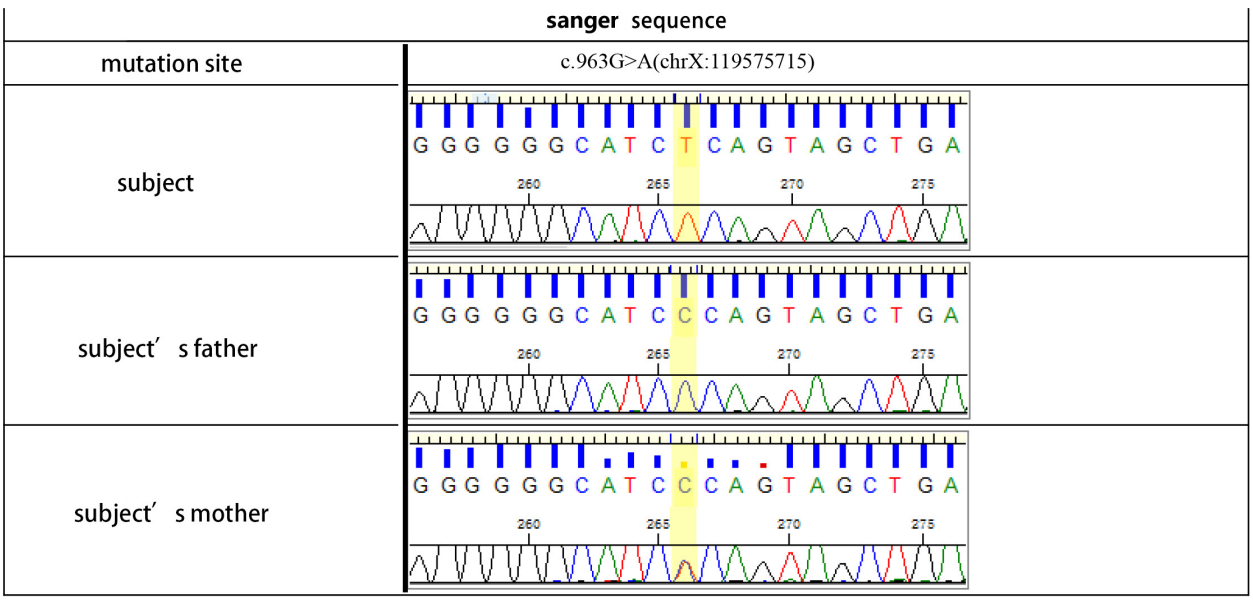

FIGURE 2 | Gene sequence of the III4 (Pt 1, subject), II3 (subject's father) and II4 (Pt 2, subject's mother).

TABLE 1 | Echocardiograph indexes of Pt 2.

	Echocardiograph indexes, mm							
	LA	**LV**	**RA**	**RV**	**IVS**	**LVPW**	**EF (%)**	**Note**
2003/12/22	31.2	42.4	Normal	Normal	13.5	PWT13.5, AWT14.0, SWT13.8	60	
2012/5/23	36	46.2	Normal	Normal	10.4	PWT10, SWT11.9	59	Mild mitral and tricuspid regurgitation
2014/8/17	32	46	31	17	15	13	50	
2015/3/8	33	40	30	18	14	12	52	
2015/11/21	33	45	30	16	13	13	56	Mild mitral and tricuspid regurgitation
2017/11/21	34	46	30	16	11	10	59	Mild mitral regurgitation
2019/3/22	36	45	34	20	10	10	51	Mild tricuspid regurgitation; mild pulmonary artery hypertension
2020/6/28	36	56	34	22	7	8	41	Mild mitral regurgitation
2020/9/25	40	59	Normal	Normal	13	11	31	Mild mitral regurgitation; Left atrial appendage thrombosis
2021/1/4	42	57	Normal	Normal	13	11	24	Mild mitral and tricuspid regurgitation; Left auricular hypercoagulability; mild pulmonary artery hypertension
2021/6/29	40	55	42	38	10	8	34	Mild mitral and tricuspid regurgitation; Moderate pulmonary artery hypertension (55 mmHg)
2021/8/16	42	59	Normal	Normal	13	11	22	Mild mitral regurgitation; Moderate tricuspid regurgitation; mild pulmonary artery hypertension (41 mmHg)

EF, ejection fraction; IVS, interventricular septum thickness; LA, left atrium; LV, left ventricle; LWPW, left ventricular posterior wall thickness; RA, right atrium; RV, right ventricle.

Family Member 3 (II6)

Pt 4 was the younger sister of Pt 2, without a medical record. The echocardiography found no anomaly. ECG showed sinus rhythm and aberrant Q wave on the I and aVL leads. The genetic test revealed that she and her two sons held the similar mutation of LAMP2 as in Pt 1. During the follow-up, the patient reported a normal life.

Family Member 4 (III5)

Pt 5, aged 8 years, was one of the sons of Pt 4. The genetic test indicated the mutation of LAMP2 as in Pt 1. No clinical manifestation was detected except higher serum concentrations of creatine kinase, lactate dehydrogenase, α-hydroxybutyrate dehydrogenase, alanine transferase, and aspartate aminotransferase. The ECG and echocardiograph suggested hypertrophic ventricles. The follow-up found no abnormity in the patient.

Family member 5Pt 6, aged 2 years, was another son of Pt 4. The genetic test revealed the similar mutation in LAMP2 as for Pt. 1, and the echocardiograph showed a thickened ventricular wall. The patient remained healthy during the follow-up.

DISCUSSION

Limited studies have shown a 4–6% rate of DD in pediatric patients with HCM, 0.7–4% in adults with HCM, 6–8% in adults with symmetric HCM, 17–30% in LV hypertrophy with pre-excitation, and 33% in HCM with vacuolar cardiomyopathy (9–11). All patients with DD develop cardiomyopathy, with males more prone to HCM, and females to HCM or dilated cardiomyopathy. In addition, most female patients present with mild symptoms and later onset compared with males (6). Electrocardiographic anomaly exists in 86–100% of male patients with DD (12), which is in accord with the present results that 5 patients of 6 evinced significant ECG disorders. Therefore, HCM accompanied with pre-excitation syndrome in a young male strongly implies DD. The underlying mechanisms remain debated, but may be associated with myocardial hypertrophy, defective autophagy, or microscopic atrioventricular connection (13).

Atrioventricular bundle passage could be a sign of DD, and 35–50% of patients with DD suffering from heart block are in need of pacemaker implantation (1). Moreover, frequent atrial fibrillation (AF), flutter, and life-threatening ventricular arrhythmias appear in 60% of DD cases (14). AF may aggravate heart failure, so when confirmed, should be watched for closely. RFA for cases of DD may not be successful due to resistance of diffuse fibrosis (1). In the present study, both Pt1 and Pt2 benefited from RFA, indicating that the fibrosis may not have been severe.

The left ventricular hypertrophy develops into dilated cardiomyopathy (DCM) in 10–33% of DD cases (6). This condition tends to quickly worsen to heart failure (15). Cardiac MRI, especially the T1 mapping and extracellular volume measurement, helps the diagnosis and prognostic assessment of DD (15, 16). Myocardial fibrosis signs in MRI determine the necessity of implantable cardioverter-defibrillator installation or heart transplantation (16).

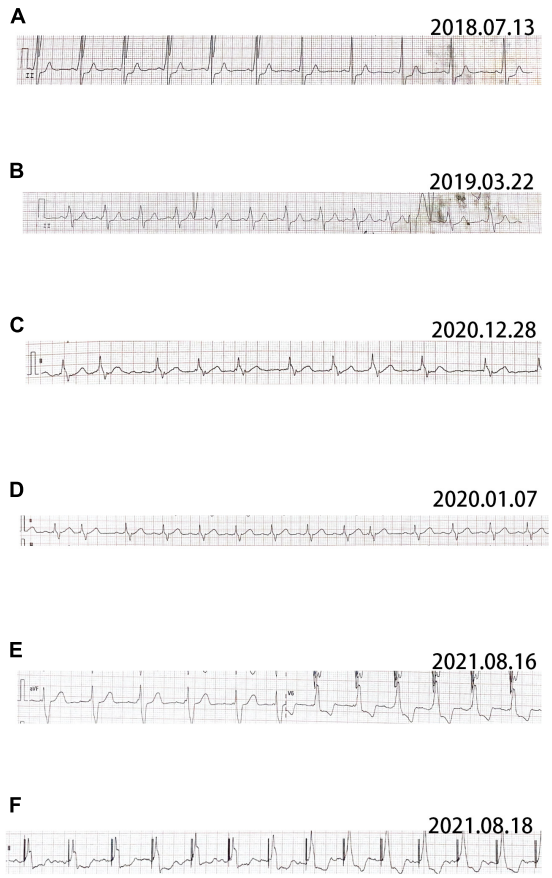

FIGURE 3 | ECG of patient 2. **(A)** The earliest ECG of patient showing sinus rhythm and complete left bundle branch block (CLBBB) with the width of QRS wave of 150 ms. **(B)** Sinus rhythm, CLBBB and frequent ventricular premature beat. **(C)** Atrial fibrillation and CLBBB. **(D)** Recovered sinus rhythm after radiofrequency ablation. **(E)** The pre-operative ECG showing sinus rhythm, CLBBB and 220 ms of QRS wave width. **(F)** Post-operative ECG showing sinus rhythm and 190 ms of QRS wave width.

Cardiac embolic stroke and ischemic thromboembolic stroke usually arise in DD (17) indicating a poor prognosis, so the anticoagulation therapy should be arranged when representative signs appear in MRI. The situation of Pt 2 in our study was relatively complicated with the onset of heart failure and left atrial appendage thrombosis. However, the anticoagulation treatment still apparently improved the condition and allowed the patient the opportunity to get RFA.

Skeletal muscle lesions are present in 80–100% of male patients with DD, which in general is mild, but turns severe occasionally and is always accompanied with 3-to-35 times higher serum creatine kinase activity (18). Females are relatively free from skeletal muscle injury and aberrant creatine kinase (to twice higher than normal). Moreover, hepatomegaly, hepatopathy, and elevated liver enzymes in childhood appear frequently in DD (1). In our results, the motor function and muscle strength of the six patents were normal, but the serum creatine kinase content become higher in Pt1 and Pt5 indicating the possible damage of skeletal muscles.

At least 110 types of mutations have been reported in the LAMP2 gene, of which c.926G > A is the commonest. Most mutations were non-functional (i.e., insignificant or a frameshift lack/insert) or splicing. Missense mutation, recombination, or synonymous substitution are rare (6). It has been reported that the eight mutations of LAMP2 accounts for the specific manifestations of DD including microdeletions, insertions, non-sense point mutations, intronic point mutations and 10-bp deletion (19). In the present study, the c.963G > A mutation was a novel discovery.

As for the treatment of DD, the ultimate strategy should be heart transplantation, especially for the female carriers (18, 20). Before the operation, a left ventricular assist device should be applied at a right time as it is crucial for maintaining the residual cardiac capacity. To avoid sudden death, cardioverter defibrillator is also a useful treatment, for which the subcutaneous is more impressive than intravenous implantation in ending ventricular tachycardia (21). With the growing utilization of molecular genetic tests in cardiomyopathy of unknown origin, more DD cases will be recognized. However, for now, genetic and protein therapies remain unavailable (22, 23).

In the present study, the DD arose earlier in the males. As seen in Pt 6, the onset age was just 2 years. All the males showed typical clinical manifestations such as LVH, and one developed Wolff-Parkinson-White syndrome. Thus, in a youth with HCM and ventricular pre-excitation, DD should be strongly considered. Liver dysfunction and skeletal muscular impairment were also more common in males in the present study; the females showed diversified cardiac manifestations, and two developed heart failure during follow-up. The definitive gender difference implies that DD occurs later in females than in males, at the age of about 30 years. The two female patients in our study displayed atrial arrhythmias at the beginning, which exacerbated the heart failure significantly. The gender-associated difference in clinical manifestations may be due to estrogen, which promotes autophagy and a lysosome pathway in multiple cells (24).

Regarding diagnosis, a family genetic screen and carrier deduction based on a genetic map should be conducted. Moreover, the cardiac MRI of the three patients in the present study identified delayed enhancement in the myocardium and high T1-mapping, which is valuable for the differential diagnosis of patients with HCM.

If clinical manifestations are not present, a close follow-up is necessary. With the advent of Wolff-Parkinson-White syndrome or atrial arrhythmias, medication or RFA should be considered. Malignant ventricular arrhythmia demands the installation of an implantable cardioverter-defibrillator. If the condition has developed into heart failure, active medication treatment should be effective. For patients who are insensitive to medication, an active CRT-D implantation is suggested.

It has been mentioned that some DD cases develop abnormalities in cerebral vessels (25), which, however, was not examined in our case series. This is a limitation of the study.

Overall, the auxiliary device implantation at an early stage would improve heart function or defer the exacerbation of cardiac performance in patients of DD. However, all these

treatments are only palliative or delay the deterioration of the condition. Without heart transplantation or future gene therapy, most patients will die within the ages of 40–50 years. Unfortunately, although we have recommended patient 2 to make an appointment for HTx, they refused to follow the suggestion for economic reasons or the lack of understanding on severity of the disease.

DATA AVAILABILITY STATEMENT

The original contributions presented in the study are included in the article/**Supplementary Material**, further inquiries can be directed to the corresponding author/s.

ETHICS STATEMENT

The studies involving human participants were reviewed and approved by the Ethics Committee of the People's Hospital of Fuyang. Written informed consent to participate in this study was provided by the participants' legal guardian/next of kin. Written informed consent was obtained from the individual(s) for the publication of any potentially identifiable images or data included in this article.

AUTHOR CONTRIBUTIONS

BN: conceptualization, supervision, and writing—review and editing. YW: data curation and writing—original draft. MJ: data curation and formal analysis. YG: formal analysis and supervision. TZ: data curation. All authors read and approved the final manuscript.

ACKNOWLEDGMENTS

We would like to thank Wenjun Li for echocardiograph examinations and Yang Zhang for CT/MRI checks.

SUPPLEMENTARY MATERIAL

The Supplementary Material for this article can be found online at: https://www.frontiersin.org/articles/10.3389/fcvm.2022.842282/full#supplementary-material

REFERENCES

1. Cenacchi G, Papa V, Pegoraro V, Marozzo R, Fanin M, Angelini C. Review: Danon disease: review of natural history and recent advances. *Neuropathol Appl Neurobiol.* (2020) 46:303–22. doi: 10.1111/nan.12587
2. Fukushima M, Inoue T, Miyai T, Obata R. Retinal dystrophy associated with Danon disease and pathogenic mechanism through LAMP2-mutated retinal pigment epithelium. *Eur J Ophthalmol.* (2020) 30:570–8. doi: 10.1177/1120672119832183
3. Danon MJ, Oh SJ, DiMauro S, Manaligod JR, Eastwood A, Naidu S, et al. Lysosomal glycogen storage disease with normal acid maltase. *Neurology.* (1981) 31:51–7. doi: 10.1212/wnl.31.1.51
4. Nishino I, Fu J, Tanji K, Yamada T, Shimojo S, Koori T, et al. Primary LAMP-2 deficiency causes X-linked vacuolar cardiomyopathy and myopathy (Danon disease). *Nature.* (2000) 406:906–10. doi: 10.1038/35022604
5. Maron BJ, Roberts WC, Arad M, Haas TS, Spirito P, Wright GB, et al. Clinical outcome and phenotypic expression in LAMP2 cardiomyopathy. *JAMA.* (2009) 301:1253–9. doi: 10.1001/jama.2009.371
6. Boucek D, Jirikowic J, Taylor M. Natural history of Danon disease. *Genet Med.* (2011) 13:563–8. doi: 10.1097/GIM.0b013e31820ad795
7. Yang J, Wang H, Chai K. Highlights of the guidelines for diagnosis and treatment of heart failure in China in 2018. *Chin J Cardiovasc Res.* (2018) 16:1057–60. doi: 10.3969/j.issn.1672-5301.2018.12.001
8. Huang C, Zhang S, Huang D, Hua W. Atrial fibrillation:current understanding and treatment recommendations-2018. *Chin J Cardiac Pacing Electrophysiol.* (2018) 32:315–68.
9. Hayashi T, Tanimoto K, Hirayama-Yamada K, Tsuda E, Ayusawa M, Nunoda S, et al. Genetic background of Japanese patients with pediatric hypertrophic and restrictive cardiomyopathy. *J Hum Genet.* (2018) 63:989–96. doi: 10.1038/s10038-018-0479-y
10. Liu Y, Wang F, Chen X, Liang Y, Deng H, Liao H, et al. Fasciculoventricular Pathways Responsible for Ventricular Preexcitation in Patients With Danon Disease. *Circulat Arrhythmia Electrophysiol.* (2018) 11:e006704. doi: 10.1161/circep.118.006704
11. Liu Y, Chen X, Wang F, Liang Y, Deng H, Liao H, et al. Prevalence and clinical characteristics of Danon disease among patients with left ventricular hypertrophy and concomitant electrocardiographic preexcitation. *Mol Genet Genomic Med.* (2019) 7:e638. doi: 10.1002/mgg3.638
12. D'Souza RS, Levandowski C, Slavov D, Graw SL, Allen LA, Adler E, et al. Danon disease: clinical features, evaluation, and management. *Circ Heart Fail.* (2014) 7:843–9. doi: 10.1161/circheartfailure.114.001105
13. Arad M, Moskowitz IP, Patel VV, Ahmad F, Perez-Atayde AR, Sawyer DB, et al. Transgenic mice overexpressing mutant PRKAG2 define the cause of Wolff-Parkinson-White syndrome in glycogen storage cardiomyopathy. *Circulation.* (2003) 107:2850–6. doi: 10.1161/01.Cir.0000075270.13497.2b
14. Guo S, Zhou L, Wang R, Lv Z, Xu H, Han B, et al. Danon disease: two patients with atrial fibrillation in a single family and review of the literature. *Exp Ther Med.* (2019) 18:1527–32. doi: 10.3892/etm.2019.7777
15. Samad F, Jain R, Jan MF, Sulemanjee NZ, Menaria P, Kalvin L, et al. Malignant cardiac phenotypic expression of Danon disease (LAMP2 cardiomyopathy). *Int J Cardiol.* (2017) 245:201–6. doi: 10.1016/j.ijcard.2017.06.031
16. Rigolli M, Kahn AM, Brambatti M, Contijoch FJ, Adler. Cardiac Magnetic Resonance Imaging in Danon Disease Cardiomyopathy. *JACC Cardiovasc Imaging.* (2021) 14:514–6. doi: 10.1016/j.jcmg.2020.08.011
17. Tsuda T, Shillingford AJ, Vetter J, Kandula V, Jain B, Temple J. Transient Ischemic Attack and Ischemic Stroke in Danon Disease with Formation of Left Ventricular Apical Thrombus despite Normal Systolic Function. *Case Rep Pediatr.* (2017) 2017:6576382. doi: 10.1155/2017/6576382
18. Miani D, Taylor M, Mestroni L, D'Aurizio F, Finato N, Fanin M, et al. Sudden death associated with danon disease in women. *Am J Cardiol.* (2012) 109:406–11. doi: 10.1016/j.amjcard.2011.09.024
19. Gill I, Kim JH, Moon JH, Yong JK, Kim NS. Identification of LAMP2 mutations in early-onset hypertrophic cardiomyopathy by targeted exome sequencing. *J Genet Med.* (2018) 15:87–91. doi: 10.5734/JGM.2018.15.2.87
20. Lotan D, Salazar-Mendiguchía J, Mogensen J, Rathore F, Anastasakis A, Kaski J, et al. Clinical profile of cardiac involvement in Danon disease: a multicenter european registry. *Circulat Genomic Precision Med.* (2020) 13:e003117. doi: 10.1161/circgen.120.003117
21. Zaki A, Zaidi A, Newman WG, Garratt CJ. Advantages of a subcutaneous implantable cardioverter-defibrillator in LAMP2 hypertrophic cardiomyopathy. *J Cardiovasc Electrophysiol.* (2013) 24:1051–3. doi: 10.1111/jce.12142

22. Khandia R, Dadar M, Munjal A, Dhama K, Karthik K, Tiwari R, et al. A comprehensive review of autophagy and its various roles in infectious, non-infectious, and lifestyle diseases: current knowledge and prospects for disease prevention, novel drug design, and therapy. *Cells.* (2019) 8:cells8070674. doi: 10.3390/cells8070674
23. Dvornikov AV, Wang M, Yang J, Zhu P, Le T, Lin X, et al. Phenotyping an adult zebrafish lamp2 cardiomyopathy model identifies mTOR inhibition as a candidate therapy. *J Mol Cell Cardiol.* (2019) 133:199–208. doi: 10.1016/j.yjmcc.2019.06.013
24. Su JW, Li SF, Tao JJ, Xu YY, Wang K, Qian XW, et al. Estrogen protects against acidosis-mediated articular chondrocyte injury by promoting ASIC1a protein degradation. *Eur J Pharmacol.* (2021) 908:174381. doi: 10.1016/j.ejphar.2021.174381
25. Nguyen HT, Noguchi S, Sugie K, Matsuo Y, Nguyen CTH, Koito H, et al. Small-vessel vasculopathy due to aberrant autophagy in LAMP-2 deficiency. *Sci Rep.* (2018) 8:3326. doi: 10.1038/s41598-018-21602-8

Conflict of Interest: The authors declare that the research was conducted in the absence of any commercial or financial relationships that could be construed as a potential conflict of interest.

frontiers | Frontiers in Cardiovascular Medicine

CASE REPORT
published: 10 June 2022
doi: 10.3389/fcvm.2022.919500

Case Report: An Unusual Case of Pheochromocytoma

Ying Liao [1†], Shanshan Shi [1,2†], Lihua Liao [1,2†], Yukun Zhao [1,2], Rongwen Lin [1] and Kaihong Chen [1]*

[1] Longyan First Affiliated Hospital of Fujian Medical University, Longyan, China, [2] The Third Clinical Medicine College, Fujian Medical University, Fuzhou, China

Pheochromocytoma is a benign catecholamine secreting tumor, which is rare and originates from the adrenal gland. It has been known for a wide range of clinical manifestations and can mimic other difficult-to-diagnose diseases. Here, we report a female patient with acquired long QT syndrome, which is a rare complication of pheochromocytoma. Although relatively rare, the presence of pheochromocytoma should be considered in the case of malignant arrhythmias and electrocardiographic changes in patients.

Keywords: syncope, pheochromocytoma, long QT syndrome, malignant arrhythmias, torsade de pointes

OPEN ACCESS

Edited by:
Leonardo Roever, Federal University of Uberlandia, Brazil

Reviewed by:
Claudio Letizia, Sapienza University of Rome, Italy
Fatemeh Khatami, Tehran University of Medical Sciences, Iran

***Correspondence:**
Kaihong Chen
chenkaihong1964@163.com

[†] These authors have contributed equally to this work and share first authorship

Specialty section:
This article was submitted to General Cardiovascular Medicine, a section of the journal Frontiers in Cardiovascular Medicine

Received: *13 April 2022*
Accepted: *11 May 2022*
Published: *10 June 2022*

Citation:
Liao Y, Shi S, Liao L, Zhao Y, Lin R and Chen K (2022) Case Report: An Unusual Case of Pheochromocytoma. Front. Cardiovasc. Med. 9:919500. doi: 10.3389/fcvm.2022.919500

INTRODUCTION

Pheochromocytoma is a benign catecholamine-secreting tumor, which is rare and originates from the adrenal gland. It has been known for a wide range of clinical manifestations and can mimic other difficult-to-diagnose diseases. Here, we report a female patient with acquired long QT syndrome (LQTs), which is a rare complication of pheochromocytoma. Although the clinical symptoms of this case are atypical, the pathologic and computed tomography (CT) scan imaging findings of this case are typical. It is worth the communication and learning of physicians.

CASE PRESENTATION

A 58-year-old woman came to an emergency department with a 6-day history of dizziness, headache, and syncope. Prodromal symptoms included palpitation and nausea but did not occur every time. She had no chest pain, dyspnea, fever, hematemesis, hematochezia, epileptic seizures, hemiplegia, aphasia, or urinary or fecal incontinence. Each syncope episode could be a spontaneously complete recovery, but it appeared to be unrelated to posture, emotion, or situation. She was presented to an emergency department at another institution but, unfortunately, was not diagnosed. However, her symptoms continued to worsen, and syncope episodes became more frequent (**Table 1**).

The patient had a medical history of hypertension. She was treated with 5 milligrams of amlodipine per day. Her blood pressure was unstable and often fluctuates, especially over the past 1 month. The patient had no history of trauma, autonomic nerve failure, epilepsy, or congenital heart disease. She did not smoke, drink, or use illegal drugs. No family history of syncope and sudden death.

Again, the patient syncope and ECG monitoring showed *torsade de pointes* (TdP) (It was a pity that the ECG was not recorded in time), which was converted with cardiopulmonary resuscitation. The patient was admitted to the coronary care unit (CCU) and further treatment was initiated. On physical examination, the temperature was 36.4°C, the respiratory rate was 20 breaths per minute,

TABLE 1 | Timeline.

July 23rd	The patient felt head pain, dizziness, accompanied by nausea and vomiting, and accompanied by palpitation and fatigue.
July 28th	Syncope occurred repeatedly for four times, with headache and palpitation before syncope.
July 29th	The patient experienced syncope three times.
Admission	
July 29th	The patient experienced syncope again, ECG monitoring showed torsade de pointes (TdP) (it was a pity that the ECG was not recorded in time), which was converted with cardiopulmonary resuscitation. The patient was admitted to the coronary care unit (CCU) and started to receive further treatment.
July 31st	Echocardiography revealed hypertrophic ventricular wall with ejection fraction (EF) of 63%.
August 1st	Coronary CT angiography (CTA) suggested mild stenosis of the left anterior descending branch. Chest CT and cerebral CT were basically normal. The unenhanced abdominal CT right adrenal heterogeneous mass (45 HU) was detected.
August 2nd	The abdominal CT scan detected a 53 × 58 mm right adrenal heterogeneous mass.
August 14th	The patient underwent endoscopic retroperitoneal adrenalectomy.
September 20th	The patient' ECG was completely normal with QTc of 404 ms.

the heart rate was 74 beats per minute, the blood pressure 117/74 mmHg, and the oxygen saturation was 98%. Her cardiopulmonary and neurological examinations were normal.

Laboratory testing showed a maximum troponin I (TNI) level of 0.32 ng per milliliter (normal value, <0.3 ng per milliliter), maximum creatinine kinase-MB (CK-MB) of 41 IU per liter (normal value, <25 IU per liter), and a maximum N-terminal pro-B-type natriuretic peptide (NT-pro BNP) of 5,138.77 pg per milliliter (normal value, <450 pg per milliliter). Her fasting blood glucose was 11.46 mmol per liter (206.3 mg per deciliter) (normal value, <7 mmol per liter) [126 mg per deciliter] and hemoglobin a1c (HbA1c) of 8.3% (normal value, <6.5 %). The patient was newly diagnosed with diabetes. Hemoglobin, blood gas analysis, D dimer, serum sodium, potassium, magnesium, calcium, renal, liver, and thyroid levels were all within normal limits. The patient's electrocardiograph (ECG) showed a sinus rhythm of 67 beats per minute, ST-segment depression in V4-V6. Most notably, it showed a QTc interval of 661 ms (**Figure 1A**). Echocardiography revealed a hypertrophic ventricular wall with an ejection fraction (EF) of 63%. Coronary CT angiography (CTA) suggested mild stenosis of the left anterior descending branch. Chest CT and cerebral CT were normal. The patient was not taking medications that caused QT prolongation.

During the hospitalization, the patient underwent an abdominal CT scan. As a result, a 53 × 58 mm right adrenal heterogeneous mass was detected. The unenhanced CT attenuation was 45 Hounsfield units (HU). Axial contrast-enhanced CT demonstrated a mass consisting of solid enhancement and cystic components (**Figures 2A,B**).

Adrenal endocrinology examinations were used for differential diagnosis. Plasm renin activity was 3.03 ng per milliliter per hour (normal value,1.31–3.95 ng per milliliter per hour), aldosterone was 35.38 ng per deciliter (normal value,7.6–30 pg per deciliter), morning adrenocorticotropic hormone (ACTH) was 2.84 ng per liter (normal value,10–90 ng per liter), cortisol at 8:00 568.4 nmol per liter (normal value,171–536 nmol per liter), cortisol at 16:00 457.4 nmol per liter (normal value,64–340 nmol per liter), cortisol at 0:00 450 nmol per liter (normal value,171–536 nmol per liter), 24-h urinary dopamine was 541.21 ug (normal value,<600 ug), 24-hr urinary norepinephrine was 659.63 ug (normal value,<90 ug), 24-h urinary adrenaline was 73.21 ug (normal value, <20 ug), and 24-h urinary vanillylmandelic acid (VMA) of 29.2 mg (normal value,<12 mg).

Two weeks later, after being prepared according to the guidelines for pheochromocytoma resection, she underwent endoscopic retroperitoneal adrenalectomy. Histopathologic examination of the adrenal mass showed that it was a typical pheochromocytoma, with large polygonal cells arranged in a thick nest and separated by a rich capillary network (zellballen appearance) (**Figure 3A**). Positive expression of tyrosine ki-67, CgA, Syn, and NSE on immunohistochemical examination (**Figure 3B**). After 1 month follow-up, the patient's ECG was completely normal with a QTc of 404 ms (**Figure 1B**). She is free of syncope but still has hypertension with amlodipine.

The patient does not experience syncope after surgery, and ECG indicates that QT returned to normal, confirming our assessment that pheochromocytoma is the cause of her problem.

Germline genetic testing found no mutation associated with inherited LQTs (KCNQ1, KCNH2, SCN5A, KCNE1, KCNE2, etc.), but found a mutation in SDHB associated with pheochromocytoma. SDHB mutation is a type of familial paraganglioma syndrome, which is characterized by paragangliomas with high metastatic risk in the mediastinum, thorax, abdomen, and pelvis.

Approximately 70–75% of patients with inherited LQTs have mutations, and more than one-third of patients with acquired LQTs also carry mutations in one of the major LQTs-related genes, of which KCNH2 is the more common. All the common long QT-related genes in the patient are negative. In combination with her characteristics, we considered it as an acquired LQT. Furthermore, we detect gene mutation associated with pheochromocytoma, confirming again that the etiology of the patient is pheochromocytoma.

DISCUSSION

Syncope is one of the most life-threatening conditions, and many people suffer from recurrent syncope without being diagnosed or treated. It is estimated that about half of people have syncope at least once in their life (1). The annual incidence of syncope in older patients was 7%, the overall prevalence was 23%, and the 2-year recurrence rate was 30%. Cardiogenic syncope is the most dangerous form, and arrhythmia is one of the most common causes of cardiogenic syncope, which is more dangerous than other etiology (2, 3).

The LQTs are an inherited or acquired heart diseases characterized by prolonged QT on the ECG, and an increased risk

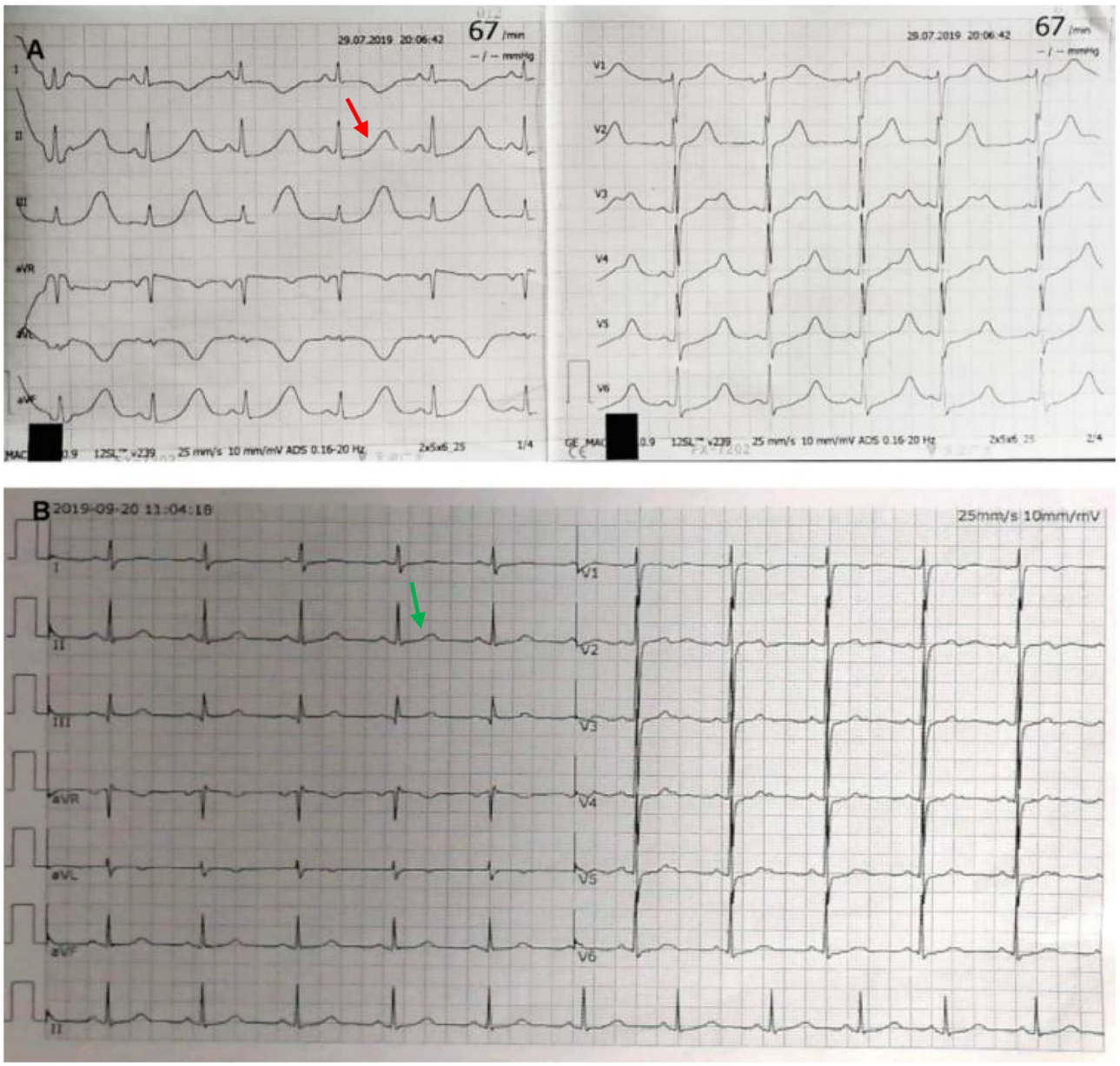

FIGURE 1 | Electrocardiograph (ECG). ECG at admission shows sinus rhythm and QTc interval of 661 ms [**(A)** red arrow]. After excision of pheochromocytoma, ECG shows normalization with QTc of 404 ms [**(B)** green arrow].

of life-threatening ventricular arrhythmias (4). Acquired LQTs are far more common than congenital LQTs and may be the result of pharmacologically affected electrolyte disturbances and endocrine imbalance (such as pheochromocytoma). LQTs are defined as prolongation of the QTc for heart rate, in adult males and children at >440 ms, or women at >460 ms. Approximately 16–35% of patients have varying degrees of QT prolongation, but QTc is rarely more than 600 ms as described in the literature. In our case, QTc at admission is 661 ms, which is very easy to induce TdP. TdP is a type of polymorphic ventricular tachycardia, which is characterized by a gradual change and distortion of the magnitude of the QRS complex wave around an isoelectric line on the ECG. It usually occurs in the setting of a prolonged QT interval.

Pheochromocytomas and paragangliomas (PPGLs) are rare neuroendocrine chromaffin tissue tumors that may produce catecholamines (5). About 80–85% of PPGLs come from the adrenal medulla, which is called pheochromocytoma, whereas about 15–20% of PPGLs come from the sympathetic or parasympathetic paravertebral ganglia, which is called

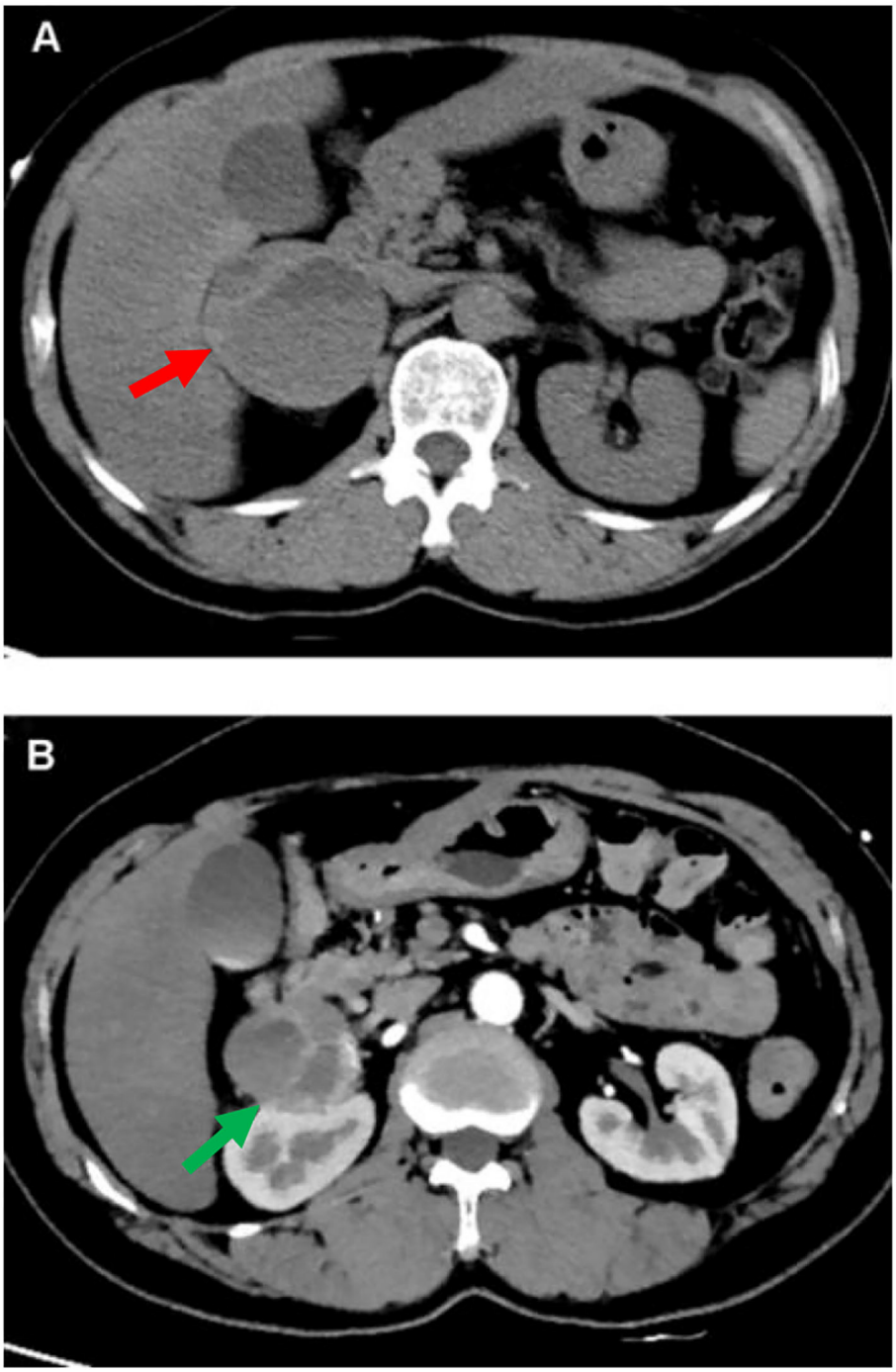

FIGURE 2 | CT of abdomen. A computed tomographic (CT) of the upper abdomen (axial view) shows a 53 mm*58 mm heterogeneous tumor of the right adrenal gland [**(A)** red arrow]. Axial contrast-enhanced CT image shows the mass compose of solid enhancing component and cystic component [**(B)** green arrow].

paragangliomas (6). The prevalence of hypertension among adult outpatients ranges from 0.1 to 0.6% (7, 8). The effects of catecholamines on different organs depend on their blood concentration and the types of adrenergic receptors in the organs. So, there are highly variable clinical symptoms and signs, which can lead to delay in diagnosis, but the most common symptoms are headaches, sweating, heart palpitations, and hypertension. Serious potential cardiovascular complications include arrhythmia, hypotension, myocardial ischemia, shock, aortic dissection, cardiomyopathy, and peripheral ischemia (9). In a retrospective study of 145 subjects, arrhythmias occurred in 15 subjects. Ventricular tachycardia was found in

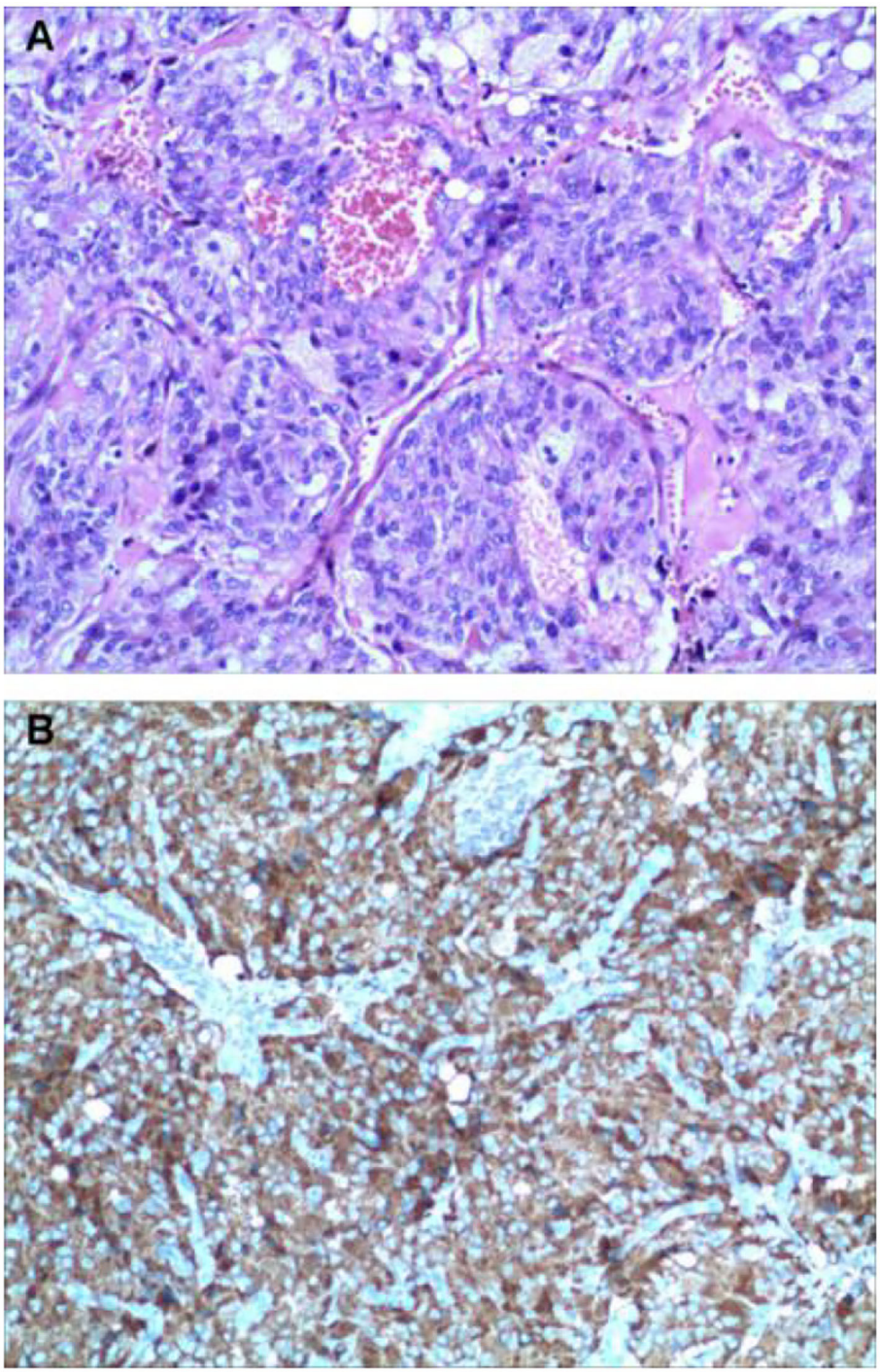

FIGURE 3 | Histologic findings. Histological evaluation of adrenal neoplasms revealed rounded to polygonal cells with abundant granular amphoteric cytoplasm arranged in well-defined nests [**(A)** hematoxylin, and eosin]. Immunohistochemical testing shows positive expression of CgA **(B)**.

2 subjects, one of whom was TdP (10). Although ventricular arrhythmias are a rare complication of PPGLS, they can occur (11–16). The mechanism of QT prolongation and TdP is not very clear. We speculate that it may have been related to the presence and relative proportion of catecholamines secreted. Adrenergic stimulation can prolong the QT interval by prolonging the duration of the action potential. In addition, the increase of myocardial heterogeneity and the triggering of early afterdepolarization (EAD) are also mechanisms.

The diagnosis of pheochromocytoma is difficult owing to the rarity of the disease, the nonspecific clinical manifestations, and the uncertainty of its location. As in our case, syncope may be the first symptom, making the diagnosis of pheochromocytoma challenging and important. This case highlights the steps to diagnose pheochromocytoma. First, if pheochromocytoma is suspected, biochemical testing should be initiated, including measurement of fractionated metanephros's and catecholamines in a 24-h urine or plasma specimen. In addition, we should also be aware of false negatives and false positives in food, drugs, and other disease states, and biochemical testing should be repeated later, during episodes of symptoms that may be caused by catecholamines.

Secondly, when there is clear biochemical diagnostic evidence, the imaging study of the adrenal gland should be started. The various imaging appearances on ultrasound, CT, MRI, and functional imaging can be complementary and have characteristics that may help distinguish them from other masses of the adrenal. If MRI or CT imaging is normal and there is a strong biochemical suspicion that it is a tumor, or there is radiological evidence that it is a paraganglioma or metastatic disease, the patient should be given iodine-123 metaiodobenzyl guanidine scan and may also undergo fludeoxyglucose positron emission tomography CT (17).

Thirdly, previous studies have shown that more than 40% of patients, who develop pheochromocytoma, carry germline mutations (18, 19). Ideally, all patients with pheochromocytoma should undergo genetic testing because the results of genetic testing can better guide the clinical treatment and prognosis (20). Genetic analysis of our case reveals gene mutation in SDHB. Patients with SDHx mutations usually have head-and-neck paragangliomas, but pheochromocytomas and retroperitoneal paragangliomas are found primarily in carriers of SDHD, SDHB, and SDHA mutations (21, 22). Fortunately, no tumor was found except in the adrenal gland. After surgery, hormone levels returned to normal and symptoms disappeared, confirming the absence of tumors elsewhere. However, the long-term clinical prognosis needs to be further evaluated with follow-up.

The PPGL is pathologically characterized by a nest of tumor cells separated by surrounding capillaries, namely Zellballen. PPGLs express generic neuroendocrine markers, of which chromogranin A and synaptophysin are most often utilized, which helps distinguish them from other neuroendocrine tumors. Malignant PPGLs are defined by the presence of chromaffin cells in tissues and sites that normally do not contain these cells (23).

If pheochromocytoma is removed timely, the prognosis is favorable. However, the prognosis is poor in patients with metastases, which especially occur in patients with large and extra-adrenal tumors. After resection, patients with PPGLs have reasonable outcomes and biochemical reaction and blood pressure control are improved. All patients with PPGLs need biochemical and potentially radiological surveillance.

PATIENT PERSPECTIVE

"As a patient, I am glad that the cause of the disease has been found and solved. My illness came suddenly. I couldn't find the cause at first and the symptoms continued to worsen, which frightened me. I was surprised to learn that my syncope and abnormal ECG were caused by a mass in the abdominal cavity because I had never found an abdominal mass before. Finally, I am very grateful to the doctor who has treated me".

CONCLUSION

In summary, there are several important points to be learned from this case. First, when evaluating patients with common syncope symptoms, physicians need to consider both rare and severe causes. Second, pheochromocytoma can be lethal if it is undiagnosed or misdiagnosis. Thus, rapid, and correct recognition is crucial. Third, if the reversible cause of TdP is identified, surgical resection of the tumor will cure and avoid unnecessary ICD implantation.

DATA AVAILABILITY STATEMENT

The original contributions presented in the study are included in the article/supplementary material, further inquiries can be directed to the corresponding author.

ETHICS STATEMENT

Written informed consent was obtained from the individual(s) for the publication of any potentially identifiable images or data included in this article.

AUTHOR CONTRIBUTIONS

All authors listed have made a substantial, direct, and intellectual contribution to the work and approved it for publication.

REFERENCES

1. Brignole M, Moya A, de Lange FJ, Deharo JC, Elliott PM, Fanciulli A, et al. Practical Instructions for the 2018 ESC Guidelines for the diagnosis and management of syncope. *Eur Heart J.* (2018) 39:e43–80. doi: 10.1093/eurheartj/ehy037
2. Shen WK, Sheldon RS, Benditt DG, Cohen MI, Forman DE, Goldberger ZD, et al. 2017 ACC/AHA/HRS guideline for the evaluation and management of patients with syncope: A report of the American College of Cardiology/American Heart Association Task Force on Clinical Practice Guidelines and the Heart Rhythm Society. *Heart Rhythm.* (2017) 14:e155–217. doi: 10.1161/CIR.0000000000000499
3. von Alvensleben JC. Syncope and palpitations: a review. *Pediatr Clin North Am.* (2020) 67:801–10. doi: 10.1016/j.pcl.2020.05.004
4. Neira V, Enriquez A, Simpson C, Baranchuk A. Update on long QT syndrome. *J Cardiovasc Electrophysiol.* (2019) 30:3068–78. doi: 10.1111/jce.14227
5. Sarkadi B, Saskoi E, Butz H, Patocs A. Genetics of pheochromocytomas and paragangliomas determine the therapeutical approach. *Int J Mol Sci.* (2022) 23. doi: 10.3390/ijms23031450

6. Garcia-Carbonero R, Matute Teresa F, Mercader-Cidoncha E, Mitjavila-Casanovas M, Robledo M, Tena I, et al. Multidisciplinary practice guidelines for the diagnosis, genetic counseling and treatment of pheochromocytomas and paragangliomas. *Clin Transl Oncol.* (2021) 23:1995–2019. doi: 10.1007/s12094-021-02622-9
7. Copeland PM. The incidentally discovered adrenal mass. *Ann Intern Med.* (1983) 98:940–5. doi: 10.7326/0003-4819-98-6-940
8. Lenders JW, Eisenhofer G, Mannelli M, Pacak K. Phaeochromocytoma. *Lancet.* (2005) 366:665–75. doi: 10.1016/S0140-6736(05)67139-5
9. Prejbisz A, Lenders JW, Eisenhofer G, Januszewicz A. Cardiovascular manifestations of phaeochromocytoma. *J Hypertens.* (2011) 29:2049–60. doi: 10.1097/HJH.0b013e32834a4ce9
10. Zelinka T, Petrak O, Turkova H, Holaj R, Strauch B, Krsek M, et al. High incidence of cardiovascular complications in pheochromocytoma. *Horm Metab Res.* (2012) 44:379–84. doi: 10.1055/s-0032-1306294
11. Cecilia GM, Emilien D, Laurent H. Acquired long QT interval complicated with Torsades de Pointes as presentation of a pheochromocytoma in a paediatric patient: a case report. *Cardiol Young.* (2015) 25:391–3. doi: 10.1017/S104795111400033X
12. Delekta J, Riahi S, Eschen O. Rare cause of ventricular tachycardia: Pheochromocytoma. *J Cardiol Cases.* (2015) 11:62–5. doi: 10.1016/j.jccase.2014.10.007
13. Oruganti SS, Gambeer Rao M, Pisapati VL. Adrenal and extra-adrenal pheochromocytomas presenting as life-threatening ventricular arrhythmias: report of three cases. *Indian Heart J.* (2016) 68:381–5. doi: 10.1016/j.ihj.2016.03.035
14. Ozyuncu N, Akturk S, Tan Kurklu TS, Erol C. Acute coronary syndrome-like presentation with prolonged QT interval: an unusual case of pheochromocytoma. *BMJ Case Rep.* (2016) 2016. doi: 10.1136/bcr-2016-216142
15. Paulin FL, Klein GJ, Gula LJ, Skanes AC, Yee R, Krahn AD, et al. Prolongation and monomorphic VT caused by pheochromocytoma. *J Cardiovasc Electrophysiol.* (2009) 20:931–4. doi: 10.1111/j.1540-8167.2008.01405.x
16. Wang L, Chen CJ, Zhao YT. An unusual etiology for acquired long QT syndrome and torsade de pointes. *Am J Emerg Med.* (2017) 35:186. doi: 10.1016/j.ajem.2016.10.048
17. Carrasquillo JA, Chen CC, Jha A, Ling A, Lin FI, Pryma DA, et al. Imaging of pheochromocytoma and paraganglioma. *J Nucl Med.* (2021) 62:1033–42. doi: 10.2967/jnumed.120.259689
18. Gunawardane PTK, Grossman A. Phaeochromocytoma and paraganglioma. *Adv Exp Med Biol.* (2017) 956:239–59. doi: 10.1007/5584_2016_76
19. Juhlin CC. Challenges in paragangliomas and pheochromocytomas: from histology to molecular immunohistochemistry. *Endocr Pathol.* (2021) 32:228–44. doi: 10.1007/s12022-021-09675-0
20. Cotesta D, Petramala L, Serra V, Pergolini M, Crescenzi E, Zinnamosca L, et al. Clinical experience with pheochromocytoma in a single centre over 16 years. *High Blood Press Cardiovasc Prev.* (2009) 16:183–93. doi: 10.2165/11530430-000000000-00000
21. Cheung VKY, Gill AJ, Chou A. Old, new, and emerging immunohistochemical markers in pheochromocytoma and paraganglioma. *Endocr Pathol.* (2018) 29:169–75. doi: 10.1007/s12022-018-9534-7
22. Benn DE, Robinson BG, Clifton-Bligh RJ. 15 years of paraganglioma: clinical manifestations of paraganglioma syndromes types 1-5. *Endocr Relat Cancer.* (2015) 22:T91–103. doi: 10.1530/ERC-15-0268
23. Tischler AS. deKrijger RR. 15 years of paraganglioma: pathology of pheochromocytoma and paraganglioma. *Endocr Relat Cancer.* (2015) 22:T123–33. doi: 10.1530/ERC-15-0261

Conflict of Interest: The authors declare that the research was conducted in the absence of any commercial or financial relationships that could be construed as a potential conflict of interest.

frontiers | Frontiers in Cardiovascular Medicine

CASE REPORT
published: 07 July 2022
doi: 10.3389/fcvm.2022.913724

The Diagnostic Challenge of Eosinophilic Granulomatosis With Polyangiitis Presenting as Acute Eosinophilic Myocarditis: Case Report and Literature Review

Hiroyuki Yamamoto[1]*, *Katsuya Hashimoto*[1], *Yoshihiko Ikeda*[2], *Jun Isogai*[3] and *Toru Hashimoto*[1]

[1] Department of Cardiovascular Medicine, Narita-Tomisato Tokushukai Hospital, Chiba, Japan, [2] Department of Pathology, National Cerebral and Cardiovascular Center, Suita, Japan, [3] Department of Radiology, Asahi General Hospital, Asahi, Japan

OPEN ACCESS

Edited by:
Jinwei Tian,
The Second Affiliated Hospital of Harbin Medical University, China

Reviewed by:
Fady Gerges,
Mediclinic Al Jowhara Hospital, United Arab Emirates
Sang-Won Lee,
Yonsei University Health System, South Korea

***Correspondence:**
Hiroyuki Yamamoto
hyamamoto19700908@gmail.com

Specialty section:
This article was submitted to General Cardiovascular Medicine, a section of the journal Frontiers in Cardiovascular Medicine

Received: *06 April 2022*
Accepted: *13 June 2022*
Published: *07 July 2022*

Citation:
Yamamoto H, Hashimoto K, Ikeda Y, Isogai J and Hashimoto T (2022) The Diagnostic Challenge of Eosinophilic Granulomatosis With Polyangiitis Presenting as Acute Eosinophilic Myocarditis: Case Report and Literature Review. Front. Cardiovasc. Med. 9:913724. doi: 10.3389/fcvm.2022.913724

Eosinophilic granulomatosis with polyangiitis (EGPA) is a systemic vasculitis involving small-to-medium-sized vessels characterized by asthma, vasculitis, and peripheral eosinophilia. EGPA-associated eosinophilic myocarditis (EM) occurs rarely, yet can be fatal if left untreated. Moreover, the accurate diagnosis of EGPA-associated EM without vasculitis is exceptionally difficult because of the overlapping features with EM of other causes. We report a case of probable EGPA with subclinical neurological involvement that presented with acute EM. The constellation of peripheral eosinophilia, left ventricular dysfunction, and normal epicardial coronary arteries raised suspicion of acute EM, which was confirmed by cardiac magnetic resonance (CMR) investigation and endomyocardial biopsy (EMB). Prompt systemic administration of corticosteroids completely restored and normalized myocardial structure and function. Although the patient's history suggested the presumed hypersensitivity myocarditis, EMB revealed EM without vasculitis, not hypersensitivity, leading to a tentative diagnosis of idiopathic hypereosinophilic syndrome. Interestingly, the characteristic findings of vasculitis on CMR imaging strongly suggested EGPA-associated EM. Although the patient had no clinical neurological manifestations, a nerve conduction study confirmed mononeuritis multiplex, leading to the final diagnosis of probable EGPA. Therefore, this case highlights the diagnostic challenge associated with EGPA and the diagnostic synergy of CMR and EMB for an exploratory diagnosis of EGPA-associated EM.

Keywords: EGPA, acute EM, hypereosinophilia, CMR, EMB, corticosteroid treatment

INTRODUCTION

Eosinophilic granulomatosis with polyangiitis (EGPA), previously known as Churg-Strauss syndrome, is a multisystem disorder characterized by necrotizing vasculitis of small-to-medium-sized vessels, with the coexistence of asthma, rhinosinusitis, and marked peripheral eosinophilia (1). EGPA-associated eosinophilic myocarditis (EM) is rare but can be fatal (1, 2). Because EM has multiple etiologies with overlapping clinical and biological features, a definitive diagnosis

of EGPA-associated EM remains challenging in the absence of clinical manifestations of vasculitis. Therefore, a promising strategy to accurately diagnose EGPA-associated EM needs to be formulated.

CASE DESCRIPTION

A 72-year-old woman was admitted to our hospital with worsening chest pain. She had a history of asthma and was treated with a fluticasone furoate/vilanterol (inhaler), theophylline (200 mg/day), ambroxol hydrochloride capsules (45 mg/day), montelukast (10 mg/day), and mequitazine (6 mg/day). Her treatment was aided with short-term use of oral prednisolone as required. The patient's general practitioner switched her from regular branded medications to generic medications 1 month prior to her admission. A week before admission, she experienced chest pain, characterized by chest tightness on exertion that disappeared on rest. Her symptoms worsened and were accompanied by dyspnea on effort (New York Heart Association class II–III). Her vital signs were as follows: blood pressure 118/73 mmHg, heart rate 87 beats/min, temperature 37.3°C, and oxygen saturation 97%. The physical and neurological examination results and chest radiographs were unremarkable. The electrocardiogram (ECG) showed pathologic Q waves in V2 to V3, and negative QRS complexes including rS morphology in the inferior leads, diagnosed as a left anterior fascicular block (**Supplementary Figure 1A**). The laboratory testing revealed a significant eosinophilia with an eosinophil percentage of 67.6% (normal < 6%) and an absolute eosinophil count (AEC) of 10,410/μL (normal < 500/μL), elevated brain natriuretic peptide level of 536 pg/mL (normal < 18.4 pg/mL), and elevated cardiac biomarkers levels as follows: creatine kinase, 473 U/L (reference: 41–153 U/L); CK-MB, 39 U/L (normal < 25 U/L); aspartate aminotransferase, 72 U/L (reference: 13–30 U/L); lactate dehydrogenase, 613 U/L (reference: 124–222 U/L); and high sensitivity cardiac troponin I, 47,875.3 pg/mL (normal < 26.2 pg/mL). The levels of the inflammatory markers were also elevated—the C-reactive protein was 0.65 mg/dL (normal < 0.3 mg/dL) and the erythrocyte sedimentation rate was >110 mm/h (reference: 3–15 mm/h). The results of renal function and urinalysis were normal. Further laboratory studies revealed elevated levels of serum IgE at 1,840 IU/mL (normal < 173 IU/mL) and rheumatoid factor at 204 IU/mL (normal < 15 IU/mL). In addition, the levels of the Th2 cytokines-related interleukins (IL) were also raised—IL-4 was 7.7 pg/mL (normal < 3.9 pg/mL) and IL-5 was 30 pg/mL (normal < 3.9 pg/mL). Anti-neutrophil cytoplasmic antibodies (ANCA) were not detected. Echocardiography revealed a mildly thickened myocardium and significant left ventricular (LV) systolic dysfunction with an ejection fraction of 43%. In addition, speckle-tracking echocardiography showed a reduced baseline global longitudinal strain of −9.9% (**Figures 1A–C** and **Supplementary Video 1**). Accordingly, we made a tentative diagnosis of acute coronary syndrome (ACS). An emergency coronary angiography was performed after pre-treatment with methylprednisolone (250 mg) that was administered to prevent allergic contrast reactions for the patient with asthma**.** The angiogram revealed normal epicardial coronary arteries. Therefore, acute EM was suspected, and cardiac magnetic resonance (CMR) was performed to assess the myocardial tissue (**Figures 2A–C** and **Supplementary Video 2**). Myocardial first-pass perfusion (FPP) imaging showed patchy and circumferential subendocardial perfusion defects (arrowheads), suggesting microvascular disorders. CMR also showed subendocardial late gadolinium enhancement (LGE) as multiple and lobulated high-signal intensity spots (arrows), which suggested vasculitis. The T2-weighted image showed a transmural high-intensity signal throughout the myocardium, corresponding to myocardial edema. Acute myocarditis was diagnosed based on the Lake–Louise criteria. These findings were consistent with acute EM. Simultaneously, an exhaustive diagnostic workup for hypereosinophilia was performed. Its differential diagnoses include hypersensitivity myocarditis (HSM), EGPA, parasitic infections, hematologic malignancies, and lymphocytic/idiopathic hypereosinophilic syndrome (HES). Considering the patient's recent medical history, HSM was initially suspected as the cause of EM. The generic drugs being administered to the patient were discontinued after admission. A subsequent endomyocardial biopsy (EMB) was performed, which demonstrated marked extravascular eosinophilic infiltrates without granulomatous and fibrinoid necrotizing vasculitis (**Figure 3A**). Numerous eosinophilic infiltrations, with degranulated eosinophils admixed with lymphocytes and myocyte necrosis, were observed in the myocardial interstitium that extended to the endocardium (**Figures 3B,C**). Moderate endocardial thickening and perivascular interstitial fibrosis were observed (data not shown). Immunostaining was performed to identify the major basic proteins revealed extensive staining in the endocardium and myocardial interstitium (**Figure 3D**). These findings led to the final diagnosis of acute EM. Subsequently, the patient was treated with intravenous methylprednisolone (1 g/day for 3 days), followed by oral prednisolone (1 mg/kg/day). The clinical response to steroid treatment was remarkable, with significant recovery of LV dysfunction, hypereosinophilia, and elevated cardiac enzyme levels within 21 days of steroid treatment (**Figures 1D–F** and **Supplementary Video 3**). Follow-up ECG showed resolution of all abnormal findings recognized during the initial ECG (**Supplementary Figure 1B**). On day 33, the patient was discharged after administration of prednisolone (15 mg/day), with a gradual tapering of the doses. On day 56, the patient remained asymptomatic, with fully recovered cardiac function observed on echocardiography (**Supplementary Figure 2** and **Supplementary Video 4**). Moreover, the abnormal findings of the CMR resolved completely (**Figures 2D–F** and **Supplementary Video 5**). On day 75, prednisolone was tapered and finally discontinued in the outpatient clinic.

Abbreviations: EGPA, eosinophilic granulomatosis with polyangiitis; EM, eosinophilic myocarditis; ECG, electrocardiogram; AEC, absolute eosinophilic count; ANCA, anti-neutrophil cytoplasmic antibodies; LV, left ventricular; ACS, acute coronary syndrome; CMR, cardiac magnetic resonance; FPP, first-pass perfusion; LGE, late gadolinium enhancement; HES, hypereosinophilic syndrome; HSM, hypersensitivity myocarditis; EMB, endomyocardial biopsy; ACR, American College of Rheumatology.

However, her asthma precipitated again 2 weeks later, which was concurrent with an eosinophilia count of 1,512/μL. Since a thorough diagnostic workup for hypereosinophilia was negative, idiopathic HES was also considered. Although the patient had no clinical neurological manifestations, her CMR findings were suggestive of vasculitis, which encouraged us to perform a nerve conduction study that revealed mononeuritis multiplex. Eventually, as per the diagnostic criteria of the American College of Rheumatology (ACR) for EGPA, the patient met four of the six items (asthma, eosinophilia >10%, mononeuritis multiplex, and extravascular eosinophilia). However, a histological diagnosis of vasculitis could not be performed because the patient refused nerve biopsies. Therefore, the final diagnosis of probable EGPA was made. The patient was restarted on prednisolone treatment (15 mg/day). At the 1-year follow-up, the patient remained clinically stable, with prednisolone tapered to 4 mg/day. As a supplement, we have presented a timeline for the case presentation (**Supplementary Figure 3**).

DISCUSSION

EGPA is classified among ANCA-positive vasculitides, and its underlying pathological mechanism remains poorly understood. The widely accepted ACR criteria for EGPA include asthma, eosinophilia (>10% in the differential count), neuropathy, non-fixed pulmonary infiltrates, paranasal sinus abnormalities, and extravascular eosinophils. According to a study, the ACR criteria for the classification of vasculitis as EGPA yielded a sensitivity of 85.0% and specificity of 99.7%, when four or more of the aforementioned conditions were applicable (3). EGPA is commonly diagnosed at ∼40 years of age and exhibits no gender predominance. Its reported prevalence is 10.7–18 per million in Europe and the United States (4, 5). EGPA progresses through three chronological phases: the prodromal phase with the occurrence of asthma and allergic manifestations; the eosinophilic phase, which is characterized by eosinophilic infiltration of the organs involving the lungs and the myocardium; and the vasculitic phase, which is characterized by organ damage due to vasculitis in small-to-medium-sized vessels in the skin, peripheral nerves, and kidneys. These three phases may overlap. Generally, EGPA has an excellent prognosis, with a 5-year survival rate of 97% (6). Cardiovascular involvement rarely occurs (about 16% of organ involvements), but is the leading cause of death in about 50% of cases (7). Although data on cardiac involvement in patients with EGPA are available in the literature, the number of reported cases of EGPA-associated EM is small (2, 8). Therefore, we conducted an updated systematic review of case reports to investigate the characteristics of EGPA-associated EM (**Table 1**). The literature search was performed using PubMed databases documented from 1983 to 2021, with the search restricted to studies published in English. We used the following MeSH terms: "eosinophilic granulomatosis with polyangiitis" or "Churg–Strauss syndrome" and "case report" and "myocarditis." Moreover, we selected cases of EGPA-associated EM confirmed by EMB and/or CMR findings. Finally, 38 cases were included (9–46). The mean age of the participants included was 47 years with no gender predominance. The main extracardiac involvement was asthma, followed by peripheral neuropathy and constitutional symptoms (94.7, 52.6, and 23.7%, respectively). At presentation, the patients were commonly diagnosed with cardiac insufficiency (51.6%), ACS (21.1%), and cardiogenic shock (13.2%). As in our case, patients with EGPA-associated EM had a high rate of ANCA-negativity and presented with marked peripheral eosinophilia. Presence of LV dysfunction (66%) and pericardial effusion (47%) were frequently observed. A higher five-factor score was indicative of poor prognosis in 39% of the patients. Considering the number of cases with a poor clinical course, including sudden cardiac death (21%) and incomplete normalized cardiac function despite intensive treatment (26%), early recognition and treatment of EGPA-associated EM is required.

Herein, we describe a previously undiagnosed case of probable EGPA with the development of acute EM, which was successfully treated with corticosteroid treatment. This case provides three clinical suggestions.

First, the clinical course, in this case, was acute EM without obvious vasculitis, which led to a delayed diagnosis of probable EGPA.

The typical symptoms of systemic vasculitis in EGPA include constitutional symptoms (fever, malaise, and weight loss), myalgia, mono/polyneuropathy (numbness, tingling, muscle weakness, and pain), skin symptoms (purpura and non-pruritic nodules), and gastrointestinal ischemic symptoms such as abdominal pain. However, none of the above symptoms, except for low-grade fever, were observed in our case. The present case exemplifies the following three diagnostic challenges of EGPA.

First, HSM was suspected based on the medication history. External factors such as exposure to allergens, infection, or vaccination can induce the development of EGPA. However, the symptoms precipitated even after discontinuation of the suspected drugs, and the histological findings on EMB confirmed that HSM was less likely. Anti-asthmatic drugs, such as leukotriene receptor antagonists and anti-IgE antibodies can trigger the development of EGPA; however, a direct causal relationship in our case was unclear. The anti-asthmatic effects of the drugs might have delayed the systemic administration of corticosteroids, resulting in the manifestation of EGPA (47).

Second, the main histopathological findings of EGPA, other than eosinophilic infiltration, were not observed in our case. EMBs in patients with EGPA-associated EM often show EM without vasculitis (2), which is probably attributed to the possibility of heterogeneous distribution of vasculitis, the small number of EMB samples, and the limited biopsy sites including the left ventricular apex and interventricular septum (**Table 1**). Besides, in the autopsy cases, it was very likely to detect evidence of vasculitis because the whole heart was able to be analyzed. Therefore, EGPA-associated EM cannot be ruled out based on the lack of histologic evidence of vasculitis in EMBs. In addition, because the histopathologic findings may vary by the phase of the disease, our patient might have been during the early vasculitic phase of the disease. Furthermore, the cases of EGPA-associated EM have a high frequency of coexisting asthma (94.7%) (**Table 1**). Therefore, inhaled corticosteroids for

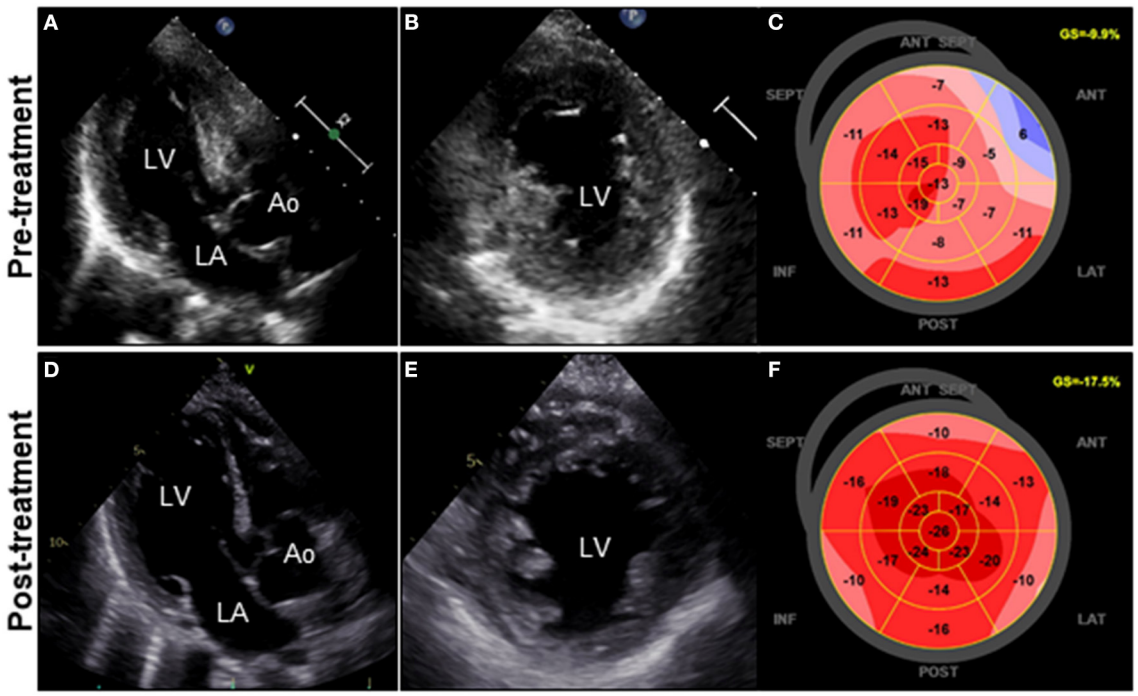

FIGURE 1 | Clinical effects of corticosteroid treatment on TTE. TTE on admission reveals diffuse and symmetrical LV wall thickening (11 mm), decreased cavity size, reduced ventricular function, and GLS values of the LV (LVDd, 44 mm; LVEF, 43%; and GLS, −9.9%; respectively) **(A–C)**. Follow-up TTE on day 21 after corticosteroid therapy reveals a significant decrease in LV wall thickness (8 mm) with concomitant improvement in cavity size, ventricular function, and GLS values of the LV (LVDd, 48 mm; LVEF, 50%; and GLS, −17.5%; respectively) **(D–F)**. Ao, aorta; GLS, global longitudinal strain; LA, left atrium; LV, left ventricle; LVDd, left ventricular end-diastolic diameter; LVEF, left ventricular ejection fraction; TTE, transthoracic echocardiography.

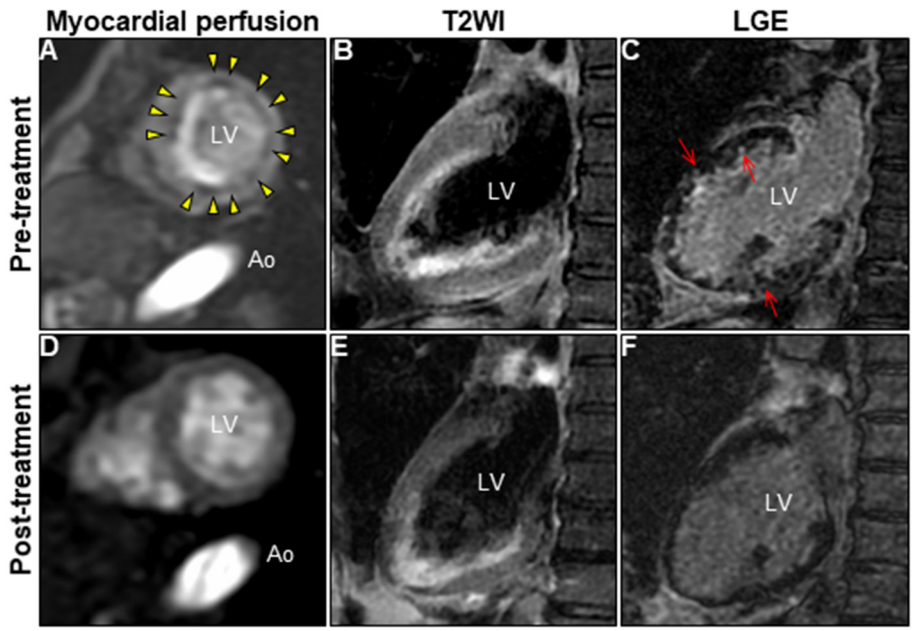

FIGURE 2 | Changes in CMR findings in patients following corticosteroid treatment. CMR findings before **(A–C)** and after corticosteroid treatment **(D–F)**. Myocardial first-pass perfusion imaging at rest **(A,D)**, T2WI of the 2-chamber view **(B,E)**, and LGE image **(C,F)**. Ao, aorta; CMR, cardiac magnetic resonance; LGE, late gadolinium enhancement; LV, left ventricle; T2WI, T2-weighted image.

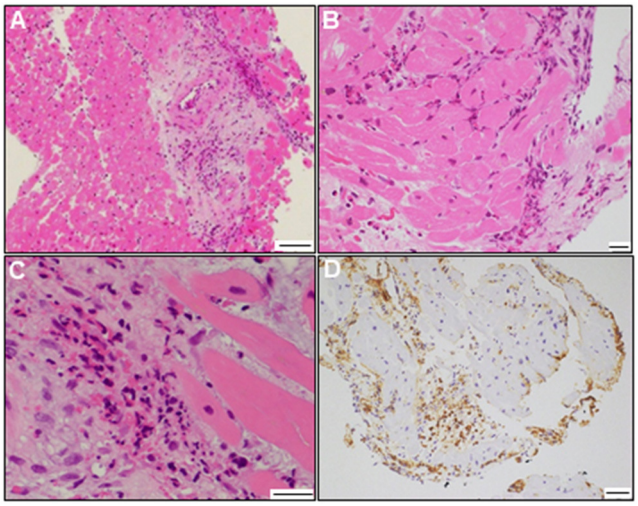

FIGURE 3 | Endomyocardial biopsy findings. Photomicrograph with hematoxylin and eosin staining **(A–C)** (bars: A, 100 μm; B and C, 20 μm). Photomicrograph showing immunostaining against the major basic protein **(D)** (bar: 50 μm).

asthma, and corticosteroid prophylaxis for allergic reactions to the contrast media, might have contributed to the absence of typical histopathologic findings in our patient. Subsequently, this patient presented with a mononeuritis multiplex which was significantly associated with systemic vasculitis (48), leading us to believe that this patient was diagnosed with probable EGPA.

A third diagnostic challenge is the potential clinical and biological overlap between EGPA and idiopathic HES. HES is a sporadic disorder that is diagnosed based on the following criteria: elevated AEC (>1,500 cells/μL on at least two occasions), and/or pathologic confirmation of tissue hypereosinophilia. With great advances in the knowledge of eosinophil biology and molecular diagnostics, the classification of HES subgroups is evolving rapidly. The following six variants of HES have been proposed (49): (i) myeloid HES, (ii) lymphocytic HES, (iii) overlap HES—eosinophilic disorders overlapping in presentation with idiopathic HES (e.g., EGPA), (iv) associated HES (eg, parasite infections, drug hypersensitivities, or immunodeficiency), (v) familial HES, and (vi) idiopathic HES—eosinophilic disorders of unknown etiology. Because AECs are high (average: 6,716; range: 1,850–30,609) and ANCAs are often undetectable (87%) in EGPA-associated EM, the clinical characteristics of EGPA-associated EM are similar to those of idiopathic HES (50). Thus, it is crucial to distinguish between the two because they differ in treatment and prognosis. EGPA and idiopathic HES can be differentiated based on vasculitis (clinical or histological). Our case review showed that patients with established EGPA-associated EM had a high prevalence of neurological involvement (52.6%, **Table 1**). Considering ANCA-negativity and the absence of significant vasculitis, our case was difficult to distinguish from idiopathic HES. Generally, asthma is not mandatory for the diagnosis of EGPA (3) and can also be found in patients with any variants of HES. Nevertheless, given that the overwhelming majority of patients with EGPA-associated EM have concomitant asthma of 94.7% as shown in **Table 1**, our case underscores the critical importance of preferentially considering EGPA as the causative etiology in cases of EM with asthma. A study analyzing 179 cases with histologically proven EM reported the prevalence of a history of asthma to be 68% in the EGPA group, 21% in the idiopathic/undefined group, and 23% in the HES group (51), which suggested that EGPA might not have been diagnosed due to the absence of obvious vasculitis in the latter two groups.

As a second clinical suggestion, both CMR and EMB were valuable for the final diagnosis of probable EGPA in our case.

CMR enables the characterization of myocardial tissue properties (inflammation, thrombus, and fibrosis) and yields high diagnostic performance in identifying acute myocarditis (81% sensitivity, 71% specificity, and 79% accuracy) (52). Typical CMR findings of EGPA-associated EM include subendocardial LGE in the apical and mid-left ventricles. In our case, the following unique CMR findings led to a strong suspicion of EGPA-associated EM. CMR revealed diffuse patchy subendocardial defects on FPP at rest, which were superimposed on abnormal lesions on LGE and T2-weighted images. Taken together, these observations were suggestive of microvascular dysfunction caused by acute inflammation, which was consistent with previous reports (53). Similar findings were observed in a patient with cardiac syndrome X, which is characterized by unexplained chest pain (54). Although coronary luminal stenosis, thrombus, or spasms have been proposed as possible causes of angina symptoms in patients with EGPA, the ACS-like symptoms reported in our case can be explained by microvascular dysfunction. Notably, in our case, multiple foci on the initial LGE were resolved following the corticosteroid treatment. Similar foci have been reported in some cases of EGPA-associated EM, and are presumed to be specific to vasculitis, which can be an indicator for EGPA-associated EM (35, 43, 55). Further studies on the relationship between foci on LGE and their respective pathologies are warranted. In addition, EMB provides useful information on the nature and distribution of inflammatory infiltrates. EGPA and HSM can be differentiated based on the histopathological findings. The histological features of EGPA include tissue eosinophilia, extravascular eosinophilic granuloma, and necrotizing vasculitis. However, the latter two are rarely seen in cardiac pathology (56) (**Table 1**), whereas HSM is characterized by interstitial prominent eosinophilic infiltrates without myocardial necrosis or fibrosis (57). The distinct pattern of endo/peri-myocardial eosinophilic infiltration and degranulation, accompanied by the presence of myocardial necrosis and fibrosis in EMB, was a crucial finding for the definitive diagnosis of acute EM and differentiating it from HSM. EMB is the golden standard for histological diagnosis of myocarditis, but it is an invasive method with limitations such as serious procedure-related complications or sampling errors. With an excellent diagnostic accuracy of CMR in acute myocarditis due to great advances in imaging technology, the usefulness of non-invasive CMR alone in diagnosing acute myocarditis has been widely reported (52, 58, 59). Therefore, a single approach of either CMR or EMB is now considered

TABLE 1 | Cases of EGPA-associated EM.

Author	Case	Age/sex	Clinical features (Extracardiac organ involvement)	Diagnosis at presentation	*Revised 2021 FFS	Laboratory findings		Cardiac Imaging		Myocardial histopathology	LGE pattern on CMR	Immunosuppressive treatment	Outcome
						AEC (%) [/mm^3]	ANCA status	LVEF [%]	PE				
Lie (9)	1	39/M	BA	SCD	na	na	na	na	na	NEM, Coronaritis	Not performed	Not performed	Died
Terasaki (10)	2	43/F	BA, CS, PNS	CI	2	16,285 (66%)	Present	Reduced	Present	EM	Not performed	GCs	Worsened
Ramakrishna (11)	3	34/F	BA, CS, ENT, PNS, Skin	Right ventricular thrombus, PN	0	3,660 (23%)	Absent	30–35	Absent	NEM, Granuloma	Not performed	pGCs/GCs	Improved
Hayashi (12)	4	26/F	BA, CS, ENT, Lung	CI	1	3,300 (29%)	Absent	19	Present	NEM	Not performed	pGCs/GCs	SCD
Schoppet (13)	5	50/F	BA, PNS	CI	2	na (39%)	na	30	Present	EM, Granuloma	Not performed	GCs/AZA	Partial cardiac recovery
Shanks (14)	6	51/F	BA, PNS, Skin	CS	2	5,600 (60%)	Absent	25	Present	EM	Not performed	GCs	Improved
Petersen (15)	7	53/F	BA, Lung	ACS	1	2,880 (60%)	Absent	na	Absent	Not performed	Diffuse SEndo	GCs	na
Ferrari (16)	8	25/M	None	CS	2	na (50%)	na	<30	Present	EM, Granuloma	Diffuse midwall	GCs/CYC	Partial cardiac recovery
Hervier (17)	9	42/na	BA, ENT	Abdominal pain	0	9,700 (60%)	Absent	na	Absent	NEM, Vasculitis	Not performed	Not performed	SCD due to VF
Setoguchi (18)	10	60/M	BA, PNS	ACS	2	Elevated	Absent	Preserved	Present	NEM, Vasculitis	Not performed	Not performed	SCD
Zardkoohi (19)	11	71/M	BA, CS, ENT, Lung, PNS	CS, ACS	2	1,850 (20%)	Absent	15	Absent	EM, Mural thrombus	Not performed	pGCs/GCs/MTX	Improved
Courand (20)	12	22/M	BA, CS, ENT, GI, Kidney, Lung	CS	2	7,700 (51%)	Absent	30	Present	Lymphocytic Myocarditis	Diffuse SEndo, patchy midwall	pGCs/GCs/pCYC/AZA	Improved
Levine (21)	13	85/F	BA, Joint, Muscle, PNS, Skin	Stroke	2	12,818 (58%)	Absent	57	Absent	EM	Partial SEndo	pGCs/GCs	SCD
McAleavey (22)	14	55/M	BA, ENT, Joint, Skin	Systemic vasculitis	0	15,750 (na)	Absent	Preserved	Present	Not performed	Partial SEndo	pGCs/GCs/CYC	Improved
Correia (23)	15	22/F	BA, CS, ENT, Lung, PNS	ACS	0	3,830 (na)	Absent	Preserved	Present	EM	Not performed	pGCs/GCs/CYC	Improved
Hara (24)	16	67/F	BA, PNS, Skin	CI, PN	2	10,450 (68%)	na	30	Absent	Not performed	SEndo	GCs/CYC	Partial cardiac recovery
Załeska (25)	17	55/M	BA, ENT, Lung	CI	1	3,880 (31%)	Absent	29	Present	Not performed	Diffuse SEndo, patchy midwall	GCs/CYC	Partial cardiac recovery
Bouiller (26)	18	63/F	BA, ENT	Chest Pain and dyspnea	0	3,480 (25%)	Absent	17	Present	EM, Mural thrombus	Patchy midwall and SEpi	pGCs/GCs/pCYC/AZA	Improved

(Continued)

TABLE 1 | Continued

Author	Case	Age/sex	Clinical features (Extracardiac organ involvement)	Diagnosis at presentation	*Revised 2021 FFS	Laboratory findings		Cardiac Imaging		Myocardial histopathology	LGE pattern on CMR	Immunosuppressive treatment	Outcome
						AEC (%) [/mm^3]	ANCA status	LVEF [%]	PE				
Bouabdallaoui (27)	19	21/M	BA, PNS	CS	2	4,470 (34%)	Absent	15	Absent	Not performed	Patchy SEndo, ICTh	pGCs/GCs	Partial cardiac recovery
Hase (28)	20	50/M	BA, ENT, Joint, Muscle, PNS, Skin	ACS	0	11,432 (55%)	Absent	30–40	Absent	EM	No LGE	GCs	No change
Beck (29)	21	75/F	BA, ENT	ACS	1	Elevated	Present	Preserved	Absent	EM	Diffuse SEndo, ICTh	GCs	Died
Ammirati (30)	22	25/M	ENT	CS	1	na (64%)	na	15	Absent	NEM	Patchy SEndo	pGCs/GCs/MTX	Partial cardiac recovery
Glaveckaite (31)	23	41/F	BA, ENT, PNS	Cardiac tamponade, PE	0	Elevated	na	<45%	Present	Not performed	Diffuse SEndo, ICTh	GCs/AZA	Improved
Bluett (32)	24	28/M	BA, CS, Lung	Perimyocarditis	1	3,400 (25%)	Absent	25	Absent	EM	Patchy SEndo	pGCs/GCs/Imanitib	Partial cardiac recovery
Plenzig (33)	25	51/M	BA, CS	SCD	2	na	na	na	na	EM, Granuloma	Not performed	na	Died
Dalia (34)	26	19/M	BA, ENT, Lung, PNS	AF with RVR	0	12,960 (45%)	Absent	55	Present	Not performed	Patchy midwall	pGCs/GCs/pCYC	Improved
Miyazaki (35)	27	60/M	BA, PNS	CI	2	15,310 (61%)	Absent	40	Absent	EM	Diffuse SEndo with Foci	pGCs/GCs/AZA	Improved
Ali (36)	28	65/F	BA, ENT, PNS, Skin	CI	2	23,000 (na)	Absent	28	Absent	EM	Patchy midwall	pGCs/GCs/AZA	Partial cardiac recovery
Ferreira (37)	29	65/F	BA, ENT, Muscle, PNS, Skin	Systemic vasculitis	1	11,280 (60%)	Absent	32	Present	Not performed	Patchy SEndo with Foci	pGCs/GCs/CYC	Improved
Dey (38)	30	60/F	BA, CS, ENT, Kidney, PNS, Skin	ACS	1	17,000 (69%)	Present	Preserved	Present	Not performed	Patchy midwall and Tm	pGCs/GCs/CYC/AZA	Improved
Chaudhry (39)	31	68/F	BA, ENT, GI, Kidney	CI, ischemic colitis	2	8,463 (39%)	Absent	20–25	Absent	NEM	Not performed	pGCs/GCs	Died
Gill (40)	32	44/F	BA, ENT, Lung	ACS	0	7,230 (42%)	na	na	Present	Not performed	Patchy SEndo	pGCs/GCs/CYC/AZA	Improved
Lopes (41)	33	22/M	BA, ENT, Lung, PNS	CI	1	11,700 (48%)	Absent	<30%	Absent	EM	Diffuse SEndo	pGCs/GCs/pCYC	Partial cardiac recovery
Civelli (42)	34	62/M	BA, CNS, GI, Kidney, Skin	CI	2	13,046 (46%)	Absent	18	Present	EM	Diffuse SEndo	pGCs/GCs/CYC	Improved
Colantuono (43)	35	19/M	BA, GI, PNS, Skin	Colitis	1	13,470 (na)	Absent	40	Absent	EM	Diffuse SEndo with Foci	pGCs/GCs/Benralizumab	Improved

(Continued)

TABLE 1 | Continued

Author	Case	Age/sex	Clinical features (Extracardiac organ involvement)	Diagnosis at presentation	*Revised 2021 FFS	Laboratory findings		Cardiac Imaging		Myocardial histopathology	LGE pattern on CMR	Immunosuppressive treatment	Outcome
						AEC (%) [/mm^3]	ANCA status	LVEF [%]	PE				
Higashitani (44)	36	46/F	BA, Lung, Muscle, PNS	Muscle weakness, CI	2	3,250 (na)	Absent	41	Present	EM	Patchy midwall	pGCs/GCs/RTX/MPZ	Partial cardiac recovery
Kurihara (45)	37	66/F	BA, PNS	CI	2	30,609 (86%)	Absent	40	Absent	EM	Not performed	GCs	na
Inaba (46)	38	61/M	BA, CNS, CS, ENT, Skin	Systemic vasculitis	0	7,788 (45%)	Present	Preserved	Absent	Not performed	Foci	pGCs/GCs/CYC/IVIG	Improved

EGPA, eosinophilic granulomatosis with polyangiitis; BA, bronchial asthma; CS, constitutional symptoms including fever, malaise, and weight loss; PNS, peripheral nervous system; ENT, ear-nose-throat; GI, gastrointestinal; CNS, central nervous system; SCD, sudden cardiac death; CI, cardiac insufficiency; PN, peripheral neuropathy; CS, cardiogenic shock; ACS, acute coronary syndrome; PE, pericardial effusion; AF with RVR, atrial fibrillation with rapid ventricular response; AEC, absolute eosinophilic count; ANCA, anti-neutrophil cytoplasmic antibodies; LVEF, left ventricular ejection fraction; LGE, late gadolinium enhancement; CMR, cardiac magnetic resonance; NEM, necrotizing eosinophilic myocarditis; EM, eosinophilic myocarditis; SEndo, subendocardial; SEpi, subepicardial; ICTh, intracardiac thrombosis; Tm, transmural; GCs, glucocorticoids; p, pulse; AZA, azathioprine; CYC, cyclophosphamide; MTX, methotrexate; RTX, rituximab; MPZ, mepolizumab, IVIG, intravenous immunoglobulin; VF, ventricular fibrillation; na, not available.

**Revised 2021 Five-Factor Score (FFS): The presence of each factor is given one point. The FFS score is converted to 0 if none of the factors are present, 1 if one factor is present, and 2 if two or more factors are present, respectively.*

sufficient for the diagnosis of acute myocarditis. However, each approach has its advantages and disadvantages in cases of acute EM that develops as the first manifestation of EGPA without clinical vasculitis as per our case. Therefore, our case underscores that the combination of CMR and EMB provides diagnostic synergy in the exploratory diagnosis of EGPA in patients with suspected acute EM.

Our final clinical suggestion is that timely corticosteroid treatment allowed significant recovery and normalization of the cardiac structure and function in our case.

The primary treatment for EGPA is systemic glucocorticoids. Additional immunosuppressive agents should be considered in patients with progressive, refractory, or relapsing diseases. Despite administering multiple immunomodulators, many cases of EGPA-associated EM were directly linked to fatal cardiac complications and incomplete recovery of cardiac function (**Table 1**). In our case, systemic and oral corticosteroids resulted in complete recovery and normalization of the cardiac structure and function within about 2 months. Considering the malignant features of EGPA-associated EM, our case underscores the significance of early recognition and treatment of this disease.

CONCLUSION

We present a case of probable EGPA with subclinical mononeuritis multiplex that developed acute EM and was successfully treated with systemic corticosteroid therapy. The EGPA-associated EM is a rare yet potentially life-threatening disorder that can be cured if treated appropriately and timely. However, without obvious vasculitis, accurate diagnosis of EGPA-associated EM is challenging. Therefore, clinicians should be aware of this rare disease and consider using both CMR and EMB diagnostic approaches for patients with suspected EM.

DATA AVAILABILITY STATEMENT

The original contributions presented in the study are included in the article/**Supplementary Materials**, further inquiries can be directed to the corresponding author/s.

ETHICS STATEMENT

Authorization for the use of case information and materials was obtained from the Institutional Review Board of Narita-Tomisato Tokushukai Hospital. The authors confirm that written consent for the submission and publication of this case report, including the images and associated movie, was obtained from the patient.

AUTHOR CONTRIBUTIONS

HY contributed in creating the clinical design and concept, interpreted the data, drafted, and revised the manuscript. HY, KH, and TH acquired the clinical data. JI performed the CMR analyses. YI performed the pathological analyses. All authors

discussed and approved the manuscript and authorized its submission for publication.

SUPPLEMENTARY MATERIAL

The Supplementary Material for this article can be found online at: https://www.frontiersin.org/articles/10.3389/fcvm.2022.913724/full#supplementary-material

Supplementary Figure 1 | ECG at admission **(A)** and on day 21 **(B)**. An initial ECG reveals evidence of pathologic Q waves in V2 to V3, and a significant left axis deviation at −57°, which is consistent with a left anterior fascicular block. Notably, the follow-up ECG after treatment of corticosteroid shows the resolution of all abnormal findings recognized during the initial ECG. ECG, electrocardiogram.

Supplementary Figure 2 | Clinical effects of the corticosteroid treatment on TTE. Follow-up TTE on day 56 after the corticosteroid therapy reveals a full recovery of the ventricular function and GLS values of the LV (LVDd, 49 mm; LVEF, 62%; GLS −16.1%, respectively) **(A–C)**. Ao, aorta; GLS, global longitudinal strain; LA, left atrium; LV, left ventricle; LVDd, left ventricular end-diastolic diameter; LVEF, left ventricular ejection fraction; TTE, transthoracic echocardiography.

Supplementary Figure 3 | A timeline for the case presentation. EGPA, eosinophilic granulomatosis with polyangiitis; EM, eosinophilic myocarditis; HES, hypereosinophilic syndrome; LGE, late gadolinium enhancement; LV, left ventricular.

Supplementary Video 1 | Pre-treatment transthoracic echocardiography. Transthoracic echocardiography at the initial presentation in a parasternal short-axis view reveals mild diffuse thickening of the left ventricular wall and decreased cavity size with a reduced ejection fraction of 43%.

Supplementary Video 2 | Pre-treatment myocardial first-pass perfusion deficits on CMR. Short-axis CMR imaging demonstrates that myocardial first-pass perfusion at rest shows patchy and circumferential subendocardial perfusion deficits. CMR: cardiac magnetic resonance.

Supplementary Video 3 | Post-treatment transthoracic echocardiography on day 21. Post-treatment follow-up transthoracic echocardiography in a parasternal short-axis view reveals significant resolution of the left ventricular wall thickening with concomitant improvement in cavity size and ventricular function with an ejection fraction of 50%.

Supplementary Video 4 | Post-treatment transthoracic echocardiography on day 56. Note the fully recovered cardiac function observed on echocardiography.

Supplementary Video 5 | Changes in myocardial first-pass perfusion deficits on CMR following corticosteroid treatment. Note the significant improvement in the abnormal first-pass perfusion deficits at admission on post-treatment follow-up CMR. CMR, cardiac magnetic resonance.

REFERENCES

1. Guillevin L, Cohen P, Gayraud M, Lhote F, Jarrousse B, Casassus P. Churg-Strauss syndrome. Clinical study and long-term follow-up of 96 patients. *Medicine*. (1999) 78:26–37. doi: 10.1097/00005792-199901000-00003
2. Neumann T, Manger B, Schmid M, Kroegel C, Hansch A, Kaiser WA, et al. Cardiac involvement in Churg-Strauss syndrome: impact of endomyocarditis. *Medicine*. (2009) 88:236–43. doi: 10.1097/MD.0b013e3181af35a5
3. Masi AT, Hunder GG, Lie JT, Michel BA, Bloch DA, Arend WP, et al. The American College of Rheumatology 1990 criteria for the classification of Churg-Strauss syndrome (allergic granulomatosis and angiitis). *Arthritis Rheum*. (1990) 33:1094–100. doi: 10.1002/art.1780330806
4. Mohammad AJ. An update on the epidemiology of ANCA-associated vasculitis. *Rheumatology*. (2020) 59(Suppl. 3):iii42–50. doi: 10.1093/rheumatology/keaa089
5. Conron M, Beynon HL. Churg-Strauss syndrome. *Thorax*. (2000) 55:870–7. doi: 10.1136/thorax.55.10.870
6. Ribi C, Cohen P, Pagnoux C, Mahr A, Arène JP, Lauque D, et al. French Vasculitis Study Group. Treatment of Churg-Strauss syndrome without poor-prognosis factors: a multicenter, prospective, randomized, open-label study of seventy-two patients. *Arthritis Rheum*. (2008) 58:586–94. doi: 10.1002/art.23198
7. Sada KE, Amano K, Uehara R, Yamamura M, Arimura Y, Nakamura Y, et al. A nationwide survey on the epidemiology and clinical features of eosinophilic granulomatosis with polyangiitis (Churg-Strauss) in Japan. *Mod Rheumatol*. (2014) 24:640–4. doi: 10.3109/14397595.2013.857582
8. Qiao L, Gao D. A case report and literature review of Churg-Strauss syndrome presenting with myocarditis. *Medicine*. (2016) 95:e5080. doi: 10.1097/MD.0000000000005080
9. Lie JT, Bayardo RJ. Isolated eosinophilic coronary arteritis and eosinophilic myocarditis. A limited form of Churg-Strauss syndrome. *Arch Pathol Lab Med*. (1989) 113:199–201.
10. Terasaki F, Hayashi T, Hirota Y, Okabe M, Suwa M, Deguchi H, et al. Evolution to dilated cardiomyopathy from acute eosinophilic pancarditis in Churg-Strauss syndrome. *Heart Vessels*. (1997) 12:43–8. doi: 10.1007/BF01747501
11. Ramakrishna G, Connolly HM, Tazelaar HD, Mullany CJ, Midthun DE. Churg-Strauss syndrome complicated by eosinophilic endomyocarditis. *Mayo Clin Proc*. (2000) 75:631–5. doi: 10.4065/75.6.631
12. Hayashi S, Furuya S, Imamura H. Fulminant eosinophilic endomyocarditis in an asthmatic patient treated with pranlukast after corticosteroid withdrawal. *Heart*. (2001) 86:E7. doi: 10.1136/heart.86.3.e7
13. Schoppet M, Pankuweit S, Maisch B. CD83+ dendritic cells in inflammatory infiltrates of Churg-Strauss myocarditis. *Arch Pathol Lab Med*. (2003) 127:98–101. doi: 10.5858/2003-127-98-CDCIII
14. Shanks M, Ignaszewski AP, Chan SY, Allard MF. Churg-Strauss syndrome with myocarditis manifesting as acute myocardial infarction with cardiogenic shock: case report and review of the literature. *Can J Cardiol*. (2003) 19:1184–8.
15. Petersen SE, Kardos A, Neubauer S. Subendocardial and papillary muscle involvement in a patient with Churg-Strauss syndrome, detected by contrast enhanced cardiovascular magnetic resonance. Heart. (2005) 91:e9. doi: 10.1136/hrt.2004.050070
16. Ferrari M, Pfeifer R, Poerner TC, Figulla HR. Bridge to recovery in a patient with Churg-Strauss myocarditis by long-term percutaneous support with microaxial blood pump. Heart. (2007) 93:1419. doi: 10.1136/hrt.2006.101881
17. Hervier B, Masseau A, Bossard C, Agard C, Hamidou M. Vasa-vasoritis of the aorta and fatal myocarditis in fulminant Churg-Strauss syndrome. *Rheumatology*. (2008) 47:1728–9. doi: 10.1093/rheumatology/ken329
18. Setoguchi M, Okishige K, Sugiyama K, Shimura T, Maeda M, Aoyagi H, et al. Sudden cardiac death associated with Churg-Strauss syndrome. *Circ J*. (2009) 73:2355–9. doi: 10.1253/circj.CJ-08-0926
19. Zardkoohi O, Hobbs R, Tan CD. A rare shock. *Am J Med*. (2011) 124:1019–22. doi: 10.1016/j.amjmed.2011.06.008
20. Courand PY, Croisille P, Khouatra C, Cottin V, Kirkorian G, Bonnefoy E. Churg-Strauss syndrome presenting with acute myocarditis and cardiogenic shock. *Heart Lung Circ*. (2012) 21:178–81. doi: 10.1016/j.hlc.2011.09.002
21. Levine AB, Kalliolias G, Heaney M, Endo Y, Gersten A, Weinsaft JW, et al. Churg-strauss syndrome with eosinophilic myocarditis: a clinical pathology conference held by the division of rheumatology at hospital for special surgery. *HSS J*. (2012) 8:313–9. doi: 10.1007/s11420-012-9276-x
22. McAleavey N, Millar A, Pendleton A. Cardiac involvement as the main presenting feature in eosinophilic granulomatosis with polyangiitis. *BMJ Case Rep*. (2013) 2013:bcr2013009394. doi: 10.1136/bcr-2013-009394
23. Correia AS, Gonçalves A, Araújo V, Almeida e Silva J, Pereira JM, Rodrigues Pereira P, et al. Churg-Strauss syndrome presenting with eosinophilic myocarditis: a diagnostic challenge. *Rev Port Cardiol*. (2013) 32:707–11. doi: 10.1016/j.repc.2012.10.017

24. Hara T, Yamaguchi K, Iwase T, Kadota M, Bando M, Ogasawara K, et al. Eosinophilic myocarditis due to Churg-Strauss syndrome with markedly elevated eosinophil cationic protein. *Int Heart J*. (2013) 54:51–3. doi: 10.1536/ihj.54.51
25. Załeska J, Wiatr E, Zych J, Szopiński J, Oniszh K, Kober J, et al. Severe congestive heart failure as the main symptom of eosinophilic granulomatosis and polyangiitis (Churg-Strauss syndrome). *Pneumonol Alergol Pol*. (2014) 82:582–9. doi: 10.5603/PiAP.2014.0077
26. Bouiller K, Samson M, Eicher JC, Audia S, Berthier S, Leguy V, et al. Severe cardiomyopathy revealing antineutrophil cytoplasmic antibodies-negative eosinophilic granulomatosis with polyangiitis. *Intern Med J*. (2014) 44:928–31. doi: 10.1111/imj.12525
27. Bouabdallaoui N, Arlet JB, Hagege AA. Cardiogenic shock, asthma, and hypereosinophilia. *Am J Emerg Med*. (2015) 33:309.e1–2. doi: 10.1016/j.ajem.2014.08.019
28. Hase H, Yamamoto T, Saito T, Yamazaki H, Kuno T, Tabei R, et al. Successful treatment using corticosteroids in early phase of eosinophilic myocarditis with eosinophilic granulomatosis with polyangiitis. *J Cardiol Cases*. (2016) 14:177–80. doi: 10.1016/j.jccase.2016.08.006
29. Beck KS, Jeong SY, Lee KY, Chang K, Jung JI. Native T1 Mapping Demonstrating Apical Thrombi in Eosinophilic Myocarditis Associated with Churg-Strauss Syndrome. *Korean Circ J*. (2016) 46:882–5. doi: 10.4070/kcj.2016.46.6.882
30. Ammirati E, Cipriani M, Musca F, Bonacina E, Pedrotti P, Roghi A, et al. A life-threatening presentation of eosinophilic granulomatosis with polyangiitis. *J Cardiovasc Med*. (2016) 17(Suppl. 2):e109–11. doi: 10.2459/JCM.0000000000000330
31. Glaveckaite S, Valeviciene N, Palionis D, Kontrimaviciute E, Lesinskas E. Heart involvement in Churg-Strauss syndrome. *Kardiol Pol*. (2017) 75:184. doi: 10.5603/KP.2017.0028
32. Bluett R, McDonnell D, O'Dowling C, Vaughan C. Eosinophilic myocarditis as a first presentation of eosinophilic granulomatosis with polyangiitis (Churg-Strauss syndrome). *BMJ Case Rep*. (2017) 2017:bcr2017221227. doi: 10.1136/bcr-2017-221227
33. Plenzig S, Heinbuch S, Held H, Verhoff MA, Lux C. A case of fatal perimyocarditis due to a rare disease. *Forensic Sci Med Pathol*. (2017) 13:454–458. doi: 10.1007/s12024-017-9920-3
34. Dalia T, Parashar S, Patel NV, Gautam A, Dai H, Bormann S. Eosinophilic myocarditis demonstrated using cardiac magnetic resonance imaging in a patient with eosinophilic granulomatosis with polyangiitis (Churg-Strauss Disease). *Cureus*. (2018) 10:e2792. doi: 10.7759/cureus.2792
35. Miyazaki M, Hattori H, Suzuki A, Serizawa N, Uto K, Fukushima K, et al. Successfully treated eosinophilic granulomatosis with polyangiitis relapse presenting as myocarditis and followed by multimodality imaging. *J Cardiol Cases*. (2018) 18:145–8. doi: 10.1016/j.jccase.2018.06.008
36. Ali D, Snead D, Dhakshinamurthy VA, Banerjee P. Rise and fall of the eosinophils in heart failure: a rare but important phenomenon seen with cardiomyopathy. *BMJ Case Rep*. (2018) 2018:bcr2017221081. doi: 10.1136/bcr-2017-221081
37. Ferreira RM, Madureira P, Pinho T, Martins E, Pimenta S, Costa L. Silent acute myocarditis in eosinophilic granulomatosis with polyangiitis. *Acta Reumatol Port*. (2018) 43:309–13.
38. Dey M, Nair J, Sankaranarayanan R, Kanagala P. Myopericarditis as a presentation of eosinophilic granulomatosus with polyangiitis (EGPA). *BMJ Case Rep*. (2019) 12:e230593. doi: 10.1136/bcr-2019-230593
39. Chaudhry MA, Grazette L, Yoon A, Correa A, Fong MW. Churg-Strauss syndrome presenting as acute necrotizing eosinophilic myocarditis: concise review of the literature. *Curr Hypertens Rev*. (2019) 15:8–12. doi: 10.2174/1573402114666180903164900
40. Gill JS, Fontana M, Knight D, Kalra SS. A case report of eosinophilic granulomatosis and polyangiitis myocarditis presenting as ST elevation myocardial infarction and showing positive response to immunotherapy. *Eur Heart J Case Rep*. (2019) 3:1–6. doi: 10.1093/ehjcr/ytz161
41. Lopes PM, Rocha BML, Cunha GJL, Ranchordas S, Albuquerque C, Ferreira AM, et al. Fulminant eosinophilic myocarditis: a rare and life-threatening presentation of eosinophilic granulomatosis with polyangiitis. *JACC Case Rep*. (2020) 2:802–8. doi: 10.1016/j.jaccas.2020.01.031
42. Civelli VF, Narang VK, Sharma R, Sharma R, Kim J, Bhandohal J, et al. A progressive case of eosinophilic myocarditis due to eosinophilic granulomatosis with polyangiitis in a caucasian male. *J Investig Med High Impact Case Rep*. (2020) 8:2324709620966855. doi: 10.1177/2324709620966855
43. Colantuono S, Pellicano C, Leodori G, Cilia F, Francone M, Visentini M. Early benralizumab for eosinophilic myocarditis in eosinophilic granulomatosis with polyangiitis. *Allergol Int*. (2020) 69:483–4. doi: 10.1016/j.alit.2020.03.001
44. Higashitani K, Yoshimi R, Sato Y, Watanabe T, Ihata A. Rituximab and mepolizumab combination therapy for glucocorticoid-resistant myocarditis related to eosinophilic granulomatosis with polyangiitis. *Mod Rheumatol Case Rep*. (2021) 6:87–92. doi: 10.1093/mrcr/rxab022
45. Kurihara K, Tsugawa J, Ouma S, Ogata T, Aoki M, Omoto M, et al. Eosinophilic granulomatosis with polyangiitis presenting with myocarditis as an initial symptom: a case report and review of the literature. *Case Rep Neurol*. (2021) 13:329–33. doi: 10.1159/000516255
46. Inaba R, Fuse Y, Kurimoto F, Suzuki S, Watanabe K. A rare case of eosinophilic granulomatosis with polyangiitis presenting as ischemic stroke and splenic infarction. *J Stroke Cerebrovasc Dis*. (2021) 30:105539. doi: 10.1016/j.jstrokecerebrovasdis.2020.105539
47. Gioffredi A, Maritati F, Oliva E, Buzio C. Eosinophilic granulomatosis with polyangiitis: an overview. *Front Immunol*. (2014) 5:549. doi: 10.3389/fimmu.2014.00549
48. Cottin V, Bel E, Bottero P, Dalhoff K, Humbert M, Lazor R, et al. Groupe d'Etudes et de Recherche sur les Maladies Orphelines Pulmonaires (GERM"O"P). Revisiting the systemic vasculitis in eosinophilic granulomatosis with polyangiitis (Churg-Strauss): a study of 157 patients by the Groupe d'Etudes et de Recherche sur les Maladies Orphelines Pulmonaires and the European Respiratory Society Taskforce on eosinophilic granulomatosis with polyangiitis (Churg-Strauss). *Autoimmun Rev*. (2017) 16:1–9. doi: 10.1016/j.autrev.2016.09.018
49. Klion A. Hypereosinophilic syndrome: approach to treatment in the era of precision medicine. *Hematology Am Soc Hematol Educ Program*. (2018) 2018:326–31. doi: 10.1182/asheducation-2018.1.326
50. Khoury P, Zagallo P, Talar-Williams C, Santos CS, Dinerman E, Holland NC, et al. Serum biomarkers are similar in Churg-Strauss syndrome and hypereosinophilic syndrome. *Allergy*. (2012) 67:1149–56. doi: 10.1111/j.1398-9995.2012.02873.x
51. Brambatti M, Matassini MV, Adler ED, Klingel K, Camici PG, Ammirati E. Eosinophilic myocarditis: characteristics, treatment, and outcomes. *J Am Coll Cardiol*. (2017) 70:2363–75. doi: 10.1016/j.jacc.2017.09.023
52. Lurz P, Eitel I, Adam J, Steiner J, Grothoff M, Desch S, et al. Diagnostic performance of CMR imaging compared with EMB in patients with suspected myocarditis. *JACC Cardiovasc Imaging*. (2012) 5:513–24. doi: 10.1016/j.jcmg.2011.11.022
53. Hansch A, Pfeil A, Rzanny R, Neumann T, Kaiser WA. First-pass myocardial perfusion abnormalities in Churg-Strauss syndrome with cardiac involvement. *Int J Cardiovasc Imaging*. (2009) 25:501–10. doi: 10.1007/s10554-009-9457-y
54. Panting JR, Gatehouse PD, Yang GZ, Grothues F, Firmin DN, Collins P, et al. Abnormal subendocardial perfusion in cardiac syndrome X detected by cardiovascular magnetic resonance imaging. *N Engl J Med*. (2002) 346:1948–53. doi: 10.1056/NEJMoa012369
55. Cui X, Peng Y, Liu J, Dong Y, Wu Z, Chen Y. Case report: area of focus of myocardial infarction with non-obstructive coronary arteries in eosinophilic granulomatosis with polyangiitis. *Front Cardiovasc Med*. (2021) 8:731897. doi: 10.3389/fcvm.2021.731897
56. Vaglio A, Buzio C, Zwerina J. Eosinophilic granulomatosis with polyangiitis (Churg-Strauss): state of the art. *Allergy*. (2013) 68:261–73. doi: 10.1111/all.12088
57. Fenoglio JJ Jr, McAllister HA Jr, Mullick FG. Drug related myocarditis. I. Hypersensitivity myocarditis. *Hum Pathol*. (1981) 12:900–7. doi: 10.1016/S0046-8177(81)80195-5
58. Ferreira VM, Schulz-Menger J, Holmvang G, Kramer CM, Carbone I, Sechtem U, et al. cardiovascular magnetic resonance in nonischemic myocardial inflammation: expert recommendations. *J Am Coll Cardiol*. (2018) 72:3158–76. doi: 10.1016/j.jacc.2018.09.072

59. Li S, Duan X, Feng G, Sirajuddin A, Yin G, Zhuang B, et al. Multiparametric cardiovascular magnetic resonance in acute myocarditis: comparison of 2009 and 2018lake louise criteria with endomyocardial biopsy confirmation. *Front Cardiovasc Med*. (2021) 8:739892. doi: 10.3389/fcvm.2021.739892

Conflict of Interest: The authors declare that the research was conducted in the absence of any commercial or financial relationships that could be construed as a potential conflict of interest.

Publisher's Note: All claims expressed in this article are solely those of the authors and do not necessarily represent those of their affiliated organizations, or those of the publisher, the editors and the reviewers. Any product that may be evaluated in this article, or claim that may be made by its manufacturer, is not guaranteed or endorsed by the publisher.

frontiers | Frontiers in Cardiovascular Medicine

TYPE Case Report
PUBLISHED 22 July 2022
DOI 10.3389/fcvm.2022.931054

OPEN ACCESS

EDITED BY
Maurizio Acampa,
Siena University Hospital, Italy

REVIEWED BY
Katrina Evers,
University Children's Hospital, Switzerland
Ibrahim El-Battrawy,
Ruhr University Bochum, Germany
Sadip Pant,
Saint Anne's Hospital, United States

*CORRESPONDENCE
Mathieu Boissan
mathieu.boissan@inserm.fr

†These authors have contributed equally to this work

SPECIALTY SECTION
This article was submitted to General Cardiovascular Medicine, a section of the journal Frontiers in Cardiovascular Medicine

RECEIVED 29 April 2022
ACCEPTED 04 July 2022
PUBLISHED 22 July 2022

CITATION
Ruiz P, Gabarre P, Chenevier-Gobeaux C, François H, Kerneis M, Cidlowski JA, Oakley RH, Lefèvre G and Boissan M (2022) Case report: Changes in the levels of stress hormones during Takotsubo syndrome.
Front. Cardiovasc. Med. 9:931054.
doi: 10.3389/fcvm.2022.931054

Case report: Changes in the levels of stress hormones during Takotsubo syndrome

Pablo Ruiz[1†], Paul Gabarre[2†], Camille Chenevier-Gobeaux[3], Hélène François[2,4], Mathieu Kerneis[5], John A. Cidlowski[6], Robert H. Oakley[6], Guillaume Lefèvre[1] and Mathieu Boissan[1,7*]

[1]Assistance Publique-Hôpitaux de Paris (AP-HP), Hôpital Tenon, Laboratoire de Biochimie, Paris, France, [2]Assistance Publique-Hôpitaux de Paris (AP-HP), Hôpital Tenon, Soins Intensifs Néphrologiques et Rein Aigu (SINRA), Paris, France, [3]Assistance Publique-Hôpitaux de Paris (AP-HP)-Centre Université de Paris, Hôpital Cochin, Department of Automated Biological Diagnostic, Paris, France, [4]Sorbonne Université, Inserm, UMR_S1155, Paris, France, [5]Sorbonne Université, ACTION Study Group, INSERM UMRS_1166, Institut de Cardiologie (AP-HP), Paris, France, [6]Signal Transduction Laboratory, National Institute of Environmental Health Sciences, National Institutes of Health, Research Triangle Park, NC, United States, [7]Sorbonne Université, Inserm, Centre de Recherche Saint-Antoine (CRSA), Paris, France

Background: Takotsubo syndrome is an acute cardiac condition usually involving abnormal regional left ventricular wall motion and impaired left ventricular contractility. It is due mainly to hyper-stimulation of the sympathetic nerve system, inducing an excess of catecholamines, usually triggered by intense psychological or physiological stress. The relationship between Takotsubo syndrome and the circulating stress hormones cortisol and copeptin (a surrogate marker of arginine vasopressin) has not been well documented.

Case summary: Here, we describe the dynamic changes in circulating cortisol and copeptin during an entire episode of Takotsubo syndrome in a post-partum woman after spontaneous vaginal delivery. The patient was diagnosed with inverted Takotsubo syndrome accompanied by HELLP syndrome. We found qualitative and quantitative changes in cortisol: a loss of circadian rhythm and a three-fold elevation in the plasma concentration of the hormone with a peak appearing several hours before circulating cardiac biomarkers began to rise. By contrast, levels of copeptin remained normal during the entire episode.

Discussion: Our findings indicate that the levels of cortisol change during Takotsubo syndrome whereas those of copeptin do not. This association between elevated cortisol and Takotsubo syndrome suggests that aberrant levels of this stress hormone may contribute to the observed cardiac pathology. We conclude that biochemical assays of circulating cortisol and cardiac biomarkers may be a useful complement to the diagnosis of Takotsubo syndrome by non-invasive cardiac imaging.

KEYWORDS

cortisol, copeptin, cardiac biomarkers, Takotsubo syndrome, case report

Introduction

Takotsubo syndrome is a type of acute heart failure that usually involves apical ballooning of the left ventricle but can also involve the right ventricle (1). This syndrome mainly affects post-menopausal women. It resembles acute coronary syndrome but usually occurs in the absence of obstructive coronary artery disease. One of the most important triggers of Takotsubo syndrome is intense psychological or physiological stress (2), which is generally considered a hallmark of the disease. Stress-induced hyperactivation of the sympathetic nervous system plays a central role in the pathophysiology by inducing excess catecholamines. Most documented cases of Takotsubo syndrome have been linked to a recognizable emotional or physiological trigger and excess catecholamine release (3–6).

The hypothalamic-pituitary-adrenal axis is the major neuroendocrine system that responds to psychological and physiological stress (7). The major stress hormones released by this system that are monitored in clinical practice are cortisol and arginine vasopressin. Although Takotsubo syndrome is a stress-induced cardiac disease, its effects on circulating cortisol and copeptin, a surrogate marker of arginine vasopressin, have not been well documented and have never been correlated with changes in cardiac biomarkers over the entire course of an episode of Takotsubo syndrome.

Here, we report a comprehensive analysis of the changes in levels of circulating stress hormones and cardiac biomarkers in a woman presenting with an unusual case of Takotsubo syndrome soon after spontaneous vaginal delivery of her baby. We found that the two stress hormones responded differently: the amount of cortisol peaked prior to the onset of cardiac necrosis, as indicated by increased levels of circulating troponin I and troponin T, while the amount of copeptin remained normal throughout the entire episode. This suggests that cortisol may be involved in the cardiac damage observed during Takotsubo syndrome and that this hormone may be a useful addition to the panel of markers used to confirm the initial diagnosis of this disease by cardiac imaging.

Methods

Levels of copeptin and cortisol in plasma samples collected in lithium heparin were assayed by using the KRYPTOR™ (ThermoFisher Scientific, Asnières sur Seine, France) and the Architect *ci 8200* (Abbott, Rungis, France) analyzers, respectively. Levels of copeptin (B·R·A·H·M·S™ Copeptin proAVP) were measured by using the TRACE technology and levels of cortisol (ARCHITECT Cortisol Reagent Kit) were measured using a mouse monoclonal antibody and a competitive one-step chemiluminescence method. Normal values of copeptin and cortisol (08:00 h) were <10 pmol/L and <550 nmol/L, respectively (manufacturer's data). Internal quality controls showed a precision of <6 % at 5 pmol/L and 100 pmol/L for copeptin and <9% at concentrations below 500 nmol/L for cortisol.

Levels of cardiac high-sensitivity troponin I (cTnIhs) and troponin T (cTnThs) in plasma samples collected in lithium heparin were assayed by using the Architect *ci 8200* (Abbott, Rungis, France) and Cobas E801 (Roche Diagnostics, Grenoble, France) analyzers, respectively. Both assays used specific antibodies for each cardiac isoform detected by chemiluminescence. Normal values of cTnIhs and cTnThs (women 99th percentile) were <15.6 ng/L and <9 ng/L, respectively (manufacturer's data). Internal quality controls showed a precision of <10% at 35 ng/L for cTnIhs and a precision of <10% at 13 ng/L for cTnThs. Plasma levels of N-terminal prohormone of brain natriuretic peptide (NT-proBNP) were assayed by a sandwich assay with ElectroChemiLuminescence (ECL) technology adapted to the Cobas E801 analyzer. Normal values of NT-proBNP (women 97.5th percentile) were <254 ng/L. Internal quality controls showed a precision of 4 % at 200 pmol/L and 850 pmol/L for NT-proBNP. Routine biochemical parameters in the blood samples were assayed by using the Architect *ci 8200* analyzer (Abbott, Rungis, France). Average values of these parameters over several days were presented as mean ± SD and compared to reference values (Z-test).

Case presentation

The details of this case were presented in a previous report (8). In brief, a 38-year-old woman (gravida 2, para 0) was admitted to the delivery unit after a normal pregnancy with no pregnancy-induced hypertension. She was in a good mood when she arrived in the labor room. She explained that this pregnancy was very important for her because of prior difficulty falling pregnant. Because of this difficulty, she had adopted a child the year before. She reported no significant medical history other than endometriosis that was responsible for an early miscarriage a few years ago. Physical examination and biochemical results at admission were normal and she delivered a healthy baby with no complications. However, just after the delivery, she became psychologically very stressed. She did not explain the reason for her distress. She only reported that a midwife acted unkindly just after the delivery.

Thirty hours after delivery, the patient complained of a strong headache accompanied by epigastric pain. Cardio-pulmonary and neurological examination was normal, but biochemical analyses indicated HELLP syndrome and acute renal failure associated with proteinuria, microangiopathic signs (thrombocytopenia, decrease of haptoglobin concentration) and hepatic cytolysis. The patient was admitted to the nephrology intensive care unit where, in addition to the typical HELLP syndrome, we found substantial elevation of

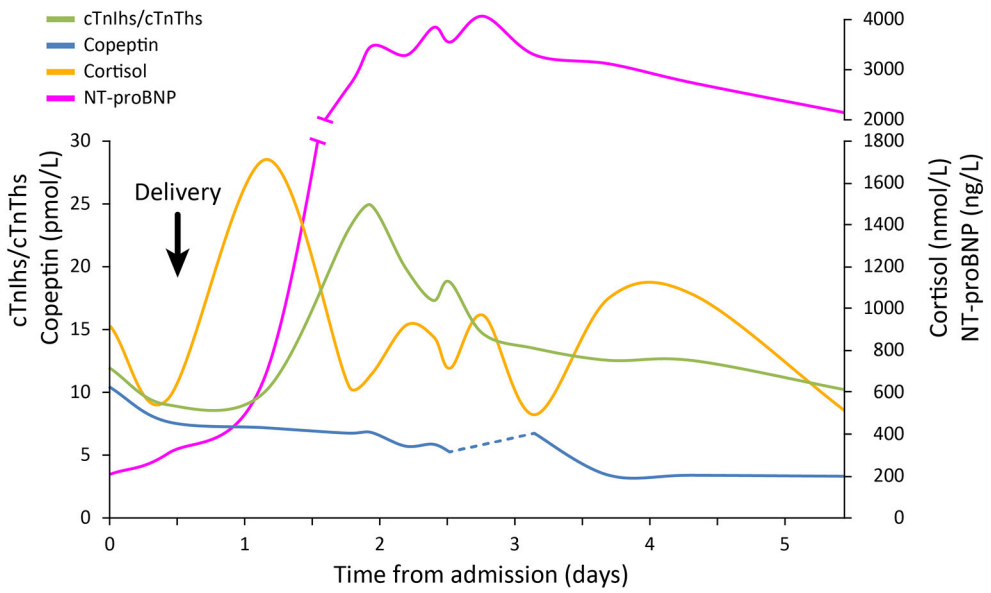

FIGURE 1
Changes in stress hormones and cardiac biomarkers during Takotsubo syndrome. Concentrations of circulating stress hormones and cardiac biomarkers were measured upon admission to hospital (day 0) and at intervals until day 5. The patient delivered her baby between day 0 and day 1 after admission. Ratio of cTnIhs/cTnThs was calculated from individual results expressed in ng/L.

the cardiac troponin I marker cTnIhs. A twelve-derivation electrocardiogram demonstrated no pathological features, but non-invasive cardiac imaging by coronary computed tomographic angiography, transthoracic echocardiography, and cardiovascular magnetic resonance imaging revealed inverted Takotsubo syndrome, a rare variant of this disease that presents with basal ballooning instead of apical ballooning.

Analysis of blood stress hormones in conserved plasma samples showed that copeptin levels remained normal throughout the entire episode of Takotsubo syndrome i.e. before and after the biological signs of cardiac involvement. The highest level of copeptin (10.5 pmol/L) was observed at admission, before delivery, but this was within the normal range, and the lowest level of copeptin (3.3 pmol/L) was observed at day 3. By contrast, the circadian rhythm of cortisol levels was probably affected from day 1 to day 3 since morning and evening concentrations were similar; for example, on day 2, cortisol was 920 nmol/L in the morning and 966 nmol/L in the evening. The normal rhythm was re-established on day 4. Quantitatively, the levels of circulating cortisol strongly increased between admission and day 1 peaking at 1,714 nmol/L very early in the morning of day 1. This elevation corresponded to a >3-fold increase in the maximal cortisol concentration usually observed at 08:00 h in healthy individuals (550 nmol/L). The peak of cortisol was observed several hours before the levels of circulating cardiac biomarkers began to increase (Figure 1). Levels of cTnIhs and cTnThs, indicative of cardiac necrosis, reached a peak 19 h after the peak of cortisol, with a ratio cTnIhs/cTnThs always >1, together with a peak in the level of natriuretic peptide NT-proBNP, indicative of cardiac stretching. Plasma concentrations of electrolytes (sodium, chloride, bicarbonates), urea, creatinine, total proteins, calcium, magnesium, and phosphorus remained within the normal ranges during the entire episode of Takotsubo syndrome from admission to day 5 (expressed as means ± SD: sodium, 137.8 ± 1.5 mmol/L; chloride, 104.6 ± 1.4 mmol/L; bicarbonates, 22.8 ± 1.7 mmol/L; urea, 4.1 ± 0.8 mmol/L; creatinine, 74.6 ± 10.9 µmol/L; total proteins, 67.9 ± 5.6 g/L; calcium, 2.13 ± 0.20 mmol/L; magnesium, 1.21 ± 0.43 mmol/L; phosphorus, 0.89 ± 0.22 mmol/L. See Table 1). By contrast, the concentrations of potassium ranging from 3.5–4.9 mmol/L (mean ± SD, 4.2 ± 0.4 mmol/L) were significantly different when compared to normal values ($P<0.05$). The calculated plasma osmolality (289–299 mosmol/L) was within the normal range (285–385 mosmol/L). Creatinine, a marker of renal failure when elevated, peaked 20 hours before the peak of cardiac biomarkers, but the increase of only 11%, corresponding to a small decrease in the estimated glomerular filtration rate from 72 to 63 mL/min/1.73 m^2, was not of the same magnitude as that of cTnIhs (+ 936 %), cTnThs (+ 233%), or NT-proBNP (+ 291 %); this moderate renal injury does not explain the huge elevation of cardiac biomarkers.

The patient was treated with a beta-blocker (labetalol) and an angiotensin-converting enzyme inhibitor (captopril), which normalized blood pressure.

10.3389/fcvm.2022.931054

TABLE 1 Changes in biochemical parameters in blood during Takotsubo syndrome.

Date	Hour	Sodium (mmol/L)	Potassium (mmol/L)	Chloride (mmol/L)	Bicarbonates (mmol/L)	TP (g/L)	Urea (mmol/L)	Creat. (μmol/L)	Calcium (mmol/L)	Phos. (mmol/L)	Mg (mmol/L)
			Pre-delivery								
Day 0	11:40 a.m.	138	4.90	106	23	58	4.7	89	N.D.	N.D.	N.D.
			Post-delivery								
Day 1	05:00 a.m.	139	4.29	106	19	74	5.2	77	N.D.	N.D.	N.D.
	07:55 p.m.	136	4.40	103	23	64	4.9	88	N.D.	N.D.	N.D.
	11:55 p.m.	136	4.40	102	23	70	4.6	98	2.07	0.87	1.82
Day 2	06:00 a.m.	137	3.60	103	24	61	4.1	76	1.86	0.68	1.87
	11:00 a.m.	138	3.50	104	26	64	3.4	72	1.90	0.66	1.43
	12:25 p.m.	138	3.90	106	23	63	3.2	70	1.90	0.70	1.32
	07:50 p.m.	136	4.41	105	24	69	2.6	70	2.06	0.71	1.13
Day 3	05:00 a.m.	136	4.30	104	24	68	3.4	69	2.19	N.D.	N.D.
Day 4	06:12 a.m.	139	4.50	107	21	70	3.8	66	2.27	0.97	1.02
Day 5	09:00 a.m.	140	4.30	105	24	77	3.8	69	2.37	1.01	0.88

TP, total proteins; Creat, creatinine; Phos, phosphorus; Mg, magnesium; N.D. not determined. Day 0 corresponds to the day of admission.

One month after discharge, transthoracic echocardiography was normal, indicating that the patient was in complete remission of her post-partum inverted Takotsubo syndrome. Three months after discharge, the patient was fully recovered, clinical examination was normal, and there was no hypertension or abnormalities in the blood analyses, thus the anti-hypertensive drugs were discontinued.

Discussion

In this case study, we measured both the circulating stress hormones copeptin and cortisol and cardiac biomarkers throughout an entire episode of Takotsubo syndrome. We found a substantial peak in the level of cortisol that preceded by 19 h a peak in biomarkers indicative of cardiac necrosis and stretching, whereas the levels of copeptin remained normal throughout. As stress is an important trigger of this syndrome and is generally considered a hallmark of the disease, our finding provides a biological correlate of stress that might be important for the pathophysiology of the syndrome and might be used to confirm the initial diagnosis of this disease by cardiac imaging.

Changes in stress hormones other than catecholamines in Takotsubo syndrome are very poorly documented in the literature. Whereas most reported studies measured stress hormones only at single timepoint, we have analyzed them throughout an episode from before its onset to its resolution. Moreover, we have compared the changes in these stress hormones with changes in cardiac biomarkers. Finally, we have documented the levels of both copeptin and cortisol. Thus the study enriches substantially the current literature on changes in these important stress hormones during Takotsubo syndrome.

Our patient became psychologically very stressed just after the delivery, which may have contributed to triggering Takotsubo syndrome. There is a general consensus that sudden and severe emotional or physical stress is a common factor in the etiology of the syndrome, by causing a surge in catecholamines that ultimately leads to acute left ventricular dysfunction [although it was reported recently that positive emotional events can also provoke Takotsubo syndrome (9)]. The Comorbidity Frequency in the Takotsubo Syndrome (COUNTS) study found that emotional and physical stress were triggers in 39 and 35%, respectively, of 1,109 patients with Takotsubo syndrome (10). In addition, this study revealed that patients with Takotsubo syndrome had a relatively high prevalence of psychological disorders (24%). Patients with Takotsubo syndrome have also been shown to have a high prevalence of chronic anxiety disorder that preceded onset of the disease (11). Moreover, anxiety and mood disorders are predictors of Takotsubo syndrome, possibly because they are associated with a higher risk of stressful events (12). Thus, chronic psychological stress may be a risk factor for Takotsubo syndrome whereas acute stress may ultimately trigger the syndrome.

Although emotional or physical stress is the most common trigger of Takotsubo syndrome, several reports have suggested other triggers of Takotsubo syndrome including hyper- and hypothyroidism. Thyrotoxicosis is the most frequent thyroid hormone condition linked to Takotsubo syndrome. Thyroid hormones sensitize the heart to catecholamines by stimulating expression of beta-adrenoceptors in cardiomyocytes. Thyrotoxicosis might then potentiate the effects of catecholamines on the myocardium, increasing its sensitivity to stress (13).

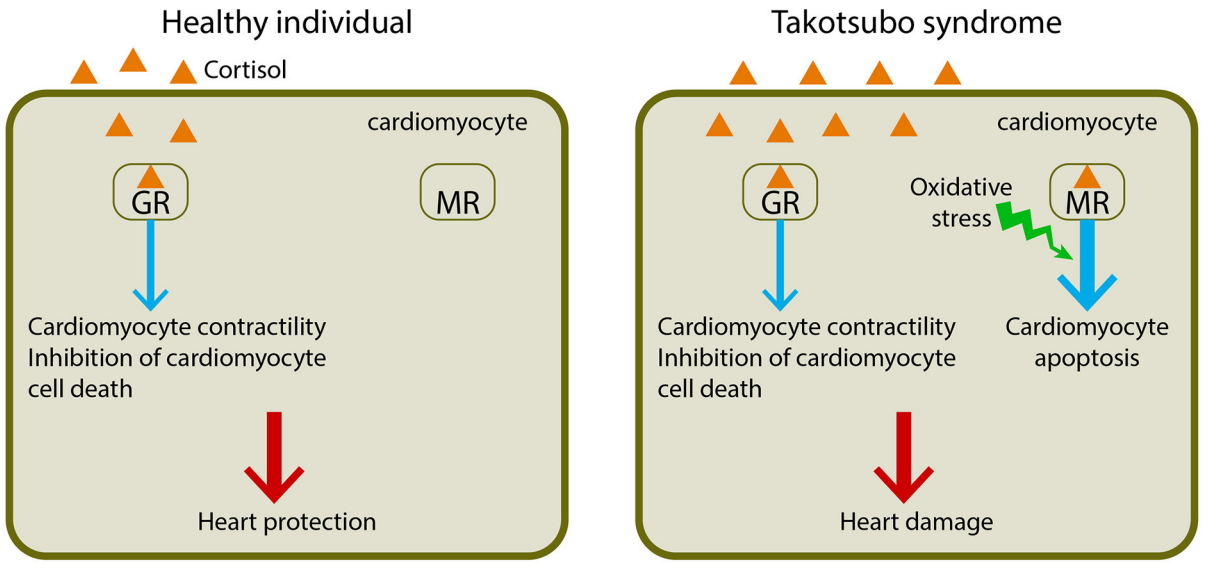

FIGURE 2
Dual effects of cortisol in cardiomyocyte function. Cortisol exerts its actions on the cardiomyocyte by binding two nuclear receptors, the glucocorticoid receptor (GR) and the mineralocorticoid receptor (MR). In a healthy individual, cortisol binds to the glucocorticoid receptor and activates its signaling, leading to enhanced cardiomyocyte contractility and inhibited cardiomyocyte death, thus protecting the heart. In a patient with Takotsubo syndrome, the increased cortisol binds not only to the glucocorticoid receptor but also to the mineralocorticoid receptor, leading to cardiomyocyte apoptosis in the presence of oxidative stress, which is often associated with Takotsubo syndrome, and thus resulting in heart damage.

Takotsubo syndrome is generally preceded by physical or emotional stress and the stress response is mainly mediated by activation of the hypothalamic-pituitary-adrenal axis. We expected, therefore, that both cortisol, released by the adrenal glands, and copeptin, released by the pituitary, would be elevated in our patient. Contrary to our expectations, however, the levels of copeptin remained normal during the entire episode of Takotsubo syndrome. This is consistent with the absence of change in sodium concentration and plasma osmolality, which arginine vasopressin would have modified by increasing water reabsorption and retention, thus resulting in hemodilution and dilutional hyponatremia. By contrast, we found qualitative and quantitative changes in cortisol: a likely loss of the circadian rhythm and a strong elevation in plasma concentration with a maximal value corresponding to a three-fold increase of the maximal concentration usually observed at 08:00h in normal individuals. In addition, cortisol peaked several hours before the circulating cardiac biomarkers began to increase. We cannot exclude the possibility that this elevated cortisol was due to pathophysiological stress associated with the postpartum HELLP syndrome rather than to emotional stress.

The rise in cortisol we measured in our patient with Takotsubo syndrome might be a protective mechanism to combat the adverse effects of excessive catecholamines on the heart and return it to homeostasis. Cortisol is a glucocorticoid steroid hormone. Glucocorticoids exert their actions on the heart by binding to the glucocorticoid receptor and the mineralocorticoid receptor in cardiomyocytes (14). In animals, increases in glucocorticoids and activation of signaling through the cardiomyocyte glucocorticoid receptor benefit the heart by enhancing cardiomyocyte contractility and inhibiting cardiomyocyte cell death (15–18). Conversely, deficient cardiac glucocorticoid receptor signaling leads to impaired contractility and left ventricular systolic dysfunction, which are the hallmarks of Takotsubo syndrome (19, 20). Thus, the increased cortisol in our patient might protect against these hallmarks.

An alternative interpretation, however, is that the rise in cortisol in our patient with Takotsubo syndrome exacerbates the heart pathology initially triggered by a catecholamine surge by activating signaling through the mineralocorticoid receptor (Figure 2), which promotes cardiomyocyte apoptosis and aggravates heart damage in the presence of oxidative stress (20–22). Growing evidence suggests Takotsubo syndrome is associated with increased production of reactive oxygen species, which may be involved in causing endothelial dysfunction leading to a transient impairment of myocardial contraction (23). The decreased potassium plasma levels from 4.4 to 3.6 mmol/L between day 1 and day 2 are consistent with this hypothesis and with a global activation of the mineralocorticoid signaling because activation of the mineralocorticoid receptor causes potassium excretion by the kidney. Ultimately, the severity and extent of the symptoms in Takotsubo syndrome may reflect the degree of imbalance between the positive and negative actions of cortisol on the heart.

Our finding that serum levels of copeptin were unaffected in our patient differs from a study of Takotsubo syndrome patients with atypical (midventricular) ballooning, which found significantly higher levels of copeptin than in patients with typical (apical) ballooning (24). Low copeptin levels were found, however, in two other studies of patients with Takotsubo syndrome (25, 26). Similar inconsistencies have been observed in studies of cortisol in patients with Takotsubo syndrome. In one study (27), evening plasma cortisol levels were elevated in 53% of patients with Takotsubo syndrome whereas the 24-h urine cortisol levels were normal in all patients, suggesting, like our study, that activation of the corticosteroid system is not sustained beyond the acute phase of the disease. Two other studies, however, found morning salivary cortisol levels were similar in patients with Takotsubo syndrome and in healthy individuals (28, 29).

Several factors may explain the divergent findings of our present study with others in the literature. First, the previous studies considered a single time-point, thus the transient elevation of cortisol may have been missed. The absolute amount of blood stress hormones is highly dependent on the interval between the onset of the disease (stress trigger) and blood sampling. One strength of our study is that blood samples for determination of these hormones were taken immediately after hospital admission and during all the hospital stay. Second, cortisol can be difficult to measure accurately because of its circadian rhythm and because most is bound to cortisol-binding globulin and albumin; only ∼10% of total plasma cortisol is unbound and biologically active (30). Plasma cortisol assays measure total cortisol (bound and unbound fractions) and their results can be misleading in patients with altered plasma protein concentrations. In our case, the plasma protein concentration of our patient was normal. Urinary and salivary cortisol measurements reflect changes in unbound plasma cortisol, but urinary cortisol is a useful index only of integrated 24-h plasma free cortisol because it is measured in urine collected over 24 h, and salivary cortisol levels reflect only 50–70% of plasma free cortisol due to the conversion of cortisol to cortisone in saliva; measurement of salivary cortisol is not yet used in routine clinical practice. Finally, the disparate findings may be attributed to differences in the analytical assays and cut-off values for what is considered normal.

Conclusion

Here, we describe the changes in circulating stress hormones and cardiac biomarkers during an unusual episode of Takotsubo syndrome in a post-partum woman after spontaneous vaginal delivery. Qualitative and quantitative changes in the levels of cortisol were seen: a loss of the circadian rhythm and strong elevation of the plasma concentration, with a peak several hours before the circulating cardiac biomarker levels began to rise. Levels of copeptin remained normal during the entire episode. Our findings indicate that measurement of the levels of the circulating stress hormone cortisol, in addition to cardiac biomarkers, by using biochemical assays routinely available in most non-specialized laboratories, may be a useful complement to the diagnosis of Takotsubo syndrome by non-invasive cardiac imaging. The beneficial or deleterious effects of cortisol on the heart in Takotsubo syndrome remain to be established in future studies.

Data availability statement

The original contributions presented in the study are included in the article/supplementary material, further inquiries can be directed to the corresponding author.

Ethics statement

Written informed consent was obtained from the individual for the publication of any potentially identifiable images or data included in this article.

Author contributions

PR and CC-G performed biological analyses. PG, HF, and MK performed physical examination and cardiac imaging. JC, RO, GL, and MB wrote the manuscript. MB supervised the study. All authors contributed to the article and approved the submitted version.

Acknowledgments

We thank Carol Featherstone of Plume Scientific Communication Services SAS for help with the preparation of the manuscript.

Conflict of interest

The authors declare that the research was conducted in the absence of any commercial or financial relationships that could be construed as a potential conflict of interest.

Publisher's note

References

1. El-Battrawy I, Santoro F, Stiermaier T, Moller C, Guastafierro F, Novo G, et al. Incidence and clinical impact of right ventricular involvement (biventricular ballooning) in takotsubo syndrome: results from the GEIST registry. *Chest.* (2021) 160:1433–41. doi: 10.1016/j.chest.2021.04.072

2. Templin C, Ghadri JR, Diekmann J, Napp LC, Bataiosu DR, Jaguszewski M, et al. Clinical features and outcomes of takotsubo (Stress) cardiomyopathy. *N Engl J Med.* (2015) 373:929–38. doi: 10.1056/NEJMoa1406761

3. Nojima Y, Kotani J. Global coronary artery spasm caused takotsubo cardiomyopathy. *J Am Coll Cardiol.* (2010) 55:e17. doi: 10.1016/j.jacc.2009.10.035

4. Munzel T, Knorr M, Schmidt F, von Bardeleben S, Gori T, Schulz E. Airborne disease: a case of a Takotsubo cardiomyopathie as a consequence of nighttime aircraft noise exposure. *Eur Heart J.* (2016) 37:2844. doi: 10.1093/eurheartj/ehw314

5. Stiermaier T, Moeller C, Oehler K, Desch S, Graf T, Eitel C, et al. Long-term excess mortality in takotsubo cardiomyopathy: predictors, causes and clinical consequences. *Eur J Heart Fail.* (2016) 18:650–6. doi: 10.1002/ejhf.494

6. Tornvall P, Collste O, Ehrenborg E, Jarnbert-Petterson H, A. Case-control study of risk markers and mortality in takotsubo stress cardiomyopathy. *J Am Coll Cardiol.* (2016) 67:1931–6. doi: 10.1016/j.jacc.2016.02.029

7. Smith SM, Vale WW. The role of the hypothalamic-pituitary-adrenal axis in neuroendocrine responses to stress. *Dialogues Clin Neurosci.* (2006) 8:383–95. doi: 10.31887/DCNS.2006.8.4/ssmith

8. Gabarre P, Ruiz P, Chenevier-Gobeaux C, Charpentier E, Soulat-Dufour L, Cohen A, et al. Inverted takotsubo syndrome with HELLP Syndrome: a case report. *Front Cardiovasc Med.* (2022) 9:832098. doi: 10.3389/fcvm.2022.832098

9. Stiermaier T, Walliser A, El-Battrawy I, Patz T, Mezger M, Rawish E, et al. Happy heart syndrome: frequency, characteristics, and outcome of Takotsubo syndrome triggered by positive life events. *JACC: Heart Failure.* (2022) 10:459–66. doi: 10.1016/j.jchf.2022.02.015

10. Pelliccia F, Parodi G, Greco C, Antoniucci D, Brenner R, Bossone E, et al. Comorbidities frequency in Takotsubo syndrome: an international collaborative systematic review including 1109 patients. *Am J Med.* (2015) 128:654. doi: 10.1016/j.amjmed.2014.11.014

11. Summers MR, Lennon RJ, Prasad A. Pre-morbid psychiatric and cardiovascular diseases in apical ballooning syndrome (tako-tsubo/stress-induced cardiomyopathy): potential pre-disposing factors? *J Am Coll Cardiol.* (2010) 55:700–1. doi: 10.1016/j.jacc.2009.10.031

12. El-Sayed AM, Brinjikji W, Salka S. Demographic and co-morbid predictors of stress (takotsubo) cardiomyopathy. *Am J Cardiol.* (2012) 110:1368–72. doi: 10.1016/j.amjcard.2012.06.041

13. Aweimer A, El-Battrawy I, Akin I, Borggrefe M, Mugge A, Patsalis PC, et al. Abnormal thyroid function is common in takotsubo syndrome and depends on two distinct mechanisms: results of a multicentre observational study. *J Intern Med.* (2021) 289:675–87. doi: 10.1111/joim.13189

14. Oakley RH, Cidlowski JA. Glucocorticoid signaling in the heart: a cardiomyocyte perspective. *J Steroid Biochem Mol Biol.* (2015) 153:27–34. doi: 10.1016/j.jsbmb.2015.03.009

15. Narayanan N, Yang C, Xu A. Dexamethasone treatment improves sarcoplasmic reticulum function and contractile performance in aged myocardium. *Mol Cell Biochem.* (2004) 266:31–6. doi: 10.1023/B:MCBI.0000049130.58074.73

16. Pearl JM, Nelson DP, Schwartz SM, Wagner CJ, Bauer SM, Setser EA, et al. Glucocorticoids reduce ischemia-reperfusion-induced myocardial apoptosis in immature hearts. *Ann Thorac Surg.* (2002) 74:830–6. doi: 10.1016/S0003-4975(02)03843-2

17. Rao MK, Xu A, Narayanan N. Glucocorticoid modulation of protein phosphorylation and sarcoplasmic reticulum function in rat myocardium. *Am J Physiol Heart Circ Physiol.* (2001) 281:H325–33. doi: 10.1152/ajpheart.2001.281.1.H325

18. Xu B, Strom J, Chen QM. Dexamethasone induces transcriptional activation of Bcl-xL gene and inhibits cardiac injury by myocardial ischemia. *Eur J Pharmacol.* (2011) 668:194–200. doi: 10.1016/j.ejphar.2011.06.019

19. Oakley RH, Ren R, Cruz-Topete D, Bird GS, Myers PH, Boyle MC, et al. Essential role of stress hormone signaling in cardiomyocytes for the prevention of heart disease. *Proc Natl Acad Sci U S A.* (2013) 110:17035–40. doi: 10.1073/pnas.1302546110

20. Oakley RH, Cruz-Topete D, He B, Foley JF, Myers PH, Xu X, et al. Cardiomyocyte glucocorticoid and mineralocorticoid receptors directly and antagonistically regulate heart disease in mice. *Sci Signal.* (2019) 12:9685. doi: 10.1126/scisignal.aau9685

21. Mihailidou AS, Loan Le TY, Mardini M, Funder JW. Glucocorticoids activate cardiac mineralocorticoid receptors during experimental myocardial infarction. *Hypertension.* (2009) 54:1306–12. doi: 10.1161/HYPERTENSIONAHA.109.136242

22. Rossier MF, Lenglet S, Vetterli L, Python M, Maturana A. Corticosteroids and redox potential modulate spontaneous contractions in isolated rat ventricular cardiomyocytes. *Hypertension.* (2008) 52:721–8. doi: 10.1161/HYPERTENSIONAHA.108.114223

23. Munzel T, Templin C, Cammann VL, Hahad O. Takotsubo Syndrome: Impact of endothelial dysfunction and oxidative stress. *Free Radic Biol Med.* (2021) 169:216–23. doi: 10.1016/j.freeradbiomed.2021.03.033

24. Burgdorf C, Schubert A, Schunkert H, Kurowski V, Radke PW. Release patterns of copeptin and troponin in Tako-Tsubo cardiomyopathy. *Peptides.* (2012) 34:389–94. doi: 10.1016/j.peptides.2012.01.022

25. Budnik M, Bialek S, Peller M, Kiszkurno A, Kochanowski J, Kucharz J, et al. Serum copeptin and copeptin/NT-proBNP ratio - new tools to differentiate takotsubo syndrome from acute myocardial infarction. *Folia Med Cracov.* (2020) 60:5–14. doi: 10.24425/fmc.2020.133481

26. Hojagergaard MA, Hassager C, Christensen TE, Bang LE, Gotze JP, Ostrowski SR, et al. Biomarkers in patients with Takotsubo cardiomyopathy compared to patients with acute anterior ST-elevation myocardial infarction. *Biomarkers.* (2020) 25:137–43. doi: 10.1080/1354750X.2019.1710767

27. Madhavan M, Borlaug BA, Lerman A, Rihal CS, Prasad A. Stress hormone and circulating biomarker profile of apical ballooning syndrome (Takotsubo cardiomyopathy): insights into the clinical significance of B-type natriuretic peptide and troponin levels. *Heart.* (2009) 95:1436–41. doi: 10.1136/hrt.2009.170399

28. Collste O, Tornvall P, Sundin O, Alam M, Frick M. No myocardial vulnerability to mental stress in Takotsubo stress cardiomyopathy. *PLoS One.* (2014) 9:e93697. doi: 10.1371/journal.pone.0093697

29. Kastaun S, Schwarz NP, Juenemann M, Yeniguen M, Nef HM, Moellmann H, et al. Cortisol awakening and stress response, personality and psychiatric profiles in patients with takotsubo cardiomyopathy. *Heart.* (2014) 100:1786–92. doi: 10.1136/heartjnl-2014-305745

30. El-Farhan N, Rees DA, Evans C. Measuring cortisol in serum, urine and saliva – are our assays good enough? *Ann Clin Biochem.* (2017) 54:308–22. doi: 10.1177/0004563216687335

frontiers | Frontiers in Cardiovascular Medicine

TYPE Case Report
PUBLISHED 09 August 2022
DOI 10.3389/fcvm.2022.947847

OPEN ACCESS

EDITED BY
Yan Zhang,
Peking University, China

REVIEWED BY
Quanyi Zhao,
Chinese Academy of Medical Sciences, China
Mao Zhang,
Stanford University, United States

*CORRESPONDENCE
Xijia Sun
xijia0822@163.com
Wenfei Tan
winfieldtan@hotmail.com

†These authors have contributed equally to this work

SPECIALTY SECTION
This article was submitted to General Cardiovascular Medicine, a section of the journal Frontiers in Cardiovascular Medicine

RECEIVED 19 May 2022
ACCEPTED 26 July 2022
PUBLISHED 09 August 2022

CITATION
Zhang Z, Jiang M, Sun X and Tan W (2022) Case report: Reducing the duration of positive-pressure ventilation for large mediastinal masses.
Front. Cardiovasc. Med. 9:947847.
doi: 10.3389/fcvm.2022.947847

Case report: Reducing the duration of positive-pressure ventilation for large mediastinal masses

Zaili Zhang, Meiru Jiang, Xijia Sun*† and Wenfei Tan*†

Department of Anesthesiology, The First Affiliated Hospital of China Medical University, Shenyang, China

Large mediastinal masses (MMs) are rare and present some challenges in hemodynamic and airway management under general anesthesia. Multiple studies have reported cardiopulmonary collapse during general anesthesia. Maintenance of spontaneous ventilation, avoidance of muscle relaxants, and awake-intubation were usually recommended during general anesthesia for high-risk patients with large MMs. However, the recent notion challenged the classic teaching that maintaining spontaneous ventilation is superior to positive-pressure ventilation (PPV). In our case reports, we present two patients with large MMs during general anesthesia. In the first case, a 21-year-old male was administered a muscle relaxant during induction, followed by PPV, but his blood oxygen saturation decreased to 40% after 20 min. Finally, his oxygen saturation was restored by a sternotomy rather than by cardiopulmonary bypass (CPB) by femoral vascular intubation. In the second case, a 33-year-old male was also administered a muscle relaxant during induction followed by PPV, but for him, sternotomy was immediately performed, with stable blood oxygen saturation. Both patients recovered well and were discharged from hospital a week after surgery. Therefore, we present a recommendation that patients with large MMs could undergo PPV after the administration of a muscle relaxant during induction, but the cardiothoracic surgeon should immediately cleave the sternum.

KEYWORDS

large mediastinal mass, positive-pressure ventilation, sternotomy, hyoxemia, case report

Introduction

Perioperative management for patients with large mediastinal masses (MMs) is challenging. There has been a focus on the mechanisms of central airway obstruction and cardiovascular instability in recent years. Several studies have recommended maintenance of spontaneous ventilation and awake intubation during general anesthesia

for high-risk patients with large MMs (1, 2). Despite more and more guidelines for the management of these patients, perioperative complications still exist. The aim of this article is to provide recommendations, including some experiences and lessons, with regard to the management of patients with large MMs. From our cases, it can be said that reducing the duration of positive-pressure ventilation (PPV) by emergency sternotomy is feasible.

Case presentation

Two high-risk patients with large MMs undergoing tumorectomy by thoracotomy at the First Affiliated Hospital of China Medical University received general anesthesia. No significant abnormalities had been observed on the pre-surgery laboratory tests (blood routine examination, liver function, renal function, hydrogen ion concentration in blood, coagulation function, and so on) and the electrocardiogram (ECG). Neither patient had a prior underlying medical history.

The first case was of a 21-year-old male admitted to our hospital because of a large MM (10.19 cm × 5.92 cm, **Figures 1a,b**); he was a high-risk patient. On 21 April 2020, he was admitted with no obvious symptoms and signs, but with a large MM shown on chest computed tomography (CT) at a local hospital. He had no history of drug allergies, contagious diseases, blood transfusion, surgery, or any other diseases. On the initial visit to the Cardiac Surgery department, his vital signs were as follows: temperature (T), 36.2°C; blood pressure (BP), 115/69 mmHg; heart rate (HR), 90 beats/min; and SPO_2, 98%. His general condition was not bad, and he had no obvious abnormality on cardiopulmonary auscultation. A diagnosis of a high-risk large anterior MM (tracheobronchial compression >50%) was made. The arch of the aorta was slightly compressed and pushed backwards, and the innominate vein and pulmonary artery were also slightly compressed. On 7 May 2020, the patient was not able to lie down prior to anesthesia without significant dyspnea. His initial vital signs in the operating room were as follows: BP, 130/80 mmHg; HR, 120 beats/min; and SPO_2, 91%. After the previous chest CT was carefully read, the patient was administered a muscle relaxant during induction followed by PPV. His blood oxygen saturation remained stable after PPV but gradually decreased to 40% after 20 min without significant changes in BP. The cardiothoracic surgeon performed cardiopulmonary bypass (CPB) by femoral vascular intubation, but the blood oxygen saturation only increased to 70%. Finally, the blood oxygen saturation increased to 100% after the cardiothoracic surgeon quickly cleaved the sternum. The pathological diagnosis of the anterior MM after surgery was T lymphoblastic lymphoma. The absence of significant neurological injury after surgery for the patient was due to the prompt rescue of the entire procedure.

The second case was of a 33-year-old male with a large MM (19.1 cm × 9.4 cm, **Figures 1c,d**); he was a high-risk patient too. On 15 February 2021, he was admitted with dyspnea and chest pain. He had no history of drug allergies, contagious diseases, blood transfusion, surgery, or any other diseases. On the initial visit to the Cardiac Surgery department, his vital signs were as follows: T, 36.6°C; BP, 139/78 mmHg; HR, 92 beats/min; and SPO_2, 98%. The breath sounds in the right lung were clear on auscultation, and the breath sounds in the left lung were weak, with audible rales. The patient had grade 3/6 systolic jet murmurs in the second intercostal space at the right margin of the sternum. The diagnoses were high-risk large anterior MM (tracheobronchial compression >50%), pericardial effusion, and pleural effusion. The left brachiocephalic vein was compressed and narrowed. The patient's pericardial effusion was improved preoperatively by pericardiocentesis. His initial vital signs in the operating room were as follows: BP, 120/70 mmHg; HR, 80 beats/min; and SPO_2, 98%. All puncture and disinfection procedures were performed under local anesthesia. Finally, the patient's sternum was immediately cleaved by the cardiothoracic surgeon after routine anesthesia induction. The patient was administered a muscle relaxant during induction followed by PPV for short periods, and he had a stable blood oxygen saturation. Ultimately, resection of the large MM was successfully performed following median sternotomy; the pathological diagnosis of the anterior MM after surgery was yolk sac tumor of the mediastinum.

Collectively, both patients recovered well and were discharged from hospital a week after surgery. Both patients reported a comfortable experience after the surgery process. In addition, they presented with no neurological injury after surgery.

Discussion

Patients with large MMs pose significant challenges due to the possible occurrence of respiratory insufficiency and hemodynamic decompensation. Li et al. (3) described that patients might be distributed into different risk categories, including low risk for asymptomatic patients, intermediate risk for those with tracheobronchial compression <50%, and high risk for those with a tracheobronchial compression >50%. Experts generally agree that low-risk patients tolerate general anesthesia without problems, while intermediate- or high-risk patients need an individualized approach. In the classic teaching, maintaining spontaneous ventilation throughout the procedure and finding a rescue position are the keys to management for intermediate- or high-risk patients (4, 5). Spontaneous ventilation can increase the transpleural pressure gradient, which can distend the intrathoracic airways and prevent collapse (6).

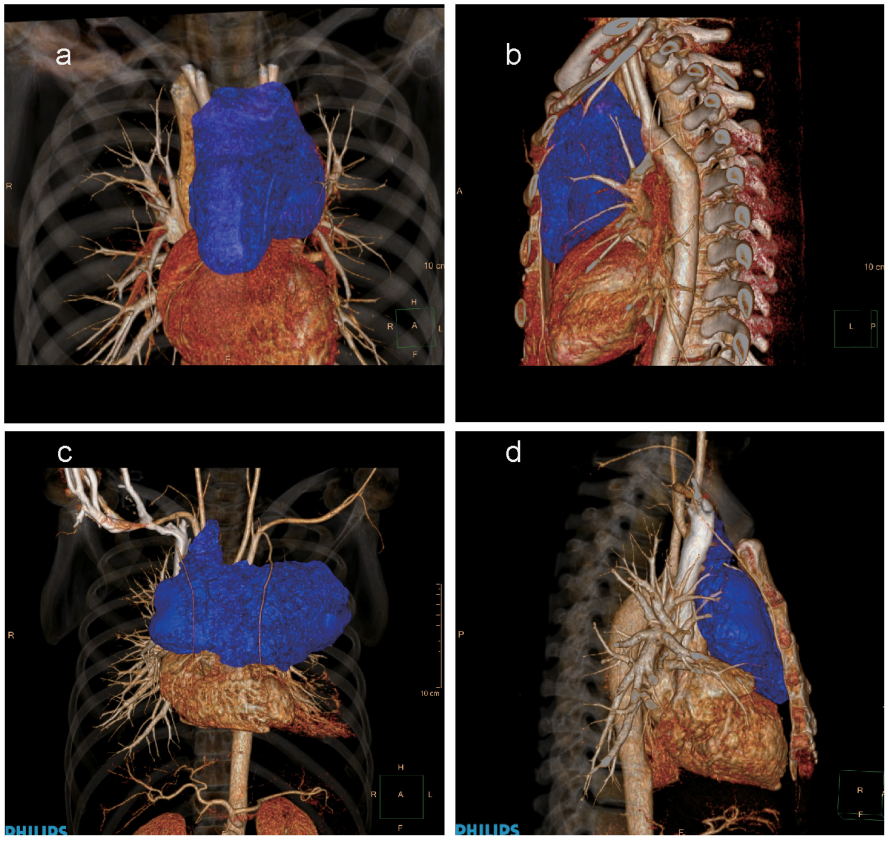

FIGURE 1
Three-dimensional computed tomography (CT) images of the large anterior mediastinal mass. **(a)** The anteroposterior CT image of the first patient (tumor represented in blue). **(b)** The lateral CT image of the first patient (tumor represented in blue). **(c)** The anteroposterior CT image of the second patient (tumor represented in blue). **(d)** The lateral CT image of the second patient (tumor represented in blue).

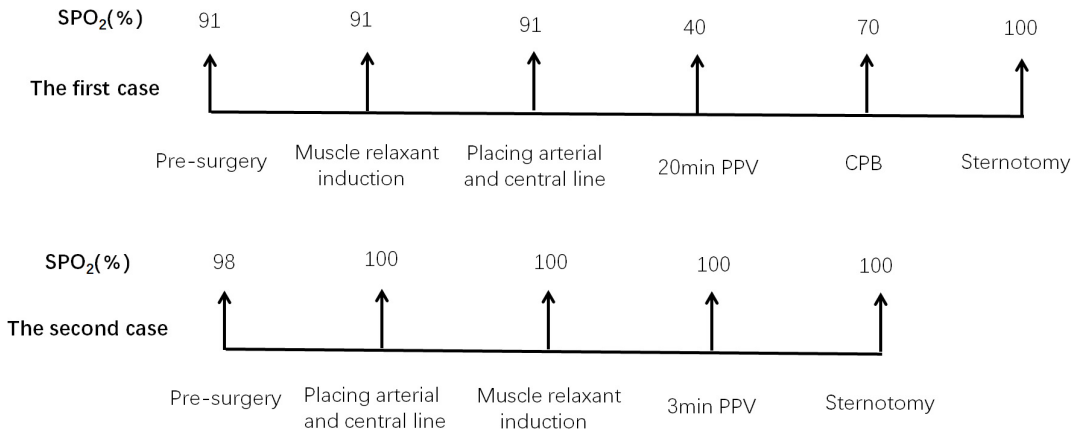

FIGURE 2
Summary of the entire process. PPV, positive-pressure ventilation; CPB, cardiopulmonary bypass.

A recent notion, published in the *New England Journal of Medicine*, challenged the classic teaching that maintaining spontaneous ventilation is superior to PPV (7). In addition, a prospective observational study also recommended that, in adult patients with large MMs and tracheobronchial compression, PPV and muscle relaxants could be instituted without

compromising central airway patency (8). We also support the notion above. However, some additional supplements should been recommended.

According to the analysis of the first case, blood oxygen saturation remained stable during the initial 20 min of PPV, and emergency sternotomy was an effective method for alleviating hypoxemia. It is suggested that PPV for short periods and emergency sternotomy are feasible for these patients. In addition, hypoxemia may be due to compression of the pulmonary artery by a large MM rather than airway collapse. For several authors, CPB is definitively the recommended modality (9). However, in the first case, hypoxemia was not significantly improved by CPB but by emergency sternotomy.

The first case had a few deficiencies. A large growing MM could not be accurately evaluated by chest CT one month before surgery. It is regrettable that we did not re-examine the chest CT and assess the symptoms. If all puncture and disinfection procedures were performed under local anesthesia, the patient's sternum was immediately cleaved by the cardiothoracic surgeon after muscle relaxant administration and PPV for short periods, and the whole anesthesia procedure may have been quite successful. As a result of the anesthesia lessons learned from the first case, we reduced the duration of PPV by performing emergency sternotomy in the second case. There is no doubt that the whole process was successful in the second case (**Figure 2**).

Based on our cases and the relevant literature, we recommend that patients with large MMs undergo PPV after induction with muscle relaxant administration, but the cardiothoracic surgeon should immediately cleave the sternum. The protocol was as follows: all puncture and disinfection procedures were performed under local anesthesia; the patient was administered a muscle relaxant during induction, and PPV for short periods; and the cardiothoracic surgeon immediately cleaved the patient's sternum and finished the tumorectomy. The anesthetic induction protocols for this study were consistent with those of Hartigan et al. (7, 8); however, reducing the duration of PPV by emergency sternotomy after administration of a muscle relaxant during induction was also our concern suggestion. Most patients with large MMs will not only have difficult induction of anesthesia but the subsequent maintenance of anesthesia and surgery are challenging too. Hartigan et al. emphasized that the duration of observation for each phase in their study was relatively brief, so they could not confirm the results of prolonged PPV. Therefore, there is no definite time for the PPV before sternotomy, but the less time the better the results.

Conclusion

In conclusion, we recommend that patients with a large MM should undergo PPV for short periods after the administration of a muscle relaxant during induction, but the cardiothoracic surgeon should cleave the sternum immediately to relieve compression.

Ethics statement

Written informed consent was obtained from the individual(s) for the publication of any potentially identifiable images or data included in this article.

Author contributions

ZZ: conceptualization, investigation, and writing – original draft. MJ: project administration and investigation. XS and WT: conceptualization and writing – review and editing. All authors contributed to the article and approved the submitted version.

Conflict of interest

The authors declare that the research was conducted in the absence of any commercial or financial relationships that could be construed as a potential conflict of interest.

Publisher's note

References

1. Stubblefield J, Moon T, Griffin J. A large anterior mediastinal mass. *Anesthesiology.* (2018) 128:637. doi: 10.1097/ALN.0000000000001931

2. Stricker PA, Gurnaney HG, Litman RS. Anesthetic management of children with an anterior mediastinal mass. *J Clin Anesth.* (2010) 22:159–63. doi: 10.1016/j.jclinane.2009.10.004

3. Li WW, van Boven WJ, Annema JT, Eberl S, Klomp HM, de Mol BA. Management of large mediastinal masses: Surgical and anesthesiological considerations. *J Thorac Dis.* (2016) 8:E175–84. doi: 10.21037/jtd.2016.02.55

4. Niimi N, Kataoka K, Hayashida M, Inada E. The dynamic collapse of the trachea during anesthesia for a pediatric patient with a large anterior mediastinal mass: A case report. *Clin Case Rep.* (2020) 8:1814–5. doi: 10.1002/ccr3.3005

5. Pearson JK, Tan GM. Pediatric anterior mediastinal mass: A review article. *Semin Cardiothorac Vasc Anesth.* (2015) 19:248–54. doi: 10.1177/1089253215578931

6. Blank RS, de Souza DG. Anesthetic management of patients with an anterior mediastinal mass: Continuing professional development. *Can J Anaesth.* (2011) 58:853–67. doi: 10.1007/s12630-011-9539-x

7. Hartigan PM, Ng JM, Gill RR. Anesthesia in a patient with a large mediastinal mass. *N Engl J Med.* (2018) 379:587–8. doi: 10.1056/NEJMc1804797

8. Hartigan PM, Karamnov S, Gill RR, Ng JM, Yacoubian S, Tsukada H, et al. Mediastinal masses, anesthetic interventions, and airway compression in adults: A prospective observational study. *Anesthesiology.* (2022) 136:104–14. doi: 10.1097/ALN.0000000000004011

9. Tanaka T, Amano H, Tanaka Y, Takahashi Y, Tajiri T, Tainaka T, et al. Safe diagnostic management of malignant mediastinal tumors in the presence of respiratory distress: A 10-year experience. *BMC Pediatr.* (2020) 20:292. doi: 10.1186/s12887-020-02183-w

frontiers | Frontiers in Cardiovascular Medicine

TYPE Case Report
PUBLISHED 07 September 2022
DOI 10.3389/fcvm.2022.970045

OPEN ACCESS

EDITED BY
Junjie Xiao,
Shanghai University, China

REVIEWED BY
Bernhard Maisch,
University of Marburg, Germany
Ashraf Hamdan,
Rabin Medical Center, Israel

*CORRESPONDENCE
Guo-zhong Zhang
zhanggz3@126.com
Bin Cong
hbydbincong@126.com

†These authors have contributed equally to this work and share first authorship

SPECIALTY SECTION
This article was submitted to General Cardiovascular Medicine, a section of the journal Frontiers in Cardiovascular Medicine

RECEIVED 15 June 2022
ACCEPTED 18 August 2022
PUBLISHED 07 September 2022

CITATION
Dong Y-m, Liu X, Yang C-t, Qi Q, Shi W-b, Li Y-m, Zuo M, Wang S-j, Bi H-t, Ma R-f, Zhang G-z and Cong B (2022) Case report: Myocarditis following COVID-19 protein subunit vaccination.
Front. Cardiovasc. Med. 9:970045.
doi: 10.3389/fcvm.2022.970045

Case report: Myocarditis following COVID-19 protein subunit vaccination

Yi-ming Dong†, Xia Liu†, Chen-teng Yang, Qian Qi, Wei-bo Shi, Ying-min Li, Min Zuo, Song-jun Wang, Hai-tao Bi, Ru-fei Ma, Guo-zhong Zhang* and Bin Cong*

Hebei Key Laboratory of Forensic Medicine, Collaborative Innovation Center of Forensic Medical Molecular Identification, Department of Forensic Medicine, Hebei Medical University, Shijiazhuang, China

We report findings in a 34-year-old female patient who presented with fulminant myocarditis 8 days after receiving the first dose of the ZF2001 RBD-subunit vaccine against coronavirus disease 2019 (COVID-19). Autopsy showed severe interstitial myocarditis, including multiple patchy infiltrations of lymphocytes and monocytes in the myocardium of the left and right ventricular walls associated with myocyte degeneration and necrosis. This report highlights the details of clinical presentations and autopsy findings of myocarditis after ZF2001 (RBD-subunit vaccine) vaccination. The correlation between vaccination and death due to myocarditis is discussed.

KEYWORDS

adverse event, myocarditis, COVID-19, protein subunit vaccine, autopsy

Introduction

Based on the rapid spread of coronavirus disease 2019 (COVID-19), there is an urgent need for effective vaccines to provide global immunity. Therefore, the world has been racing to develop safe and effective COVID-19 vaccines. Currently, there are six types of COVID-19 vaccines, such as inactivated vaccine, viral vector-based vaccine, subunit vaccine, live-attenuated vaccine, DNA vaccine, and mRNA vaccine (1).

Extensive clinical data suggest a strong association between COVID-19 mRNA vaccination with and myocarditis or myopericarditis (2, 3). There have been several reports of cases of myocarditis and pericarditis following COVID-19 mRNA vaccination, mainly in young males (4–6). However, myocarditis and pericarditis after COVID-19 recombinant protein vaccination has rarely been reported. This report describes a case of myocarditis following ZF2001 (Anhui Zhifei Longcom/Chinese Academy of Sciences) vaccination in a 36-year-old female patient.

Case presentation

A 36-year-old woman received her first dose of the COVID-19 vaccine (ZF2001) in April 2021. She developed nausea, vomiting, and diarrhea on the 3rd day after

vaccination and fever on the 5th day, with the highest temperature of 39.8°C accompanied by chills, dizziness, and nausea. On the 8th day, she visited a local doctor due to vomiting and fever. Her nasopharyngeal swab test for the new coronavirus nucleic acid was negative for the new coronavirus *ORF1ab* gene and the new coronavirus *N* gene. Cardiopulmonary computerized tomography (CT) showed no abnormalities. Abdomen CT showed fatty liver. She was given levofloxacin anti-infective treatment for 3 days, but her fever was persistent. On the 10th day after vaccination, blood chemistry tests showed an elevated myocardial enzyme (peak creatin-kinase 404 U/L, creatin-kinase MB 30 U/L, and lactate dehydrogenase 228 U/L), increased neutrophil ratio (79.1%), increased erythrocyte sedimentation rate (ESR) (70 mm/h), increased fibrinogen content (5.62 g/L), increased activated partial thromboplastin time (36.0 s). Electrocardiogram (ECG) showed bigamy and right bundle branch block. Chlamydia pneumoniae, Mycoplasma pneumoniae, herpes simplex virus, respiratory syncytial virus, adenovirus, and Coxsackie B virus antibody tests were negative. She was diagnosed with acute myocarditis. On the 11th day, her body temperature was 35.5°C and the arterial blood pressure was 81/59 mmHg. ECG monitoring showed bundle branch block and frequent premature and ventricular contractions. Blood tests showed elevated biomarkers of myocardial damage (peak creatin-kinase 1472 U/L, creatin-kinase MB 112 U/L, and lactate dehydrogenase 578 U/L). Fulminant myocarditis complicated by heart failure, arrhythmia, and a state of shock were considered. Supportive treatments with continued anti-infection medication were given. The right subclavian vein was catheterized, and arterial blood pressure and cardiac output were monitored. The patient suffered from sudden onset convulsions/seizure actives and received anti-seizure medication. ECG showed accelerated ventricular spontaneous rhythm and widened QRS, indicating severe myocardial damage. Color Doppler ultrasound showed poor cardiac function and abnormal ventricular wall motion, which further supported the diagnosis of fulminant myocarditis. The patient underwent right femoral vein puncture due to heart failure and renal insufficiency to perform bedside hemofiltration. On the 12th day, bedside ultrasound showed that the overall systolic function of the heart was reduced. The patient developed lactose acidosis and her blood pressure dropped. Blood tests showed raised biomarkers of myocardial damage (peak creatin-kinase 1727 U/L, creatin-kinase MB 223 U/L, and lactate dehydrogenase 3261 U/L). The patient developed ventricular fibrillation, bilateral mydriasis, loss of light reflex, persistently low blood pressure, and received chest compressions and extracorporeal membrane oxygenation (ECMO) therapy. Her condition deteriorated rapidly despite intensive medical treatments and supportive care. The patient died 12 days after COVID-19 vaccination.

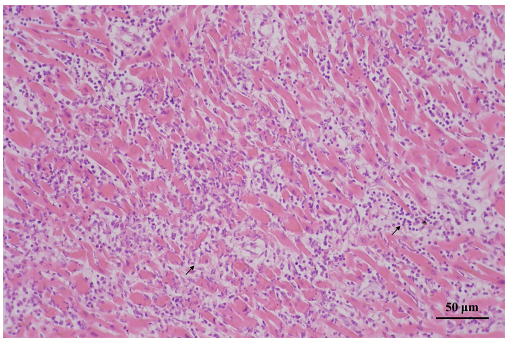

FIGURE 1
Myocardial degeneration and necrosis; myocardial interstitium is mainly infiltrated by lymphocytes and monocytes (arrows).

A forensic autopsy was requested by her family because of the temporal relationship between COVID-19 vaccination and her death. The post-mortem study revealed light yellow effusion in the bilateral pleural cavities, 400 ml in the left, and 350 ml in the right. There was no thrombus in the pulmonary arteries. There was 70 ml of light-yellow effusion in the pericardial sac. The heart weighed 338.1 g, and the left anterior descending coronary artery and the right coronary artery had mild atherosclerosis. The spleen capsule was slightly shrunken, and the cut surface was pale. There was focal peripancreatic tissue hemorrhage, but no obvious hemorrhage was seen on the cut surface. No special structural finding was observed in the other organs.

Histological examination revealed that the left anterior descending coronary artery and the right coronary artery had mild atherosclerotic stenosis; the heart showed multi-focal inflammatory infiltration, mainly lymphocytes and monocytes associated myocyte degeneration and necrosis of both left and right ventricular walls (**Figure 1**). Histological examination of the tissues confirmed myocarditis. Immunohistochemical staining of heart section showed occasional spike RBD positive cardiomyocytes, infiltrating immune cells and vascular endothelial cells (**Figures 2A–C**). The lungs showed edema with local inflammatory cell infiltration (**Supplementary Figure 1**). Intracerebral vascular filling was poor, and the perivascular space was enlarged (**Supplementary Figure 2A**). The liver showed steatosis. The liver showed autolysis (**Supplementary Figure 2B**). In addition, Toluidine blue staining of the larynx, epiglottis, gastrointestinal, myocardium, lungs, and other tissues showed no mast cell infiltration or degranulation (**Supplementary Figure 3**).

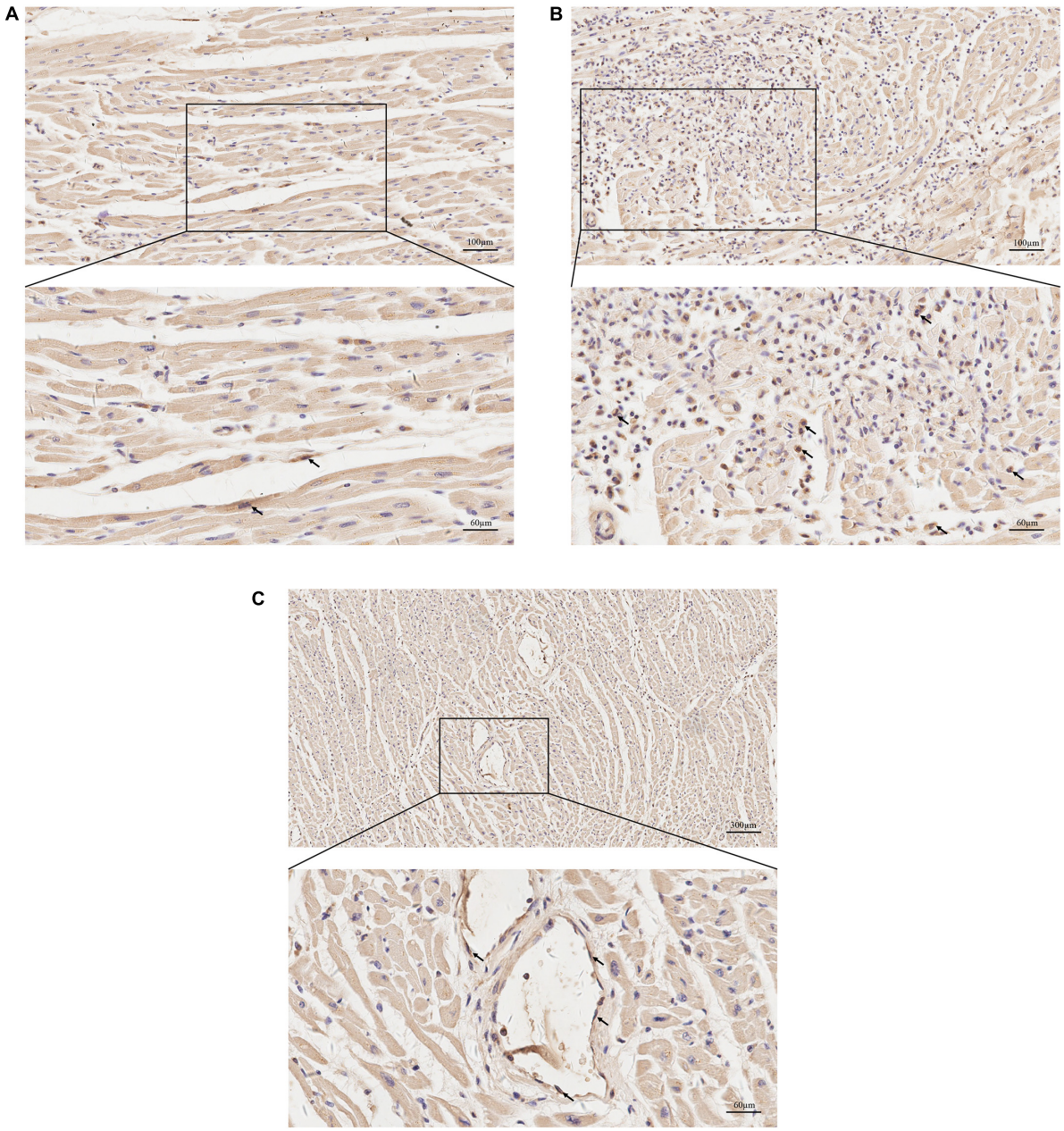

FIGURE 2
Immunohistochemical staining for protein expression of spike receptor binding domain (RBD) in heart sections. **(A)** Representative images of immunohistochemical staining of heart section showed occasional spike RBD positive cardiomyocytes (arrows). **(B)** Representative images showing spike RBD expression in the infiltrating immune cells in myocardium (arrows). **(C)** Representative images showing spike RBD expression in the vascular endothelial cells in myocardium (arrows).

Discussion

On July 9, 2021, the WHO Global Advisory Committee on Vaccine Safety (GACVS) COVID-19 subcommittee published a report on myocarditis and pericarditis following COVID-19 mRNA vaccination, usually after the second dose of mRNA COVID-19 vaccine (7). Data showed that the estimated incidence of cardiac inflammation per 100,000 doses of CoronaVac (inactivated virus vaccine) and BNT162b2 (mRNA vaccine) was 0.31 (95% CI, 0.13–0.66) and 0.57 (CI, 0.36–0.90), respectively (8). Literature also reported that the risk of myocarditis and pericarditis increased after vaccination with an mRNA COVID-19 vaccine, and some scholars have proposed that the use of viral vector vaccine alternatives

may reduce the occurrence of myocardial damage after vaccination (9).

Current studies suggest that the possible pathogenesis of mRNA COVID-19 vaccine-induced myocarditis is mainly molecular mimicry and delayed allergic reaction (10). An important underlying mechanism of myocarditis after mRNA COVID-19 vaccination is the molecular mimicry between the spike protein of the novel severe acute respiratory syndrome coronavirus (SARS-CoV-2) and self-antigens (11). The surface spike protein of SARS-CoV-2 serves as an mRNA vaccine-encoded immunogenic target that may induce immune cross-reactivity through molecular mimicry of live virus infection (12). Elevated levels of cardioreactive autoantibodies have been reported in patients with myocarditis following COVID-19 vaccination (13). These antibodies may target multiple antigens, and when cells cannot distinguish between foreign and self-peptides, pro-inflammatory cytokine responses are dysregulated, resulting in immune damage to the host. Another possible hypothesis is delayed hypersensitivity. Phagocytic and eosinophilic infiltration and mild peripheral eosinophilia were found in cardiac tissue of patients following COVID-19 vaccination (4). In fact, the patients may have been sensitized by the first dose of the vaccine and may have then experienced delayed hypersensitivity reactions following the second dose. This would explain why most patients did not develop symptoms of myocarditis until 2–4 days after the second dose of the vaccine.

Most reported patients with myocarditis following COVID-19 vaccination were vaccinated with mRNA vaccines, and myocarditis caused by other types of COVID-19 vaccines was rarely reported. A case-control study of the risk of carditis associated with two different types of COVID-19 vaccines found an increased risk of myocarditis after mRNA COVID-19 vaccination, but no association between inactivated virus vaccines and myocarditis was reported in the literature (8). The patient reported in this article was vaccinated with the protein subunit COVID-19 vaccine (ZF2001). ZF2001, produced by Anhui Zhifei Longcom Biologic Pharmacy Co., Ltd., is an RBD-dimer subunit vaccine with conditional approval in China. SARS-CoV-2 RBD antigen was manufactured in the CHO cell lines as a liquid formulation containing 25 μg per 0.5 mL, and aluminum hydroxide was used as an adjuvant for the antigen (14, 15). To our knowledge, this is the first reported case of myocarditis following this type of COVID-19 vaccine.

Myocarditis can be one of the clinical symptoms in patients with COVID-19 infection (16). In addition, there are many other viruses can cause myocarditis. Viral myocarditis may be followed by bacterial and fungal infections. Non-infectious factors such as drugs and allergic reactions can also lead to myocarditis (17). Therefore, SARS-CoV-2 and common myocarditis-causing viruses, such as Coxsackie group B virus, parvovirus B19, and herpes virus, should be tested in patients with suspected post- COVID-19 vaccinated myocarditis to rule out SARS-CoV-2 and viral infections. In this case, the new coronavirus *ORF1a* gene test was negative, and the new coronavirus *N* gene test was negative, indicating that the patient did not have COVID-19 infection. In addition, the antibody tests for respiratory syncytial virus, adenovirus, Coxsackie B virus, herpes simplex virus, and hepatitis virus were also negative. Clinical presentation showed that there was a clear temporal relationship between the protein subunit of COVID-19 vaccine and the occurrence of myocarditis in this patient. Although potential cause of myocarditis due to viral infection cannot be completely excluded because no viral culture/viral DNA/RNA detection were performed, myocarditis could be a severe side effect of the protein subunit of COVID-19 vaccine.

Conclusion

We reported a case of fulminant myocarditis following the first dose of the ZF2001 RBD-subunit vaccine against COVID-19. There has been increasing data supporting the association between vaccination and myocarditis, but the exact mechanism by which different types of COVID-19 vaccines mediate the development of myocarditis is still unclear. Further research is needed to address the specific mechanism of myocarditis after COVID-19 vaccination and to discover specific biomarker that can indicate myocarditis or myocardial damage after COVID-19 vaccination.

Data availability statement

The original contributions presented in this study are included in the article/**Supplementary material**, further inquiries can be directed to the corresponding authors.

Ethics statement

The studies involving human participants were reviewed and approved by the Medical Ethics Committee of Hebei Medical University. The patients/participants provided their written informed consent to participate in this study.

Author contributions

Y-MD wrote the manuscript, while G-ZZ and BC critically revised it. Y-MD, XL, C-TY, QQ, W-BS, Y-ML, MZ, S-JW, H-TB, R-FM, G-ZZ, and BC collected the data upon which the manuscript was based, discussed the results, and reviewed and approved the manuscript. All authors contributed to the report and approved the submitted version.

Funding

This work was supported by the Hebei Province Key R&D Program for People's Livelihood Science and Technology Project (20377742D) and Science and Technology Research Project of Hebei Province Colleges and Universities (ZD2021073).

Conflict of interest

The authors declare that the research was conducted in the absence of any commercial or financial relationships that could be construed as a potential conflict of interest.

Publisher's note

Supplementary material

The Supplementary Material for this article can be found online at: https://www.frontiersin.org/articles/10.3389/fcvm.2022.970045/full#supplementary-material

References

1. Bisgin A, Sanlioglu AD, Eksi YE, Griffith TS, Sanlioglu S. Current update on severe acute respiratory syndrome coronavirus 2 vaccine development with a special emphasis on gene therapy viral vector design and construction for vaccination. *Hum Gene Ther.* (2021) 32:541–62. doi: 10.1089/hum.2021.052

2. Husby A, Hansen JV, Fosbøl E, Thiesson EM, Madsen M, Thomsen RW, et al. SARS-CoV-2 vaccination and myocarditis or myopericarditis: population based cohort study. *BMJ.* (2021) 375:e068665. doi: 10.1136/bmj-2021-068665

3. Gargano JW, Wallace M, Hadler SC, Langley G, Su JR, Oster ME, et al. Use of mRNA COVID-19 vaccine after reports of myocarditis among vaccine recipients: update from the advisory committee on immunization practices – United States, june 2021. *MMWR Morb Mortal Wkly Rep.* (2021) 70:977–82. doi: 10.15585/mmwr.mm7027e2

4. Verma AK, Lavine KJ, Lin CY. Myocarditis after Covid-19 mRNA vaccination. *N Engl J Med.* (2021) 385:1332–4.

5. Larson KF, Ammirati E, Adler ED, Cooper LT Jr., Hong KN, Saponara G, et al. Myocarditis after BNT162b2 and mRNA-1273 vaccination. *Circulation.* (2021) 144:506–8.

6. Kim HW, Jenista ER, Wendell DC, Azevedo CF, Campbell MJ, Darty SN, et al. Patients with acute myocarditis following mRNA COVID-19 vaccination. *JAMA Cardiol.* (2021) 6:1196–201.

7. Montgomery J, Ryan M, Engler R, Hoffman D, McClenathan B, Collins L, et al. Myocarditis following immunization with mRNA COVID-19 vaccines in members of the US military. *JAMA Cardiol.* (2021) 6:1202–6. doi: 10.1001/jamacardio.2021.2833

8. Lai FTT, Li X, Peng K, Huang L, Ip P, Tong X, et al. Carditis after COVID-19 vaccination with a messenger RNA vaccine and an inactivated virus vaccine : a case-control study. *Ann Intern Med.* (2022) 175:362–70. doi: 10.7326/M21-3700

9. Li M, Yuan J, Lv G, Brown J, Jiang X, Lu ZK. Myocarditis and pericarditis following COVID-19 vaccination: inequalities in age and vaccine types. *J Pers Med.* (2021) 11:1106. doi: 10.3390/jpm11111106

10. Hajra A, Gupta M, Ghosh B, Ashish K, Patel N, Manek G, et al. Proposed pathogenesis, characteristics, and management of COVID-19 mRNA vaccine-related myopericarditis. *Am J Cardiovasc Drugs.* (2022) 22:9–26.

11. Bozkurt B, Kamat I, Hotez PJ. Myocarditis with COVID-19 mRNA vaccines. *Circulation.* (2021) 144:471–84.

12. Segal Y, Shoenfeld Y. Vaccine-induced autoimmunity: the role of molecular mimicry and immune crossreaction. *Cell Mol Immunol.* (2018) 15:586–94.

13. Caforio AL, Pankuweit S, Arbustini E, Basso C, Gimeno-Blanes J, Felix SB, et al. Current state of knowledge on aetiology, diagnosis, management, and therapy of myocarditis: a position statement of the European society of cardiology working group on myocardial and pericardial diseases. *Eur Heart J.* (2013) 34:2636–48; 2648a–48d. doi: 10.1093/eurheartj/eht210

14. Yang S, Li Y, Dai L, Wang J, He P, Li C, et al. Safety and immunogenicity of a recombinant tandem-repeat dimeric RBD-based protein subunit vaccine (ZF2001) against COVID-19 in adults: two randomised, double-blind, placebo-controlled, phase 1 and 2 trials. *Lancet Infect Dis.* (2021) 21:1107–19. doi: 10.1016/S1473-3099(21)00127-4

15. Dai L, Gao L, Tao L, Hadinegoro SR, Erkin M, Ying Z, et al. Efficacy and safety of the RBD-dimer-based Covid-19 vaccine ZF2001 in adults. *N Engl J Med.* (2022) 386:2097–111. doi: 10.1056/NEJMoa2202261

16. Castiello T, Georgiopoulos G, Finocchiaro G, Claudia M, Gianatti A, Delialis D, et al. COVID-19 and myocarditis: a systematic review and overview of current challenges. *Heart Fail Rev.* (2022) 27:251–61. doi: 10.1007/s10741-021-10087-9

17. Fung G, Luo H, Qiu Y, Yang D, McManus B. Myocarditis. *Circ Res.* (2016) 118:496–514.

frontiers | Frontiers in Cardiovascular Medicine

TYPE Case Report
PUBLISHED 23 September 2022
DOI 10.3389/fcvm.2022.893742

OPEN ACCESS

EDITED BY
Junjie Xiao,
Shanghai University, China

REVIEWED BY
Tommaso Gori,
Johannes Gutenberg University Mainz, Germany
Vincenzo Sucato,
University of Palermo, Italy

*CORRESPONDENCE
Balazs Odler
balazs.odler@medunigraz.at

SPECIALTY SECTION
This article was submitted to General Cardiovascular Medicine, a section of the journal Frontiers in Cardiovascular Medicine

RECEIVED 28 March 2022
ACCEPTED 02 August 2022
PUBLISHED 23 September 2022

CITATION
Krall M, Gollmer J, Pollheimer MJ, Reiter C, Kolland M, Kirsch AH, Kronbichler A, Eller K, Rosenkranz AR and Odler B (2022) Myocardial infarction with non-obstructive coronary arteries in a patient double-seropositive for anti-glomerular basement membrane and anti-neutrophil cytoplasmic antibodies: A case report. *Front. Cardiovasc. Med.* 9:893742. doi: 10.3389/fcvm.2022.893742

Myocardial infarction with non-obstructive coronary arteries in a patient double-seropositive for anti-glomerular basement membrane and anti-neutrophil cytoplasmic antibodies: A case report

Marcell Krall[1], Johannes Gollmer[2], Marion J. Pollheimer[3], Clemens Reiter[4], Michael Kolland[1], Alexander H. Kirsch[1], Andreas Kronbichler[5], Kathrin Eller[1], Alexander R. Rosenkranz[1] and Balazs Odler[1]*

[1]Division of Nephrology, Department of Internal Medicine, Medical University of Graz, Graz, Austria, [2]Division of Cardiology, Department of Internal Medicine, Medical University of Graz, Graz, Austria, [3]Institute of Pathology, Medical University of Graz, Graz, Austria, [4]Division of General Radiology, Department of Radiology, Medical University of Graz, Graz, Austria, [5]Department of Medicine, University of Cambridge, Cambridge, United Kingdom

We report a case of a patient double-seropositive for anti-glomerular basement membrane (anti-GBM) and anti-neutrophil cytoplasmic antibodies (ANCA) who reported retrosternal chest pain during a regular hemodialysis session associated with ST-segment depression in electrocardiogram and an increase of serum high-sensitivity troponin T. Urgent coronary angiography excluded obstructive coronary artery disease, suggesting the diagnosis of ischemia with non-obstructive coronary arteries. This case illustrates an unusual presentation of cardiovascular involvement in a patient with double-positive ANCA/anti-GBM disease, emphasizing the possible relevance of coronary microvascular dysfunction and the need for close cardiovascular follow-up in this patient population.

KEYWORDS

MINOCA, ANCA, anti-GBM, double-positive, coronary, therapy

Introduction

Anti-neutrophil cytoplasm antibody (ANCA)-associated vasculitides (AAV) and anti-glomerular basement membrane (GBM) disease are rare entities (1, 2). The coincidence of positivity for anti-GBM and ANCA antibodies with clinical features of both diseases represents a life-threatening entity (3). Cardiovascular (CV) events are among the leading causes of death in AAV; thus, a more complex understanding of CV manifestations and their risk factors is required (4). In line, cardiac involvement is an underdiagnosed manifestation in AAV, and involvement of the coronary arteries is only rarely reported (5–9). Our case illustrates that myocardial infarction with non-obstructive coronary arteries (MINOCA) might be an important contributor to cardiac complications seen in patients with AAV and/or anti-GBM disease.

Case presentation

A 61-year-old Caucasian man presented to our university clinic with acute kidney injury. He was diagnosed with scleritis of the right eye approximately 13 years before current admission and had received azathioprine (AZA) for immunosuppression due to suspected myeloperoxidase (MPO)-ANCA positive granulomatosis with polyangiitis (GPA)

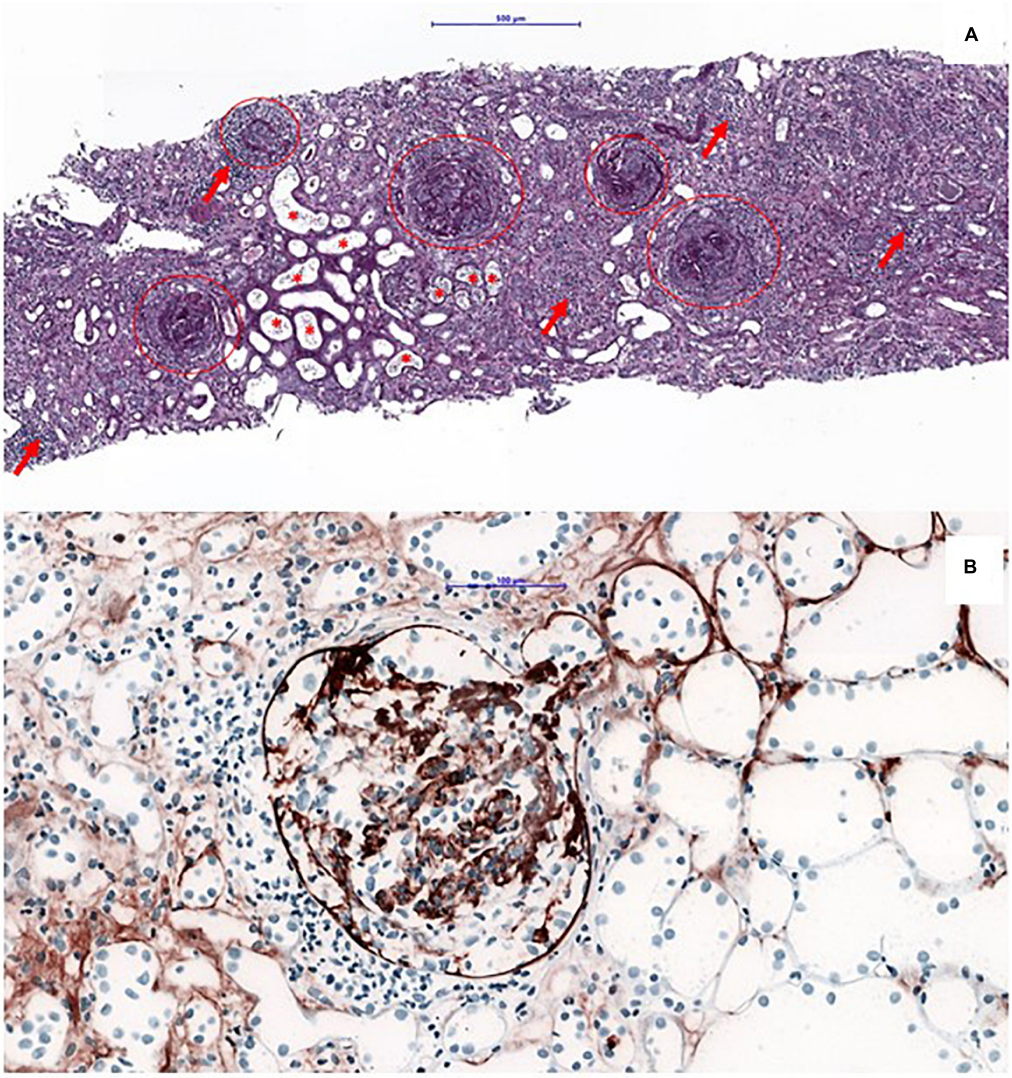

FIGURE 1
Kidney biopsy: an overview of a PAS-stained kidney biopsy, showing large cellular crescent present in all glomeruli (as highlighted by the circles), in line with a severe presentation of anti-glomerular basement membrane (anti-GBM) disease. Concomitant tubulo-interstitial nephritis (arrows) and signs of severe acute tubular injury with red blood cells within the tubular lumina (asteriks). Bar = 500 μm **(A)**. Immunohistochemical staining with the antibody against IgG, showing a linear staining pattern of the glomerular basement membrane **(B)**.

without evidence of further organ involvements. Besides, he had arterial hypertension treated with angiotensin-converting enzyme inhibitor/hydrochlorothiazide and had been diagnosed with prostate cancer 2 years before current admission (treated by radiotherapy and gonadotropin-releasing hormone analog).

The AZA therapy had been discontinued 19 months prior to presentation due to an influenza infection. Thereafter, on admission, a nephritic syndrome was present. Laboratory investigations revealed an increase of MPO-ANCA and anti-glomerular basement membrane (anti-GBM) antibody titers

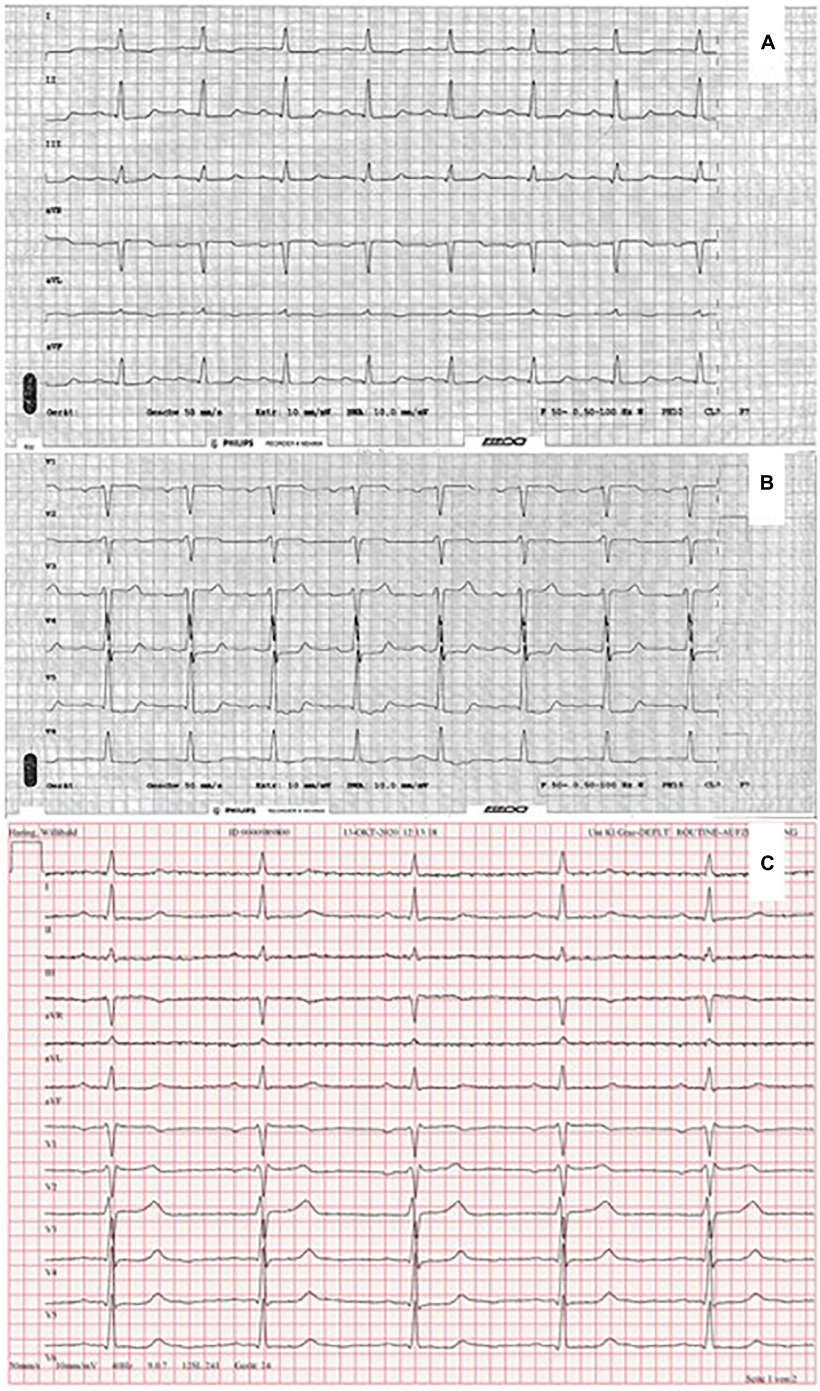

FIGURE 2
Electrocardiogram showing ST-segment depression in II, III, aVF **(A)**, and V4–V6 **(B)**. Electrocardiogram (with a paper speed of 50 mm/s) 1 month before MINOCA **(C)**.

(>100 and 244 U/ml, respectively). Thus, a kidney biopsy was performed, and the diagnosis of double-positive disease was made (**Figures 1A,B**).

Plasma exchange (14 sessions), high-dose corticosteroids, and cyclophosphamide (CYC – cumulative dose of 3.3 g) were initiated. However, he progressed to end-stage kidney disease and required hemodialysis (HD). In addition, 2 doses of rituximab (RTX) 500 mg each 2 weeks apart were given followed by 500 mg every 6 months as maintenance immunosuppressive therapy.

After 4 weeks of HD initiation, during a regular HD session, the patient reported retrosternal chest pain. Electrocardiogram (ECG) showed ST depressions in leads II, III, aVF, and V4 to V6 (**Figures 2A,B**), which changes were absent in a previous ECG 1 month before (**Figure 2C**). High-sensitive troponin T (hs-Tn) was elevated (the baseline level: 1,514 pg/ml; normal range: <14 pg/ml); thus, the diagnosis of non-ST elevation myocardial ischemia was made (**Figure 3**). Bed-side echocardiography revealed mildly reduced ejection fraction (40%) with diffuse hypokinesia and pronounced abnormalities in inferior, inferolateral, and anterolateral segments. Urgent coronary angiography (CA) excluded obstructive coronary artery disease (CAD) in major epicardial vessels and did not show signs of ruptured plaque or dissection, suggesting the diagnosis of MINOCA (**Figures 3A–E**). Cardiac magnetic resonance (CMR) imaging was performed to exclude acute (peri) myocarditis. Cine imaging revealed severe left ventricular and atrial dilatation with global hypokinesia and reduced left ventricular ejection fraction, aortic and mitral insufficiency but preserved right ventricular function. Native myocardial T1-values were globally elevated, myocardial T2-values were within the normal ranges, T2-weighted images showed no signs of edema, and no late enhancement was visualized, therefore not fulfilling diagnostic criteria of an acute myocarditis (10) but consistent with diffuse myocardial fibrosis in dilated cardiomyopathy. Myocarditis was also ruled out by positron emission computed tomography. Notably, ANCA positivity was seen throughout the disease course, while hs-Tn decreased significantly a few weeks after the cardiac event (**Figure 4**).

Discussion

Double-positive disease is a life-threatening disorder characterized by small vessel vasculitis affecting the kidneys and the lungs with a coincidence of anti-GBM disease and AAV (11). Cardiac involvement is a known disease manifestation in AAV, predominantly in those with MPO-ANCA positivity, and associated with increased mortality (12). On the contrary,

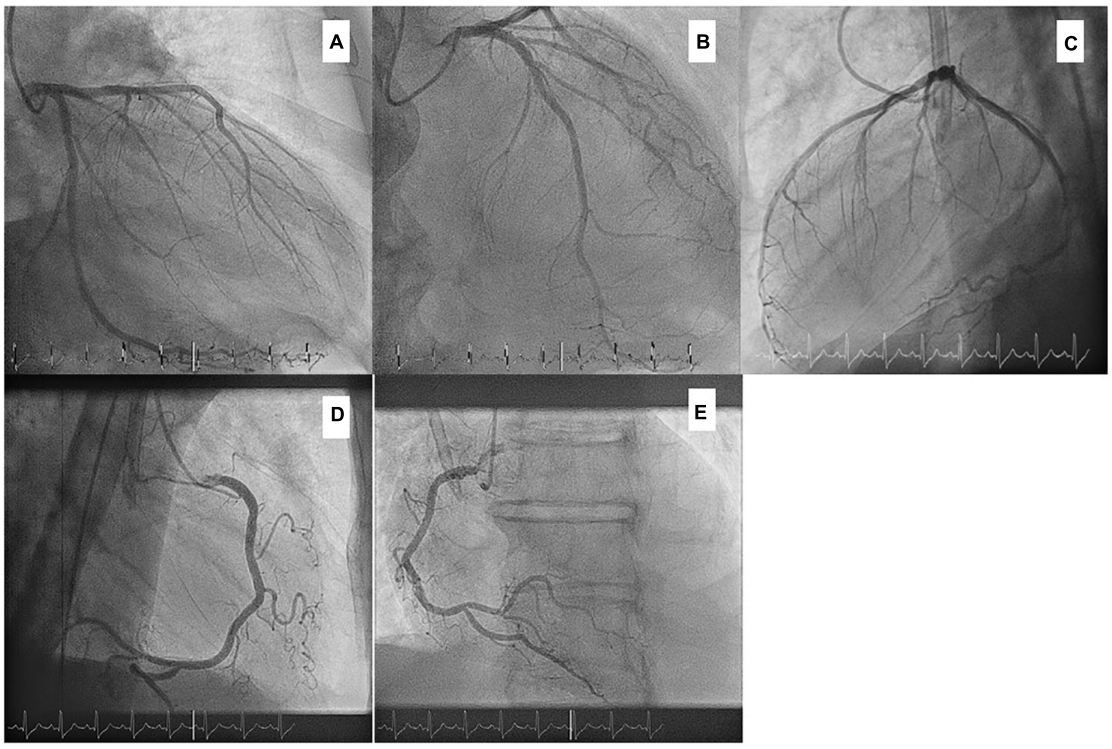

FIGURE 3
Coronary angiography without significant obstructive coronary artery disease. **(A)** cranial, 40° **(B)** RAO, 20°; caudal, 30° **(C)** LAO, 90° **(D)** RAO, 90° **(E)** LAO, 30°.

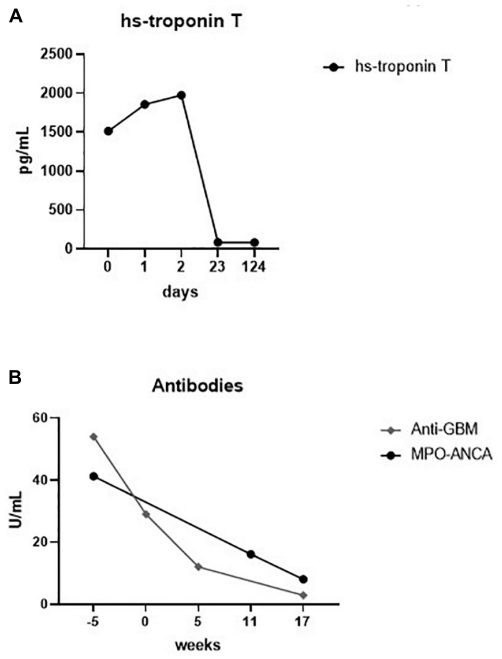

FIGURE 4
Laboratory charts of the time-dependent development of high-sensitive (hs) troponin T **(A)** and myeloperoxidase anti-neutrophil cytoplasm (MPO-ANCA) and anti-glomerular basement membrane (anti-GBM) antibodies **(B)**. Zero on both scales indicates the time point of chest pain.

CV complications are rarely reported in patients with anti-GBM disease. Only one case of anti-GBM disease with cardiac involvement was reported in our literature review (13).

Myocardial infarction with non-obstructive coronary arteries represents a major health problem and is often misdiagnosed, leading to possible undertreatment (14). Patients with small-vessel vasculitis have a high CV event rate, even exceeding high-risk populations, such as those with chronic kidney disease (4). Recently, there has been an increasing interest to identify patients at risk since they have a higher risk of developing major cardiovascular events and being hospitalized due to heart failure or repeated CA (15–17). Adequate diagnosis is challenging; however, if clinical surrogate markers of myocardial ischemia without evidence of obstructive CAD are present, the diagnosis of MINOCA can be considered (18). Dilated cardiomyopathy as a possible cause of chest pain in our patient cannot be excluded entirely. However, he had typical angina pectoris with dynamic ischemic ECG changes and a high-serum level of hs-Tn (again, later falling despite chronic HD), while invasive angiography did not reveal coronary stenosis (≥50%). In accordance, the absence of myocarditis and tear on angiography also underlines the clinical diagnosis of MINOCA. Importantly, the use of CYC is a considerable risk factor in cardiotoxicity; however, its triggering minimum dose is not known. Registry data reveal an association between high-dose CYC (>36 g) and ischemic heart disease in patients with GPA (19).

A study by Pugnet et al. analyzed patients with GPA who underwent CMR (20). In patients, who had simultaneous CA with normal coronary findings, subendocardial late gadolinium enhancement (LGE) with perfusion defects, suggesting ischemic lesions possibly due to small vessel vasculitis, was seen. In our case, CMR showed no late enhancement, suggesting the absence of inflammation.

Mechanisms contributing to the development of MINOCA seem to be heterogeneous but characterized mainly by coronary vasospasm and microvascular dysfunction (14, 21). In our patient, invasive functional CA and pharmacological reactivity testing was not performed; thus, the contributing mechanism behind his symptoms remains unclear. Nevertheless, strong evidence on the association between coronary vascular dysfunction and small vessel disease exists (22). In patients with AAV, ANCA-activated neutrophils induce endothelial injury, which might lead to coronary vascular dysfunction and promote the induction of epicardial vessel spasm in predisposed coronary segments. In addition, the endothelial impairment resulting in altered vascular tone enhances smooth muscle contractility and might be responsible for myocardial ischemia *via* decreased coronary flow and perfusion pressure. Moreover, similar to patients with systemic lupus erythematosus, systemic inflammation in AAV patients might also contribute to coronary vasomotor abnormalities (23). A recent European multicenter study has found that patients with double-positive disease have a relapse rate comparable to patients with AAV alone, suggesting the importance of long-term follow-up and maintenance immunosuppressive therapy in this patient population (11). In our patient, a preexisting extrarenal vasculitis with continuous ANCA positivity might be a possible endogenous contributor responsible for his myocardial ischemia besides the predominant clinical phenotype of anti-GBM disease.

As coronary microvascular dysfunction might have a significant impact on the patients' quality of life as well as a clinical outcome, sufficient therapeutic strategies are of particular interest (24, 25). Since – to our knowledge – no studies are published dealing with this entity in patients with AAV and/or double-positive ANCA/anti-GBM disease, it is unclear which medical treatment might be the most sufficient. Recent major guidelines issued by the leading cardiology societies have provided a guidance on various pharmacological treatment options of MINOCA related to the underlying mechanism (14, 26). Accordingly, angiotensin-converting enzyme inhibitors or angiotensin receptor blockers might depict a useful option to reduce systemic inflammation and endothelial dysfunction (27). Calcium antagonists might be used in patients with evidence of either epicardial or microvascular spasm who underwent acetylcholine testing (14). As patients with AAV face increased CV risk even in the early phase of the disease, adequate lifestyle changes and rigorous CV risk management are of particular importance (28, 29).

There are some clear limitations to this presented case that merit notification. Invasive testing of coronary artery spasm and microvascular dysfunction, which might have provided direct evidence on some of the possible mechanisms of MINOCA, have not been performed in this case; therefore, MINOCA remains a "working diagnosis." Also, certain underlying conditions, such as coronary thrombosis with a quick spontaneous lysis of the thrombus or uncontrolled blood pressure, cannot be fully excluded. Finally, our patient was on dialysis, and, thus, the contribution of prominent accumulation of uremic toxins over time as a specific trigger of microvascular dysfunction might also be occurred.

Conclusion

In summary, we report a case of a patient double-seropositive for anti-GBM and ANCA antibodies with extrarenal vasculitis who presented with MINOCA. Now, studies improving our understanding of underlying mechanisms associated with excessive CV mortality in AAV patients are essential. Coronary microvascular dysfunction or vasospastic angina due to endothelial injury and/or systemic inflammation might be a significant contributor of MINOCA in patients with AAV and/or double-positive disease, who can be at higher risk to develop this condition. Given the increased risk of adverse CV outcomes associated with AAV, this entity might be an important and reversible cause, which needs a multidisciplinary care approach and further exploration in addition to traditional CV risk factors.

Data availability statement

The original contributions presented in this study are included in the article/supplementary material, further inquiries can be directed to the corresponding author.

Ethics statement

The studies involving human participants were reviewed and approved by the Ethics Committee of the Medical University of Graz. The patients/participants provided their written informed consent to participate in this case study. Written informed consent was obtained from the individual(s) for the publication of any potentially identifiable images or data included in this article.

Author contributions

MaK and BO wrote the first draft of the manuscript. JG described the coronary angiography and ECG. CR evaluated and interpreted the cardiac MRI findings. MP performed the histological work-up. MaK, AKi, AKr, KE, and AR contributed to the data acquisition and drafting of the manuscript. All authors contributed to the article and approved the submitted version.

Conflict of interest

The authors declare that the research was conducted in the absence of any commercial or financial relationships that could be construed as a potential conflict of interest.

Publisher's note

References

1. McAdoo SP, Pusey CD. Anti-glomerular basement membrane disease. *Clin J Am Soc Nephrol.* (2017) 12:1162–72. doi: 10.2215/CJN.01380217

2. Kitching AR, Anders H-J, Basu N, Brouwer E, Gordon J, Jayne DR, et al. ANCA-associated vasculitis. *Nat Rev Dis Primers.* (2020) 6:71. doi: 10.1038/s41572-020-0204-y

3. Philip R, Dumont A, Martin Silva N, de Boysson H, Aouba A, Deshayes S. ANCA and anti-glomerular basement membrane double-positive patients: a systematic review of the literature. *Autoimmun Rev.* (2021) 20:102885. doi: 10.1016/j.autrev.2021.102885

4. Kronbichler A, Leierer J, Gauckler P, Shin JI. Comorbidities in ANCA-associated vasculitis. *Rheumatology.* (2020) 59:iii79–83. doi: 10.1093/rheumatology/kez617

5. Florian A, Slavich M, Blockmans D, Dymarkowski S, Bogaert J. Cardiac involvement in granulomatosis with polyangiitis (Wegener Granulomatosis). *Circulation.* (2011) 124:e342–4. doi: 10.1161/CIRCULATIONAHA.111.030809

6. Mathur K, Saini A, Bah T, Katikaneni P. Case report: acute ST elevation myocardial infarction in fulminant systemic p-ANCA vasculitis: a rare catastrophic complication. *BMJ Case Rep.* (2016) 2016:bcr2016215628. doi: 10.1136/bcr-2016-215628

7. Yoshida M, Nakaya I, Sakuma T, Soma J. Cardiac small vessel vasculitis in a case of microscopic polyangiitis. *Intern Med.* (2014) 53:2655–6. doi: 10.2169/internalmedicine.53.2556

8. Kim YK, Chekka P, Mysore M, Childress J, Alfaraidhy M, Thomas A, et al. Isolated antineutrophil cytoplasmic antibody-associated coronary

vasculitis and valvulitis. *JACC Case Rep.* (2021) 3:309. doi: 10.1016/j.jaccas.2020.12.007

9. Cuminetti G, Regazzoni V, Vizzardi E, Bonadei I, de Jong MMJ, Lorusso R, et al. Cardiac ANCA-associated vasculitis mimicking an acute coronary syndrome. *Int J Cardiol.* (2016) 214:200–1. doi: 10.1016/j.ijcard.2016.03.117

10. Ferreira VM, Schulz-Menger J, Holmvang G, Kramer CM, Carbone I, Sechtem U, et al. Cardiovascular magnetic resonance in nonischemic myocardial inflammation. *J Am Coll Cardiol.* (2018) 72:3158–76. doi: 10.1016/j.jacc.2018.09.072

11. McAdoo SP, Tanna A, Hrušková Z, Holm L, Weiner M, Arulkumaran N, et al. Patients double-seropositive for ANCA and anti-GBM antibodies have varied renal survival, frequency of relapse, and outcomes compared to single-seropositive patients. *Kidney Int.* (2017) 92:693. doi: 10.1016/j.kint.2017.03.014

12. Wallace ZS, Fu X, Harkness T, Stone JH, Zhang Y, Choi H. All-cause and cause-specific mortality in ANCA-associated vasculitis: overall and according to ANCA type. *Rheumatology.* (2020) 59:2308–15. doi: 10.1093/rheumatology/kez589

13. Solak Y, Selcuk NY, Polat I, Atalay H, Turkmen K. Dilated cardiomyopathy in a patient with antibody-negative Goodpasture's syndrome and pulmonary relapse. *Saudi J Kidney Dis Transpl.* (2010) 21:332.

14. Kunadian V, Chieffo A, Camici PG, Berry C, Escaned J, Maas AHEM, et al. An EAPCI expert consensus document on ischaemia with non-obstructive coronary arteries in collaboration with European society of cardiology working group on coronary pathophysiology & microcirculation endorsed by coronary vasomotor disorders international study group. *Eur Heart J.* (2020) 41:3504. doi: 10.1093/eurheartj/ehaa503

15. Radico F, Zimarino M, Fulgenzi F, Ricci F, Di Nicola M, Jespersen L, et al. Determinants of long-term clinical outcomes in patients with angina but without obstructive coronary artery disease: a systematic review and meta-analysis. *Eur Heart J.* (2018) 39:2135–46. doi: 10.1093/eurheartj/ehy185

16. Shimokawa H, Suda A, Takahashi J, Berry C, Camici PG, Crea F, et al. Clinical characteristics and prognosis of patients with microvascular angina: an international and prospective cohort study by the Coronary Vasomotor Disorders International Study (COVADIS) Group. *Eur Heart J.* (2021) 42:4592–600. doi: 10.1093/eurheartj/ehab282

17. Jespersen L, Abildstrom SZ, Hvelplund A, Madsen JK, Galatius S, Pedersen F, et al. Burden of hospital admission and repeat angiography in angina pectoris patients with and without coronary artery disease: a registry-based cohort study. *PLoS One.* (2014) 9:e93170. doi: 10.1371/journal.pone.0093170

18. Beltrame JF, Tavella R, Jones D, Zeitz C. Management of ischaemia with non-obstructive coronary arteries (INOCA). *BMJ.* (2021) 375:e060602. doi: 10.1136/bmj-2021-060602

19. Faurschou M, Mellemkjaer L, Sorensen IJ, Svalgaard Thomsen B, Dreyer L, Baslund B. Increased morbidity from ischemic heart disease in patients with Wegener's granulomatosis. *Arthritis Rheum.* (2009) 60:1187–92. doi: 10.1002/art.24386

20. Pugnet G, Gouya H, Puéchal X, Terrier B, Kahan A, Legmann P, et al. Cardiac involvement in granulomatosis with polyangiitis: a magnetic resonance imaging study of 31 consecutive patients. *Rheumatology.* (2017) 56:947–56. doi: 10.1093/rheumatology/kew490

21. Del Buono MG, Montone RA, Camilli M, Carbone S, Narula J, Lavie CJ, et al. Coronary microvascular dysfunction across the spectrum of cardiovascular diseases. *J Am Coll Cardiol.* (2021) 78:1352–71. doi: 10.1016/j.jacc.2021.07.042

22. Ford TJ, Rocchiccioli P, Good R, McEntegart M, Eteiba H, Watkins S, et al. Systemic microvascular dysfunction in microvascular and vasospastic angina. *Eur Heart J.* (2018) 39:4086. doi: 10.1093/eurheartj/ehy529

23. Weber BN, Stevens E, Barrett L, Bay C, Sinnette C, Brown JM, et al. Coronary Microvascular Dysfunction in Systemic Lupus Erythematosus. *J Am Heart Assoc.* (2021) 10:e018555. doi: 10.1161/JAHA.120.018555

24. Sucato V, Novo G, Saladino A, Rubino M, Caronna N, Luparelli M, et al. Ischemia in patients with no obstructive coronary artery disease: classification, diagnosis and treatment of coronary microvascular dysfunction. *Coron Artery Dis.* (2020) 31:472–6. doi: 10.1097/MCA.0000000000000855

25. Bajaj NS, Singh A, Zhou W, Gupta A, Fujikura K, Byrne C, et al. Coronary microvascular dysfunction, left ventricular remodeling, and clinical outcomes in patients with chronic kidney impairment. *Circulation.* (2020) 141:21–33. doi: 10.1161/CIRCULATIONAHA.119.043916

26. Tamis-Holland JE, Jneid H, Reynolds HR, Agewall S, Brilakis ES, Brown TM, et al. Contemporary diagnosis and management of patients with myocardial infarction in the absence of obstructive coronary artery disease: a scientific statement from the American heart association. *Circulation.* (2019) 139:e891–908. doi: 10.1161/CIR.0000000000000670

27. Ruilope LM, Redón J, Schmieder R. Cardiovascular risk reduction by reversing endothelial dysfunction:ARBs, ACE inhibitors, or both? Expectations from the ONTARGET trial programme. *Vasc Health Risk Manag.* (2007) 3:1–9.

28. Massicotte-Azarniouch D, Petrcich W, Walsh M, Canney M, Hundemer GL, Milman N, et al. Association of anti-neutrophil cytoplasmic antibody-associated vasculitis and cardiovascular events: a population-based cohort study. *Clin Kidney J.* (2022) 15:681. doi: 10.1093/ckj/sfab229

29. Floyd L, Morris AD, Woywodt A, Dhaygude A. Cardiovascular disease and ANCA-associated vasculitis: are we missing a beat?. *Clin Kidney J.* (2022) 15:618. doi: 10.1093/ckj/sfac009

frontiers | Frontiers in Cardiovascular Medicine

TYPE Case Report
PUBLISHED 29 September 2022
DOI 10.3389/fcvm.2022.1014250

OPEN ACCESS

EDITED BY
Pietro Enea Lazzerini,
University of Siena, Italy

REVIEWED BY
Sankha Shubhra Chakrabarti,
Institute of Medical Sciences, Banaras Hindu University, India
Francesco Sessa,
University of Catania, Italy

*CORRESPONDENCE
Chia-Pin Lin
chiapinlin@hotmail.com

SPECIALTY SECTION
This article was submitted to General Cardiovascular Medicine, a section of the journal Frontiers in Cardiovascular Medicine

RECEIVED 08 August 2022
ACCEPTED 13 September 2022
PUBLISHED 29 September 2022

CITATION
Chan CC, Lin CP, Chang CJ and Chu PH (2022) Case report: Sudden cardiorespiratory collapse in a healthy male after coronavirus disease 2019 vaccination at a vaccination center. *Front. Cardiovasc. Med.* 9:1014250. doi: 10.3389/fcvm.2022.1014250

Case report: Sudden cardiorespiratory collapse in a healthy male after coronavirus disease 2019 vaccination at a vaccination center

Cze Ci Chan, Chia-Pin Lin*, Chi-Jen Chang and Pao-Hsien Chu

Department of Cardiology, Linkou Medical Center, Chang Gung Memorial Hospital, Taoyuan City, Taiwan

Since 2020, new vaccines were developed to fight the coronavirus disease 2019 (COVID-19). Vaccination is important in preventing mortality and achieving herd immunity. However, due to vast vaccination, fatal adverse events could be seen. We report a case of a previously healthy, young male who had a cardiopulmonary arrest 2 min after receiving the Oxford-AstraZeneca (ChAdOx1 nCoV-19) COVID-19 vaccination. After targeted temperature management, a coronary angiogram was performed after neurological recovery and showed severe stenosis at the proximal left anterior descending artery. Stenting was done and he was discharge. No similar case of sudden cardiorespiratory collapse immediately after COVID-19 vaccination has been reported. Our patient did not have any effort-related angina or dyspnea on exertion before this event. The sudden cardiorespiratory collapse was probably related to underlying coronary artery disease, complicated with a vasovagal event. We stress the importance of coronary angiography in out of hospital cardiac arrest patients after neurological recovery. In the era of COVID-19 vaccination, even though fatal adverse events following immunization are rare, heightened awareness of severe side effects needing medical attention is very important.

KEYWORDS

coronary artery disease, sudden collapse, COVID-19 ChAdOx1 nCoV-19 vaccine, COVID-19 vaccination adverse effect, cardiovascular adverse events, case report

Introduction

Since 2020, the coronavirus disease 2019 (COVID-19) pandemic has placed a heavy burden on healthcare systems worldwide. The number of cases continues to increase daily, and several measures have been taken to combat this virus. New vaccines were developed with extraordinary speed to stop the virus and prevent more deaths. Taiwan has now approved four vaccines, Moderna, BioNTech, Oxford-AstraZeneca and Medigen (1). In July 2021, total number of people with at least one dose of COVID-19

vaccine in Taiwan and worldwide were 6.43 million (24.6%) and 2.15 billion (26.8%) respectively. Two hundred and forty thousand people are vaccinated daily then to cope with the rapidly spreading disease in Taiwan, with the majority being vaccinated with either Moderna or Oxford-AstraZeneca vaccine (2). Although the vaccines are beneficial in reducing COVID-19 severity, some rare complications have been reported (3). Here, we report a case of sudden collapse after vaccination at a vaccination center, with the aim of generating awareness among clinicians and other healthcare workers regarding rare but potentially fatal events.

Case description

A previously healthy 35-year-old male, non-smoker, who had a cardiopulmonary arrest 2 min after receiving the Oxford-AstraZeneca (ChAdOx1 nCoV-19) COVID-19 vaccination was referred to our hospital. The patient was a physical education teacher at a high school with a normal body mass index of 22.5 kg/m^2. No prior chest pain or syncope events were ever experienced. At the vaccination center, he collapsed 2 min after being injected, and cardiopulmonary resuscitation (CPR) was performed immediately. The automated external defibrillator showed shockable rhythm, and he was defibrillated four times before return of spontaneous circulation. The total duration of CPR was 15 min. Intubation was done at a local medical hospital 30 min later, and he was then transferred to our hospital for further management after 3 h. Upon arrival, he was unconscious, with a Glasgow Coma Scale score of E1V1M3, and intermittent general tonic clonic seizure activity was noted. Anaphylaxis was highly suspected at first, but no significant skin-mucosal tissue involvement was noticed on physical examination. There were no signs of respiratory compromise or gastrointestinal symptoms at the vaccination center. A tryptase test was done to rule out anaphylaxis, and it was within normal limits. He had an elevated troponin I level of 1.04 ng/ml (reference range <0.3) approximately 4 h after cardiopulmonary arrest, however, electrocardiography did not show ST-elevation. Transthoracic echocardiography showed a left ventricular ejection fraction of 73% without regional wall motion abnormalities. He was then admitted to the intensive care unit for targeted temperature management. Followed up troponin I levels increased to 5.226 ng/mL 6 h later but decreased to 2.231 ng/mL the next day. He had normal cholesterol, low- density lipoprotein, triglyceride and glycohemoglobin levels. No events of life-threatening arrhythmias were recorded in the intensive care unit. After 3 days, he regained consciousness and was extubated 1 day later. A coronary angiogram was performed, which showed severe stenosis at the proximal left anterior descending artery (**Figure 1A**). The stenosis was pre-dilated with a semi-compliant 2.5 mm balloon, and then intravascular ultrasound was used to determine the plaque composition, as well as the length and size of the stent. A fibrotic plaque was identified with a length of around 35 mm (**Figure 2A**). The distal lumen of the artery was 4.0 mm with a plaque burden of <50%. A 4.0 mm non-compliant balloon was used for further pre-dilatation of the stenosis, followed by stenting with a 4.0 mm × 38 mm drug eluting stent (**Figure 1B**). Final post-dilatation of the stent was done with the 4.0 mm non-compliant balloon. Post-stenting intravascular ultrasound showed an adequate landing zone and stent expansion without stent edge dissection or stent malapposition (**Figure 2B**). He was discharged 2 days later without significant complications. At a follow-up visit 3 months after discharge he was asymptomatic, and he remained on dual-antiplatelet therapy.

Discussion

To the best of our knowledge, no similar case of sudden cardiorespiratory collapse immediately after COVID-19 vaccination has been reported. According to the Council for International Organizations of Medical Sciences (CIOMS) and the World Health Organization (WHO) Working Group on Vaccine Pharmacovigilance, an adverse event following immunization (AEFI) is defined as any untoward medical occurrence following immunization which does not necessarily have a causal relationship to the vaccine. The adverse event may be any unfavorable or unintended sign, abnormal laboratory finding, symptom or disease. CIOMS and WHO have defined five cause-specific AEFI, including (i) reaction to a vaccine product, (ii) reaction to a defect in vaccine quality, (iii) reaction to an immunization error, (iv) reaction related to anxiety, and (v) coincidental event, to differentiate vaccine- and vaccination-related reactions from coincidental events by assignment of causality (4). Most reported AEFIs are not serious, however, uncommon adverse reactions such as anaphylaxis, myocarditis and thrombosis have been reported after administering a vaccine (3). In the phase 3 trial of the Oxford-AstraZeneca (ChAdOx1 nCoV-19) COVID-19 vaccine, the incidence rates of adverse events were similar in the vaccinated and placebo groups, with the most common being general pain, headache, and injection-site pain. The incidence rates of serious and medically attended adverse events such as potential immune-mediated conditions were reported to be low and similar to the placebo group. In addition, no anaphylaxis events were reported (5). However, real world studies of Oxford-AstraZeneca (ChAdOx1 nCoV-19) COVID-19 vaccine have however reported severe hypersensitivity reactions with major cardiovascular parameter changes (6).

Another common adverse effect shortly after many types of vaccination among adolescents and young adults is syncope (vasovagal or vasodepressor), which may complicate non-allergic systemic reactions. A vasovagal event is more likely

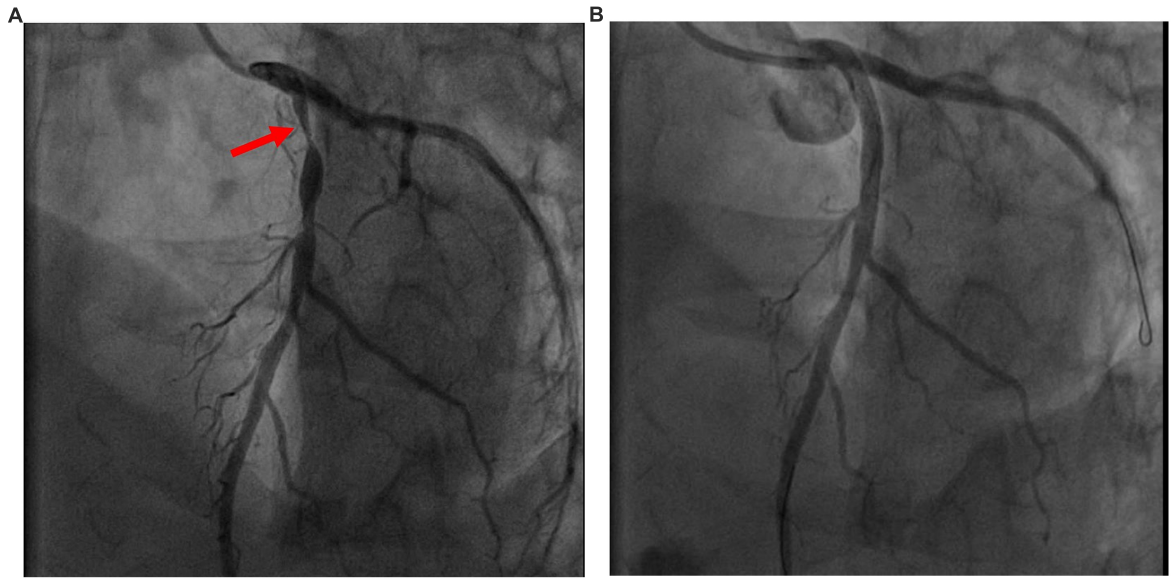

FIGURE 1
(A) Pre- intervention image. Coronary angiogram showed severe proximal left anterior descending artery stenosis (red arrowhead). **(B)** Post-intervention image. Post- stenting coronary angiogram.

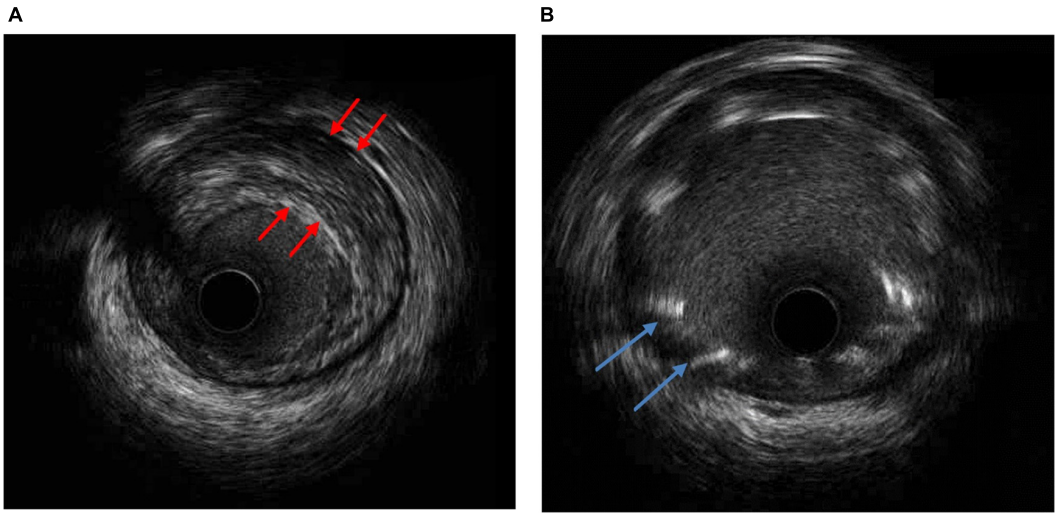

FIGURE 2
(A) Intravascular ultrasound (IVUS) of the narrowest lesion site showing a fibrotic plaque (red arrowhead). **(B)** IVUS post-stenting with fair stent expansion without stent edge dissection or stent malapposition (blue arrowhead).

to be triggered by anxiety and pain, causing a drop in heart rate, and blood pressure, rather than the COVID-19 vaccine itself. The Centers for Disease Control and Prevention in the United States reported the rate of post-immunization syncope in 2006 among people >5 years of age was 0.054/100 000 doses distributed and about 80% of syncope events usually self-resolve and occur within 15 min after vaccination (7). In 2018, WHO proposed a new term "immunization stress-related response (ISRR)" to cover the entire spectrum of manifestations (symptoms and signs) of a stress response before, during or immediately after immunization. ISRR may demonstrate as acute stress responses, vasovagal reactions or dissociative neurological symptom reactions with or without non-epileptic seizures. Early presentations of an ISRR may be an acute stress response due to sympathetic involvement with increased heart rate and blood pressure and symptoms may vary from mild feelings of worry to difficulty in breathing. Occasionally, this may be followed by an over-compensatory parasympathetic

response in which heart rate and/or blood pressure fall sharply resulting in a vasovagal reaction characterized by symptoms ranging from dizziness to syncope (8). In this patient, it is difficult to distinguish if the syncopal event or a new-onset ventricular arrhythmia led to cardiac arrest. However, as no life-threatening arrhythmias were noted throughout hospitalization, it is deemed more likely that the vasovagal reaction caused a transient ischemia of the myocardium due to a very high-grade chronic stable lesion, initiating tachyarrhythmias leading to cardiac arrest (9). To define the relationship between AEFI and COVID-19 vaccination, the causality WHO algorithm could be adopted to determine the direct link between vaccination and adverse effects as shown in many studies (10, 11). According to the WHO algorithm, our case has consistent causal association to immunization and the vasovagal event is likely to be an immunization anxiety-related reaction.

Other most frequently discussed major cardiovascular (CV) complications after COVID-19 vaccination include myocarditis, pericarditis and vascular thrombotic events, however, rare cases of acute coronary syndrome and cardiac arrest have also been reported (12, 13). In a study of data from the WHO, Kaur et al. reported that the most common CV adverse events observed with the COVID-19 vaccines under study were tachycardia, palpitations and flushing. A case series in the UK on the AstraZeneca vaccine reported 167 cases of cardiac arrest (including 35 fatalities), 386 cases of myocardial infarction (MI) (including 51 fatalities), and 79 cases of acute MI (including 13 fatalities) (14). In 2 studies showing CV complications associated with COVID-19 vaccines, the time gap between vaccination and the incidence of MI varied from 15 min to 2 days, with several possible mechanisms proposed such as immune thrombotic thrombocytopenia, a series of allergic reactions leading to occlusion of coronary arteries, and high demand and low supply due to vaccination stress in weaker patients, where else the time gap for myocarditis varied from 24 h to 7 days after receiving Oxford-AstraZeneca (ChAdOx1 nCoV-19) COVID-19 vaccine (15, 16). However, it is still unclear whether there is any link between COVID-19 vaccines and MI, and further longitudinal studies are needed to clarify this issue.

Besides COVID-19 vaccination and its AEFIs, the timing of coronary angiography and percutaneous coronary intervention after successful resuscitation from out-of-hospital cardiac arrest (OHCA) without ST-segment elevation electrocardiography was another issue in our case. Given that he did not have electrocardiographic evidence of myocardial ischemia and as he had a normal left ventricle systolic function without regional wall motion abnormalities on transthoracic echo, coronary angiography could possibly have been foregone. The prevalence of coronary artery disease (CAD) has been reported to be around 60–70% among those successfully resuscitated from OHCA without ST-segment elevation myocardial infarction (STEMI) (17, 18). Although most studies do not support a routine early invasive strategy in OHCA patients without STEMI or signs of refractory cardiogenic shock, performing coronary angiography after neurological recovery to try and identify the cause of the arrest seemed to be reasonable in our case owing to the high incidence of CAD in these studies (17–19).

Conclusion

With the increasing number of people receiving COVID-19 vaccinations, rare but serious AEFIs have been reported. We hope that this case report will raise awareness among healthcare providers worldwide that in the era of COVID-19 vaccination, even though fatal AEFIs are rare, heightened awareness of severe side effects needing medical attention is very important.

Data availability statement

The raw data supporting the conclusions of this article will be made available by the authors, without undue reservation.

Ethics statement

Written informed consent was obtained from the individual(s) for the publication of any potentially identifiable images or data included in this article.

Author contributions

CC took care of the patient and wrote the report. C-PL and C-JC performed the cardiac angiography and intravascular ultrasound. P-HC revised in the report. All authors contributed to the article and approved the submitted version.

Conflict of interest

The authors declare that the research was conducted in the absence of any commercial or financial relationships that could be construed as a potential conflict of interest.

Publisher's note

References

1. Ministry of Health and Welfare. *Taiwan FDA Granted Emergency Use Authorization (EUA) for Four COVID-19 Vaccines in Taiwan*. (2021). Available online at: https://www.mohw.gov.tw/cp-115-64023-2.html (accessed September 12, 2022).

2. OCHA. *Coronavirus (COVID-19) Vaccinations Dataset*. (2021). Available online at: https://ourworldindata.org/covid-vaccinations?country=TWN~{}OWID_WRL (accessed September 12, 2022).

3. Ho, JS, Sia CH, Ngiam JN, Loh PH, Chew NW, Kong WK, et al. A review of COVID-19 vaccination and the reported cardiac manifestations. *Singapore Med J.* (2021). doi: 10.11622/smedj.2021210 [Epub ahead of print].

4. WHO. *Serious Adverse Events Following Immunization (AEFI)*. (2018). Available online at: https://www.who.int/groups/global-advisory-committee-on-vaccine-safety/topics/aefi/serious-aefi (accessed September 12, 2022).

5. Falsey AR, Sobieszczyk ME, Hirsch I, Sproule S, Robb ML, Corey L, et al. Phase 3 Safety and Efficacy of AZD1222 (ChAdOx1 nCoV-19) Covid-19 Vaccine. *N Engl J Med.* (2021) 385:2348–60. doi: 10.1056/NEJMoa2105290

6. Kaur U, Bala S, Joshi A, Reddy NTS, Japur C, Chauhan M, et al. Persistent health issues, adverse events, and effectiveness of vaccines during the second wave of COVID-19: a cohort study from a tertiary hospital in North India. *Vaccines.* (2022) 10:1153. doi: 10.3390/vaccines10071153

7. CDC. Syncope after immunization – United States, January 2005–July 2007. *Mortal Morbid Wkly Rep.* (2008) 57:457–60.

8. WHO. *Immunization Stress-Related Response. A Manual for Program Managers and Health Professionals to Prevent, Identify and Respond to Stress Related Responses Following Immunization*. Geneva: WHO (2019).

9. Myerburg RJ, Junttila MJ. Sudden cardiac death caused by coronary heart disease. *Circulation.* (2012) 125:1043–52. doi: 10.1161/CIRCULATIONAHA.111.023846

10. Pomara C, Sessa F, Ciaccio M, Dieli F, Esposito M, Giammanco GM, et al. COVID-19 vaccine and death: causality algorithm according to the WHO eligibility diagnosis. *Diagnostics.* (2021) 11:955. doi: 10.3390/diagnostics11060955

11. Sessa F, Salerno M, Esposito M, Di Nunno N, Zamboni P, Pomara C. Autopsy findings and causality relationship between death and COVID-19 vaccination: a systematic review. *J Clin Med.* (2021) 10:5876. doi: 10.3390/jcm10245876

12. Maadarani O, Bitar Z, Elzoueiry M, Nader M, Abdelfatah M, Zaalouk T, et al. Myocardial infarction post COVID-19 vaccine - coincidence, Kounis syndrome or other explanation - time will tell. *JRSM Open.* (2021) 12:20542704211025259. doi: 10.1177/20542704211025259

13. Sung JG, Sobieszczyk PS, Bhatt DL. Acute myocardial infarction within 24 hours after COVID-19 vaccination. *Am J Cardiol.* (2021) 156:129–31. doi: 10.1016/j.amjcard.2021.06.047

14. AstraZeneca. *COVID-19 Vaccine Astrazeneca Analysis Print*. (2022). Available online at: https://assets.publishing.service.gov.uk/government/uploads/system/uploads/attachment_data/file/972833/COVID-19_AstraZeneca_Vaccine_Analysis_Print.pdf (accessed September 12, 2022).

15. Shiravi AA, Ardekani A, Sheikhbahaei E, Heshmat-Ghahdarijani K. Cardiovascular complications of SARS-CoV-2 vaccines: an overview. *Cardiol Ther.* (2022) 11:13–21. doi: 10.1007/s40119-021-00248-0

16. Singh R, Chakrabarti SS, Gambhir IS, Verma A, Kumar I, Ghosh S, et al. Acute cardiac events after ChAdOx1 nCoV-19 corona virus vaccine: report of three cases. *Am J Ther.* (2022) 29:e579–85. doi: 10.1097/MJT.0000000000001472

17. Lemkes JS, Janssens GN, van der Hoeven NW, Jewbali LSD, Dubois EA, Meuwissen MM, et al. Coronary angiography after cardiac arrest without ST segment elevation: one-year outcomes of the COACT randomized clinical trial. *JAMA Cardiol.* (2020) 5:1358–65. doi: 10.1001/jamacardio.2020.3670

18. Desch S, Freund A, Akin I, Behnes M, Preusch MR, Zelniker TA, et al. Angiography after out-of-hospital cardiac arrest without ST-segment elevation. *N Engl J Med.* (2021) 385:2544–53. doi: 10.1056/NEJMoa2101909

19. Kern KB, Radsel P, Jentzer JC, Seder DB, Lee KS, Lotun K, et al. Randomized pilot clinical trial of early coronary angiography versus no early coronary angiography after cardiac arrest without st-segment elevation: the PEARL study. *Circulation.* (2020) 142:2002–12. doi: 10.1161/CIRCULATIONAHA.120.049569

frontiers | Frontiers in Cardiovascular Medicine

TYPE Case Report
PUBLISHED 11 October 2022
DOI 10.3389/fcvm.2022.915874

OPEN ACCESS

EDITED BY
Yan Zhang,
Peking University, China

REVIEWED BY
Jaganmohan Tharakan,
Cardiologist Researcher India, India
Mao Zhang,
Stanford University, United States

*CORRESPONDENCE
Songlin Zhang
anyecho11try@163.com

SPECIALTY SECTION
This article was submitted to General Cardiovascular Medicine, a section of the journal Frontiers in Cardiovascular Medicine

RECEIVED 08 April 2022
ACCEPTED 29 August 2022
PUBLISHED 11 October 2022

CITATION
Zhou T, Liu C and Zhang S (2022) Case report: Conquer a complex variant: Coronary-pulmonary artery fistulas, atrial septal defect and bicuspid pulmonary valve, under beating heart surgery.
Front. Cardiovasc. Med. 9:915874.
doi: 10.3389/fcvm.2022.915874

Case report: Conquer a complex variant: Coronary-pulmonary artery fistulas, atrial septal defect and bicuspid pulmonary valve, under beating heart surgery

Ting Zhou[1], Chaobing Liu[2] and Songlin Zhang[2]*

[1]Department of Cardiothoracic Surgery, The First College of Clinical Medical Science, China Three Gorges University, Yichang, China, [2]Department of Cardiothoracic Surgery, Yichang Central People's Hospital, Yichang, China

Coronary artery to pulmonary artery fistula (CPAF) is a congenital or acquired abnormal channel between arteries, with a left-to-right cardiac shunting, which may lead to myocardial ischemia, arrhythmia, thrombotic complications, and heart failure. CPAF is usually detected by coronary angiography but few reports have used beating-heart surgery as a detection method. The patient in this case report is a 39-year-old male diagnosed with atrial septal defect (ASD), bicuspid pulmonary valve, and moderate tricuspid regurgitation (TR). He is asymptomatic. In preoperative evaluation, significant CPAF was suspected using echocardiography. The patient refused coronary angiography due to allergic history. Therefore, the cardiac team designed and performed on-pump beating-heart surgery (OPBHS) to detect and repair these disorders, and suggested OPBHS as a myocardial protection strategy for the patient at low surgical risk. A rare and complex cardiovascular case with CPAFs from two branches of the left anterior descending coronary (LAD) artery to the main pulmonary artery (MPA) with ASD, bicuspid pulmonary valve, and moderate TR has not yet been reported in the literature, and its embryological hypothesis has been further analyzed in this report.

KEYWORDS

CPAF, on-pump beating heart surgery, ASD, bicuspid pulmonary valve, moderate tricuspid regurgitation

Abbreviations: CPAF, Coronary artery to pulmonary artery fistula; LAD, left anterior descending coronary; PA, pulmonary artery; ASD, atrial septal defect; OPBHS, on-pump beating heart surgery; ECG, electrocardiogram; CRBBB, complete right bundle branch block; TR, tricuspid regurgitation; TTE, Transthoracic echocardiography; TEE, transesophageal echocardiography; CPB, cardiopulmonary bypass; I/R injury, ischemia and reperfusion injury; NYHA, New York Heart Association; CABG, coronary artery bypass grafting.

Introduction

Coronary artery to pulmonary artery fistula (CPAF) is a congenital or acquired abnormal channel between the coronary artery and the pulmonary artery with a left-to-right cardiac shunting, which may lead to myocardial ischemia, arrhythmia, thrombotic complications, and heart failure (1, 2). From the reported literature, coronary to PA fistula comprises 16% of all coronary cameral fistulae. Coronary cameral fistulae have been reported in 0.1–0.5% of routine coronary angiograms and the vast majority of them are small and asymtomatic (2, 3).

We report a rare congenital cardiovascular variant with two CPAFs from two branches of the left anterior descending coronary (LAD) to the main pulmonary artery (MPA), coexisting with a bicuspid pulmonary valve and atrial septal defect (ASD), which has not yet been reported in the literature.

The patient was a 39-year-old male diagnosed with ASD, bicuspid pulmonary valve, and moderate TR, and he was asymptomatic. In the preoperative evaluation using echocardiography, a hemodynamically significant coronary-PA fistula was highly suspected. The patient refused to undergo a coronary angiography due to their allergic history to penicillin. This unique situation provided diagnostic and therapeutic challenges to the surgical team. As such, the cardiac team designed and performed OPBHS to detect and repair the CPAFs, ASD, bicuspid pulmonary valve, and moderate TR.

We present the following case in accordance with the CARE Reporting checklist (available at http://dx.doi.org/10.21037/acr-20-100).

Case report

A 39-year-old male, went to see a doctor with a cold, and a systolic ejection murmur (Levine 2 of 6) over his left upper sternal border was detected. Therefore, he was referred to our tertiary medical center for further evaluation. He was asymptomatic. His past medical history was paroxysmal hypertension, and he was an active smoker, without a family history of heart disease. Clinical examination suggested ASD with a moderate left-to-right shunt and no pulmonary artery hypertension (PAH). The laboratory tests were within the normal range and included: cardiac enzymes, N-terminal pro-B-type natriuretic peptide, inflammatory markers, lipid panel, and coagulation function. The 12-lead electrocardiogram (ECG) showed a sinus rhythm and a complete right bundle branch block (CRBBB), without signs of compromised myocardial perfusion or left ventricular hypertrophy. A chest CT scan reported a widening of the left and right pulmonary arteries and minor fibrosis of both lungs. Transthoracic echocardiography (TTE) (**Figure 1**) revealed a secundum ASD with a diameter of 25 mm, a bicuspid pulmonary valve, a widening of the pulmonary artery, and the right atrium and ventricle were dilated.

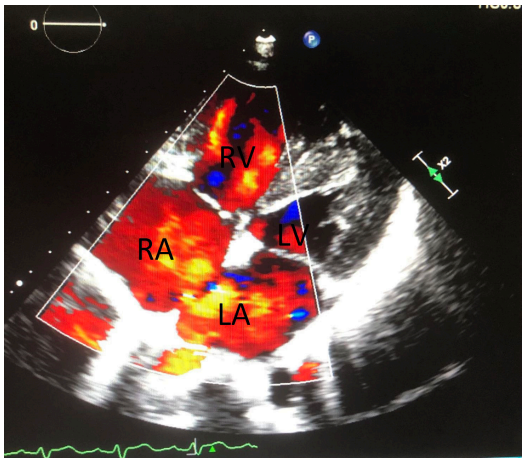

FIGURE 1
Shows the atrial septal defect.

Additionally, transesophageal echocardiography (TEE) showed moderate tricuspid regurgitation (TR). Furthermore, TEE showed obvious high velocity continuous and dominant diastolic aliasing in the color flow Doppler signals in the MPA (**Figure 2**). The logical conclusions were that there might be either a small AP window, anomalous coronary from PA, coronary PA fistula, or atypical PDA. Combining the image of a large proximal left anterior descending artery (LAD) at origin, the surgical team suspected the diagnosis was LAD to PA fistula. Nevertheless, a transthoracic/transesophageal echo has the rare ability to visualize clear imaging of the fistulous connection. Furthermore, due to allergic history to penicillin, the patient refused to undergo coronary angiography.

After careful preoperative evaluation, there were three reasons for the choice of on-pump beating-heart surgery (OPBHS). First and foremost, to investigate the continuous aliasing of the color Doppler signals in the MPA, we can directly detect any coronary-PA fistula under beating-heart surgery. Furthermore, if the coronary –PA fistula existed, it could be treated effectively along with the ASD, bicuspid pulmonary valve, and moderate TR. Finally, considering the myocardial protection, OPBHS might reduce the risk of ischemia and reperfusion (I/R) injury. The total procedure was displayed in the **Figure 3**.

Operative procedure

Through a small incision, using a median sternotomy, the OPBHS was performed. After opening the pericardium, the proximal segment of the LAD was about 10 mm in diameter and tortuous. Two branches of the LAD terminated at the

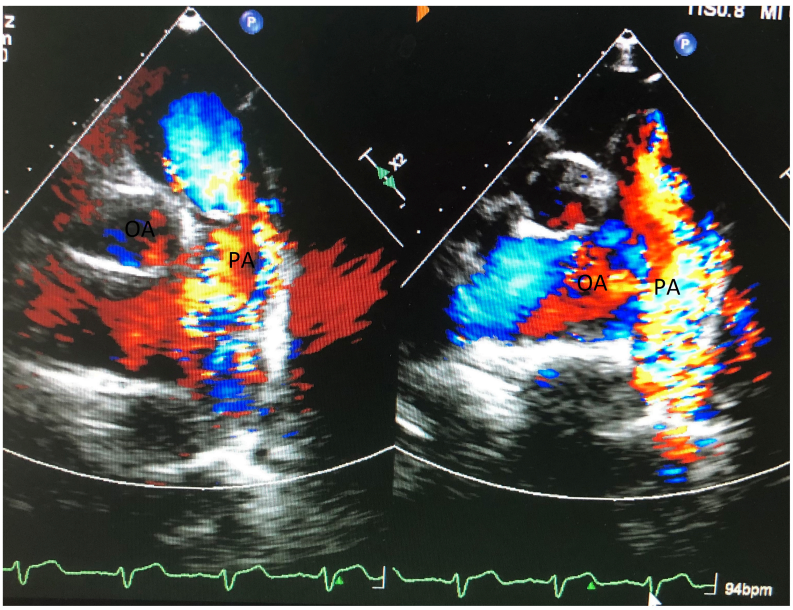

FIGURE 2
Shows obvious high velocity continuous and dominant diastolic aliasing color flow Doppler signals in MPA.

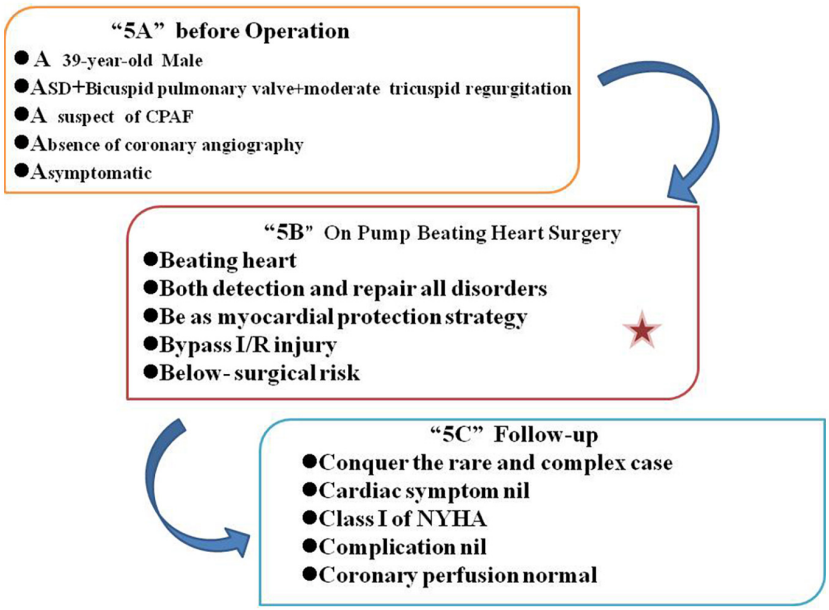

FIGURE 3
Total procedures.

trunk of the pulmonary artery (PA). The diameters of the two branches were 8 and 7 mm, respectively. The width of the MPA is about 30 mm.

First, the secundum ASD was repaired, with a 25*20 mm polyester patch. The MPA was opened through a transverse incision. Under the beating heart, two fistulas were found, just above the pulmonary valve in the MPA, with two left-to-right cardiac shunts. The size of the orifices of the two fistulas was 8 and 7 mm, respectively. They originated from two branches of the LAD that drained into the MPA. The lengths of their communications were 30 and 35 mm, respectively. The diameter of fistulous tracks was 8 and 7 mm, respectively. Therefore,

coronary-pulmonary artery fistulas were large and significant and warranted surgery.

The heart team evaluated the condition of the patient and informed their authorized person of the unexpected finding of coronary to PA fistulae requiring surgical correction. After obtaining consent, the procedure was carried out. Two fistulous tracts arising from the LAD were traced, draining to the MPA, and clamped. The ECG monitor showed no ST changes so the left ventricular contractility remained unchanged. A surgical ligature of the two fistulous tracts was performed. The orifices of the fistulous tracts were closed with a 4-0 polypropylene suture from within the MPA.

The repairs of the bicuspid pulmonary valve and tricuspid valve were performed uneventfully. A 20 mm-probe could easily cross the right ventricular outflow. No residual defects or regurgitation was detected on the TEE after intracardiac manipulation.

The post-operative period was uneventful. Post-operative investigations showed normal cardiac enzymes and normal ECG. An echocardiographic evaluation revealed normal cardiac LV function and no significant residua. The patient was reviewed after 2 months. He did not have any cardiac symptoms, was carrying out normal activities, and was in the New York Heart Association (NYHA) class I. He was satisfied with the surgery and its outcomes.

All procedures performed in studies involving human participants were in accordance with the ethical standards of the institutional and/or national research committee(s) and with the Helsinki Declaration (as revised in 2013). Written informed consent was obtained from the patient.

Discussion

It is reasonable to assume the patient had a congenital coronary to PA fistula from two branches of the LAD to the MPA, associated with an ostium secundum ASD and bicuspid pulmonary valve. Based on the Hackensellner involution-persistence hypothesis (4), we propose that the two fistulas might be two persistent anlages from truncus arteriosus. Other congenital heart defects have been associated with coronary fistula, varying from 0.5 to 5%. A large flow in the fistulas may cause myocardial ischemia or infarction. Therefore, the surgery was deemed to be required (1, 2, 5).

We propose the potential origin and reason of the case. Although there is no family history, it might be possible that the patient carries some genetic mutations leading to this rare case. In recent research from the UK NHS Genomic Medicine Centre, a heterozygous GDF2 variant lead to vascular malformation such as hereditary hemorrhagic telangiectasia (HHT), and it might be one of the genetic mutations for coronary-pulmonary fistula (6). Mutations in the *RBM10* gene are a cause of ASD, and might be responsible for PA fistula, according to a molecular study by Han and his colleague (7).

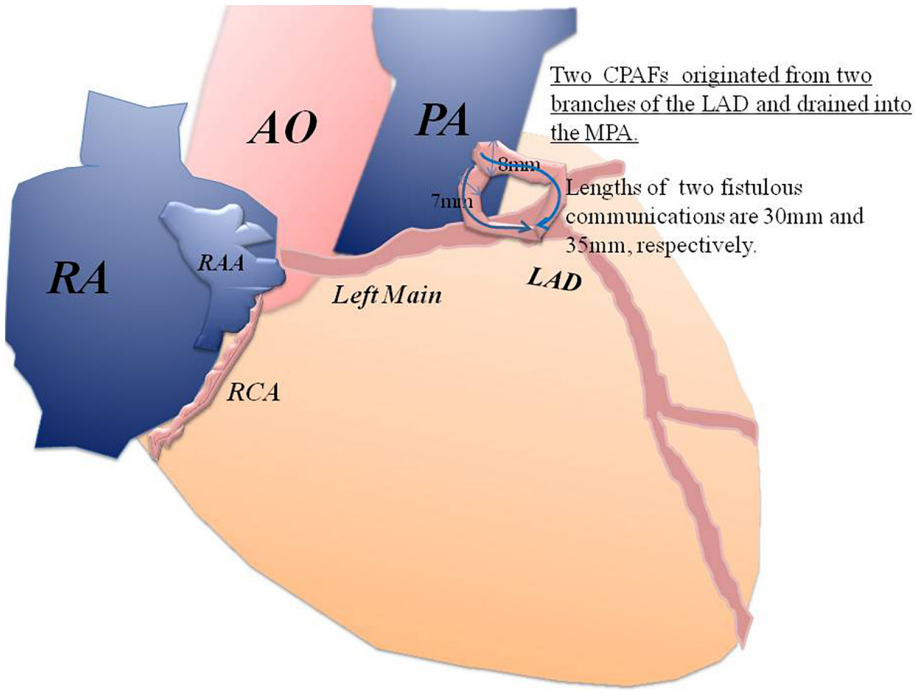

FIGURE 4
A sketch of the two CPAFs that originated from two branches of the LAD and drained into the MPA.

To deeply understand this complex case, we analyzed the patient's hemodynamic results, the moderate left-to-right ASD shunt overload, and abraded the tricuspid valve. Despite the additional volume from two Coronary-PA fistulas and ASD, under the obstruction of the bicuspid pulmonary valve, fortunately, the pulmonary artery gradually widened without PAH.

In our case, CPAFs were successfully detected and treated under OPBHS. The clinical advantages of the OPBHS included:(1) a near-physiologic state, maintaining continuous coronary blood flow avoiding ischemia and reperfusion injury; (2) CPAFs were identified and carefully evaluated under direct vision; and (3) ligature of two fistulous tracts was performed under direct vision, preventing downstream coronary steal and left-to-right shunt. The patient was easily weaned off CPB. No ST changes or significant arrhythmia were detected by ECG monitoring.

OPBHS was initiated as a myocardial protection strategy to prevent ischemia/reperfusion injury. It was first applied by Wei and his colleagues in 1993 for a patient undergoing mitral valve replacement (8).

Usually, OPBHS is reserved for high surgical risk with LV dysfunction/chronic kidney disease (9–13). With the outcomes of our case, this technique may be possible for patients with low surgical risk.

Limitations

The surgical team summarized the experience of this case, analyzing the total diagnosis and treatment process. The preoperative assessment could be more comprehensive. A 39-year-old male, without coronary angiogram due to patient refusal, even though asymptomatic, with cardiac enzymes in the normal range, without signs of ischemia on ECG, and with variable coronary risk factors (hypertension, active smoker), could have a guarded coronary treadmill evaluation and myocardial perfusion scan.

In a small incision, taking surgical photos was inconvenient and increased the risk of contamination of the surgical field. In this situation, we prioritized patient safety and did not take representative intraoperative photographs. However, we do believe that the rare variant should be reported. To give readers a better understanding, we have provided a sketch (**Figure 4**).

Conclusion

We report a rare and complex case with two coronary-pulmonary artery fistulas from two branches of the LAD to the MPA, ASD, and a bicuspid pulmonary valve. Furthermore, it was successfully diagnosed and repaired under OPBHS. The patient was asymptomatic and the small coronary-pulmonary artery fistula might be clinically missed. Therefore, the use of OPBHS to directly detect, evaluate and treat CPAFs is relevant. OPBHS as a myocardial protection strategy is feasible for patients with low surgical risk. The precise role of OPBHS in myocardial protection needs further study.

Data availability statement

The original contributions presented in this study are included in the article/supplementary material, further inquiries can be directed to the corresponding author.

Ethics statement

The studies involving human participants were reviewed and approved by the Medical ethics committee of Yichang Central People's Hospital. The ethics committee waived the requirement of written informed consent for participation.

Author contributions

All authors listed have made a substantial, direct and intellectual contribution to the work, and approved it for publication.

Acknowledgments

We are grateful for the patient's collaboration, especially in the follow-up. We also appreciate the Department of Cardiothoracic Surgery at the Yichang Central People's Hospital.

Conflict of interest

The authors declare that the research was conducted in the absence of any commercial or financial relationships that could be construed as a potential conflict of interest.

Publisher's note

References

1. George B, Sood MR. Coronary-pulmonary artery fistula with lung hypoplasia and a bicuspid aortic valve: a case report. *JRSM Cardiovasc Dis*. (2022) 11:20480040221082905. doi: 10.1177/20480040221082905

2. Kim H, Beck KS, Choe YH, Jung JM. Coronary-to-pulmonary artery fistula in adults: natural history and management strategies. *Korean J Radiol.* (2019) 20:1491–7. doi: 10.3348/kjr.2019.0331

3. Zhang LJ, Zhou CS, Wang Y, Jin Z, Yu W, Zhang Z, et al. Prevalence and types of coronary to pulmonary artery fistula in a Chinese population at dual-source CT coronary angiography. *Acta Radiol.* (2014) 55:1031–9. doi: 10.1177/0284185113512299

4. Vaidyanathan KR, Theodore SAC, Sankar MN, Cherian KM. Coronary artery to pulmonary artery fistula with dual origin–embryological, clinical and surgical significance. *Eur J Cardiothorac Surg.* (2007) 31:318–9. doi: 10.1016/j.ejcts.2006.11.0186

5. Rubimbura V, Girod G, Delabays A, Meier D, Rotzinger DC, Muller O, et al. Case report: coronary-pulmonary fistula closure by percutaneous approach: learning from mistakes. *Front Cardiovasc Med.* (2022) 8:779716. doi: 10.3389/fcvm.2021.779716

6. Balachandar S, Graves TJ, Genomics England Research Consortium. Identification and validation of a novel pathogenic variant in GDF2 (BMP9) responsible for hereditary hemorrhagic telangiectasia and pulmonary arteriovenous malformations. *Am J Med Genet A.* (2022) 188:959–64. doi: 10.1002/ajmg.a.62584

7. Daicheng H, Shiwen X, Jingxuan Z, Junbo H, Bo WA. Frameshift RBM10 variant associated with TARP syndrome. *Front Genet.* (2022) 13:922048. doi: 10.3389/fgene.2022.922048

8. Wei H, Mingwu C, Wensheng W. Beating heart mitral valve replacement in 2 cases under mild hypothermia cardiopulmonary bypass. *Guangxi Med Coll J.* (1993) 10:320–1.

9. Zhang S, Huang S, Tiemuerniyazi X, Song Y, Feng W. A meta-analysis of early, mid-term and long-term mortality of on-pump vs. off-pump in redo coronary artery bypass surgery. *Front Cardiovasc Med.* (2022) 9:869987. doi: 10.3389/fcvm.2022.869987

10. Velioglu Y, Isik M. Early-term outcomes of off-pump versus on-pump beating-heart coronary artery bypass surgery. *Thorac Cardiovasc Surg.* (2019) 67:546–53. doi: 10.1055/s-0039-1679923

11. Ueki C, Sakaguchi G, Akimoto T, Ohashi Y, Sato H. On-pump beating-heart technique is associated with lower morbidity and mortality following coronary artery bypass grafting: a meta-analysis. *Eur J Cardiothorac Surg.* (2016) 50:813–21. doi: 10.1093/ejcts/ezw129

12. Mo A, Lin H. Surgical correction of ruptured aneurysms of the sinus of Valsalva using on-pump beating-heart technique. *J Cardiothorac Surg.* (2010) 5:37. doi: 10.1186/1749-8090-5-37

13. Wejner-Mik, P, Lipiec P, Peruga JZ, Jaszewski R, Pawłowski W, Kasprzak J. Optimal treatment of coronary-to-pulmonary artery fistula: surgery, coil or stent graft? *Postepy Kardiologii Interwencyjnej.* (2013) 9:282–5. doi: 10.5114/pwki.2013.37510

frontiers | Frontiers in Cardiovascular Medicine

TYPE Case Report
PUBLISHED 14 October 2022
DOI 10.3389/fcvm.2022.996481

OPEN ACCESS

EDITED BY
Antonio Sorgente,
EpiCURA, Belgium

REVIEWED BY
Giuseppe Mascia,
University of Genoa, Italy
Petr Peichl,
Institute for Clinical and Experimental Medicine (IKEM), Czechia

*CORRESPONDENCE
Guangzhi Chen
chengz2003@163.com
Yan Wang
newswangyan@tjh.tjmu.edu.cn

SPECIALTY SECTION
This article was submitted to General Cardiovascular Medicine, a section of the journal Frontiers in Cardiovascular Medicine

RECEIVED 17 July 2022
ACCEPTED 09 September 2022
PUBLISHED 14 October 2022

CITATION
He M, Qiu J, Bai Y, Wang Y and Chen G (2022) Massive pleural effusion following high-power and short-duration radiofrequency ablation for treatment of atrial fibrillation: A case report and review of the literature.
Front. Cardiovasc. Med. 9:996481.
doi: 10.3389/fcvm.2022.996481

Massive pleural effusion following high-power and short-duration radiofrequency ablation for treatment of atrial fibrillation: A case report and review of the literature

Miaomiao He, Jie Qiu, Yang Bai, Yan Wang* and Guangzhi Chen*

Division of Cardiology, Department of Internal Medicine, Tongji Hospital, Tongji Medical College, Huazhong University of Science and Technology, Wuhan, China

Postpericardial injury syndrome (PPIS) is defined as pericarditis or pericardial effusion that results from recent myocardial infarction or intracardiac interventions. These symptoms typically include fever, leukocytosis, a high erythrocyte sedimentation rate, and elevated C-reactive protein levels. Additionally, pericardial effusion and pleural effusion may be present. It is considered to be a common complication in cardio-surgery with an occurrence of 3–30%. In the past 20 years, a high number of patients with atrial fibrillation have suffered from PPIS following radiofrequency catheter ablation. However, previous reports focused on identifying cardiac tamponade and pericardial effusion as their main clinical manifestations. Solitary pulmonary involvement following PPIS with the radiofrequency catheter ablation may occur. We report a case of PPIS that presented pleural effusion as the dominant feature soon after the operation and systematic review to illustrate the clinical characteristics of PPIS.

KEYWORDS

atrial fibrillation, radiofrequency catheter ablation, postpericardial injury syndrome, diagnosis, pleural effusion

Introduction

Radiofrequency catheter ablation (RFCA) involves pulmonary vein isolation and left atrial ablations, which are a crucial part of non-pharmacological treatment for drug-refractory atrial fibrillation (AF) (1–3). RFCA has become more widely used in the treatment of uncontrolled AF in the past few years (4, 5). As a result of RFCA, complications such as left atrial esophageal fistula and cardiac tamponade have declined over the past 10 years, especially when performed by an experienced surgeon (6, 7).

Postpericardial injury syndrome (PPIS) is defined as pericarditis or pericardial effusion that results from myocardial infarction or intracardiac interventions (8). These

symptoms typically include fever, leukocytosis, a high erythrocyte sedimentation rate, and elevated C-reactive protein levels. Additionally, pericardial effusion and pleural effusion may be present. The first described PPIS for cardiac surgeries was reported in 1958 (9). It is considered to be a common complication in cardio-surgery with an occurrence of 3–30% (10, 11). PPIS following RFCA of AF has been frequently reported over the past 20 years. But the majority of reported cases concerning PPIS focused on simultaneous pleural and pericardial effusion as first clinical manifestations. There is no reported case of solitary pulmonary involvement except for a new case from our center. Hence, considering the challenging nature of this disease, we here present an unusual case of PPIS manifested by massive pleural effusions alone and a systematic review to illustrate clinical characteristics of PPIS.

Case presentation

A 65-year-old woman underwent CA at our center because of increasing palpitation symptoms despite antiarrhythmic drug therapy. She had a history of hypertension, and chronic AF and had symptomatic AF confirmed by the 12-lead ECG for 1 year (Figure 3A). On admission, her routine clinical assessment and physical examination revealed irregular heart sounds, jugular venous pulsations, and hypertension. Preprocedural transesophageal echocardiography showed normal biventricular function with patent foramen ovale and no thrombus in the LA appendage. A chest computed tomography demonstrated no significant abnormalities, as shown in Figure 1A.

After a successful routine single transseptal puncture, under electroanatomic mapping data using a 3D mapping system (CARTO3, Biosense Webster, Inc, Diamond Bar, CA), all four pulmonary veins were isolated and the additional ablation was technically successful using a ThermoCool SmartTouch irrigation-tip contact force radiofrequency ablation catheter (Biosense Webster Inc, Irvine, CA), including groof of the left atrium, BOX isolation of posterior wall, superior vena cava, and right atrial cavotricuspid isthmus. Depending on the ablation index, ablation was initiated at a power of 60 W for a duration of 8–10 s on the left posterior wall and 11–20 s on the other parts of the left atrial wall. We ablated the cavotricuspid isthmus and other parts of the right atrial wall with 40 W and adjusted the target ablation index between 400 and 500 if needed. The superior vena cava was ablated with 40 W and the target ablation index was adjusted between 250 and 350 as necessary. To avoid excessive drops in impedance, we adjusted the contact force by 5–10 *g* for each application (Figure 2). A total of 7,000 U heparin

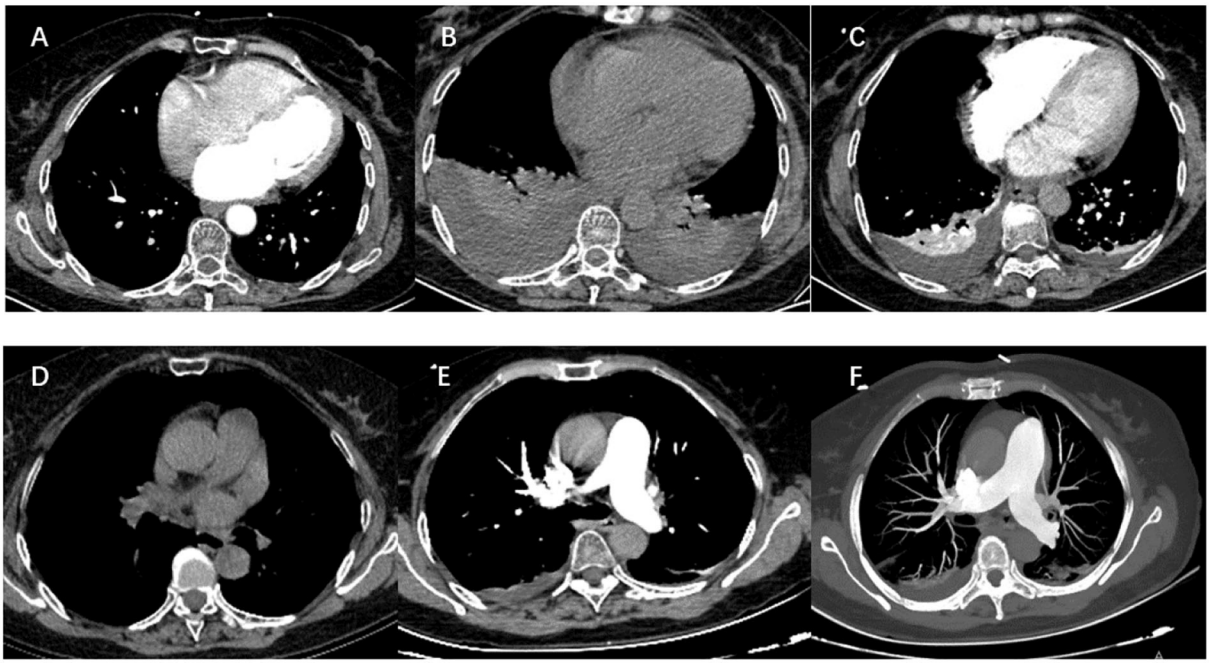

FIGURE 1
The dramatic transition of a thoracic CT scan (soft-tissue window) and pulmonary computed tomography angiography. **(A)** Preoperative tests: CT revealed clear lung fields bilaterally. **(B)** Three days after operation: CT scan showing large bilateral pleural effusions without pericardial effusion. **(C)** Nine days after the operation: there is a resolution of the left pleural effusion and a marked decrease in the right pleural effusion. **(D)** Nineteen days after operation: there is no pleural effusion on CT images. **(E,F)** Pulmonary computed tomography angiography ruled out pulmonary embolism.

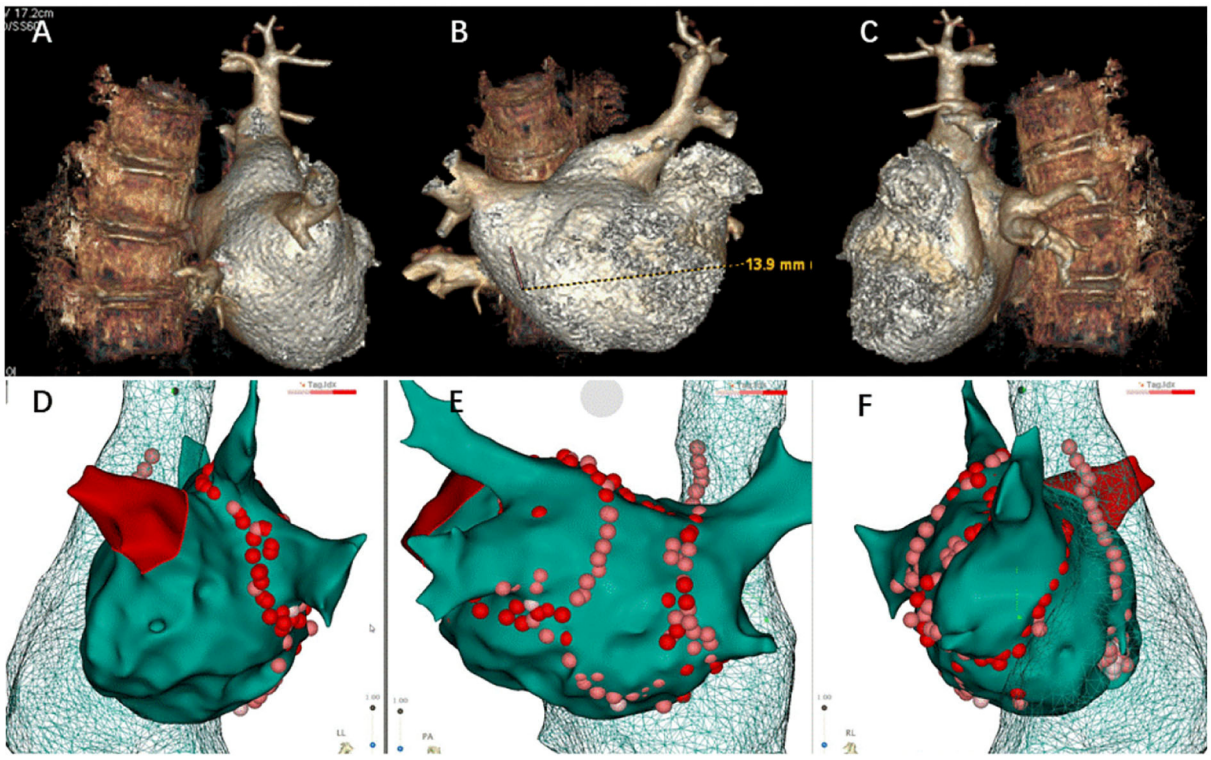

FIGURE 2
Three-dimensional reconstruction of pulmonary vein and ablation circle (red-colored) using the CARTO3® system. **(A)** Three-dimensional reconstruction of the pulmonary vein in left lateral view. **(B)** Three-dimensional reconstruction of the pulmonary vein in posteroanterior view. **(C)** Three-dimensional reconstruction of the pulmonary vein in right lateral view. **(D)** Ablation circle in left lateral view. **(E)** Ablation circle in posteroanterior view. **(F)** Ablation circle in right lateral view.

was given during the procedure. The scheduled procedure was completed without complications. The vital signs were stable during ablation.

On the following day, there was a progressive worsening of symptoms associated with chest distress and dyspnea (Figure 3B). Upon physical examination, her neck veins were non-distended, her lungs were distant, and her heart sounds were clear. She was afebrile, with a normal sinus rhythm of 120 breaths per minute, blood pressure of 135/76 mmHg, and respiratory rate of 20 breaths per minute. There was a mild rise in the inflammatory markers (C-reactive protein [CRP]). High sensitivity cardiac troponin T was elevated at 2,546.1 pg/ml (Table 1). Significant laboratory findings included a white blood cell count of 16.82 × 10^9/L with 87.4% neutrophils. A transthoracic echocardiogram (TTE) showed normal left ventricular function (ejection fraction 60%) without pericardial effusion, but a new-onset small right pleural effusion was detected. An oral diuretic was prescribed, which improved the symptoms. The patient was started on glucocorticoids, antibiotic therapy, and oxygen inhalation by mask.

Her health condition did not improve after treatment for 3 days. As shown in Figure 1B, massive bilateral pleural effusion alone was observed in a chest computed tomography. There was no pericardial effusion in the post-procedure TTE. Pulmonary computed tomography angiography ruled out pulmonary embolism (Figure 1). After the exclusion of infectious, metabolic, and toxic causes of pleural effusion, the criteria for PPIS were considered because our patient was found to have pleural effusions along with pleuritic chest distress and elevated levels of inflammatory markers. Then the patient was continued on glucocorticoid and antibiotic therapy. The pathological changes were resolved and the chest CT reverted to normal after 3 days of treatment, and the patient was able to be discharged out of the hospital; the chest CT is shown in Figure 1C.

At a 1-month follow-up, recovery of the patient was uneventful, and the chest CT scan displayed full expansion of the lungs with almost complete resolution of the massive pleural effusion (Figure 1D).

Literature review

Methods

A systematic electronic literature search for primary evidence was performed in the PubMed database. Keywords used in electronic searching include "post-cardiotomy

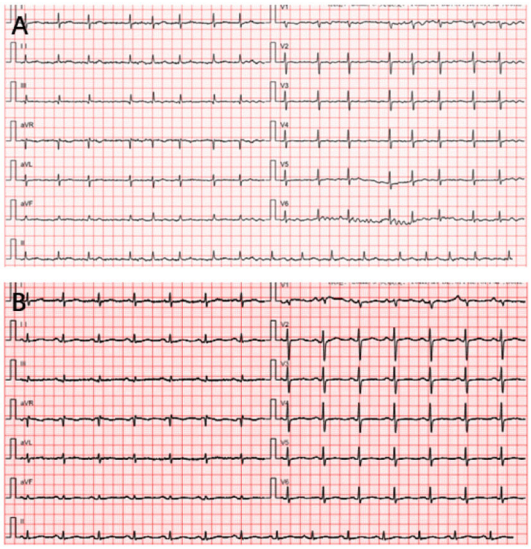

FIGURE 3
Patient's electrocardiogram (ECG). **(A)** The preprocedure ECG reveals atrial fibrillation. **(B)** The postoperative ECG of the patient when she felt palpitations and chest discomfort.

syndrome", or "post-cardiac injury syndrome", or "Dressler's syndrome," or "pericardial effusion, and CA." No language restrictions were applied. In addition to the articles searched by keywords, the reference lists of all relevant articles were also examined. Articles satisfying the following criteria were included in this study: (1) the main clinical manifestation after the operation is pleural effusion and (2) CA treatment in patients with AF. Studies that meet the following criteria were excluded: (1) studies not in the English language; (2) studies published only in abstract or review form; and (3) data unavailable, or not relevant. Other ablation-related complications such as cardiac tamponade, left atrial esophageal fistula, pericarditis, and pericardial effusion were not enrolled in this study.

Results

Based on the key terms used for the search, 561 articles were initially identified between 1993 and 2022. We excluded 33 non-English studies during the screening of abstracts; 524 articles that did not meet the inclusion criteria were also ruled out. After screening titles and corresponding contents, 11 published studies were identified as fulfilling the inclusion criteria. The extracted data included the name of the author, year of publication, age and gender of patients, type of AF, the onset of catheter-related complications, laboratory examination, outcomes, and therapeutic strategies. The extracted data are compiled in Table 2.

Data of 17 diagnosed patients with PPIS including 16 (94.1%) from the 11 articles and one new case from our center were collected. There were eight female and nine male patients with a mean age of 62.1 years (range: 24–82 years). Of the 17 patients, nine had paroxysmal AF and seven had non-paroxysmal AF. The presence of symptoms associated with PPIS usually initiated within 3 h to 3 months after RFCA, with an average of 15 days after ablation. The predominant symptoms included pleural effusion and pericardial effusion, which mostly occurred in the first week (52.9%, 9/17). Most patients had dyspnea (11/17, 64.7%), chest pain (12/17, 70.5%), and fever (12/17, 70.5%). Interestingly, 12 cases with pleural effusion presented pericardial effusion except for a new case. Another specific clinical sign is that low power delivery (20–40 W) over a long duration (20–40 s) was performed in the majority of cases. Elevated markers of inflammation and elevated WBC are also important clinical signs and were present in 76.4% of cases (13/17) and 52.9% of cases (9/17), respectively. In one case, the appearance of resistant ascites and progressive prominent symptoms of congestion pointing to the diagnosis of constrictive pericarditis arose 1 month after the ablation of AF (22). Therapeutic strategies for pleural effusion following ablation of AF were based on nonsteroidal anti-inflammatory drugs (NSAIDS) (8/17, 47.1%), glucocorticoids (8/17, 47.1%), and antibiotic therapy (6/17, 35.2%). Pericardiocentesis was presented in 9 cases, and thoracentesis was presented in 6 cases. No mortality occurred during a mean follow-up of 2.3 (0.5–24) months.

Discussion

In this study, we present the first case of PPIS characterized as massive pleural effusion alone after RFCA of AF. In our case, a symptom cluster of chest tightness and breathlessness occurred the day after the operation. Contrast radiography suggested massive bilateral pleural effusion in the absence of pericardial effusion. Cardiac tamponade and cardiac perforation were ruled out by echocardiography. Pulmonary computed tomography angiography also ruled out pulmonary embolism (Figure 1). PPIS after the operation was considered when both elevated leukocyte count and increased C-reactive protein. RFCA is currently the most commonly used ablation technique for the treatment of AF, aiming at eliminating AF and maintaining sinus rhythm in long term. Conventional thermal radiofrequency ablation for AF is low power delivery (20–40 W) over a long duration (20–40 s). Recently, there has been increasing interest to use relatively higher power (45–70 W) over a short duration (5–10 s) (23). The goal was to achieve a high rate of transmural trauma with minimal destruction of surrounding tissues, resulting in lower rates of recurrence and higher efficiency of this solution. Compared with conventional radiofrequency ablation, a large number of studies confirmed

TABLE 1 Several laboratory data cases showing the change in leukocytosis and vital sign.

	WBC (10^9/L)	Hb (g/L)	NT-proBNP (pg/mL)	EF (%)	T (°C)	HR (Times / minute)	R (Times / minute)
1 week before operation	8.77	130	732	68	36.3	105	20
1 day after operation	16.82	116	217	60	36	57	20
3 days after operation	16.26	117	173	64	36.6	61	21
1 week after operation	18.1	118	113	67	36.3	72	19

WBC, white blood cell; Hb, hemoglobin; NT-proBNP, N-terminal pro-B-type natriuretic peptide; EF, ejection fraction; T, temperature; HR, heart rate; R, respiratory rate.

that HPSD may create transmural lesions but lessen injurious heating of deeper structures (24–26). This particular patient was successfully treated with 60 W RFCA. The sinus rhythm of the patient recovered following the completion of pulmonary vein isolation and did not complain any discomfort, which suggested that the operation process was smooth and safe.

Most likely, the primary cause of PPIS is an autoimmune phenomenon, but the precise mechanism remains unknown (27). There are two theories to explain the origin of this syndrome. The first theory is that antibodies against contractile proteins actin and myosin (AMA) and circulate immunocomplex were produced after surgical trauma, resulting in the exposure of endogenous antigens (28, 29). It has been reported that the epicardium after myocardial injury contributed to an inflammatory response by generating cytokines, which led to modulate revascularization and repair of damaged tissue and incite an inflammatory reaction (30). Some studies have confirmed that the presence of specific auto-antibodies experienced a 4-fold increase in the postoperative period, which provides evidence supporting the autoimmune etiology. The second theory is that autoimmune reaction is accelerated by a recent or reactivated viral infection (31). Concomitant mechanical injury of the pericardium is necessary for both theories. In the articles included in the present systematic review, the case in which clinical signs included massive pleural effusion was performed with the application of postoperative thoracentesis and thoracostomy tube placement. Although the patients in our case presented with massive pleural effusion alone, the treatment of chest drain insertion was not given. One reason is that the patient's vital signs were stable, and her oxygen saturation was above 95% under oxygen inhalation. Another is that the patient had a better response to therapy. Within 3 days of treatment with glucocorticoids, antibiotic therapy, and NSAIDS, the patient showed a gradual decrease in the large volumes of pleural fluid, and thoracic CT became normal at recheck examination 2 weeks after discharge. On-demand use of NSAIDs and glucocorticoids, a rapid symptomatic improvement in the case presented strongly argues for an immune-mediated mechanism.

A comprehensive systematic review of PPIS has shown that there was a predominance of CA of AF to ablation-associated PPIS (71.4%) (19). This reflects the fact that AF ablation was associated with a higher risk of PPIS than other RFCA procedures because of larger defects in the myocardium and a higher probability of injury to the adjacent vessels and pleura (15, 32). It has been reported that the incidence of PPIS is correlated to the extent and progression of myocardial damage.

The incidence of PPIS is greater in procedures that involve an extensive area of the myocardium. As is well known, CA of AF usually causes extensive linear lesions of the atrial myocardium, particularly following persistent AF ablation (33). These may have caused the increased incidence of PPIS. However, with all the recent advances in techniques of zero X-ray ablation approach, CF-sensing catheters, and ablation index (34–36), an attempt is being made to reduce the incidence of complications of tamponade and radiation. In the smart AF trial, the incidence of cardiac tamponade was 2.5% among 161 patients (37). In the Toccastar Trial, the tamponade incidence was much lower (38). The results of one recent clinical trial show that the use of AI was associated with a lower observed rate of tamponade (36).

Petey et al. reported a similar case to ours in 2008. Their case was also simple, with exudative pleural effusion following pulmonary vein isolation for paroxysmal AF. However, their case developed PPIS after the thoracoscopic procedure, which is different from our case. In 2013, Yang Liu et al. published an article on the main complications associated with RFCA of cardiac arrhythmia, especially the incidence of PPIS. Only 6 cases of PPIS have been reported in the literature, of whom five were involved in CA of AF. This is because AF ablation carries a higher risk of cardiac perforation than other RFCA procedures. These patients became symptomatic of dyspnea, fever, pleural effusion, or pericardial effusion. Pericardial effusion was present in three of the four patients who had pleural effusions. In a notable departure from a paper published in 2013, radiofrequency ablation AF by use of the Carto3 system was performed in our case rather than the EnSite system. The relatively higher power (60 W) over a short duration was used in our case, rather than low power delivery (35 W) over a long duration. These advances could further decrease the incidence of cardiac perforation.

The incidence of PPIS seems strongly to age, gender, and underlying disease-related. Some studies suggest that elder

TABLE 2 Clinical characteristics of all cases reported in the literature.

Reference	Basic information					Clinical manifestation																Elevated CRP/ESR	Elevated WBC	Treatment					Follow-up
	Age	Sex	Type of AF	Watt of AF	Time of PPIS	Vomiting	Dyspnea	Fever	Chest pain	Cough	Pleural rub	Pulmonary infiltrates	Pneumonia	Pleural effusion			Pericardial rub	Pericardial effusion	Cardiac perforation	Cardiac Tamponade				NSAID	Steroids	Colchicine	Antibiotic therapy	Pericardiocentesis	Thoracentesis	
														Bilateral	Unilateral (side)	Time of detection														
Wood et al. (12)	54	M	persistent AF	12W	5 DAYS	NO	YES	YES	YES	NO	NO	NO	NO	YES	NO	5DAYS	NO	YES	NA	YES	YES	NA	YES	NO	NO	YES	YES	YES	3 MON
Luckie et al. (13)	56	M	AF	NA	8 WEEKS	NO	YES	YES	YES	NO	NO	NO	NO	NO	NO	~	YES	MODERATE	NO	NO	YES	NO	YES	YES	YES	NO	NO	NO	6 WEEKS
Goossens et al. (14)	68	F	paroxysmal AF	25-35W	4 DAYS	NO	YES	YES	YES	NA	NA	NO	NO	YES	NO	2 WEEKS	NO	YES	NO	YES	YES	NA	YES	YES	NO	NO	YES	YES	NA
Liu et al. (15)	60	F	paroxysmal AF	35W	2 DAYS	NO	YES	YES	NO	NO	NO	NO	YES	YES	NO	2 DAYS	NO	YES	YES	NO	YES	YES	YES	NO	NO	NO	YES	NO	1 MON
Liu et al. (15)	77	F	paroxysmal AF	35W	3 DAYS	NO	YES	YES	NO	NO	NO	YES	YES	YES	NO	3 DAYS	NO	YES	YES	NO	YES	YES	NO	YES	NO	YES	YES	NO	1 MON

(Continued)

10.3389/fcvm.2022.996481

TABLE 2 (Continued)

Reference	Basic information					Clinical manifestation														Elevated CRP/ESR	Elevated WBC	Treatment						Follow-up
	Age	Sex	Type of AF	Watt of AF	Time of PPIS	Vomiting	Dyspnea	Fever	Chest pain	Cough	Pleural rub	Pulmonary infiltrates	Pneumonia	Pleural effusion			Pericardial rub	Pericardial effusion	Cardiac perforation	Cardiac Tamponade			NSAID	Steroids	Colchicine	Antibiotic therapy	Pericardiocentesis	Thoracentesis	
														Bilateral	Unilateral (side)	Time of detection													
Liu et al. (15)	56	M	paroxysmal AF	35W	2 DAYS	YES	NO	YES	YES	NO	NO	YES	YES	NO	YES (left)	2 DAYS	NO	YES	YES	NO	NO	NO	YES	NO	NO	NO	NO	NO	1 MON
Liu et al. (15)	67	M	persistent AF	35W	4 DAYS	NO	YES	NO	YES	NO	YES	YES	NO	YES	NO	4 DAYS	NO	YES	YES	NO	NO	NO	NO	NO	NO	NO	NO	NO	1 MON
Liu et al. (15)	62	F	paroxysmal AF	35W	3H	NO	NO	NO	YES	NO	YES	NO	NO	NO	YES (left)	3H	NO	YES	YES	NO	NO	NO	NO	NO	NO	NO	YES	NO	1 MON
Torihashi et al. (16)	49	M	persistent AF	25-30W	2 WEEK	NO	NO	NO	YES	NO	NO	NO	NO	NO	NO	~	YES	LARGE	NO	YES	YES	YES	YES	NO	NO	NO	YES	NO	4 DAY
Yukumi et al. (17)	24	M	paroxysmal AF	NA	3 MONTHS	NO	NO	YES	YES	NO	NO	NO	NO	NO	YES (right)	3 MONTHS	NO	YES	NO	NO	YES	YES	YES	NO	YES	NO	NO	YES	1 MON

(Continued)

10.3389/fcvm.2022.996481

TABLE 2 (Continued)

Reference	Basic information					Clinical manifestation															Elevated CRP/ESR	Elevated WBC	Treatment					Follow-up
	Age	Sex	Type of AF	Watt of AF	Time of PPIS	Vomiting	Dyspnea	Fever	Chest pain	Cough	Pleural rub	Pulmonary infiltrates	Pneumonia	Pleural effusion			Pericardial rub	Pericardial effusion	Cardiac perforation	Cardiac Tamponade			NSAID	Steroids	Colchicine	Antibiotic therapy	Pericardiocentesis	Thoracentesis	
														Bilateral	Unilateral (side)	Time of detection													
Han et al. (18)	68	F	paroxysmal AF	30W	1 DAY	NO	YES	YES	YES	YES	NO	YES	YES	NO	NO	~	NO	NO	NO	NO	YES	YES	NO	YES	NO	YES	NO	NO	1 MON
Li et al. (19)	82	M	persistent AF	NA	14 DAYS	NO	NO	YES	NO	NO	NA	YES	NO	YES	NO	14 DAYS	NO	YES	NO	NO	YES	NO	NO	YES	NO	YES	NO	YES	1 MON
Li et al. (19)	78	M	persistent AF	NA	3 DAYS	NO	YES	YES	NO	YES	NA	MASSIVE	NO	YES	NO	3 DAYS	NO	SMALL	NO	NO	YES	YES	NO	YES	NO	YES	NO	NO	1 MON
Fong et al. (20)	59	F	paroxysmal AF	NA	3 WEEK	NO	NO	YES	NO	YES	NO	NO	NO	NO	NO	~	NO	LARGE	NO	NO	YES	YES	NO	YES	NO	NO	YES	NO	2 WEEK

(Continued)

10.3389/fcvm.2022.996481

TABLE 2 (Continued)

Reference	Basic information					Clinical manifestation																Elevated CRP/ESR	Elevated WBC	Treatment						Follow-up
	Age	Sex	Type of AF	Watt of AF	Time of PPIS	Vomiting	Dyspnea	Fever	Chest pain	Cough	Pleural rub	Pulmonary infiltrates	Pneumonia	Pleural effusion			Pericardial rub	Pericardial effusion		Cardiac perforation	Cardiac Tamponade			NSAID	Steroids	Colchicine	Antibiotic therapy	Pericardiocentesis	Thoracentesis	
														Bilateral	Unilateral (side)	Time of detection														
Rosati et al. (21)	62	F	persistent AF	35W	2 WEEK	NO	YES	YES	YES	YES	NA	NO	NO	NO	YES (left)	1 MON	NO	MODERATE		NA	NO	NA	YES	YES	NO	YES	NO	YES	YES	2 WEEK
Fukasawa et al. (22)	69	M	paroxysmal AF	35-40W	1 MON	NO	YES	NO	YES	NO	NA	NO	NO	YES	NO	3 MONTHS	NA	YES		NO	YES	YES	NA	NO	NO	YES	NO	YES	YES	24 MON
This study	65	F	persistent AF	60W	3 DAYS	NO	YES	NO	YES	NO	NO	NO	NO	YES	NO	3 DAYS	NO	SAMLL		NO	NO	YES	YES	NO	YES	NO	YES	NO	NO	2 WEEK

F, female; M, male; W, watt; Mon, month; AF, atrial fibrillation; PPIS, post-pericardiotomy syndrome; CRP, C-reactive protein; ESR, erythrocyte sedimentation rate; WBC, white blood cell; NSAID, Nonsteroidal anti-inflammatory drugs.

10.3389/fcvm.2022.996481

individuals were more prone to develop cardiac perforation-related PPIS, which is probably because aging may be associated with an increased inflammatory response (39). Multivariate analysis revealed that the incidence of acute pericarditis post-ablation in females increased by 40% compared with that of male patients. One possible explanation for this is that as the thickness of the left atrial wall decrease, so too does the increased risk of pericardial compilations in females, especially in patients with AF (40). Additionally, the risk of developing acute pericarditis was 40% higher in obese patients (41). Pleural incision, anemia, and rheumatoid arthritis were also identified as independent risk factors (10, 42). In an attempt to preclude the onset of this complication, high-risk individuals should have priority to be paid close attention.

Diagnosis depends upon clinical suspicion and the exclusion of other clinical conditions that may mimic this syndrome, such as pulmonary embolism, pneumonia, and congestive heart failure. Transthoracic echocardiography is a readily available imaging modality performed at the bedside to assess cardiac anatomy, function, and hemodynamics. It is the golden standard in the determination of accurate diagnosis and the tool of choice for emergent bedside evaluation for cardiac tamponade (43). In practice, the fluoroscopic check of cardiac motion provides a useful tool for the early recognition of pleural effusion. CT can provide information on pericardial thickening, calcification, effusions, and lead perforations. Badger et al. found that quantification of left atrial structural remodeling with delayed-enhancement magnetic resonance imaging has been overestimated in patients undergoing RFCA in the acute stage because of an inflammatory process induced by radiofrequency energies (44). Therefore, both pericardial and pleural effusions typically result from thermal injury. Additionally, routine laboratory tests and radiographic investigations usually show non-abnormalities in patients with PPIS, such as leukocyturia, pleural effusion, or pericardial effusion. Treatment strategies for PPIS aim at decreasing pericardial inflammation and improving symptoms. Based on the European Society of Cardiology 2015 guidelines, nonsteroid anti-inflammatory agents (NSAIDs) and colchicine are the preferred drugs for the treatment of PPIS. Aspirin has become the first choice for NSAIDs because of its analgesic and anti-inflammatory effects. Steroids are second-line agents for symptom control, which should be tapered when inflammatory markers are normalized and clinically significant symptoms are reduced (28, 45, 46). Colchicine-resistant patients or steroid-dependent patients should choose other therapeutic options such as anakinra or intravenous immunoglobulins (47). The combination of colchicine and NSAIDs in the treatment of PPIS has been reported to be associated with lower rates of pericardiocentesis and reduced clinically significant symptoms (28, 48, 49).

Typically, the treatment of PPIS was well-received, and the results are promising, but hospital stay may be prolonged, and healthcare costs may be increased. Initial investigations of clinically suspected PPIS were serum inflammatory levels and echocardiography. When the results of those tests are inconclusive, computerized tomography can provide additional diagnostic information. The diagnosis of PPIS diagnosis remains difficult in cases following cardiac catheter intervention because patients had no clinical signs of manifest heart disease. Therefore, cardiologists and pulmonologists should be aware of this rare but potentially important complication (50).

Conclusion

We report a rare case of PPIS that is characterized as massive pleural effusion alone after RFCA of AF. To reduce potential progression, timely diagnostics and preventive strategies for PPIS after RFCA of AF are of great importance. PPIS should be considered in a patient who presents with massive pleural effusion alone following RFCA, especially after an infectious cause and pulmonary embolism have been excluded.

Data availability statement

The original contributions presented in the study are included in the article/supplementary material, further inquiries can be directed to the corresponding authors.

Ethics statement

Written informed consent was obtained from the individual(s) for the publication of any potentially identifiable images or data included in this article.

Author contributions

YW and GC performed the operation and revised the study. MH drafted the manuscript. GC and YB organized the study and edited the manuscript. All authors have read and agreed to the published version of the manuscript.

Funding

This study was supported by grants from Tongji Hospital Returns from Studying Abroad Startup Foundation (2022hgry008 and 2022hgry023).

Conflict of interest

The authors declare that the research was conducted in the absence of any commercial or financial relationships that could be construed as a potential conflict of interest.

Publisher's note

References

1. Calkins H, Kuck KH, Cappato R, Brugada J, Camm AJ, Chen SA, et al. 2012 HRS/EHRA/ECAS expert consensus statement on catheter and surgical ablation of atrial fibrillation: recommendations for patient selection, procedural techniques, patient management and follow-up, definitions, endpoints, and research trial design. *J Interv Card Electrophysiol.*. (2012) 33:171–257. doi: 10.1007/s10840-012-9672-7

2. Blanc JJ, Almendral J, Brignole M, Fatemi M, Gjesdal K, González-Torrecilla E, et al. Consensus document on antithrombotic therapy in the setting of electrophysiological procedures. *Europace.* (2008) 10:513–27. doi: 10.1093/europace/eun104

3. Gupta A, Perera T, Ganesan A, Sullivan T, Lau DH, Roberts-Thomson KC, et al. Complications of catheter ablation of atrial fibrillation: a systematic review. *Circ Arrhythm Electrophysiol.* (2013) 6:1082–8. doi: 10.1161/CIRCEP.113.000768

4. Calkins H, Hindricks G, Cappato R, Kim YH, Saad EB, Aguinaga L, et al. 2017 HRS/EHRA/ECAS/APHRS/SOLAECE expert consensus statement on catheter and surgical ablation of atrial fibrillation: Executive summary. *Europace.* (2018) 20:157–208. doi: 10.1093/europace/eux275

5. Li W, Sun J, Yu Y, Guo K, Wang QS, Zhang PP, et al. What is the role of left bundle branch block in atrial fibrillation-induced cardiomyopathy? *Int J Cardiol.* (2015) 184:382–4. doi: 10.1016/j.ijcard.2015.02.060

6. Ngo L, Ali A, Ganesan A, Woodman R, Adams R, Ranasinghe I: Ten-year trends in mortality and complications following catheter ablation of atrial fibrillation. *Eur Heart J.* (2022) 11:e022009. doi: 10.1161/JAHA.121.022009

7. Dagres N, Hindricks G, Kottkamp H, Sommer P, Gaspar T, Bode K, et al. *et al*: Complications of atrial fibrillation ablation in a high-volume center in 1,000 procedures: still cause for concern? *J Cardiovasc Electrophysiol.* (2009) 20:1014–9. doi: 10.1111/j.1540-8167.2009.01493.x

8. Imazio M, Hoit BD. Post-cardiac injury syndromes. An emerging cause of pericardial diseases. *Int J Cardiol.* (2013) 168:648–52. doi: 10.1016/j.ijcard.2012.09.052

9. Ito T, Engle MA, Goldberg HP: Postpericardiotomy syndrome following surgery for nonrheumatic heart disease. *Circulation.* (1958) 17:549-556. doi: 10.1161/01.CIR.17.4.549

10. Deftereos SG, Beerkens FJ, Shah B, Giannopoulos G, Vrachatis DA, Giotaki SG, et al. Colchicine in cardiovascular disease: in-depth review. *Circulation.* (2022) 145:61–78. doi: 10.1161/CIRCULATIONAHA.121.056171

11. Agarwal SK, Vallurupalli S, Uretsky BF, Hakeem A. Effectiveness of colchicine for the prevention of recurrent pericarditis and post-pericardiotomy syndrome: an updated meta-analysis of randomized clinical data. *Eur Heart J Cardiovasc Pharmacother.* (2015) 1:117–25. doi: 10.1093/ehjcvp/pvv001

12. Wood MA, Ellenbogen KA, Hall J, Kay GN. Post-pericardiotomy syndrome following linear left atrial radiofrequency ablation. *J Interv Card Electrophysiol.* (2003) 9:55–7. doi: 10.1023/A:1025376605807

13. Luckie M, Jenkins N, Davidson NC, Chauhan A. Dressler's syndrome following pulmonary vein isolation for atrial fibrillation. *Acute Card Care.* (2008) 10:234–5. doi: 10.1080/17482940701843722

14. Goossens K, Caenepeel A, De Greef Y. Delayed tamponade triggering Dressler's syndrome after pulmonary vein isolation. *Acta Cardiol.* (2012) 67:595–8. doi: 10.1080/AC.67.5.2174137

15. Liu Y, Wang C, Zhao R, Wan D, Xie H, Jin G, et al. Incidence and clinical characteristics of postcardiac injury syndrome complicating cardiac perforation caused by radiofrequency catheter ablation for cardiac arrhythmias. *Int J Cardiol.* (2013) 168:3224–9. doi: 10.1016/j.ijcard.2013.04.011

16. Torihashi S, Shiraishi H, Hamaoka T, Imai M, Kuroyanagi A, Nakanishi N, et al. Two cases of delayed cardiac tamponade due to pericarditis after pulmonary vein (PV) isolation for atrial fibrillation. *Internal Med (Tokyo, Japan).* (2015) 54:791–6. doi: 10.2169/internalmedicine.54.2537

17. Yukumi S, Ichiki H, Funada J, Suzuki H, Morimoto M, Fujita T, et al. Postcardiac injury syndrome following vascular interventional radiofrequency ablation for paroxysmal atrial fibrillation. *Respir Med Case Rep.* (2015) 15:89–91. doi: 10.1016/j.rmcr.2015.03.008

18. Han J, Zhang Y, Zhou D, Zhang B, Wu T, Zheng L. Uncommon presentation of postcardiac injury syndrome induced by radiofrequency catheter ablation for atrial fibrillation: only pulmonary parenchymal inflammation. *J Cardiol Cases.* (2016) 14:17–20. doi: 10.1016/j.jccase.2016.03.002

19. Li W, Sun J, Yu Y, Wang ZQ, Zhang PP, Guo K, et al. Clinical features of post cardiac injury syndrome following catheter ablation of arrhythmias: systematic review and additional cases. *Heart Lung Circ.* (2019) 28:1689–96. doi: 10.1016/j.hlc.2018.09.001

20. Fong HK, Abdullah O, Gautam S: Cough as the sole manifestation of pericardial effusion. *BMJ Case Rep.* (2018) 2018:bcr2017222327. doi: 10.1136/bcr-2017-222327

21. Rosati F, Hassan SMA, Reid K, Dejong P, Bisleri G. Left atrium perforation with lung injury after catheter ablation. *J Card Surg.* (2020) 35:2860–2. doi: 10.1111/jocs.14917

22. Fukasawa K, Umetani K, Yano T, Sano K. Constrictive pericarditis following atrial fibrillation catheter ablation with cardiac tamponade. *Heart Rhythm Case Reports.* (2021) 7:836–9. doi: 10.1016/j.hrcr.2021.09.007

23. Qiu J, Wang Y, Wang DW, Hu M, Chen G. Update on high-power short-duration ablation for pulmonary vein isolation. *J Cardiovasc Electrophysiol.* (2020) 31:2499–508. doi: 10.1111/jce.14649

24. Bhaskaran A, Chik W, Pouliopoulos J, Nalliah C, Qian P, Barry T, et al. Five seconds of 50-60 W radio frequency atrial ablations were transmural and safe: an in vitro mechanistic assessment and force-controlled in vivo validation. *Europace.* (2017) 19:874–80. doi: 10.1093/europace/euw077

25. Bourier F, Duchateau J, Vlachos K, Lam A, Martin CA, Takigawa M, et al. High-power short-duration versus standard radiofrequency ablation: Insights on lesion metrics. *J Cardiovasc Electrophysiol.* (2018) 29:1570–5. doi: 10.1111/jce.13724

26. Ali-Ahmed F, Goyal V, Patel M, Orelaru F, Haines DE, Wong WS. High-power, low-flow, short-ablation duration-the key to avoid collateral injury? *J Interv Card Electrophysiol.* (2019) 55:9–16. doi: 10.1007/s10840-018-0473-5

27. Engle MA, McCabe JC, Ebert PA, Zabriskie J. The postpericardiotomy syndrome and antiheart antibodies. *Circulation.* (1974) 49:401–6. doi: 10.1161/01.CIR.49.3.401

28. Adler Y, Charron P, Imazio M, Badano L, Barón-Esquivias G, Bogaert J, et al. 2015 ESC Guidelines for the diagnosis and management of pericardial diseases: The Task Force for the Diagnosis and Management of Pericardial Diseases of the European Society of Cardiology (ESC)Endorsed by: The European Association for Cardio-Thoracic Surgery (EACTS). *Eur Heart J.* (2015) 36:2921–64. doi: 10.5603/KP.2015.0228

29. Imazio M, Brucato A, Rovere ME, Gandino A, Cemin R, Ferrua S, et al. Contemporary features, risk factors, and prognosis of the post-pericardiotomy syndrome. *Am J Cardiol.* (2011) 108:1183–7. doi: 10.1016/j.amjcard.2011.06.025

30. Ramjee V, Li D, Manderfield LJ, Liu F, Engleka KA, Aghajanian H, et al. Epicardial YAP/TAZ orchestrate an immunosuppressive response following myocardial infarction. *J Clin Invest.* (2017) 127:899–911. doi: 10.1172/JCI88759

31. Lessof MH. Psotcardiotomy syndrome: pathogenesis and management. *Hosp Pract.* (1976) 11:81–6. doi: 10.1080/21548331.1976.11706998

32. Koller ML, Maier SK, Bauer WR, Schanzenbächer P. Postcardiac injury syndrome following radiofrequeny ablation of atrial flutter. *Z Kardiol.* (2004) 93:560–5. doi: 10.1007/s00392-004-0093-1

33. January CT, Wann LS, Calkins H, Chen LY, Cigarroa JE, Cleveland JC, et al. 2019 AHA/ACC/HRS Focused Update of the 2014 AHA/ACC/HRS Guideline for the management of patients with atrial fibrillation: a Report of the American College of Cardiology/American Heart Association Task Force on Clinical Practice Guidelines and the Heart Rhythm Society in

collaboration with the society of thoracic surgeons. *Circulation.* (2019) 140:e125–51. doi: 10.1161/CIR.0000000000000665

34. Mascia G, Giaccardi M. A new era in zero X-ray ablation. *Arrhythmia Electrophysiol Rev.* (2020) 9:121–7. doi: 10.15420/aer.2020.02

35. Giaccardi M, Anselmino M, Del Greco M, Mascia G, Paoletti Perini A, Mascia P, et al. Radiation awareness in an Italian multispecialist sample assessed with a web-based survey. *Acta Cardiol.* (2021) 76:307–11. doi: 10.1080/00015385.2020.1733303

36. Reinsch N, Füting A, Buchholz J, Ruprecht U, Neven K. Influence of ablation index on the incidence of cardiac tamponade complicating pulmonary vein isolation. *Herz.* (2021) 46:228–34. doi: 10.1007/s00059-020-04988-y

37. Natale A, Reddy VY, Monir G, Wilber DJ, Lindsay BD, McElderry HT, et al. Paroxysmal AF catheter ablation with a contact force sensing catheter: results of the prospective, multicenter SMART-AF trial. *J Am Coll Cardiol.* (2014) 64:647–56. doi: 10.1016/j.jacc.2014.04.072

38. Reddy VY, Dukkipati SR, Neuzil P, Natale A, Albenque JP, Kautzner J, et al. Randomized, controlled trial of the safety and effectiveness of a contact force-sensing irrigated catheter for ablation of paroxysmal atrial fibrillation: results of the TactiCath Contact Force Ablation Catheter Study for Atrial Fibrillation (TOCCASTAR) Study. *Circulation.* (2015) 132:907–15. doi: 10.1161/CIRCULATIONAHA.114.014092

39. Wu D, Meydani SN. Age-associated changes in immune and inflammatory responses: impact of vitamin E intervention. *J Leukoc Biol.* (2008) 84:900–14. doi: 10.1189/jlb.0108023

40. Michowitz Y, Rahkovich M, Oral H, Zado ES, Tilz R, John S, et al. Effects of sex on the incidence of cardiac tamponade after catheter ablation of atrial fibrillation: results from a worldwide survey in 34 943 atrial fibrillation ablation procedures. *Circ Arrhythm Electrophysiol.* (2014) 7:274–80. doi: 10.1161/CIRCEP.113.000760

41. Darmoch F, Alraies MC, Al-Khadra Y, Moussa Pacha H, Soud M, Chami T, et al. National trends of acute pericarditis post-atrial fibrillation ablation. *Int J Clin Pract.* (2020) 74:e13434. doi: 10.1111/ijcp.13434

42. Hoffman M, Fried M, Jabareen F, Vardinon N, Turner D, Burke M, et al. Anti-heart antibodies in postpericardiotomy syndrome: cause or epiphenomenon? A prospective, longitudinal pilot study. *Autoimmunity.* (2002) 35:241–5. doi: 10.1080/08916930290028166

43. Bucekova E, Simkova I, Hulman M. Postpericardiotomy syndrome - post-cardiac injury syndrome. *Bratisl Lek Listy.* (2012) 113:481–5. doi: 10.4149/BLL_2012_106

44. Badger TJ, Oakes RS, Daccarett M, Burgon NS, Akoum N, Fish EN, et al. Temporal left atrial lesion formation after ablation of atrial fibrillation. *Heart rhythm.* (2009) 6:161–8. doi: 10.1016/j.hrthm.2008.10.042

45. Vaduganathan M, Bhatt DL, Cryer BL, Liu Y, Hsieh WH, Doros G, et al. Proton-pump inhibitors reduce gastrointestinal events regardless of aspirin dose in patients requiring dual antiplatelet therapy. *J Am Coll Cardiol.* (2016) 67:1661–71. doi: 10.1016/j.jacc.2015.12.068

46. Yadlapati R, Kahrilas PJ. When is proton pump inhibitor use appropriate? *BMC Med.* (2017) 15:36. doi: 10.1186/s12916-017-0804-x

47. Imazio M, Lazaros G, Brucato A, Gaita F. Recurrent pericarditis: new and emerging therapeutic options. Nature reviews. *Cardiology.* (2016) 13:99–105. doi: 10.1038/nrcardio.2015.115

48. Alraies MC, AlJaroudi W, Shabrang C, Yarmohammadi H, Klein AL, Tamarappoo BK. Clinical features associated with adverse events in patients with post-pericardiotomy syndrome following cardiac surgery. *Am J Cardiol.* (2014) 114:1426–30. doi: 10.1016/j.amjcard.2014.07.078

49. Wolk B, Dandes E, Martinez F, Helguera M, Pinski SL, Kirsch J. Postcardiac injury syndrome following transvenous pacer or defibrillator insertion: CT imaging and review of the literature. *Curr Probl Diagn Radiol.* (2013) 42:141–8. doi: 10.1067/j.cpradiol.2012.12.001

50. Laohaburanakit P. Exudative pleural effusion following thoracoscopic pulmonary vein isolation for paroxysmal atrial fibrillation. *Chest.* (2008) 133:1246–7. doi: 10.1378/chest.07-2028

frontiers | Frontiers in Cardiovascular Medicine

TYPE Case Report
PUBLISHED 28 October 2022
DOI 10.3389/fcvm.2022.1007213

OPEN ACCESS

EDITED BY
Leonardo Roever,
Federal University of Uberlândia, Brazil

REVIEWED BY
Mark G. Davies,
The University of Texas Health Science Center at San Antonio, United States
Daqiao Guo,
Fudan University, China

*CORRESPONDENCE
Hiroyuki Yamamoto
hyamamoto19700908@gmail.com

SPECIALTY SECTION
This article was submitted to General Cardiovascular Medicine, a section of the journal Frontiers in Cardiovascular Medicine

RECEIVED 30 July 2022
ACCEPTED 26 September 2022
PUBLISHED 28 October 2022

CITATION
Yamamoto H, Fukushima Y, Ikeda Y, Suda T, Goto M, Isogai J, Hashimoto T, Takahashi T and Ogino H (2022) Decisive diagnostic clue for infectious abdominal aortic aneurysm caused by *Arthrobacter russicus* in a diabetic elderly woman with renal dysfunction: A case report and literature review. *Front. Cardiovasc. Med.* 9:1007213. doi: 10.3389/fcvm.2022.1007213

Decisive diagnostic clue for infectious abdominal aortic aneurysm caused by *Arthrobacter russicus* in a diabetic elderly woman with renal dysfunction: A case report and literature review

Hiroyuki Yamamoto[1]*, Yasuto Fukushima[2], Yoshihiko Ikeda[3], Tomoyuki Suda[4,5], Mieko Goto[2], Jun Isogai[6], Toru Hashimoto[1], Takashi Takahashi[2] and Hidemitsu Ogino[4]

[1]Department of Cardiovascular Medicine, Narita-Tomisato Tokushukai Hospital, Chiba, Japan, [2]Laboratory of Infectious Diseases, Graduate School of Infection Control Sciences and Omura Satoshi Memorial Institute, Kitasato University, Tokyo, Japan, [3]Department of Pathology, National Cerebral and Cardiovascular Center, Suita, Japan, [4]Department of Surgery, Narita-Tomisato Tokushukai Hospital, Chiba, Japan, [5]Department of General Surgery, Shonan Kamakura General Hospital, Kanagawa, Japan, [6]Department of Radiology, Asahi General Hospital, Asahi, Japan

Infectious aortic aneurysm (IAA) can be a rare but potentially fatal sequela of infectious inflammatory disease of the aortic wall with a high incidence of rupture. The definitive diagnosis is based on vascular imaging of the aneurysm using contrast-enhanced computed tomography (CE-CT) and identification of the causative microorganism from positive blood cultures (BCs). However, IAA remains extremely difficult to diagnose and treat in patients with prior antimicrobial treatment or with renal dysfunction. Here we describe a case of an 85-year-old woman with IAA caused by *Arthrobacter russicus* presenting with abdominal pain and fever that was initially diagnosed as a presumptive urinary tract infection and treated with empiric antimicrobial therapy. However, persistent abdominal pain with increased serological inflammation necessitated further evaluation. Unenhanced multimodality imaging considering the renal dysfunction revealed infectious aortitis of the infrarenal abdominal aorta, together with the initial culture results, leading to the tentative diagnosis of *Klebsiella pneumoniae* aortitis. Thereafter, serial monitoring with unenhanced magnetic resonance angiography (MRA) using thin-slab maximum intensity projection (TS-MIP) revealed acute aortic expansion strongly suggestive of a pseudoaneurysm that was successfully treated with early surgical repair under adequate infection control. Despite negative Gram staining and tissue culture results for the excised aortic wall, a definitive diagnosis of IAA secondary to *A. russicus* rather than *K. pneumoniae* was finally made by confirming the histologic findings consistent with IAA

and the identification of *A. russicus* 16S rRNA on the resected aortic wall. The patient also developed a vascular graft infection during the postoperative course that required long-term systemic antimicrobial therapy. This case highlights the value of unenhanced MRA in the early detection of IAA in patients with renal dysfunction and the importance of a molecular diagnosis for identifying the causative microorganism in cases of culture- or tissue-negative IAA.

KEYWORDS

infectious aortic aneurysm, abdominal aorta, MRA, renal dysfunction, 16S rRNA, *Arthrobacter russicus*

Introduction

Infectious aortic aneurysm (IAA) is a rare but serious infectious inflammatory disease of the aortic wall that often requires prompt surgical intervention because of a high associated mortality rate with antimicrobial therapy alone (1). However, various obstacles, including negative blood and tissue cultures, non-specific symptoms and signs, IAA mimics, and high perioperative mortality rates of open surgery, pose a diagnostic and therapeutic challenge in patients with IAA (1–3).

Case description

An 85-year-old woman was admitted to our hospital with a 3-day history of abdominal pain and fever. Her medical history included a cerebral infarction, Parkinson's disease, dementia, and diabetes. Her vital signs were as follows: blood pressure, 186/86 mmHg; heart rate, 90 beats/min; blood temperature, 38.4°C; respiratory rate, 18 breaths/min; oxygen saturation, 99% on ambient air; height, 150 cm; and weight, 43.5 kg. An abdominal examination revealed no significant pulsatile mass, rebound tenderness, audible vascular murmur, or costovertebral angle tenderness except for mild tenderness in the periumbilical region. Chest X-ray findings were unremarkable. An initial laboratory workup revealed an elevated leukocyte count of 10,200/μL (neutrophils, 89.5%), elevated levels of C-reactive protein (18.04 mg/dL; normal, < 0.14 mg/dL), fasting blood glucose (188 mg/dL; normal, < 110 mg/dL), and glycated hemoglobin (8.3%; normal, < 6.0%). Severe renal dysfunction with a calculated creatinine clearance of 19.6 mL/min was observed. A urine dipstick test revealed glucose 4 +, blood 1 +, protein 1 +, and bacteria 2 +. We initially suspected gastroenteritis, pyelonephritis, or a liver abscess.

Contrast-enhanced computed tomography (CE-CT) was omitted due to the patient's severe renal dysfunction. Abdominal ultrasonography revealed multiple gallstones and obvious intestinal gas but no intrahepatic mass, hydronephrosis, or flap in the abdominal aorta. After the collection of a urine culture and two sets of blood cultures (BCs), the patient was intravenously administered ceftriaxone 1 g daily for a presumptive urinary tract infection. Persistent abdominal pain with increased serological inflammation prompted further abdominal evaluation on day 4. Unenhanced CT revealed a non-aneurysmal dilation of the infrarenal abdominal aorta with increased soft tissue mass around the aorta (**Figures 1A**, **2A**). Unenhanced magnetic resonance imaging (MRI) further characterized the periaortic tissue's properties. T2 and diffusion-weighted imaging (DWI) showed a high-intensity area around the aorta with diffusion restriction (**Figures 1B,C**). Furthermore, gallium-67 single-photon emission computed tomography (Ga-SPECT)-CT showed abnormal uptake in the corresponding area, confirming active inflammation (**Figure 1D**).

We initially suspected inflammatory aortitis, including autoimmune- or immunoglobulin G4-related disease (IgG4-RD). However, serum immunological examination results were within normal ranges, suggesting less likelihood of inflammatory diseases. Urine culture and BCs conducted on admission revealed the presence of *Klebsiella pneumoniae* susceptible to conventional antimicrobials but naturally resistant to ampicillin. Accordingly, a tentative diagnosis of *K. pneumoniae* abdominal aortitis was made. The dose of ceftriaxone was increased to 2 g twice daily, and oral levofloxacin (250 mg/day) was added. Insulin therapy was initiated to manage the hyperglycemia. The echocardiographic and endoscopic examination findings were unremarkable. Thereafter, the patient's symptoms disappeared, the serological

Abbreviations: BCs, blood cultures; CE-CT, contrast-enhanced computed tomography; CT, computed tomography; DWI, diffusion-weighted imaging; Ga-SPECT, gallium-67 single-photon emission computed tomography; IgG4-RD, immunoglobulin G4-related disease; IAA, infectious aortic aneurysm; MRA, magnetic resonance angiography; MRI, magnetic resonance imaging; PET/CT, ^{18}F-flourodeoxyglucose positron emission tomography/computed tomography; rRNA, ribosomal RNA; TS-MIP, thin-slab maximum intensity projection.

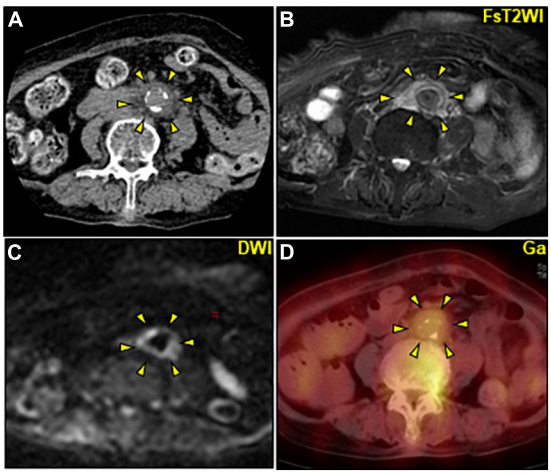

FIGURE 1
Multimodality imaging of periaortic mass of the abdominal aorta. **(A–D)** Axial images. **(A)** Unenhanced CT image showing a non-dilated abdominal aorta with a maximum diameter of 17 mm including mural calcification surrounded by circumferential heterogeneous soft-tissue density (arrowheads). **(B,C)** Unenhanced abdominal magnetic resonance image. **(B)** FsT2WI showing significantly high signal intensity and marked thickening of the periaortic tissue of the abdominal aorta (arrowheads) with inhomogeneous diffusion restriction on DWI **(C)**. **(D)** Ga-single photon emission computed tomography/CT image revealing an active accumulation of Ga (arrowheads) corresponding to the periaortic mass. CT, computed tomography; DWI, diffusion-weighted imaging; FsT2WI, fat-suppressed T2-weighted image; Ga, gallium citrate-67.

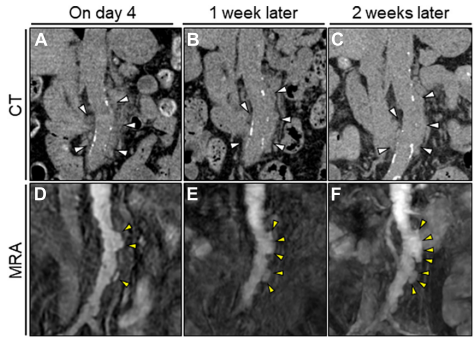

FIGURE 2
Serial unenhanced CT and MRA assessment of the abdominal aorta. **(A–C)** Serial unenhanced reconstructed coronal CT image showing no significant change in the periaortic mass of the abdominal aorta (white arrowheads). **(D)** Initial TS-MIP image of the original MRA image showing several asymmetric aortic dilatations in the abdominal aorta (yellow arrowheads). **(D–F)** Serial TS-MIP of the original MRA image showing rapid aortic expansion with multilobular protrusion of the abdominal aorta to the left side (yellow arrowheads). CT, computed tomography; MRA, magnetic resonance angiography; TS-MIP, thin-slab maximum intensity projection.

inflammation decreased, and all the subsequent repeated BCs remained sterile. The periaortic soft tissue lesion appeared stable on serial CT imaging (Figures 2A–C). Nevertheless, serial unenhanced magnetic resonance angiography (MRA) with thin-slab maximum intensity projection (TS-MIP) demonstrated acutely progressive morphological changes of the abdominal aorta characterized by multilobular and saccular features strongly suggestive of infectious pseudoaneurysm formation (Figures 2D–F). Additionally, an aortic mural thrombus was observed on the anterior wall of the descending thoracic aorta (Supplementary Figure 1A). She was treated accordingly with anticoagulation therapy (apixaban, 2.5 mg twice daily).

Owing to the elevated risk of aortic rupture, early surgery was planned by a multidisciplinary team after confirmation of a stable inflammatory response following antimicrobial treatment. On day 30, she underwent open surgical repair of the infected aortic lesion using an *in situ* graft (GORE-TEX Vascular Graft) (Figures 3A,B). Pathology of the excised aorta revealed severely calcified atherosclerosis with inflammatory cell infiltrations predominantly consisting of neutrophils, fresh mural thrombus, and partial pseudoaneurysm formation but without obvious bacteria (Figures 3C–3H). The accumulation of nuclear debris suggestive of infection was also noted. Despite negative Gram staining and tissue culture results for the aortic wall, *Arthrobacter russicus* sequences were obtained via 16S rRNA sequencing (Supplementary Figures 2–4), leading to the potential causative microorganism. A careful interview revealed that she was a farm worker with multiple exposures to soil and frequent episodes of foreign body ingestion related to dementia. Given the unsanitary living conditions and impaired immunity prone to aortic infections including severe atherosclerosis, diabetes, and renal failure, it was highly likely that this microorganism was the causative agent of the IAA in this patient. The early postoperative MRA revealed abnormal intensity around the vascular graft highly suggestive of vascular graft infection (Supplementary Figure 1B). Therefore, the antimicrobial therapy was switched to intravenous meropenem (0.5 g twice daily) plus vancomycin (0.5 g daily) for 60 days.

After follow-up blood examination and MRA confirmed the resolution of an inflammatory response to the infection (Supplementary Figures 1C,D), the antimicrobial therapy was de-escalated to oral cefalexin (250 mg every 8 h). Her subsequent clinical course was excellent, with no infection recurrence; however, the aortic mural thrombus size remained unchanged. On day 180, she was transferred to a nursing home for rehabilitation because of dementia and advanced disuse atrophy from prolonged bed rest. A summarized illustration of the case presentation is provided in Supplementary Figure 5.

Discussion

Here we describe the first case of IAA caused by *A. russicus*, successfully treated using an early surgical intervention

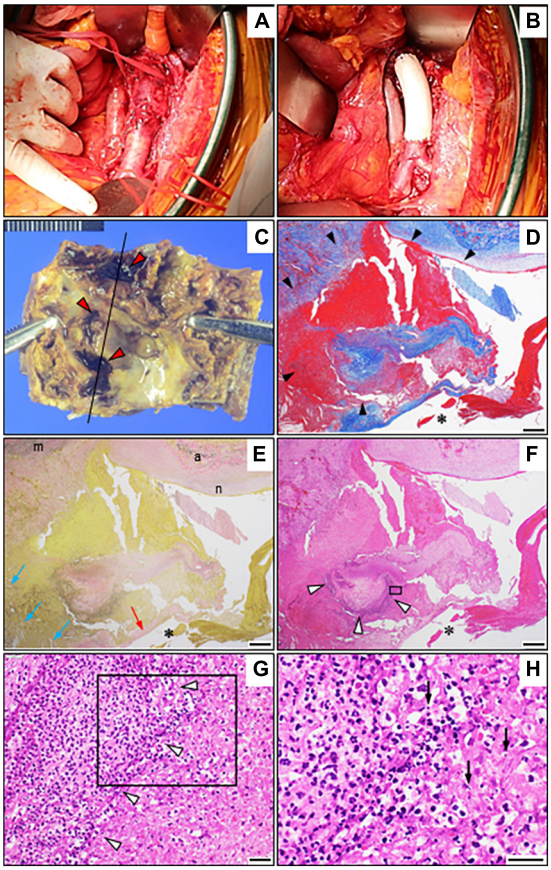

FIGURE 3
Operative view and pathological findings. **(A,B)** Intraoperative view before **(A)** and after **(B)** the repair using a Dacron graft. **(C)** The resected abdominal aortic aneurysm shows severely calcified plaque as well as several recesses with adherent mural thrombi (red arrowheads). **(D–F)** Photomicrographs of the resected abdominal aorta (longitudinal sections around the black line in **C**) with Masson's trichrome stain **(D)**, Elastica van Gieson staining **(E)**, and hematoxylin and eosin staining **(F)** showing marked inflammatory infiltration of the aortic wall (white arrowheads) and pseudoaneurysm formation (black arrowheads) due to loss of the normal structure of the aortic wall as well as cholesterol crystals (blue arrows). **(G)** A high-power view with hematoxylin and eosin staining showing intense perivascular inflammatory infiltrates (magnified view of the black box in **F**) but no microorganisms (white arrowheads). **(H)** Notably, the magnified view of the black box in **(G)** shows the accumulation of nuclear debris (arrows). Bars: **(D–F)**, 500 μm; and **(G,H)**, 20 μm. *Vascular lumen. The red arrow depicts a fibrous cap, while "m," "a," and "n" depict the media, adventitia, and neointima, respectively.

concurrent with long-term antimicrobial therapy. Our case report offers three clinical implications. First, unenhanced MRI/MRA was feasible for diagnosing IAA in our patient with renal dysfunction. An IAA refers to an arterial dilation secondary to destruction of the infected aortic wall. IAA (thoracic and abdominal) accounts for 0.7–4.5% of all aortic aneurysms (1). Most IAA cases affect elderly men over 65 years of age with severe atherosclerosis (4). Although the aortic intima is extremely resistant to infection due to its barrier mechanism, any situation that damages it is a crucial predisposing factor for aortic infection (2). Aortic infection can occur via several mechanisms: (1) bacteremic seeding of an existing intimal injury, atherosclerotic plaque, and preexisting aneurysm (5–7); (2) septic embolization of the aortic vasa vasorum (8); (3) an infected foci extending to the aortic wall (9); and (4) direct bacterial inoculation during aortic injury (10). Although the microbiological spectrum involved in IAA has evolved over time and depends on geographical conditions, *Staphylococcus* spp. (50–60%) and *Salmonella* spp. (30–40%) remain the most common causative species underlying IAA owing to their high affinity for the arterial wall (1, 11, 12).

Untreated IAA can cause rupture, aortofistulous communication, mural thrombosis, distal ischemia, sepsis, or multiorgan failure. Of these, rupture, the most fatal sequela, occurs in 50–80% of all cases, with a significantly higher mortality rate of 42% in cases of IAA with free or contained rupture vs. without rupture (1, 13). Therefore, this disease requires a prompt diagnosis and appropriate timely treatment. However, the high suspicion of IAA remains challenging due to the non-specific signs and symptoms. CE-CT is the cornerstone for diagnosing IAA because it can provide detailed information about lesion size and location as well as the surrounding structures. The typical CT findings indicative of IAA include a saccular or multilobulated aneurysm, a periaortic soft tissue mass, periaortic fat stranding, and periaortic air or fluid accumulation.

A variety of microorganisms can cause IAA. Distinct IAA phenotypes specific to each microorganism may exist because of differences in pathogenicity and virulence. Although most pathogen-specific features of IAA imaging on CT remain poorly understood, the IAA features on CT that may suggest the involvement of several specific pathogens have been reported in the following three categories: (1) characteristics of IAA: while most pathogens are associated with the rapid aneurysmal expansion, *Helicobacter cinaedi* is a low virulence bacterium that contributes to the promotion of atherosclerosis via macrophage-driven proinflammatory response and hence slowly progressive over months to years (14, 15); (2) periaortic involvement: *Clostridium septicum* can survive and proliferate in tissues under anaerobic condition that may be strongly associated with the presence of periaortic gas on CT (16). Specific feature of *Mycobacterium tuberculosis* includes enlargement of periaortic lymph nodes with central hypodensity suggesting of necrotic lymphadenopathy due to the nature of direct infection from the adjacent lymph nodes (17); and (3) surrounding organ involvement: psoas abscess and lumbar osteomyelitis are reportedly frequently associated with the IAA associated with *Salmonella* spp. (11 and 19%, respectively) (18, 19). However, we faced two diagnostic challenges to reaching an accurate diagnosis in the present case. As a result, the diagnosis was delayed.

The first diagnostic challenge was the presence of significant renal dysfunction in our patient, which required us to preclude iodinated contrast media exposure. The other diagnostic challenge was that CT findings observed in our case were similar between IAA and IgG4-RD. IgG4-RD is a life-threatening inflammatory vasculopathy that frequently affects individuals of middle to advanced ages by involving large and medium-sized vessels simultaneously, which often occurs in the infrarenal segment of the abdominal aorta (20, 21). Various serious aortic complications such as intra-abdominal bleeding, intra-aneurysmal thrombus, and abdominal aortic stenosis resulting from aneurysmal development or rupture can occur. These conditions require prompt and comprehensive treatment consisting of corticosteroid and immunosuppressant therapy, vascular graft, or surgical resection (22). Although the two distinct disorders share similar age at onset and radiological findings, it is critical to differentiate between the two because they differ significantly in terms of requisite treatment approaches. Admittedly, the unenhanced MRI/MRA scan was valuable for addressing the above issues in this case. MRI can enable soft tissue characterization and provide variable information on disease activity before aortic luminal changes occur. DWI, which can measure the random motion of water protons, is frequently used to detect acute inflammation such as acute stroke, tumors, and abscesses (23). It can also identify the active phase of inflammatory aortitis or acute infection (24, 25). Because of the limited spatial resolution of DWI, its use in combination with other MRI sequences may be valuable for evaluating aortitis without involving radiation exposure or contrast agents. In addition, unenhanced MRA can provide valuable morphological information about the aortic lumen (e.g., vessel stenosis, vessel dilation, and mural thrombus) comparable to CT angiography results (26). Because of its superior soft tissue imaging characteristics, MRA can help discriminate aortitis mimics such as aortic dissection, penetrating ulcers, or mural hematomas. Furthermore, TS-MIP of the original MRA can help clinicians screen for the development of aneurysms and monitor existing aneurysms. Indeed, the TS-MIP findings of multilobular or eccentric acute aortic expansion observed in this case were characteristic of IAA and helpful in distinguishing it from IgG4-RD. IAA and IgG4-RD can also be differentiated based on histopathological findings (22).

Moreover, ^{18}F-flourodeoxyglucose positron emission tomography/computed tomography (PET/CT) is a potential alternative for evaluating IAA. Although PET/CT is very sensitive for detecting metabolic activity, its diagnostic accuracy is limited due to difficulty distinguishing IAA from inflammatory aortic aneurysm and false positive results including malignancy and non-specific findings. However, a recent retrospective study analyzing 29 patients with abdominal aneurysms who underwent both PET/CT and CE-CT reported that a combination of specific imaging features (e.g., dorsal sparing of metabolic activity or wall thickening of aneurysm in PET/CT; fat stranding or fluid collections in CE-CT) and metabolic activity (intensity and site) can identify the etiology of each aneurysm with high accuracy among abdominal aortic aneurysms (infectious, inflammatory, and non-infectious/non-inflammatory) (27, 28). Therefore, the combined use of PET/CT and CE-CT may improve the diagnostic accuracy of the IAA and further studies are warranted.

In our case, IAA was confirmed based on histologic findings and the identification of *A. russicus* 16S rRNA on the resected aortic wall. Advanced age, poorly controlled diabetes, and renal

TABLE 1 Literature review of *Arthrobacter*-associated cardiovascular diseases.

Author	Bernasconi E (ref no. 32)	Durand C (ref no. 33)	Present case
Report year	2004	2021	This report
Age, years, sex	39, Male	52, unknown	85, female
Underlying condition	Injectable drug use	Injectable drug use	Diabetes mellitus, renal dysfunction
Clinical symptoms	Fever, fatigue, myalgia, weight loss	Fever, weakness, weight loss	Fever, abdominal pain
Diagnosis	Endocarditis of native mitral valve	Endocarditis of mitral and aortic valves	Infectious abdominal aortic aneurysm and aortic mural thrombus of the descending thoracic aorta
Surgical intervention(s)	None	Mitral valve replacement, aortic vegetectomy	*In situ* graft replacement
Species identified	*Arthrobacter woluwensis*	*Arthrobacter woluwensis*	*Arthrobacter russicus*
Identification assay	16S rRNA sequencing analysis of blood specimen	16S rRNA sequencing analysis of tissue specimen	16S rRNA sequencing analysis of tissue specimen
Antimicrobial treatment	TEIC	OX + GM, DAP + ST, TEIC + ST, followed by LZD + ST	CTRX + LVFX, MEPM + VCM followed by CFX
Treatment outcome	Cured	Cured	Cured (despite perioperative vascular graft infection)

CFX, cefalexin; CTRX, ceftriaxone; DAP, daptomycin; GM, gentamicin; LVFX, levofloxacin; LZD, linezolid; MEPM, meropenem; OX, oxacillin; rRNA, ribosomal RNA; ST, sulfamethoxazole/trimethoprim; TEIC, teicoplanin; VCM, vancomycin.

dysfunction, which are closely associated with atherosclerosis, might have provided a rich nidus for aortic infection. Therefore, this case report emphasizes the importance of considering IAA as a possible source of unexplained abdominal pain and fever among elderly patients with severe atherosclerosis and the use of unenhanced MRI/MRA to evaluate and monitor aortic diseases in patients with renal dysfunction wherein iodinated contrast media exposure is undesirable.

As a second clinical implication, to the best of our knowledge, this is the first case of IAA caused by *A. russicus*. The 16S rRNA sequencing was also helpful to identify this microorganism. *Arthrobacter* spp. (Gram-positive, aerobic, non-motile, and coryneform rods) are widely distributed in the environment, especially the soil (29). The microorganisms belong to the genus *Arthrobacter* of the family *Micrococcaceae* of the order *Micrococcales*. These bacteria are isolated from animals and wastewater materials (30). *A. russicus*, firstly reported in 2004 (31), was recovered from air in the Russian space station. The first identification of *Arthrobacter* from human specimens (urine, skin, blood, vagina, and eye) was reported in 1996 (29). The incidence of *Arthrobacter* human infections is underestimated since its biochemical identification method is based on a single strain and the bacteria are difficult to isolate (29, 32, 33).

Table 1 summarizes the *Arthrobacter*-associated cardiovascular disease cases including the present case. Two cases of *A. woluwensis* endocarditis have been reported (32, 33): although conventional phenotyping using morphological and biochemical features initially led to misidentification of the causative organism in both cases, 16S rRNA sequencing on tissue or blood culture samples ultimately succeeded in identifying *A. woluwensis* as the true causative organism of IE in both cases. Therefore, 16S rRNA sequencing was required to identify *Arthrobacter* spp. as per our case. While drug injection appeared to be the entry site in two cases of *A. woluwensis* endocarditis (**Table 1**), the entry site remained unclear in the present case because this seems very rare among Japanese elderly individuals. Presumably, this patient might have repeatedly developed silent *Arthrobacter* bacteremia via translocation of this microorganism from the gastrointestinal tract to the portal bloodstream after the ingesting of soil or wastewater before hospitalization.

We misdiagnosed this case as IAA caused by *K. pneumoniae* because of the initial positive urine culture and BCs for *K. pneumoniae*. However, *K. pneumoniae* is rarely the causative microorganism of IAA, with limited case reports of presumably hypervirulent strains (34, 35). Based on this patient's clinical course, all negative blood culture results after the initial antimicrobial treatment, and the negative Gram staining and molecular examination results, we concluded that this microorganism caused transient bacteremia in our case because data were lacking to support *K. pneumoniae* as the primary causative microorganism of the IAA. Therefore, our experience with this case suggests that the microorganism yielded from initial positive BCs is not always the true causative agent of the IAA. Furthermore, the frequency of positive BCs in patients with IAA varies significantly (2, 4, 11, 19, 36–38). Given the high frequency of negative BCs (up to 50% of cases), negative BCs alone are inadequate for ruling out the presence of IAA. Additionally, Gram staining and tissue cultures of the excised specimen can be negative in patients who previously received broad-spectrum antimicrobial therapy.

Similar to the present case, molecular diagnosis by 16S rRNA sequencing may be helpful for estimating the causative microorganism in cases, where IAA is strongly suspected despite negative tissue culture and repeated BCs. Recently, metagenomic next-generation sequencing and analysis may be a promising alternative (39).

A final clinical implication is that the long-term systemic antimicrobial therapy effectively controlled postoperative vascular graft infection in this case. In principle, surgery is required to treat IAA. Surgical procedures include open surgery to remove the infected tissue with/without *in situ* graft repair, extra-anatomic bypass, and endovascular stent graft insertion. Each procedure is determined based on the infected aneurysm location, infection degree, and patient condition. Since the perioperative mortality rate for the IAA in the acute setting remains high (3), endovascular stent graft insertion can be an acceptable alternative to conventional open surgery or a bridge to subsequent open surgical repair in high-risk surgical patients with severe sepsis or hemodynamic instability. Recent nationwide studies revealed that the results of the endovascular approach were comparable to those of open surgery (40, 41). In this case, despite IAA removal with *in situ* graft repair under adequate infection control with antimicrobial agents, the patient developed a serious postoperative vascular graft infection that was fortunately controlled with long-term systemic antimicrobial therapy. However, *in situ* graft infections caused by inadequate infection clearance can lead to a poor prognosis and a high mortality rate (nearly 100%) within 2 years (42). Although a postoperative antimicrobial duration of 6 weeks to 6 months is generally recommended (1), there are no specific criteria for discontinuing antimicrobial therapy in patients with IAA. Furthermore, this patient had residual aortic mural thrombus despite receiving anticoagulation therapy. Therefore, our patient remains under long-term surveillance for recurrent infections and the risk of aortic mural thrombus–related complications.

Limitations

Limited to small numbers, the antimicrobial susceptibility patterns among clinical isolates related to *Arthrobacter* spp. have been reported (29). However, the antimicrobial susceptibility of *Arthrobacter* was unknown in our case since

we could not recover the microorganism from the tissue and blood. Therefore, the present case received empiric antimicrobial therapy. Fortunately, long-term challenging therapy (ceftriaxone and levofloxacin, meropenem and vancomycin, followed by cefalexin) resolved the clinical symptoms, imaging findings, and blood laboratory data of inflammatory responses. Choosing optimal antimicrobial therapies for *Arthrobacter* infections remains challenging because of the difficulty isolating and identifying the phenotype (32, 33).

Future directions

Considering the difficulty of identification of *Arthrobacter* spp. by conventional biochemical approaches, the frequency of these microorganism infections in patients with IAA may remain underestimated. Therefore, prospective evaluation of the complementary use of molecular testing for the identification of *Arthrobacter* infection in all cases of IAA is further warranted.

Conclusion

Herein, we report the first case of IAA caused by *A. russicus* that was successfully treated with a combination of surgery and long-term antimicrobial therapy. Unenhanced MRA/MRI was useful for identifying IAA and determining its treatment response in this patient with renal dysfunction. In addition, 16S rRNA sequencing analysis allowed us to identify *A. russicus* as the causative organism of IAA. *A. russicus* can cause IAA, but is difficult to identify by conventional biochemical characterization. Therefore, a molecular diagnosis should be performed to identify the causative microorganism in patients with culture-negative IAA, considering the possibility of *A. russicus*.

Data availability statement

The datasets presented in this study can be found in online repositories. The names of the repository and accession number(s) can be found below: NCBI GenBank; LC715707 and LC715708.

Author contributions

HY contributed to the clinical design and study concept. HY, TS, TH, and HO acquired the clinical data. YF and MG performed the microbiological analyses. YI performed the pathological analyses. JI performed the radiological analyses. HY, JI, and TT interpreted the data and drafted the manuscript. All authors discussed, read, and approved the manuscript and its submission for publication.

Acknowledgments

We thank Haruno Yoshida (Laboratory of Infectious Diseases, Graduate School of Infection Control Sciences and Ōmura Satoshi Memorial Institute, Kitasato University, Tokyo, Japan) for her helpful assistance (submission and registration onto the DNA Data Bank of Japan database).

Conflict of interest

The authors declare that the research was conducted in the absence of any commercial or financial relationships that could be construed as a potential conflict of interest.

Publisher's note

All claims expressed in this article are solely those of the authors and do not necessarily represent those of their affiliated organizations, or those of the publisher, the editors and the reviewers. Any product that may be evaluated in this article, or claim that may be made by its manufacturer, is not guaranteed or endorsed by the publisher.

Supplementary material

The Supplementary Material for this article can be found online at: https://www.frontiersin.org/articles/10.3389/fcvm.2022.1007213/full#supplementary-material

References

1. Wilson WR, Bower TC, Creager MA, Amin-Hanjani S, O'Gara PT, Lockhart PB, et al. Vascular graft infections, mycotic aneurysms, and endovascular infections: a scientific statement from the American Heart Association. *Circulation.* (2016) 134:e412–60. doi: 10.1161/CIR.0000000000000457

2. Oderich GS, Panneton JM, Bower TC, Cherry KJ Jr., Rowland CM, Noel AA, et al. Infected aortic aneurysms: aggressive presentation, complicated early outcome, but durable results. *J Vasc Surg.* (2001) 34:900–8. doi: 10.1067/mva.2001.118084

3. Kim HH, Kim DJ, Joo HC. Outcomes of open repair of mycotic aortic aneurysms with in situ replacement. *Korean J Thorac Cardiovasc Surg.* (2017) 50:430–5. doi: 10.5090/kjtcs.2017.50.6.430

4. Lopes RJ, Almeida J, Dias PJ, Pinho P, Maciel MJ. Infectious thoracic aortitis: a literature review. *Clin Cardiol.* (2009) 32:488–90. doi: 10.1002/clc.20578

5. Reddy DJ, Shepard AD, Evans JR, Wright DJ, Smith RF, Ernst CB. Management of infected aortoiliac aneurysms. *Arch Surg.* (1991) 126:873–8.

6. Itatani K, Miyata T, Komiyama T, Shigematsu K, Nagawa H. An ex-situ arterial reconstruction for the treatment of an infected suprarenal abdominal aortic aneurysm involving visceral vessels. *Ann Vasc Surg.* (2007) 21:380–3. doi: 10.1016/j.avsg.2006.06.013

7. Ernst CB, Campbell HC Jr., Daugherty ME, Sachatello CR, Griffen WO Jr. Incidence and significance of intra-operative bacterial cultures during abdominal aortic aneurysmectomy. *Ann Surg.* (1977) 185:626–33. doi: 10.1097/00000658-197706000-00003

8. Shaikholeslami R, Tomlinson CW, Teoh KH, Molot MJ, Duke RJ. Mycotic aneurysm complicating staphylococcal endocarditis. *Can J Cardiol.* (1999) 15:217–22.

9. Hsu RB, Lin FY. Psoas abscess in patients with an infected aortic aneurysm. *J Vasc Surg.* (2007) 46:230–5. doi: 10.1016/j.jvs.2007.04.017

10. Samore MH, Wessolossky MA, Lewis SM, Shubrooks SJ Jr., Karchmer AW. Frequency, risk factors, and outcome for bacteremia after percutaneous transluminal coronary angioplasty. *Am J Cardiol.* (1997) 79:873–7. doi: 10.1016/s0002-9149(97)00006-4

11. Brown SL, Busuttil RW, Baker JD, Machleder HI, Moore WS, Barker WF. Bacteriologic and surgical determinants of survival in patients with mycotic aneurysms. *J Vasc Surg.* (1984) 1:541–7.

12. Hsu RB, Tsay YG, Wang SS, Chu SH. Surgical treatment for primary infected aneurysm of the descending thoracic aorta, abdominal aorta, and iliac arteries. *J Vasc Surg.* (2002) 36:746–50. doi: 10.1067/mva.2002.126557

13. Müller BT, Wegener OR, Grabitz K, Pillny M, Thomas L, Sandmann W. Mycotic aneurysms of the thoracic and abdominal aorta and iliac arteries: experience with anatomic and extra-anatomic repair in 33 cases. *J Vasc Surg.* (2001) 33:106–13. doi: 10.1067/mva.2001.110356

14. Khan S, Rahman HN, Okamoto T, Matsunaga T, Fujiwara Y, Sawa T, et al. Promotion of atherosclerosis by *Helicobacter* cinaedi infection that involves macrophage-driven proinflammatory responses. *Sci Rep.* (2014) 15:4680. doi: 10.1038/srep04680

15. Kushimoto K, Yonekura R, Umesue M, Oshiro Y, Yamasaki H, Yoshida K, et al. Infected thoracic aortic aneurysm caused by *Helicobacter cinaedi*. *Ann Vasc Dis.* (2017) 10:139–42. doi: 10.3400/avd.cr.16-00126

16. Ito F, Inokuchi R, Matsumoto A, Kumada Y, Yokoyama H, Ishida T, et al. Presence of periaortic gas in Clostridium septicum-infected aortic aneurysm aids in early diagnosis: a case report and systematic review of the literature. *J Med Case Rep.* (2017) 11:268. doi: 10.1186/s13256-017-1422-0

17. Mearelli F, Burekovic I, Zanetti M, Altamura N, Carlo G, Biolo G, et al. Disseminated tuberculosis in an immunocompetent patient. *Int J Infect Dis.* (2013) 17:e784–6. doi: 10.1016/j.ijid.2013.02.026

18. Guo Y, Bai Y, Yang C, Wang P, Gu L. Mycotic aneurysm due to *Salmonella* species: clinical experiences and review of the literature. *Braz J Med Biol Res.* (2018) 51:e6864. doi: 10.1590/1414-431X20186864

19. Soravia-Dunand VA, Loo VG, Salit IE. Aortitis due to *Salmonella*: report of 10 cases and comprehensive review of the literature. *Clin Infect Dis.* (1999) 29:862–8. doi: 10.1086/520450

20. Ozawa M, Fujinaga Y, Asano J, Nakamura A, Watanabe T, Ito T, et al. Clinical features of IgG4-related periaortitis/periarteritis based on the analysis of 179 patients with IgG4-related disease: a case-control study. *Arthritis Res Ther.* (2017) 19:223. doi: 10.1186/s13075-017-1432-8

21. Perugino CA, Wallace ZS, Meyersohn N, Oliveira G, Stone JR, Stone JH. Large vessel involvement by IgG4-related disease. *Medicine.* (2016) 95:e3344. doi: 10.1097/MD.0000000000003344

22. Yamamoto H, Ito Y, Isogai J, Ishibashi-Ueda H, Nakamura Y. Immunoglobulin G4-related multiple giant coronary artery aneurysms and a single left gastric artery aneurysm. *JACC Case Rep.* (2020) 2:769–74. doi: 10.1016/j.jaccas.2020.03.015

23. Andre JB, Bammer R. Advanced diffusion-weighted magnetic resonance imaging techniques of the human spinal cord. *Top Magn Reson Imaging.* (2010) 21:367–78. doi: 10.1097/RMR.0b013e31823e65a1

24. Doi S, Kuroiwa Y, Kusumoto K, Yamashita A, Furukoji E, Tai H, et al. Therapeutic response of immunoglobulin 4-related aortitis and pancreatitis demonstrated by diffusion-weighted MRI. *Radiol Case Rep.* (2019) 14:1132–5. doi: 10.1016/j.radcr.2019.06.020

25. Dumont RA, Keen NN, Bloomer CW, Schwartz BS, Talbott J, Clark AJ, et al. Clinical utility of diffusion-weighted imaging in spinal infections. *Clin Neuroradiol.* (2019) 29:515–22. doi: 10.1007/s00062-018-0681-5

26. Hartlage GR, Palios J, Barron BJ, Stillman AE, Bossone E, Clements SD, et al. Multimodality imaging of aortitis. *JACC Cardiovasc Imaging.* (2014) 7:605–19. doi: 10.1016/j.jcmg.2014.04.002

27. Husmann L, Huellner MW, Ledergerber B, Eberhard N, Kaelin MB, Anagnostopoulos A, et al. Diagnostic accuracy of PET/CT and contrast enhanced CT in patients with suspected infected aortic aneurysms. *Eur J Vasc Endovasc Surg.* (2020) 59:972–81. doi: 10.1016/j.ejvs.2020.01.032

28. Husmann L, Huellner MW, Gruenig H, Ledergerber B, Messerli M, Mestres CA, et al. Imaging characteristics and diagnostic accuracy of FDG-PET/CT, contrast enhanced CT and combined imaging in patients with suspected mycotic or inflammatory abdominal aortic aneurysms. *PLoS One.* (2022) 17:e0272772. doi: 10.1371/journal.pone.0272772

29. Funke G, Hutson RA, Bernard KA, Pfyffer GE, Wauters G, Collins MD. Isolation of *Arthrobacter* spp. from clinical specimens and description of *Arthrobacter cumminsii* sp. nov. and *Arthrobacter woluwensis* sp. nov. *J Clin Microbiol.* (1996) 34:2356–63. doi: 10.1128/jcm.34.10.2356-2363.1996

30. Funke G, von Graevenitz A, Clarridge JE III, Bernard KA. Clinical microbiology of coryneform bacteria. *Clin Microbiol Rev.* (1997) 10:125–59. doi: 10.1128/CMR.10.1.125

31. Li Y, Kawamura Y, Fujiwara N, Naka T, Liu H, Huang X, et al. *Rothia aeria* sp. nov., *Rhodococcus baikonurensis* sp. nov. and *Arthrobacter russicus* sp. nov., isolated from air in the Russian space laboratory Mir. *Int J Syst Evol Microbiol.* (2004) 54:827–35. doi: 10.1099/ijs.0.02828-0

32. Bernasconi E, Valsangiacomo C, Peduzzi R, Carota A, Moccetti T, Funke G. *Arthrobacter woluwensis* subacute infective endocarditis: case report and review of the literature. *Clin Infect Dis.* (2004) 38:e27–31. doi: 10.1086/381436

33. Durand C, Kouchit Y, Prots L, Degand N, Dellamonica P, Demonchy E, et al. A case of infective endocarditis caused by *Arthrobacter woluwensis*. *Eur J Clin Microbiol Infect Dis.* (2021) 40:1329–31. doi: 10.1007/s10096-021-04154-0

34. Chuang YC, Lee MF, Yu WL. Mycotic aneurysm caused by hypermucoviscous *Klebsiella pneumoniae* serotype K54 with sequence type 29: an emerging threat. *Infection.* (2013) 41:1041–4. doi: 10.1007/s15010-013-0447-6

35. Chen YJ, Chen SY, Wang JT, Hsueh PR. Mycotic aneurysm caused by gas-forming serotype K5 *Klebsiella pneumoniae*. *Int J Infect Dis.* (2009) 13:e47–8. doi: 10.1016/j.ijid.2008.06.008

36. Sörelius K, Budtz-Lilly J, Mani K, Wanhainen A. Systematic review of the management of mycotic aortic aneurysms. *Eur J Vasc Endovasc Surg.* (2019) 58:426–35. doi: 10.1016/j.ejvs.2019.05.004

37. Hsu RB, Lin FY. Surgical pathology of infected aortic aneurysm and its clinical correlation. *Ann Vasc Surg.* (2007) 21:742–8. doi: 10.1016/j.avsg.2007.01.015

38. Bennett DE. Primary mycotic aneurysms of the aorta. Report of case and review of the literature. *Arch Surg.* (1967) 94:758–65. doi: 10.1001/archsurg.1967.01330120012004

39. Huang ZD, Zhang ZJ, Yang B, Li WB, Zhang CJ, Fang XY, et al. Pathogenic detection by metagenomic next-generation sequencing in osteoarticular infections. *Front Cell Infect Microbiol.* (2020) 10:471. doi: 10.3389/fcimb.2020.00471

40. Sörelius K, Mani K, Björck M, Sedivy P, Wahlgren CM, Taylor P, et al. Endovascular treatment of mycotic aortic aneurysms: a European multicenter study. *Circulation.* (2014) 130:2136–42. doi: 10.1161/CIRCULATIONAHA.114.009481

41. Sörelius K, Wanhainen A, Furebring M, Björck M, Gillgren P, Mani K, et al. Nationwide study of the treatment of mycotic abdominal aortic aneurysms comparing open and endovascular repair. *Circulation.* (2016) 134:1822–32. doi: 10.1161/CIRCULATIONAHA.116.024021

42. Batt M, Jean-Baptiste E, O'Connor S, Bouillanne PJ, Haudebourg P, Hassen-Khodja R, et al. In-situ revascularisation for patients with aortic graft infection: a single centre experience with silver coated polyester grafts. *Eur J Vasc Endovasc Surg.* (2008) 36:182–8. doi: 10.1016/j.ejvs.2008.02.013

frontiers | Frontiers in Cardiovascular Medicine

TYPE Case Report
PUBLISHED 02 November 2022
DOI 10.3389/fcvm.2022.1020672

OPEN ACCESS

EDITED BY
Leonardo Roever,
Federal University of Uberlandia, Brazil

REVIEWED BY
Ajay Kumar Mishra,
Saint Vincent Hospital, United States
Roney Orismar Sampaio,
University of São Paulo, Brazil

*CORRESPONDENCE
Yushi Wang
yushi@jlu.edu.cn

SPECIALTY SECTION
This article was submitted to General Cardiovascular Medicine, a section of the journal Frontiers in Cardiovascular Medicine

RECEIVED 16 August 2022
ACCEPTED 14 October 2022
PUBLISHED 02 November 2022

CITATION
Wang S, Wang J, Liu J, Zhang Z, He J and Wang Y (2022) A case report and review of literature: Tuberculous pericarditis with pericardial effusion as the only clinical manifestation. *Front. Cardiovasc. Med.* 9:1020672. doi: 10.3389/fcvm.2022.1020672

A case report and review of literature: Tuberculous pericarditis with pericardial effusion as the only clinical manifestation

Shipeng Wang, Jingyue Wang, Junqian Liu, Zhiyu Zhang, Jiahuan He and Yushi Wang*

Department of Cardiology, The First Hospital of Jilin University, Changchun, China

Tuberculosis is a main cause of pericardial disease in developing countries. However, in patients with atypical clinical presentation, it can lead to misdiagnosis, missed diagnosis, and delayed treatment. In this study, we report a case of a 61-year-old woman admitted to the cardiac intensive care unit with "weakness and loss of appetite" and a large pericardial effusion shown by echocardiography. After hospitalization, a pericardiocentesis was performed, and the pericardial fluid was hemorrhagic. However, the Xpert MTB/RIF and T-SPOT tests were negative, and repeated phlegm antacid smears and culture of pericardial fluid did not reveal antacid bacilli. The patient eventually underwent thoracoscopic pericardial biopsy, which revealed extensive inflammatory cells and significant granulomas. Combined with the fact that the patient's pericardial effusion was exudate, the patient was considered to be suspected of tuberculous pericarditis (TBP) and given empirical anti-tuberculosis treatment the patient's symptoms improved and the final diagnosis was TBP. In this case report, it is further shown that a negative laboratory test cannot exclude tuberculosis infection. In recurrent unexplained pericardial effusions, the pericardial biopsy is feasible. In countries with a high burden of tuberculosis, empirical antituberculosis therapy may be used to treat the pericardial effusion that excludes other possible factors.

KEYWORDS

tuberculosis, tuberculous pericarditis (TBP), pericardial effusion (PE), diagnosis, case, review

Introduction

Tuberculosis (TB) is one of the top 10 leading causes of death worldwide and the leading cause of death by a single source of infection. According to the World Health Organization (WHO) global TB report 2021 version (1), China had the second highest incidence of TB in the world in 2020, accounting for 8.5% of TB globally. While extrapulmonary TB accounts for 15% of all TB cases, an epidemiological study indicated that nearly one-third of HIV-negative TB patients in China have extrapulmonary TB (2). TB is caused by mycobacterium tuberculosis and is mainly transmitted through the respiratory system. Mycobacterium tuberculosis mainly affects the lungs and causes pulmonary tuberculosis, but the rest of the body can also be infected. The clinical presentation of tuberculosis is variable, and symptoms are often atypical, which makes it more challenging to diagnose early. Tuberculous pericarditis (TBP) is a rarely seen form of extrapulmonary TB, accounting for 1–2% of all TB infections. TBP is the most common cause of massive pericardial effusion in developing countries. It is also the most common cause of constrictive pericarditis in adults, which has a poor prognosis and high mortality rate owing to constrictive pericarditis (3). Therefore, early diagnosis and intervention of TBP are crucial to treat the disease and improve the prognosis. In this article, we describe a patient with TBP who was admitted to the cardiovascular intensive care unit with massive pericardial effusion, her clinical presentation, diagnostic process, and treatment. We share our experience in the diagnosis of TBP.

Case presentation

A 61-year-old Chinese woman presented with weakness and loss of appetite for the previous 20 days. She had a medical history of cholecystitis and underwent a cholecystectomy several years ago. Physical examination showed that the patient had a temperature of 36.7°C, blood pressure of 128/76 mmHg, and a heart rate of 77 beats/min. There were coarse breath sounds in both lungs and diminished breath sounds in both lower lungs; a small number of wet rales could be heard, and diminished heart sounds with enlarged heart borders due to pericardial effusion.

The electrocardiogram (**Figure 1**) suggested a sinus heart rate with low voltage in the limb leads. The patient's laboratory data at admission are shown in **Table 1**. Echocardiography indicated moderate to severe pericardial effusion (**Figure 2**), and echo-free areas were seen in the pericardial cavity. The diastolic fluid width was measured as 14 mm in the anterior wall of the right ventricle, 16 mm in the posterior wall of the left ventricle, 19 mm in the lateral wall of the left ventricle, and 20 mm in the apical part of the left ventricle. A bedside color doppler ultrasound showed bilateral pleural effusions. After admission, the patient had a fever intermittently, with a temperature of up to 38.3°C without chills and shivering. The patient's temperature was elevated within 24 h of admission, meaning that the possibility of community-acquired pneumonia could not be excluded. After blood cultures were retained, the patient was also given empirical anti-infective treatment with moxifloxacin. However, as the patient's improvement in relevant tests was considered not to exclude tuberculosis, the use of fluoroquinolones alone should be avoided, and the patient's moxifloxacin was discontinued and changed to ampicillin. The patient's blood culture later indicated no bacterial growth. A computed tomography (CT) scan of the lungs revealed sporadic inflammation in both lungs, inflammatory nodules in the upper left and lower right lung lobes, calcification in the upper left lobe (**Figure 3**), and bilateral pleural effusions. Furthermore, the mediastinal lymph nodes were enlarged and partially calcified. Pericardiocentesis and drainage were used to relieve the patient's symptoms, such as chest tightness and shortness of breath. The patient's pericardial effusion was hematogenous, with routine results as follows: protein 53.96 g/L; Reye's test positive; total erythrocyte count 214300.00 $\times$ 10^6/L; total leukocyte count 3762.00 $\times$ 10^6/L; percentage of single nucleated cells 84%; adenosine deaminase (ADA) 32.0 U/L; lactate dehydrogenase (LDH) 326 U/L; and carcinoembryonic antigen (CEA) 0.47 ng/ml.

The above results indicated that the patient's pericardial effusion was exudate. The pericardial effusion smear did not find acid-fast bacilli, and Xpert MTB/RIF (Xpert Mycobacterium TB/RIF test is a new test, which is helpful for rapid diagnosis of TB and drug resistance, thus bringing revolutionary changes to TB control.) and T-SPOT tests (The T-SPOT test is a unique TB blood test designed to reduce variability and maximize sensitivity, even in people with low immune function.) were negative. The exfoliated cells of the pericardial effusion showed lymphocytes and lobulated nuclei, and no cancer cells were found. Female tumor markers such as CEA, cancer antigen (CA) 125, CA 199, and neuron-specific enolase were below the reference values to exclude tumor-derived pericardial effusion. Further positron emission tomography/computed tomography (PET/CT) was performed, which showed inhomogeneous thickening of the pericardium, enhanced metabolism, mediastinal lymph nodes, and uterine metabolism fibroids. Therefore, we could almost exclude the possibility that pericardial effusion was caused by a tumor. The patient's thyroid function test suggested that her free triiodothyronine (FT3) of 2.31 pmol/L was only mildly depressed, and it was unlikely that the pericardial effusion was caused by hypothyroidism. To rule out the possibility that the patient's pericardial effusion was caused by autoimmune disease, we further performed autoimmune marker screening, and the patient's antinuclear antibodies (ANA), anti-neutrophil cytoplasmic antibodies (ANCA), and antiphospholipid. The antiphospholipid syndrome antibodies were all negative, which essentially excluded autoimmune diseases.

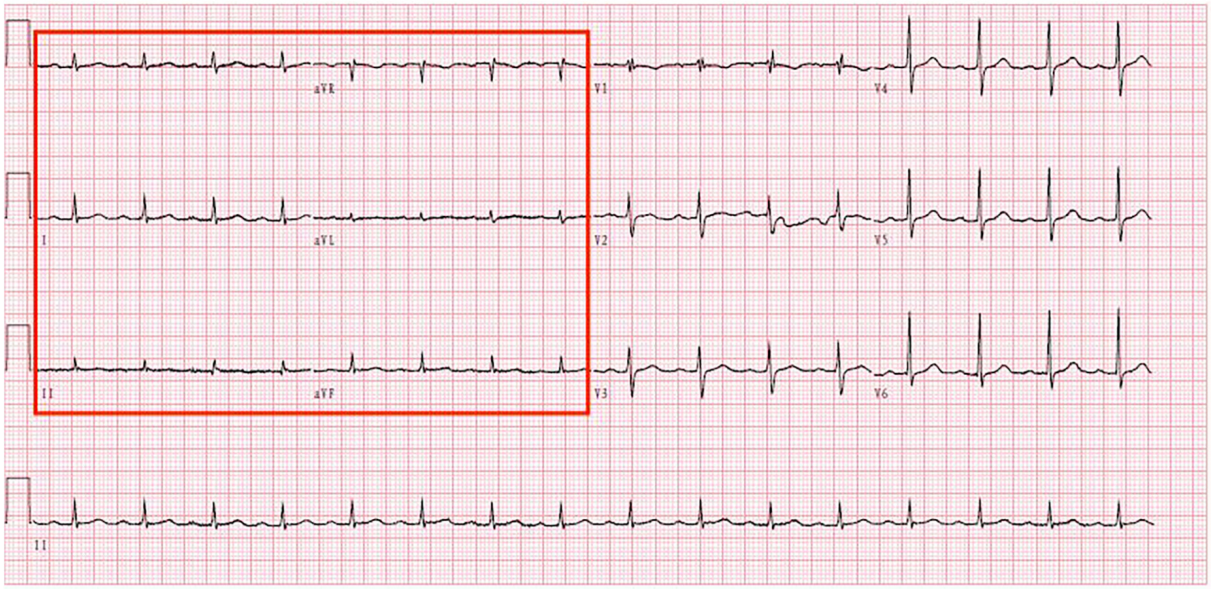

FIGURE 1
Electrocardiogram shows that the patient has low voltage in the limb leads.

Three days after admission, the patient had no fluid flow from the pericardial drainage tube, so the pericardial drainage tube was removed. Seven days after admission, the patient's bedside color doppler ultrasound showed that the right pleural effusion was less than at the time of admission. However, there was still a considerable amount of pleural effusion on the left side. We gave the patient left-sided thoracic puncture drainage, and the drainage fluid was light-red. Routine examination of the pleural fluid showed protein 42.83 g/L; a positive Reye's test; total red blood cell count of 67,500.00 $\times$ 10^6/L; total white blood cell count of 1359.00 $\times$ 10^6/L; and percentage of single nucleated cells 97%. Its property was approximately the same as that of pericardial effusion, which was an exudate and the possibility of extravasation of a large amount of pericardial effusion could not be excluded. After receiving symptomatic supportive treatment, the patient's symptoms showed improvement, and the family refused to undertake further specific investigations to determine the cause.

However, 2 months later, the patient was readmitted with malaise, chest pain, and low-grade fever. She had been treated with cephalosporin at a local hospital before admission, but the outcome was poor. A small amount of pericardial effusion was again detected by echocardiography at the time of admission. To determine the cause of the pericardial effusion, the patient was referred to the department of thoracic surgery for a biopsy of the pericardial mass. Pathological findings showed granulomatous lesions and fibrous hyperplasia of the mediastinal lymph nodes (**Figure 4**) and granulomatous lesions of the pericardial fibrofatty tissue (**Figure 5**). Furthermore, the patient's pulmonary CT indicated a nodular calcified shadow in the left upper lung and enlarged and partially calcified lymph nodes in the mediastinum and part of the bilateral hilum. The patient was considered to have stable tuberculosis in the upper lobe of the left lung, and the pericardial puncture fluid was exudate with increased leukocytes, mainly monocytes, and mildly elevated ADA. TBP can be suspected according to the diagnostic criteria, and the patient was advised to go to an infectious disease hospital for further treatment. The dosing regimen was: isoniazid 300 mg orally one time a day (QD), rifampicin 600 mg orally QD, ethambutol 100 mg orally QD, and pyrazinamide 100 mg orally QD. The four drugs were administered for 8 weeks and then reduced to isoniazid and rifampicin to continue the treatment for 6 months. According to the PET-CT results, the patient's pericardium had become unevenly thickened. To avoid progression to constrictive pericarditis, the patient was given prednisolone 50 mg, and the dose was gradually reduced. After 8 months, we followed up with the patient by telephone; her symptoms, such as weakness and chest pain, were improved following the anti-tuberculosis treatment.

Discussion

We have reported the case of a patient who was diagnosed with TBP by pericardial biopsy after all laboratory tests were negative. The patient presented with fatigue and loss of appetite as the primary clinical manifestations, and an echocardiogram showed moderate to large pericardial effusion. The drainage fluid after the puncture was a hemorrhagic

10.3389/fcvm.2022.1020672

TABLE 1 The patient's laboratory data.

Parameter	Values		Unit
	Day 1	References value	
WBC	6.06	3.5–9.5	10^9/L
NE#	4.53	1.80–6.30	10^9/L
NE	0.75	0.4–0.75	%
LY#	0.96	1.1–3.2	10^9/L
LY	0.16	0.2–0.5	%
Hb	82	115–150	g/L
PLT	342	125–350	10^9/L
AST	25.5	13.0–35.0	U/L
ALT	47.3	7.0–40.0	U/L
TB	8.6	0.0–21.0	μmol/L
DBIL	2.3	0.0–6.8	μmol/L
IBIL	6.3	5.0–20.0	μmol/L
Lac	0.6	0.5–2.2	mmol/L
Fib	4.34	1.8–4.0	g/L
TP	60.3	68–85	g/L
GLU	5.8	3.9–6.1	mmol/l
BUN	2.36	3.1–8.8	mmol/L
sCr	50.1	41–81	μmol/L
TG	0.88	0.28–1.8	mmol/L
D-dimer	> 5000	100–600	ng/ml
CKMB	< 1.0	0–4.3	ng/ml
Tn	< 0.05	0–0.05	ng/ml
PT	14.7	9.0–13.0	S
INR	1.24	0.8–1.2	–
APTT	24.5	21–33	S
PCT	< 0.05	0–0.5	ng/mL
CPR	54.23	0–3.5	mg/L
TSH	1.781	0.35–4.94	μIU/ml
FT3	2.31	2.43–6.01	pmol/L
FT4	12.43	9.01–19.05	pmol/L

WBC, white blood cell; NE, neutrophils; LY, lymphocyte; Hb, hemoglobin; PLT, platelets; AST, aspartate aminotransferase; ALT, alanine transaminase; TB, total bilirubin; DBIL, direct bilirubin; IBIL, indirect bilirubin; Lac, lactic acid; Fib, fibrinogen; TP, Total proteins; GLU, glucose; BUN, blood urea nitrogen; sCr, serum creatinine; TG, triglyceride; CKMB, creatine kinase MB; Tn, troponin; PT, prothrombin time; INR, international normalized ratio; APTT, activated partial thromboplastin time; PCT, procalcitonin; CRP, C-reactive protein; TSH, thyroid-stimulating hormone; FT3, free triiodothyronine; FT4, free thyroxine.

exudate. Tuberculosis and cancer are common causes of pericardial effusion, and TB is the most frequent cause in developing countries (4).

Extrapulmonary tuberculosis (EPTB) can affect any part of the body; it is often missed or misdiagnosed because clinical manifestations may be atypical, diagnostic tissue samples are readily unavailable, and bacterial levels are low, making diagnosis difficult (5). Pleura and lymph nodes are the most common sites of EPTB lesions, followed by bones, joints, intestines, peritoneum, kidneys, the genitourinary system, and meninges (6). A study on the epidemiology of extrapulmonary TB in Chinese inpatients suggested that skeletal TB may be the predominant form of extrapulmonary TB in China, accounting for nearly 41% of its EPTB; this discrepancy may be related to BCG vaccination nationwide in China (2). In contrast, pericardial TB is a rare type of EPTB, usually caused by retrograde dissemination of mycobacterium tuberculosis from the peripheral trachea, peripheral bronchi, or mediastinal lymph nodes *via* lymphatics or hematogenous dissemination of the primary TB infection (7). EPTB can present different physical signs and symptoms depending on the organ involved, the disease's aggressiveness, and the host's immune response. TBP can be divided into four stages, with corresponding clinical manifestations (8, 9). The mortality rate of TBP 6 months after diagnosis is 17–40% (10). Therefore, an early and effective diagnosis of TBP can help improve the disease cure rate and reduce mortality.

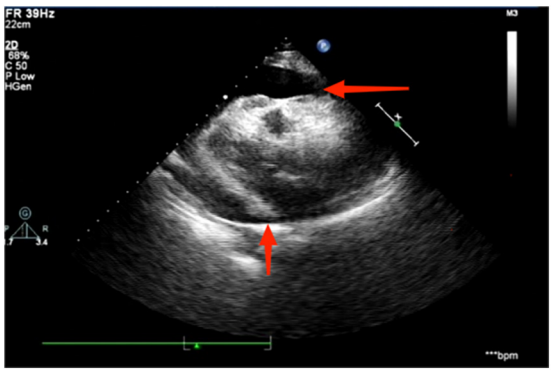

FIGURE 2
Echocardiography suggests the presence of a moderate to large pericardial effusion, as indicated by the red arrowhead.

To facilitate diagnosis in TB-endemic countries, there are uniform diagnostic criteria for confirmed and suspected TBP based on clinical and laboratory findings (11). Currently, the most widely used laboratory tests for diagnosing TBP include T-SPOT, Xpert MTB/RIF, ADA, etc. The overall sensitivity and specificity of T-SPOT are 91 and 88%, respectively (12), while the corresponding figures for Xpert MTB/RIF are 68 and 99% (13). Hence, the latter is more specific than T-SPOT but has lower sensitivity when negative. The threshold value of ADA remains controversial; ≥ 40 U/L is usual when diagnosing the possible presence of TBP in patients, and the sensitivity and specificity of the test are 84.0 and 80.0%, respectively, at the threshold value of 40 U/L (14). Pericardial fluid culture is also a widely used test for diagnosing TBP; however, it is usually not preferred because it is time-consuming, and in 27–48% of cases, no tuberculous fraction is found in the pericardial fluid (15). Notably, this patient differed from typical patients with tuberculous cystitis in having no typical TB symptoms. She also recorded negative T-SPOT and Xpert MTB/RIF tests, ADA of

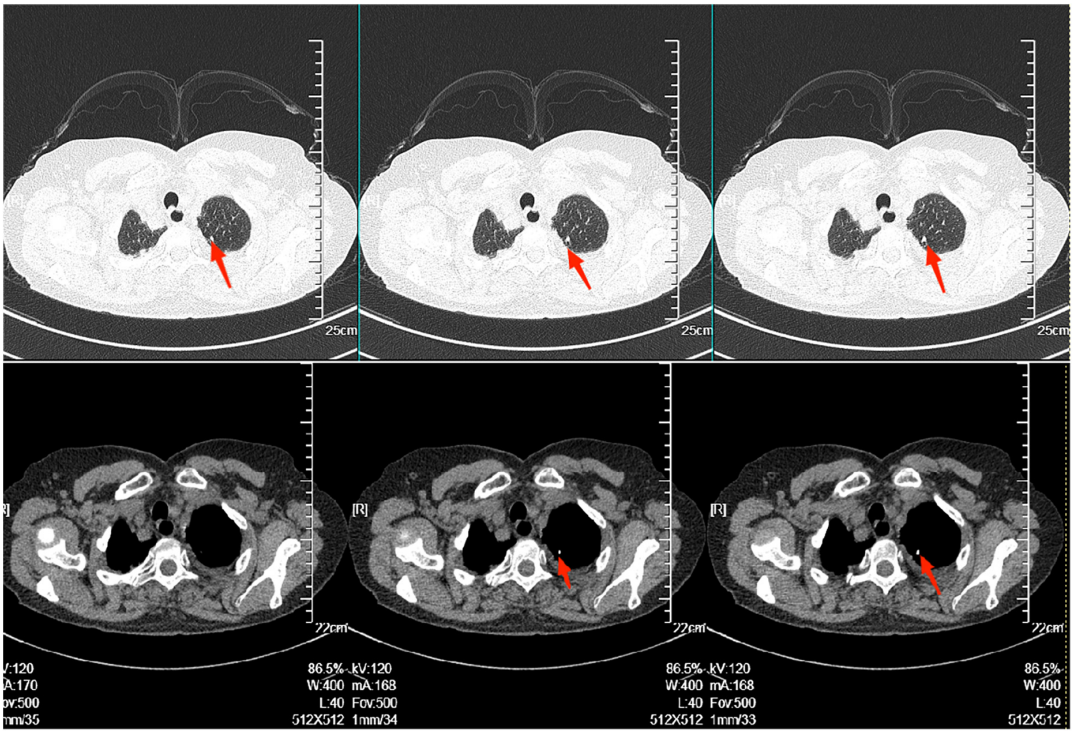

FIGURE 3
There was scattered inflammation in both lungs, inflammatory nodules in the upper left and lower right lobes. Calcification in the left upper lobe, as shown in the red arrow in the figure. The radiologist considered it to be stable tuberculosis.

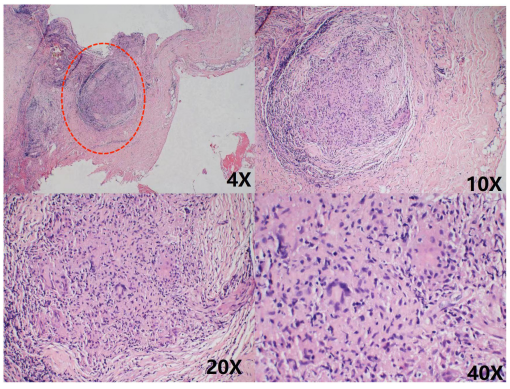

FIGURE 4
Chronic inflammatory cell infiltration was seen in the connective tissue granulomatous lesions and fibrous tissue hyperplasia were seen in the lymph nodes No necrosis was observed. As shown in the red circle.

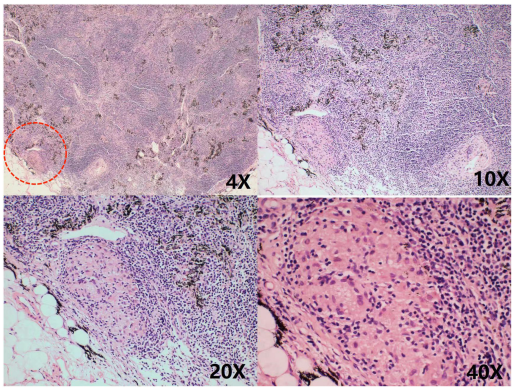

FIGURE 5
Granulomatous lesions are seen within the fibrofatty tissue, as shown in the red circle.

32 U/L in the pericardial fluid, and negative results for the culture of antacid bacilli in the pericardial fluid, which do not form the basis for a TBP diagnosis. A meta-analysis found the overall sensitivity and specificity of interferon-gamma (IFN-γ) to be 97 and 99%, respectively. However, IFN-γ is relatively expensive and is not commonly used as a laboratory test (16).

The patient was discharged with symptomatic treatment, but she was readmitted 1 month later with malaise, chest pain with hypothermia, and echocardiography indicated a small pericardial effusion. A single-center study involving 174 patients suggested that pericardial tissue biopsy is feasible for recurrent pericardial effusions to improve the likelihood of diagnosis in patients (17). Ultimately, this patient was diagnosed with

TBP when a pericardial biopsy was performed to identify the source of the pericardial effusion, and a granuloma was found.

The current treatment for TB pericarditis is a "quadruple" regimen of rifampin, isoniazid, pyrazinamide, and ethambutol for 2 months, followed by isoniazid and rifampin for 4 months (3). Adjuvant corticosteroid therapy reduces the hospitalization rate for TBP and the incidence of patients progressing to constrictive pericarditis, but it increases cancer incidence in HIV-positive patients (18). Meanwhile, some studies have suggested that routine pericardiocentesis with prolonged drainage reduces the incidence of constrictive pericarditis (19, 20). In countries with a high burden of tuberculosis, ATT may be used to treat the pericardial effusion that excludes other possible factors (21). However, the efficacy and safety of empirical ATT need further study.

Our study also has a few limitations. The diagnosis of EPTB is a challenge. We have no definitive diagnostic evidence - mycobacterium tuberculosis was found or pericardial biopsy found caseous granuloma. There is still much room for exploration in the way of laboratory test of extra-pulmonary tuberculosis.

In conclusion, negative routine laboratory tests for the pericardial effusion of unknown origin does not exclude tuberculosis pericarditis. And a biopsy of the pericardial effusion may help clarify the diagnosis based on excluding other causes. Empirical anti-TB treatment may be considered after non-TB causes have been ruled out to the extent possible.

Data availability statement

The original contributions presented in this study are included in the article/supplementary material, further inquiries can be directed to the corresponding author.

Author contributions

SW conceived the idea and conceptualized the case. JW, JL, ZZ, and JH collected the data. SW analyzed the data and drafted the manuscript, which was then reviewed by YW. All authors contributed to the article and approved the submitted version.

Conflict of interest

The authors declare that the research was conducted in the absence of any commercial or financial relationships that could be construed as a potential conflict of interest.

Publisher's note

References

1. World Health Organization. *Global Tuberculosis Report 2021*. Geneva: World Health Organization (2021).

2. Pang Y, An J, Shu W, Huo F, Chu N, Gao M, et al. Epidemiology of extrapulmonary tuberculosis among inpatients, China, 2008-2017. *Emerg Infect Dis.* (2019) 25:457–64. doi: 10.3201/eid2503.180572

3. Adler Y, Charron P, Imazio M, Badano L, Barón-Esquivias G, Bogaert J, et al. 2015 ESC Guidelines for the diagnosis and management of pericardial diseases: the task force for the diagnosis and management of pericardial diseases of the European society of cardiology (ESC)endorsed by: the European association for cardio-thoracic surgery (EACTS). *Eur Heart J.* (2015) 36:2921–64. doi: 10.5603/KP.2015.0228

4. Vakamudi S, Ho N, Cremer PC. Pericardial effusions: causes, diagnosis, and management. *Prog Cardiovasc Dis.* (2017) 59:380–8. doi: 10.1016/j.pcad.2016.12.009

5. Sharma SK, Mohan A, Kohli M. Extrapulmonary tuberculosis. *Expert Rev Respir Med.* (2021) 15:931–48. doi: 10.1080/17476348.2021.1927718

6. Prakasha SR, Suresh G, D'Sa IP, Shetty SS, Kumar SG. Mapping the pattern and trends of extrapulmonary tuberculosis. *J Glob Infect Dis.* (2013) 5:54–9. doi: 10.4103/0974-777X.112277

7. Spodick DH. Tuberculous pericarditis. *AMA Arch Intern Med.* (1956) 98:737–49. doi: 10.1001/archinte.1956.00250300055008

8. Chang SA. Tuberculous and infectious pericarditis. *Cardiol Clin.* (2017) 35:615–22. doi: 10.1016/j.ccl.2017.07.013

9. Ntsekhe M, Mayosi BM. Tuberculous pericarditis with and without HIV. *Heart Fail Rev.* (2013) 18:367–73. doi: 10.1007/s10741-012-9310-6

10. Mayosi BM, Wiysonge CS, Ntsekhe M, Gumedze F, Volmink JA, Maartens G, et al. Mortality in patients treated for tuberculous pericarditis in sub-Saharan Africa. *S Afr Med J.* (2008) 98:36–40.

11. Mayosi BM, Burgess LJ, Doubell AF. Tuberculous pericarditis. *Circulation.* (2005) 112:3608–16. doi: 10.1161/CIRCULATIONAHA.105.543066

12. Luo Y, Xue Y, Guo X, Lin Q, Tang G, Yu J, et al. Diagnostic value of pleural fluid T-SPOT for tuberculous pleurisy: an updated meta-analysis. *Tuberculosis (Edinb).* (2020) 122:101941. doi: 10.1016/j.tube.2020.101941

13. Andrianto, A, Mertaniasih NM, Gandi P, Al-Farabi MJ, Azmi Y, Jonatan M, et al. Diagnostic test accuracy of Xpert MTB/RIF for tuberculous pericarditis: a systematic review and meta-analysis. *F1000Res.* (2020) 9:761. doi: 10.12688/f1000research.22770.1

14. Reuter H, Burgess LJ, Carstens ME, Doubell AF. Adenosine deaminase activity–more than a diagnostic tool in tuberculous pericarditis. *Cardiovasc J S Afr.* (2005) 16:143–7.

15. Kyriakakis CG, Mayosi BM, de Vries E, Isaacs A, Doubell AF. An approach to the patient with suspected pericardial disease. *S Afr Med J.* (2016) 106:151–5. doi: 10.7196/SAMJ.2016.v106i2.10328

16. Liu C, Cui YL, Ding CM, Cui YL, Ding CM, Wu YH, et al. Diagnostic accuracy of interferon-gamma in pericardial effusions for tuberculous pericarditis: a meta-analysis. *J Thorac Dis.* (2018) 10:854–60. doi: 10.21037/jtd.2017.12.107

17. Yildirim M, Ustaalioglu R, Erkan M, Ustaalioglu BB, Demirbag H, Yasaroglu M, et al. The diagnostic value of pericardial fluid and pericardial biopsy: single center experiences. *Heart Surg Forum.* (2016) 19:E23–7. doi: 10.1532/hsf.1328

18. Mayosi BM, Ntsekhe M, Bosch J, Pandie S, Jung H, Gumedze F, et al. Prednisolone and Mycobacterium indicus pranii in tuberculous pericarditis. *N Engl J Med.* (2014) 371:1121–30. doi: 10.1056/NEJMoa1407380

19. Liebenberg JJ, Dold CJ, Olivier LR. A prospective investigation into the effect of colchicine on tuberculous pericarditis. *Cardiovasc J Afr.* (2016) 27:350–5. doi: 10.5830/CVJA-2016-035

20. Reuter H, Burgess LJ, Louw VJ, Doubell AF. The management of tuberculous pericardial effusion: experience in 233 consecutive patients. *Cardiovasc J S Afr.* (2007) 18:20–5.

21. Wang C, Fang L, Zhu W, Lin X, Guo X, Chen A, et al. Empirical anti-tuberculous therapy for the massive pericardial effusion of unknown etiology. *Curr Med Res Opin.* (2021) 37:1507–13. doi: 10.1080/03007995.2021.1940909

frontiers | Frontiers in Cardiovascular Medicine

TYPE Case Report
PUBLISHED 10 November 2022
DOI 10.3389/fcvm.2022.1020762

OPEN ACCESS

EDITED BY
Leonardo Roever,
Federal University of Uberlândia, Brazil

REVIEWED BY
Hui Chen,
First Affiliated Hospital of Xi'an Medical University, China
Agnes S. Kim,
UConn Health, United States
Carmelo Bernabeu,
Spanish National Research Council (CSIC), Spain

*CORRESPONDENCE
Qian Gao
gaojingqian@hotmail.com
Zhenguo Zhai
zhaizhenguo2011@126.com

SPECIALTY SECTION
This article was submitted to General Cardiovascular Medicine, a section of the journal Frontiers in Cardiovascular Medicine

RECEIVED 16 August 2022
ACCEPTED 13 October 2022
PUBLISHED 10 November 2022

CITATION
Liu D, Xu F, Gao Q and Zhai Z (2022) Case report: Pulmonary arterial hypertension in *ENG*-related hereditary hemorrhagic telangiectasia.
Front. Cardiovasc. Med. 9:1020762.
doi: 10.3389/fcvm.2022.1020762

Case report: Pulmonary arterial hypertension in *ENG*-related hereditary hemorrhagic telangiectasia

Dong Liu[1,2], Feiya Xu[2,3], Qian Gao[2]* and Zhenguo Zhai[1,2,3]*

[1]Peking University China-Japan Friendship School of Clinical Medicine, Beijing, China, [2]Department of Pulmonary and Critical Care Medicine, Center of Respiratory Medicine, China-Japan Friendship Hospital, National Center for Respiratory Medicine, Institute of Respiratory Medicine, Chinese Academy of Medical Sciences, National Clinical Research Center for Respiratory Diseases, Beijing, China, [3]Department of Pulmonary and Critical Care Medicine, Capital Medical University, Beijing, China

A young adult woman presented with exertional dyspnea and she had had recurrent epistaxis for more than 10 years. On physical examination, cyanosis was noted on the lips, and telangiectasias were seen on the oral mucosa and fingertips. Routine investigations revealed iron deficiency anemia and slightly elevated bilirubin. The result of right heart catheterization was indicative of pulmonary arterial hypertension (PAH). Pulmonary angiography showed arteriovenous malformations of the left upper pulmonary artery, and anterior cerebral artery malformation was seen in cranial computed tomographic angiogram. Genetic testing revealed that she and her three daughters carried heterozygous variant of ENG c.1195-1196del p.Arg399GlyfsTer2, which is characterized by pulmonary and cerebral arteriovenous malformations. In addition, our patient had pulmonary hypertension (PH) that is commonly associated with ACVRL1 mutations, revealing her phenotype was not consistent with isolated ENG genetic mutations. Here, we report a case with hereditary hemorrhagic telangiectasia (HHT) combined with PAH, which is associated with interesting differential diagnosis and etiological analysis. We have discussed the relationship between PH and HHT and the characteristics of PAH in HHT patients.

KEYWORDS

exertional dyspnea, pulmonary hypertension, hereditary hemorrhagic telangiectasia (HHT), pulmonary arterial hypertension, ENG

Case presentation

A 31-year-old woman complained of "shortness of breath for 2 years with exertion, worsening for 10 months." Two years ago, in the fifth month of her fourth pregnancy, she suffered exertional dyspnea accompanied by edema of both lower extremities, which was relieved after delivery. In the past 10 months, the patient's exercise capacity decreased progressively with onset of palpitations, and she had to take rest when climbing to the second floor. She was admitted to a local hospital. The pulmonary systolic pressure was estimated to be 110 mmHg by echocardiography. Computed

tomographic pulmonary angiogram (CTPA) showed that the main pulmonary artery was widened, and no filling defect was found. Her symptoms improved with diuretic.

She had had recurrent epistaxis for more than 10 years, and her eldest and second daughters also had a history of epistaxis. Vital signs revealed a temperature of 36.5°C, heart rate of 85 beats per minute, respiratory rate of 21 breaths per minute, and blood pressure of 119/70 mmHg. Cyanosis was noted on the lips, and telangiectasias were seen on the oral mucosa and fingertips (**Figure 1**). Auscultation revealed P2 > A2 in the pulmonary auscultation area and grade 3/6 systolic murmurs in tricuspid valve area. No pitting edema of extremities was observed. Arterial blood gas analysis on room air is normal. Fecal occult blood was weakly positive. Complete blood count and decreased ferritin were suggestive of iron deficiency anemia. Liver function revealed slightly elevated bilirubin and brain natriuretic peptide, troponin were normal. Immunoglobulin levels were normal, but with mildly decreased levels of complement3 and complement4. Coagulation function showed reduced activity of protein C. Laboratory data in detail are shown in **Table 1**.

The result of right heart contrast echocardiography was consistent with pulmonary arteriovenous malformations (AVMs). The result of echocardiography was indicative of pulmonary hypertension (PH). Electronic gastroscopy showed chronic non-atrophic gastritis but no gastric vascular malformations. Pulmonary function showed mild diffusion dysfunction. No obvious filling defect or vascular malformations were observed on CTPA (**Figure 2A**), but several ground-glass opacities were seen on the lung window of CTPA, where one of 7.8 mm × 7.5 mm in diameter was located in the right upper lung lobes (**Figure 2B**). The result of right heart catheterization (RHC) is shown in **Table 2**. Pulmonary angiography showed AVMs of the left upper pulmonary artery (**Figure 3A**), and anterior cerebral artery malformation was seen in cranial computed tomographic angiogram (**Figure 3B**). Genetic testing revealed the patient carried heterozygous variants in the ENG c.1195-1196del p.Arg399GlyfsTer2. Except her son, all her three daughters carried a heterozygous variant at the ENG c.1195-1196del locus.

As a young adult woman, our patient's main clinical symptom at presentation was exertional dyspnea, and she had recurrent epistaxis, multiple mucocutaneous telangiectasias, and organ involvement. According to Curacao diagnostic criteria (1), together with the results of RHC, the diagnosis of hereditary hemorrhagic telangiectasia (HHT) combined with pulmonary arterial hypertension (PAH) could be made.

She was treated with macitentan 10 mg once daily, furosemide 20 mg once daily, spironolactone 20 mg once daily, and polysaccharide iron complex 300 mg once daily.

Four months later, the patient returned to our hospital. The patient's exercise tolerance was improved. Repeat RHC revealed in **Table 2**. Although the mean pulmonary artery pressure (PAP) of the patient did not change significantly, she reported feeling better and meantime pulmonary blood volume and pulmonary vascular resistance (PVR) improved.

Discussion

Hereditary hemorrhagic telangiectasia is an autosomal dominant inherited disease characterized by multisystemic vascular dysplasia (2). The main genetic mutations are in endoglin (ENG), activin receptor-like kinase1 (ACVRL1), and mothers against decapentaplegic homolog 4 (SMAD4) (3). HHT1 is caused by mutations in ENG gene, while HHT2 is caused by ACVRL1 gene mutations, where TGF-β superfamily signaling pathway has been recognized to play a vital role (4). For our patient, one heterozygous variant was detected in the ENG gene, and the c.1195-1196del variant was located in the ENG gene of exon 9, which was a pathogenic variant according to the American College of Medical Genetics (ACMG) criteria (5). The mutation of ENG c.1195-1196del could cause a frameshift at amino acid 399 of the encoded protein, resulting in an early stop codon at amino acid 400. All types of mutations have been reported, including missense, non-sense, deletions, insertions, and splice site. Most families with HHT have unique mutations, and more than 900 mutations are described (6). According to the analysis of ExAC database and gnomAD database, the population frequency of this variant locus has not been recorded, but this variant was reported in a patient with spontaneous hemothorax (7).

Although PH is increasingly recognized as an important complication of HHT recently (8), whether PH is secondary to HHT or HHT is combined with PH in our patient was required to be discussed. At present, it is believed that the main pathogenesis of HHT-related PH occurs in two ways. First, multiple pulmonary AVMs bring about significant right-to-left shunt, resulting in high hemodynamics and increased cardiac preload. Reverse transmission of pressure leads to PH of a post-capillary subtype. One large study of 175 children confirmed HHT and found that 22% of children with HHT had pulmonary AVMs (9). But PH is not always associated with pulmonary AVMs. Our patient has no obvious hypoxemia and erythrocytosis, which means the right-to-left shunting in pulmonary arteries is not severe. These signs are

Abbreviations: ACMG, American College of Medical Genetics; AVMs, arteriovenous malformations; BMPR2, bone morphogenetic protein receptor type II; CTEPH, chronic thromboembolic pulmonary hypertension; CTPA, computed tomographic pulmonary angiogram; HHT, hereditary hemorrhagic telangiectasia; HPAH, hereditary pulmonary arterial hypertension; HRCT, high resolution chest tomography; IPAH, idiopathic pulmonary arterial hypertension; PAP, pulmonary artery pressure; PAH, pulmonary arterial hypertension; PAWP, pulmonary artery wedge pressure; PCH, pulmonary capillary hemangiomatosis; PH, pulmonary hypertension; PVOD, pulmonary veno-occlusive disease; PVR, pulmonary vascular resistance; TBLB, transbronchial lung biopsy; RHC, right heart catheterization.

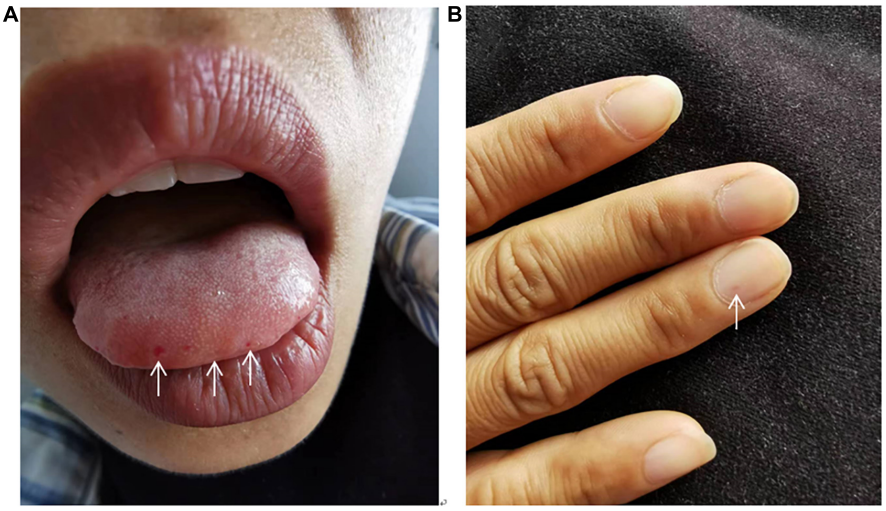

FIGURE 1
Abnormal inspection. Cyanosis was noted on the lips, and telangiectasias were seen on the oral mucosa **(A)** and fingertips **(B)**.

consistent with the results of pulmonary artery angiography. Second, others may feature significantly increased PAP and PVR with normal pulmonary artery wedge pressure (PAWP), which defines pre-capillary PH, whose histological features are not significantly different from idiopathic pulmonary arterial hypertension (IPAH). A cohort study of 578 HHT patients found that HHT2 patients were more likely to have post-capillary PH than HHT1 patients (10) because such patients often have hepatic AVMs. Trembath et al. found that ACVRL1 gene mutations may lead to the occlusion of pulmonary artery, which results in hereditary PAH (HPAH) and clinical manifestations, such as AVMs (3). Pre-capillary PH in HHT patients is relatively rare and mainly occurs in patients with ACVRL1 gene mutations (4). Therefore, HHT-related PH has primarily been associated with ACVRL1 gene, leading us to wonder whether HHT was the only contributing factor to her PH.

TABLE 1 Laboratory data.

Arterial blood gas analysis	**pH 7.45, PCO_2 30 mmHg, PO_2 95 mmHg, SO_2 98%**
Complete blood count	hemoglobin 103 g/L, mean corpuscular volume 74.9 fl, mean corpuscular hemoglobin 22.8 pg, mean corpuscular hemoglobin concentration 305 g/L.
Anemia test	ferritin 4.1 ng/ml, normal folic acid, vitamin B12, anti-intrinsic factor antibody.
Liver function	total bilirubin 31.54 umol/L, direct bilirubin 9.32 umol/L.
Cardiac biomarkers	normal
Anticoagulation test	protein C activity 56%, normal activity of protein S and antithrombin-III.
Antinuclear antibody	normal
Rheumatoid antibody	normal
Vasculitis antibody	normal
Tumor markers	normal
Complement	complement3 62.80 mg/dl, complement4 9.25 mg/dl.

Reference ranges are as follows: hemoglobin, 115–150 g/L; mean corpuscular volume, 82–100 fl; mean corpuscular hemoglobin, 27–34 pg; mean corpuscular hemoglobin concentration, 316–354 g/L; ferritin, 11.0–306.8 ng/ml; total bilirubin, 5.00–21.00 umol/L; direct bilirubin, 0–7.00 umol/L; protein C activity, 70–130%; complement3, 70.00–128.00 mg/dl; complement4, 16.00–47.00 mg/dl.

Genetic testing provides clues for a definite diagnosis, but when the patient's phenotype could not be fully explained by the genotype, it is necessary to review the patient's medical history and test results to make the best clinical judgment. The etiology can be traced back as follows: (1) Reduced protein C activity and normal activity of protein S and antithrombin-III were found. She did not take warfarin recently, which may interfere with the activity of protein C. The available evidence could not support the diagnosis of hereditary thrombophilia. But she was in a potential hypercoagulable state, which was a risk factor for pulmonary veno-occlusive disease (PVOD)/pulmonary capillary hemangiomatosis (PCH). Although EIF2AK4 gene mutation was not found in our patient, PVOD/PCH could not be completely ruled out due to her manifestations of PAH in the absence of left-sided heart disease, combined with ground-glass nodules and decreased lung diffusion capacity. Unfortunately, high-resolution chest tomography (HRCT) and transbronchial lung biopsy (TBLB) were not underwent. (2) The four times of pregnancies kept the pulmonary blood vessels in a state of higher circulation over an extended period of time. Although the abnormal state was not continuous, the remodeling of the pulmonary capillaries

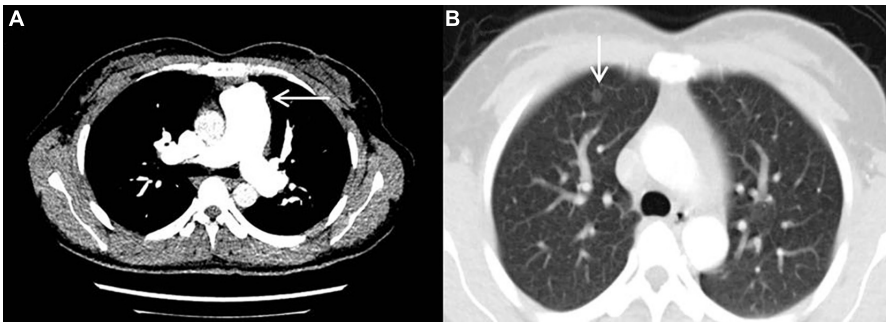

FIGURE 2
Computed tomography pulmonary angiography. **(A)** No obvious filling defect or vascular malformations were observed. **(B)** The ground-glass opacity that was 7.8 mm × 7.5 mm in diameter and located in the right upper lung lobes was seen.

likely could not be recovered. (3) A small amount of right-to-left shunt can be seen in the patient's right heart contrast echocardiography, but it is currently hard to confirm whether it is a congenital or secondary change. Whether patent foramen ovale worked in the progress of PH is uncertain. (4) Pre-capillary PH could be the result of chronic thromboembolic pulmonary hypertension (CTEPH) (11), but no significant ventilation and blood flow mismatch were observed in ventilation/perfusion scintigraphy, which was vital for the diagnosis of CTEPH. (5). In addition, chronic anemia caused by epistaxis led to increased cardiac output and may also have contributed to the development of PH.

Although PAH in HHT patients with ENG gene mutation is not first reported, the diagnosis and etiological analysis in this group is still challenging. On the one hand, hereditary PAH in patients with pulmonary AVMs in combination with HHT is difficult to be distinguished clinically from IPAH, as it is usually associated with dysfunction of ALK-1, the product of ACVRL1 gene (12). Some studies found approximately 70% of cases with HPAH are associated with bone morphogenetic protein receptor type II (BMPR2) gene mutation and less than 1% of patients with HHT suffered HPAH caused by a mutation in the ACVRL1 gene (8, 13). However, HPAH patients with ACVRL1 gene mutations are frequently asymptomatic and not combined with HHT (14). Besides, several less common HHT gene mutations were identified in HPAH patients, such as ENG gene and growth differentiation factor 2 (GDF2) gene (15). On the other hand, as a rare complication of HHT, PAH could be likely related to high-output heart failure. A case of 55-year-old woman with HHT combined with high-output heart failure was reported, and her PVR was elevated to 5.5 Woods units prior to the treatment (16). Compared with relatively temporary high circulation state of our patient, she was in a persistent state due to the presence of hepatic AVMs. Besides, a case of 26-year-old woman with HHT with pre-capillary PH was reported. After she underwent the therapy of pre-capillary PH, high cardiac output and PAWP were surprisingly unveiled (17), which suggested that high cardiac-output state could be masked.

TABLE 2 The results of right heart catheter in two admissions.

	First admission	Second admission
Right atrial pressure	5/1 (2) mmHg	6/2 (3) mmHg
Right ventricular pressure	63/0 (21) mmHg	53/−2 (21) mmHg
Pulmonary artery pressure	63/23 (33) mmHg	51/18 (32) mmHg
Pulmonary artery wedge pressure	7 mmHg	10 mmHg
Pulmonary blood volume	5.39 L/min	8.15 L/min
Pulmonary vascular resistance	4.82 Wood units	2.70 Wood units

In summary, PH could result from multiple different issues and is likely multifactorial. Standardized diagnosis, seeking causes, and early identification of risk factors are essential to improve the prognosis of patients. Additional causes should be suspected and sought out when unusual clinical phenomena occur. As a rare disease, if HHT was combined with PH, it could easily be diagnosed as idiopathic PAH or attributed to HHT alone if one is not mindful of other potential contributions. Therefore, it is vital to evaluate the underlying reversible causes.

Limitations

This was a retrospective study and the lack of information was the shortcoming of our study. Up to the time we chose this case, the patient had been hospitalized twice and we read all the data in the electronic medical record, but the patient did not complete all important examinations, including brain magnetic resonance imaging, HRCT, and TBLB.

Future directions

In patients with HHT, the pathogenesis of PH is complex and multifactorial and the phenotypes are diverse. It is

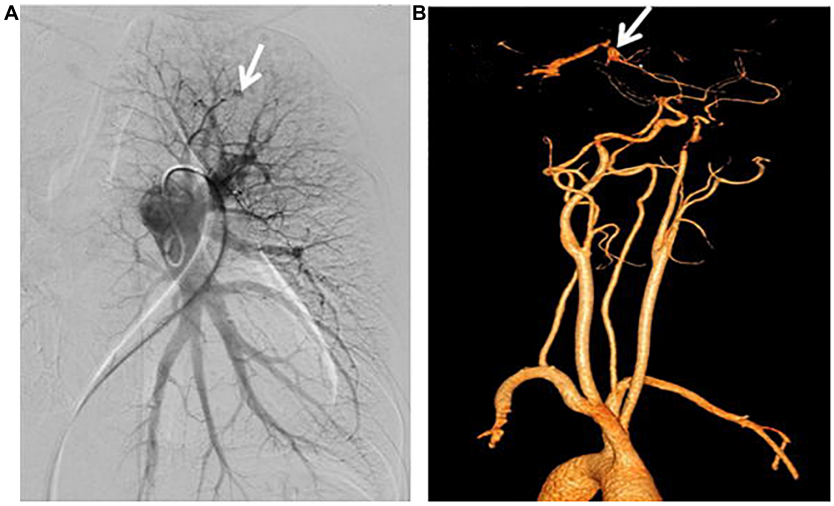

FIGURE 3
Pulmonary angiography and cranial computed tomographic angiogram. **(A)** Arteriovenous malformations of the left upper pulmonary artery were shown. **(B)** Anterior cerebral artery malformations were revealed.

not clear how to identify whether PH is secondary to HHT or HHT is combined with PH accurately. It is difficult to tell the differences between HHT-related PAH and PAH in the general population. Further researches are required to explore the pathogenesis of PH in HHT patients.

Conclusion

We report such an ENG-related case of HHT combined with PAH in a young adult woman with minor pulmonary AVMs for the first time. We found that even if high-output heart failure was not continuous in HHT patients, irreversible pulmonary vascular remodeling might occur and pre-capillary PH was caused.

Data availability statement

The original contributions presented in this study are included in the article/supplementary material, further inquiries can be directed to the corresponding author/s.

Ethics statement

Written informed consent was obtained from the individual(s) for the publication of any potentially identifiable images or data included in this article.

Author contributions

DL collected the patient's information, summarized the literature data, and wrote the manuscript. FX collected the patient's information and wrote the manuscript. QG and ZZ were the major contributors in revising the manuscript. All authors read and approved the final manuscript.

Funding

This study was supported by the CAMS Innovation Fund for Medical Sciences (CIFMS) (No. 2020-I2M-B-095) and Chinese Academy of Medical Sciences Innovation Fund for Medical Sciences (2021-I2M-1-049).

Conflict of interest

The authors declare that the research was conducted in the absence of any commercial or financial relationships that could be construed as a potential conflict of interest.

Publisher's note

References

1. Shovlin CL, Guttmacher AE, Buscarini E, Faughnan ME, Hyland RH, Westermann CJ, et al. Diagnostic criteria for hereditary hemorrhagic telangiectasia (Rendu-Osler-Weber syndrome). *Am J Med Genet.* (2000) 91:66–7. doi: 10.1002/(sici)1096-8628(20000306)91:13.0.co;2-p

2. Guttmacher AE, Marchuk DA, White RI Jr. Hereditary hemorrhagic telangiectasia. *N Engl J Med.* (1995) 333:918–24. doi: 10.1056/NEJM199510053331407

3. Trembath RC, Thomson JR, Machado RD, Morgan NV, Atkinson C, Winship I, et al. Clinical and molecular genetic features of pulmonary hypertension in patients with hereditary hemorrhagic telangiectasia. *N Engl J Med.* (2001) 345:325–34.

4. Lam S, Guthrie KS, Latif MA, Weiss CR. Genetic counseling and testing for hereditary hemorrhagic telangiectasia. *Clin Genet.* (2022) 101:275–84. doi: 10.1111/cge.14050

5. Miller DT, Lee K, Chung WK, Gordon AS, Herman GE, Klein TE, et al. ACMG SF v3.0 list for reporting of secondary findings in clinical exome and genome sequencing: a policy statement of the American college of medical genetics and genomics (ACMG). *Genet Med.* (2021) 23:1381–90. doi: 10.1038/s41436-021-01172-3

6. Bayrak-Toydemir P, McDonald J. *HHT Mutation Database.* (2022). Available online at: https://arup.utah.edu/database/HHT/ (accessed April 2, 2022).

7. Ishikawa T, Pollak S, Pflugradt R, Bohnert M, Grosse Perdekamp M, Thierauf A, et al. Pulmonary arteriovenous malformation causing sudden death due to spontaneous hemothorax. *Int J Legal Med.* (2010) 124:459–65. doi: 10.1007/s00414-009-0401-4

8. Bofarid S, Hosman AE, Mager JJ, Snijder RJ, Post MC. Pulmonary vascular complications in hereditary hemorrhagic telangiectasia and the underlying pathophysiology. *Int J Mol Sci.* (2021) 22:3471. doi: 10.3390/ijms22073471

9. Van Gent MW, Post MC, Snijder RJ, Westermann CJ, Plokker HW, Mager JJ, et al. Real prevalence of pulmonary right-to-left shunt according to genotype in patients with hereditary hemorrhagic telangiectasia: a transthoracic contrast echocardiography study. *Chest.* (2010) 138:833–9. doi: 10.1378/chest.09-1849

10. Vorselaars V, Velthuis S, van Gent M, Westermann C, Snijder R, Mager J, et al. Pulmonary hypertension in a large cohort with hereditary hemorrhagic telangiectasia. *Respiration.* (2017) 94:242–50. doi: 10.1159/000458447

11. Shovlin CL, Sulaiman NL, Govani FS, Jackson JE, Begbie ME. Elevated factor VIII in hereditary haemorrhagic telangiectasia (HHT): association with venous thromboembolism. *Thromb. Haemost.* (2007) 98:1031–9.

12. Abdalla SA, Gallione CJ, Barst RJ, Horn EM, Knowles JA, Marchuk DA, et al. Primary pulmonary hypertension in families with hereditary haemorrhagic telangiectasia. *Eur Respir J.* (2004) 23:373–7. doi: 10.1183/09031936.04.00085504

13. Vorselaars VMM, Hosman AE, Westermann CJJ, Snijder RJ, Mager JJ, Goumans MJ, et al. Pulmonary arterial hypertension and hereditary haemorrhagic telangiectasia. *Int. J. Mol. Sci.* (2018) 19:3203.

14. Rosenzweig EB, Morse JH, Knowles JA, Chada KK, Khan AM, Roberts KE, et al. Clinical implications of determining BMPR2 mutation status in a large cohort of children and adults with pulmonary arterial hypertension. *J. Heart Lung Transplant.* (2008) 27:668–74. doi: 10.1016/j.healun.2008.02.009

15. Aldred MA, Morrell NW, Guignabert C. New mutations and pathogenesis of pulmonary hypertension: progress and puzzles in disease pathogenesis. *Circ Res.* (2022) 130:1365–81. doi: 10.1161/CIRCRESAHA.122.320084

16. Murray E, Taylor J, Hountras PA. Case of high-output heart failure. *Chest.* (2022) 161:e23–8. doi: 10.1016/j.chest.2021.07.2180

17. Liu D, Sindhu K, Witkin A, Patel L, Channick R. Pulmonary hypertension in a patient with hereditary hemorrhagic telangiectasia. *R I Med J (2013).* (2017) 100:29–31.

frontiers | Frontiers in Cardiovascular Medicine

TYPE Case Report
PUBLISHED 17 November 2022
DOI 10.3389/fcvm.2022.970783

OPEN ACCESS

EDITED BY
Junjie Xiao,
Shanghai University, China

REVIEWED BY
Hardik Dineshbhai Desai,
Gujarat Adani Institute of Medical Sciences, India
Raja Joshi,
Sir Ganga Ram Hospital, India

*CORRESPONDENCE
Ziming Wan
wanziming001@163.com

SPECIALTY SECTION
This article was submitted to General Cardiovascular Medicine, a section of the journal Frontiers in Cardiovascular Medicine

RECEIVED 18 July 2022
ACCEPTED 31 October 2022
PUBLISHED 17 November 2022

CITATION
Wan Z (2022) Case report: Severe dry cough associated with superior vena cava syndrome—Caused recurrent chylothorax.
Front. Cardiovasc. Med. 9:970783.
doi: 10.3389/fcvm.2022.970783

Case report: Severe dry cough associated with superior vena cava syndrome—Caused recurrent chylothorax

Ziming Wan*

Department of Nephrology, The First Affiliated Hospital of Chongqing Medical University, Chongqing, China

Introduction: Symptomatic pleural effusion is occasionally caused by superior vena cava syndrome. Dyspnea and pleuritic chest pain are common symptoms of pleural effusion. However, the current literature has not reported a causal linkage between chylous pleural effusion and dry cough.

Case presentation: A patient with uremia suffered from an unexplained severe dry cough, which could be triggered by postural changes. Medical examinations ruled out the possibility of chronic bronchitis, gastroesophageal reflux, chest tumor, tuberculosis, asthma, chronic obstructive pulmonary disease, and allergy history. Examinations showed that the patient had chylous pleural effusion. The cough symptoms were relieved after extraction of the pleural effusion but soon reappeared with the recurrence of chylothorax. Enhanced computed tomography showed that the patient had superior vena cava occlusion. After recanalization of the superior vena cava by percutaneous balloon dilatation, the patient no longer had chylothorax, and the severe cough was eliminated.

Conclusion: Super vena cava syndrome can cause chylothorax and further stimulate severe dry cough. Cough is not a specific symptom. Chest imaging and pleural fluid analysis can help narrow down the diagnosis.

KEYWORDS

chylothorax, dry cough, enhanced computed tomography, superior vena cava syndrome, case report

Introduction

Pleural effusion refers to the fluid accumulated in the pleural cavity and is usually divided into transudate and exudate. Thoracentesis and pleural effusion analysis are often performed to determine the cause. Chylous pleural effusion, or chylothorax, is a non-inflammatory exudate rich in triglycerides (1). Chylothorax is usually caused by the destruction of the thoracic duct due to trauma, thoracic tumors, severe infection, and occasionally by superior vena cava syndrome. In cases of chylous collection of > 500 mL, shortness of breath, chest tightness, palpitation, and dyspnea may occur (2).

Patients with chronic coughs are very common in the respiratory department outpatient clinic, but they are often ignored by clinicians. Many patients are generally diagnosed with bronchitis or chronic bronchitis, which is ineffective after cough and expectorant treatment or a variety of antibiotics. The diagnosis of a chronic cough generally follows the sequence of simple examination before complex examination and common diseases before rare diseases. Chronic cough is not a specific symptom. The most frequent causes include eosinophilic bronchitis, postnasal drip syndrome, gastroesophageal reflux disease, cough variant asthma, and upper airway cough syndrome. Cough receptors are found not only in the throat, trachea, bronchus, and other parts of the respiratory system, but also in the esophagus, paranasal sinuses, external auditory canal, pleura, pericardium, and other parts (3). Therefore, diseases of the above systems or parts may produce cough symptoms. The key to chronic cough treatment lies in determining the etiology.

No previous studies have reported a causal and therapeutic linkage between large chylous pleural effusion and cough. This article reports a severe dry cough case caused by superior vena cave occlusion-induced recurrent chylothorax.

Case report

A 50-year-old man sought treatment in several hospitals because of a severe dry cough. The cough first appeared in December 2020 without obvious inducement, accompanied by a small amount of white foam sputum and sticky sputum. During 1 month, the patient's cough gradually worsened, with dyspnea after activities and paroxysmal dyspnea at night. Cough symptoms were associated with postural changes, such as standing up from sitting, bending over, or turning over during sleep, which could trigger severe coughs, and the patient even had transient amaurosis (self-reported syncope three times). The patient was hospitalized at Xinqiao Hospital of Army Military Medical University (Chongqing, China) on 11 January 2021, and discharged on 21 January 2021. Computed tomography (CT) of the chest showed bilateral pleural effusion (**Figure 1A**), which was later tested to be chylous fluid (**Table 1**). The cough was relieved after extracting the pleural fluid. However, the relief could only last for 1 day until the pleural effusion reappeared. The patient had to have pleural effusion extracted every other day to relieve his cough, and the amount of pleural effusion was very large (800–1,000 mL each time). It was suspected that the severe cough was related to recurrent pleural effusion. To determine the cause of such a serious pleural effusion, the patient received enhanced CT, which found an occlusion in the superior vena cava. Because the patient had a long history of dialysis because of uremia, he was recommended to go to the nephrology department to treat his superior vena cava occlusion.

The patient then visited the Department of Nephrology of our hospital. The patient was diagnosed with chronic kidney disease stage 5 in 2003 and received kidney transplantations in 2003 and 2017. The second transplantation failed. He had undergone dialysis for 8 years. In the first 6 months, a right internal jugular vein long-term catheter was used for dialysis, which was later changed to a left brachiocephalic arteriovenous fistula. Physical examination showed that the patient had erythema and edema on the face and neck, diffuse varicosities across the anterior chest, and distended jugular veins. Subsequent CT venography and digital subtraction angiography showed occlusion of the superior vena cava (**Figure 1B**) and extensive venous collateral vessels within the lower neck and superior mediastinum. The patient was admitted for hospitalization on 20 February 2021. To determine the cause of pleural effusion, 40 mL of pleural fluid was drawn from the right thoracic drainage tube and sent for pleural effusion analysis, exfoliated cell examination (thoracic tumor), and bacterial culture (tuberculosis infection).

The results of the pleural effusion analysis returned on 21st February, showing chyle positivity with elevated lymphocytes (**Table 1**). No abnormality was found in exfoliated cell examination. Ward rounds showed that the patient's temperature was normal, superficial lymph nodes were not palpable, the breath sounds were low and clear, and no rales were heard. Routine blood tests showed that leukocytes (7.77×10^9/L) and neutrophils (86.5%) were elevated. Because the inflammatory indicators increased in the pleural effusion and blood samples, the patient was given piperacillin-tazobactam (4.5 g q12 h) as treatment. At 1:00 p.m. that day, the patient experienced transient syncope. Sudden loss of consciousness occurred after coughing induced by positional changes from lying to sitting. The patient fell to the ground, without limb twitching, incontinence, or foaming at the mouth. The patient improved spontaneously after 5 s and did not complain of dizziness, headache, palpitations, chest tightness, or dyspnea. His blood pressure was 105/63 mmHg, and his heart rate was 88 times/min. No special treatment was carried out for this syncope.

On 22 February, several tests, including the detection of anti-tuberculosis antibody, sputum smear, sputum culture, and detection of acid-fast bacilli in sputum, were performed. The patient had been taking immunosuppressants since renal transplantation, which might increase the susceptibility to tuberculosis infection. Tuberculosis infection is a possible cause of chylothorax, so we decided to further search for evidence of tuberculosis infection. The bacterial culture of the pleural effusion showed positive results for *Staphylococcus lugdunensis*, so the antibiotic treatment was continued.

On 23 February, 1,000 mL of effusion was extracted from both lungs through thoracentesis. The pleural fluid analysis showed that the total cell counts decreased, suggesting that the antibiotic treatment was effective. Antibody tests for tuberculosis (gold labeled immunoassay) were weakly positive (+/-), but no *Mycobacterium tuberculosis* was detected in sputum specimens (sandwich cup method). According to the

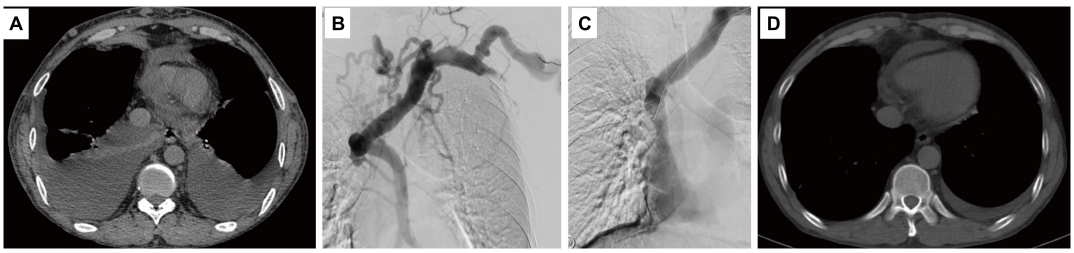

FIGURE 1
Computed tomography shows pleural effusion **(A)** and angiography shows superior vena cava occlusion **(B)**. Balloon dilatation was performed **(C)** and pleural effusion no longer appeared after 4 months **(D)**.

current examination results, the possibility of tuberculosis infection could be ruled out. Therefore, we speculated that superior vena cava occlusion was the most likely cause of recurrent chylothorax.

On 24th February, percutaneous balloon dilatation was performed to recanalize the superior vena cava (Figure 1C). The superior vena cava was clearly visualized and unobstructed. The collateral circulation mostly disappeared, and the stenosis was relieved.

The patient recovered well in the following days. Physical examination showed that the swelling of the face and neck obviously subsided. Three days after the operation (March 1), the patient received an ultrasound examination for the detection of pleural effusion. The results showed a flaky anechoic area in the bilateral chest, with a maximum depth of 46 mm in the right chest and 40 mm in the left chest. The location of the pleural fluid was not determined due to the small amount. On 3rd March, the patient received a chest CT again. Only a small amount of pleural effusion was found, and most of the lungs were dilated. The patient was discharged on the same day.

Follow-up was conducted after 4 months and 12 months. Chest CT showed no pleural effusion (Figure 1D). The patient reported that cough symptoms were eliminated. Based on the results, we can confirm that the obstruction of the superior vena cava caused the patient to develop recurrent chylothorax, and further stimulated severe postural change-related cough.

TABLE 1 Results of pleural effusion analysis.

	Jan 21, 2021	Feb 21, 2021	Feb 23, 2021
Color	Right: clear yellow Left: milky	Yellowish red and cloudy	Yellowish white and cloudy
Rivalta test	+	+	2+
Chyle test	+	+	+
Total cells (/L)	N/A	3.61×10^9	1.33×10^9
Nucleated cells (/L)	N/A	6.1×10^8	3.3×10^8
Lymphocytes	N/A	90%	96%
Total protein (g/L)	29.5	N/A	26
Albumin (g/L)	N/A	13	13
Lactic dehydrogenase (U/L)	129.5	89	88
Adenosine deaminase (U/L)	4	1.4	4.6

Discussion

In general, symptomatic pleural effusion mainly causes dyspnea or pleuritic chest pain. The rarity of the present case is that a severe chronic cough related to postural changes is the main symptom. In this case, the patient's complex complications increase the difficulty of diagnosis. The patient had received kidney transplantation twice because of uremia and had complications, including renal hypertension, renal hypoproteinemia, hyperlipidemia, and pericardial effusion. Chest imaging examination is helpful to narrow down the diagnosis. Fortunately for this case, thoracentesis, and pleural effusion analysis were performed immediately after the discovery of pleural effusion, which suggested that the cough symptoms were caused by chylothorax. We found another rare case report of chronic cough and recurrent pleural effusion (4). Similarly, in that case, the doctors performed chest radiography after excluding other common causes of cough and found pleural effusion. The pleural effusion was exudate. After consecutive examinations, the patient was diagnosed with constrictive pericarditis. These two cases illustrate that the diagnosis of unexplained cough can be very challenging.

Although it took several days to determine the cause of chylothorax, the exploration direction in the diagnosis process was clear. The three most likely causes were thoracic tumor, tuberculosis infection, and superior vena cava syndrome. Thoracic tumors were first excluded by enhanced CT and exfoliated cell examination of the pleural effusion. Infection also did not seem to be the cause because a large amount of pleural effusion is often related to a very serious infection. The current case only showed a slight increase in inflammatory indicators, and his body temperature remained normal. Combined with a bacterial culture of pleural effusion, tuberculosis antibody screening, and tuberculosis detection in sputum specimens,

the presence of tuberculosis was ruled out. Considering the patient's dialysis history, the obvious physical appearance of central vein occlusion, and the angiography evidence, superior vena cava syndrome was the most likely cause of chylothorax. Finally, the recanalization operation eliminated the symptoms of chylothorax and cough at the same time, which confirmed our diagnosis.

In summary, super vena cava syndrome can cause chylothorax and further stimulate severe dry cough. Chest imaging and pleural fluid analysis can help narrow down the diagnosis of cough.

Patient perspective

The ultimate cause of the patient's cough was superior vena cava obstruction, which is a common complication in dialysis patients. However, no nephrologist had established a correlation between dialysis and cough during the patient's routine dialysis. The reason is that pleural effusion caused by the superior vena cava is not common, and cough caused by pleural effusion is extremely rare. Patients with cough symptoms usually go to the respiratory department for diagnosis and treatment. In this case, the patient had visited several hospitals before finally being diagnosed in our hospital and had been unable to receive effective treatment. The patient's quality of life quality was seriously affected, and the patient showed obvious anxiety and disappointment. The patient was finally diagnosed and effectively treated in our hospital. On the second day after the operation, the patient reported that his cough and dyspnea after activities had improved significantly. During the follow-up, both large pleural effusion and cough no longer recur. The patient and his family were very satisfied and expressed thanks to the relevant medical staff.

Data availability statement

The original contributions presented in this study are included in the article/supplementary material, further inquiries can be directed to the corresponding author.

Ethics statement

Ethical review and approval was not required for the study on human participants in accordance with the local legislation and institutional requirements. The patients/participants provided their written informed consent to participate in this study. Written informed consent was obtained from the individual(s) for the publication of any potentially identifiable images or data included in this article.

Author contributions

ZW was the responsible physician in the treatment process of the patient and collected all the data, wrote the article, and approved it for publication.

Funding

This research was funded by the Joint Medical Research Project of Science, Technology, and Health in Chongqing Municipality (grant no. 2020FYYX063 to ZW).

Conflict of interest

The author declares that the research was conducted in the absence of any commercial or financial relationships that could be construed as a potential conflict of interest.

Publisher's note

All claims expressed in this article are solely those of the authors and do not necessarily represent those of their affiliated organizations, or those of the publisher, the editors and the reviewers. Any product that may be evaluated in this article, or claim that may be made by its manufacturer, is not guaranteed or endorsed by the publisher.

References

1. Agrawal V, Doelken P, Sahn SA. Pleural fluid analysis in chylous pleural effusion. *Chest.* (2008) 133:1436–41. doi: 10.1378/chest.07-2232

2. McGrath EE, Blades Z, Anderson PB. Chylothorax: aetiology, diagnosis and therapeutic options. *Respir Med.* (2010) 104:1–8. doi: 10.1016/j.rmed.2009.08.010

3. Weldon DR. Differential diagnosis of chronic cough. *Allergy Ashtma Proc.* (2005) 26:345–51.

4. Crandall MA, Mulvagh SL. 68-year-old woman with chronic cough and recurrent pleural effusions. *Mayo Clin Proc.* (2010) 85:479–82. doi: 10.4065/mcp.2009.0257

frontiers | Frontiers in Cardiovascular Medicine

TYPE Case Report
PUBLISHED 25 November 2022
DOI 10.3389/fcvm.2022.1036603

OPEN ACCESS

EDITED BY
Tianshu Liu,
Fudan University, China

REVIEWED BY
Teruhiko Imamura,
University of Toyama, Japan
Marco Giuseppe Del Buono,
Agostino Gemelli University Polyclinic (IRCCS), Italy

*CORRESPONDENCE
Xiaoping Hong
hong_xiaoping@hotmail.com

†These authors have contributed equally to this work

SPECIALTY SECTION
This article was submitted to General Cardiovascular Medicine, a section of the journal Frontiers in Cardiovascular Medicine

RECEIVED 05 September 2022
ACCEPTED 24 October 2022
PUBLISHED 25 November 2022

CITATION
Chen Y, Chen Y, Xie J, Liu D and Hong X (2022) Multisystem immune-related adverse events due to toripalimab: Two cases-based review.
Front. Cardiovasc. Med. 9:1036603.
doi: 10.3389/fcvm.2022.1036603

Multisystem immune-related adverse events due to toripalimab: Two cases-based review

Yanran Chen[1†], Yulan Chen[2,3†], Jingyi Xie[2,3], Dongzhou Liu[2,3] and Xiaoping Hong[1,2,3*]

[1]The Second Clinical Medical College, Jinan University, Shenzhen, China, [2]Department of Rheumatology and Immunology, Shenzhen People's Hospital, The Second Clinical Medical College, Jinan University, Shenzhen, China, [3]The First Affiliated Hospital, Southern University of Science and Technology, Shenzhen, China

Immune checkpoint inhibitors (ICIs) have significantly improved the survival of patients with advanced tumors. However, immune-related adverse events (irAEs) caused by ICIs, especially high-grade irAEs, are of growing concern. High-grade multisystem irAEs due to toripalimab, a programmed cell death-1 (PD-1) inhibitor, have been rarely reported. Two patients with malignant metastatic tumors were treated with anti-PD-1 immunotherapy. However, both patients developed high-grade multisystem irAEs based on myocarditis, with chest discomfort and malaise as the main clinical manifestation. Both patients had an elevation of cardiac enzymes, abnormal electrocardiography and left ventricular wall motion. Patient 2 was also diagnosed with organizing pneumonia. Immunotherapy was suspended. High-dose intravenous methylprednisolone was immediately initiated. The patients' symptoms were significantly relieved in a short period of time. Immunosuppressants were discontinued at the 6th month follow-up in patient 1 without relapse. However, patient 2 was lost to follow up due to financial reasons. To the best of our knowledge, this is the first report regarding ICI-associated myocarditis-pneumonia due to toripalimab, indicating the significance of early recognition and management of high-grade multisystem irAEs in clinical practice.

KEYWORDS

immune checkpoint inhibitors, PD-1, immune-related adverse events, myocarditis, pneumonia

Introduction

Immune checkpoint inhibitors (ICIs) have dramatically extended the survival of patients with advanced tumors. However, immune-related adverse events (irAEs) caused by ICIs, especially high-grade irAEs, pose a significant threat to patients' lives, with an incidence ranging from 54 to 76% (1). Excessive immune activation by ICIs can

occasionally induce multiple irAEs in different organs (2). The incidence of multisystem high-level irAEs may be underestimated due to the high rate of misdiagnosis that may result from its individualized clinical presentation.

Toripalimab, a human monoclonal antibody against programmed cell death-1 (PD-1), has been developed and received conditional approval as salvage treatment for unresectable or metastatic melanoma in China since 2018 (3). Yet high-grade multisystem irAEs caused by toripalimab have been rarely reported. Here we report two Chinese patients with advanced tumors who experienced a severe storm of multisystem irAEs after receiving toripalimab treatment, indicating the significance of early diagnosis and timely management of multisystem irAEs due to toripalimab.

Case presentation

Case 1

A 43 years-old Chinese female patient had a 6-year history of mixed liposarcoma of the right upper extremity with bilateral lower extremity metastases. The patient received 240 mg of toripalimab every 2 weeks from May 2019. After four cycles of toripalimab treatment, she presented to the emergency department at our institution with complaints of a 5-day generalized rash and malaise, as well as a sudden onset of severe chest pain with palpitation and dyspnea lasting for 2 h. She denied a history of diabetes mellitus, cardiovascular diseases, or thyroid diseases. Blood pressure on admission was 101/58 mmHg and the heart rate was irregular with a frequency of 131 beats/min. The respiratory rate was 36 breaths/min with normal oxygen saturation. Physical examination revealed generalized multiforme-like rash as well as muffled heart sounds and a grade II/VI holosystolic murmur typical of mitral regurgitation. Neurological examination revealed a grade IV muscle strength in her both lower limbs.

Laboratory tests showed that serum creatine phosphokinase (CPK) was 2,370 U/L (normal 25∼192 U/L), with increased levels of creatine kinase isoenzyme MB (CK-MB 53.6 ng/ml, normal 2∼4.99 ng/ml), cardiac troponin I (cTnI 7.49 ng/ml, normal 0∼0.02 ng/ml), cardiac troponin T (cTnT 5.43 ng/ml, normal 0∼0.014 ng/ml), myoglobin (214 ng/ml, normal 0∼46.6 ng/ml), lactate dehydrogenase (LDH 616 U/L, normal 110∼240 U/L), alanine aminotransferase (ALT 73 U/L, normal 0–40 U/L), aspartate aminotransferase (AST 212 U/L, normal 0–45 U/L), and N-terminal pro brain natriuretic peptide (NT-proBNP 4999 pg/ml, normal 0∼450 pg/ml). Further tests revealed decreased levels of free triiodothyronine (2.44 pmol/L, normal 3.28∼6.47 pmol/L) and free thyroxine (3.72 pmol/L, normal 7.64∼11.3 pmol/L), with elevated levels of thyrotropin (68.29 mIU/L, normal 0.38∼5.91 mIU/L), anti-thyroid peroxidase antibodies (94.99 mIU/ml, normal 0∼34 mIU/ml), and anti-thyroglobulin antibodies (572 IU/ml, normal 0∼115 IU/ml) (Table 1). There was no evidence of infection, and her autoimmune antibodies, including myositis-associated and myositis-specific antibodies, were also negative. Electrocardiogram showed paroxysmal ventricular tachycardia (104 beats/min). Emergency coronary angiography and left heart catheterization were unremarkable. Echocardiography revealed the myocardial motion of the anterior wall and the apical segment of the anterior septum of the left ventricle was diminished. The left atrium and left ventricle were enlarged (anterior-posterior left atrial diameter was 38 mm). In contrast, the right atrium and right ventricle were normal, with moderate mitral and tricuspid regurgitation and a small amount of pericardial effusion, with an ejection fraction (EF) of 55%. Electromyography demonstrated varying degrees of myogenic damage in the proximal muscles of the extremities, without abnormal changes in the distal muscles. Thyroid ultrasound

TABLE 1 Laboratory findings on admission.

Parameter	Case 1	Case 2	Reference range
Leukocytes (10^9/L)	5.83	7.56	04–10
Erythrocytes (10^{12}/L)	2.9	3.44	3.5–5
Hemoglobin (g/L)	90	102	110–150
Platelets (10^9/L)	98	401	100–300
CPK (U/L)	2,370	1,365	25–192
CK–MB (ng/ml)	53.6	21.32	2–4.99
cTnI (ng/ml)	7.49	0.24	0–0.02
cTnI (ng/ml)	5.43	1.872	0–0.014
ALT (U/L)	73	14.8	0–45
AST (U/L)	212	27.6	0–40
Albumin (g/L)	36.3	31.2	35–55
IgG (g/L)	8.01	7.16	8–18
ALP (U/L)	68	71	15–121
Creatinie (μmol/L)	103	56	44–133
Urea nitrogen (mmol/L)	3.65	6	2.5–7.5
CRP (mg/L)	3.8	4.37	<5
PCT (ng/ml)	<0.05	<0.05	<0.05
ANA (AU/ml)	<32	2152	<32
Anti-dsDNA	Negative	Negative	Negative
pANCA	Negative	Negative	Negative
cANCA	Negative	Negative	Negative
Anti-Ro60	Negative	Positive	Negative
Anti-Ro52	Negative	Positive	Negative
Anti-SS-B	Negative	Negative	Negative
Anti-U1-snRNP	Negative	Positive	Negative

CPK, creatine phosphokinase; CK-MB, creatine kinase-MB; cTnI, cardiac troponin I; cTnT, cardiac troponin T; ALT, alanine aminotransferase; AST, aspartate aminotransferase; IgG, immunoglobulin G; ALP, alkaline phosphatase; CRP, C-reactive protein; PCT, procalcitonin; ANA, anti-nuclear antibodies; Anti-dsDNA, anti-double-stranded (ds) DNA antibody; pANCA, perinuclear anti-neutrophil cytoplasmic antibody; cANCA, cytoplasmic anti-neutrophil cytoplasmic antibody; Anti-SS-B, anti-Sjögren's syndrome antigen B antibody; Anti-U1-snRNP, anti-U1-small nuclear ribonucleic particle antibody.

and chest computed tomography (CT) scan showed no abnormalities. Cardiac magnetic resonance (MR) and muscle biopsy was not allowed due to the rapid deterioration of chest pain. She was transferred to the intensive care unit.

The patient was finally diagnosed with multisystem irAEs resulting from anti-PD-1 therapy according to the results of the multidisciplinary discussion. The diagnoses of ICI-associated myocarditis (grade 4), myositis (grade 3), Hashimoto's thyroiditis (grade 2), and skin toxicity (grade 2) were made based on the National Cancer Institute Common Toxicity Criteria for Adverse Events (NCI-CTCAE). On day 3, intravenous methylprednisolone (200 mg/day) was initiated for 3 days, with oral levothyroxine replacement therapy (50 μg/day). Her chest pain and dyspnea were significantly relieved and the rash disappeared within 10 days. CPK, CK-MB, and troponin gradually decreased (**Figure 1**). On day 7, laboratory tests showed serum CPK to be 284 U/L, cTnI 0.279 ng/ml, cTnT 1.367 ng/ml, myoglobin 34 ng/ml, CK-MB 7.91 ng/ml, and NT-proBNP 1792 pg/ml. Echocardiography suggested an increase in EF to 60%.

Her methylprednisolone was gradually tapered. After 3 weeks, methylprednisolone was reduced to 48 mg/day, and she again developed chest pain and malaise. Laboratory tests showed a normal CPK level but an elevated CK-MB level to 28.7 ng/ml. Therefore, azathioprine (50 mg/day) was added, and her symptoms were gradually relieved within 2 weeks. Methylprednisolone was gradually tapered accordingly and was discontinued after 12 weeks, with azathioprine (100 mg/day) as maintenance therapy. At 6-month follow-up, laboratory tests revealed CPK to be 212 U/L, CK-MB 3.84 ng/ml, CTnI 0.08 ng/ml, and CTnT 0.016 ng/ml (**Figure 1**). At the time of writing this report, she was only taking oral levothyroxine (75 μg/day) replacement therapy and refused to receive any other anti-PD-1 therapies due to the potential risk for recurrence of severe multisystem irAEs, without evidence of tumor progression.

Case 2

A 64 years-old Chinese woman was diagnosed with advanced pancreatic adenocarcinoma with multiple metastases (liver, adrenal glands, and multiple lymph nodes) in January 2021. Due to her intolerance to chemotherapy, toripalimab (240 mg every 2 weeks) was initiated and clinical improvement was gradually achieved. Before the sixth treatment, she developed chest tightness and malaise that lasted for 2 days, without fever or cough. She took amlodipine for 7 years due to hypertension, and she denied prior history of lung diseases or autoimmune diseases. Physical examination on admission showed that the patient had an oxygen saturation of 87% (room air, at rest) and wet rales in the right lower lungs, with normal cardiac auscultation.

Laboratory tests showed that serum CPK was 1322 U/L, CK-MB 101.2 ng/ml, CTnI 0.72 ng/ml, CTnT 1.872 ng/ml, myoglobin 146.3 ng/ml, and NT-proBNP 3964.8 pg/ml. The white blood cell count was 9.18×10^9/L (normal $4\sim10 \times 10^9$/L), and calcitonin (<0.05 ng/ml, normal <0.05 ng/ml) and C-reactive protein (2.73 mg/L, normal <5 mg/L) levels were normal. Arterial blood gas analysis showed an oxygenation index of 281. Further examination revealed positive anti-nuclear antibodies (ANA, 2152 AU/ml, normal 0∼32 AU/ml) by chemiluminescent immunoassay and positive anti-U1-small nuclear ribonucleic particles (snRNP), anti-Ro60, and anti-Ro52 antibodies by line immunoassay (**Table 1**). Her electrocardiogram showed a complete right bundle branch conduction block. The echocardiogram showed reduced anterior interventricular wall segmental motion in the left ventricle with an EF of 49%. Chest CT of the chest showed consolidative opacities predominantly in the right basal parenchyma and a small amount of right pleural fluid. Lymphocyte subpopulation testing of the patient's bronchoalveolar lavage fluid showed that $CD3^+$ T cells accounted for 95.8% of lymphocytes, without evidence of infection. Lung biopsy showed alveolar wall edema suggestive of alveolitis, with a large amount of fibrinous exudate and lymphocytic infiltrate in the alveolar space, with no hyaline membrane formation (**Figure 2**). No malignant cells were seen in the patient's bronchoalveolar lavage fluid or lung tissue biopsy.

The patient was diagnosed with ICI-associated myocarditis (grade 3) and ICI-associated pneumonia (grade 3) based on NCI CTCAE. Intravenous methylprednisolone (200 mg/day) was started on the second day of admission, along with intravenous immunoglobulin (20 g/day) for 3 days. The patient's chest tightness improved and the oxygenation index increased to 323. On day 4 of admission, the patient was discharged without a repeated CT scan according to her wish.

Discussion

Immune checkpoint inhibitors such as those targeting PD-1, PD-1 ligand 1 (PD-L1), and cytotoxic T lymphocyte-associated antigen 4 (CTLA-4) have been the most significant breakthroughs in cancer immunotherapy in recent years. These ICIs enhance immune surveillance and reduce the immune escape of cancer cells by "releasing the brakes" on the T-cell activation pathway, which may affect multiple organs. The NCI-CTCAE classifies irAEs into five levels, from mild, moderate, severe, life-threatening, to fatal (4). The most common fatal irAEs include myocarditis, pneumonia, encephalitis, and fulminant hepatitis, with a mortality ranging from 0.3 to 1.3% (2). Toripalimab is a relatively new ICI developed in China and was generally well-tolerated in clinical trials in Chinese patients with advanced malignancies. The high-grade irAEs (grade 3

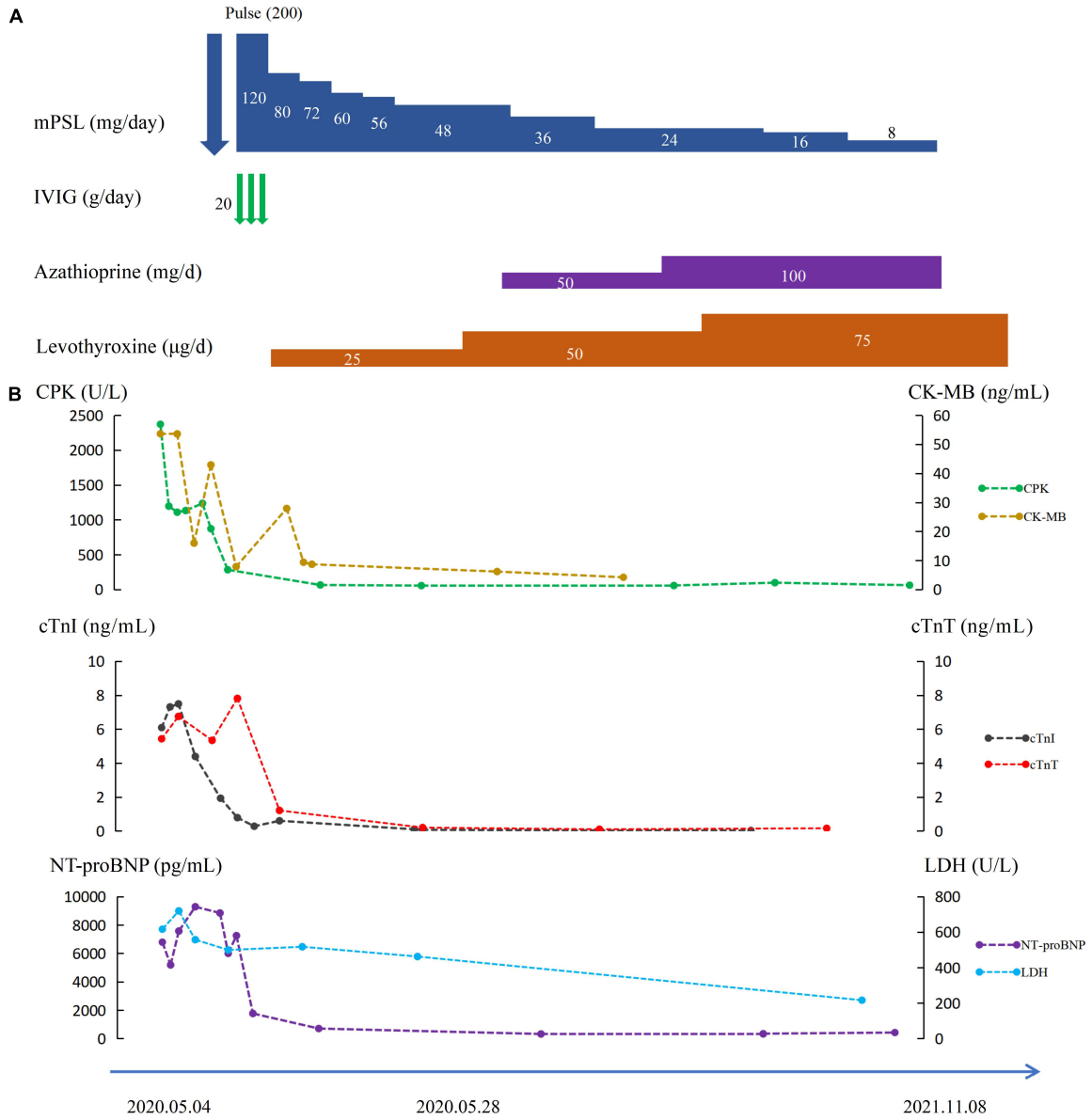

FIGURE 1
(A) Electrocardiogram of patient 1 on admission. **(B)** Clinical course of patient.

or higher) associated with toripalimab was most common in the hematologic and hepatic system (3). Multisystem irAEs and fatal irAEs, such as myocarditis and pneumonia, caused by toripalimab have been rarely reported. Here we report two Chinese patients with advanced tumors who suffered from fatal multisystem irAEs after receiving toripalimab treatment. To the best of our knowledge, this is the first study describing a patient who concurrently experienced ICI-associated myocarditis and pneumonia, which indicates the significance of early recognition and management of multisystem irAEs due to toripalimab.

Cardiac immune-related events include the development of myocarditis, pericarditis, pericardial effusion, arrhythmias, myocardial infarction, and heart failure. The mechanisms by which ICIs cause myocarditis are unclear. Most of the existing studies have been attributed to the presence of shared antigens between the tumor and myocardium (5). Several studies have confirmed that PD-1 is found in the myocardium of patients with ICI-associated myocarditis with expansion of T cell clones. T cell receptors bind to homologous muscle antigens and tumor antigens, causing damage similar to viral myocarditis (5, 6). Even though ICI-associated myocarditis only seems to account for about 2.4% of all irAEs (5, 7), its mortality rate may reach 50% (8). The first 3 months of receiving ICIs are considered as a high-risk period for developing immune

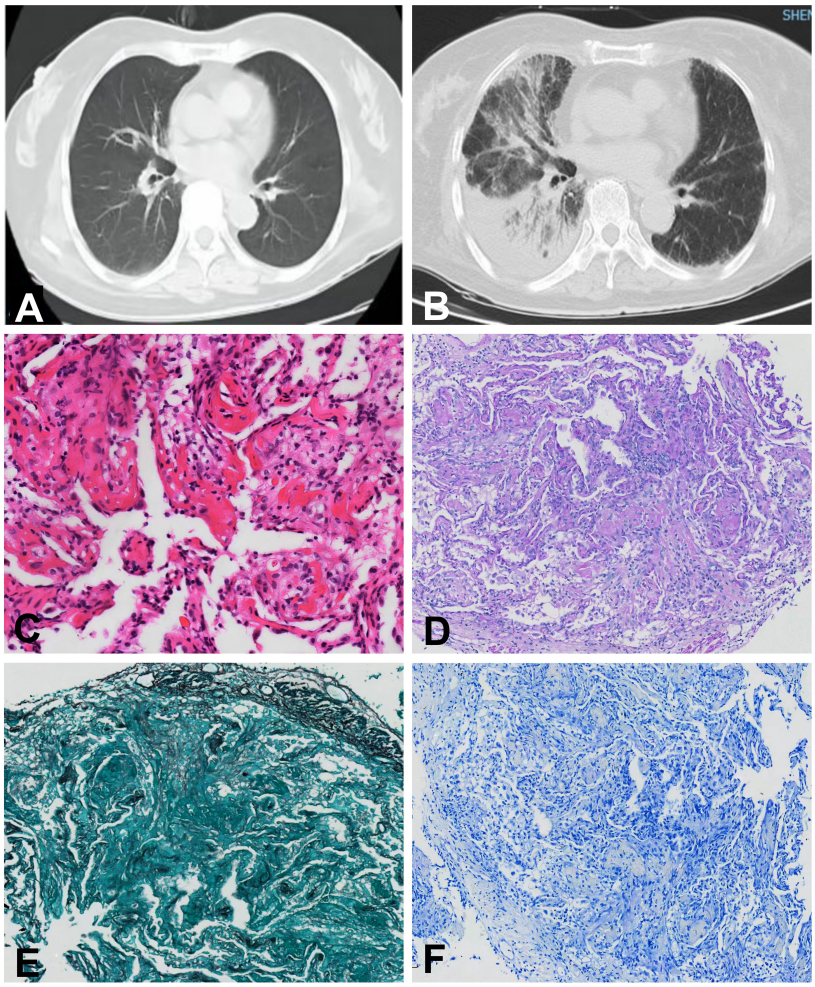

FIGURE 2
Chest computed tomography and histopathological changes of the lung biopsy in case 2. Chest computed tomography before **(A)** and after **(B)** onset of pneumonia. **(C)** Hematoxylin-eosin staining (×20). **(D)** Periodic acid-Schiff staining (×10). **(E)** Hexosamine silver staining (×10). **(F)** Antacid staining (×10).

myocarditis (7–9). Mahmood et al. (7) showed that the median time from the first exposure to ICIs to the onset of myocarditis was 34 days. Remarkably, cases of immune myocarditis that received combination immunotherapy occurred even after the first receipt (10). PD-1/PD-L1 inhibitors are more likely to cause myocarditis and pericardial disease than CTLA-4 inhibitors (11). Accordingly, both patients in this study developed myocarditis within the first 3 months of receiving toripalimab, suggesting an extra attention should be paid during the high-risk period after toripalimab treatment. Therefore, informing patients receiving ICIs for the first time is recommended to pay special attention to symptoms such as chest pain and palpitations and to seek prompt medical attention. For patients with a history of ICIs and symptoms such as chest tightness, chest pain, and weakness, clinicians should consider ICIs-cardiomyopathy and perform electrocardiography, cardiac enzymology, and echocardiography.

The initial symptoms of ICI-associated myocarditis are heterogeneous and may include vague manifestations such as discomfort, fatigue, and weakness associated with the primary diseases, which are difficult to distinguish and can be easily overlooked. Almost all patients with myocarditis had elevated troponin and CPK levels, and 89% of cases showed electrocardiographic arrhythmias, including atrial fibrillation, premature ventricular beats, conduction block, and ventricular tachycardia. Cardiac ultrasound was suggested as a baseline assessment tool because about three-fourth of the patients showed abnormal left ventricular EF values after the onset of the disease (12). Enhancement of cardiac MR is an important modality in the available non-invasive diagnosis of myocarditis and 48% of patients with myocarditis may demonstrate late gadolinium enhancement (13). Endomyocardial biopsy is the gold standard for the diagnosis of myocarditis, which is characterized by myocardial infiltrates,

including CD4 and CD8-positive T lymphocytes as well as macrophages (14). However, myocardial biopsy has its technical limitations, especially in cases of patchy or focal myocardial infarction-associated myocarditis (15). Furthermore, coronary angiography can help make a differential diagnosis in some cases with myocarditis that mimic coronary artery diseases, as demonstrated in patient 1 in this study. Most patients with clinically advanced tumors refuse to undergo this invasive procedure after a difficult tumor identification and treatment. Enhanced MR is considered an important non-invasive tool for diagnosing myocarditis, but patients prefer to spend their limited treatment costs on anti-tumor drugs due to their high price. In addition, although cardiac MR and endomyocardial biopsy was not performed in these two patients, myocardial abnormalities, such as significantly elevated levels of myocardial enzymes, ventricular dysfunction and arrhythmias, strongly supported the diagnosis of myocarditis.

Shao et al. reported an overall incidence of 4.5% for ICI-associated pneumonia (16). The incidence of severe pneumonia (grade 3 or higher) was reported to be 0.8–1.5% (17). Studies have shown that lung cancer patients treated with PD-1 or PD-L1 inhibitors were more likely to develop pneumonia compared to CTLA-4 inhibitors (2.7 vs. 1%) (17–19). ICI-associated pneumonia mainly includes organizing pneumonia (OP), non-specific interstitial pneumonia, hypersensitivity pneumonia, diffuse alveolar injury, acute interstitial pneumonia, and acute respiratory distress syndrome (20–22). OP was the predominant type of ICI-associated pneumonia, accounting for 77.8% of cases (22). Bronchoalveolar lavage and transbronchial lung biopsy were recommended in patients with ICI-associated pneumonia (14, 23). Based on Naidoo et al. criteria for ICI-associated pneumonia (24), the diagnosis of OP (grade 3) can be made in case 2. In addition, the incidence of thyroid dysfunction due to anti-PD-1 antibody treatment (5–10%) is higher than that after CTLA-4 inhibitors (0–5%) (25–27). Thyroiditis caused by ICIs usually causes transient hyperthyroidism, which often progresses to hypothyroidism. Notably, in this study, the diagnoses of myocarditis, myositis, Hashimoto's thyroiditis, and skin toxicity were concurrently made in patient 1, and ICI-associated myocarditis and pneumonia was made in patient 2, which indicates multisystem irAEs in both of these two patients.

In a clinical study including 623 patients, 5.8% of patients experienced multisystem irAEs due to ICIs, with

TABLE 2 Case reports regarding multisystem immune-related adverse events (irAEs) based on myocarditis induced by programmed cell death-1 (PD-1) inhibitors.

Case	Gender/ Age	Tumor	PD-1 inhibitor	Time[#]	Symptom	irAE	Treatment	Outcome
1 (36)	M/78	Melanoma	Pembrolizumab	5	Limb weakness	Myocarditis, myositis	PSL, PLEX	Dead due to respiratory failure
2 (37)	M/80	Melanoma	Nivolumab	2	Anorexia	IM3OS	PSL, IVIG, IA, PLEX	CPK levels normalized within 4 months
3 (38)	M/63	Melanoma	Nivolumab	2	Muscle pain	Myocarditis, myositis	PSL	Dead due to heart failure
4 (39)	F/55	Melanoma	Nivolumab	4	Ophthalmoplegia	IM3OS	PSL, IVIG, IA, PLEX	Weaned off ventilatory support at the 6 months
5 (40)	F/47	Melanoma	Toripalimab	4	Diplopia	IM3OS	PSL, IVIG, ventilator, PM	CPK levels normalized within 2 months
6 (41)	M/75	LUAD	Pembrolizumab	3	Asthenia	IM3OS, hepatitis, pneumonia	PSL, IVIG, IA, PLEX, IFX, ventilator	Dead due to respiratory failure
7 (42)	F/53	Thymoma	Pembrolizumab	4	Cough	Myocarditis, MG, liver and kidney dysfunction	PSL, IVIG, euthyrox, pyridostigmine	CPK levels normalized within 6 months
8 (43)	M/66	Thymoma, LUAD	Sintilimab	3	Fatigue, myalgia	Myocarditis, MG	PSL, IVIG, PLEX, euthyrox, pyridostigmine	CPK levels normalized within 3 months
9 (44)	F/48	Thymoma	Pembrolizumab	2	Shortness of breath	Myocarditis, MG	PSL, IVIG, IFX, PM, ventilator, ECMO	Dead due to heart failure
10 (45)	F/45	Thymoma	Pembrolizumab	2	Quadriparesis	Myocarditis, MG, liver dysfunction	PSL, IVIG, IA, ventilator, PM, ECMO	Dead due to hypoxic brain damage

[#]Time between initiation of PD-1 inhibitors and irAE (weeks). PSL, prednisolone; PLEX, plasma exchange; IM3OS, myocarditis with myositis and myasthenia gravis overlap syndrome; IVIG, intravenous immunoglobulin; IA, immunoadsorption; PM, pacemaker; LUAD, lung adenocarcinoma; IFX, infliximab; ECMO, extracorporeal membrane oxygenation; MG, myasthenia gravis.

the combination of hepatitis-thyroiditis (10%) and dermatitis-pneumonia (10%) being the most common (28). ICI-associated myocarditis was most commonly accompanied by myositis (29%) and hepatitis (21%), followed by thyroiditis (12%) (9). It has been shown that myositis was the second frequent rheumatic and musculoskeletal irAEs (accounting for 36.1%), in which the mortality was 24% for myositis and 56.7% for concurrent myocarditis (29). The mechanism of myocarditis-myositis is unclear. Still, the theory of shared antigens between myocardium, skeletal muscle, and tumors has also been highlighted in the previous studies (6, 29). Importantly, myocarditis with myositis and/or myasthenia gravis overlap syndrome was reported to have a 60% mortality rate and is a hot issue in ICI-associated cardiomyopathy involving multisystem irAEs (30, 31). Therefore, it is reasonable to speculate that patients with multisystem irAEs based on myocarditis could have a higher mortality. Early recognition and diagnosis of multisystem irAEs are pivotal in the management of patients undergoing ICI treatment. Multisystem irAEs based on myocarditis reported previously are summarized in **Table 2**. Furthermore, to our knowledge, case 2 is the first report of myocarditis-pneumonia caused by toripalimab.

Low-grade irAEs respond rapidly to steroid therapy and generally do not result in hospitalization or termination of treatment with ICIs. Permanent discontinuation of ICIs is recommended for patients with severe myositis or myocarditis and myositis-carditis overlap (32). Patients with ICI-associated myocarditis required immediate initiation of intravenous corticosteroid therapy and consideration of escalation to immunoglobulin, cyclophosphamide, rituximab, azathioprine, or methotrexate if patients do not respond well to corticosteroid alone (4, 14). Infliximab is the recommended second-line agent for ICI-associated myocarditis. Both abciximab and tacrolimus have been reported (1, 33), and tofacitinib has recently been reported to have significant efficacy in immune-associated myocarditis (34). Notwithstanding, even based on the above treatment, the mortality rate of myocarditis still reaches 50% (35). Hence, an early recognition and intervention of myocarditis is beneficial to improve the prognosis. Notably, both patients in this study had a positive response to glucocorticoids. Patient 1 experienced a recurrence of symptoms during glucocorticoid tapering, and a positive effect was obtained with the addition of azathioprine. In case 2, the patient also showed improvement after methylprednisolone and immunoglobulin therapy.

Conclusion

In conclusion, we described two Chinese patients with advanced tumors suffering from severe multisystem irAEs based on after receiving toripalimab treatment. Improved awareness and an early identification of multisystem irAEs are of great importance in management of patients undergoing treatment of ICIs.

Data availability statement

The original contributions presented in this study are included in the article/supplementary material, further inquiries can be directed to the corresponding author.

Ethics statement

Written informed consent was obtained from the individual(s) for the publication of any potentially identifiable images or data included in this article.

Author contributions

XH initiated and reviewed the manuscript. YRC and YLC were involved in the data collection and writing of the manuscript. JX provided the clinical details. DL was responsible for steering the direction of the manuscript. All authors read and approved the final manuscript for submission.

Funding

This work was supported by Shenzhen Key Medical Discipline Construction Fund (No. SZXK011).

Acknowledgments

We greatly appreciate the patients and their family for their kind cooperation.

Conflict of interest

The authors declare that the research was conducted in the absence of any commercial or financial relationships that could be construed as a potential conflict of interest.

Publisher's note

References

1. Martins F, Sykiotis GP, Maillard M, Fraga M, Ribi C, Kuntzer T, et al. New therapeutic perspectives to manage refractory immune checkpoint-related toxicities. *Lancet Oncol.* (2019) 20:e54–64. doi: 10.1016/S1470-2045(18)30828-3

2. Wang DY, Salem JE, Cohen JV, Chandra S, Menzer C, Ye F, et al. Fatal toxic effects associated with immune checkpoint inhibitors: a systematic review and meta-analysis. *JAMA Oncol.* (2018) 4:1721–8. doi: 10.1001/jamaoncol.2018.3923

3. Keam SJ. Toripalimab: first global approval. *Drugs.* (2019) 79:573–8. doi: 10.1007/s40265-019-01076-2

4. Thompson JA, Schneider BJ, Brahmer J, Andrews S, Armand P, Bhatia S, et al. NCCN guidelines insights: management of immunotherapy-related toxicities, version 1.2020. *J Natl Compr Canc Netw.* (2020) 18:230–41. doi: 10.6004/jnccn.2020.0012

5. Johnson DB, Balko JM, Compton ML, Chalkias S, Gorham J, Xu Y, et al. Fulminant myocarditis with combination immune checkpoint blockade. *N Engl J Med.* (2016) 375:1749–55. doi: 10.1056/NEJMoa1609214

6. Palaskas N, Lopez-Mattei J, Durand JB, Iliescu C, Deswal A. Immune checkpoint inhibitor myocarditis: pathophysiological characteristics, diagnosis, and treatment. *J Am Heart Assoc.* (2020) 9:e013757. doi: 10.1161/JAHA.119.013757

7. Mahmood SS, Fradley MG, Cohen JV, Nohria A, Reynolds KL, Heinzerling LM, et al. Myocarditis in patients treated with immune checkpoint inhibitors. *J Am Coll Cardiol.* (2018) 71:1755–64. doi: 10.1016/j.jacc.2018.02.037

8. Moslehi JJ, Salem JE, Sosman JA, Lebrun-Vignes B, Johnson DB. Increased reporting of fatal immune checkpoint inhibitor-associated myocarditis. *Lancet.* (2018) 391:933. doi: 10.1016/S0140-6736(18)30533-6

9. Atallah-Yunes SA, Kadado AJ, Kaufman GP, Hernandez-Montfort J. Immune checkpoint inhibitor therapy and myocarditis: a systematic review of reported cases. *J Cancer Res Clin Oncol.* (2019) 145:1527–57. doi: 10.1007/s00432-019-02927-x

10. Guo CW, Alexander M, Dib Y, Lau PKH, Weppler AM, Au-Yeung G, et al. A closer look at immune-mediated myocarditis in the era of combined checkpoint blockade and targeted therapies. *Eur J Cancer.* (2020) 124:15–24. doi: 10.1016/j.ejca.2019.09.009

11. Esposito R, Fedele T, Orefice S, Cuomo V, Prastaro M, Canonico ME, et al. An emergent form of cardiotoxicity: acute myocarditis induced by immune checkpoint inhibitors. *Biomolecules.* (2021) 11:785. doi: 10.3390/biom11060785

12. Escudier M, Cautela J, Malissen N, Ancedy Y, Orabona M, Pinto J, et al. Clinical features, management, and outcomes of immune checkpoint inhibitor-related cardiotoxicity. *Circulation.* (2017) 136:2085–7. doi: 10.1161/CIRCULATIONAHA.117.030571

13. Zhang L, Awadalla M, Mahmood SS, Nohria A, Hassan MZO, Thuny F, et al. Cardiovascular magnetic resonance in immune checkpoint inhibitor-associated myocarditis. *Eur Heart J.* (2020) 41:1733–43. doi: 10.1093/eurheartj/ehaa051

14. Brahmer JR, Lacchetti C, Schneider BJ, Atkins MB, Brassil KJ, Caterino JM, et al. Management of immune-related adverse events in patients treated with immune checkpoint inhibitor therapy: American society of clinical oncology clinical practice guideline. *J Clin Oncol.* (2018) 36:1714–68. doi: 10.1200/JCO.2017.77.6385

15. Friedman CF, Proverbs-Singh TA, Postow MA. Treatment of the immune-related adverse effects of immune checkpoint inhibitors: a review. *JAMA Oncol.* (2016) 2:1346–53. doi: 10.1001/jamaoncol.2016.1051

16. Shao J, Wang C, Ren P, Jiang Y, Tian P, Li W. Treatment- and immune-related adverse events of immune checkpoint inhibitors in advanced lung cancer. *Biosci Rep.* (2020) 40:BSR20192347. doi: 10.1042/BSR20192347

17. Nishino M, Giobbie-Hurder A, Hatabu H, Ramaiya NH, Hodi FS. Incidence of programmed cell death 1 inhibitor-related pneumonitis in patients with advanced cancer: a systematic review and meta-analysis. *JAMA Oncol.* (2016) 2:1607–16. doi: 10.1001/jamaoncol.2016.2453

18. Wolchok JD, Neyns B, Linette G, Negrier S, Lutzky J, Thomas L, et al. Ipilimumab monotherapy in patients with pretreated advanced melanoma: a randomised, double-blind, multicentre, phase 2, dose-ranging study. *Lancet Oncol.* (2010) 11:155–64. doi: 10.1016/S1470-2045(09)70334-1

19. Suresh K, Voong KR, Shankar B, Forde PM, Ettinger DS, Marrone KA, et al. Pneumonitis in non-small cell lung cancer patients receiving immune checkpoint immunotherapy: incidence and risk factors. *J Thorac Oncol.* (2018) 13:1930–9. doi: 10.1016/j.jtho.2018.08.2035

20. Nishino M, Ramaiya NH, Awad MM, Sholl LM, Maattala JA, Taibi M, et al. PD-1 inhibitor-related pneumonitis in advanced cancer patients: radiographic patterns and clinical course. *Clin Cancer Res.* (2016) 22:6051–60. doi: 10.1158/1078-0432.CCR-16-1320

21. Naidoo J, Wang X, Woo KM, Iyriboz T, Halpenny D, Cunningham J, et al. Pneumonitis in patients treated with anti-programmed death-1/programmed death ligand 1 therapy. *J Clin Oncol.* (2017) 35:709–17. doi: 10.1200/JCO.2016.68.2005

22. Larsen BT, Chae JM, Dixit AS, Hartman TE, Peikert T, Roden AC. Clinical and histopathologic features of immune checkpoint inhibitor-related pneumonitis. *Am J Surg Pathol.* (2019) 43:1331–40. doi: 10.1097/PAS.0000000000001298

23. Puzanov I, Diab A, Abdallah K, Bingham CO III, Brogdon C, Dadu R, et al. Managing toxicities associated with immune checkpoint inhibitors: consensus recommendations from the society for immunotherapy of cancer (SITC) toxicity management working group. *J Immunother Cancer.* (2017) 5:95. doi: 10.1186/s40425-017-0300-z

24. Naidoo J, Page DB, Li BT, Connell LC, Schindler K, Lacouture ME, et al. Toxicities of the anti-PD-1 and anti-PD-L1 immune checkpoint antibodies. *Ann Oncol.* (2015) 26:2375–91. doi: 10.1093/annonc/mdv383

25. Gonzalez-Rodriguez E, Rodriguez-Abreu D. Spanish group for cancer I-B. immune checkpoint inhibitors: review and management of endocrine adverse events. *Oncologist.* (2016) 21:804–16. doi: 10.1634/theoncologist.2015-0509

26. Barroso-Sousa R, Barry WT, Garrido-Castro AC, Hodi FS, Min L, Krop IE, et al. Incidence of endocrine dysfunction following the use of different immune checkpoint inhibitor regimens: a systematic review and meta-analysis. *JAMA Oncol.* (2018) 4:173–82. doi: 10.1001/jamaoncol.2017.3064

27. Hasegawa S, Ikesue H, Nakao S, Shimada K, Mukai R, Tanaka M, et al. Analysis of immune-related adverse events caused by immune checkpoint inhibitors using the Japanese adverse drug event report database. *Pharmacoepidemiol Drug Saf.* (2020) 29:1279–94. doi: 10.1002/pds.5108

28. Shankar B, Zhang J, Naqash AR, Forde PM, Feliciano JL, Marrone KA, et al. Multisystem immune-related adverse events associated with immune checkpoint inhibitors for treatment of non-small cell lung cancer. *JAMA Oncol.* (2020) 6:1952–6. doi: 10.1001/jamaoncol.2020.5012

29. Allenbach Y, Anquetil C, Manouchehri A, Benveniste O, Lambotte O, Lebrun-Vignes B, et al. Immune checkpoint inhibitor-induced myositis, the earliest and most lethal complication among rheumatic and musculoskeletal toxicities. *Autoimmun Rev.* (2020) 19:102586. doi: 10.1016/j.autrev.2020.102586

30. Steven NM, Fisher BA. Management of rheumatic complications of immune checkpoint inhibitor therapy - an oncological perspective. *Rheumatology.* (2019) 58:vii29–39. doi: 10.1093/rheumatology/kez536

31. Pathak R, Katel A, Massarelli E, Villaflor VM, Sun V, Salgia R. Immune checkpoint inhibitor-induced myocarditis with myositis/myasthenia gravis overlap syndrome: a systematic review of cases. *Oncologist.* (2021) 26:1052–61. doi: 10.1002/onco.13931

32. Kostine M, Finckh A, Bingham CO, Visser K, Leipe J, Schulze-Koops H, et al. EULAR points to consider for the diagnosis and management of rheumatic immune-related adverse events due to cancer immunotherapy with checkpoint inhibitors. *Ann Rheum Dis.* (2021) 80:36–48. doi: 10.1136/annrheumdis-2020-217139

33. Ma R, Wang Q, Meng D, Li K, Zhang Y. Immune checkpoint inhibitors-related myocarditis in patients with cancer: an analysis of international spontaneous reporting systems. *BMC Cancer.* (2021) 21:38. doi: 10.1186/s12885-020-07741-0

34. Liu Y, Jiang L. Tofacitinib for treatment in immune-mediated myocarditis: the first reported cases. *J Oncol Pharm Pract.* (2020). [Epub ahead of print]. doi: 10.1177/1078155220947141

35. Heinzerling L, Ott PA, Hodi FS, Husain AN, Tajmir-Riahi A, Tawbi H, et al. Cardiotoxicity associated with CTLA4 and PD1 blocking immunotherapy. *J Immunother Cancer.* (2016) 4:50. doi: 10.1186/s40425-016-0152-y

36. Haddox CL, Shenoy N, Shah KK, Kao JC, Jain S, Halfdanarson TR, et al. Pembrolizumab induced bulbar myopathy and respiratory failure with necrotizing myositis of the diaphragm. *Ann Oncol.* (2017) 28:673–5. doi: 10.1093/annonc/mdw655

37. Kimura T, Fukushima S, Miyashita A, Aoi J, Jinnin M, Kosaka T, et al. Myasthenic crisis and polymyositis induced by one dose of nivolumab. *Cancer Sci.* (2016) 107:1055–8. doi: 10.1111/cas.12961

38. Behling J, Kaes J, Münzel T, Grabbe S, Loquai C. New-onset third-degree atrioventricular block because of autoimmune-induced myositis under treatment with anti-programmed cell death-1 (nivolumab) for metastatic melanoma. *Melanoma Res.* (2017) 27:155–8. doi: 10.1097/CMR.0000000000000314

39. So H, Ikeguchi R, Kobayashi M, Suzuki M, Shimizu Y, Kitagawa K. PD-1 inhibitor-associated severe myasthenia gravis with necrotizing myopathy and myocarditis. *J Neurol Sci.* (2019) 399:97–100. doi: 10.1016/j.jns.2019.02.023

40. Luo YB, Tang W, Zeng Q, Duan W, Li S, Yang X, et al. Case report: the neuromusclar triad of immune checkpoint inhibitors: a case report of myositis, myocarditis, and myasthenia gravis overlap following toripalimab treatment. *Front Cardiovasc Med.* (2021) 8:714460. doi: 10.3389/fcvm.2021.714460

41. Fuentes-Antrás J, Peinado P, Guevara-Hoyer K, Díaz Del Arco C, Sánchez-Ramón S, Aguado C. Fatal autoimmune storm after a single cycle of anti-PD-1 therapy: a case of lethal toxicity but pathological complete response in metastatic lung adenocarcinoma. *Hematol Oncol Stem Cell Ther.* (2020). doi: 10.1016/j.hemonc.2020.04.006

42. Shen L, Chen H, Wei Q. Immune-therapy-related toxicity events and dramatic remission after a single dose of pembrolizumab treatment in metastatic thymoma: a case report. *Front Immunol.* (2021) 12:621858. doi: 10.3389/fimmu.2021.621858

43. Xing Q, Zhang ZW, Lin QH, Shen LH, Wang PM, Zhang S, et al. Myositis-myasthenia gravis overlap syndrome complicated with myasthenia crisis and myocarditis associated with anti-programmed cell death-1 (sintilimab) therapy for lung adenocarcinoma. *Ann Transl Med.* (2020) 8:250. doi: 10.21037/atm.2020.01.79

44. Portolés Hernández A, Blanco Clemente M, Escribano García D, Velasco Calvo R, Núñez García B, Oteo Domínguez JF, et al. Checkpoint inhibitor-induced fulminant myocarditis, complete atrioventricular block and myasthenia gravis-a case report. *Cardiovasc Diagn Ther.* (2021) 11:1013–9. doi: 10.21037/cdt-21-147

45. Hyun JW, Kim GS, Kim SH, Cho JY, Kim HJ, Lee GK, et al. Fatal simultaneous multi-organ failure following pembrolizumab treatment for refractory thymoma. *Clin Lung Cancer.* (2020) 21:e74–7. doi: 10.1016/j.cllc.2019.10.008

frontiers | Frontiers in Cardiovascular Medicine

TYPE Case Report
PUBLISHED 01 December 2022
DOI 10.3389/fcvm.2022.1043427

OPEN ACCESS

EDITED BY
Junjie Xiao,
Shanghai University, China

REVIEWED BY
Bernhard Maisch,
University of Marburg, Germany
Blanca Domenech-Ximenos,
Hospital Clinic of Barcelona, Spain

*CORRESPONDENCE
Xiangxiang Jing
ljjxx2000@126.com

SPECIALTY SECTION
This article was submitted to General Cardiovascular Medicine, a section of the journal Frontiers in Cardiovascular Medicine

RECEIVED 13 September 2022
ACCEPTED 15 November 2022
PUBLISHED 01 December 2022

CITATION
Chen Q, Yang D, Liu L and Jing X (2022) Right atrial cardiac lipoma with distinctive imaging characteristics. A rare case report and literature review.
Front. Cardiovasc. Med. 9:1043427. doi: 10.3389/fcvm.2022.1043427

Right atrial cardiac lipoma with distinctive imaging characteristics. A rare case report and literature review

Qiqing Chen, Dayan Yang, Lili Liu and Xiangxiang Jing*

Department of Ultrasonography, Hainan General Hospital (Hainan Affiliated Hospital of Hainan Medical University), Haikou, China

Cardiac lipomas are rare primary cardiac tumors that are often only detected incidentally during other examinations. Lipomas of the right atrium are particularly rare. In this report, we describe the case of a patient presenting with a mixed cystic-solid lipoma in the right atrium. The symptoms, imaging findings, and treatment strategies associated with this case are discussed herein. This 65-year-old female patient reported to our hospital due to exertional chest tightness, shortness of breath, and occasional chest pain for over 1 year. She subsequently underwent transthoracic echocardiography and contrast-enhanced ultrasonography, both of which revealed a cystic-solid mass in the right atrium. The transthoracic computed tomography scan showed a dense patchy shadow in the right atrium. The mass was completely excised from the atrial septum, and subsequent histopathological examination confirmed its identity as a lipoma. Surgical resection remains the primary treatment approach for cardiac lipomas, and multimodal imaging is of key importance for the diagnosis and follow-up monitoring of affected patients.

KEYWORDS

contrast-enhanced ultrasonography, transthoracic echocardiography, diagnosis, cardiac lipomas, multimodal imaging

Introduction

Cardiac lipomas are rare primary cardiac tumors, the majority of which are asymptomatic (1). Clinical manifestations in affected patients generally vary as a function of tumor size and location, with some patients experiencing symptoms attributable to the compression of heart chambers by a large tumor volume or the involvement of the myocardium or heart valves that ultimately lead to their presentation for symptom. Transthoracic echocardiography remains the significant imaging approach when diagnosing cardiac tumors. Cardiac lipomas are rare, and

largely present as solid, sessile masses with a soft texture and deformable shape that varies with the cardiac cycle upon imaging examination. Here, we describe a rare case report of a cystic-solid lipoma of the right atrium that was pathologically diagnosed as a lipoma following surgical excision. In addition to evaluating two-dimensional transthoracic echocardiography (2D-TTE), contrast-enhanced ultrasound (CEUS) and transthoracic computed tomography (CT), we additional discuss our experiences and associated surgical and pathological findings.

Case report

Medical history and physical examination

A 65-year-old female presented to the hospital with chest tightness and dyspnea that had been present for more than 1 year and were aggravated by exercise, co-occurring with dull, non-radiating chest pain that was relieved following rest for about 20 min. Transthoracic echocardiography conducted in another hospital revealed a space-occupying lesion, leading to her presentation to our hospital for additional treatment. On physical examination, the patient exhibited a heart rate of 76 bpm and a blood pressure of 128/85 mmHg. She had no history of diabetes, hypertension, or coronary heart disease. Specialist examination did not reveal any abnormal uplift in the precordial area nor any abnormalities in the valve areas, although slightly enlarged cardiac dullness was detected. No obvious murmur was heard in each valve area. Electrocardiography results revealed sinus rhythm with low voltage of the limb leads. Routine hematological, biochemical, and thyroid function test results were normal.

Echocardiography examination

Two-dimensional transthoracic echocardiography (2D-TTE, Philips EPIQ CVx-Philips Medical Systems, Andover, MA, USA) revealed mild dilatation of the right atrium, with a predominantly cystic-solid mixed echogenic lesion that was present the right atrium with a rounded shape and a pedicle attached to the right atrium (**Figures 1A, B**). The atrial septum measured approximately 40 mm × 44 mm proximal to the fossa ovalis on the side of the right atrium, and significant echoic enhancement was observed for the solid portion of this mass (about 30 mm × 15 mm in size). No apparent obstruction or hemodynamic abnormalities were observed in the Valvular orifice (**Figure 1C**). No obvious abnormalities were apparent upon sonogram-based examination of the inferior vena cava (**Figure 1D**). Echocardiography confirmed the presence of a right atrial cystic solid mixed echogenic space-occupying lesion of uncertain etiology that was primarily cystic, with significantly enhanced echoic signal in the solid regions.

Contrast-enhanced ultrasonography

The patient next underwent contrast-enhanced ultrasonography (Philips EPIQ CVx-Philips Medical Systems, Andover, MA, USA). After initiating the intracardiac contrast mode, the depth, gain, and instrument frame rate were adjusted such that the target lesions were clearly visible, after which the mechanical index (MI) was set to 1.0. Then, using SonoVue (Bracco, Italy) as an acoustic contrast agent, 5 mL of 0.9% sodium chloride was mixed with SonoVue microbubbles, and 2.4 mL of this mixture was gradually injected *via* the patient's left cubital vein to observe the filling of the cardiac cavity, the lesion site, and myocardial tissue contrast-enhanced performance. The resultant dynamic image was stored for analysis. CEUS results revealed high contrast enhancement in the solid echoic mass in the center of the right atrial tumor, while no contrast enhancement was evident in the surrounding anechoic area (**Figure 2**). No abnormal contrast enhancement was observed in the other cardiac chambers or the myocardium. Accordingly, this right atrial cystic-solid mixed space-occupying lesion was tentatively diagnosed as a potential cardiac teratoma.

Transthoracic computed tomography

The patient subsequently underwent chest CT examination, which showed low levels of inflammation in the middle lobe of the right lung, the lower lingual segment of the upper lobe of the left lung, and the lower lobes of both lungs (**Figure 3A**). In addition, the chest CT scan also exhibited a dense patchy shadow in the right atrium (about 26 mm × 14 mm in size) (**Figure 3B**). When measuring the lesion area in Hounsfield Units (HU), it exhibited a density of 394.6 HU, which was significantly higher than the density of normal fatty tissue. Although further conclusions regarding the etiology of this tumor could not be drawn based on these findings.

Surgical and pathological findings

After the above examinations had been completed, the patient underwent elective right atrial tumor resection. Intraoperative examination revealed moderate cardiac enlargement, and a spherical mass with a size of about 3.0 cm × 4.0 cm could be seen in the right atrium, the tumor was connected to the right atrial side of the right atrial septum under the oval fossa with a small tumor pedicle (**Figures 4A, B**). Subsequent dissection thereof resulted in the outflow of a large volume of dark red liquid, after which a solid yellow-white

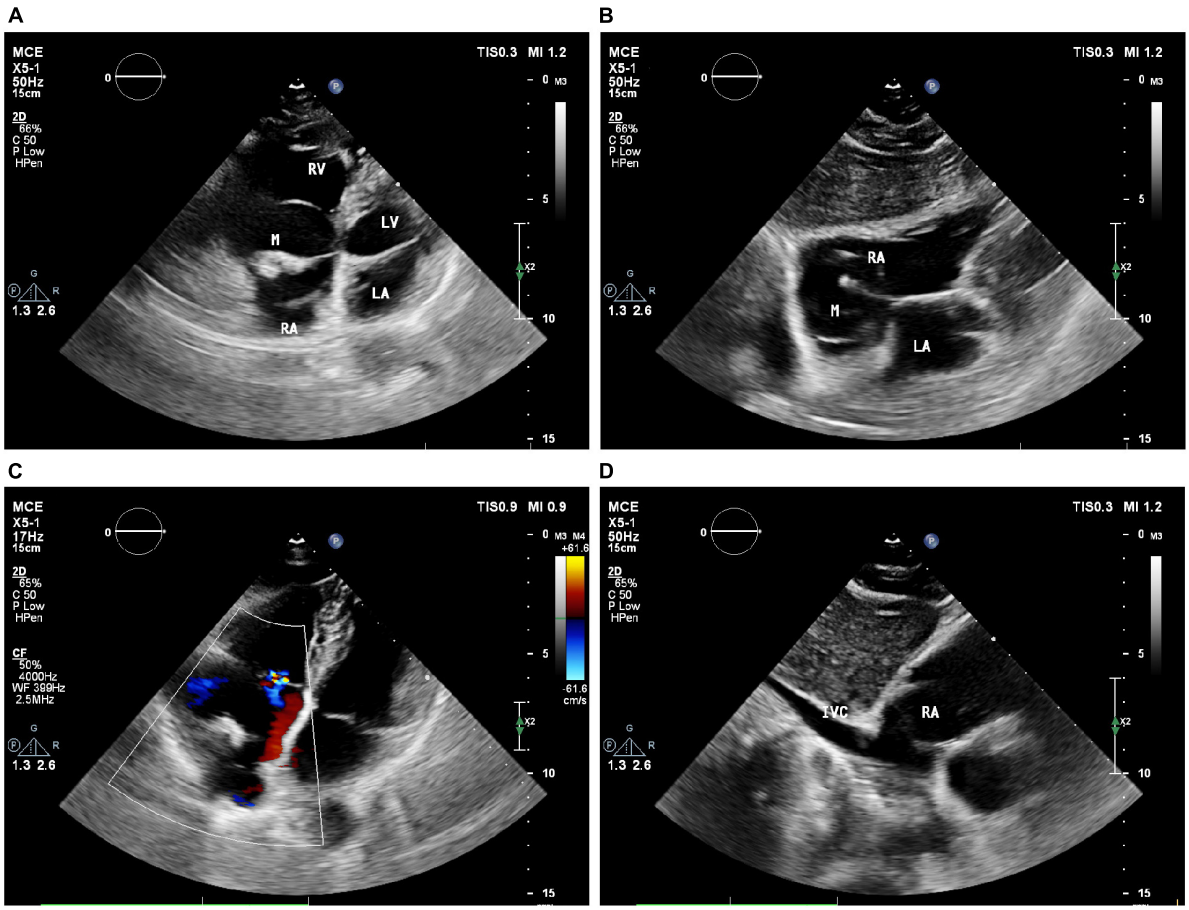

FIGURE 1
Echocardiography showed a large cystic-solid mixed echogenic lesion in the right atrium. Apical four-chamberview **(A)** and subxiphoid four-chamber view **(B)** showed that the mass was attached to the right atrial surface of the atrial septum. Ultrasound findings of tricuspid valve orifice **(C)** andinferior vena cava **(D)**. M = (intracardiac mass).

tumor with a rough texture was observed attached to one side of the cyst wall (**Figures 4C, D**). Postoperative pathological examination *via* light microscopy revealed large sheets of mature adipocytes interspersed between the myocardium, leading to the diagnosis of a cardiac lipoma (**Figures 4E, F**).

Follow-up

Seven days after tumor excision, TTE revealed a normal chamber size and appropriate wall motion, with only limited levels of physiologic regurgitation of the tricuspid valve, and a left ventricular ejection fraction of 60%.

Discussion

Cardiac lipomas are rare, comprising just 2.4% of all benign cardiac tumors (2). These masses are histologically similar to lipomas detected in other parts of the body, and originate from the mesoderm. Roughly 50, 25, and 25% of cardiac lipomas are of subendocardial, subepicardial, and myocardial origin, respectively (3). As most patients harboring cardiac lipomas do not experience any symptoms, these masses are often only detected incidentally (4). When patients do experience symptoms, they are directly associated with tumor size and location, with myocardial tumors impacting the cardiac conduction system, potentially causing intractable arrhythmias. In contrast, myocardial involvement can lead to conduction disturbances and other forms of arrhythmia including premature beats or atrial fibrillation. When large tumors are present within the heart cavities, this can result in abnormal cardiac hemodynamics, while heart valve involvement can result in valvular insufficiency or stenosis and associated clinical symptoms.

Transthoracic echocardiography (TTE) can provide detailed insight regarding the size, shape, location, activity, and secondary hemodynamic changes associated with a given tumor

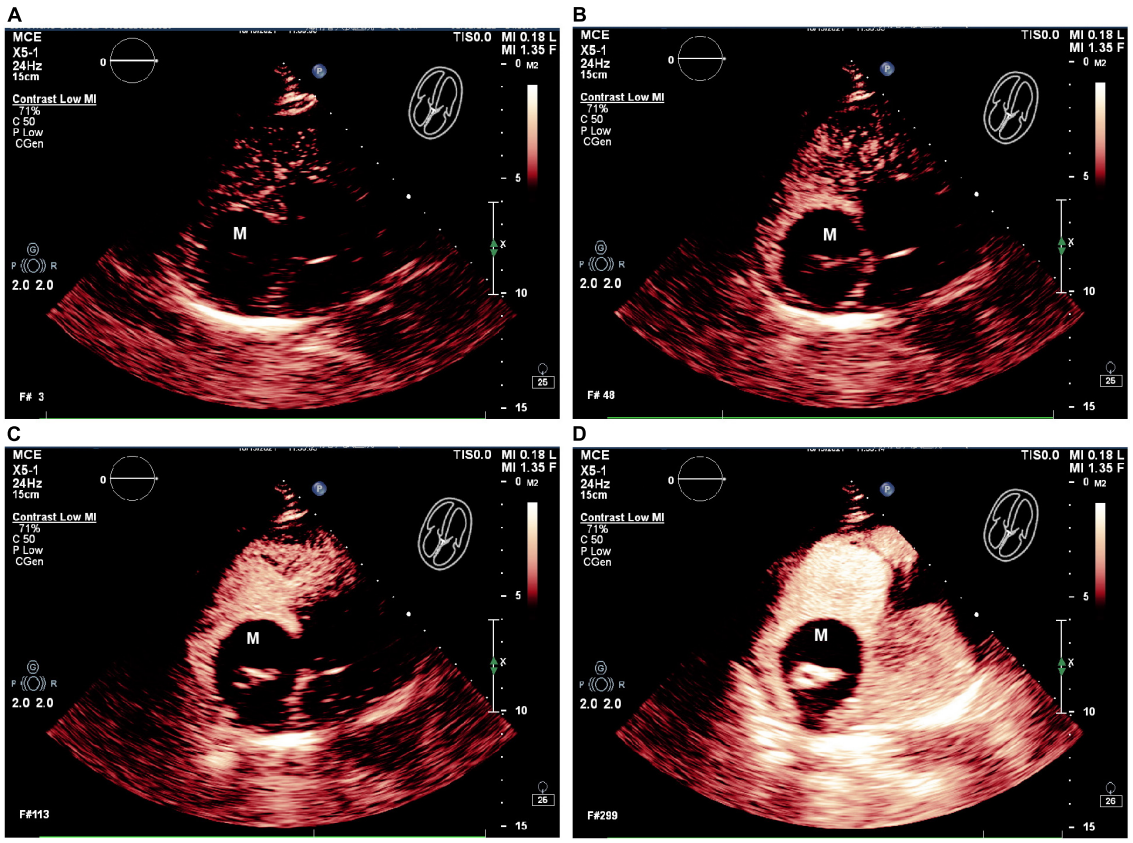

FIGURE 2
The RA mass was seen on contrast enhancement ultrasound (CEUS). **(A–D)** CEUS results showed that in different cardiac cycles, which the solid echo mass in the right atrium tumor revealed high contrast enhancement, and no contrast enhancement is evident in the surrounding anechoic area. M = (intracardiac mass).

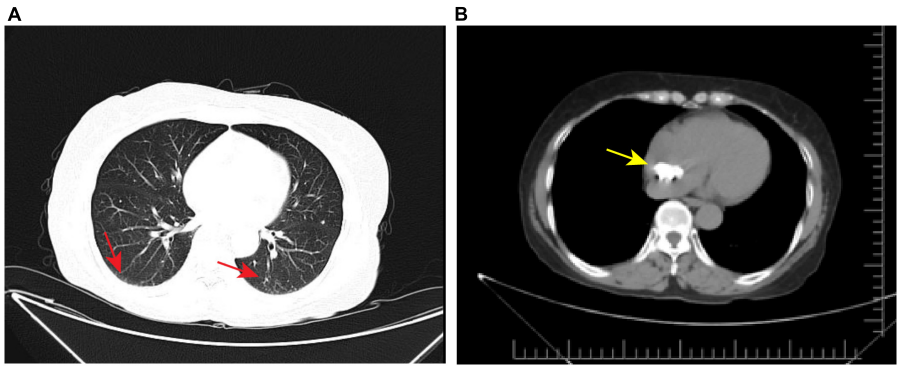

FIGURE 3
Axial view of chest computed tomography. **(A)** Chest CT showed low levels of inflammation in both lungs (red arrow). **(B)** Chest CT also showed a dense patchy shadow in the RA (yellow arrow).

(5). As TTE is non-invasive, repeatable, and does not expose patients to any radiation, it is the imaging modality of choice. CEUS can offer insight regarding tumor vascularity. Cardiac lipomas generally contain relatively few blood vessels, while extensive vascularization may be indicative of malignancy. Surgical resection is the primary approach used to treat cardiac lipomas.

Literature reports suggest that cardiac lipomas are generally round, homogeneous masses with an internal echoic signal and performance that is associated with their localization

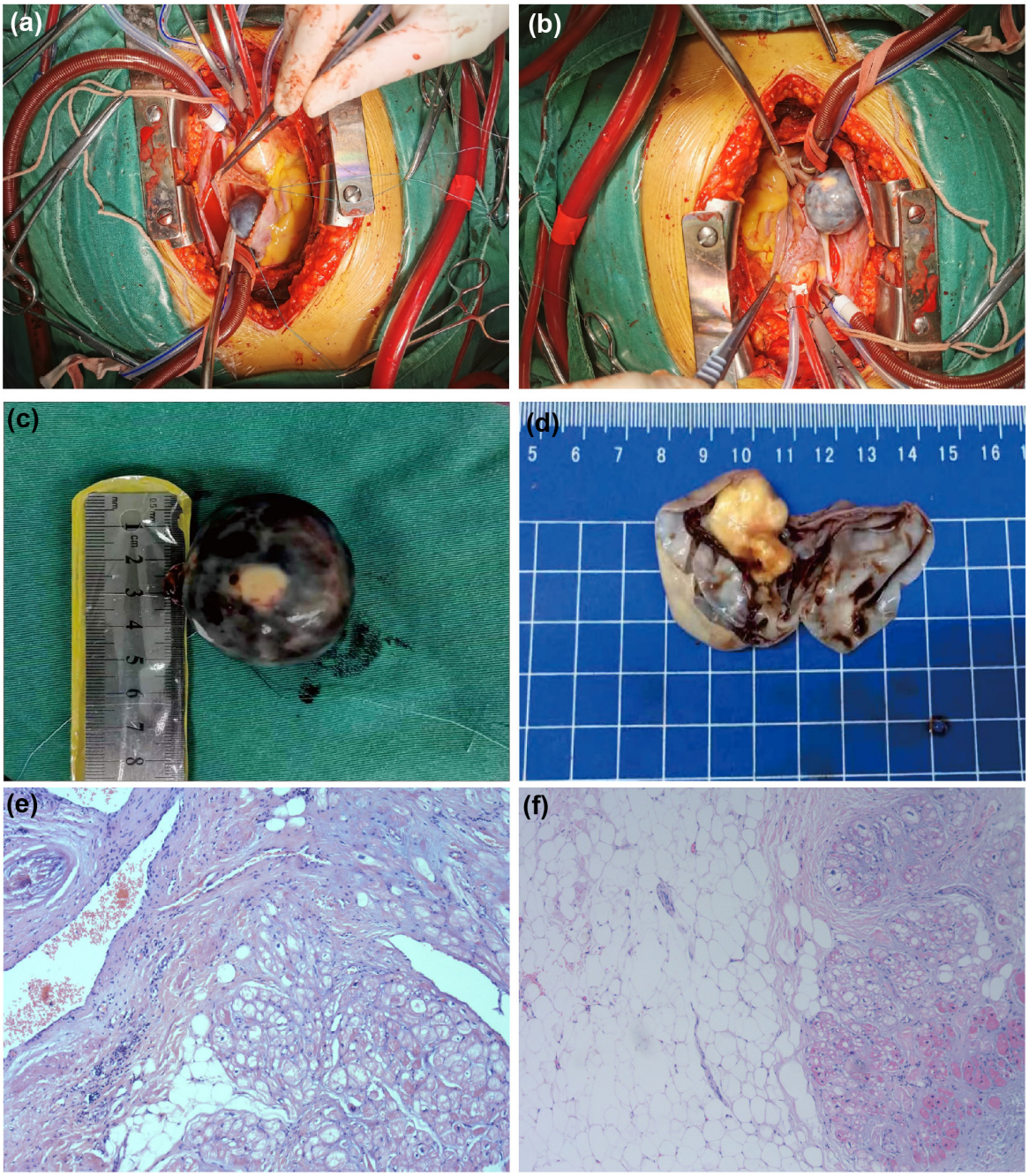

FIGURE 4
Surgical and pathological results. The tumor was spherical mass **(A)** and that was connected to the right atrial side of the right atrial septum under the oval fossa with a small tumor pedicle **(B)**. **(C)** The *ex vivo* tumor was black spherical. **(D)** It can be observed that the yellowish white solid tumor with rough texture is attached to one side of the cyst wall after dissecting the tumor. **(E,F)** Stained with hematoxylin and eosin (H&E) at 10 magnification: the tumor comprised mature adipocytes with entrapped myocardial cells.

(6). Intracardiac lipomas are generally hyperechoic and may have capsules, whereas pericardial lipomas are often poorly-defined hypoechoic masses with morphological characteristics that vary with the cardiac cycle. TTE can enable the further establishment of tumor location and the involvement of valves and surrounding tissue structures, while CEUS largely reveals limited contrast agent perfusion (4). The ultrasonographic findings observed in the present case are distinct from those reported previously in cases of cardiac lipoma. In this patient, TTE revealed a round cystic-solid space-occupying lesion with

TABLE 1 Literature review of cardiac lipoma case reports.

Case reports	Location	Size of lipoma	TTE	CEUS	Management
Fang (4)	RV	4.0 x 1.6 cm	hyperechoic solid mass	Slight enhancement	Surgical
Cao (8)	LV	5.0 × 3.0 cm	solid mass	no enhancement	Surgical
Dan et al. (10)	IVS	3.6 × 2.0 cm	homogeneous parenchymal mass	/	Surgical
Hsiao et al. (9)	pericardium	6.2 × 2.5 cm	homogenous large mas	/	Surgical
Arı (2)	LV	2.1 × 1.6 cm	solid mass	/	Surgical
Li (7)	LV wall	1.9 × 1.4 × 1.2 cm	irregular echo dense mass	/	Surgical

RV, right ventricular; LV, left ventricular; IVS, interventricular septum.

a clear boundary that did not deform with the cardiac cycle. Contrast echocardiography of the left heart further exhibited the presence of a cystic-solid mixed heterogeneous space-occupying lesion in the right atrium, with a solid echoic mass within the lesion exhibiting contrast agent hyperperfusion whereas no contrast agent perfusion was evident in the surrounding anechoic area. These imaging results are likely to result in the preliminary misdiagnosis of this mass as a cardiac teratoma.

The confluence of several factors led to the initial misdiagnosis of the present case, and it is important that these factors be reviewed to guide the evaluation of patients exhibiting similar clinical manifestations. Firstly, this case exhibited 2D-TTE findings distinct from those typically associated with cardiac lipoma cases, as prior literature reports suggest that cardiac lipomas often appear as solid hyperechoic masses with an uneven signal and a clear boundary that deforms with the cardiac cycle (4). In this case, however, we observed a mixed cystic-solid mass that did not deform with the cardiac cycle. We are not aware of any similar reports in the relevant literature, which is summarized in **Table 1** (2, 4, 7–10). Secondly, common cardiac lipomas generally exhibit low levels of contrast enhancement upon CEUS examination. In this case, however, CEUS revealed high levels of contrast enhancement in the solid region of this mass together with an absence of any contrast enhancement in the anechoic region. Thirdly, cardiac teratomas are a relatively rare form of cardiac tumor and are more common in pediatric patients (11, 12), comprising ∼1% of all cardiac tumors in adults. Cardiac teratomas may present as polycystic mixed echoic masses, with some cysts being filled with hyperechoic components including fat or bone. Reported ultrasonographic findings associated with cardiac teratomas are similar to those observed in the present case, accounting for the initial misdiagnosis of this patient. However, pathological examination was ultimately able to provide a more accurate definitive diagnosis in this case.

It is important to differentiate between cardiac lipomas, such as those observed in the present case, and several other diseases. Cardiac liposarcomas are extremely rare and account for only ∼1% of all primary cardiac malignancies (13–16). Affected patients may experience symptoms including chest pain, tightness, and difficulty breathing at an earlier time point, and they frequently present with tumors that have already undergone distant metastasis. 2D-TTE examination of cardiac liposarcomas generally reveals an irregularly shaped heterogeneous hyperechoic mass, with larger tumors potentially harboring necrotic regions. On CEUS examination, cardiac liposarcomas typically exhibit heterogeneous regions of high enhancement, with no enhancement in necrotic areas. Well-differentiated liposarcomas are often indistinguishable from cardiac lipomas on 2D-TTE examination, leading to the potential for misdiagnosis such that only pathological examination can facilitate accurate identification. Cardiac metastases, which most frequently arise from primary tumors of the liver (17), may also exhibit a presentation similar to that of cardiac lipomas. The most frequently involved areas include the right heart and pericardium. These metastases are typically irregularly shaped, with a wide base, little activity, heterogeneous echoic signal, and evidence of refractory pericardial effusion. CEUS examination may reveal internal inhomogeneous hyperenhancement and hypervascular masses. Cardiac myxomas are lobulated structures with low-to-moderate echoic signal and low contrast enhancement on CEUS examination that usually occur at the fossa ovalis of the interatrial septum. Cardiac lymphomas are primarily hypoechoic or slightly hyperechoic, with unclear borders, uneven echoic signal, lower levels of liquefaction and calcification, and an irregular "cauliflower-like" shape (18). Varying degrees of secondary pericardial effusion may be evident in cases of pericardial involvement. When this disease is more advanced, adjacent tissues and blood vessels are frequently affected. CEUS examination generally exhibits high levels of contrast enhancement. Atrial thrombus formation may also mimic some of the characteristics of cardiac lipomas, primarily occurring in patients with a history of rheumatic heart disease, atrial fibrillation, or venous thrombosis. Echocardiography reveals an irregularly shaped mass with a wide base and an inhomogeneous echoic signal that does

not oscillate with the cardiac cycle. CEUS examination of atrial thrombi generally fails to reveal any contrast medium perfusion, and fresh thrombi can form with limited contrast medium perfusion.

Conclusion

While some cardiac tumors are associated with obvious or distinctive ultrasonographic findings, others do not exhibit these obvious features such that they may be more difficult to identify or diagnose. As cardiac lipomas generally have an insidious onset, their diagnosis is largely reliant on imaging examinations. Echocardiography is of particular value when diagnosing cardiac masses, and left cardiac contrast echocardiography is particularly advantageous as a means of distinguishing between benign and malignant tumors. Contrast echocardiography is a safe and sensitive approach that can offer insight regarding the blood supply of a given lesion, thus supporting differential diagnosis efforts. In summary, the present case emphasizes the importance of considering clinical manifestations, laboratory test results, and multimodal imaging findings when diagnosing patients with cardiac lipomas or other cardiac tumors.

Data availability statement

The original contributions presented in this study are included in the article/supplementary material, further inquiries can be directed to the corresponding author.

Ethics statement

Written informed consent was obtained from the individual(s) for the publication of any potentially identifiable images or data included in this article.

Author contributions

XJ contributed to the conception of the case report. QC contributed to writing the manuscript. DY and LL contributed to the clinical data collection. All authors contributed to the article and approved the submitted version.

Funding

We gratefully acknowledge the financial support from National Natural Science Foundation of China (Grant Nos. 82160337, 81760317, and 81871365) and Hainan Province Scienceand Technology Special Fund (Grant Nos. ZDYF2020138, ZDYF2019136, and ZDYF2020140).

Acknowledgments

The authors gratefully thank Shengxiong Lin of cardiovascular surgery for his technical support on the intraoperative digital photos.

Conflict of interest

The authors declare that the research was conducted in the absence of any commercial or financial relationships that could be construed as a potential conflict of interest.

Publisher's note

References

1. Karangelis D, Palios J, Tzertzemelis D, Economidou S, Panagiotou M. Surgical resection of a cardiac lipoma of the right ventricle. *Ann Card Anaesth.* (2019) 22:452–4. doi: 10.4103/aca.ACA_87_18

2. Arı H, Arı S, Göncü MT, Koca V, Bozat T. Biventricular lipoma (first case in literature). *Int J Cardiol.* (2011) 150:e98–100. doi: 10.1016/j.ijcard.2010.02.058

3. Rainer WG, Bailey DJ, Hollis HW Jr. Giant cardiac lipoma: refined hypothesis proposes invagination from extracardiac to intracardiac sites. *Tex Heart Inst J.* (2016) 43:461–4. doi: 10.14503/THIJ-15-5342

4. Fang L, He L, Chen Y, Xie M, Wang J. Infiltrating lipoma of the right ventricle involving the interventricular septum and tricuspid valve: report of a rare case and literature review. *Medicine (Baltimore).* (2016) 95:e2561. doi: 10.1097/MD.00000000-00002561

5. Shamsi F, Bajwa G, Ghalib H. Left ventricular lipoma: a rare case", case report. *J Cardiothorac Surg.* (2020) 15:85. doi: 10.1186/s13019-020-01122-1

6. Liu W, Bu H. Strategies to rare primary cardiac lipomas in the left ventricle in a patient: case report. *BMC Cardiovasc Disord.* (2022) 22:316. doi: 10.1186/s12872-022-02748-w

7. Li FP, Wang XF, Xiao J, Xiao YB. Myocardial lipomatous infiltration of the left ventricular wall. *J Card Surg.* (2010) 25:513–5. doi: 10.1111/j.1540-8191.2010.01021.x

8. Cao S, Tan T, Zhou Y, Zhou Q. Giant left ventricular infiltrating lipoma. *Circ Cardiovasc Imaging.* (2019) 12:e009361. doi: 10.1161/CIRCIMAGING.119.009361

9. Hsiao PG, Hsieh MJ, Hsueh C, Chen TH, Chang RY, Chu PH. An unusual giant subepicardial lipoma: a case report. *Med J South Taiwan.* (2018) 14:104–8. doi: 10.6726/MJST.201812_14(2).0006

10. Dan L, Weitie W, Zhicheng Z, Wang Y, Xu R, Liu K. Cardiac lipoma in the interventricular septum: a case report. *J Cardiothorac Surg.* (2015) 10:69. doi: 10.1186/s13019-015-0275-0

11. Cohen R, Mirrer B, Loarte P, Navarro V. Intrapericardial mature cystic teratoma in an adult: case presentation. *Clin Cardiol.* (2013) 36:6–9. doi: 10.1002/clc.22051

12. Agwar FD, Gemechu TW. Mature teratoma in the right ventricle. *Ann Thorac Surg.* (2021) 112:e111–3. doi: 10.1016/j.athoracsur.2020.12.040

13. Kong F, Zhang W, Guo Q. Multiple well-differentiated cardiac liposarcoma with a concomitant myocardial lipoma: a case report. *Mol Clin Oncol.* (2018) 9:617–21. doi: 10.3892/mco.2018.1741

14. Wang X, Yu X, Ren W, Li D. A case report: a giant cardiac atypical lipoma associated with pericardium and right atrium. *BMC Cardiovasc Disord.* (2019) 19:247. doi: 10.1186/s12872-019-1221-1

15. Liu L, Fang A, Cheng S, Guo G, Zhang S, Chen X, et al. Diagnosis and survival analyses of patients with space-occupying cardiac lesions: a 10-year retrospective single-center study. *Quant Imaging Med Surg.* (2022) 12:4081–94. doi: 10.21037/qims-21-1151

16. Mao F, Dong Y, Ji Z, Cao J, Wang WP. Contrast-enhanced ultrasound guided biopsy of undetermined abdominal lesions: a multidisciplinary decision-making approach. *Biomed Res Int.* (2017) 2017:8791259. doi: 10.1155/2017/8791259

17. Lee JH, Kim HS, Park JH, Park JS. Intraductal papillary mucinous neoplasm of the biliary tract with cardiac metastasis: a case report. *Medicine (Baltimore).* (2021) 100:e24310. doi: 10.1097/MD.0000000000024310

18. Yang D, Wu T, Gao L, Liu L, Liu F, Jing X. Cardiac lymphoma diagnosed by multi-modality imaging: a case report. *Front Cardiovasc Med.* (2022) 9:771538. doi: 10.3389/fcvm.2022.771538

frontiers | Frontiers in Cardiovascular Medicine

TYPE Case Report
PUBLISHED 20 December 2022
DOI 10.3389/fcvm.2022.1079670

OPEN ACCESS

EDITED BY
Guo-Wei Tu,
Fudan University, China

REVIEWED BY
Hiroki Nagasawa,
Juntendo University Shizuoka Hospital, Japan
Qun Lu,
Xi'an Jiaotong University, China

*CORRESPONDENCE
Feng Zhu
✉ alexzhujunchi@hotmail.com

†These authors share first authorship

SPECIALTY SECTION
This article was submitted to General Cardiovascular Medicine, a section of the journal Frontiers in Cardiovascular Medicine

RECEIVED 25 October 2022
ACCEPTED 02 December 2022
PUBLISHED 20 December 2022

CITATION
Shen T, Fang H, Tang T, Tang H, Hu X and Zhu F (2022) Case report: Delayed cardiac rupture with congenital absence of pericardium after blunt trauma.
Front. Cardiovasc. Med. 9:1079670.
doi: 10.3389/fcvm.2022.1079670

Case report: Delayed cardiac rupture with congenital absence of pericardium after blunt trauma

Tuo Shen†, He Fang†, Tao Tang†, Hongtai Tang, Xiaoyan Hu and Feng Zhu*

Burns and Trauma ICU, The First Affiliated Hospital, Naval Medical University, Shanghai, China

A 66 years old male was admitted to our hospital after a serious car accident. The patient presented with severe shock after admission. After the examination, the patient was diagnosed with hemopneumothorax and myocardial contusion, accompanied by spleen rupture. After emergency surgery and a series of symptomatic treatments, the patient's condition gradually stabilized. One week later, the patient suddenly presented with severe shock. Massive hemothorax was found on the left side of the chest. Surgical exploration revealed cardiac rupture and accidental absence of congenital pericardium. According to the literature review, congenital absence of pericardium (CAP) is relatively rare. Although there are certain imaging features, the clinical diagnosis is very difficult. However, this patient did not show the characteristics in the literature and had some other atypical features. The role of CAP in the occurrence and development of the patient's heart injury and rupture is worthy of discussion. What we learned from this case is that we should look for potential risks in the telltale signs of a patient's condition.

KEYWORDS

congenital absence of pericardium, delayed cardiac rupture, myocardial contusion, blunt trauma, chest trauma, case report

Introduction

Congenital absence of pericardium (CAP) (see **Figure 1**) is rare in clinical practice (1). It includes complete and partial pericardial absence, and left pericardial absence is common. The absence of pericardium often lacks typical imaging manifestations and clinical signs, and some patients may present with shortness of breath, chest pain, dizziness, and other discomfort. Some patients may die suddenly of unknown causes, and some patients may be accidentally diagnosed during surgeries (2).

Chest trauma is the third most common cause of trauma. Chest trauma has a high morbidity and mortality, associated with 25% of trauma-related deaths (3). The incidence of cardiac contusion in blunt chest trauma ranges from 3 to 56% (4).

Blunt cardiac rupture is a very rare condition with a high mortality rate, and the incidence of blunt cardiac rupture is 1/2,400 in the United States (5). Delayed blunt cardiac rupture is less common clinically.

Congenital absence of pericardium was incidentally discovered in the treatment of a patient with delayed blunt cardiac rupture.

Case presentation

A 66 years old male was admitted to the hospital due to a rear-end crash, in which case, the patient in the back seat was squeezed in the chest by the front seat. The patient complained of multiple body pain with chest tightness and shortness of breath. He had no previous history of coronary heart disease, angina pectoris or myocardial infarction. The patient developed severe shock in the emergency room with a blood pressure of 78/40 mmHg. The electrocardiogram (ECG) indicated a high wall myocardial infarction (see **Figure 2**). The troponin was 8.434 μg/L (see **Figure 3**). Computed tomography (CT) indicated "multiple rib fracture on the left side, hydropneumothorax on the left side, no obvious abnormality in the skull and abdomen"(see **Figures 4**, **5**). Closed thoracic drainage was given. The drainage volume was reduced and stabilized after drainage of 1,300 ml bloody fluid. Resuscitation with adequate fluids and high doses of vasoactive drugs, however, is not effective. Bedside ultrasonography indicated a large amount of ascites, and the abdominocentesis got blood that doesn't clot. Emergency laparotomy revealed splenic rupture and contusion of pancreatic tail, and splenectomy was performed. After symptomatic treatment, the circulation was gradually stabilized. One week later, the thoracic drainage volume was 40 ml for 2 consecutive days, and the thoracic drainage tube was removed. The next day, however, the patient was suddenly agitated and sweating profuse, followed by no response and weak pulsation of the aorta. Resuscitation was initiated Immediately, meanwhile, bedside ultrasound showed a large pleural effusion on the left side. Closed thoracic drainage was performed to drain a large amount of blood continuously, and exploratory thoracotomy was performed in emergency. Intraoperative exploration revealed massive hematocele and blood clots in the thoracic cavity. After the removal of the hematocele and clots, the left heart was bare and the pericardium was absent (see **Figure 1**). We found widespread contusion on the lateral posterior wall of the left ventricle with a 5mm laceration where was sustained bleeding. The bleeding was stopped by pressing, and the blood pressure was controlled before suture and repair. Severe and extensive contusion and necrosis of myocardial tissue resulted in failure of repair and death. The figure below shows a timeline of the patient's medical history (see **Figure 6**).

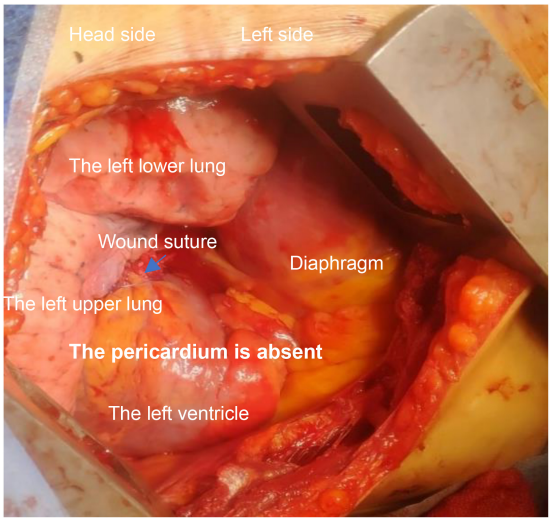

FIGURE 1
Intraoperative observations: right side decubitus position; left heart exposed; left side posterior wall rupture has been sutured; there is still continuous bleeding.

Discussion

Congenital absence of pericardium is often difficult to diagnose, and it has no specific symptoms and signs, so it is often ignored. CAP has certain imaging diagnostic features (6, 7): (1) pulmonary parenchyma between the main pulmonary artery and the ascending aorta; (2) pulmonary parenchyma between the base of the heart and the left diaphragmatic muscle; (3) pulmonary parenchyma between the ascending main aorta and the right pulmonary artery; (4) "SNOOPY" sign on chest radiograph. Even so, it is still very difficult to clinically diagnose CAP. Sergio et al. (6), reviewed the imaging examinations of 12,888 patients and found only 1 case with partial pericardial defect (left heart) with conditions (1) and (2), and 10 cases with false positive results. Reviewing the radiographic findings of this patient after the injury, we did find some evidence of CAP (see **Figure 4**), but did not find any obvious radiographic features in accordance with the literature.

Computed tomography and magnetic resonance imaging (MRI) are the gold standard for the diagnosis of CAP (7), but it is still difficult to make a diagnosis in the absence of symptoms and experience, so that in many cases the diagnosis is made during surgeries. In this case, CAP was missed by CT. Due to severe lung contusion, the patient was dependent on ventilator support. We didn't have the opportunity to perform MRI or any other examinations.

The pericardium supports and protects the heart, limiting its expansion, cushioning the impact of violent heart injury, mitigating the injury, and preventing the heart from rapidly rupturing when pressure rises.

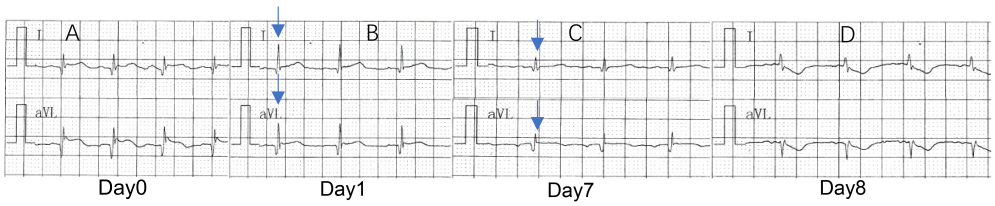

FIGURE 2
(A) Sinus rhythm, abnormal Q-wave and ST-segment elevation on I and aVL, suggesting acute high lateral myocardial infarction. **(B)** Sinus rhythm, abnormal Q-waves on I and aVL, suggesting high lateral myocardial infarction. **(C)** Sinus rhythm, no obvious abnormality on I and aVL. **(D)** Sinus tachycardia, ST-segment depression on I and aVL, suggesting increased myocardial ischemia. Analyses the ECG results, 1 day before cardiac rupture, QRS voltage on I and aVL was significantly lower.

Due to the lack of pericardial protection, after a violent injury to the chest, the myocardium may suffer more severe contusion under the compression of the front and rear chest wall structures. Shah et al. (8), suggested that cardiac injury should be highly suspected in any patient with blunt chest trauma and multiple injuries, and that baseline chest radiographs, ECG, and cardiac enzyme measurements should be part of the routine evaluation of these patients to rule out cardiac injury, and echocardiography should be performed if clinically necessary. The imaging manifestations of blunt myocardial contusion are atypical, and the electrocardiographic findings are sometimes indistinguishable from myocardial infarction. In this patient, the early ECG showed a high lateral wall myocardial infarction and his myocardial enzymes increased significantly. Excluding the history of coronary heart disease and myocardial infarction, the diagnosis of cardiac contusion was relatively accurate in combination with the mechanism of injury and the extensive hemothorax and multiple rib fractures. But it was hard to diagnose an acute heart rupture. In the presence of the pericardium, cardiac rupture may be accompanied by pericardium tamponade. Most patients died at the scene or in the early stages of rescue. In the blunt injury, simultaneous rupture of the heart and pericardium is rare. Coincidentally, this patient happened to have no pericardium. A heart rupture at the time of the injury can be very difficult to determine. The small rupture in the heart may have closed during the patient's hypotension. Even if that was what really happened, we could not diagnose acute cardiac rupture due to the lack of effective early evaluation methods. Moreover, due to the complexity of the condition, no further evaluation was performed in the case of no significant change in treatment strategy. Meanwhile, combined with the Flotrac/Vigileo system, the patient's cardiac function was relatively stable 1 week after the injury. As the patient's condition improved, the cardiac preload and afterload increased. But the damaged myocardium gradually dissolved. The ventricular wall became weak. The patients' intolerance to endotracheal intubation and airway response to stimulation such as sputum aspiration after recovery will lead to fluctuations in blood pressure, which increased the burden on the left heart imperceptibly. Without the restriction and protection of

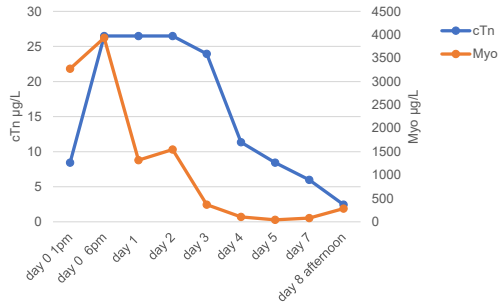

FIGURE 3
Time courses of troponin (cTn) and myoglobin (Myo).

the pericardium, the blunt heart was more likely to rupture. During the final cardiac surgery, we found extensive bruising of the myocardium surrounding the rupture. This suggests that the heart rupture may be secondary to myocardial contusion. Unfortunately, we did not have the opportunity to conduct autopsy or pathological examination after the operation.

The patient's condition changed suddenly, progressed rapidly, and the clinical diagnosis was not clear. Generally, patients with heart rupture often die of tamponade at an early stage. Due to the absence of the pericardium, the patient showed symptoms of heart failure and shock during the process of heart rupture. After a large amount of transfusion and fluid rehydration, there was still a chance to perform thoracotomy exploration, which to a certain extent created a rescue opportunity for clinicians.

Our early assessment for cardiac contusion was flawed in this patient. Evaluation by echocardiography was necessary. We can evaluate the motion of the ventricular wall and observe the pericardial effusion. By chance, maybe, we could find the CAP. Unfortunately, the emergency room and intensive care unit were not equipped to perform echocardiography.

The patient still showed signs of the onset of a ruptured heart. ECG changes before and after the onset still had a certain suggestive effect (see **Figure 2**). The patient's I lead and aVL leads showed significant amplitude changes the day before the

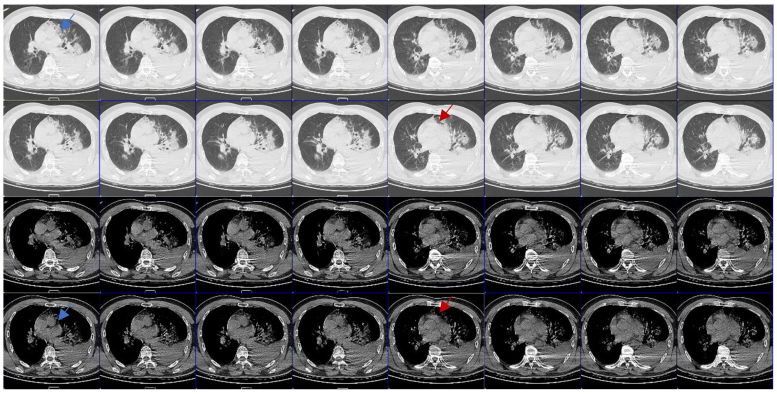

FIGURE 4
Computed tomography (CT) images in different window settings: As the blue arrow shows, there is no obvious pericardial structure in the left area of pulmonary artery, which is closely related to lung tissue and has irregular edge; as the red arrow shows, there is an abnormal notch near the pulmonary artery, which is rare when the pericardium is intact.

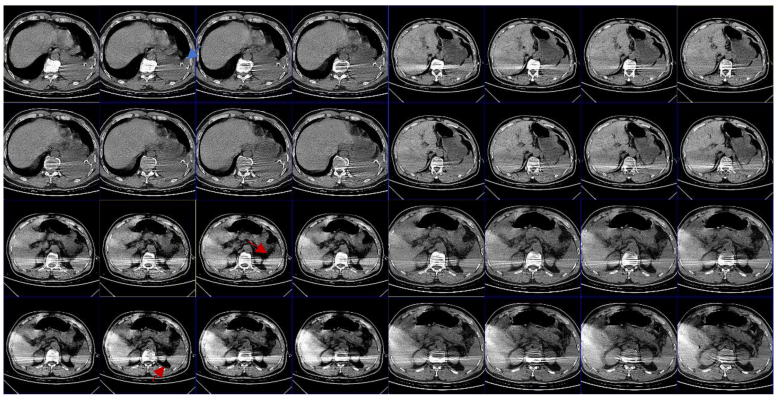

FIGURE 5
Abdominal CT: the blue arrow shows intrathoracic drain; the red arrow shows that there appears to be exudate around the spleen; the splenic hilum appears to be intact.

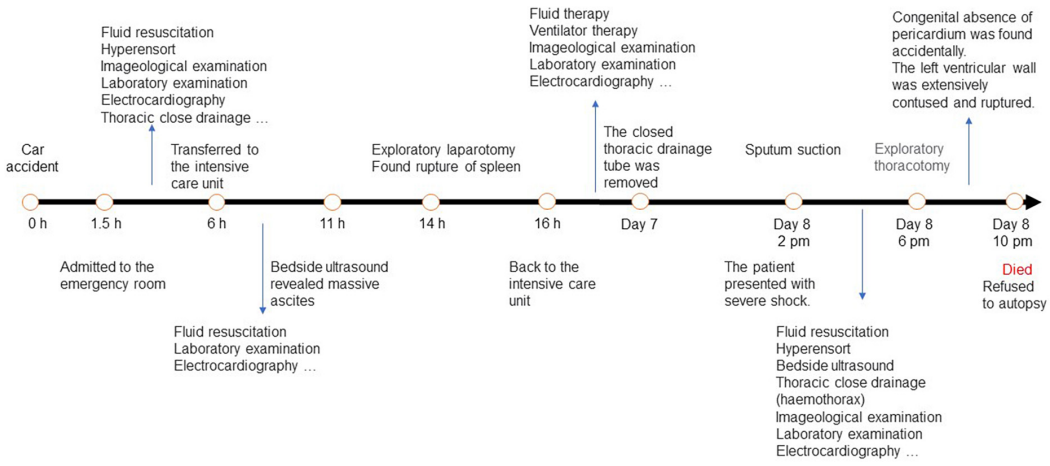

FIGURE 6
Timeline.

onset of the disease. Dynamic comparison of ECG changes could enable us to warn of the potential risk of heart rupture in advance and make adequate clinical response measures.

Conclusion

1. The clinical diagnosis of CAP is very difficult. Routine imaging examinations sometimes lack specificity. Therefore, the diagnosis should be made with the help of clinical experience and targeted tests.
2. Without the protective effect of the pericardium, the heart is more vulnerable to injury and more likely to cause serious adverse events in both complete and partial pericardial absence during chest trauma.
3. In the treatment of patients with chest trauma, the presence of cardiac contusion should be vigilant. For patients with severe cardiac contusion, there is still a risk of delayed rupture even in about 1 week after injury. Therefore, it is necessary to systematically evaluate the severity of cardiac contusion.
4. In the rescue stage of patients with severe chest trauma, we can use ECG, echocardiography, chest CT and laboratory tests to evaluate cardiopulmonary injuries. For patients with cardiac contusion, it is still necessary to regularly evaluate with the help of various methods in the subsequent treatment. Such as MRI, coronary angiography, etc.
5. We should observe the change process of auxiliary examination dynamically, especially the change of some indexes closely related to injury.

Data availability statement

The original contributions presented in this study are included in the article/**Supplementary material**, further inquiries can be directed to the corresponding author.

Ethics statement

Written informed consent was obtained from the individual(s) for the publication of any potentially identifiable images or data included in this article.

Author contributions

FZ came up with the idea. TS drafted the manuscript. HF and TT collected and summarized the medical records. HT, XH, and FZ revised the manuscript. All authors read and approved the final manuscript.

Conflict of interest

The authors declare that the research was conducted in the absence of any commercial or financial relationships that could be construed as a potential conflict of interest.

Publisher's note

Supplementary material

The Supplementary Material for this article can be found online at: https://www.frontiersin.org/articles/10.3389/fcvm.2022.1079670/full#supplementary-material

References

1. Yazdan-Ashoori P, Jimenez-Juan L, Pereira L, Ahmed S. It's never too late: spotting congenital absence of the pericardium in an older adult. *CJC Open.* (2020) 2:702–4. doi: 10.1016/j.cjco.2020.06.017

2. Symeonides P. Sometimes surgery is the only way to make a diagnosis and treat the patient: a case of congenital partial absence of pericardium. *Eur J Case Rep Intern Med.* (2017) 4:000593. doi: 10.12890/2017_000593

3. Verma N, White C, Mohammed T. Blunt cardiothoracic trauma: common injuries and diagnosis. *Semin Roentgenol.* (2018) 53:171–7. doi: 10.1053/j.ro.2018.02.007

4. Sybrandy K, Cramer M, Burgersdijk C. Diagnosing cardiac contusion: old wisdom and new insights. *Heart.* (2003) 89:485–9. doi: 10.1136/heart.89.5.485

5. Teixeira P, Inaba K, Oncel D, DuBose J, Chan L, Rhee P, et al. Blunt cardiac rupture: a 5-year NTDB analysis. *J Trauma.* (2009) 67:788–91. doi: 10.1097/TA.0b013e3181825bd8

6. Sergio P, Bertella E, Muri M, Zangrandi I, Ceruti P, Fumagalli F, et al. Congenital absence of pericardium: two cases and a comprehensive review of the literature. *BJR Case Rep.* (2019) 5:20180117. doi: 10.1259/bjrcr.20180117

7. Vosko I, Zhan Y, Nabi F, Zoghbi W. Snoopy's heart: a case of complete congenital absence of the pericardium. *Methodist Debakey Cardiovasc J.* (2019) 15:226–7. doi: 10.14797/mdcj-15-3-226

8. Shah S, Huda S, Raj V. Blunt chest wall trauma and troponin elevation: is it a cardiac contusion or a myocardial infarction?. *Am J Med.* (2021) 134:e113–4. doi: 10.1016/j.amjmed.2020.06.049

frontiers | Frontiers in Cardiovascular Medicine

TYPE Case Report
PUBLISHED 05 January 2023
DOI 10.3389/fcvm.2022.1046498

OPEN ACCESS

EDITED BY
Junjie Xiao,
Shanghai University, China

REVIEWED BY
Yehia Saleh,
Houston Methodist Hospital,
United States
Stefan Simović,
University of Kragujevac, Serbia

*CORRESPONDENCE
María Ascensión Sanromán Guerrero
ascensan08@hotmail.com

SPECIALTY SECTION
This article was submitted to General Cardiovascular Medicine, a section of the journal Frontiers in Cardiovascular Medicine

RECEIVED 16 September 2022
ACCEPTED 02 December 2022
PUBLISHED 05 January 2023

CITATION
Sanromán Guerrero MA, Sánchez EH, Ruanes BdN, Fernández-González P, Ugalde SA, Leal AG, Fernández MS, Rodríguez JJA, Martinez Garcia L, Escudero R, Méndez MÁF, Zamorano Gómez JL, Llorente BM and Vivancos-Gallego MJ (2023) Case report: From monkeypox pharyngitis to myopericarditis and atypical skin lesions.
Front. Cardiovasc. Med. 9:1046498.
doi: 10.3389/fcvm.2022.1046498

Case report: From monkeypox pharyngitis to myopericarditis and atypical skin lesions

María Ascensión Sanromán Guerrero[1]*, Elena Hernández Sánchez[1], Belén de Nicolás Ruanes[2], Pablo Fernández-González[2], Sonia Antoñana Ugalde[1], Alejandra González Leal[1], Marcelo Sanmartín Fernández[1], Jose Javier Alarcón Rodríguez[3], Laura Martinez Garcia[4], Rosa Escudero[5], Maria Ángeles Fernández Méndez[3], Jose Luis Zamorano Gómez[1], Beatriz Montero Llorente[6] and Maria Jesús Vivancos-Gallego[5]

[1]Department of Cardiology Medicine, Hospital Ramón y Cajal, Madrid, Spain, [2]Department of Dermatology, Hospital Ramón y Cajal, Madrid, Spain, [3]Department of Radiology, University Hospital Ramón y Cajal, Madrid, Spain, [4]Department of Microbiology, University Hospital Ramón y Cajal and IRYCIS, Universidad de Alcalá, CIBERESP, Madrid, Spain, [5]Department of Infectious Diseases, University Hospital Ramón y Cajal and IRYCIS, Universidad de Alcalá, CIBERINFEC, Madrid, Spain, [6]Department of Clinical Pharmacology, Hospital Ramón y Cajal, Madrid, Spain

Background: A global outbreak of the human monkeypox virus (HMPXV), first identified in May 2022, was declared a health emergency of international concern on 23 July 2022. Before the global outbreak, monkeypox cases were mostly confined to central and west African countries, where this virus is prevalent. Close contact, mainly sexual contact, is supposed to be the main route of transmission, and it is remarkable that the incidence is higher in men who have sexual relationships with other men.

Case summary: A 40-year-old Caucasian man arrived at the emergency department complaining of oppressive epigastric pain extending to the chest after a diagnosis of pharyngitis, which was suspected to be caused by the human monkeypox virus. Based on the clinical symptoms, physical examination, serum cardiac biomarkers, and electrocardiographic findings, he was diagnosed with myopericarditis. The real-time PCR for human monkeypox in skin lesions, urine, plasma, and the oropharyngeal swab was positive. The peak of troponin I was 20.6 ng/ml, and the electrocardiogram showed an upward concavity in the ST segment in diffuse leads, which was in agreement with the previous diagnosis. The presence of edema, subepicardial, and myocardial late gadolinium enhancement, and increased values on T1 mapping in the cardiac MRI were in agreement with the diagnosis of myopericarditis. Antiviral treatment with tecovirimat was started with excellent tolerability. After 6 days, the patient recovered and was discharged.

10.3389/fcvm.2022.1046498

Discussion: To our knowledge, this is one of the first reported cases of myopericarditis due to human monkeypox infection, which was confirmed by a cardiac MRI following modified Lake Louise criteria. The short span between the onset of the mucocutaneous symptoms and the myocardial damage suggests a pathogenic association. Furthermore, the active viral replication in plasma samples and the negative results on real-time PCR for other viruses support this clinical association.

KEYWORDS

myocarditis, pericarditis, tecovirimat, monkeypox, Lake Louise criteria, plasma

Introduction

Before April 2022, human monkeypox virus (HMPXV) infection had mostly been reported in Africa, where it was an endemic disease. The World Health Organization declared the HMPXV outbreak a public health emergency of international concern (PHEIC) on 23 July 2022. Currently, numerous cases occur worldwide after close or sexual contact, which is supposed to be the main transmission route. Skin lesions are detected in 95% of the affected people, influencing the anogenital area the most, followed by the arms and trunk in 50% of the cases. Mucosal lesions are reported in 41% of the cases. To date, gay or bisexual men are the most affected population group, suggesting the amplification of the spreading of the disease in sexual networks (1, 2).

Of the 528 cases worldwide, complications associated with HMPXV infection have been reported: one case of epiglottitis and two cases of myocarditis. Only 5% received specific treatment for HMPXV: tecovirimat (2%), cidofovir (2%), and vaccinia immune globulin (<1%) (1).

In this study, we report a case of myopericarditis after pharyngitis caused by an HMPXV infection, followed by the onset of atypical skin lesions. Without the requirement for vasoactive pharmaceutical treatment, a benign clinical course was observed. Nevertheless, tecovirimat was administered during hospitalization for heart damage, demonstrating its safety and a complete resolution of symptoms. In conclusion, despite the need for further research, this antiviral treatment is increasingly recommended for use in this clinical setting of heart damage.

Case report

We present the case of a 40-year-old Caucasian man who sought emergency medical attention on 26 August 2022 due to odynophagia, a swollen right submandibular lymph node, cervical pain, and a fever of up to 38°C. He reported having had high-risk sexual contact (exclusively oral intercourse) 2 weeks before the onset of the symptoms. His male partner was diagnosed with genital HMPXV 5 days later with a positive real-time PCR for *orthopoxvirus*. Until that moment, our patient was asymptomatic. He had previously been diagnosed with human papillomavirus condyloma, for which he had been treated with cryotherapy and imiquimod. There were no known drug allergies. The patient lived in a suburban area of Madrid with his mother and no animals. He had never been vaccinated for smallpox. Informed consent was given prior to writing and publishing this case report.

The physical exam revealed swollen tonsils and uvula. Multiple coalescing ulcerations covered the right tonsil with a necrotic base and confluent lesions, which showed a necrotic center and white margins (Figure 1A). No anogenital or skin lesions were present at this initial visit. During his stay at the hospital, a small number of millimetric umbilicated pustules with an erythematous base on the trunk and the proximal region of the limbs also appeared (Figure 1B).

With verbal consent, swabs from nasopharyngeal, rectal, and urine samples were taken by the Dermatology Department at the Emergency Room (ER). Given that the patient did not present alarming signs, he was prescribed amoxicillin and anti-inflammatory drugs (ibuprofen) and was discharged.

Two hours later, he suddenly woke up at home, in his bed, due to an oppressive epigastric pain extending to the chest. The pain lasted approximately one and a half hours and prompted his return to the ER. At the time of admission, the temperature was 36.3°; blood pressure, 102/70 mm Hg; heart rate, 75 beats per minute; and basal oxygen saturation, 95%. There were no heart murmurs in the cardiac auscultation. No signs of edema were observed.

The chest x-ray revealed no significant findings (Figure 1C). The electrocardiogram (ECG) on arrival showed a diffuse ST elevation with an upward concavity in leads (I, II, AVL, V4, V5, and V6), a negative T wave in III, and a diffusely depressed PR segment (Figure 1D). The initial troponin I determination was 9.7 ng/ml (Architect Abbot), and the C-reactive protein level was 10.5 mg/L (normal value < 5 mg/L). The transthoracic echocardiogram revealed a preserved left

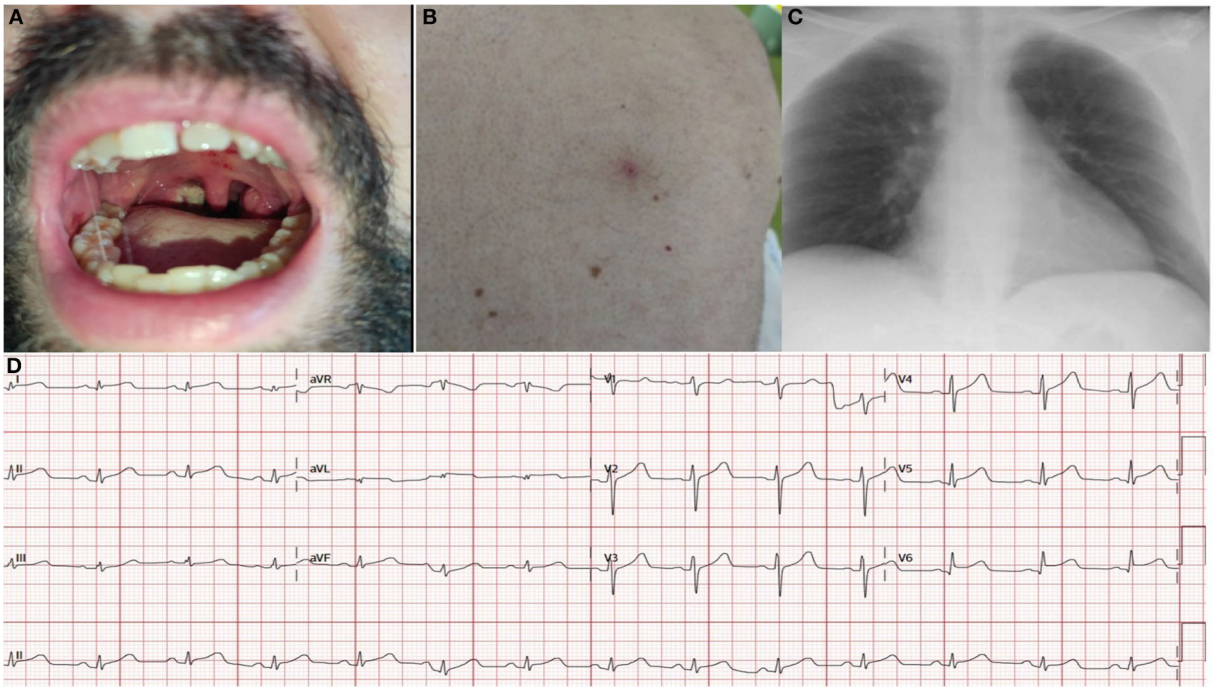

FIGURE 1
Skin lesions **(A, B)**, chest x-ray **(C)** at admission and electrocardiogram at admission **(D)**. At admission, the electrocardiogram revealed sinus rhythm with diffuse ST elevation with upward concavity in leads (I, II, III, AVF, V4, V5, and V6) and diffuse depressed PR segment.

ventricular ejection fraction. No regional wall abnormalities, no significant valve diseases, and no pericardial effusion was observed (Supplementary Video 1).

The patient was later admitted to the coronary care unit; he remained asymptomatic and hemodynamically stable. Chest pain was controlled with intravenous anti-inflammatory drugs (50 mg of dexketoprofen every 8 h) and 0.5 mg of colchicine every 12 h. No more drugs were administered. Forty-eight hours later, the HMPXV infection was confirmed by the Microbiology Department at our hospital. Samples sent for testing included urine and plasma; swabs were taken from a suspected skin lesion, and rectal and pharyngeal samples were collected. A microbiological diagnosis was made by real-time PCR (3). In addition, he was screened for sexually transmitted infections (STIs), including *Chlamydia trachomatis* and *Neisseria gonorrhoeae,* in a pharyngeal swab, a rectal swab, and a first-void urine sample, as well as HBV, HIV, HCV, and syphilis serology, which came back negative.

During admission to the coronary care unit, the Infectious Diseases team monitored the patient, and other potential causes of acute myopericarditis were discarded. Differential diagnoses included viral and bacterial infections, non-infectious causes such as drug abuse, hypersensitivity reactions, and systemic disorders.

Cardiac Magnetic Resonance (CMR) performed on day 6 showed a preserved left ejection fraction (56%) with no regional wall abnormalities. An increased myocardial and pericardial signal intensity on the T2 STIR sequence was suggestive of edema (Figure 2A). On the T1 mapping, an average native T1 of 1,160 ms was observed, and on the T2 mapping, an average T2 of 60 ms was observed. In addition, the quantitative assessment of the cardiac ECV (extracellular volume) was 35%. The T1 and T2 mapping values were measured on a 1.5 Tesla MR Philips machine within a single breath-hold using a modified Look-Locker with inversion recovery (MOLLI) and gradient and spin echo (Gra-SE) sequences, respectively. Normal native myocardial T1 values lie between 1,025 and 1,075 ms, whereas T2 values lie between 50 and 57 ms (internally validated). A color-coded image of T2 mapping (Figure 2B), native T1 (Figure 2C), and enhanced T1 mapping (Figure 2D) were also performed. Late gadolinium enhancement (LGE) images, obtained by using a balanced fast field echo (FFE) sequence, showed subepicardial and mesocardial enhancement of the myocardium and mild signs of pericarditis, which were considered consistent with acute myopericarditis (Figures 3A–D). The patient met all modified Lake Louise criteria for myocarditis: T2 criteria (myocardial edema shown on a T2 STIR sequence and T2 mapping) and T1 criteria (non-ischemic myocardial injury shown on an LGE sequence and T1 mapping). Signs of mild pericarditis were also exhibited.

According to the CMR results, the myocardial injury and inflammatory markers, as well as the remarkable

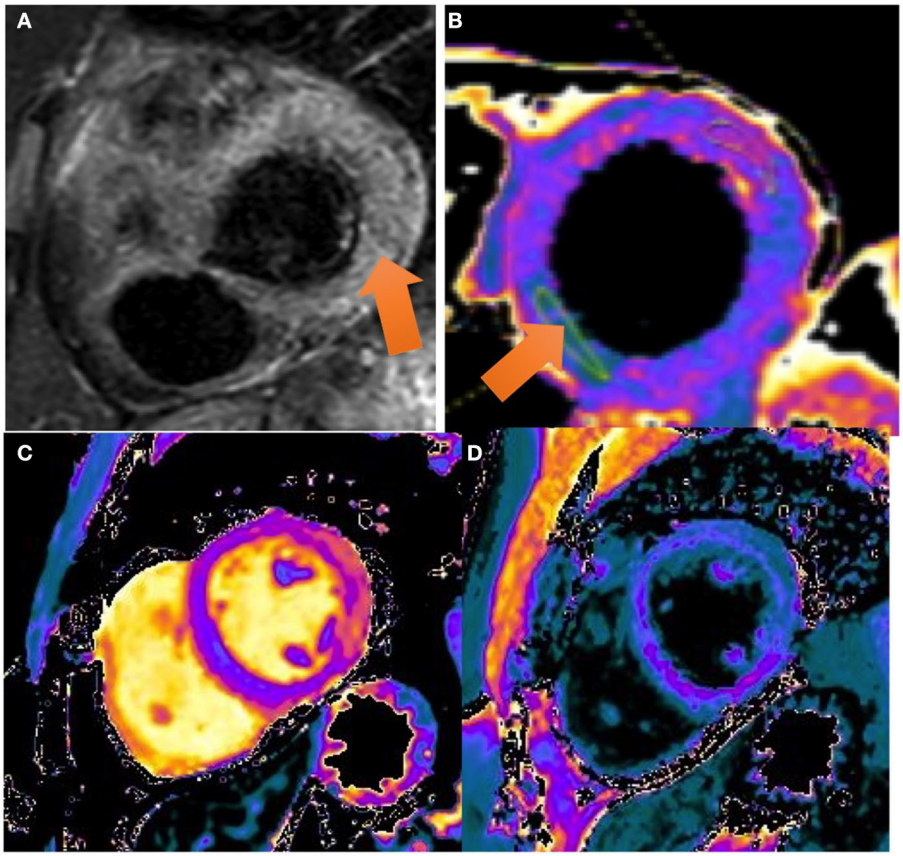

FIGURE 2
CMR images: the balanced FFE (fast field echo) sequences acquired along the short axis **(A, B)** and two chamber **(C)** and four chamber **(D)** views demonstrate myocardial late gadolinium enhancement with epicardial predominance in the lateral and inferior wall and mesocardial predominance in the septum and anterior wall (view arrows).

electrocardiographic findings, supported the diagnosis of acute myopericarditis. Moreover, the temporary association with an active HMPXV infection and ruling out other possibilities of causes of myopericarditis suggested a myopericarditis associated with an *orthopoxvirus* infection. Therefore, a myocardial biopsy or coronariography was not required.

As potential HMPXV infection complications (systemic involvement and myocardial damage) occurred in this patient, requiring hospitalization, tecovirimat was requested from a drug agency. Following the Infectious Diseases Department's instructions, the treatment started 48 h after admission: 600 mg of oral Tecovirimat every 12 h for 14 days. No adverse events were reported. During his stay at the hospital, the previous electrocardiographic findings became normal (Figure 4A), whereas the oropharyngeal lesions increased in size and coalesced into large ulcerations located on both tonsils and the uvula (Figures 4B, C).

After the resolution of the symptoms and the improvement in the inflammatory response and the myocardial injury markers (Table 1), the patient was discharged with close monitoring and follow up by both the Cardiology, Infectious Diseases, and Dermatology departments. The patient's last visit was on 5 October and he had completely recovered. Transthoracic echocardiogram and pharyngeal examination were normal without swollen submandibular adenopathy, and he remained asymptomatic. Pharyngeal samples for HMPXV tested positive on 5 September and 12 September and finally negative on 20 September. A new CMR will be performed 6 months after the episode, approximately on 20 March 2023.

Discussion

We present a case of myopericarditis associated with HMPXV infection treated with tecovirimat. Notably, four cases have been previously published, and only one of them was also treated with antiviral therapy (1, 2, 4–6).

This case reveals four aspects worth highlighting: an atypical clinical presentation, the frequent positive samples for HMPXV from different locations, a well-documented myopericarditis as

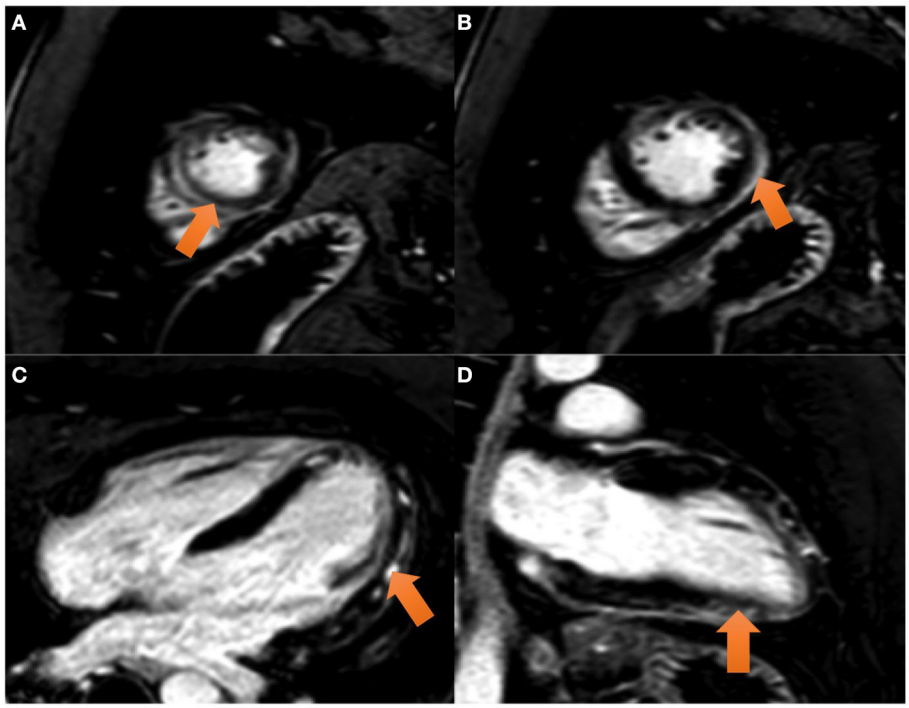

FIGURE 3
CMR images: **(A)** T2 STIR sequence: a high ratio (> 2) is seen in the intensity between the myocardium and the skeletal muscle compatible with a generalized edema. Color-coded image of T2 mapping in LV mid-chamber. The arrow marks an increased T2 value (T2 = 60 ms) in the lateral and inferolateral wall. **(B)** Color-coded image of T2 mapping in LV mid-chamber. The arrow marks an increased T2 value (T2 = 60 ms) in the lateral and inferolateral wall. **(C, D)** T1 mapping and T1 enhanced mapping, respectively. In T1 mapping, extensive area of increased T1 value (view pink and orange areas) in lateral and inferolateral walls. On quantitative analysis, values on the native T1 map were 1,160 ms (normal value 1,025–1,075 ms). In T1 enhanced mapping, these areas area correlated with increased extracellular volume (ECV).

an unusual complication, and the use of tecovirimat with a good clinical course.

The clinical signs of the HMPXV are frequently reported as cutaneous or genital lesions (1, 2). We observed some differences: pharyngeal involvement with large lymphadenopathy was a prominent initial finding, followed by myopericarditis prior to the rare atypical rash with minute pustular lesions.

The detection of HMPXV DNA in a pharyngeal swab sheds light on the transmission mechanisms of the infection, and the positive HMPXV DNA in plasma samples deserves special consideration since it can explain the systemic findings and myocardial involvement.

In this case, the diagnosis of myopericarditis was confirmed by cardiac magnetic resonance following modified Lake Louise criteria. Even though the temporal association does not prove causality, the short span between the onset of the mucocutaneous symptoms and the myocardial damage suggests a pathogenic association. Furthermore, the negative results with real-time PCR regarding other viruses commonly related to myocarditis and oral lesions support this clinical association. As previously mentioned, active viral replication in plasma samples was shown. This strengthens the systemic viral presence and possible heart damage (7, 8). This report highlights myopericarditis as a potential complication of monkeypox and aims to raise clinicians' awareness.

The clinical course of the HMPXV infection has been uniformly benign in most patients (1, 2). An antiviral treatment, tecovirimat, prevents the dissemination of the HMPXV in the host by inhibiting the activity of the orthopoxvirus VP37 envelope-wrapping protein, thereby preventing the formation of competent enveloped virions and virus particles from exiting human cells (9).

Tecovirimat has been recently approved (January 2022) for treating systemic symptoms of the monkeypox infection and is the sole treatment approved by the EMA to date. It may be indicated in severe forms of the disease (myocarditis, encephalitis, and other conditions needing hospital admission), immunocompromised patients, or patients presenting with mucocutaneous lesions with an atypical location and poor pain control (10–12).

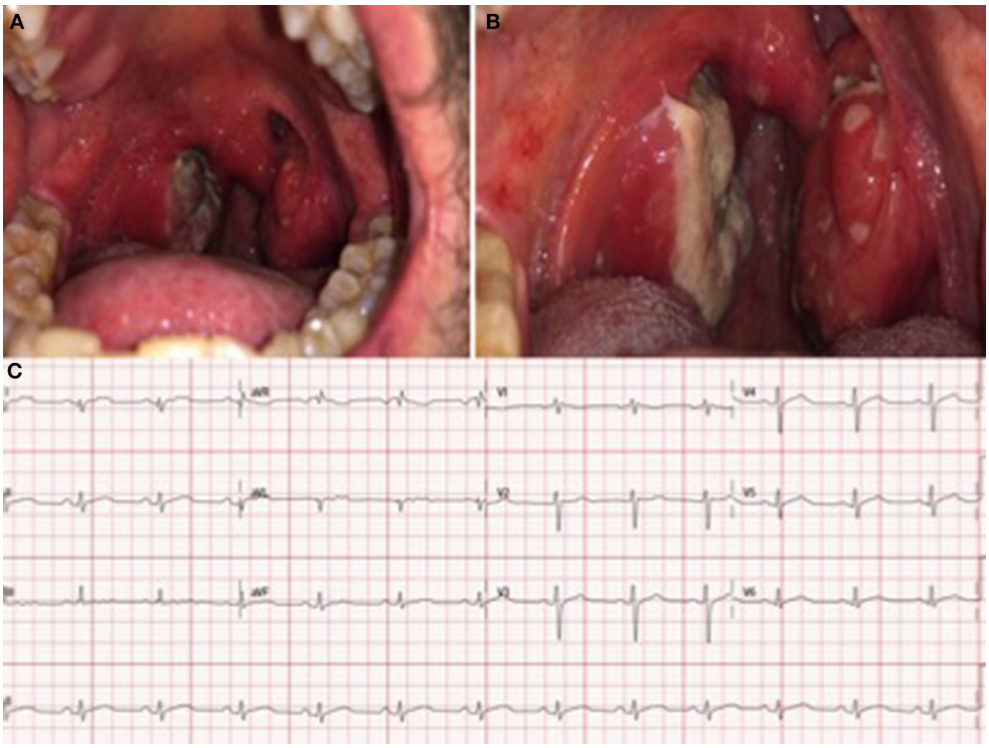

FIGURE 4
(A) Enlargement and coalescence of oral ulcerations on the tonsils and uvula 48 and 96 h after the diagnosis, respectively **(B)**. **(C)** Electrocardiogram at discharge: Sinus rhythm without significant findings.

TABLE 1 Trajectory of biomarkers.

	Day 1	Day2	Day 3	Day 4	Day 6
CRP (mg/l)	84.4	93.9	110.5	74.7	37.6
Tn-I (ng/ml)	20.6	11.8	4.8	0.7	0.1
WBC (10^3/ml)	9.36	9.92	11.10	11.80	11.40
Fibrinogen (mg/dl)	502,10	300	N/A	N/A	N/A
BNP (pg/ml)	<16	N/A	N/A	N/A	N/A

Moreover, although we do not have conclusive evidence on the use of tecovirimat for monkeypox-related myopericarditis, it appears to be safe, as it led to clinical recovery (13, 14).

Limitations

There is a lack of evidence regarding the pathophysiology, mechanisms, and efficacy of available antiviral treatments in HMPXV myopericarditis. These data are still emerging.

According to the available clinical evidence of myopericarditis due to other viral agents, the two most plausible mechanisms by which HMPXV can lead to myocarditis are direct damage to cardiomyocytes due to active replication of *orthopoxvirus* or muscle damage secondary to the autoimmune mechanism by molecular mimicry with viral proteins.

Similarly, previous vaccine studies against smallpox described myopericarditis cases as rare complications after vaccination (15–17). Mechanisms proposed to explain vaccine-related myopericarditis were damage that are directly attributable to the virus as the smallpox vaccine is a live-attenuated virus or an immune-mediated injury vaccine due to immune activation with peaks on days 8–9 (18–20).

The diagnosis of myopericarditis is challenging, but based on the clinical features of fever, chest pain, diffuse upward concave ST elevation, elevated inflammatory markers, the findings in the CMR, and positive *orthopoxvirus* DNA on a plasma sample, the first mechanism is more plausible.

Pathological confirmation of myopericarditis due to monkeypox with cardiac biopsy probably would have contributed to clarifying the diagnosis, but due to its inherent risks and lack of benefit in this patient, it was not pursued.

Conclusions

Here, we present a case of mild myopericarditis with a favorable clinical course, which is consistent with previous reports. Based on our experience, tecovirimat may be beneficial in this setting; however, further research is needed in this field.

Patients perspective

Since his clinical admission, the patient has been involved in all clinical decisions concerning him and is in agreement with all therapeutic methods and different alternatives. He has always been grateful for the treatment he received and was happy to be at the disposal of every scientific contribution.

On 9 September 2022, a reexamination was carried out on the patient's progress and clinical response to tecovirimat. A complete remission of the oral ulcers was observed. The submandibular right lymph node had also been progressively diminishing in size since the third day of starting the treatment with tecovirimat. The health status was excellent; thus, the treatment with tecovirimat was continued for 14 days. We observed no adverse or unanticipated events.

Data availability statement

The raw data supporting the conclusions of this article will be made available by the authors, without undue reservation.

Ethics statement

The patients/participants provided written informed consent to participate in this study.

Author contributions

MAS, ES, AL, SU, MV-G, BR, and MSF wrote this clinical report. JR and MM provided and interpreted CMR images. MSF, SU, AL, MAS, ES, RE, MV-G, BR, PF-G, and JZ offered clinical assistance to the patient. LM performed the real time PCR in plasma. All the authors reviewed the manuscript. All authors contributed to the article and approved the submitted version.

Funding

This research was supported by the CIBER—Consorcio Centro de Investigación Biomédica en Red-(CB21/13/00084), Instituto de Salud Carlos III, Ministerio de Ciencia e Innovación.

Conflict of interest

The authors declare that the research was conducted in the absence of any commercial or financial relationships that could be construed as a potential conflict of interest.

Publisher's note

Supplementary material

The Supplementary Material for this article can be found online at: https://www.frontiersin.org/articles/10.3389/fcvm.2022.1046498/full#supplementary-material

References

1. Thornhill John P, Barkati S, Walmsley S, Rockstroh, Antinori A, Luke B, et al. Monkeypox virus infection in humans across 16 countries April-June 2022. *N Engl J Med.* (2022) 387:679–91. doi: 10.1056/NEJMoa2207323

2. Tarín-Vicente EJ, Alemany A, Agud-Dios M, Ubals M, Suñer C, Antón A, et al. Clinical presentation and virological assessment of confirmed human monkeypox virus cases in Spain: a prospective observational cohort study. *Lancet.* (2022) 400:661–9. doi: 10.1016/S0140-6736(22)01436-2

3. Kurth A, Nitsche A. Detection of human-pathogenic poxviruses. *Methods Mol Biol.* (2011) 665:257–78. doi: 10.1007/978-1-60761-817-1_15

4. Pinho AI, Braga M, Vasconcelos M, Oliveira C, Santos LD, Guimarães AR, et al. Acute myocarditis - a new manifestation of monkeypox infection? *J Am Coll Cardiol Case Rep.* (2022). doi: 10.1016/j.jaccas.2022.08.033

5. Tan DHS, Jaeranny S, Li M, Sukhdeo SS, Monge JC, Callejas MF, et al. Atypical clinical presentation of monkeypox complicated by myopericarditis. *Open Forum Infect Dis.* (2022) 9:ofac394. doi: 10.1093/ofid/ofac394

6. Rodriguez-Nava G, Kadlecik P, Filardo TD, Ain DL, Cooper JD, McCormick DW, et al. Myocarditis attributable to monkeypox virus infection in 2 patients, Unites States, 2022. *Emerg Infect Dis.* (2022) 28:2508–12. doi: 10.3201/eid2812.221276

7. Calaforio AL, Pankuweit S, Arbustini E, Basso C, Gimeno-Blanes J, Felix SB et al. Current state of knowledge on aetiology, diagnosis, management, and therapy of miocarditis: a position Statement of the European Society of Cardiology Working group on Myocardial and Pericardial diseases. *Eur Heart J.* (2013) 34:2636–2648. doi: 10.1093/eurheartj/eht210

8. Ferreira VM, Schulz-Menger J, Holmvang G, Kramer CM, Carbone I, Sechtem U, et al. Cardiovascular magnetic resonance in nonischemic myocardial inflammation: expert recommendations. *J Am Coll Cardiol.* (2018) 72:3158–76. doi: 10.1016/j.jacc.2018.09.072

9. Matias WR, Koshy JM, Nagami EH, Kovac V, Moeng LR, Shenoy ES et al. Tecovirimat for the treatment of human monkeypox: an initial series from Massachusetts, United States. *Open Forum Infect Dis.* (2022) 9:ofac377. doi: 10.1093/ofid/ofac377

10. Sherwart A, T Brooks J, Birnkrant D, Kim P. Tecovirimat and treatment of MPX-Past, present and future considerations. *N Engl J Med.* (2022) 387:579–81. doi: 10.1056/NEJMp2210125

11. Laudisoit A, Tepage F, Colebunders R. Oral tecovirimat for the treatment of smallpox. *N Engl J Med.* (2018) 379:44–53. doi: 10.1056/NEJMoa1705688

12. Desai AN, Thompson GR III, Neumeister SM, Arutyunova AM, Trigg K, Cohen SH. Compassionate use of tecovirimat for the treatment of monkeypox infection. *JAMA.* (2022) 22:e2215336. doi: 10.1001/jama.2022.15336

13. Baker RO, Bray M, Huggins JW. Potential antiviral therapeutics for smallpox, MPX and other Orthopoxvirus infections. *Antiviral Res.* (2003). doi: 10.1016/S0166-3542(02)00196-1

14. Hoy SM. Tecovirimat: first global approval. *Drugs.* (2018) 78:1377–82. doi: 10.1007/s40265-018-0967-6

15. Engler RJM, Nelson MR, Collins LC Jr, Spooner C, Hemann BA, Gibbs BT, et al. A prospective study of the incidence of myocarditis/pericarditis and new onset cardiac symptoms following smallpox and influenza vaccination. *PLoS ONE.* (2015) 10:e0118283. doi: 10.1371/journal.pone.0118283

16. Jacobson IG, Smith TC, Smith B, Wells TS, Reed RJ, Ryan MAK. US Military service members vaccinated against smallpox in 2003 and 2004 experience a slightly higher risk of hospitalization postvaccination. *Vaccine.* (2008) 26:4048–56. doi: 10.1016/j.vaccine.2008.05.044

17. Morgan J, Roper MH, Sperling L, Schieber RA, Heffelfinger JD, Casey CG, et al. Myocarditis, pericarditis, and dilated cardiomyopathy after smallpox vaccination among civilians in the United States, January-October 2003. *Clin Infect Dis.* (2008) 46:S242–50. doi: 10.1086/524747

18. McNalley MC, Qamar Y. Cardiac complications of progressive generalized vaccinia: report of a case. *Dis Chest.* (1966) 49:333–5. doi: 10.1378/chest.49.3.333

19. Bengtsson E, Lundström R. Postvaccinal myocarditis. *Cardiologia.* (1957) 30:1–8. doi: 10.1159/000165631

20. Cohen JI, Hohman P, Fulton R, Turk S-P, Qin J, Thatcher K, et al. Kinetics of serum cytokines after primary or repeat vaccination with the smallpox vaccine. *J Infect Dis.* (2010) 201:1183–91. doi: 10.1086/651453

Appendix

Timeline.

12 August 2022	High-risk sexual contact with a male partner.
16 August 2022	Exploration by a dermatologist due to high-risk sexual contact with a partner. Diagnosed of MPX by reactive polymerase chain reaction assay. Asymptomatic patient. No swabs or samples were taken.
26 August 2022	Odynophagia, fever, right submandibular adenopathy, cervical pain. Swollen tonsils and ulcerative lesions on the right tonsil. Anti-inflammatory drugs and amoxicillin were prescribed.
27 August 2022	Chest pain elevated cardiac markers. Diagnosis of myopericarditis. Anti-inflammatory treatment was initiated, and colchicine was.
28 August 2022	Tecovirimat started.
1 September 2022	Cardiac magnetic resonance was performed. Hospital discharge.
7 September 2022	Blood test. No blood test abnormalities.
9 September 2022	Follow-up by the Infectious Diseases Department. No side effects with tecovirimat. Almost completely recovered. Persistently swollen submandibular adenopathy.
10 September 2022	End of tecovirimat.
18 September 2022	End of quarantine.
20 September 2022	Pharyngeal samples for HPMX were taken on and were negative.
5 October 2022	The patient was fully recovered and asymptomatic.

frontiers | Frontiers in Cardiovascular Medicine

TYPE Case Report
PUBLISHED 25 January 2023
DOI 10.3389/fcvm.2023.1091603

OPEN ACCESS

EDITED BY
Pietro Enea Lazzerini,
University of Siena, Italy

REVIEWED BY
Giuseppe Mascia,
University of Genoa, Italy
Cecilia Castor Praga,
Autonomous University of Nuevo León, Mexico

*CORRESPONDENCE
Aleksandra Milovančev
✉ aleksandra.milovancev@mf.uns.ac.rs
Milovan Petrović
✉ milovan.petrovic@mf.uns.ac.rs

SPECIALTY SECTION
This article was submitted to General Cardiovascular Medicine, a section of the journal Frontiers in Cardiovascular Medicine

RECEIVED 07 November 2022
ACCEPTED 09 January 2023
PUBLISHED 25 January 2023

CITATION
Milovančev A, Miljković T, Ilić A, Stojšić Milosavljević A, Petrović M, Roklicer R, Lakičević N, Trivić T and Drid P (2023) Disrupting arrhythmia in a professional male wrestler athlete after rapid weight loss and high-intensity training—Case report. *Front. Cardiovasc. Med.* 10:1091603. doi: 10.3389/fcvm.2023.1091603

Disrupting arrhythmia in a professional male wrestler athlete after rapid weight loss and high-intensity training—Case report

Aleksandra Milovančev[1,2]*, Tatjana Miljković[1,2], Aleksandra Ilić[1,2], Anastazija Stojšić Milosavljević[1,2], Milovan Petrović[1,2]*, Roberto Roklicer[3], Nemanja Lakičević[4], Tatjana Trivić[3] and Patrik Drid[3]

[1]Faculty of Medicine, University of Novi Sad, Novi Sad, Serbia, [2]Department of Cardiology, Institute of Cardiovascular Diseases of Vojvodina, Sremska Kamenica, Serbia, [3]Faculty of Sport and Physical Education, University of Novi Sad, Novi Sad, Serbia, [4]Sport and Exercise Sciences Research Unit, University of Palermo, Palermo, Italy

Introduction: Physiological heart adaptations may lead to increased susceptibility to arrhythmia in athletes. Furthermore, vigorous training and method like rapid weight loss (RWL) in combat sports could pose additional risks. This case represents how routine cardiovascular screening during high-risk methods like RWL and high-intensity training (HIT) reveal abrupt ventricular arrhythmias in a young athlete.

Case report: We report a case of a 20-year-old male wrestler athlete who developed disrupting arrhythmia during RWL and HIT. The study included: a medical exam, 12 lead electrocardiograms (ECG), transthoracic echocardiogram (ECHO), and 24 h of continuous ECG monitoring in baseline, phase one (P1), (in which the athlete had to simulate RWL through vigorous training and dietary intervention and HIT) and phase two (P2), (with the same HIT protocol performed without the RWL procedure). Baseline laboratory analyses were without abnormalities, ECG showed sinus rhythm with one premature atrial contraction (PAC) and ECHO showed signs of concentric remodeling with preserved systolic, diastolic function, and global longitudinal strain. After P1 RWL simulation, he lost 5.15% of body weight in 3 days, which resulted in lower blood glucose levels, higher urea, creatinine, creatine kinase (CK), CK-MB levels, and slightly increased levels of NT pro-BNP, ECG revealed sinus rhythm with one ventricular premature beat (VPB), 24-h continuous electrocardiogram (ECG) revealed frequent ventricular premature beats (PVB) 2,150/ 24 h, with two couplets, and 8 PAC. After an advised 4-week period of de-training continuous 24 h, ECG monitoring was improved with only occasional PVB. The 24 h continuous ECG monitoring was repeated after HIT and revealed even more frequent PVB, 5% of all beats for 24 h, 4,205 in total, and almost all VPB were in bigeminy and trigeminy. The athlete was advised against RWL and extremely vigorous exercise and for regular, frequent checkups with occasional ECG monitoring during and after exercise.

Conclusion: The short and long-term implication of abrupt ventricular arrhythmias provoked by intensive training and methods like RWL is unknown. We postulate that cardiovascular screening is necessitated, especially during high-risk methods like RWL and HIT, in helping us prevent adverse outcomes and come to individual-based clinical making decisions for each athlete.

KEYWORDS

rapid weight loss, arrhythmia, wrestling, combat athletes, heart, case report

1. Introduction

Wrestling is one of the oldest Olympic sports, with Greco-Roman and freestyle wrestling being internationally recognized as competitive forms of wrestling. As a combat sport, wrestling is exceedingly mentally and physiologically demanding (1). Rapid weight loss (RWL) is highly prevalent in wrestling (2). Many wrestlers engage in RWL before weigh-in, followed by rapid weight gain (RWG) after weigh-in/before a competition to get a real or perceived advantage over their lighter opponents. In terms of combat sports, athletes practicing RWL usually reduce ∼2–10% of their body weight in a time of 1–7 days (3), but in practice, there is no universally applied RWL procedure but rather many variations of the same theme (4). For example, our study reports an athlete who loses more than 5% in 3 days. Methods to induce RWL are similar to those found in other combat sports and are centered around active and passive dehydration, gut content manipulation, and glycogen depletion (2, 5). Concerns about acute health risks from the continued use of RWL have mainly focused on the loss of more than 5% of body mass using extreme dehydration or food deprivation on days 1 or 2 before weigh-in. Health risk that may be caused by RWL depends on various factors, such as the total amount of body mass (BM) reduction, the time for this reduction, and the frequency of episodes and/or strategies used for RWL (6). Despite the documented health risks and consequences that can even lead to death (7), it is still practiced (8).

An athlete's heart physiologically adapts morphology and function to cope with the demands of exercise. These changes pose the risk of different electrical disturbances, which are the main cause of adverse cardiovascular events in athletes (9). Regular medical checkups are usually done in rest or on a treadmill with continuous electrocardiogram (ECG) monitoring. There is a gap in knowledge of whether are there heart rhythm disturbances or myocardial injuries during procedures like RWL or vigorous training.

The aim of this study was to assess the effects of 3-day RWL on rhythm disturbances and biomarkers of myocardial injury in a young male, apparently healthy wrestler. We herein describe a case of a professional wrestler athlete with acute onset of ventricular arrhythmias after RWL and high-intensity training.

2. Case description

2.1. Athlete overview

A professional male wrestler (age 20, height 177.5 cm, weight 77.5 kg) volunteered to participate after providing informed written consent and permission to publish obtained data. A wrestler had 14 years in sport, though last 7 years he has been competing in wrestling, on the national level. He usually performs RWL a couple of times a year, and loses 3–6% of his body weight in 3–5 days. The athlete was without a medical history of previous disorders. The medical exam was performed 7 days before RWL, baseline 12 lead electrocardiogram (ECG) was without abnormalities, transthoracic echocardiogram (ECHO) showed signs of concentric remodeling with preserved systolic, diastolic function, and global longitudinal strain (Table 1). Laboratory analyses were without any abnormalities (Table 2). The experiment protocol was conducted and supervised by assistants and professors of Faculty of Sport and Physical Education, University of Novi Sad. The medical assessment and interpretation were conducted by cardiologists with experience in sports cardiology.

This study was conducted in accordance with the Helsinki declaration. Ethical approval was obtained from the ethics committee of the University of Novi Sad, Novi Sad, Serbia (Ref. No. 46-06-02/2020-1).

2.2. Protocol (dietary, training)

This study included two phases (Figure 1, timeline). Phase one (P1), in which the athlete had to lose 5% of his body in 3 days through vigorous training and dietary intervention. The day of training (testing) was the last day of the RWL period, after which the measurements were performed. In Phase two (P2), the same high-intensity training protocol was performed with no RWL procedure included. The total duration of the training was 90 min. The respondent was familiar with the testing procedure and was instructed to perform the protocol with the same sparring partner on both periods (P1 and P2).

2.2.1. Warm-up

Participant started with a warm-up that consisted of 5 min of foam rolling, followed by 5 min of dynamic stretching. Standard and sport-specific warm-ups were conducted for the next 7 min after which 8 min of gymnastic and acrobatic elements were performed by wrestler (total warm-up time = 25 min).

2.2.2. Testing protocol

The main part of the training consisted of an intensive throwing technique (15 s) interspersed with low-intensity aerobic running (45 s). In fact, the participant initially began a low-intensity circular run (45 s). Five seconds before the throwing part of the test, the respondent was instructed to place himself at a point 9 m away from his sparring partner. At the sound signal, he had to run to his sparring partner as fast as possible and perform the throwing technique. Immediately after the throw, as fast as possible, he had to return to the starting point of 9 m. Participant had to perform at least 4 shoulder throws together with sprints during this period of 15 s. When the throwing part was completed, respondent started a new set of low-intensity running. After the subject completed the set of 10 min, a 3-min break was applied. Four sets of the explained protocol have been realized (total duration of testing protocol = 40 min).

2.2.3. Cool down

At the end of the test protocol, the cool down phase was employed. This phase consisted of 12 min of low-intensity circular running.

2.3. RWL procedure

2.3.1. First day

After the baseline assessment (in the morning) the respondent implemented the following meal and training plan. The subject had one can of tuna for lunch. Furthermore, plenty of fluid during the

10.3389/fcvm.2023.1091603

TABLE 1 Baseline echocardiographic parameters.

Parameters	
LVEDd (mm)	44
LVEDd/BSA (mm/m^2)	22.8
LVEDs (mm)	29
LVEDs/BSA (mm/m^2)	15.03
IVS (mm)	10
PLW (mm)	10
EDV (ml)	90
EDVI (ml/m^2)	46.63
ESV (ml)	36
ESVI (ml/m^2)	18.65
SV (ml)	54
SVI (ml/m^2)	27.98
RWT (mm)	0.45
LVM (g)	156
LVMI (g/m^2)	81
Aortic root (mm)	27
Cuspis separation (mm)	21
Ascending aorta (mm)	29
EF%	60
FS%	34.1
E-wave (m/s)	0.75
A (m/s)	0.5
E/A ratio	1.5
e' sep (cm/s)	0.1
E/e'sep ratio	6.8
e' lat (cm/s)	0.12
E/e' lat ratio	6.25
e'average (cm/s)	0.11
E/e' average	6.82
LAVs (ml)	52
LAVsI (ml/m2)	26.94
GLVS (%)	−18.6
RVEDd (mm)	27
TAPSE (mm)	22
RVSP (mmHg)	29
MR	mild
TR	mild

A, late atrial contraction; E, early wave; E/A ratio, peak early wave to atrial late wave ratio; e'average, average peak early velocity; E/e' average, early wave to average peak early velocity; E/e' sep, early wave to septal peak early velocity; E/e' lat ratio, early wave to lateral peak early velocity; e' lat, lateral peak early velocity; e' sep, septal peak early velocity; E/e' lat ratio, early wave to lateral peak early velocity; EDV-LV, End-diastolic volume; EDVI-LV, End-diastolic volume/ body surface area; EF, ejection fraction; ESV-LV End-systolic volume; ESVI–LV, End-systolic volume/ body surface area; FS, fraction of shortening; GLVS- global left ventricular strain, IVS, inter-ventricular septum, LVHL, left ventricle hypertrophy level, LAVs, left atrium volume at end-systole, LAVsI, left atrium volume index; LVM, left ventricle mass; LVMI, left ventricle mass index, LVEDd, LV end-diastolic diameter, LVEDd/BSA, LV end-diastolic diameter and body surface area ratio; LVEDs, LV end-systolic diameter; LVEDs/BSA, LV end-systolic diameter and body surface area ratio; MR, Mitral regurgitation; PLW, posterolateral wall; RVEDd, Right ventricular End-diastolic diameter; RWT, relative wall thickness; TAPSE, Tricuspid annular plane systolic excursion; TR, Tricuspid regurgitation; SV, Stroke volume; SVI, stroke volume/body surface area.

TABLE 2 Comparison of analyzed baseline P1 and P 2 parameters.

Parameter	Baseline	P1	P2
Body composition			
Body height (cm)	177.5	177.5	177.5
Body mass (kg)	77.7	73.7	77.4
BMI (kg/m^2)	25.2	23.8	25
Fat mass (%)	17.6	13.9	16.7
Muscle mass (%)	41.9	43.9	42.3
Visceral body fat (%)	7	6	7
Basal metabolic rate (kcal)	1,775	1,720	1,768
Laboratory analysis			
GLUC (mmol/l) (4.1–6.1)	6	3.9	5.8
CKI (U/L) (26–100)	226	424	486
MBI (U/L) (7–25)	28	53	19
BUN (mmol/l) (2.5–7.5)	6.8	8.3	4.3
URCA (umol/l) (208–428)	341	484	379
CRE (umol/l) (62–106)	92	100	111
LDI (U/L) (125–220)	210	327	204
AST (U/L) (5–34)	21	39	31
ALT (U/L) (5–55)	40	32	42
S-HS Troponin I (ng/L) (≤10)	10	10	10
S-NT-proBNP (pg/ml) (≤125)	12.1	26.8	8.7
WBC (10^9/L) (4–11)	6.23	22.61	12.77
NEUT (10^9/L) (2–7.6)	2.18	20.28	10.36
LYMPH (10^9/L) (1.32–3.57)	3.18	1.17	1.55
MONO (10^9/L) (0.30–0.82)	0.71	1.14	0.84
EO (10^9/L) (0.04–0.54)	0.15	0.01	0.01
BASO (10^9/L) (0.01–0.08)	0.01	0.01	0.01
RBC (10^{12}/L) (4.50–6.50)	5.38	5.31	5.2
HGB (g/L) (130–170)	158	155	153
HCT (L/L) (0.400–0.540)	0.461	0.448	0.438
MCV (fL) (80.0–100.0)	85.5	84.4	84.2
MCH (pg) (27.0–32.0)	29.4	29.2	29.4

(Continued)

10.3389/fcvm.2023.1091603

TABLE 2 (Continued)

Parameter	Baseline	P1	P2
MCHC (g/L) (320–360)	343	346	349
RDW-SD (fL) (37.0–54.0)	41.2	40.2	40.2
RDW-CV (%) (11.0–16.0)	13.3	13	13.1
PLT (10^9/L) (150–400)	172	202	183
MPV (fL) (6.0-11.0)	9.4	10.3	9.8
PDW (fL) (9.0–17.0)	10.6	11.7	10.3
P-LCR (%) (13.0–43.0)	20.7	26.4	22.8
PCT (L/L) (0.0015–0.0050)	0.0016	0.0021	0.0018

ALT, alanine aminotransferase, AST, aspartate aminotransferase, BASO, basophils; BL, baseline measurement; BMI, body mass index; BUN, blood urea nitrogen, CKI, creatine kinase; CRE- Creatinine, EO, eosinophils; GLUC, blood glucose level; HCT, hematocrit level; HGB, hemoglobin level; LDI, Lactate dehydrogenase; LYMPH, lymphocytes; MBI, creatine kinase-MB isoenzyme; MCH, mean corpuscular hemoglobin; MCHC, mean corpuscular hemoglobin concentration; MCV, mean corpuscular volume; MONO, monocytes; MPV, mean platelet volume; NEUT, neutrophils; P1, phase one (rapid weight loss & high intensity training); P2, phase two (high intensity training); PCT, procalcitonin; PDW, platelet distribution width; P-LCR, platelet-large cell ratio; PLT, platelet; RBC, red blood cells; RDW-CV, range of variation of red blood cell volume that is reported as a part of a standard complete blood count; RDW-SD, differences in the volume and size of red blood cells (standard deviation); S-HS Troponin I, high sensitivity cardiac troponin; S-NT-proBNP, NT-pro B-type Natriuretic Peptide; Potassium, potassium concentration; S-Sodium, sodium concentration; URCA, Uric acid, WBC, white blood cells.

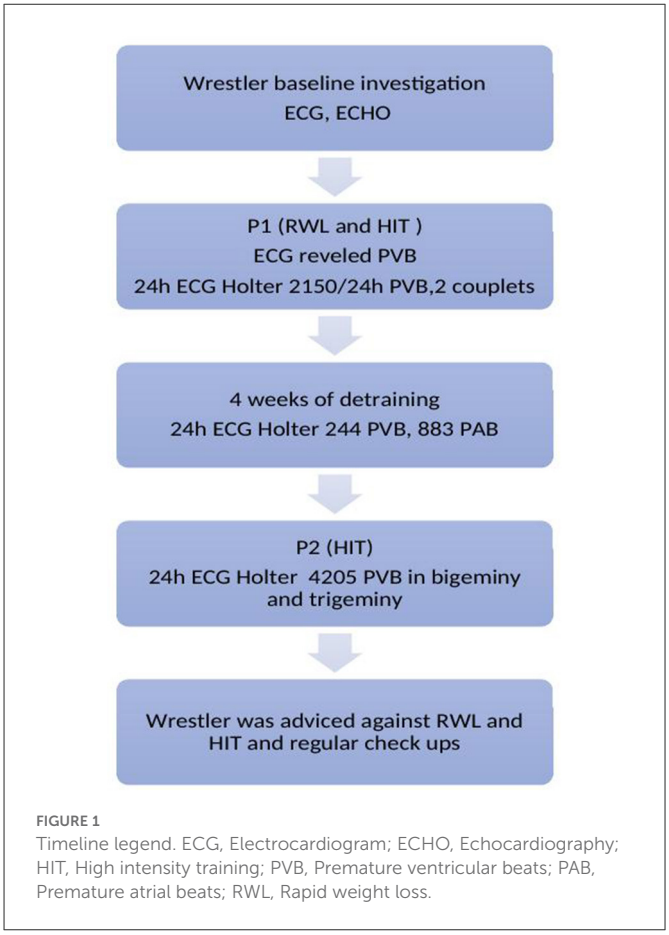

FIGURE 1
Timeline legend. ECG, Electrocardiogram; ECHO, Echocardiography; HIT, High intensity training; PVB, Premature ventricular beats; PAB, Premature atrial beats; RWL, Rapid weight loss.

rest of the day was consumed (lemon and grape juices, and a lot of water ingestion). Prior to the evening training session, participant performed a low intensity activity (active rest) as walking, after which he attended the regular wrestling training session. For dinner, the respondent had a meal consisting of one green apple.

2.3.2. Second day

On the second day, many caffeine rich drinks were consumed. The first beverage in the morning was a cup of green tea. A glass of squeezed ginger, lemon and grape was the second beverage ahead of the morning workout. The training session in the morning included 45 min of low intensity aerobic running. For lunch, the respondent had a meal consisting of slice of fish, half portion of rice, and lettuce. During the afternoon, the subject rested until the evening training session with no more fluid intake on this day. The training session in the evening consisted of low intensity running (45 min of jogging interspersed with gymnastic and acrobatic elements) in a plastic suit (in order to induce extensive sweating). Immediately after the training, the respondent used sauna-—3 sets of 5 min spent in heated environment with 2–5 min break (spending time outside the sauna).

2.3.3. Third day

On the final day, the above explained training session was performed in the morning. No liquids were consumed prior and/or during the test protocol (before the final measurement). 2 h after the procedure, weight measurement and medical assessments (12 lead ECG, ECHO, blood sampling and 24 h continuous ECG monitoring) were carried out. Once the examinations were completed, the respondent was allowed to begin the process of rehydration and food intake. There were no changes in protocol.

3. Results

After P1, the wrestler lost 5.15% of BW in 3 days. Laboratory analyses during the experiment are presented in Table 2. The RWL resulted in lower blood glucose levels and higher urea and uric acid levels as a sign of dehydration and higher levels of AST and LDI. High levels of myocyte enzyme damage (increased CK) were reported after P1 and P2, including MBI after P2. Troponin levels remained the same, but NT pro-BNP was higher after the RWL when compared to baseline and P2. Creatinine levels were increased after P2.

After P1 and P2 complete blood count showed substantially increased leukocytes and neutrophils count, with slightly declined lymphocytes.

Echocardiography after P1 and P2 showed preserved systolic and diastolic function and no signs of ischemia or myocardial injury with preserved left ventricular global longitudinal strain.

Electrocardiograms are presented in Figure 2. Baseline ECG showed sinus rhythm, heart rate (HR) of 52 beats per minute (bpm), and one ectopic premature atrial complex (PAC). After P1, ECG revealed sinus rhythm with one ventricular premature beat (VPB).

10.3389/fcvm.2023.1091603

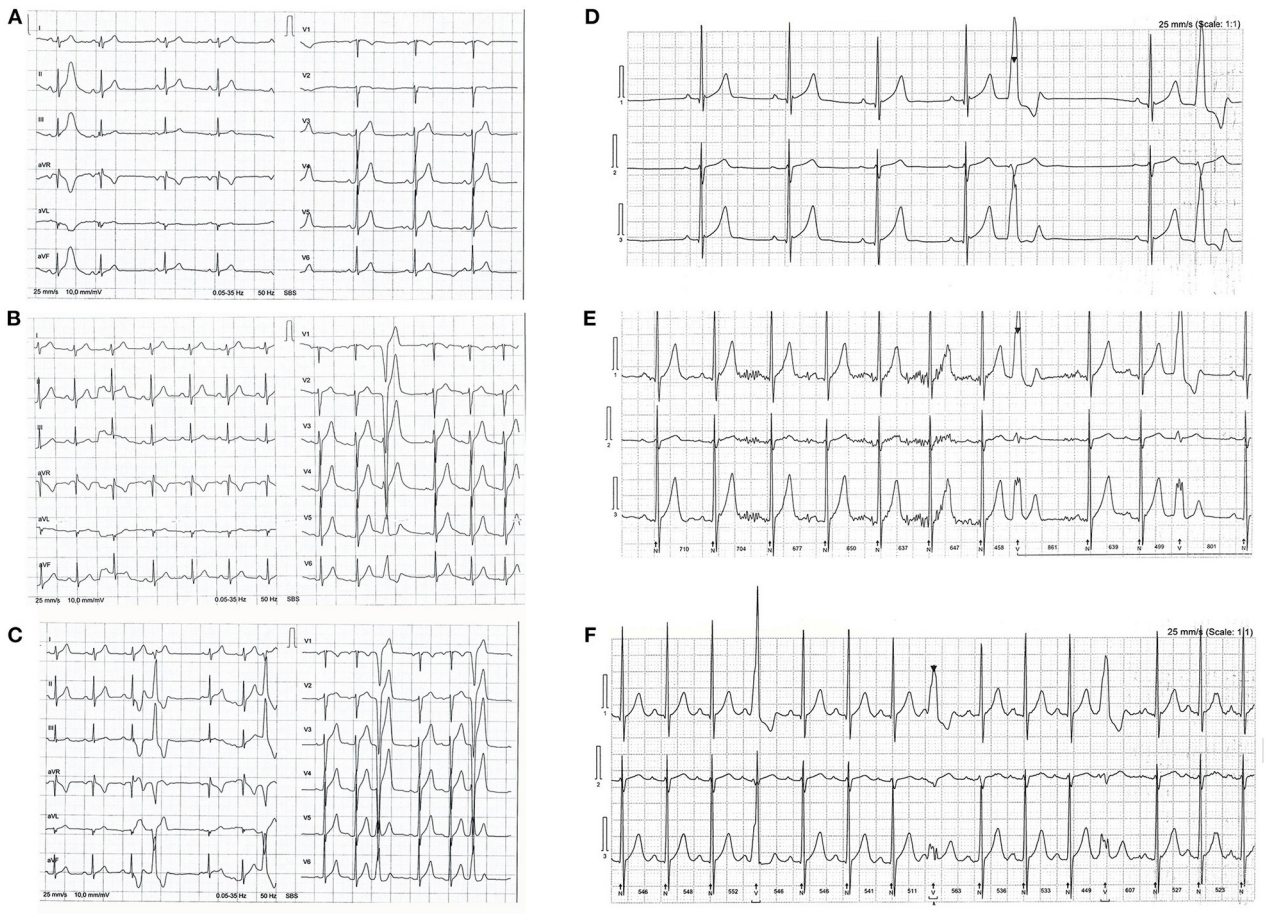

FIGURE 2
(A) Shows a baseline electrocardiogram (ECG). Sinus rhythm and one ectopic premature atrial beat. **(B)** Shows an ECG after P1, phase one (rapid weight loss & high intensity training); sinus rhythm and one ectopic premature ventricular beat (PVB). **(C)** Shows an P2, phase two (high intensity training) ECG with sinus rhythm and PVB in trigeminy. Three lead ECG Holter monitoring after P1 shows ectopic PVB in bigeminy in **(D)** and trigeminy in **(E)**, frequent ectopic PVB after P2 in **(F)**.

Continuous 24 h ECG monitoring revealed the sinus rhythm with an average heart rate HR of 79/ bpm, minimum HR of 46/bpm, and maximal HR of 131/bpm, with frequent 2150 VPB in total for 24 h, with 2 couplets, and 8 PAC. As a therapeutic measure, a period of de-training was recommended. After 4-week period, 24 hours of continuous ECG monitoring revealed practically normal reports: sinus rhythm, average HR 68/bpm, maximal 101/bpm, and minimum 36/bpm, with occasional 244 VPB, 883 PAC, 39 in couplets, 39 times in salvos no longer than 4 beats. After P2, 24 h of ECG monitoring revealed sinus rhythm, maximal HR 126/bpm, min 49/bpm, average 79/min, with even more frequent VPB, 5% of all beats for 24 h, 4205 in total, almost all VPB was in bigeminy and trigeminy. Although the athlete was asymptomatic, he was advised against RWL and extremely vigorous exercise and for regular, frequent checkups with ECG monitoring during and after exercise. On the first check-up after 3 months, he was asymptomatic and engaged in a regular training routine.

4. Discussion

We reported a case of a male wrestler who developed disrupting arrhythmia during RWL and HIT. Physiological adaptation of an athlete's heart might be related to arrhythmic expression, plus certain procedures like RWL and HIT can pose an additional risk. The magnitude of the problem is unknown because there is no regular screening during these procedures.

Problematic RWL practices in wrestling were documented in the scientific literature nearly 100 years ago (10). In the wake of the tragic deaths of young wrestlers in the USA, the conversation around the health and wellbeing of combat sports athletes intensified, and the American College of Sports Medicine (ACSM) published an updated position statement on weight loss in wrestlers (11) while the National Collegiate Athletic Association (NCAA) introduced a Wrestling Weight Certification Program in 1997 (12) in the attempt to prevent extreme weight making in this sport. The newly introduced rules (i) limited weight loss to $\leq$1.5% of body weight per week; (ii) established a minimal competitive weight for each wrestler based on a lower limit of 5% body fat (males); (iii) moved weighins to 1 to 2 h pre-competition; (iv) added 3.2 kg to each weight category limit; (v) banned the use of unsafe RWL methods; (vi) randomized the order of weight class competition (instead of heavier athletes competing later), and (vii) obligated athletes to pass a hydration test (urine specific gravity $\leq$1.020) at the weigh-in.

Features of RWL (mainly ionic disturbances) and high-intensity training (high adrenergic tone, high ventricular wall stress) may

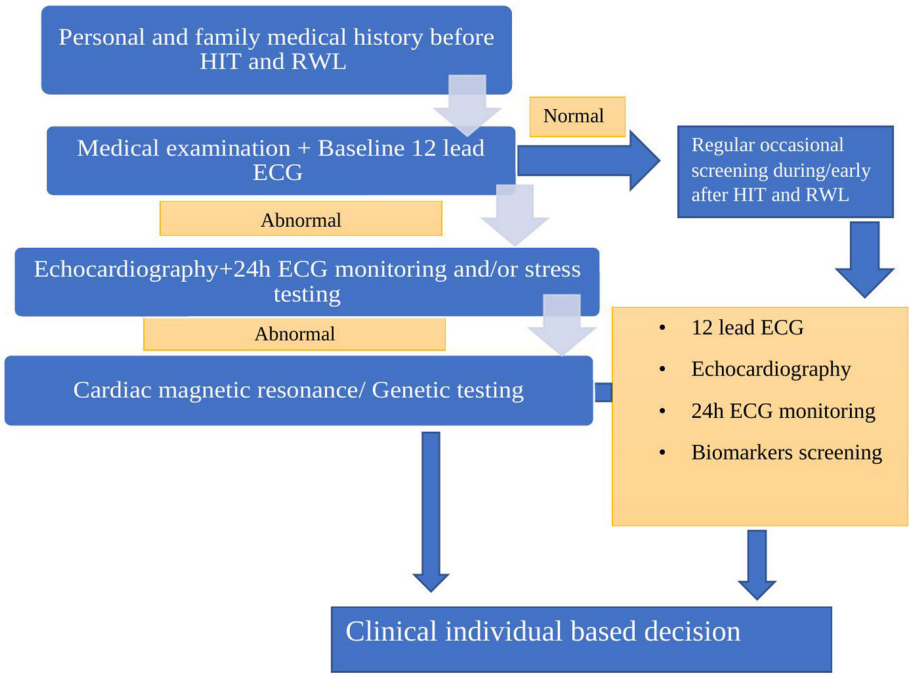

Legend: ECG- Electrocardiogram, HIT-High intensity training, RWL- Rapid weight loss

FIGURE 3
Suggested cardiovascular screening for athletes engaged in HIT and RWL.

predispose ischemia and arrhythmia. The authors (13) found an increase in heart rate observed as higher sympathetic modulation after RWL and concluded a higher cardiovascular risk in athletes as a result of RWL. The features of RWL affect the hemodynamics of the cardiovascular system, provoke plasmatic volume decrease, increase rest heart rate, lowers blood ejection, and finally result in a decreasing capacity to sustain work at a constant rate (11). In our case report athlete has experienced lower blood glucose levels after P1, this could be largely due to significantly lower energy intake during RWL. We can see that glucose levels after P2 are similar to baseline levels. Exercise is known to improve insulin sensitivity, although an increase in catecholamines might result in hyperglycemia just post-intense exercise (14).

Abnormally elevated values of blood urea nitrogen and uric acid were measured after P1. Creatinine is increased after P1 but even more, above the reference range after P2. Creatinine levels may increase after intense exercise as a result of exercise-induced muscle breakdown (15). A systematic review of 10 studies (16) found that creatinine, blood urea nitrogen, and urine-specific gravity values were significantly increased after RWL in the majority of the included studies. In a study by Cicioglu et al. (17) a decrease of −5.30% in total body water was reported after RWL. However, dehydration is present also in prolonged exercise. In a study by Bongers et al. (18) subjects were dehydrated on average 0.6 ± 0.3% and 2.9 ± 0.7% after acute and prolonged exercise, respectively ($p < 0.001$). Dehydration during RWL and subsequent acute kidney damage despite various degrees of weight loss characterize RWL. In addition, strength prolonged exercise accompanied by dehydration activates renin–angiotensin–aldosterone system which in these conditions may result in ischemic kidney injury (19). The estimated glomerular filtration rate significantly decreased after prolonged exercise (18). In another study (20), a significant correlation between creatinine and reduced lean body mass during RWL was observed.

Athlete's exhibited 2-fold increased CK after P1 and almost 3-fold after P2 in addition to elevated MBI above the reference value. CK and LDI are fragments of myosin heavy chain and are related to muscle damage. It is known that intense exercise leads to muscle tissue injury causing CK to be released into the bloodstream (21). Vigorous exercise results in elevations of plasma MBI in a significant proportion of athletes. Increases in these enzymes are not considered to be associated with myocardial injury but rather with muscle damage. Marked increases in CK activity are often associated with an increase in AST associated with higher muscular activity (22).

Troponin levels remained the same, but NT pro-BNP was higher after the RWL when compared to baseline and P2, though did not exceed reference ranges. NT-proBNP are mostly are released from cardiac chambers in response to volume or pressure overload and myocardial strain (23). Elevation in this biomarker can be early marker of imposed stress on myocardium during RWL. But further research in this field is needed.

Physical exercise may affect changes in the immune system. In a study that included 800 healthy young individuals exercise significantly increased white blood cells, segmented neutrophils, band neutrophils, eosinophils and to a lesser extent lymphocytes (24). In a study by Shariat et al. young judoists experienced significant increase in white blood cell count after RWL. Leukocytes after P1 follow 2-fold increase when compared to P2. Psychophysical stress during RWL could contribute to significant increases in cortisol

and testosterone levels, that could additionally increase and mobilize leukocytes during RWL.

Cardiac remodeling poses the risk of increased arrhythmias at the atrial and ventricular levels. The concept of the athlete's heart as a proarrhythmic has been described previously (9). In a large-scale study by Spirito et al. (25), the findings indicated that wrestling has a high impact on LV wall thickness size but a relatively small impact on cavity dimension, suggesting that wrestling has a disproportionate influence on wall thickness relative to cavity dimension, which is comparable with our study results. In a similar fashion, Cohen and colleagues (26) found the left ventricular posterior wall, interventricular septal, and left ventricular internal dimensions to be significantly larger in high school wrestlers who had seasonal variations in the weight of 9% than in non-athletic controls during systole ($p < 0.05$) and diastole ($p < 0.025$). Left ventricular remodeling might promote arrhythmia in these athletes. Continuous vigorous exercise may result in right heart remodeling and cardiac structure and function alteration (27). Sustained volume overload in endurance sports may result in acute right heart chambers dilatation and chronic replacement of the myocardium with fibrotic areas that could be a substrate for ventricular arrhythmias (28). Although wrestling is categorized as a strength sport, many sports include frequently overlap between isotonic and isometric exercise, and thus pose mutual risks. Differentiating physiological responses following sport participation from pathology conditions could be challenging. Characteristics of exercise-induced remodeling may resemble very early features of arrhythmogenic right ventricular cardiomyopathy (ARVC), inherited cardiomyopathy linked to fatal arrhythmias (29), and sometimes it is difficult to differentiate between these two entities (27). In these individuals, cardiac magnetic resonance (CMR) a powerful imaging technique may enhance the evaluation of cardiac structure and function (30) and help in the differentiation between physiological and pathological conditions. In a study evaluating the overlap between typical features of ARVC and sport-related peculiarities by CMR, 16% of young athletes had abnormally increased RV volumes, one of the diagnostic criteria for ARVC. However, the diagnosis of ARVC is complex and involves subsequent diagnostics and fulfillment of the Task Force Criteria (TFC) (31). In a study investigating ventricular arrhythmias in 4,263 athletes, the prevalence of mostly isolated frequent and monomorphic ventricular arrhythmias was 4.19% in a healthy heart without structural cardiomyopathy, with the mean daily number of 1,101 +/−2,693 (range 0–16,678) (32). An increasing number of PVBs, specific morphology (site of origin), and characteristics should raise the red flag for investigation in underlying heart disease. There is no absolute threshold in athletes in the number of PVBs that is used as a cut-off for underlying disease. Biffi (33) et al. found that >2,000 PVCs per day in asymptomatic athletes were associated with a 30% of chance of finding an underlying structural or cardio-genetic disease. A meta-analysis of ten studies found that PVB in the recovery phase of an exercise test, not during exercise, was correlated with a higher risk of adverse cardiovascular events in the long term (34).

In another study, elite athletes with ventricular arrhythmias during exercise had evidence of impaired RV function, myocardial fibrosis, and additional LV contraction abnormalities in life-threatening arrhythmic events. The authors concluded that ventricular arrhythmias are more commonly associated with cardiovascular abnormalities in young competitive and female athletes and if present, they require a thorough investigation and follow-up. They postulated that these phenotypes imitate arrhythmogenic cardiomyopathy and may potentially be provoked by vigorous exercise in susceptible individuals (35).

5. Conclusion

We know that physiological adaptation and heart remodeling can yield the risk of arrhythmia, especially in susceptible individuals, whilst regularly practiced methods like RWL and HIT pose the additional risk that may possibly confer unfavorable prognosis even in asymptomatic individuals. We postulate that cardiovascular screening is necessitated, especially during high-risk methods like RWL and HIT, in helping us prevent adverse outcomes and come to individual-based clinical making decisions (Figure 3).

5.1. Limitations

This study is single case report which *per se* has its limitation as lack of ability to generalize, potential of over interpretation etc. Although the research in this area is scarce, preliminary conclusions and hypothesis that screening is necessitate part of different procedures the athletes is involved may highlight the need for research in this area.

Data availability statement

The original contributions presented in the study are included in the article/supplementary material, further inquiries can be directed to the corresponding authors.

Ethics statement

The studies involving human participants were reviewed and approved by Ethics Committee of the University of Novi Sad, Novi Sad, Serbia (Ref. No. 46-06-02/2020-1). The patients/participants provided their written informed consent to participate in this study. Written informed consent was obtained from the individual(s) for the publication of any potentially identifiable images or data included in this article.

Author contributions

AM, MP, and PD conceived and designed the research. RR, TM, and AI conducted experiments. ASM and TT analyzed data and interpreted the results of the experiments. AM and NL drafted the manuscript and prepared tables. All authors edited and revised the manuscript and approved the final version of the manuscript.

Funding

This work has been supported by the Provincial Secretariat for Higher Education and Scientific Research (142-451-3098).

Acknowledgments

We thank the athlete and all who participated in this experiment.

Conflict of interest

The authors declare that the research was conducted in the absence of any commercial or financial relationships that could be construed as a potential conflict of interest.

Publisher's note

References

1. Chaabene H, Negra Y, Bouguezzi R, Mkaouer B, Franchini E, Julio U, et al. Physical and physiological attributes of wrestlers: an update. *J Strength Cond Res.* (2017) 31:1411–42. doi: 10.1519/JSC.0000000000001738

2. Castor-Praga C, Lopez-Walle JM, Sanchez-Lopez J. Multilevel evaluation of rapid weight loss in wrestling and taekwondo. *Front Sociol.* (2021) 6:637671. doi: 10.3389/fsoc.2021.637671

3. Artioli GG, Saunders B, Iglesias RT, Franchini E. It is time to ban rapid weight loss from combat sports. *Sports Med.* (2016) 46:1579–84. doi: 10.1007/s40279-016-0541-x

4. Khodaee M, Olewinski L, Shadgan B, Kiningham RR. Rapid weight loss in sports with weight classes. *Curr Sports Med Rep.* (2015) 14:435–41. doi: 10.1249/JSR.0000000000000206

5. Alderman BL, Landers DM, Carlson J, Scott JR. Factors related to rapid weight loss practices among international-style wrestlers. *Med Sci Sports Exerc.* (2004) 36:249–52. doi: 10.1249/01.MSS.0000113668.03443.66

6. Artioli GG, Gualano B, Franchini E, Scagliusi FB, Takesian M, Fuchs M, et al. Prevalence, magnitude, and methods of rapid weight loss among judo competitors. *Med Sci Sports Exerc.* (2010) 42:436–42. doi: 10.1249/MSS.0b013e3181ba8055

7. Franchini E, Brito CJ, Artioli GG. Weight loss in combat sports: physiological, psychological and performance effects. *J Int Soc Sports Nutr.* (2012) 9:52. doi: 10.1186/1550-2783-9-52

8. Lakicevic N, Roklicer R, Bianco A, Mani D, Paoli A, Trivic T, et al. Effects of rapid weight loss on judo athletes: a systematic review. *Nutrients.* (2020) 12:1220. doi: 10.3390/nu12051220

9. Heidbuchel H. The athlete's heart is a proarrhythmic heart, and what that means for clinical decision making. *EP Europace.* (2018) 20:1401–11. doi: 10.1093/europace/eux294

10. Kenney HE. The problem of weight making for wrestling meets. *J Health Phys Educ.* (1930) 1:24–49. doi: 10.1080/23267240.1930.10623427

11. Oppliger RA, Case HS, Horswill CA, Landry GL, Shelter AC. American College of Sports Medicine position stand. Weight loss in wrestlers. *Med Sci Sports Exerc.* (1996) 28:ix–xii. doi: 10.1097/00005768-199610000-00049

12. Association NCA. *NCAA Wrestling Weight-Certification Program*. Indianapolis: National Collegiate Athletic Association (1998) 1–32.

13. Nascimento-Carvalho B. do, Mayta MAC, Izaias JE, Doro MR, Scapini K, Caperuto E, et al. Cardiac sympathetic modulation increase after weight loss in combat sports athletes. *Rev Bras Med Esporte.* (2018) 24:413–7. doi: 10.1590/1517-869220182406182057

14. Marliss EB, Vranic M. Intense exercise has unique effects on both insulin release and its roles in glucoregulation: implications for diabetes. *Diabetes.* (2002) 51(Suppl 1):S271–283. doi: 10.2337/diabetes.51.2007.S271

15. Junglee NA, Lemmey AB, Burton M, Searell C, Jones D, Lawley JS, et al. Does proteinuria-inducing physical activity increase biomarkers of acute kidney injury? *Kidney Blood Press Res.* (2012) 36:278–89. doi: 10.1159/000343417

16. Lakicevic N, Paoli A, Roklicer R, Trivic T, Korovljev D, Ostojic SM, et al. Effects of rapid weight loss on kidney function in combat sport athletes. *Medicina.* (2021) 57:551. doi: 10.3390/medicina57060551

17. Cicioglu H, Isik O, Yildirim I, Ünveren A, Karagöz S. The effects of dehydration before competition upon body compositions, leptin hormone and ghrelin hormone among elite wrestlers. *Biomed Res India.* (2017) 28:10.

18. Bongers CCWG, Alsady M, Nijenhuis T, Tulp ADM, Eijsvogels TMH, Deen PMT, et al. Impact of acute versus prolonged exercise and dehydration on kidney function and injury. *Physiol Rep.* (2018) 6:e13734. doi: 10.14814/phy2.13734

19. Roncal-Jimenez C, Lanaspa MA, Jensen T, Sanchez-Lozada LG, Johnson RJ. Mechanisms by which dehydration may lead to chronic kidney disease. *Ann Nutr Metab.* (2015) 66 Suppl 3:10–3. doi: 10.1159/000381239

20. Karila T a. M, Sarkkinen P, Marttinen M, Seppälä T, Mero A, Tallroth K. Rapid weight loss decreases serum testosterone. *Int J Sports Med.* (2008) 29:872–7. doi: 10.1055/s-2008-1038604

21. Baird MF, Graham SM, Baker JS, Bickerstaff GF. Creatine-kinase- and exercise-related muscle damage implications for muscle performance and recovery. *J Nutr Metab.* (2012) 2012:960363. doi: 10.1155/2012/960363

22. Kindermann W. Creatine kinase levels after exercise. *Dtsch Arztebl Int.* (2016) 113:344. doi: 10.3238/arztebl.2016.0344a

23. Sedaghat-Hamedani F, Kayvanpour E, Frankenstein L, Mereles D, Amr A, Buss S, et al. Biomarker changes after strenuous exercise can mimic pulmonary embolism and cardiac injury–a metaanalysis of 45 studies. *Clin Chem.* (2015) 61:1246–55. doi: 10.1373/clinchem.2015.240796

24. Sand KL, Flatebo T, Andersen MB, Maghazachi AA. Effects of exercise on leukocytosis and blood hemostasis in 800 healthy young females and males. *World J Exp Med.* (2013) 3:11–20. doi: 10.5493/wjem.v3.i1.11

25. Spirito P, Pelliccia A, Proschan MA, Granata M, Spataro A, Bellone P, et al. Morphology of the "athlete's heart" assessed by echocardiography in 947 elite athletes representing 27 sports. *Am J Cardiol.* (1994) 74:802–6. doi: 10.1016/0002-9149(94)90439-1

26. Cohen CR, Allen HD, Spain J, Marx GR, Wolfe RW, Harvey JS. Cardiac structure and function of elite high school wrestlers. *Am J Dis Child.* (1987) 141:576–81. doi: 10.1001/archpedi.1987.04460050118044

27. Mascia G, Arbelo E, Porto I, Brugada R, Brugada J. The arrhythmogenic right ventricular cardiomyopathy in comparison to the athletic heart. *J Cardiovasc Electrophysiol.* (2020) 31:1836–43. doi: 10.1111/jce.14526

28. Trivax JE, McCullough PA. Phidippides cardiomyopathy: a review and case illustration. *Clin Cardiol.* (2012) 35:69–73. doi: 10.1002/clc.20994

29. Corrado D, Link MS, Calkins H. Arrhythmogenic right ventricular cardiomyopathy. *N Engl J Med.* (2017) 376:61–72. doi: 10.1056/NEJMra1509267

30. Situ Y, Birch SCM, Moreyra C, Holloway CJ. Cardiovascular magnetic resonance imaging for structural heart disease. *Cardiovasc Diagn Ther.* (2020) 10:361–75. doi: 10.21037/cdt.2019.06.02

31. Marcus FI, McKenna WJ, Sherrill D, Basso C, Bauce B, Bluemke DA, et al. Diagnosis of arrhythmogenic right ventricular cardiomyopathy/dysplasia: proposed modification of the task force criteria. *Eur Heart J.* (2010) 31:806–14. doi: 10.1093/eurheartj/ehq025

32. Tranchita E, Minganti C, Borrione P, Parisi A. Ventricular premature beats prevalence in young Italian athletes: an observational study. *Medicina dello Sport.* (2017) 70:191–9. doi: 10.23736/S0025-7826.17.03141-6

33. Biffi A, Pelliccia A, Verdile L, Fernando F, Spataro A, Caselli S, et al. Long-term clinical significance of frequent and complex ventricular tachyarrhythmias in trained athletes. *J Am Coll Cardiol.* (2002) 40:446–52. doi: 10.1016/S0735-1097(02)01977-0

34. Lee V, Perera D, Lambiase P. Prognostic significance of exercise-induced premature ventricular complexes: a systematic review and meta-analysis of observational studies. *Heart Asia.* (2017) 9:14–24. doi: 10.1136/heartasia-2016-010854

35. Fuchs T, Torjman A, Galitzkaya L, Leitman M, Pilz-Burstein R. The clinical significance of ventricular arrhythmias during an exercise test in non-competitive and competitive athletes. *Isr Med Assoc J.* (2011) 13:735–9.

frontiers | Frontiers in Cardiovascular Medicine

TYPE Case Report
PUBLISHED 26 January 2023
DOI 10.3389/fcvm.2022.1046436

OPEN ACCESS

EDITED BY
Junjie Xiao,
Shanghai University, China

REVIEWED BY
Thomas Theologou,
Istituto Cardiocentro Ticino, Ospedale Regionale di Lugano, Switzerland
Chengming Fan,
Central South University, China

*CORRESPONDENCE
Namakkal S. Rajasekaran
✉ rajnsr@uabmc.edu
Muralidharan Thoddi Ramamurthy
✉ muralidharantr@sriramachandra.edu.in

SPECIALTY SECTION
This article was submitted to General Cardiovascular Medicine, a section of the journal Frontiers in Cardiovascular Medicine

RECEIVED 16 September 2022
ACCEPTED 20 December 2022
PUBLISHED 26 January 2023

CITATION
Thoddi Ramamurthy M, Kumar Balakrishnan V, Sunny S, Rajkumar A, Sundaram S, Krishnamurthy P, Boopathy Senguttuvan N, Murali A, Santhosham JDR, Periandavan K and Rajasekaran NS (2023) Case report: Metastatic myxoid liposarcoma arising from the right atrium extends as cardiac tamponade—A rare case of atrial oncology.
Front. Cardiovasc. Med. 9:1046436.
doi: 10.3389/fcvm.2022.1046436

Case report: Metastatic myxoid liposarcoma arising from the right atrium extends as cardiac tamponade—A rare case of atrial oncology

Muralidharan Thoddi Ramamurthy[1]*, Vinod Kumar Balakrishnan[1], Sini Sunny[2], Abinayaa Rajkumar[3], Sandhya Sundaram[1], Preetam Krishnamurthy[1], Nagendra Boopathy Senguttuvan[1], Arunan Murali[4], J. D. Roy Santhosham[4], Kalaiselvi Periandavan[3] and Namakkal S. Rajasekaran[2,5]*

[1]Department of Cardiology, Sri Ramachandra Medical University and Research Institute, Chennai, Tamil Nadu, India, [2]Division of Molecular and Cellular Pathology, Department of Pathology, University of Alabama at Birmingham, Birmingham, AL, United States, [3]Department of Medical Biochemistry, University of Madras, Taramani Campus, Chennai, Tamil Nadu, India, [4]Department of Radiology, Sri Ramachandra Medical University and Research Institute, Chennai, Tamil Nadu, India, [5]Division of Cardiovascular Medicine, Department of Medicine, University of Utah, Salt Lake City, UT, United States

The reported incidence of liposarcomas in ~2,000 cases annually results in about 30% of myxoid liposarcomas. Cardiac myoxid liposarcomas are very rare; their presentation could be cardiac tamponade, due to direct compression of the tumor and/or pericardial effusion. In this report, we describe a patient who presented with pericardial effusion secondary to myoxid liposarcomas from the right atrium, an extremely rare presentation of liposarcomas in the heart. We also present non-invasive imaging through echocardiography, CECT thorax and FDG PET scans, followed by a CT-guided mass biopsy. Histopathology of the right atrial mass demonstrated myxoid liposarcoma positive for the S100 tumor marker.

KEYWORDS

liposarcoma—diagnosis, cardiac tamponade, right atrium (RA), cardiac tumor diagnosis, FDG (18F-fluorodeoxyglucose)-PET/CT

History of presentation

A 53-year-old woman, with a history of having been hypertensive for 8 years but displaying no prior record of cardiac illness, came to the hospital with complaints of shortness of breath (class IV) for 1 week. This was aggravated 2 days prior to her visit, associated with orthopnea, a dry cough, and a low-grade intermittent fever. On examination, Pulsus paradoxus and Kussmaul's signs were present.

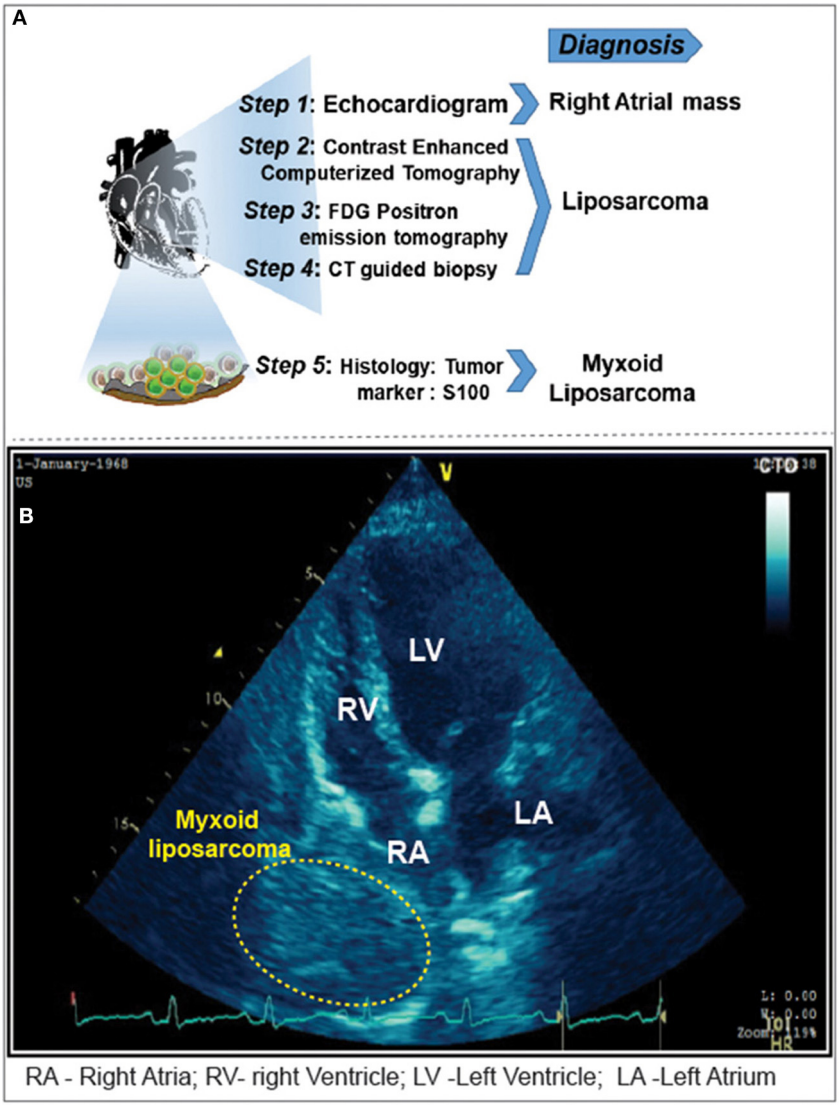

FIGURE 1
(A) Imaging modalities and approaches carried out for the diagnosis of cardiac tamponade. **(B)** Pericardiocentesis followed by 2D-Echocardiogram revealed a 5 x 4 cm sized mass adjacent to the right atrium. Yellow highlighted area locates the myxoid liposarcoma in the right atrium.

Medical history

The ECG showed sinus tachycardia with non-specific ST-T changes. Moreover, the echocardiogram showed massive pericardial effusion with features suggestive of cardiac tamponade and homogenous mass adjacent to the right atrium (Figures 1A, B). Emergency pericardiocentesis was done, and hemorrhagic pericardial fluid was sent for analysis. The patient became asymptomatic; a chest roentgenogram revealed bilateral minimal pleural effusion. Anti-tuberculous treatment was initiated, given the high suspicion of tuberculosis and mildly raised adenosine deaminase levels in the pericardial fluid sample.

CECT thorax (Figures 2A, B) revealed minimally enhancing mass lesion in the right atrial wall with a small intraluminal component projecting into the right atrial chamber, with multiple enlarged retroperitoneal lymph nodes. As it was initially suspected to be lymphoma, a PET CT scan (Figures 2C–F) was performed to rule out metastasis, which showed mildly FDG-avid hypodensity along the lateral wall of the right atrium with mass effect over it.

Abbreviations: CECT, contrast enhanced computerized tomography; FDG–PET, fluoro deoxy glucose—positron emission tomography; PET–CT scan, positron emission tomography—computed tomography.

10.3389/fcvm.2022.1046436

Investigations

CT-guided biopsy from the right atrial mass was subjected to histopathological examination. The findings revealed the presence of myxoid liposarcoma (Figure 3A). The histological findings were further confirmed by tumor markers Pan CK and S100, denoting that the sample stained positive for S100 (Figures 3A, B).

Management

Anti-tuberculous treatment was terminated. The case was discussed on the tumor board and a decision to obtain a biopsy from the mesenteric lymph node adjacent to the left iliac artery with laparoscopic assistance was made. However, the patient and her family were not in agreement; hence, she was discharged against medical advice.

Discussion

Primary cardiac tumors are rare (1–3), found in about 0.001–0.3% of autopsies performed (4–6). Exact incidence of these tumors are unknown or not reported, but 1 in 500 cardiac surgical cases found to have primary cardiac tumors, out of which 75% are benign and about 25% are malignant (7, 8). Of these malignant tumors, around 75% are sarcomas (4, 9). Cardiac sarcoma is classified into right heart sarcomas, left heart sarcomas, and pulmonary artery sarcomas (10). Right heart sarcomas are generally bulkier, exophytic, infiltrate easily, remain asymptomatic, and cause heart failure belatedly and metastasize earlier (11). Therefore, the clinical diagnosis is challenging. The heart is an unusual site for liposarcoma and very few cases of metastatic primary cardiac sarcomas have been reported to date. WHO classification was proposed in 2004 for cardiac tumors (12). This may arise in either of the atria, but also from ventricles and the pericardium. Pericardial involvement may manifest as pericardial effusion or irregular nodules over pericardium (13, 14).

Non-invasive imaging plays a critical role in the diagnosis and surgical interventions of cardiac tamponade (15). Although echocardiography is a simple non-invasive method for cardiac mass evaluation, the area of tissue that could be covered using standard transducers may not be sufficient to assess the extent of the tumor mass (16). In the present case, our multimodal approach involving FDG PET scan followed by CT-guided biopsy facilitated the accurate assessment of size, location, depth of infiltration, and lesion margins of cardiac mass. Histopathology (H&E) of liposarcomas showed a traditional myxoid pattern of the matrix, round lipoblast cells with a hyperchromatic nucleus in the periphery. These cells had scanty cytoplasm, displaced by clear, large lipid droplets appearing as signet-ring shapes. Immunohistochemistry confirmed the S100, a known marker of malignant cells (17, 18). Thus, we recommend the use of an FDG-PET scan followed by histological analysis for the evaluation of size, morphology, tissue characteristics, and clinical correlation of cardiac masses.

Even though there are more innovations in diagnosis (19), the imaging characteristics of myxoid liposarcomas remain inconclusive. Usually, the malignancy tends to arise in atria as a large infiltrating mass; in time, it infiltrates into the ventricles and pericardium. Usually, the pericardium is the most vulnerable site for effusion and tumor nodules (14). While the exact cause of liposarcoma is unclear, variation in arterial pressure, genetic mutations in adipocytes,

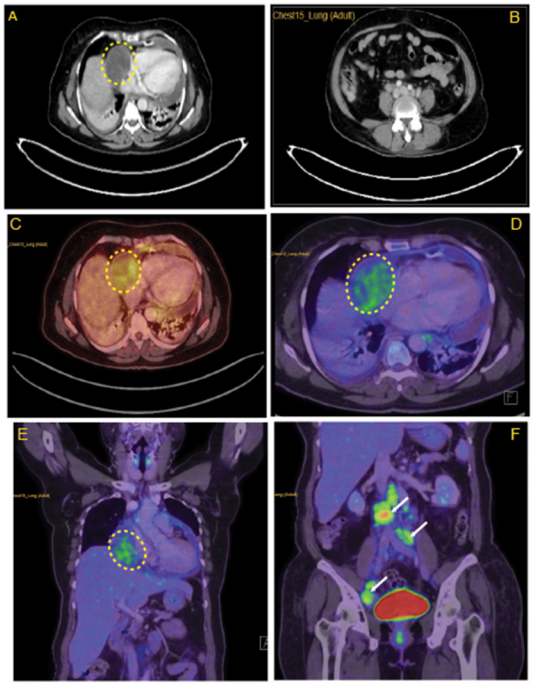

FIGURE 2
Lymph node characteristics in the right atrium. **(A)** CECT thorax revealing minimally enhancing mass lesion in the right atrial wall. **(B)** Multiple enlarged retroperitoneal lymph nodes. **(C)** Horizontal sections of FDG PET scan revealing mildly FDG avid hypodensity (5.8 × 5 cm, SUV max −3.40) along the lateral wall of the right atrium with mass effect over it. **(D)** Coronal section of FDG PET scan revealing mildly FDG avid mass over the lateral wall of the right atrium. **(E)** Enlarged FDG avid lymph nodes at perivascular, aortocaval, retrocaval, and bilateral common iliac and external iliac levels **(F)**. Yellow highlighted area locates the myxoid liposarcoma in the right atrium. White arrows in **(F)** indicates metastasis in abdomen areas.

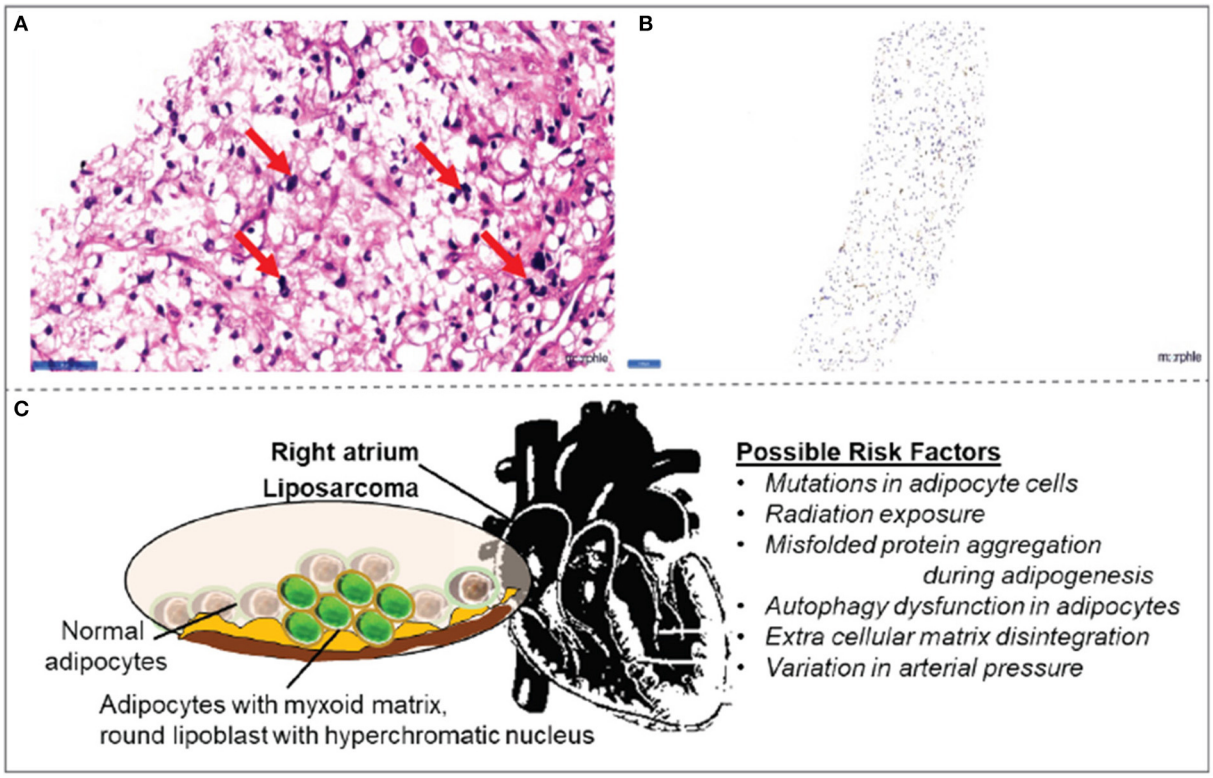

FIGURE 3
Histopathology observations in right atrial mass **(A)** biopsy collected from right atrial mass demonstrated signet-ring-shaped lipoblasts in mucoid matrix suggestive of myxoid liposarcoma. **(B)** The tumor cells are positive for the S100 tumor marker. **(C)** Schematic illustration of possible risk factors associated with myxoid liposarcomas in the right atrium.

misfolded protein aggregation during adipogenesis, autophagy dysfunction, and extracellular matrix disintegration are likely to be the molecular mechanisms of the pathology (Figure 3C). In the present case, cardiac tamponade was characterized by pericardial effusion occurring in the right atrium. Of note, the myxoid liposarcoma is positive for S100 tumor markers even in the atrium itself, without any signs of infiltration to ventricles, a very rare occurrence.

Diagnosing myxoid liposarcomas remains a challenge (20, 21). Imaging modalities like echocardiography, cardiac MRI, and CT scans are extremely useful tools for identifying these tumors. FDG-PET scan is the newly evolved tool to diagnose both the tumor and metastasis (22, 23). In this case, we progressed schematically using an echocardiogram for diagnosing cardiac tamponade along with right atrial mass, then imaging with CECT thorax and FDG-PET scan, followed by CT-guided biopsy of the mass. There are limited data and guidelines for the diagnosis and treatment of this rare condition. Total or partial surgical resection may rarely benefit for patients with cardiac tumors. Here, since the sarcoma invaded the whole right atrium of the patient at the time of first hospitalization, a surgical resection or reconstruction was unlikely. However, because the patient was discharged against medical advice, there was no follow-up due to loss of communication.

Data availability statement

The raw data supporting the conclusions of this article will be made available by the authors, without undue reservation.

Ethics statement

The studies involving human participants were reviewed and approved by CSP-MED/20/FEB/59/53 DATED 07.03.2020. The patients/participants provided their written informed consent to participate in this study. Written informed consent was obtained from the individual(s) for the publication of any potentially identifiable images or data included in this article.

Author contributions

MTR and NSR contributed to the intellectual content and revised the manuscript. VK drafted the manuscript. VK and NB were responsible for acquisition and interpretation of the data. SSunn and AR reconstructed the images, prepared the legends, and updated the literature. SSund and PK reviewed the histology data and interpreted the results. JS was responsible for acquisition of CT biopsy. AM performed and interpreted PET scanning. All authors made substantial contribution to the preparation of the manuscript, as well as read and approved the final version of the manuscript.

Acknowledgments

We thank Snekha N. Rajasekaran for language editing. Department of Pathology and School of Medicine at University of Alabama at Birmingham (UAB) provided travel support to NSR (PATH-MCP#3111315-PDF#2085) for this collaborative research.

Conflict of interest

The authors declare that the research was conducted in the absence of any commercial or financial relationships that could be construed as a potential conflict of interest.

Publisher's note

References

1. Silverman N. Primary cardiac tumors. *Ann Surg.* (1980) 191:127. doi: 10.1097/00000658-198002000-00001

2. Maraj S, Pressman GS, Figueredo VM. Primary cardiac tumors. *Int J Cardiol.* (2009) 133:152-6. doi: 10.1016/j.ijcard.2008.11.103

3. Simpson L, Kumar SK, Okuno SH, Schaff HV, Porrata LF, Buckner JC, et al. Malignant primary cardiac tumors: review of a single institution experience. *Cancer.* (2008) 112:2440–6. doi: 10.1002/cncr.23459

4. Reardon MJ, DeFelice CA, Sheinbaum R, Baldwin JC. Cardiac autotransplant for surgical treatment of a malignant neoplasm. *Ann Thorac Surg.* (1999) 67:1793–5. doi: 10.1016/S0003-4975(99)00343-4

5. Patel J, Sheppard MN. Pathological study of primary cardiac and pericardial tumours in a specialist UK Centre: surgical and autopsy series. *Cardiovasc Pathol.* (2010) 19:343–52. doi: 10.1016/j.carpath.2009.07.005

6. Yanagawa B, Chan EY, Cusimano RJ, Reardon MJ. Approach to surgery for cardiac tumors: primary simple, primary complex, and secondary. *Cardiol Clin.* (2019) 37:525–31. doi: 10.1016/j.ccl.2019.07.001

7. Blackmon SH, Reardon MJ. Surgical treatment of primary cardiac sarcomas. *Texas Heart Inst J.* (2009) 36:451.

8. Reardon MJ, Walkes J-C, Benjamin R. Therapy insight: malignant primary cardiac tumors. *Nat Clin Pract Cardiovasc Med.* (2006) 3:548–53. doi: 10.1038/ncpcardio0653

9. Orbach D, Rey A, Oberlin O, Toledo JSd, Terrier-Lacombe MJ, Unnik Av, et al. Soft tissue sarcoma or malignant mesenchymal tumors in the first year of life: experience of the international society of pediatric oncology (SIOP) malignant mesenchymal tumor committee. *J Clin Oncol.* (2005) 23:4363–71. doi: 10.1200/JCO.2005.12.009

10. Blackmon SH, Patel A, Reardon MJ. Management of primary cardiac sarcomas. *Expert Rev Cardiovasc Ther.* (2008) 6:1217–22. doi: 10.1586/14779072.6.9.1217

11. Ramlawi B, Leja MJ, Saleh WKA, Al Jabbari O, Benjamin R, Ravi V, et al. Surgical treatment of primary cardiac sarcomas: review of a single-institution experience. *Ann Thorac Surg.* (2016) 101:698–702. doi: 10.1016/j.athoracsur.2015.07.087

12. Amano J, Nakayama J, Yoshimura Y, Ikeda U. Clinical classification of cardiovascular tumors and tumor-like lesions, and its incidences. *Gen Thorac Cardiovasc Surg.* (2013) 61:435–47. doi: 10.1007/s11748-013-0214-8

13. Lococo F, Cesario A, Meacci E, Vita L, Porziella V, Margaritora S, et al. Huge primary pericardial liposarcoma. *Thorac Cardiovasc Surg.* (2011) 59:172–3. doi: 10.1055/s-0030-1250187

14. Wang J-G, Wei Z-M, Liu H, Li Y-J. Primary pleomorphic liposarcoma of pericardium. *Interact CardioVasc Thorac Surg.* (2010) 11:325–7. doi: 10.1510/icvts.2010.239723

15. O'Connor MJ. Imaging the itis: endocarditis, myocarditis, and pericarditis. *Curr Opin Cardiol.* (2019) 34:57–64. doi: 10.1097/HCO.0000000000000577

16. Sinagra G, Merlo M, Pinamonti B. *Dilated Cardiomyopathy: From Genetics to Clinical Management.* (2019). doi: 10.1007/978-3-030-13864-6

17. Salama I, Malone P, Mihaimeed F, Jones JL. A review of the S100 proteins in cancer. *Eur J Surg Oncol.* (2008) 34:357–64. doi: 10.1016/j.ejso.2007.04.009

18. Gaynor R, Irie R, Morton D, Herschman H, Jones P, Cochran A. S100 protein: a marker for human malignant melanomas? *Lancet.* (1981) 317:869–71. doi: 10.1016/S0140-6736(81)92142-5

19. Abaricia S, Hirbe AC. Diagnosis and treatment of myxoid liposarcomas: histology matters. *Curr Treat Opt Oncol.* (2018) 19:1–13. doi: 10.1007/s11864-018-0590-5

20. Narendra S, Valente A, Tull J, Zhang S. DDIT3 gene break-apart as a molecular marker for diagnosis of myxoid liposarcoma—assay validation and clinical experience. *Diagn Mol Pathol.* (2011) 20:218–24. doi: 10.1097/PDM.0b013e3182107eb9

21. Anderson WJ, Jo VY, editors. Pleomorphic liposarcoma: updates and current differential diagnosis. *Semin Diagn Pathol.* (2019) 36:122–8. doi: 10.1053/j.semdp.2019.02.007

22. Paydary K, Seraj SM, Zadeh MZ, Emamzadehfard S, Shamchi SP, Gholami S, et al. The evolving role of FDG-PET/CT in the diagnosis, staging, and treatment of breast cancer. *Mol Imaging Biol.* (2019) 21:1–10. doi: 10.1007/s11307-018-1181-3

23. Almuhaideb A, Papathanasiou N, Bomanji J. 18F-FDG PET/CT imaging in oncology. *Ann Saudi Med.* (2011) 31:3–13. doi: 10.4103/0256-4947.75771

frontiers | Frontiers in Cardiovascular Medicine

TYPE Case Report
PUBLISHED 03 February 2023
DOI 10.3389/fcvm.2023.1110269

OPEN ACCESS

EDITED BY
Gian Marco Rosa,
San Martino Hospital (IRCCS), Italy

REVIEWED BY
Guorong Lyu,
The Second Affiliated Hospital of Fujian Medical University, China
Kun Sun,
Shanghai Jiao Tong University, China

*CORRESPONDENCE
Zaiwang Zhang
✉ zhangzaiwang666@sohu.com
Wei Li
✉ 1546529103@qq.com

†These authors have contributed equally to this work and share first authorship

SPECIALTY SECTION
This article was submitted to General Cardiovascular Medicine, a section of the journal Frontiers in Cardiovascular Medicine

RECEIVED 28 November 2022
ACCEPTED 13 January 2023
PUBLISHED 03 February 2023

CITATION
Wu Y, Cai Z, Cheng J, Zhang B, Wang G, Li W and Zhang Z (2023) An adult female patient with single atrium and single ventricle undergoing appendectomy: A case report. *Front. Cardiovasc. Med.* 10:1110269. doi: 10.3389/fcvm.2023.1110269

An adult female patient with single atrium and single ventricle undergoing appendectomy: A case report

Yu Wu[1†], Zenghua Cai[1†], Jianzheng Cheng[1†], Bo Zhang[2], Guoji Wang[1], Wei Li[2*] and Zaiwang Zhang[1*]

[1]Department of Anesthesiology, The 980th Hospital (Bethune International Peace Hospital) of the Joint Logistic Support Force, Shijiazhuang, China, [2]Department of General Surgery, The 980th Hospital (Bethune International Peace Hospital) of the Joint Logistic Support Force, Shijiazhuang, China

Appendicitis is one of the common diseases, and appendectomy is one of the most commonly performed procedures. Single atrium and single ventricle are rare heart diseases, and very few patients survive to adulthood. We report a patient with single atrial and single ventricles undergoing appendectomy with transverse abdominis plane block and dexmedetomidine sedation anesthesia with smooth postoperative appendectomy.

KEYWORDS

appendicitis, single atrium and single ventricle, adult patient, anesthesia, low metabolic equivalent

Introduction

Appendicitis is one of the most common surgical emergencies and appendectomy is one of the most commonly performed surgical procedures. The annual incidence of acute appendicitis (90–100)/100,000 people in developed countries are reported in the literature (1), about 50,000 appendectomies are performed annually in the UK and 300,000 in the USA (2). Chronic inflammatory lesions of the appendix, such as hyperplasia of the fibrous connective tissue of the duct wall, narrowing or occlusion of the duct lumen, distortion of the appendix, and adhesions to the surrounding tissues evolve into chronic appendicitis after acute appendicitis intervention or self-healing, which can reoccur or have multiple acute attacks.

Case present

We now report a female patient, 20 years old, 44 Kg, with recurrent intermittent lower abdominal pain for more than 2 years, with exacerbation occurring 3 times, which improved significantly with interventions such as anti-inflammatory treatment when symptoms appeared. Half a month ago the symptoms reappeared and the patient was hospitalized for surgical treatment (**Figure 1**).

The patient had a history of cyanotic since birth and low activity tolerance. Due to the poor economic conditions, the family could not pay the bills in the early years. As she grew up, the best chance to cure her illness has been lost. Comprehensive consideration,

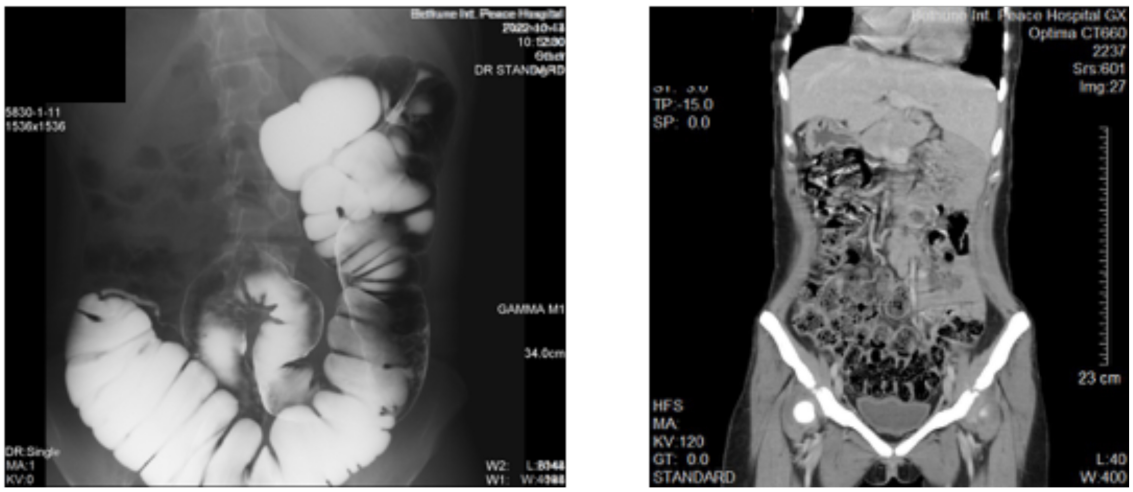

FIGURE 1
Imaging images of the patient's abdomen. **(Left)** Barium examination. **(Right)** Full abdominal CT scan.

she has not received surgical intervention. At the present, her metabolic equivalent (MET) was 4.0 [1 MET = 3.5 ml/(kg·min) of oxygen consumption] (3), and New York Heart Association Classification was Grade III. Electrocardiogram: sinus rhythm; P-wave peak, bimodal and widened; right-sided electrical axis, cis-clockwise transposition; RavR > 0.5 mV; right ventricular high voltage; ST-T abnormalities. Echocardiogram: (1). Her heart is located on the left side of the chest. Single ventricular end-diastolic volume was 63 ml, single ventricular end-systolic volume was 28 m1, and ejection fraction was 56%. The transverse diameter of the single atrium was about 50 mm, and the transverse diameter of the single ventricle was about 42 mm; (2). Muscular stenosis of the funnelus with an internal diameter of 1.6 mm, CDFI: flow rate of 376 cm/s, a pressure difference of 57 mmHg; Pulmonary valve thickened with a limited opening, annular diameter 10.2 mm, proximal aortic diameter 8.2 mm, distal aortic diameter 13.3 mm, CDFI: pulmonary artery opening velocity 327 cm/s, differential pressure 43 mmHg, moderate aortic regurgitation (3). Only one set of atrioventricular echoes could be detected, CDFI: flow rate of 436 cm/s, residence difference of 76 mmHg, moderate atrioventricular valve reflux (**Figure 2**).

Her oxygen saturation in room air (SpO2) was 72%, hemoglobin was 209 g/L, red blood cells were $8.84 \times 10^{\wedge 12}$/L, prothrombin time was 15.2 s, prothrombin activity was 65%, international normalized ratio (INR) was 1.35, total bilirubin was 60.8 umol/L, direct bilirubin was 9.2 umol/L, and other hematologic and biochemical tests were approximate. After a week of anti-inflammatory treatment to control the appendiceal inflammation, an open appendectomy under the left side's transverse abdominal plane nerve block was proposed according to the patient's wishes.

The patient was fasted for 8 hours and admitted to the operating room, where she was monitored for rhythm, heart rate, blood pressure, pulse oximetry, and arterial blood gas analysis followed by face mask oxygenation to improve oxygenation. The patient's arterial blood gas analysis on admission showed: pH 7.363, PCO_2 36.4 mmHg, PO_2 39 mmHg, BEecf −5 mmol/L, HCO_3 20.7 mmol/L, TCO_2 22 mmol/L, sO_2 72%; after 10 min of oxygenation: pH 7.356, PCO_2 37.2 mmHg, PO_2 50 mmHg, BEecf −5 mmol/L, HCO_3 20.8 mmol/L, TCO_2 22 mmol/L, sO_2 84%; meanwhile, her venous blood gas analysis showed: pH 7.353, PCO_2 37.3 mmHg, PO_2 48 mmHg, BEecf −5 mmol/L, HCO_3 20.8 mmol/L, TCO_2 22 mmol/L, sO_2 81%. A left transversus abdominis plane block was performed with 20 ml of 0.125% ropivacaine under ultrasound guidance. After the patient's sensation in the left lower abdomen was different from that in the right lower abdomen, the general surgeon used 0.5% lidocaine for local injection and intravenous pumping of dexmedetomidine 0.2 ug/kg/h. After the patient's local abdominal wall sensation disappeared, the abdominal cavity was opened layer by layer by incision, and the blind end of the appendix was carefully searched for with long forceps and removed without any obvious adverse sensation during the operation. The operation lasted 45 min, 200 ml of Ringer's fluid was infused, and bleeding was about 10 ml (**Figure 3**).

Discussion

The patient's multiple appendicitis episodes severely affected her daily life and became another significant burden for her co-morbid heart disease. Although theoretically, this appendicitis could still be relieved with medications and other interventions, the patient's desire for surgery was strong and we respected the patient's wishes to finalize our treatment decisions with a patient-centered approach (4). Recurrence after conservative treatment of acute appendicitis is also a concern for both physicians and patients. The APPAC trial with a 72.7% success rate of conservative treatment was reported to have a recurrence rate of 27.3, 34.0, 35.2, 37.1, and 39.1% at 1–5 years after 5 years of follow-up (5). The recurrence rate in real-world studies may be lower. Data from the National Health Insurance in Taiwan, China showed that 15.1% of nearly 240,000 first-time hospitalizations for acute appendicitis received non-surgical treatment, with an average follow-up of 6.5 years and 7.1% of recurrences (6). 1.5% of nearly 240,000 cases of uncomplicated acute appendicitis in 11 years were treated non-operatively, 5.9% failed, and

Abbreviations: UK, United Kingdom; USA, United States of America; MET, metabolic equivalent; CDFI, color doppler flow imaging; INR, international normalized ratio; APPAC trial, appendicitis acuta trial.

10.3389/fcvm.2023.1110269

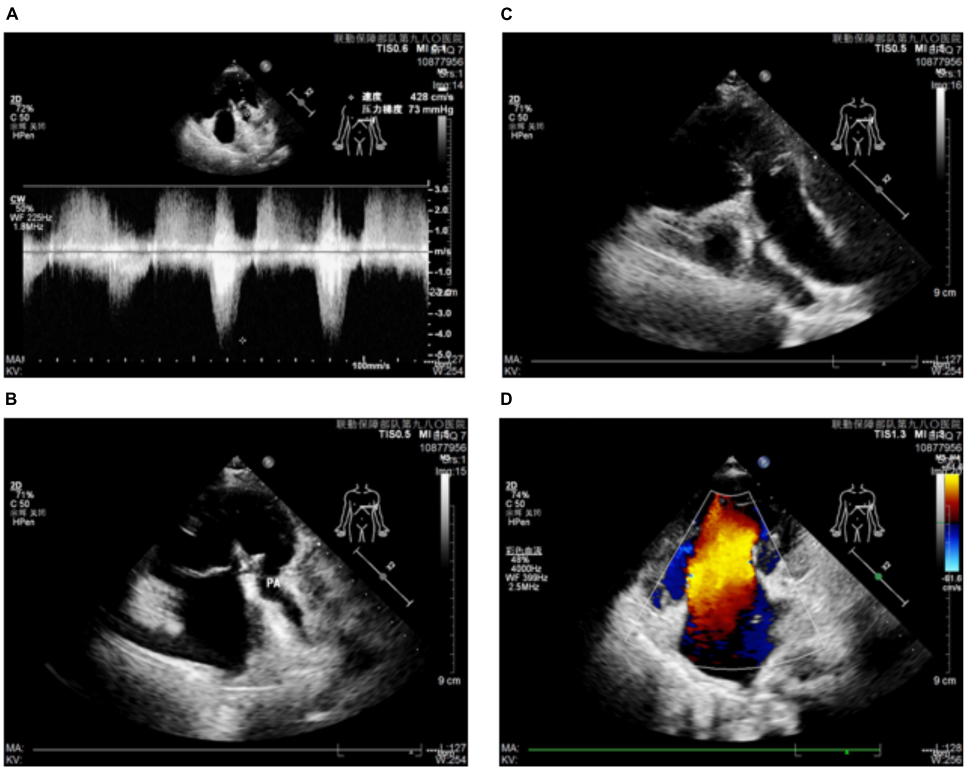

FIGURE 2
Ultrasound imaging of the patient's heart. **(A,B)** Patient's atrial ventricle and pulmonary artery imaging and pressure. **(C)** Images of the patient's atrium ventricle and aorta. **(D)** Atrial ventricular flow imaging of the patient.

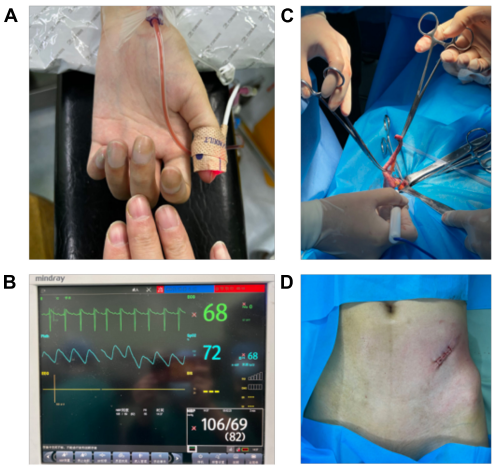

FIGURE 3
Images of patients during surgery. **(A)** Compared with the fingers of normal people, the finger color of the patient was purple. **(B)** Patient's heart rate, blood pressure, and pulse oxygen saturation. **(C)** The moment when the patient's appendix was removed. **(D)** Postoperative incision of the patient.

4.4% recurred (median follow-up > 7 years), with a lower recurrence rate in women than in men, California, USA (7). Darwazeh et al. (8) systematically reviewed 21 non-operative treatments for appendiceal abscess or cellulitis with a mean follow-up of 45.9 months and a recurrence rate of 0∼24% with a mean of 12.4%. Surgery should be recommended for cases with multiple (≥ 2) recurrences, subacute or chronic appendicitis that appears to be successfully treated conservatively but still has abdominal pain, or the occurrence of postoperative stump inflammation. During this procedure, the surgeon visually observes inflammation in the appendix. Studies have shown that the surgeon's intraoperative visual determination of the type of appendiceal pathology is approximately 80% accurate (9). Postoperative pathology also confirmed the patient's diagnosis of chronic appendicitis.

In patients with a common atrium and single ventricle, arterial and venous blood are mixed in the common cardiac chamber and decreased pulmonary blood flow is due to infundibular stenosis. Patients with single atrium and single ventricle heart disease are rare and account for 1∼2% of all congenital heart malformations. Without corrective surgery, it will die in the neonatal period or infancy, and survival into adulthood is unusual (10). Patients with single atrium and single ventricle hearts require surgery in infancy or childhood to ensure balanced pulmonary and systemic blood flow (11). Due to the disturbance of the homeostasis of their hemodynamic state, few patients can live an almost normal life without any surgical intervention. Only about 10 cases worldwide have been reported for patients with single ventricle surviving to late adulthood, one of them up to 62 years of age and the others up to 50 years of age (12). Survival to adulthood in patients with a single ventricle combined with a single atrium is even rarer, with only a very few cases reported so far (13, 14). There have been few reported cases of patients successfully surviving into adulthood with concurrent surgical treatment. In addition to a primigravida with a single atrium and single ventricle (15), and a patient with anomalous hepatic venous drainage and azygos continuation of inferior vena cava (16).

It is a miracle that the patient survived to adulthood, which may be related to the tolerable pressure of the pulmonary artery trans-valve. The patient also paid attention to the prevention of infectious diseases such as colds and the amount of exercise she took. According to relevant calculations, the patient's metabolic equivalent is currently assessed at 4 points, and she can almost perform simple daily life independently. Interventions in such patients focus on maintaining the patient's cardiac and pulmonary circulatory homeostasis and reducing disturbances to cardiac function that she has tolerated for many years. Considering that the patient had chronic appendicitis and that the local inflammation and adhesions of the appendix were not too severe, the general surgeon, cardiac surgeon, and anesthesiologist unanimously decided to use regional block anesthesia instead of general anesthesia to maintain the balance of cardiac and pulmonary function in this patient. A patient with Marfan syndrome receiving transversus abdominis plane blocks with analgesic results has been reported (17) and administration of dexmedetomidine might reduce the adverse effects of general anesthesia in infants with congenital heart disease undergoing surgery and extracorporeal circulation (18). The surgical showed that ultrasound-guided transversus abdominis plane block and dexmedetomidine had a less hemodynamic impact on this patient, and reduced the patient's tension, anxiety, and discomfort, creating conditions for a successful surgery. The patient had almost no adverse effects during the operation, and the appendectomy was completed successfully.

Data availability statement

The original contributions presented in this study are included in this article/supplementary material, further inquiries can be directed to the corresponding authors.

Ethics statement

Written informed consent was obtained from the individual(s) for the publication of any potentially identifiable images or data included in this article.

Author contributions

YW and BZ took the responsibility of communicating with the patient's family and obtaining authorization for this manuscript. YW was responsible for drafting the manuscript. WL revised the manuscript. ZZ, ZC, and JC were responsible for literature searches and final proofreading. All authors contributed to the article and approved the submitted version.

Funding

This study was supported by Scientific Project of Traditional Chinese Medicine Bureau of Hebei Province (No. 2023339).

Acknowledgments

The authors would like to express their gratitude to the patient and the parents.

Conflict of interest

The authors declare that the research was conducted in the absence of any commercial or financial relationships that could be construed as a potential conflict of interest.

Publisher's note

References

1. Bhangu A, Søreide K, Di Saverio S, Assarsson J, Drake F. Acute appendicitis: modern understanding of pathogenesis, diagnosis, and management. *Lancet.* (2015) 386:1278–87. doi: 10.1016/S0140-6736(15)00275-5

2. Moris D, Paulson EK, Pappas TN. Diagnosis and management of acute appendicitis in adults: a review. *JAMA.* (2021) 326:2299–311. doi: 10.1001/jama.2021.20502

3. Franklin BA, Brinks J, Berra K, Lavie C, Gordon N, Sperling L. Using metabolic equivalents in clinical practice. *Am J Cardiol.* (2018) 121:382–7. doi: 10.1016/j.amjcard.2017.10.033

4. Hasday SJ, Chhabra KR, Dimick JB. Antibiotics vs Surgery for acute appendicitis: toward a patient-centered treatment approach. *JAMA Surg.* (2016) 151:107–8. doi: 10.1001/jamasurg.2015.4065

5. Salminen P, Tuominen R, Paajanen H, Rautio T, Nordström P, Aarnio M, et al. Five-Year Follow-up of Antibiotic Therapy for Uncomplicated Acute Appendicitis in the APPAC Randomized Clinical Trial. *JAMA.* (2018) 320:1259–65. doi: 10.1001/jama.2018.13201

6. Liang TJ, Liu S, Tsai C, Kang C, Huang W, Chang H, et al. Analysis of recurrence management in patients who underwent nonsurgical treatment for acute appendicitis. *Medicine.* (2016) 95:e3159. doi: 10.1097/MD.0000000000003159

7. McCutcheon BA, Chang D, Marcus L, Inui T, Noorbakhsh A, Schallhorn C, et al. Long-term outcomes of patients with nonsurgically managed uncomplicated appendicitis. *J Am Coll Surg.* (2014) 218:905–13. doi: 10.1016/j.jamcollsurg.2014.01.003

8. Darwazeh G, Cunningham SC, Kowdley GCA. Systematic review of perforated appendicitis and phlegmon: interval appendectomy or Wait-and-See? *Am Surg.* (2016) 82:11–5. doi: 10.1177/000313481608200107

9. Strong S, Blencowe N, Bhangu A, National Surgical Research Collaborative. How good are surgeons at identifying appendicitis? Results from a multi-centre cohort study. *Int J Surg.* (2015) 15:107–12. doi: 10.1016/j.ijsu.2015.01.032

10. Moodie DS, Ritter D, Tajik A, O'Fallon W. Long-term follow-up in the unoperated univentricular heart. *Am J Cardiol.* (1984) 53:1124–8. doi: 10.1016/0002-9149(84)90648-9

11. Goyal R, Batra RK, Jangde A, Kumar G. A case of single atrium and single ventricle physiology with bilateral cleft lip and palate for lip repair surgery. *J Anaesthesiol Clin Pharmacol.* (2012) 28:384–5. doi: 10.4103/0970-9185.98355

12. Oliver JM, Fdez-de-Soria R, Dominguez F, Ramos F, Calvo L, Ros J, et al. Spontaneous long-term survival in single ventricle with pulmonary hypertension. *Am Heart J.* (1990) 119:201–2. doi: 10.1016/S0002-8703(05)80105-X

13. Lohithalingam P, Lakmini KMS, Weerasinghe S, Pereira T, Premaratna R. Long-term survival of a patient with single atrium and single ventricular heart: a case report. *Ceylon Med J.* (2018) 63:80–1. doi: 10.4038/cmj.v63i2.8673

14. Klisiewicz A, Michałek P, Szymański P, Hoffman P. Univentricular heart, common atrium, single atrio-ventricular valve– –is it possible in humans?. *Kardiol Pol.* (2004) 61:274–6.

15. Wei C, Xue X, Zhu G, Li M, Liu H, Peng H. A primigravida with single atrium and single ventricle. *Int J Gynaecol Obstet.* (2013) 123:160–1. doi: 10.1016/j.ijgo.2013.06.017

16. Xiao Y, Qiao W, Zhan Y, Zhang J, Ren W. Single ventricle and single atrium with anomalous hepatic venous drainage and azygos continuation of inferior vena cava in an adult patient. *J Clin Ultrasound.* (2015) 43:458–61. doi: 10.1002/jcu.22217

17. Katakura Y, Sakurai A, Endo M, Hamada T, Nomoto M, Yamada H, et al. Safe and effective analgesia with bilateral continuous TAP block for a patient with marfan syndrome after open abdominal aortic aneurysm repair. *Masui.* (2016) 65:621–3.

18. Huang J, Gou B, Rong F, Wang W. Dexmedetomidine improves neurodevelopment and cognitive impairment in infants with congenital heart disease. *Per Med.* (2020) 17:33–41. doi: 10.2217/pme-2019-0003

frontiers | Frontiers in Cardiovascular Medicine

TYPE Case Report
PUBLISHED 21 March 2023
DOI 10.3389/fcvm.2023.1076118

OPEN ACCESS

EDITED BY
Xiaofeng Yang,
Temple University, United States

REVIEWED BY
Nikhil Agrawal,
University of Texas Health Science Center at Houston, United States
Lilia M. M. Sierra-Galan,
The American British Cowdray Medical Center, Mexico

*CORRESPONDENCE
Meiping Lu
meipinglu@zju.edu.cn

†These authors have contributed equally to this work

SPECIALTY SECTION
This article was submitted to General Cardiovascular Medicine, a section of the journal Frontiers in Cardiovascular Medicine

RECEIVED 28 October 2022
ACCEPTED 28 February 2023
PUBLISHED 21 March 2023

CITATION
Xuan W, Wang Z, Lin J, Zou L, Xu X, Yang X, Xu Y, Zhang Y, Zheng Q, Xu X and Lu M (2023) Case report: Aggressive progression of acute heart failure due to juvenile tuberculosis-associated Takayasu arteritis with aortic stenosis and thrombosis.
Front. Cardiovasc. Med. 10:1076118.
doi: 10.3389/fcvm.2023.1076118

Case report: Aggressive progression of acute heart failure due to juvenile tuberculosis-associated Takayasu arteritis with aortic stenosis and thrombosis

Wenjie Xuan[1,2†], Zhaoling Wang[1†], Jinjing Lin[1,2†], Lixia Zou[1], Xisheng Xu[1], Xinghui Yang[3], Yiping Xu[1], Yan Zhang[1], Qi Zheng[1], Xuefeng Xu[1] and Meiping Lu[1*]

[1]Department of Rheumatology Immunology and Allergy, Children's Hospital of Zhejiang University School of Medicine, National Clinical Research Center for Child Health, Hangzhou, China, [2]Department of Pediatrics, Shaoxing People's Hospital (Shaoxing Hospital, Zhejiang University School of Medicine), Shaoxing, China, [3]Department of Radiology, Children's Hospital of Zhejiang University School of Medicine, National Clinical Research Center for Child Health, Hangzhou, China

Background: Takayasu arteritis (TA) is a chronic granulomatous vasculitis with unknown pathophysiology. TA with severe aortic obstruction has a poor prognosis. However, the efficacy of biologics and appropriate timing of surgical intervention remain controversial. We report a case of tuberculosis (TB)-associated TA with aggressive acute heart failure (AHF), pulmonary hypertension (PH), thrombosis, and seizure, who failed to survive after surgery.

Case presentation: A 10-year-old boy who developed a cough with chest tightness, shortness of breath, hemoptysis with reduced left ventricular ejection fraction, PH, and increased C-reactive protein and erythrocyte sedimentation rate was hospitalized at the pediatric intensive care unit of our hospital. He had strongly positive purified protein derivative skin test and interferon-gamma release assay result. Computed tomography angiography (CTA) showed occlusion of proximal left subclavian artery and stenosis of descending aorta and upper abdominal aorta. His condition did not improve after administration of milrinone, diuretics, antihypertensive agents, and intravenous methylprednisolone pulse followed by oral prednisone. Intravenous tocilizumab was administered for five doses, followed by two doses of infliximab, but his HF worsened, and CTA on day 77 showed complete occlusion of the descending aorta with large thrombus. He had a seizure on day 99 with deterioration of renal function. Balloon angioplasty and catheter-directed thrombolysis were performed on day 127. Unfortunately, the child's heart function continued to deteriorate and died on day 133.

Abbreviations

TA, Takayasu arteritis; TB, tuberculosis; AHF, acute heart failure; PH, pulmonary hypertension; ESR, erythrocyte sedimentation rate; CRP, C-reactive protein; CT, computed tomography; BCG, Bacillus Calmette-Guerin; BP, blood pressure; NT-proBNP, N-terminal pro-brain natriuretic peptide; PPD, purified protein derivative; ANA, antinuclear antibody; ANCA, antineutrophil cytoplasmic antibody; CTA, computed tomography angiography; LVEF, left ventricular ejection fraction; IVMP, intravascular methylprednisolone pulse; TCZ, tocilizumab; MRA, magnetic resonance angiography; FLAIR, fluid-attenuation inversion recovery; EULAR, European League Against Rheumatism; PRES, posterior reversible encephalopathy syndrome; MPR, multiplanar reconstruction; MIP, maximum intensity projection; VR, volume rendered.

Conclusion: TB infection may be related to juvenile TA. The biologics, thrombolysis, and surgical intervention failed to achieve the anticipated effect in our case with aggressive AHF due to severe aortic stenosis and thrombosis. More studies are needed to determine the role of biologics and surgery in such dire cases.

KEYWORDS

juvenile, Takayasu arteritis, acute heart failure, pulmonary hypertension, thrombosis, surgery

Introduction

Takayasu arteritis (TA) is a chronic, granulomatous vasculitis that predominantly involves the aorta and its main branches (1). TA may lead to fatal complications, such as heart failure (HF), myocardial infarction, dissecting aneurysm, and stroke (2). Juvenile TA is less common and has an insidious onset. The pathogenesis of TA may be related to infection, genetic susceptibility, and immune abnormalities. Tuberculosis (TB) was one of the leading causes of death from a single infectious pathogen, with an estimated 2 million TB deaths in 2019 in the world (3). The prevalence of TB was relatively high in Southeast Asia (44%), Africa (25%), and Western Pacific (18%) (3). Studies have shown that TA is closely associated with TB infection in adults, of which 9.9% had TB (4). Pedreira and Santiago (5) reported that active or latent TB accounted for 6.3%–20% or 20%–82% of patients with TA, respectively. However, there was no difference in clinical presentation in TA with or without TB infection (6). TB-associated juvenile TA is rare (7, 8). Treatment of juvenile TA is based on the approaches used for adults, but the rapid onset and severity of the disease in children means that treatment options are very limited, and the efficacy of biologics or surgical interventions is controversial (9, 10). Herein, we reported an aggressive case of TB-associated TA in a Chinese boy, who presented with refractory acute heart failure (AHF), pulmonary hypertension (PH), and seizure due to severe aortic stenosis and associated thrombosis. Balloon angioplasty and catheter-directed thrombolysis were attempted, but unfortunately, those did not prevent his demise on day 133.

Case presentation

A 10-year-old Chinese boy was transferred to the pediatric intensive care unit (PICU) of our hospital with AHF, PH, and hypertension. Ten months prior to this admission, he presented to the local healthcare providers with "chest pain," increased erythrocyte sedimentation rate (ESR: 39–52 mm/h), and C-reactive protein (CRP: 22.6–29.1 mg/L), and chest computed tomography (CT) scan demonstrated calcified left hilar lymph nodes. Chest pain improved after antibiotic therapy for 1 week (no detail regarding the medications).

On this admission, he returned to the local hospital with a 2-week history of cough, chest tightness, and shortness of breath. He was diagnosed with AHF, PH, and hypertension and transferred to our hospital. The patient had received routine vaccinations including Bacillus Calmette-Guerin (BCG). His growth and development were normal.

Physical examination on admission showed the following: heart rate 120/min, respiratory rate 26/min, and blood pressure (BP) 159/103 mmHg in his right arm, 124/93 mmHg in his left arm, 87/55 mmHg in his right leg, and 121/106 mmHg in the left leg. Distended jugular veins and weak left radial artery pulsation were found. Class IV systolic murmur in the precordial region was heard. There was no enlargement of liver and spleen. Laboratory evaluations revealed increased N-terminal pro-brain natriuretic peptide (NT-proBNP: 19052 pg/mL), CRP (8.45 mg/L), ESR (32 mm/h), serum creatinine (86 μmol/L), and urea (15.68 mmol/L) with decreased blood potassium (2.9 mmol/L), sodium (128 mmo1/L), and hemoglobin (84 g/L). The purified protein derivative (PPD) skin test and interferon-gamma release assay (IGRA) result were strongly positive. However, all microbiological analyses including TB culture and pathogenic microorganism sequencing were negative. Serum immunoglobulin and complements (C3 and C4) were normal. Antinuclear antibody (ANA) and antineutrophil cytoplasmic antibody (ANCA) were negative. Echocardiography revealed reduced left ventricular ejection fraction (LVEF: 40%) with left heart dilatation, PH (75 mmHg), and moderate mitral insufficiency. Chest x-ray showed significant cardiomegaly (**Figure 1A**). Chest CT showed calcified left hilar lymph nodes, enlarged mediastinal lymph nodes, patchy and slightly high-density shadows in both lungs, and a small amount of bilateral pleural effusion. CT angiography (CTA) showed occlusion of the proximal left subclavian artery and stenosis of the lumen of the descending and upper abdominal aorta with extensive thickening of the vascular wall (**Figures 1B,C**). Whole exome sequencing did not indicate any abnormal mutations. Based on the radiological findings and laboratory examinations, he was diagnosed as TB-associated TA (11) complicated with AHF and PH.

The boy was initially treated with bed rest, oxygen inhalation, milrinone, diuretics, captopril, bosentan, and antibiotics including anti-TB medications. He developed hemoptysis on day 8. Intravenous methylprednisolone pulse (IVMP) therapy (10 mg/kg/day) was given on days 22–24, followed by 1 mg/kg of daily oral prednisone. Metoprolol was added on day 28. However, subxiphoid and right upper abdominal pain was recurrent during hospitalization and worsened on day 29. AHF, PH, BP, heart rate, cardiac function, chest tightness, and shortness of breath did not improve notably. On day 32, intravenous tocilizumab (TCZ) was initiated at a dose of 8 mg/kg following the 0-, 2-, and 4-week regimen (**Figure 2**). Coughing

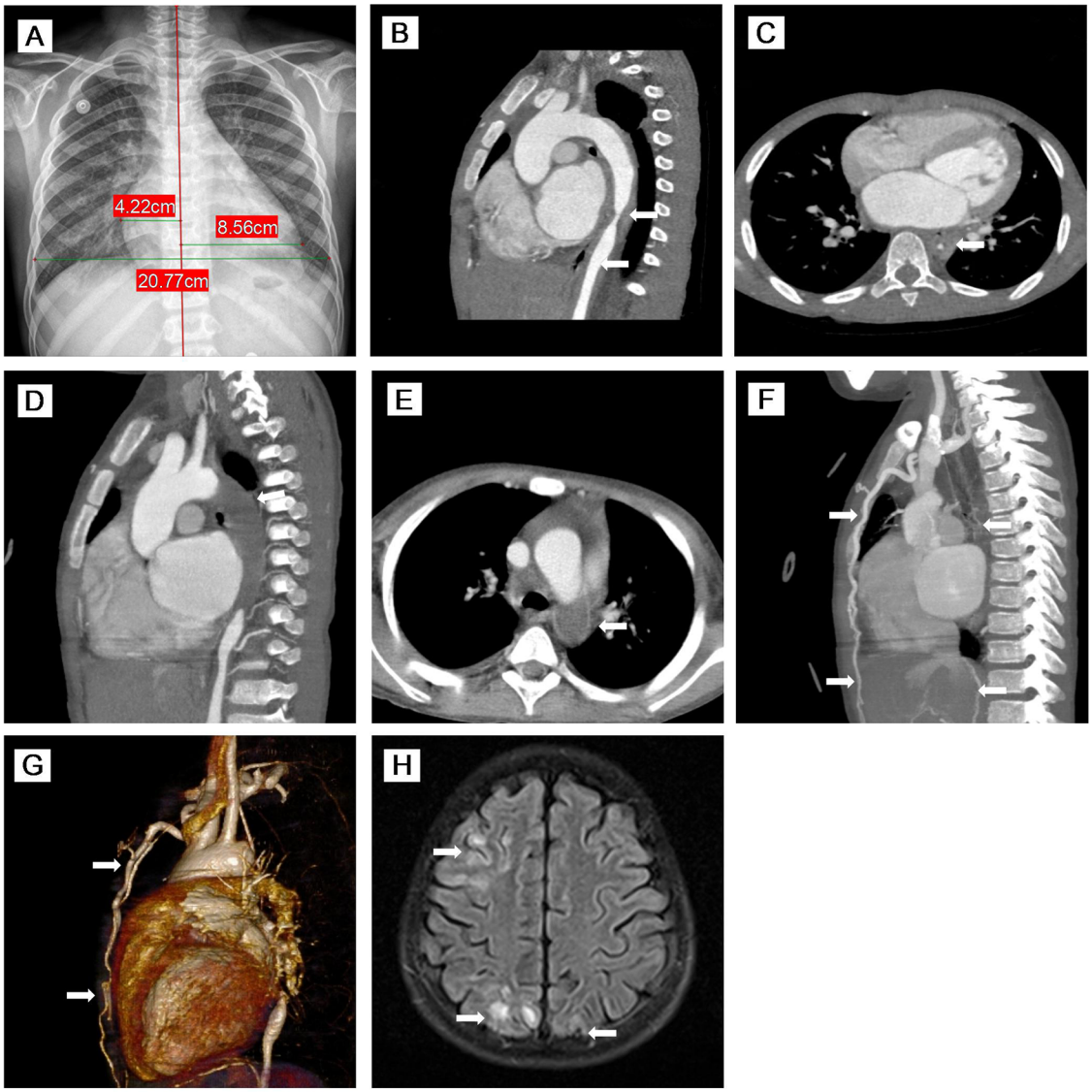

FIGURE 1
(A) Chest x-ray showed significant cardiomegaly. (B–E) MPR images of thoracic CTA. (B) Sagittal view of CTA demonstrated stenosis of the descending aorta and upper abdominal aorta with thickening of the vascular wall. (C) Axial view of CTA showed that the descending aorta was stenosed to 3.1 mm. (D, E) Sagittal oblique view and axial view of CTA indicated complete occlusion of the descending aorta with large thrombus (76 mm in length). (F,G) MIP image and VR reconstruction of CTA revealed complete occlusion of the descending aorta with large thrombus (76 mm in length) and extensive collateral circulation (twisted and dilated right intrathoracic artery, numerous open collateral vessels in the neck and upper mediastinum). (H) Axial view of brain MR imaging revealed high signals on T2 FLAIR images of cortical and subcortical areas of both the occipital lobes and right frontal-parietal lobe. MPR, multiplanar reconstruction; CTA, computed tomography angiography; MIP, maximum intensity projection; VR, volume rendered; MR, magnetic resonance; FLAIR, fluid-attenuation inversion recovery.

and hemoptysis resolved. Chest tightness, shortness of breath, abdominal pain, BP (115/82 mmHg on the right arm) and heart rate (102 beats/min), LVEF (45%), and PH (47 mmHg) were slightly improved after three doses of TCZ. He was discharged on day 60.

The child was re-admitted on day 66 due to worsening HF with lower LVEF (30%), higher PH (70 mmHg), and normal CRP and ESR. During this admission, his BP fluctuated from 175/105–123/74 mmHg, and hemoptysis recurred. Repeated CTA on day 77 and day 92 showed complete occlusion of the descending aorta with large thrombus (76 mm in length) (Figures 1D,E) and extensive collateral circulation (twisted and dilated right intrathoracic artery, numerous open collateral vessels in the neck and upper mediastinum) (Figures 1F,G). In addition to the same medications as the first admission, subcutaneous low-molecular-weight heparin was started on day 78. IVMP therapy (10 mg/kg/day) was administered again on days 93–95.

The patient developed seizure and loss of consciousness while afebrile on day 99. Seizure was controlled with intravenous diazepam. Cranial magnetic resonance angiography (MRA) showed narrowed lumen of the anterior, middle, and posterior cerebral arteries. Brain MR imaging revealed strong signals on T2

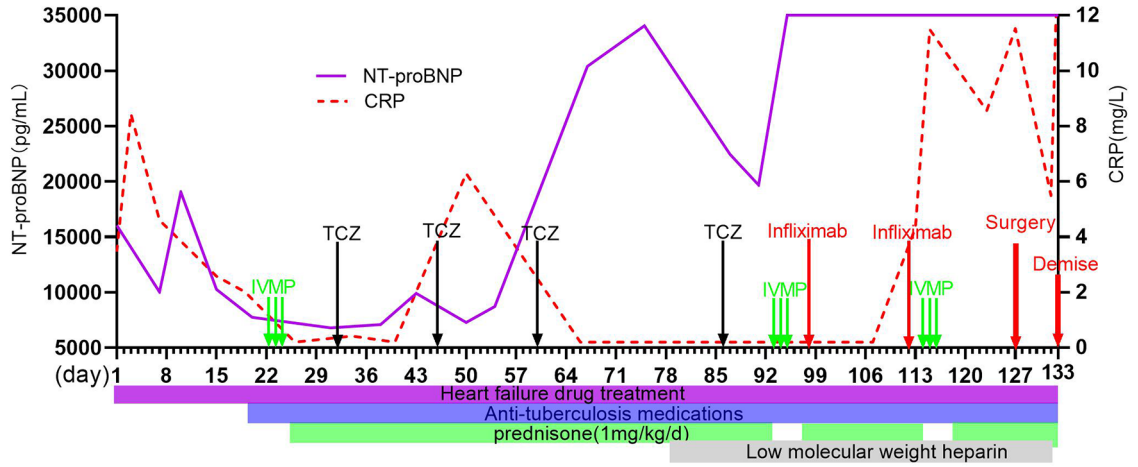

FIGURE 2
Clinical course of this case and sequential changes in NT-proBNP and CRP. NT-proBNP, N-terminal pro-brain natriuretic peptide; CRP, C-reactive protein; IVMP, intravascular methylprednisolone pulse; TCZ, tocilizumab.

fluid-attenuation inversion recovery (FLAIR) images of the cortical and subcortical areas of both the occipital lobes and right frontal-parietal lobe (**Figure 1H**). After failing to respond to another two doses of TCZ, intravenous infliximab was given for two doses on day 98 and day 112, and IVMP therapy (10 mg/kg/day) again on days 114–116. However, there were still no signs of improvement, and his renal function worsened. Given the complete occlusion of the aorta with large thrombus and aggravating life-threatening HF without response to any medication, balloon angioplasty was performed and catheter-directed thrombolysis with urokinase and heparin was started on day 127. Four days after surgery, the patient worsened suddenly with increased shortness of breath, decreased heart rate, and dropping of oxygen saturation to 60%. The patient died on day 133 (**Figure 2**).

Discussion and conclusion

In our case, the boy presented with hypertension and differential limb systolic pressure of >10 mmHg, increased ESR of 32 mm/h, and CRP of 8.45 mg/L. CTA showed the involvement of the left subclavian artery, descending aorta, and abdominal aorta. All microbiological analyses in our case were negative except for the positive PPD skin test and IGRA result. Treatment with antibiotics including anti-TB medications was ineffective. There was no evidence of other immune inflammatory diseases such as systemic lupus erythematosus and ANCA-associated vasculitis based on the clinical and laboratory features. TA was diagnosed according to the diagnostic criteria developed by the European League Against Rheumatism (EULAR)/Paediatric Rheumatology International Trials Organisation/Paediatric Rheumatology European Society (11). The clinical course was complicated with refractory HF, PH, thrombosis, and central nervous system involvement and renal dysfunction.

HF is the leading cause of death in adult TA patients (12). Zhang et al. (13) analyzed 163 adult patients with TA, including 61 cases with HF. During a median follow-up period of 887 days, all 11 fatal cases were in the HF group. AHF is less common but more malignant than chronic HF in TA patients. Fan et al. (14) reported five children with TA complicated with AHF, of which two patients had improved, two died, and one was lost to follow-up. Our case with AHF due to severe stenosis of descending aorta failed to all treatments and succumbed to his disease.

PH is another serious complication of TA, and the incidence rate is approximately 0%–17.8%. PH occurs because of (i) precapillary causes, such as pulmonary disease, chronic hypoxia, and chronic thromboembolic disease, and (II) postcapillary causes, such as left heart disease, aortic regurgitation, or disease associated with pulmonary arteritis (15, 16). PH is mostly asymptomatic clinically, while some patients may present with dyspnea, decreased activity tolerance, low oxygen saturation, occasional pulmonary hemorrhage, and, in severe cases, hemoptysis and HF (15). In our case, he presented with cough, chest tightness, shortness of breath, hemoptysis with persistent lower LVEF, and high NT-proBNP but without pulmonary artery involvement in CTA. It indicated that the refractory PH and hemoptysis may be secondary to left heart failure/dysfunction as a result of severe stenosis or complete occlusion of the descending aorta.

The patient developed seizure with abnormal cranial MRA and T2 FLAIR images on day 99. Seizures may be caused by stroke, hypertensive encephalopathy, posterior reversible encephalopathy syndrome (PRES), and other reasons. Neurological symptoms in TA are usually associated with decreased blood flow due to steno-occlusive lesions and/or shifting of the blood flow (steal) (17, 18). PRES is extremely rare in TA. The mechanism of PRES is not fully understood but may be related to the blood–brain barrier disruption with fluid transudation caused by high BP (19). In our case, the patient received long-term intravenous methylprednisolone and several IVMP and suffered from persistent hypertension. Seizures may be related to both hypertension induced PRES and narrowed lumen of arteries according to imaging findings.

TABLE 1 Review of surgical modalities and outcomes in juvenile Takayasu arteritis involving aorta.

First author, year (reference)	Sex	Age	Heart failure	Involved vessels	Surgical modalities	Outcome	Follow-up
Fan et al., 2018 (14)	F	Adolescent	Yes	Stenosis of distal thoracic aorta	Stent implantation	Improvement	3 years
Fan et al., 2018 (14)	F	Adolescent	Yes	Stenosis from thoracic to abdominal aorta	Balloon angioplasty	Improvement	6 months
Sugawara et al., 2020 (22)	F	8 years	Yes	Occlusion of descending aorta	Axillo-external iliac artery bypass	Improvement	10 years
Nakata et al., 2022 (9)	F	1 year	Yes	Occlusion of distal thoracic aorta	Graft interpose	Improvement	2 months
Pavic et al., 2019 (10)	M	3.5 months	Yes	Thrombosis of distal aorta and iliac arteries	Thrombectomy	Death	—

F, female; M, male.

The EULAR recommendations for the management of TA included glucocorticoids and conventional synthetic disease-modifying antirheumatic drugs, followed by TCZ or TNF-inhibitors (20). In our case, TCZ at the first hospitalization led to a slight transient improvement. However, his HF worsened with increased aortic stenosis and complete occlusion of the descending aorta despite five doses of TCZ. Changing TCZ to a TNF-inhibitor (infliximab) also failed to reverse the condition. Our case indicated that efficacy of biologics was poor in TA with severe stenosis or occlusion of aorta induced HF. As aortic obstruction may contribute to aggressive HF, which could result in death from cardiopulmonary failure, a desperate final attempt to reverse the clinical course was made with surgical intervention.

Previous studies revealed that surgery was helpful to relieve vascular obstruction in patients with severe ischemia of vital organs and limbs, intractable hypertension, and refractory HF (20, 21). Although in most cases surgery is beneficial, it is always accompanied by risks (**Table 1**). Two of five cases of juvenile TA complicated with HF survived with surgery (14). An 8-year-old patient with TA who underwent surgical treatment for the complication of aortic occlusion and HF was stable with 10 years of follow-up (22). Nakata et al. (9) reported that a 1-year-old girl with TA-induced long-segment occlusion of the distal thoracic aorta developed cardiogenic shock but survived after surgery. However, another case of a 3.5-month-old boy with TA died after surgery (10). In general, surgical intervention should not be performed until TA patients reach an inactive state with normal ESR, CRP, and stable imaging (23). In most TA patients, increased ESR and CRP correlated with active disease status. However, about 20% of TA patients have normal laboratory parameters despite having active disease (24). There was evidence that the disease activity significantly might increase the risks of anastomotic dehiscence or restenosis (25). This issue makes it difficult for the clinicians to determine the optimal time in surgical intervention. In our case, given the progressive HF and associated decline in renal function, balloon angioplasty and catheter-directed thrombolysis with urokinase and heparin were done in a desperate final attempt to save his life. Unfortunately, the boy died 6 days after surgery. This case suggested that TA with severe HF due to severe aortic stenosis and occlusion had very poor prognosis. The optimal time for surgical intervention remains problematic.

In summary, TB infection may be related to juvenile TA. It is a must to investigate early in all TA, even if there are no signs or symptoms, especially in TB-endemic countries. TA patients with aggressive AHF due to severe aortic stenosis and thrombosis have a poor prognosis, and biologics are of limited efficacy. Our case pointed out that timing of surgical intervention with balloon angioplasty and catheter-directed thrombolysis may be critical in disease outcome, but it is extremely difficult to pinpoint when the optimal time may be. More studies are needed to better address this issue.

Data availability statement

The original contributions presented in the study are included in the article/Supplementary Material, further inquiries can be directed to the corresponding author.

Ethics statement

Written informed consent was obtained from both parents of the patient to publish this case report.

Author contributions

WX, ZW, JL, XiX, LZ, YX, YZ, QZ, XuX, and ML contributed to the study design, literature review, and substantially revised the manuscript. XY performed the CTA and evaluated the figures. WX wrote and drafted the manuscript. ZW revised the figure. JL: created the table. All authors contributed to the article and approved the submitted version.

Funding

This work was supported by the National Science Foundation of China (No. 82070027) and the Key Program of Zhejiang Province Science and Technology Plan Project (No. 2023C03032).

Acknowledgments

We would like to thank Lawrence Kwok Leung Jung from the Division of Rheumatology, Children's National Medical Center in Washington, DC, for revising the manuscript and Can Lai from the Department of Radiology, Children's Hospital of Zhejiang

University School of Medicine, National Clinical Research Center for Child Health, for revising the figures.

Conflict of interest

The authors declare that the research was conducted in the absence of any commercial or financial relationships that could be construed as a potential conflict of interest.

Publisher's note

References

1. Ozen S, Pistorio A, Iusan SM, Bakkaloglu A, Herlin T, Brik R, et al. EULAR/PRINTO/PRES criteria for Henoch–Schonlein purpura, childhood polyarteritis nodosa, childhood Wegener granulomatosis and childhood Takayasu arteritis: Ankara 2008. Part II: final classification criteria. *Ann Rheum Dis*. (2010) 69:798–806. doi: 10.1136/ard.2009.116657

2. Tian Y, Chen Y. Stroke in Takayasu arteritis with concomitant tuberculosis: an unusual pediatric case report. *BMC Pediatr*. (2022) 22:50. doi: 10.1186/s12887-022-03125-4

3. Chakaya J, Khan M, Ntoumi F, Aklillu E, Fatima R, Mwaba P, et al. Global tuberculosis report 2020—reflections on the global TB burden, treatment and prevention efforts. *Int J Infect Dis*. (2021) 113:S7–12. doi: 10.1016/j.ijid.2021.02.107

4. Zhang Y, Fan P, Luo F, Zhang HM, Song L, Ma WJ, et al. Tuberculosis in Takayasu arteritis: a retrospective study in 1105 Chinese patients. *J Geriatr Cardiol*. (2019) 16:648–55. doi: 10.11909/j.issn.1671-5411.2019.08.003

5. Pedreira ALS, Santiago MB. Association between Takayasu arteritis and latent or active *Mycobacterium tuberculosis* infection: a systematic review. *Clin Rheumatol*. (2020) 39:1019–26. doi: 10.1007/s10067-019-04818-5

6. Lim AY, Lee GY, Jang SY, Gwag HB, Choi SH, Jeon E, et al. Comparison of clinical characteristics in patients with Takayasu arteritis with and without concomitant tuberculosis. *Heart Vessels*. (2016) 31:1277–84. doi: 10.1007/s00380-015-0731-8

7. Khemiri M, Douira W, Barsaoui S. Co-occurrence of Takayasu's arteritis and tuberculosis: report of a Tunisian pediatric case. *Ann Pediatr Cardiol*. (2016) 9:75–8. doi: 10.4103/0974-2069.171398

8. Benjaminsen E, Reigstad A, Cengija V, Lilleby V, Carlsson M, Filosto M. Stroke as the sole manifestation of Takayasu arteritis in a 15-year-old boy with latent tuberculosis. *Case Rep Neurol Med*. (2016) 2016:8736248. doi: 10.1155/2016/8736248

9. Nakata T, Tachi M, Suehiro S, Oda T. Paediatric Takayasu's arteritis complicated by thrombotic occlusion of the distal thoracic aorta. *Interact Cardiovasc Thorac Surg*. (2022) 34:504–6. doi: 10.1093/icvts/ivab302

10. Pavic R, Blazekovic R, Divkovic D, Marjanovic K, Sipl M. Aggressive progression of Takayasu's arteritis in infancy: a case report. *Acta Clin Croat*. (2019) 58:535–9. doi: 10.20471/acc.2019.58.03.19

11. de Souza AW, de Carvalho JF. Diagnostic and classification criteria of Takayasu arteritis. *J Autoimmun*. (2014) 48–49:79–83. doi: 10.1016/j.jaut.2014.01.012

12. Li J, Zhu M, Li M, Zheng W, Zhao J, Tian X, et al. Cause of death in Chinese Takayasu arteritis patients. *Medicine*. (2016) 95:e4069. doi: 10.1097/MD.0000000000004069

13. Zhang Y, Fan P, Zhang H, Ma W, Song L. Clinical characteristics and outcomes of chronic heart failure in adult Takayasu arteritis: a cohort study of 163 patients. *Int J Cardiol*. (2021) 325:103–8. doi: 10.1016/j.ijcard.2020.10.031

14. Fan L, Zhang H, Cai J, Ma W, Song L. Middle aortic syndrome because of pediatric Takayasu arteritis admitted as acute heart failure: clinical course and therapeutic strategies. *J Hypertens*. (2018) 36:2118–9. doi: 10.1097/hjh.0000000000001847

15. Direskeneli H. Pulmonary hypertension in Takayasu's arteritis: should be monitored closely. *Int J Cardiol*. (2019) 276:238–9. doi: 10.1016/j.ijcard.2018.10.074

16. Sari A, Sener YZ, Firat E, Armagan B, Erden A, Oksul M, et al. Pulmonary hypertension in Takayasu arteritis. *Int J Rheum Dis*. (2018) 21:1634–9. doi: 10.1111/1756-185x.13354

17. Bond KM, Nasr D, Lehman V, Lanzino G, Cloft HJ, Brinjikji W. Intracranial and extracranial neurovascular manifestations of Takayasu arteritis. *AJNR Am J Neuroradiol*. (2017) 38:766–72. doi: 10.3174/ajnr.A5095

18. Pallangyo P, Misidai N, Hemed NR, Swai HJ, Mkojera Z, Bhalia S, et al. Takayasu arteritis mistaken for epilepsy: a case presenting with convulsive syncope. *J Med Cases*. (2020) 11:37–40. doi: 10.14740/jmc3424

19. Jadib A, Salam S, Harmoumi Y, Chahidi EOL, Soussi O, Laoudiyi D, et al. Posterior reversible encephalopathy syndrome revealing Takayasu's arteritis in a child. *Radiol Case Rep*. (2021) 16:3969–72. doi: 10.1016/j.radcr.2021.09.034

20. Hellmich B, Agueda A, Monti S, Buttgereit F, de Boysson H, Brouwer E, et al. 2018 Update of the EULAR recommendations for the management of large vessel vasculitis. *Ann Rheum Dis*. (2020) 79:19–30. doi: 10.1136/annrheumdis-2019-215672

21. Mason JC. Surgical intervention and its role in Takayasu arteritis. *Best Pract Res Clin Rheumatol*. (2018) 32:112–24. doi: 10.1016/j.berh.2018.07.008

22. Sugawara H, Goto H, Akamatsu D, Hamada Y, Tsuchida K, Yoshida Y, et al. Midaortic syndrome due to Takayasu arteritis in a child with acute decompensated cardiac failure managed by an emergency axillo-external iliac artery bypass: a follow-up case report of long-term outcomes. *Ann Vasc Surg*. (2020) 64:408.e5–e9. doi: 10.1016/j.avsg.2019.09.026

23. Mason JC. Takayasu arteritis: surgical interventions. *Curr Opin Rheumatol*. (2015) 27:45–52. doi: 10.1097/BOR.0000000000000127

24. Maksimowicz McKinnon K, Clark TM, Hoffman GS. Limitations of therapy and a guarded prognosis in an American cohort of Takayasu arteritis patients. *Arthritis Rheum*. (2007) 56:1000–9. doi: 10.1002/art.22404

25. Fields CE, Bower TC, Cooper LT, Hoskin T, Noel AA, Panneton JM, et al. Takayasu's arteritis: operative results and influence of disease activity. *J Vasc Surg*. (2006) 43:64–71. doi: 10.1016/j.jvs.2005.10.010

frontiers | Frontiers in Cardiovascular Medicine

TYPE Case Report
PUBLISHED 06 April 2023
DOI 10.3389/fcvm.2023.1091420

OPEN ACCESS

EDITED BY
Leonardo Roever,
Federal University of Uberlandia, Brazil

REVIEWED BY
Knosalla Christoph,
German Heart Center Berlin, Germany
Sebastiano Cicco,
University of Bari Aldo Moro, Italy

*CORRESPONDENCE
Yuriy Pya
piayury@gmail.com
Abdurashid Mussayev
abdurashid.mussayev@gmail.com

SPECIALTY SECTION
This article was submitted to General Cardiovascular Medicine, a section of the journal Frontiers in Cardiovascular Medicine

RECEIVED 07 November 2022
ACCEPTED 17 March 2023
PUBLISHED 06 April 2023

CITATION
Pya Y, Mussayev A, Novikova S, Bekbossynova M, Alimbayev S, Khissamutdinov N, Kapyshev T, Kuanyshbek A and Lesbekov T (2023) Case report: A novel surgical technique for rapid valve-in-ring implantation into the native aortic annulus during left ventricular assist device implantation.
Front. Cardiovasc. Med. 10:1091420.
doi: 10.3389/fcvm.2023.1091420

Case report: A novel surgical technique for rapid valve-in-ring implantation into the native aortic annulus during left ventricular assist device implantation

Yuriy Pya[1]*, Abdurashid Mussayev[2]*, Svetlana Novikova[1], Makhabbat Bekbossynova[3], Serik Alimbayev[2], Nail Khissamutdinov[3], Timur Kapyshev[4], Aidyn Kuanyshbek[4] and Timur Lesbekov[1]

[1]Department of Cardiac Surgery, National Research Cardiac Surgery Center, Astana, Kazakhstan, [2]Department of Interventional Cardiology, National Research Cardiac Surgery Center, Astana, Kazakhstan, [3]Department of Cardiology, National Research Cardiac Surgery Center, Astana, Kazakhstan, [4]Department of Anesthesiology, Resuscitation and Intensive Care (Adult), Astana, Kazakhstan

The implantation of a left ventricular assist device (LVAD) has become an essential requirement for managing patients with end-stage heart failure. However, aortic valve insufficiency is a contraindication for LVAD implantation in patients with end-stage heart failure, partly because of the decreasing efficiency of mechanical circulatory support and the eventual development of right ventricular failure. Herein, we present the first case of performing transcatheter aortic valve replacement in valve-in-ring along with LVAD implantation for the treatment of a 60-year-old male suffering from refractory heart failure due to dilated cardiomyopathy and pure aortic insufficiency in need of a new aortic bioprosthesis. A balloon-expandable bioprosthetic transcatheter heart valve was implanted into a previously sewn annulus ring into the aortic root *via* transaortic access. Subsequently, a centrifugal-flow LVAD was implanted. Postoperatively, the patient was in New York Heart Association Functional Class (NYHA) II with 6-min walk test of 310 m. The patient has completed 6 months of follow-up with no events. This novel and feasible surgical technique reduced the cardiopulmonary bypass time and duration of surgery. Furthermore, it avoids the risk of redo sternotomy and decreases the chances of paravalvular leakage and worsening of aortic regurgitation.

KEYWORDS

left ventricular assist device (LVAD), native aortic valve, ring annuloplasty, transcatheter aortic valve replacement, valve-in-ring, balloon expandable valve, heart failure

1. Introduction

In patients with end-stage heart failure who are refractory to medical treatment and non-definitive surgical management, left ventricular assist device (LVAD) is an effective alternative to heart transplantation, especially with limited donor availability (1, 2).

Abbreviations

AI, aortic insufficiency; AR, aortic regurgitation; LVAD, left ventricular assist device; NYHA, New York Heart Association Functional Class; TAVR, transcatheter aortic valve replacement; THV, transcatheter heart valve; ViR, valve-in-ring.

Recent studies show that continuous flow LVADs can improve the survival of end-stage heart failure patients and have been in current clinical use as a destination therapy or as a bridge-to-transplant (1–3). However, the use of LVAD has been reported to cause aortic insufficiency (AI), as early as 6 months, requiring continuous hemodynamic monitoring of the aortic valve (AV) post implantation (1, 3). The pathophysiology of this LVAD-associated AI is partly related to the impact of the LVAD, causing degenerative changes and remodeling of the AV (4, 5). In addition, the following AV hemodynamic abnormalities have been implicated in LVAD-associated AI: (i) reduced AV opening, (ii) local flow stasis, (iii) high shear stress, (iv) inversion of the transvalvular pressure gradient, and (v) pancyclic pressure gradient (4). LVAD implantation also induces anatomical alterations, such as retraction and aortic cusp malcoaptation, fibrosis, and aortic wall remodeling, which ultimately lead to AI (5). Surgical repair is the only option in such cases, and AV closure (AVC) or replacement (AVR) are considered safe and reliable for treating conditions that could lead to right ventricular failure (5–7).

The surgical repair of the AV in the context of LVAD-associated anatomical remodeling generally includes ring annuloplasty (8). However, reports show that AV regurgitation can develop even after AV repair within a few months of LVAD implantation with concomitant annuloplasty (3, 8, 9). Hence, concomitant AVR with ring annuloplasty during LVAD implantation has been adopted and reported with feasible outcomes (8, 9). Minimizing or mitigating the risks associated with the surgical settings, in addition to increased cardiopulmonary bypass time, is highly desirable. In lieu of such challenges, transaortic transcatheter aortic valve replacement (TAVR) has been considered a suitable treatment, which aids in preventing ischemia at the cross-clamping site. The increased evidence of positive clinical outcomes of TAVR with improved transcatheter heart valve (THV) designs, especially for highly comorbid patients with a high-surgical-risk status, has encouraged more clinicians to consider its use for the management of severe aortic regurgitation (AR) patients, including those with AI (10).

We present a novel technique that combines the implantation of a THV with a newly attached annuloplasty ring, valve-in-ring (ViR) followed by concomitant LVAD implantation. In this method, THV deployment is performed through the transapical route before LVAD implantation; we used a balloon-expandable biological transcatheter valve prosthesis, Myval THV (Meril Life Sciences, Pvt. Ltd., India). This Conformité Européenne (CE)-marked THV is composed of a cobalt alloy (MP35N) frame with a hybrid honeycomb cell design. This case report presents the novel surgical technique that modifies and improves upon the previous techniques of AV repair.

2. Case report

A 60-year-old male with refractory heart failure due to idiopathic dilated cardiomyopathy [New York Heart Association Functional Class (NYHA) III., INTERMACS IV] was admitted to our institution. The patient had a history of heart failure since 2012 that was treated by implanting a cardiac resynchronization therapy defibrillator (CRT-D) in 2012 and pulse generator replacement in 2017. Echocardiography demonstrated a very low left ventricular ejection fraction (LVEF) of 23%, dilated left ventricle with end-diastolic volume of 424 ml and an elevated left ventricular end-diastolic diameter (LVEDD) of 8.7 cm, severe mitral regurgitation (MR), and mild to moderate eccentric AI (**Figure 1**). The etiology of dilated cardiomyopathy was confirmed as idiopathic after ruling out the common causes. In view of nonavailability of donors and long waiting period for transplant, LVAD was considered in this patient as a bridge-to-transplant. The patient's clinical profile suggested his candidature for LVAD implant with concomitant AVR; hence, the patient was recommended for the same. Preoperative multislice computed tomography (MSCT) analysis was performed to assess the feasibility for a transfemoral procedure using the Structural Heart v.10.3 software (NRCSC). MSCT analysis revealed, the aortic annulus area was 702.1 mm^2, area-derived annular diameter was 29.9 mm, annular perimeter was 96.5 mm, and the right and left coronary artery heights were 15.4 and 13.3 mm, respectively (**Supplementary Figures S1 and S2**). The aortic root analysis was validated using the 3mensio software (Pie Medicals, Netherlands) at an independent Core lab (TAVI Core Lab, Meril Life Sciences Pvt. Ltd., India).

2.1. Surgical procedure

The surgery was carried out using median sternotomy under cardiopulmonary bypass support with aortic cross-clamping after inducing cardioplegia. The pericardium was cut open and by oblique aortotomy, the aortic leaflets were excised and the valve was exposed. The basal attachment of AV leaflets was sewn using an Ethibond 2/0 suture (Johnson & Johnson Medical N.V., Belgium) to the ventricular myocardium (Valvar Hinge) using three stitches, each leaflet bearing one stitch. A flexible annuloplasty ring [CARBOMEDICS AnnuloFlex TM32 flexible ring (Sorin Group Italia S.r.L., Italy)] was fixed with the native annulus using the same stitches to provide a sturdy base for valve replacement, as illustrated in **Supplementary Figure S3** (11) and in **Figure 2**.

Thereafter, the extra-large size (30.5 mm) of the balloon-expandable THV was deployed such that it provides a coverage of 70% aortic root and 30% left ventricular outflow tract (LVOT). The balloon-expandable THV was dilated using the Navigator THV Delivery System filled with a nominal volume of 36 ml saline, as shown in **Figure 3**. The deployment was performed according to the manufacturer's instructions. Subsequently, the aortic cross-clamp was removed and the Navigator THV Delivery System was retracted. The total cross-clamping time was 15 min.

After a successful TAVR, the HeartMate 3^{TM} LVAD (Abbott Vascular, United States) was implanted (**Figure 4**) through the standard apical to ascending aorta approach.

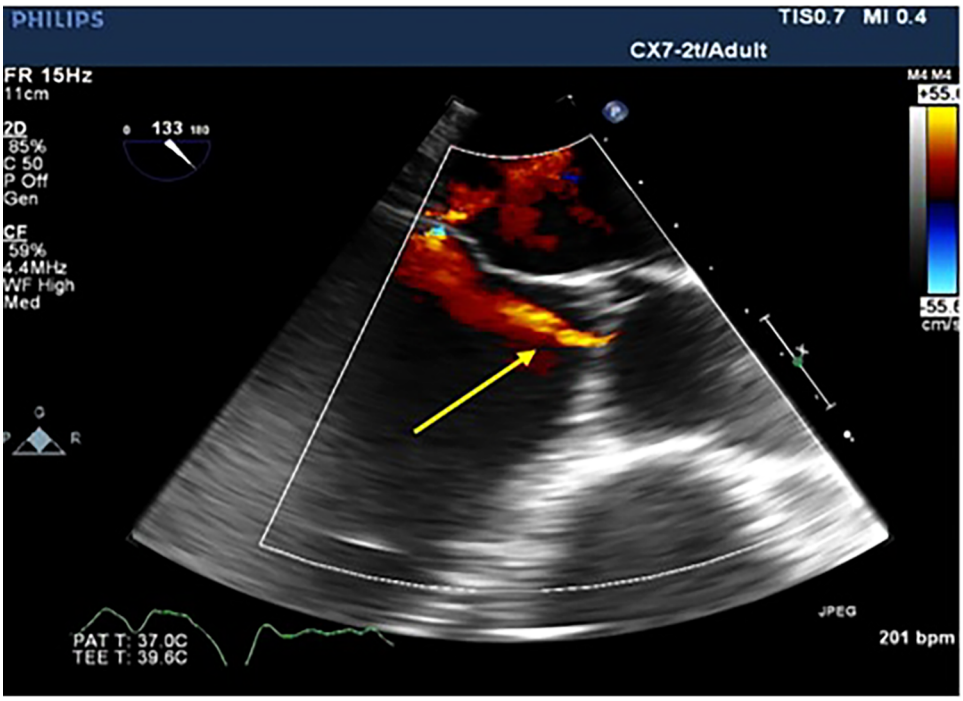

FIGURE 1
Transesophageal echocardiographic long access view of the aortic valve showing aortic regurgitation jet (yellow arrow).

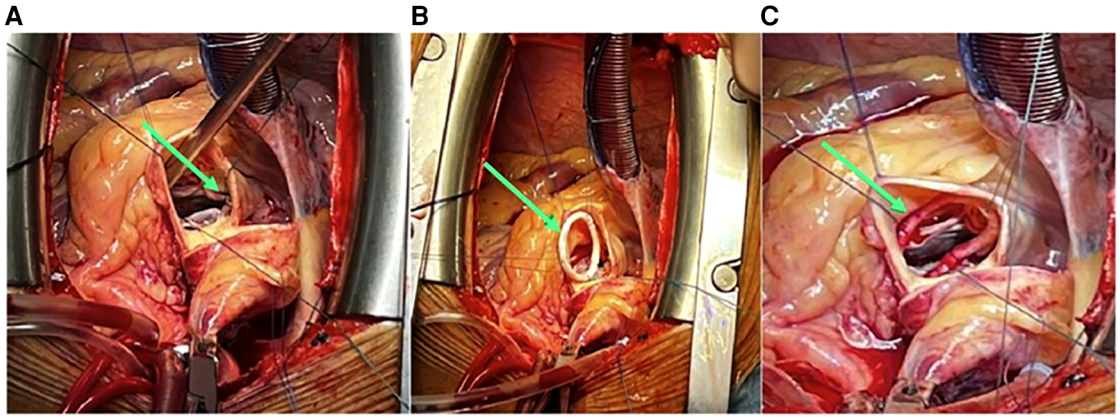

FIGURE 2
(A) Native annulus stitching with 2/0 Ethibond sutures (green arrow). (B) Carbomedics Annuloflex flexible ring #32 stitching (green arrow). (C) Carbomedics Annuloflex ring #32 positioning and fixation (green arrow).

2.2. In-hospital outcomes

The patient was removed from cardiopulmonary bypass after 100 min and operative time (measured as skin-to-skin time) was 190 min. As a result, the patient was extubated 4 h later and stayed in the ICU for 1 day. The patient was discharged and taken to the rehabilitation department 3 days after the surgery. Postoperative echocardiography and fluoroscopy results confirmed the adequate valve positioning without any transvalvular or periprosthetic regurgitation, as shown in **Supplementary Figure S4**. Postoperatively, the patient was in NYHA II with a 6-min walk test of 310 m. Currently, the patient has completed 6 months of follow-up with no events.

3. Discussion

In this case, a concomitant annuloplasty and implantation of a transcatheter AV were performed along with LVAD placement in a patient having stage D heart failure with reduced ejection fraction (23%). Despite the hybrid procedure, we achieved satisfactory procedural outcomes with no device-related or procedure-related

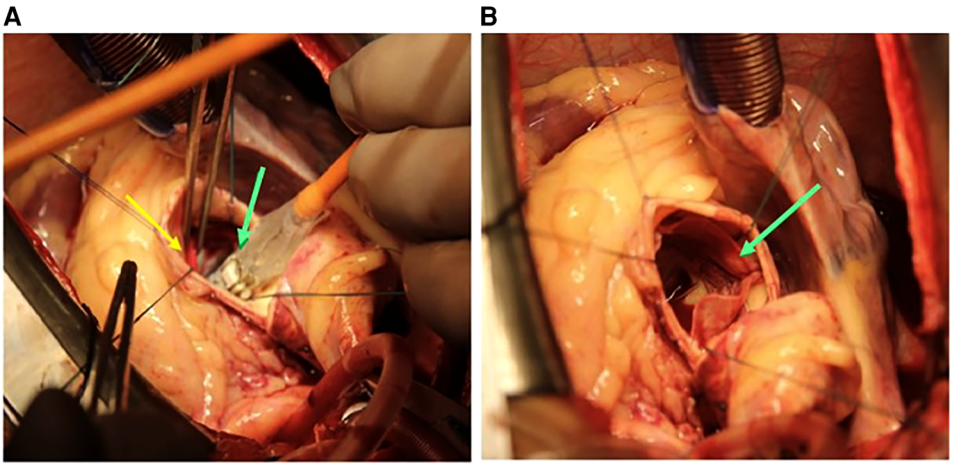

FIGURE 3
(A) Deployment of the 30.5 mm Myval THV (green arrow) positioning into the ring (yellow arrow). (B) Deployed THV (green arrow). THV, transcatheter heart valve.

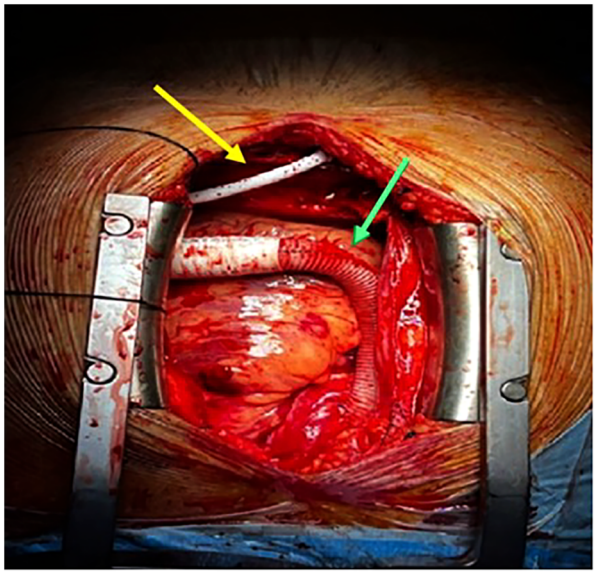

FIGURE 4
Implantation of HeartMate 3™ LVAD, LVAD HM3 outflow graft (green arrow), and LVAD HM3 driveline cable (yellow arrow). LVAD, left ventricular assist device.

complications including deployment failure or postoperative residual AR. In this case, we performed the first ever direct transaortic TAVR using balloon-expandable THV into a newly sewn flexible annuloplasty ring (ViR) on the native AV annulus during the LVAD implantation procedure. The considerable decrease in ischemia time is the key benefit of this new procedure. This technique resolves the issues of late severe AR associated with LVAD implantation, including the risks of redo sternotomy after LVAD, and retains the structural suitability for a possible need of future TAVR. In addition, the availability of extra-large sizes (30.5 and 32 mm) of this balloon-expandable THV enabled better size selection, given that if these sizes were not available, the 29 mm THV would have been used although being excessively oversized, which might not have generated optimal outcomes.

The selection of the treatment modality is a complex decision, as there is a lack of consensus regarding the optimal management of LVAD-related AR. Chung et al. performed ViR implantation in a patient with severe LVAD-associated AR who received a self-expanding AV bioprosthesis and reported excellent post-procedural hemodynamic outcomes. This case report offers encouraging evidence for considering the suitability of TAVR at a later stage following LVAD implantation in such critical heart failure patients (9). Dranishnikov et al. performed simultaneous AVR and LVAD implantation in 19 patients, in whom they reported longer cardiopulmonary bypass times for AVR cases using biological AV with prior LVAD, compared to patients with LVAD alone (12). They also stated that simultaneous AVR with LVAD implantation does not worsen the prognosis (12), which provides considerable impetus to performing concomitant AVR with LVAD implantation for treating stage D heart failure patients with AI (12). The use of a bioprosthetic AV in cases of LVAD-associated AI has been reported with acceptable perioperative and early (30-day) outcomes (9, 12, 13). Hence, a bioprosthetic, balloon-expandable THV was used for the ViR technique as a potential solution in our case.

Rapid deployment (RD)-AVR and TAVR have a shorter cross-clamping time and an overall procedural time, which minimizes the risk of intraoperative myocardial ischemia (5, 14, 15). Rahmanian et al. examined 163 patients undergoing RD-AVR and reported the mean cross-clamping and cardiopulmonary times as 55 ± 23 and 88 ± 38 min respectively, which were relatively lesser than those of the control group (77 ± 22 and 105 ± 38 min), respectively, whereas in-hospital mortality rates of both the RD-AVR and control groups were similar [1.8%, ($n = 3$/

163); $p = 1.000$] (16). Similar outcomes were reported by White et al., who retrospectively observed patients undergoing RD-AVR and conventional AVR (295 patients in each group). Their key findings were as follows: (i) reduced cross-clamping (73.8 ± 37.5 and 107 ± 14.9 min) and procedural times (3.4 ± 1.0 and 3.7 ± 0.5 h); (ii) higher rates of new permanent pacemaker implantation leading to longer hospital stay in the RD-AVR group (~7%); and (iii) similar rates of early myocardial infarction, stroke, and early mortality in both groups (17). Holloway et al. performed RD-AVR using a 23-mm Edwards INTUITY valve (Edwards Lifesciences, Irvine, CA, United States) in an AI patient undergoing concomitant LVAD implantation (14). In the case-series reported by Gangahanamaiah and Marasco (18), RD-AVR was performed using the Perceval valve (LivaNova, London, United Kingdom).

Overall, though RD-AVR is considered a safe treatment for end-stage heart failure, it is more expensive. Moreover, performing RD-AVR using balloon-expandable valves has not shown feasibility yet, since the newly inserted AV prosthesis exerts excessive radial force on the LVOT, which leads to the need for permanent pacemaker (18, 19). Moreover, a higher mortality rate has been reported for AV closure + repair with LVAD, compared to AVR with LVAD (6). AV repair in LVAD-assisted surgery fails if TAVR is required in future. To overcome these case-specific challenges, an initial ring annuloplasty to repair the AV with LVAD was performed by Chung et al. which allows the prospects of a subsequent ViR TAVR procedure (9).

The use of a balloon-expandable biological THV in the cases of LVAD failure-associated AI has rarely been reported, particularly for aortic ViR procedures. We believe that more data should be accumulated from high-volume cardiology centers by surgeons who may consider using this technique to perform aortic ViR procedures in LVAD recipients having AR and/or AI to understand the clinical effectiveness of this technique.

3.1. Limitations

There are a few limitations of this technique. The first is the absence of a specific aortic annulus ring constructed for this procedure, which might affect the stabilization of the aortic annulus or may not achieve the leaflet coaptation. The second is that our novel technique may not be suitable for treating congenital malformations of the aortic root, such as bicuspid aortic valve or Marfan syndrome.

3.2. Future directions

Patients with end-stage heart failure have limited treatment options and experience aortic valve dysfunction/insufficiency post-LVAD implantation. Furthermore, paucity of the literature on balloon-expandable valves provides an opportunity to investigate the field and afford patient-specific treatment options, if necessary. This cutting-edge technique offers a breakthrough for high-risk, younger patients and may serve as a potential platform for future interventions. In addition to dealing with aortic insufficiency, balloon-expandable valves also lower the need for a permanent pacemaker and improve hemodynamic outcomes, as seen in this case. This novel and feasible surgical technique shortens the ischemia time, avoids the risk of redo sternotomy, reduces the possibility of paravalvular leakage, and prevents the progression of aortic regurgitation.

4. Conclusion

This novel technique of direct transaortic transcatheter valve-in-ring with LVAD implantation can be considered in elderly, high-risk heart failure patients, particularly those with prior cardiac surgeries, complex valvular anatomy, and poor ejection fraction. Planning and execution of preoperative and perioperative strategies must be combined with vigilant postoperative management of an LVAD patient. The key benefit of this new procedure is that it enables the surgeons to reduce the ischemia time. Furthermore, the issues of late severe AR associated with LVAD implantation and redo sternotomy are resolved. The valve anatomy is maintained, thus allowing the possible scope for a future TAVR after LVAD if necessary, and decreasing the risk associated with multiple cardiothoracic surgeries and improving patient prognosis.

Data availability statement

The original contributions presented in the study are included in the article/**Supplementary Material**, further inquiries can be directed to the corresponding authors.

Ethics statement

The studies involving human participants were reviewed and approved by the Institutional Ethics Committee of National Research Cardiac Surgery Center, Astana, Kazakhstan. The patients/participants provided their written informed consent to participate in this study. Written informed consent was obtained from the individual(s) for the publication of any potentially identifiable images or data included in this article.

Author contributions

YP: substantial contributions to the conception and design of the work. AM: the acquisition, analysis and interpretation of data for the work, and agreement to be accountable for all aspects of the work in ensuring that questions related to the accuracy or integrity of any part of the work are appropriately investigated and resolved. SN and SA: drafting the work and revising it critically for important intellectual content. MB and TK: final approval of the version to be published. NK: the acquisition, analysis and interpretation of data for the work. AK: agreement

to be accountable for all aspects of the work in ensuring that questions related to the accuracy or integrity of any part of the work are appropriately investigated and resolved. TL: substantial contributions to the conception or design of the work. All authors contributed to the article and approved the submitted version.

Conflict of interest

The authors declare that the research was conducted in the absence of any commercial or financial relationships that could be construed as a potential conflict of interest.

Publisher's note

All claims expressed in this article are solely those of the authors and do not necessarily represent those of their affiliated organizations, or those of the publisher, the editors and the reviewers. Any product that may be evaluated in this article, or claim that may be made by its manufacturer, is not guaranteed or endorsed by the publisher.

Supplementary material

The Supplementary Material for this article can be found online at: https://www.frontiersin.org/articles/10.3389/fcvm.2023.1091420/full#supplementary-material.

SUPPLEMENTARY FIGURE 1
Annulus (A) and Left (B) ventricular outflow tract measurement by multidetector row computed tomography. The resulting annular plane is seen.

SUPPLEMENTARY FIGURE 2
The heights of right (A) and left (B) coronary artery from basal plane measurement by multidetector row computed tomography.

SUPPLEMENTARY FIGURE 3
Pictorial representation of Ethibond sutures with flexible ring[11].

SUPPLEMENTARY FIGURE 4
A- Transcatheter heart valve leaflets (yellow arrow); Color Doppler with no signs of PVL; B- Annular ring (yellow arrow); Transcatheter heart valve (green arrow); Left ventricular assist device (blue arrow).

References

1. Bellumkonda L, Bonde P. Ventricular assist device therapy for heart failure—past, present, and future. *Int Anesthesiol Clin*. (2012) 50(3):123–45. doi: 10.1097/AIA.0b013e31826233a9

2. Brown MA, Sheikh FH, Ahmed S, Najjar SS, Molina EJ. Intra-aortic balloon pump as a bridge to durable left ventricular assist device. *J Am Heart Assoc*. (2021) 10(15):e019376. doi: 10.1161/JAHA.120.019376

3. Kyriakopoulos CP, Kapelios CJ, Stauder EL, Taleb I, Hamouche R, Sideris K, et al. LVAD as a bridge to remission from advanced heart failure: current data and opportunities for improvement. *J Clin Med*. (2022) 11(12):3542. doi: 10.3390/jcm11123542

4. Barth M, Mrozek L, Niazy N, Selig JI, Boeken U, Sugimura Y, et al. Degenerative changes of the aortic valve during left ventricular assist device support. *ESC Heart Fail*. (2022) 9(1):270–82. doi: 10.1002/ehf2.13767

5. Iadanza A, D'Ascenzi F, Torrisi A, Sinicropi G, Neri E, Bernazzali S, et al. TAVR in patients with left ventricular assist device: case report and literature review. *Structural Heart*. (2019) 3(1):11–7. doi: 10.1080/24748706.2018.1540071

6. Robertson JO, Naftel DC, Myers SL, Prasad S, Mertz GD, Itoh A, et al. Concomitant aortic valve procedures in patients undergoing implantation of continuous-flow left ventricular assist devices: an INTERMACS database analysis. *J Heart Lung Transplant*. (2015) 34(6):797–805. doi: 10.1016/j.healun.2014.11.008

7. Mancini D, Colombo PC. Left ventricular assist devices: a rapidly evolving alternative to transplant. *JACC*. (2015) 65(23):2542–55. doi: 10.1016/j.jacc.2015.04.039

8. Adamson RM, Dembitsky WP, Baradarian S, Chammas J, May-Newman K, Chillcott S, et al. Aortic valve closure associated with HeartMate left ventricular device support: technical considerations and long-term results. *J Heart Lung Transplant*. (2011) 30(5):576–82. doi: 10.1016/j.healun.2010.11.007

9. Chung MJ, Ganapathi AM, Vora AN, Schroder JN, Kiefer TL, Hughes GC. Valve-in-ring transcatheter aortic valve replacement after left ventricular assist device therapy. *Ann Thorac Surg*. (2020) 109(3):e163–5. doi: 10.1016/j.athoracsur.2019.06.094

10. Ancona MB, Moroni F, Romano V, Agricola E, Esposito A, Ajello S, et al. Impianto transcatetere di valvola aortica per insufficienza aortica nei pazienti con assistenza ventricolare sinistra [Transcatheter aortic valve implantation for aortic insufficiency in patients with left ventricular assistance]. *G Ital Cardiol*. (2021) 22(3 Suppl 1):395–425. doi: 10.1714/3578.35633

11. Patel PA, Gutsche JT, Vernick WJ, Giri JS, Ghadimi K, Weiss SJ, et al. The functional aortic annulus in the 3D era: Focus on transcatheter aortic valve replacement for the perioperative echocardiographer. *J Cardiothorac Vasc Anesth*. (2015) 29(1):240–5

12. Dranishnikov N, Stepanenko A, Potapov EV, Dandel M, Siniawski H, Mladenow A, et al. Simultaneous aortic valve replacement in left ventricular assist device recipients: single-center experience. *Int J Artif Organs*. (2012) 35(7):489–94. doi: 10.5301/ijao.5000102

13. John R, Naka Y, Park SJ, Sai-Sudhakar C, Salerno C, Sundareswaran KS, et al. Impact of concurrent surgical valve procedures in patients receiving continuous-flow devices. *J Thorac Cardiovasc Surg*. (2014) 147(2):581–9. doi: 10.1016/j.jtcvs.2013.10.024

14. Holloway DD, Jones LC, Howell SJ, Rich JD, Pham DT. LVAD with concomitant rapid deployment valve implantation—a case report. *J Cardiothorac Surg*. (2019) 14(1):126. doi: 10.1186/s13019-019-0944-5

15. Chien S, Clark C, Maheshwari S, Koutsogiannidis CP, Zamvar V, Giordano V, et al. Benefits of rapid deployment aortic valve replacement with a mini upper sternotomy. *J Cardiothorac Surg*. (2020) 15:226. doi: 10.1186/s13019-020-01268-y

16. Rahmanian BP, Kaya S, Eghbalzadeh K, Menghesha H, Madershahian N, Wahlers T. Rapid deployment aortic valve replacement: excellent results and increased effective orifice areas. *Ann Thorac Surg*. (2018) 105:24–30. doi: 10.1016/j.athoracsur.2017.07.047

17. White A, Bozso JS, Lakey O, Hong Y, Wang S, Nagendran J, et al. Rapid deployment valves versus conventional tissue valves for aortic valve replacement. *J Thorac Cardiovasc Surg*. (2022) 163(6):2036–42. doi: 10.1016/j.jtcvs.2020.06.022

18. Gangahanamaiah S, Marasco SF. Rapid deployment of an aortic valve prosthesis during ventricular assist device implantation. *J Heart Lung Transplant*. (2019) 38(4):478–80. doi: 10.1016/j.healun.2018.09.023

19. Barnhart GR, Accola KD, Grossi EA, Woo J, Mumtaz MA, Sabik JF, et al. TRANSFORM (Multicenter experience with rapid deployment Edwards INTUITY valve system for aortic valve replacement) US clinical trial: performance of a rapid deployment aortic valve. *J Thorac Cardiovasc Surg*. (2017) 153:241–51. doi: 10.1016/j.jtcvs.2016.09.062

frontiers | Frontiers in Cardiovascular Medicine

TYPE Case Report
PUBLISHED 20 April 2023
DOI 10.3389/fcvm.2023.1123305

OPEN ACCESS

EDITED BY
Pietro Enea Lazzerini,
University of Siena, Italy

REVIEWED BY
Ulrich Ronellenfitsch,
University Hospital Halle (Saale), Germany
Cassius Iyad Ochoa Chaar,
Yale University, United States

*CORRESPONDENCE
Chen-June Seak
✉ julianseak@hotmail.com

RECEIVED 13 December 2022
ACCEPTED 03 April 2023
PUBLISHED 20 April 2023

CITATION
Wong AC, Chou Y-M, Goh ZNL, Chang K-F and Seak C-J (2023) Case report: Aortoesophageal fistula—an extremely rare but life-threatening cardiovascular cause of hematemesis. Front. Cardiovasc. Med. 10:1123305. doi: 10.3389/fcvm.2023.1123305

Case report: Aortoesophageal fistula—an extremely rare but life-threatening cardiovascular cause of hematemesis

Alexis Ching Wong[1], Yu-Mou Chou[2,3], Zhong Ning Leonard Goh[1], Kuang-Fu Chang[3,4] and Chen-June Seak[1,2,3]*

[1]Department of Emergency Medicine, New Taipei Municipal Tucheng Hospital, New Taipei City, Taiwan, [2]Department of Emergency Medicine, Lin-Kou Medical Center, Chang Gung Memorial Hospital, Taoyuan, Taiwan, [3]College of Medicine, Chang Gung University, Taoyuan, Taiwan, [4]Department of Medical Imaging and Intervention, New Taipei Municipal Tucheng Hospital, New Taipei City, Taiwan

Aortoesophageal fistula (AEF) is an extremely rare cardiovascular etiology of hematemesis and upper gastrointestinal bleeding. As such, its recognition and diagnosis are challenging and may be delayed when such patients present to the emergency department (ED). Without timely surgical intervention, AEF is almost always fatal. Awareness of AEF as a possible diagnosis and consequently early identification of these patients presenting to the ED are therefore crucial in optimizing clinical outcomes. We report a 45-year-old male presenting to the ED with the classical triad of an AEF (Chiari's triad)—midthoracic pain or dysphagia, a sentinel episode of minor hematemesis, then massive hematemesis with risk of exsanguination. The case report highlights the importance of considering the differential diagnosis of AEF when evaluating patients presenting to the ED with hematemesis, especially if they have predisposing risk factors such as prior aortic or esophageal surgeries, aortic aneurysms, or thoracic malignancies. Patients suspected of having AEF should be prioritized for early computed tomography angiography to expedite diagnosis and treatment.

KEYWORDS

aortoesophageal fistula, haematemesis, upper gastrointestinal bleeding, Chiari's triad, emergency department, computed tomography angiography

Introduction

Gastrointestinal bleeding is a common presentation seen in the emergency department (ED). Upper gastrointestinal bleeding (UGIB), in which the source of bleeding is proximal to the ligament of Treitz, accounts for approximately 70%–80% of all gastrointestinal hemorrhages (1). UGIB typically manifests as hematemesis, occasionally accompanied by hematochezia and melena. Since peptic ulcer disease (i.e., non-variceal) and esophageal varices represent the vast majority of UGIB etiologies, the possibility of vascular abnormalities is often overlooked (2).

One such rare vascular etiology causing hematemesis is aortoesophageal fistula (AEF). AEFs can be classified as primary or secondary. Primary AEFs directly originate from the native aorta due to various circumstances such as aortic aneurysm (54.2%), foreign body ingestion (19.2%), and advanced esophageal carcinoma (17.0%), in addition to radiotherapy and infections (e.g., syphilis, tuberculosis); secondary AEFs are sequelae of prior vascular interventions such as thoracic aortic or esophageal surgeries (4.7%) and

graft placement (3, 4). We report a patient with underlying esophageal cancer who presented to the ED with hematemesis and was subsequently diagnosed with a primary AEF.

Case report

A 45-year-old Chinese male with underlying recently diagnosed squamous cell carcinoma of the esophagus (stage T4bN2M0) presented to the ED with frank hematemesis. He was hypotensive (blood pressure 95/51 mmHg) and tachycardic (pulse rate 129 beats/min) on ED arrival, while point-of-care full blood count revealed gross anemia (Hb 3.6 g/dl). The patient was resuscitated accordingly with intravenous fluid boluses pending activation of a massive transfusion protocol. He was also treated for the provisional diagnosis of UGIB secondary to bleeding esophageal tumor with tranexamic acid and proton pump inhibitors. The other hematological and biochemical blood investigations returned normal. Further review of his past medical records revealed that the patient had just completed his first cycle of concurrent chemoradiotherapy a month prior, with the initial tumor staging imaging studies showing no tumor invasion of the adjacent vascular structures.

The patient was transfused with 6 units of packed cells in the ward. There was a symptom-free latent interval of 6 h, until the patient developed another bout of hematemesis and suffered a cardiovascular collapse while awaiting esophagoduodenoscopy. Cardiopulmonary resuscitation was performed in accordance with Advanced Cardiac Life Support protocols. He eventually achieved a return of spontaneous circulation after 36 min but required intubation and inotropic support. The patient was transfused with another 6 units of packed cells and 12 units of fresh frozen plasma. Computed tomography angiography (CTA) thereafter demonstrated an AEF with aortic pseudoaneurysm, as well as massive contrast extravasation at the distal esophagus suggestive of an active hemorrhage (**Figures 1**, **2**). Yet another 6 units of packed cells, 6 units of fresh frozen plasma, and 12 units of platelets were transfused. Nevertheless, he finally succumbed to recurrent hematemesis leading to fatal exsanguination before definitive surgical intervention could be performed (9 h post herald bleed).

Discussion

AEF is an extremely rare cardiovascular etiology of hematemesis and UGIB. As such, its recognition and diagnosis

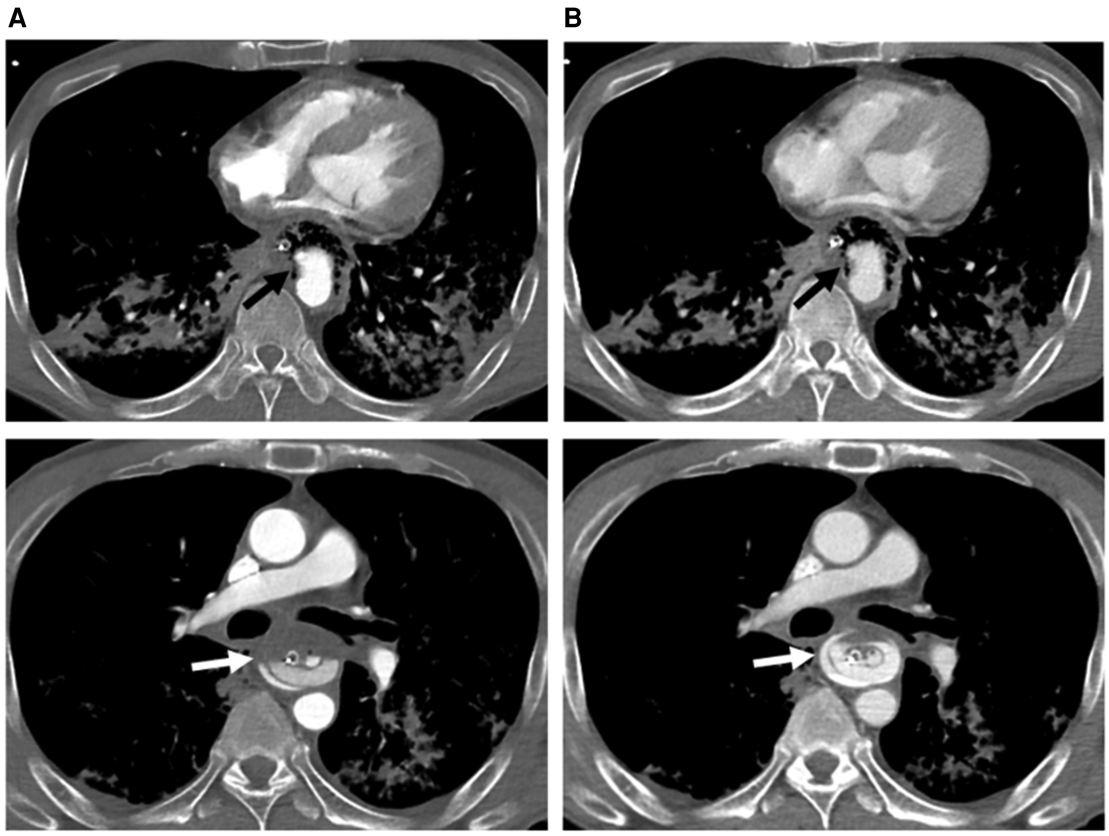

FIGURE 1
Axial computed tomography angiography of arterial (A) and venous (B) phases at two different levels below the carina, demonstrating a descending aortic pseudoaneurysm (black arrow) protruding into the esophagus (with a nasogastric tube *in situ*) through an aortoesophageal fistula (evidenced by direct communication of esophagus and aorta). There is a progressive increase in amount of contrast material (white arrow) in the esophagus, indicating rupture of the pseudoaneurysm and active bleeding.

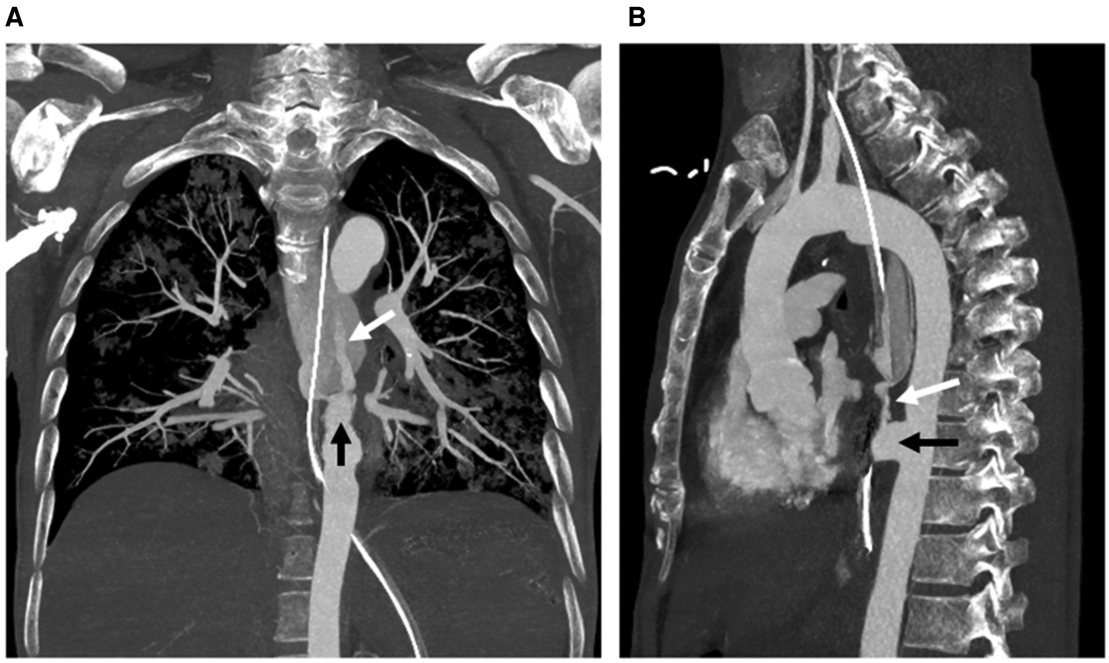

FIGURE 2
Coronal (A) and sagittal (B) maximum intensity projection images from computed tomography angiography show a descending aortic pseudoaneurysm (black arrow) at the level of the aortoesophageal fistula, complicated with rupture and contrast material extravasation (white arrow) into the esophagus (with a nasogastric tube *in situ*).

are challenging and may be delayed when such patients present to the ED. Without timely surgical treatment, AEF is almost always fatal; even with surgical intervention, AEF patients face a high mortality rate of 77% (5). Awareness of AEF as a possible diagnosis and consequently early identification of these patients presenting to the ED are therefore crucial in optimizing their clinical outcomes.

On retrospective review of our patient's clinical course, his progression illustrates the classical triad of an AEF (Chiari's triad)—midthoracic pain or dysphagia, a sentinel episode of minor hematemesis, and a symptom-free interval followed by fatal exsanguination due to recurrent hematemesis. The symptom-free interval during which there is spontaneous cessation of hematemesis has been described in up to 80% of AEF patients (6). In our case, this latent interval lasted approximately 6 h, possibly attributable to the transient occlusion of the AEF *via* a combination of periaortic hematomas, intravascular hypotension, and arterial wall spasm (7).

CTA is the investigation modality of choice to confirm the diagnosis of AEF, as it can objectively demonstrate contrast extravasation. OGDS may be useful in excluding other common causes of UGIB, as well as revealing a bulging pulsatile lesion or submucosal hematoma *via* direct visualization that is suggestive of bleeding into the esophageal wall (8, 9). Nevertheless, esophagoduodenoscopy can be hazardous due to the risk of dislodging the occluding periaortic hematoma responsible for hemostasis and precipitating fatal hemorrhage (10–12).

Clinicians should keep in mind that the diagnosis of AEF is possible in patients presenting with hematemesis to the ED, especially if they have underlying risk factors of previous aortic surgery, aortic aneurysms, and thoracic cancer. Patients suspected to have AEF can be prioritized for CTA to clinch the definitive diagnosis, and subsequent arrangements for surgical interventions can be expedited. While an earlier CTA may or may not have improved the survival chances of our patient, establishing the diagnosis quickly would have been beneficial in allowing our ED team to counsel the patient's family regarding his prognosis accordingly—in recognition of this, our ED now prioritizes CTA over esophagoduodenoscopy in patients who present with frank hematemesis and concurrently have known risk factors for AEF (aortic aneurysm, foreign body ingestion, and advanced esophageal carcinoma).

The definitive treatment of AEFs is usually a combination of aortic (thoracic endovascular aortic repair, graft replacement, graft repair) and esophageal (esophagectomy, esophageal stent, esophageal repair) surgeries (13). In the acute setting of massive hematemesis, the Sengstaken-Blakemore tube (SBT) has been reported to be effective in securing hemostasis *via* the gastroesophageal balloon's tamponade effect, to buy time for definitive surgery (7, 14). Nevertheless, deploying the SBT is not without its complications, such as aspiration pneumonitis, airway obstruction, mucosal ulceration, esophageal perforation, and broncho-esophageal fistulas (15–17).

Surgical treatment options of AEF include open surgery and thoracic endovascular aortic repair (TEVAR); the latter is a minimally invasive technique which deploys an endoluminal aortic stent to rapidly control the bleeding with a favorable 30-day mortality rate of 27.5% (18, 19). TEVAR however does not

address the esophageal lesion in AEFs, which may form a nidus for infections and subsequently lead to stent graft infection, mediastinitis, sepsis, re-hemorrhage, and stroke (20, 21). In contrast, open surgery allows for the debridement of infected mediastinum and esophageal repair in addition to aortic wall reconstruction; the trade-off is a high operative mortality rate of up to 55% (22). Combining TEVAR as bridging therapy with follow-up definitive open repair has been found to yield the lowest mortality rate at 25% (19), though esophageal cancer patients like ours may benefit more from palliative esophageal stents with survival of up to 8 months (23).

Conclusion

AEF is a rare and life-threatening cardiovascular cause of UGIB. It should be included in the list of differential diagnoses when evaluating patients presenting to the ED with hematemesis, especially if they have predisposing risk factors such as prior aortic or esophageal surgeries, aortic aneurysms, or thoracic malignancies. Patients suspected of having AEF should be prioritized for early CTA to expedite the diagnosis. Minimally invasive procedures such as SBT or TEVAR are pivotal to achieve initial hemostasis, which should be followed by definitive open surgery once the patient is stable.

Data availability statement

The original contributions presented in the study are included in the article/Supplementary Material, further inquiries can be directed to the corresponding author.

Ethics statement

The studies involving human participants were reviewed and approved by The Institutional Review Board of the Chang Gung Memorial Hospital (IRB no: 2212130011). Written informed consent for participation was not required for this study in accordance with the national legislation and the institutional requirements. Written informed consent was obtained from the next of kin for the publication of any potentially identifiable images or data included in this article.

Author contributions

Conceptualization: ACW, Y-MC, ZNL G, K-FC, C-JS. **Data curation:** Y-MC, K-FC, C-JS. **Funding acquisition:** C-JS. **Methodology:** ACW, Y-MC, ZNLG, K-FC, C-JS. **Investigation:** Y-MC, K-FC, C-JS. **Resources:** C-JS. **Supervision:** C-JS. **Validation:** ZNLG, C-JS. **Visualization:** ZNLG, C-JS. **Writing-original draft:** ACW, ZNLG, K-FC, C-JS. **Writing—review & editing:** C-JS, ZNLG. All authors contributed to the article and approved the submitted version.

Funding

This work was supported by Ministry of Science and Technology of Taiwan [MOST 109-2314-B-182A-102-] and Chang Gung Memorial Hospital in Taiwan [CMRPVVL0071 and CORPVVL0061]. The funders had no role in study design, data collection and analysis, decision to publish, or preparation of the manuscript.

Conflict of interest

The authors declare that the research was conducted in the absence of any commercial or financial relationships that could be construed as a potential conflict of interest.

Publisher's note

References

1. DeLaney M, Greene CJ. Emergency department evaluation and management of patients with upper gastrointestinal bleeding. *Emerg Med Pract.* (2015) 17:1–18.

2. Stanley AJ, Laine L. Management of acute upper gastrointestinal bleeding. *Br Med J.* (2019) 364:I536. doi: 10.1136/bmj.l536

3. Hollander JE, Quick G. Aortoesophageal fistula: a comprehensive review of the literature. *Am J Med.* (1991) 91:279–87. doi: 10.1016/0002-9343(91)90129-L

4. Barrios Carvajal M, Díaz-Tobarra M, Martí-Obiol R, López Mozos F, Ortega Serrano J. Combined treatment of an aortoesophageal fistula after aortoplasty for aortic stenosis. *Ann Thorac Surg.* (2015) 100:1091–3. doi: 10.1016/j.athoracsur.2014.11.038

5. Yang Y, Hu D, Peng D. Primary aortoesophageal fistula: a fatal outcome. *Am J Emerg Med.* (2018) 36:343.e1–e3. doi: 10.1016/j.ajem.2017.11.008

6. Carter R, Mulder GA, Snyder EN Jr, Brewer LA 3rd. Aortoesophageal fistula. *Am J Surg.* (1978) 136:26–30. doi: 10.1016/0002-9610(78)90195-2

7. Seet E, Beevee S, Cheng A, Lim E. The sengstaken-blakemore tube: uses and abuses. *Singapore Med J.* (2008) 49:e195–7.

8. Saers SJF, Scheltinga MRM. Primary aortoenteric fistula. *Br J Surg.* (2005) 92:142–52. doi: 10.1002/bjs.4928

9. Maher MM, Murphy J, Dervan P, O'Connell D. Aorto-oesophageal fistula presenting as a submucosal oesophageal haematoma. *Br J Radiol.* (1998) 71:972–4. doi: 10.1259/bjr.71.849.10195014

10. Ctercteko G, Mok CK. Aorta-esophageal fistula induced by a foreign body: the first recorded survival. *J Thorac Cardiovasc Surg.* (1980) 80:233–5. doi: 10.1016/S0022-5223(19)37796-7

11. Baron RL, Koehler RE, Gutierrez FR, Forrest JV, Weyman PJ. Clinical and radiographic manifestations of aortoesophageal fistulas. *Radiology*. (1981) 141:599–605. doi: 10.1148/radiology.141.3.7302210

12. Benson MJ, Rouse D, van Someren N, Wingate DL, Swain CP. Fatal hemorrhage from an aorto-esophageal fistula precipitated by flexible endoscopy. *Gastrointest Endosc*. (1991) 37:193–6. doi: 10.1016/S0016-5107(91)70686-X

13. Takeno S, Ishii H, Nanashima A, Nakamura K. Aortoesophageal fistula: review of trends in the last decade. *Surg Today*. (2020) 50:1551–9. doi: 10.1007/s00595-019-01937-z

14. Assink J, Vierhout BP, Snellen JP, Benner PM, Paul MA, Cuesta MA, et al. Emergency endovascular repair of an aortoesophageal fistula caused by a foreign body. *J Endovasc Ther*. (2005) 12:129–33. doi: 10.1583/04-1401R.1

15. Avgerinos A, Armonis A. Balloon tamponade technique and efficacy in variceal haemorrhage. *Scand J Gastroenterol Suppl*. (1994) 207:11–6. doi: 10.3109/00365529409104188

16. Chong CF. Esophageal rupture due to sengstaken-blakemore tube misplacement. *World J Gastroenterol*. (2005) 11:6563–5. doi: 10.3748/wjg.v11.i41.6563

17. Chien JY, Yu CJ. Images in clinical medicine. Malposition of a sengstaken-blakemore tube. *N Engl J Med*. (2005) 352:e7. doi: 10.1056/NEJMicm040003

18. Li S, Gao F, Hu HO, Shi J, Zhang J. Risk factors for mortality in patients with aortoesophageal fistula related to aortic lesions. *Gastroenterol Res Pract*. (2020) 2020:4850287. doi: 10.1155/2020/4850287

19. Canaud L, Ozdemir BA, Bee WW, Bahia S, Holt P, Thompson M. Thoracic endovascular aortic repair in management of aortoesophageal fistulas. *J Vasc Surg*. (2014) 59:248–54. doi: 10.1016/j.jvs.2013.07.117

20. Zhan Y, Xu Z. Massive hemorrhage from an aortoesophageal fistula caused by esophageal stent implantation: a case report and literature review. *Medicine (Baltimore)*. (2019) 98:e18303. doi: 10.1097/MD.0000000000018303

21. Lee S, Srinivasa RN, Rigberg DA, Yanagawa J, Benharash P, Moriarty JM. Aortoesophageal fistula involving the central aortic arch salvaged with emergent percutaneous TEVAR, great vessel coverage and in vivo graft fenestration. *Diagn Interv Radiol*. (2021) 27:122–5. doi: 10.5152/dir.2020.20033

22. Kieffer E, Chiche L, Gomes D. Aortoesophageal fistula: value of in situ aortic allograft replacement. *Ann Surg*. (2003) 238:283–90. doi: 10.1097/01.sla.0000080828.37493.e0

23. Aday U, Ali Çetin D, Çiyiltepe H, Gündeş E, Bozdağ E, Senger AS. Cause of mortality in aortoesophageal fistula: oesophageal sepsis. A case report. *Prz Gastroenterol*. (2017) 12:222–5. doi: 10.5114/pg.2017.70476

frontiers | Frontiers in Cardiovascular Medicine

TYPE Case Report
PUBLISHED 09 May 2023
DOI 10.3389/fcvm.2023.1108768

OPEN ACCESS

EDITED BY
Junjie Xiao,
Shanghai University, China

REVIEWED BY
Yunshan Cao,
Gansu Provincial Hospital, China
Sandeep Sainathan,
University of Miami Health System,
United States

*CORRESPONDENCE
M. Westhoff
michael.westhoff@lkhemer.de

SPECIALTY SECTION
This article was submitted to General Cardiovascular Medicine, a section of the journal Frontiers in Cardiovascular Medicine

RECEIVED 26 November 2022
ACCEPTED 16 March 2023
PUBLISHED 09 May 2023

CITATION
Westhoff M, Hardebusch T, Litterst P, Breithecker A, Haas M, Kuniss M, Neumann T, Guth S and Wiedenroth CB (2023) Successful simultaneous stenting of a pulmonary artery and vein in pulmonary vascular stenosis due to silicosis. Case report and literature review. Front. Cardiovasc. Med. 10:1108768. doi: 10.3389/fcvm.2023.1108768

Successful simultaneous stenting of a pulmonary artery and vein in pulmonary vascular stenosis due to silicosis. Case report and literature review

M. Westhoff[1,2]*, T. Hardebusch[1], P. Litterst[1], A. Breithecker[3], M. Haas[4], M. Kuniss[4], T. Neumann[4], S. Guth[5] and C. B. Wiedenroth[5]

[1]Department of Pulmonology, Klinik für Pneumologie, Schlaf und Beatmungsmedizin, Lungenklinik Hemer, Zentrum für Pneumologie und Thoraxchirurgie, Hemer, Germany, [2]Universität Witten/Herdecke University, Witten, Germany, [3]Department of Radiology, Kerckhoff Heart and Thorax Center, Bad Nauheim, Germany, [4]Department of Cardiology, Kerckhoff Heart and Thorax Center, Bad Nauheim, Germany, [5]Department of Thoracic Surgery, Kerckhoff Heart and Thorax Center, Bad Nauheim, Germany

A 58-year-old patient was admitted to the emergency department due to severe respiratory insufficiency. Anamnesis revealed that the patient had experienced increasing stress dyspnea for a few months. Upon imaging, an acute pulmonary embolism was excluded, but peribronchial and hilar soft tissue proliferation with compression of central parts of the pulmonary circulation was found. The patient had a history of silicosis. The histology report showed tumor-free lymph node particles with prominent anthracotic pigment and dust depositions without evidence of IgG4-associated disease. The patient was administered steroid therapy and underwent simultaneous stenting of the left interlobular pulmonary artery and the upper right pulmonary vein. As a result, a significant improvement in symptoms and physical performance was achieved. The diagnosis of inflammatory or, in particular, fibrosing mediastinal processes can be challenging and important clinical symptoms must be taken into account, especially if the pulmonary vasculature is involved. In such cases, the possibility of interventional procedures should be examined in addition to drug therapy options.

KEYWORDS
mediastinal fibrosis, silicosis, pulmonary artery stenosis, pulmonary vein stenosis, pulmonary hypertension, stenting

1. Introduction

Inflammatory and especially fibrosing mediastinal processes can lead to significant differential diagnostic challenges and key clinical symptoms, especially if pulmonary vascular involvement is present (1–4). In cases of definitively confirmed pulmonary arterial and/or venous stenosis, it is important to clarify whether interventional procedures are an option in addition to drug therapy (5–7).

The following case description reveals the chameleon-like clinical symptoms of an extremely rare case of simultaneous pulmonary artery (PA) and pulmonary vein (PV) stenosis as a result of silicosis, the considerable challenges in confirming the diagnosis, and the currently existing therapeutic options for the treatment of pulmonary vascular co-involvement in fibrosing mediastinal diseases.

2. Case description

In June 2020, a 58-year-old patient with known history of silicosis first presented due to increasing dyspnea under stress. The blood gases in the referring clinic showed hyperventilation and hypoxemia (pH 7.47, pCO_2 32 mmHg, pO_2 52 mmHg). Upon imaging, consolidations were detected in the lower and middle lobes of the right lung as well as in the upper lobe of the left lung, which were initially interpreted as a result of a possible previous infection.

Due to severe dyspnea (RR 29/min) with persistent hypoxemia under low-flow oxygen and now manifest hypercapnic respiratory insufficiency ($PaCO_2$ 66 mmHg, pH 7.23) high-flow oxygen therapy (HFNC) with intermittent non-invasive ventilation (NIV) was initiated. ECG showed sinus tachycardia (103 bpm) with normal axis. There was also no indication of IgG4-associated disease. There was no improvement with antibiotic therapy, so that under the suspicion of exacerbated inflammatory lung disease, steroid therapy (initially 1 g/day for 3 day followed by 1 mg/kg/day) was initiated along with diuretic therapy due to a tendency for peripheral edema in connection with known hypertensive heart disease. These measures led to an impressive improvement of the respiratory and clinical situation and normalization of blood gases when breathing room air; under these conditions, the 6-min walking distance was 400 m without ventilatory insufficiency or hypoxemia. The lung function test showed an obstructive respiratory disease (FEV1/FVC 56%, FEV1 57%-pred., Reff 128%-pred.), the diffusion capacity for carbon monoxide was reduced (53%-pred.).

In August 2020, a follow-up thoracic CT scan showed a complete regression of basal consolidations in the right lower lobe and clear regression of the remaining inflammatory changes. Steroid therapy was continued at 50 mg/day, reduced in dose over time, and discontinued in October 2020 (see timeline, **Figure 1** and **Table 1**).

3. Further diagnostic assessment, treatment, and clinical course

In December 2020, the patient again developed progressive exercise dyspnea with a productive cough and fatigue. Blood gas analysis showed hypoxemic respiratory insufficiency (pH 7,48, PaO_2 50 mmHg, $PaCO_2$ 32 mmHg). Body plethysmography revealed an irreversible moderate obstructive ventilation disorder with reduced diffusion capacity (DLCO 60%-pred.).

Echocardiography revealed that systolic pulmonary arterial pressure was increased to 65 mmHg. Cardiopulmonary exercise testing (CPET) (**Figure 1**) showed a limited load (79 W, 60% of normal) as well as reduced ventilatory capacity, deconditioning, a pseudorestrictive breathing pattern, and abnormal diffusion with an $AaDO_2$ of 50.3 mmHg, characteristic of pulmonary vasculopathy. Scintigraphy showed reduced perfusion in both lungs. There was no evidence of PA embolism in angio-CT scans of the thorax, but there was a compression of central regions of the left pulmonary arterial tree, with soft tissue proliferation on both sides, hilar and peribronchial (**Figure 2**), largely identical to the first imaging results from June 2020. Also striking was a compression-related concentric high-grade stenosis of the outflow portion of the left lower lobe artery, a moderate compression of the bronchus intermedius and the lower lobe bronchus, and a rupture of the middle lobe bronchus.

Rigid bronchoscopy with endobronchial ultrasound (EBUS) revealed extensive peribronchial compactions walling in surrounding tissue without recognizable boundaries as well as calcifications in the lymph nodes. Macroscopically, the biopsies were anthracotic. Histology revealed tumor-free lymph node particles with prominent anthracotic pigment and dust depositions. There were practically no positively labeled cells upon staining of MUM 1 as a marker of plasma cells or B cells. A conspicuous proliferation of IgG- or IgG4-positive plasma cells could be ruled out.

To further clarify the suspected vascular compression with consequent reduction of perfusion, selective pulmonary angiography supplemented by high-resolution angio-CT of the thorax was performed. The compression-related stenosis of the left lower lobe artery was confirmed, and stenosis of the right upper PV was also detected. Furthermore, a segmental pulmonary embolism was observed in the region of the right lower lobe. Moderate precapillary pulmonary hypertension with a PAm of 27 mmHg, pulmonary capillary wedge pressure of 4 mmHg, and a PVR of 4.4 WU was detected using right heart catheterization. Under load (40 W) there was a significant increase in PAm to 61 mmHg and in PVR to 5.1 WU.

Under renewed steroid therapy, simultaneous percutaneous intervention on the left interlobular PA and the right upper PV was carried out on March 11, 2021, by means of balloon dilatation and stent insertion (**Figure 3**): the left interlobar pulmonary artery was stented using an AndraTex Optimus CoCr Stent (L in 12×23 mm) after predilatation with Medtronic Admiral Xtreme 8.0×40 mm and 10.0×40 mm balloons. The right upper pulmonary vein was stented using a Cordis Palmaz Genesis (9×17 mm) after predilatation with a Cordis Powerflex Pro (6×20 mm). Post-procedural results were documented with selective angiography. Post-intervention the patient developed reperfusion edema of the left lower lobe of the lung that was quickly brought under control by NIV and negative fluid balance. A three-month dual anti-platelet therapy and oral anticoagulation (for 3 months at reduced dosage) were prescribed. Steroid therapy was gradually reduced to <5 mg/day. In the clinical course up to September 2022, CPET (**Figure 1**) showed increasing improvement in findings with significantly increased resilience (138 W, 92% normal), a decrease in diffusion disturbances, and an improved respiratory efficiency compared to the CPET before PA- and PV-stenting and the follow-up CPETs in 2021. Echocardiographically a normalization of PA pressure was seen.

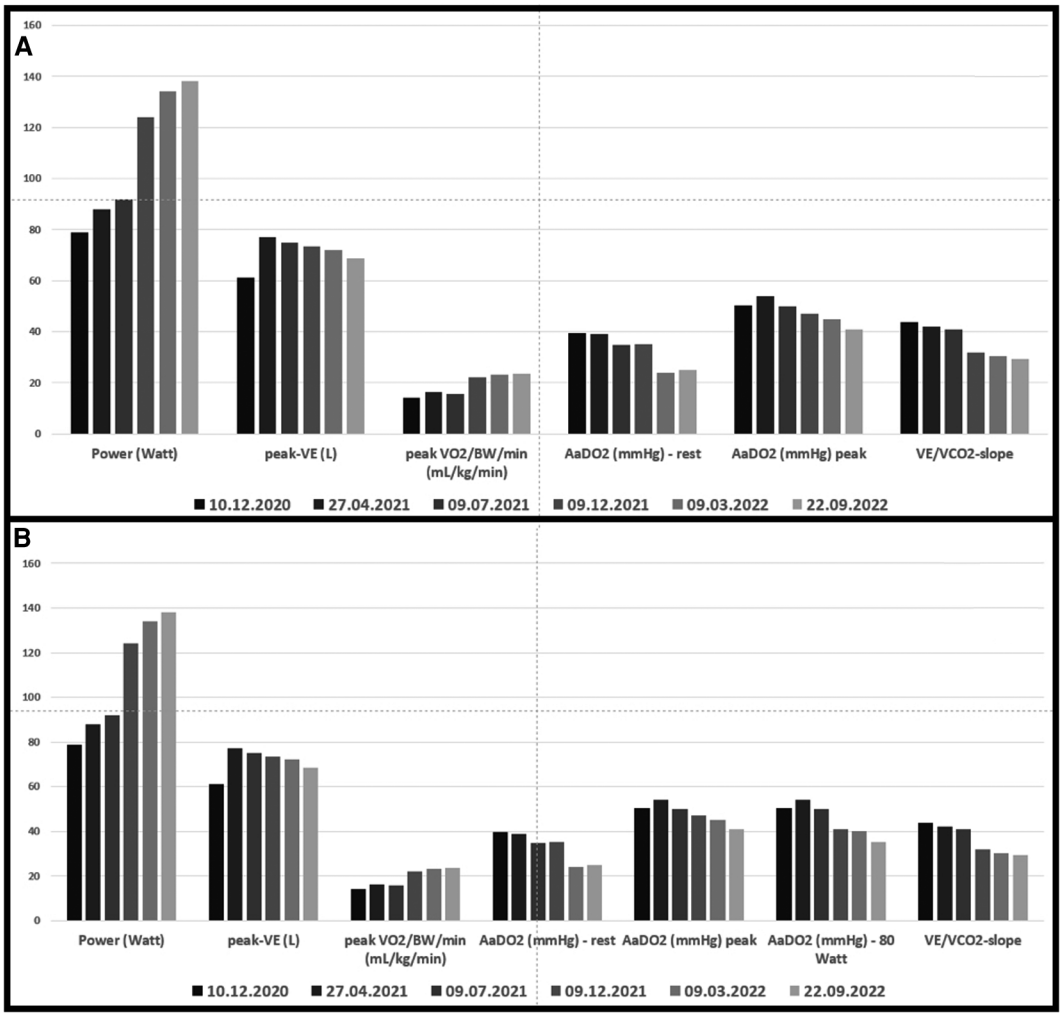

FIGURE 1
(A) Cardio-pulmonary exercise data. Grey bars before and green bars after intervention in 3/2021; (B) data from a) with the addition of $AaDO_2$ at 80 Watt (maximal power achieved at the pre-interventional cardio-pulmonary exercise test).

4. Discussion

The present case report is the first description of simultaneous, successful stenting of concurrent stenosis of a pulmonary artery and vein with pulmonary hypertension in the context of mediastinal fibrosis with lymph node enlargement due to silicosis with anthracofibrosis. A similar stenting of pulmonary artery and vein stenosis in mediastinal fibrosis caused be Histoplasmosis was already described in 2001 by Doyle et al. (27). The diagnosis of vascular stenosis resulting from mediastinal fibrosis in the setting of silicosis is supported by the known occupational load, the bronchoscopically visible anthracotic mucosal changes, the CT findings with lymph node enlargement, including calcifications, and the histological changes with evidence of prominent anthracotic pigment and dust depositions as well as exclusion of other causes.

Initially, the pronounced clinical symptoms—swelling of the bronchial mucosa as is characteristic of anthracosilicosis, detection of infiltrates in the right lower lobe, and acute hypoxemic and hypercapnic insufficiency—were interpreted as signs of pneumonia complicated by cardiac decompensation with simultaneous pulmonary hypertension, especially since there was significant clinical improvement with diuretic therapy and non-invasive ventilation as well as complementary steroid therapy. Retrospectively, and with knowledge of the pulmonary vascular status, the transient respiratory deterioration and the pronounced bronchial mucosal thickening and bronchial stenosis can be explained by the impairment of pulmonary perfusion as well as intermittent pulmonary congestion as a result of PV stenosis. Similar findings for pulmonary hypertension, pulmonary venous congestion, and occasionally also additional pleural effusions and hemoptysis have already been described in connection with pulmonary vascular stenosis, mainly in the context of fibrosing mediastinitis (19, 20, 28–31). Wang et al. describe the dyad, triad, and tetralogy of pulmonary hypertension in fibrosing mediastinitis (PH-FM), which can even be seen in a chest radiograph. The FM dyad includes predominant main PA and lobe atelectasis. FM triad refers to the FM dyad plus pleural

TABLE 1 Case reports without interventions.

	Total cases	Cases of isolated PV stenosis	Cases of isolated PA stenosis	Cases of PV and PA stenosis	Disease
Beaconsfield et al., 1998 (8)	*N* = 1		*N* = 1		Tuberculosis
Chang et al., 2012 (9)	*N* = 1			*N* = 1	Fibrosing Mediastinitis
Cimenoglu et al., 2019 (10)	*N* = 1		*N* = 1		Fibrosing Mediastinitis
Co et al., 2018 (4)	*N* = 1			*N* = 1	Fibrosing Mediastinitis
Cohen et al., 1996 (11)	*N* = 1		*N* = 1		Tuberculosis
Cosio et al., 1973 (12)	*N* = 1		*N* = 1		Fibrosing Mediastinitis
Damuth et al., 1980 (13)	*N* = 1		*N* = 1		Sarcoidosis
Gustafson et al., 2012 (14)	*N* = 1		*N* = 1		Fibrosing Mediastinitis (Histoplasmosis)
Hasegawa et al., 2012 (15)	*N* = 1		*N* = 1		Sarcoidosis
Kolbe et al., 1997 (16)	*N* = 1		*N* = 1		Fibrosing Mediastinitis
Lee et al., 2014 (17)	*N* = 1		*N* = 1		Fibrosing Mediastinitis
Leong et al., 2008 (18)	*N* = 1	*N* = 1			Fibrosing Mediastinitis
Li et al., 2018 (19)	*N* = 1	*N* = 1			Fibrosing Mediastinitis
Mahnken et al., 2001 (20)	*N* = 1	*N* = 1			Silicosis
Mangla et al., 1985 (21)	*N* = 1		*N* = 1		Sarcoidosis
Nelson et al., 1965 (22)	*N* = 1		*N* = 1		Fibrosing Mediastinitis
Ojeifo et al., 2015 (23)	*N* = 1		*N* = 1		Tuberculosis
Papandreou et al., 1992 (24)	*N* = 1		*N* = 1		Fibrosing Mediastinitis
Perez et al., 1999 (25)	*N* = 1		*N* = 1		Coccidioidomycosis
Songster et al., 2020 (26)	*N* = 1			*N* = 1	Fibrosing Mediastinitis (Histoplasmosis)
Yazaki et al., 2021 (27)	*N* = 1	*N* = 1			Anthracofibrosis
Totals	**21**	**4**	**14**	**3**	

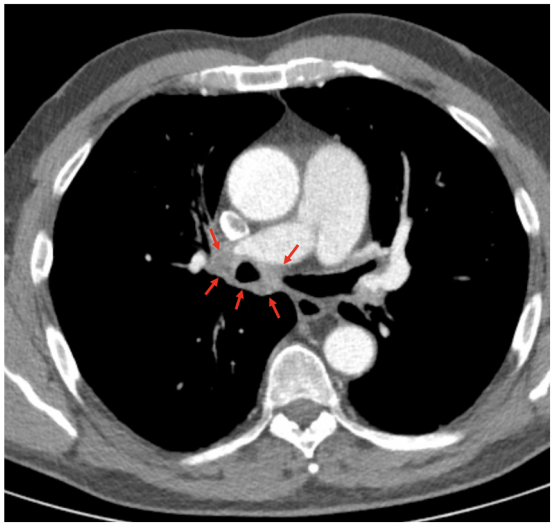

FIGURE 2
Preinterventional computed tomography showing perihilar soft tissue proliferation circumferentially located around the right main stem bronchus (red arrows).

effusion or pulmonary congestion/interstitial pulmonary edema. FM tetralogy includes the mentioned 4 signs (9). Clinical indications of relevant stenosis of the pulmonary arteries were found in the CT of the thorax by the increasing vascular rarefication of the left lower lobe of the lung and the accordingly reduced perfusion in the scintigram. Pulmonary venous stenosis could only be diagnosed using pulmonary angiography and a supplementary high-resolution CT with appropriate contrast agent administration. This underlines the importance of employing high-quality and differential diagnostics for the assessment of pulmonary vascular involvement.

With differential diagnosis it is possible to essentially exclude fibrosing mediastinitis in undefined mediastinal processes. This is a rare disease caused by extensive fibroinflammatory changes with compression of vessels, especially the pulmonary vessels and the superior vena cava but also in individual cases the coronary vessels and esophagus (1, 2, 5, 15), that is characterized by a potentially lethal course. In most cases, fibrosing mediastinitis is infection associated (mostly histoplasmosis, occasionally in tuberculosis, coccidioidomycosis), non-infection associated (e.g., sarcoidosis, IgG4-related, silicosis), iatrogenic (e.g., radiotherapy, chest surgery) disease or it is idiopathic (3, 7, 9, 13, 15, 23, 32–34). In addition, further manifestations of multifocal fibrosis may be present (1).

The initially successful steroid therapy was suggestive of a steroid-sensitive, IgG4-associated disease; on the other hand, positive effects of steroids are also described that are independent of IgG4 (1, 2, 15). However, there were no clear indications, in particular serological or histological, in the present case. Here, the silicotic changes were particularly impressive.

In the present case, only the interventional treatment of vascular stenosis by means of stent implantation in the pulmonary artery and vein proved to be effective, both acutely and in the long term.

Besides echocardiography and B-type natriuretic peptide, CPET proved to be a sensitive non-invasive tool to detect functional impairment before stenting, as well as functional improvement after the intervention with normalization of parameters initially indicating pulmonary hypertension. Using

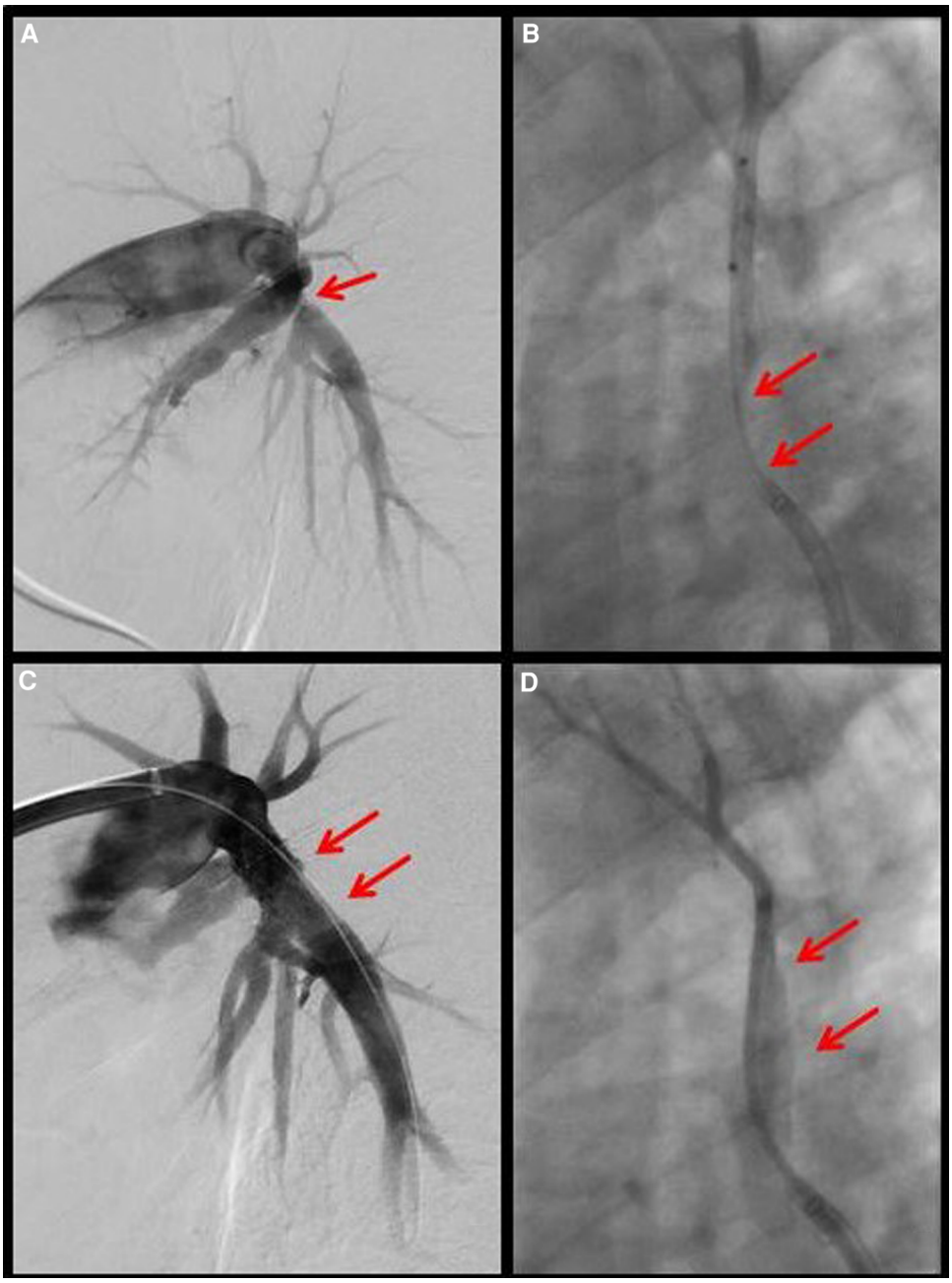

FIGURE 3
Intervention on the left interlobular pulmonary artery with high-grade stenosis before (A) and good flow after (B) stent insertion. Intervention on the highly stenosed upper right pulmonary vein (C) with good outflow after stent insertion (D).

these tools for surveillance, repeated angiographies may be avoided. However, suspicious findings and clinical deterioration should be clarified by imaging.

More than three decades ago, hybrid procedures with intraoperative stent insertion (23, 34–37) were performed in individual cases for the treatment of congenital PA and PV stenosis. Subsequently, interventional therapies in the form of balloon angioplasty and stenting were applied mainly for PV stenosis after ablation in atrial fibrillation (38, 39). In contrast, the clinical evidence on confirmed PA and PV stenosis in the context of fibrosing mediastinal processes is scarce, especially with regard to interventional therapy; there are primarily individual case reports, some with literature reviews (**Tables 1**, **2**) (5, 19, 27, 29, 44). Fender et al. (5) describe in their overview several cases of successful percutaneous intervention but also refer to the limited experience with such procedures worldwide. In 2011 Albers et al. (7) reported a larger study of 58 patients with fibrosing mediastinitis, 46 of whom had PV and/or PA stenosis. In 53% of the cases, both vascular structures were involved. In addition, 12 patients had superior vena cava stenosis. Thirty patients were treated with multiple stenting of pulmonary veins and arteries. Reinterventions were required in

TABLE 2 Case reports with and without interventions (*16 cases without information about intervention).

	Total cases	Cases of isolated PV stenosis	Cases of isolated PA stenosis	Cases of PV and PA stenosis	Cases with dilatation ± stenting	PV stenosis, dilatation only	PV stenosis, dilatation and stenting	PA stenosis, dilatation only	PA stenosis, dilatation and stenting	Disease
Ahn et al., 2015 (40)	*N* = 1		*N* = 1		*N* = 1				*N* = 1	Silicosis
Albers et al., 2011 (7)	*N* = 46	n.a.	n.a.	*N* = 31	*N* = 30		*N* = 16		*N* = 19	Fibrosing Mediastinitis
Argueta et al., 2019 (33)	*N* = 2		*N* = 1		*N* = 1				*N* = 1	Fibrosing Mediastinitis (Coccidioidomycosis)
Condado et al., 2016 (41)	*N* = 5		*N* = 2	*N* = 3	*N* = 3		*N* = 1		*N* = 3	Sarcoidosis
Duan et al., 2022 (42)	*N* = 30	*N* = 30			*N* = 30		*N* = 30			Fibrosing Mediastinitis
Doucet et al., 2015 (43)	*N* = 1	*N* = 1			*N* = 1		*N* = 1			Fibrosing Mediastinitis (Histoplasmosis)
Doyle et al., 2001 (44)	*N* = 4	*N* = 2	*N* = 1	*N* = 1	*N* = 4		*N* = 3		*N* = 2	Fibrosing Mediastinitis
Ferguson et al., 2010 (45)	*N* = 4	*N* = 1	*N* = 3		*N* = 4		*N* = 1		*N* = 3	Fibrosing Mediastinitis
Guerrero et al., 2001 (46)	*N* = 1		*N* = 1		*N* = 1				*N* = 1	Fibrosing Mediastinitis
Li et al., 2020 (29)	*N* = 1		*N* = 1		*N* = 1				*N* = 1	Fibrosing Mediastinitis
Liu et al., 2015 (47)	*N* = 8		*N* = 8		*N* = 8				*N* = 8	Sarcoidosis
Ingraham et al., 2022 (6)	*N* = 1		*N* = 1		*N* = 1				*N* = 1	Fibrosing Mediastinitis
Kandzari et al., 2000 (48)	*N* = 1		*N* = 1		*N* = 1				*N* = 1	Fibrosing Mediastinitis
Peikert et al., 2011 (3)	*N* = 43	*N* = 10	*N* = 33		*N* = 4	*N* = 1			*N* = 3	Fibrosing Mediastinitis (incl. Histoplasmosis)
Ponamgi et al., 2015 (49)	*N* = 8	*N* = 8			*N* = 8	*N* = 3	*N* = 5			Fibrosing Mediastinitis
Satpathy et al., 2011 (50)	*N* = 1		*N* = 1		*N* = 1				*N* = 1	Fibrosing Mediastinitis (Histoplasmosis)
Seckeler et al., 2021 (32)	*N* = 1		*N* = 1		*N* = 1				*N* = 1	Fibrosing Mediastinitis (Coccidioidomycosis)
Shapiro et al., 2005 (51)	*N* = 1	*N* = 1			*N* = 1	*N* = 1				Fibrosing Mediastinitis
Smith et al., 2011 (52)	*N* = 1		*N* = 1		*N* = 1				*N* = 1	Fibrosing Mediastinitis
Thiessen et al., 2007 (53)	*N* = 1		*N* = 1		*N* = 1				*N* = 1	Fibrosing Mediastinitis
Unger et al., 2015 (30)	*N* = 1	*N* = 1			*N* = 1		*N* = 1			Fibrosing Mediastinitis
Valentin et al., 2016 (54)	*N* = 1		*N* = 1		*N* = 1				*N* = 1	Fibrosing Mediastinitis
Welby et al., 2021 (55)	*N* = 9		*N* = 9		*N* = 9				*N* = 9	Fibrosing Mediastinitis
Westhoff et al.,	*N* = 1	*N* = 1	*N* = 1	*N* = 1	*N* = 1		*N* = 1		*N* = 1	Silicosis
Yang et al., 2021 (56)	*N* = 1			*N* = 1	*N* = 1		*N* = 1		*N* = 1	Fibrosing Mediastinitis
Zhang et al., 2018 (28)	*N* = 1	*N* = 1			*N* = 1		*N* = 1			Silicosis, Anthracofibrosis
Zhou et al., 2019 (57)	*N* = 5	*N* = 5			*N* = 5		*N* = 5			Fibrosing Mediastinitis
Totals	**180***	**61**	**68**	**35**	**122**	**5**	**66**	**0**	**60**	

10.3389/fcvm.2023.1108768

five patients. In a retrospective analysis, Peikert et al. (3) observed a total of 80 cases of fibrosing mediastinitis between 1985 and 2006, 34 of which had vascular involvement. However, only 3 patients underwent angioplasty including stenting of the PA, while one patient received balloon dilatation of the PV. A more recent overview of 30 cases with PV dilatation and stent implantation was provided by Duan et al. (see also below) (42).

In the context of silicosis, however, reports of PA or PV stenosis as a result of extensive fibrosis and/or lymph node enlargement (19, 20, 28) are rare. In a recent report, Yazaki et al. described a patient with dyspnea and pulmonary hypertension as a result of occlusion of the upper right PA (28). Similar to our case, the endoscopic imaging was characteristic of anthracofibrosis, and this diagnosis was supported by right heart catheterization and pulmonary angiography. The therapy administered with tadalafil seems rather unusual in view of the findings (28). Zhang et al. (20) reported for the first time in 2018 the successful percutaneous treatment of a case of PA stenosis with concomitant pulmonary hypertension in the context of mediastinal anthracofibrosis originating from silicosis. Here, pulmonary hypertension was particularly noteworthy. The definitive diagnosis could only be made by pulmonary angiography showing evidence of bilateral stenosis, which was successfully treated by balloon dilatation and stenting. Dilatation or stenting of stenosis of the pulmonary veins in silicosis and simultaneous arterial interventions have not yet been described.

A search of the literature produced a total of 120 cases of mediastinal fibrosis that were treated by dilatation of the pulmonary vessels, including 3 cases with both PA and PV stenosis (**Table 2**). In 71 of those 120 cases there was dilatation of PV stenoses with or without supplementary stenting, and in 60 cases PA dilatations were performed with or without stenting. In addition to the present case with simultaneous intervention, there is another in which both PA and PV stenting took place; however, this was a case of fibrosing mediastinitis (44) (**Table 2**).

The further clinical course after pulmonary vascular interventions shows a significant functional improvement in the majority of cases but can also be characterized by residual stenosis or restenosis. A number of studies provided detailed data about reduction of the degrees of stenosis, symptom relief, reduction of pulmonary pressure, re-stenosis, and survival. In the report by Albers et al. (7), 32 patients (87%), including patients with compression of the vena cava, experienced improvement in symptoms. This was also reflected in a significant decrease in pulmonary arterial pressures. There was a large variation in the period of persistent symptomatic improvement (2 to 144 months). Fifteen percent of the 40 patients treated by intervention died during follow-up. Five-year survival in patients with bilateral vascular involvement was significantly more favorable for patients with intervention than in those without (89.5% vs. 52.5%). In contrast, there was no significant difference between the two groups in cases of unilateral disease. In a case series described by Ponamgi et al. (49), there were 3 deaths among 8 patients with multiple dilated and stented pulmonary veins. Of 25 dilated veins, restenosis occurred in 11 during follow-up. Zhou et al. (57) reported in 2019 on 5 patients with fibrosing mediastinitis and PV stenosis treated by balloon dilatation and stent implantation. A total of 11 compression stenoses were treated without complications except for a cardiac arrest triggered by vagal stimulation. In the long-term course, one patient experienced renewed higher-grade stenosis at the proximal stent end as a result of fibrotic compression, while another patient developed in-stent thrombosis due to a cessation of anticoagulation. A re-evaluation at 6 months showed a significant improvement in the degree of stenosis and trans-stenotic pressure gradients in all cases. Pulmonary hypertension associated with pulmonary venous stenosis was improved post-interventionally, with a decrease in mean PA pressure from 45.0 ± 9.0 mmHg to 38.7 ± 8.4 mmHg ($p < 0.05$). Welby et al. (55) observed a significant increase of 54%–79% ($p = 0.005$) in lumen width after stenting of PA stenosis, with a simultaneous decrease in the stenosis gradient by an average of 9.38 mmHg ($p = 0.005$). The openness rate after one year was 90%, and 89% of patients reported an improvement in dyspnea. Re-interventions were required in 2 out of 9 patients. In the recent case study by Duan et al. (42) of 30 patients with fibrosing mediastinitis in the period 2018–2020, a total of 63 PV stenoses were treated in 32 angioplasty sessions and 44 stents were implanted in 41 pulmonary veins after prior balloon angioplasty. This strategy showed a significant improvement in clinical and functional findings in the WHO functional class with a simultaneous decrease in pulmonary arterial pressure by 5.4 mmHg, as was also observed in the present case. However, a significant number of post-interventional complications such as hemoptysis (18.8%) and lung injuries (44%) were described.

5. Conclusions

In summary, in cases of progressive dyspnea and concomitant mediastinal fibrosis, differential diagnostic clarification of the cause of fibrosis is required. In rare cases, this may be silicosis. Furthermore, especially in the presence of pulmonary hypertension, concomitant pulmonary vascular stenosis in the context of fibrosis must be taken into account. As in the current case, venous and arterial stenosis can be successfully treated by intervention. In the long term, this is reflected in a reduction in the extent of stenosis and pulmonary arterial pressures. In individual cases, however, residual stenosis may be present, or restenosis may occur.

Data availability statement

The data analyzed in this study is subject to the following licenses/restrictions: The authors obtained written informed consent from the patient for publication. However, requests to access these datasets should be directed to Michael Westhoff, michaelwesthoff.mail@t-online.de.

Ethics statement

Written informed consent was obtained from the individual(s) for the publication of any potentially identifiable images or data included in this article.

Author contributions

MW: conception of the manuscript; acquisition, analysis, and interpretation of the data; drafting of the manuscript and revising the manuscript critically for important intellectual content; final approval of the manuscript to be published; agreement to be accountable for all aspects of the work. TH: acquisition, analysis, and interpretation of the data; revising the manuscript critically for important intellectual content; final approval of the manuscript to be published; agreement to be accountable for all aspects of the work. PL: acquisition, analysis, and interpretation of the data; revising the manuscript critically for important intellectual content; final approval of the manuscript to be published; agreement to be accountable for all aspects of the work. AB: acquisition, analysis, and interpretation of the data; revising the manuscript critically for important intellectual content; final approval of the manuscript to be published; agreement to be accountable for all aspects of the work. MH: acquisition, analysis, and interpretation of the data; revising the manuscript critically for important intellectual content; final approval of the manuscript to be published; agreement to be accountable for all aspects of the work. MK: acquisition, analysis, and interpretation of the data; revising the manuscript critically for important intellectual content; final approval of the manuscript to be published; agreement to be accountable for all aspects of the work. TN: acquisition, analysis, and interpretation of the data; revising the manuscript critically for important intellectual content; final approval of the manuscript to be published; agreement to be accountable for all aspects of the work. SG: acquisition, analysis, and interpretation of the data; revising the manuscript critically for important intellectual content; final approval of the manuscript to be published; agreement to be accountable for all aspects of the work. CW: conception of the manuscript; acquisition, analysis, and interpretation of the data; drafting of the manuscript and revising the manuscript critically for important intellectual content. All authors contributed to the article and approved the submitted version.

Funding

Funded by the Gesellschaft zur Förderung der Lungenklinik Hemer e.V.

Acknowledgments

We are grateful to Elizabeth Martinson, of the KHFI Editorial Office for her editorial assistance.

Conflict of interest

MW has received speaker fees and/or consultant honoraria from Actelion/Janssens, Boehringer Ingelheim, Insmed, Novartis, Vitalaire, Löwenstein Medical. TH has no conflict of interest. PL has no conflict of interest. AB has received speaker fees from MSD. MH has received speaker fees from Daiichi-Sankyo and Pfizer. MK has no conflict of interest. TN has no conflict of interest. SG has received speaker fees from Actelion, Bayer, GSK, MSD and Pfizer. CW has received speaker fees and/or consultant honoraria from Actelion, AOP Orphan Pharmaceuticals AG, Bayer AG, BTG, MSD, and Pfizer.

Publisher's note

References

1. Westhoff M. Riedel-Struma und fibröse Mediastinitis. Ihre Beziehungen zur multifokalen Fibrose [Riedel's struma and fibrous mediastinitis. Their relation to multifocal fibrosis]. *Dtsch Med Wochenschr*. (1988) 113:348–51. doi: 10.1055/s-2008-1067644

2. Westhoff M. Riedel-Struma und fibröse Mediastinitis. Positive therapeutische Beeinflussbarkeit durch Corticoide. [Riedel's struma and fibrous mediastinitis. Positive therapeutic responsiveness to corticoids]. *Dtsch Med Wochenschr*. (1988) 113:337–41. doi: 10.1055/s-2008-1067641

3. Peikert T, Colby TV, Midthun DE, Pairolero PC, Edell ES, Schroeder DR, et al. Fibrosing mediastinitis: clinical presentation, therapeutic outcomes, and adaptive immune response. *Medicine (Baltimore)*. (2011) 90:411–23. doi: 10.1097/MD.0b013e318237c8e6

4. Co MLF, Patel HN, Agdamag AC, Okwuosa TM. Fibrosing mediastinitis-related pulmonary artery and vein stenosis-limiting chemotherapy. *BMJ Case Rep*. (2018) 2018:bcr2017221905. doi: 10.1136/bcr-2017-221905

5. Fender EA, Widmer RJ, Knavel Koepsel EM, Welby JP, Kern R, Peikert T, et al. Catheter based treatments for fibrosing mediastinitis. *Catheter Cardiovasc Interv*. (2019) 94:878–85. doi: 10.1002/ccd.28152

6. Ingraham BS, Packer DL, Holmes DR, Reddy YNV. The hemodynamic spectrum of pulmonary vein stenosis from fibrosing mediastinitis. *Catheter Cardiovasc Interv*. (2022) 99:198–200. doi: 10.1002/ccd.29955

7. Albers EL, Pugh ME, Hill KD, Wang L, Loyd JE, Doyle TP. Percutaneous vascular stent implantation as treatment for central vascular obstruction due to fibrosing mediastinitis. *Circulation*. (2011) 123:1391–9. doi: 10.1161/CIRCULATIONAHA.110.949180

8. Doyle TP, Loyd JE, Robbins IM. Case report: tuberculous pulmonary arteritis–an unusual cause of right pulmonary artery stenosis. *Clin Radiol*. (1998) 53:229–31. doi: 10.1016/S0009-9260(98)80109-8

9. Yazaki K, Yoshida K, Hyodo K, Kanazawa J, Saito T, Hizawa N. Pulmonary hypertension caused by fibrosing mediastinitis. *JACC Asia*. (2022) 2:218–34. doi: 10.1016/j.jacasi.2021.11.016

10. Zhang R, Ma G, Xu X, Liang L. Pulmonary arterial bypass surgery for fibrosing mediastinitis causing severe pulmonary hypertension. *Ann Thorac Surg*. (2019) 107: e411–3. doi: 10.1016/j.athoracsur.2018.09.067

11. Mahnken AH, Breuer C, Haage P. Pulmonary artery reconstruction for tuberculosis. *Ann Thorac Surg*. (1996) 61:1257–9. doi: 10.1016/0003-4975(95)01063-7

12. Li Y, Meng X, Wang Y, Yang Y, Lu X. Pulmonary arterial stenosis with wide splitting of the second heart sound due to mediastinal fibrosis. *Am J Cardiol*. (1973) 31:372–6. doi: 10.1016/0002-9149(73)90270-1

13. Li YJ, Pan X, Wang C, He B. Sarcoidosis complicated with major pulmonary artery obstruction and stenosis. *Intern Med*. (2012) 51:2775–80. doi: 10.2169/internalmedicine.51.7693

14. Gustafson MR, Moulton MJ. Fibrosing mediastinitis with severe bilateral pulmonary artery narrowing: rV-RPA bypass with a homograft conduit. *Tex Heart Inst J*. (2012) 39:412–25.

15. Chang SH, Shih CW, Lei MH. Idiopathic mediastinal fibrosis with involvement of the pulmonary vessels and left main coronary artery. *Catheter Cardiovasc Interv*. (2012) 79:1019–22. doi: 10.1002/ccd.23154

16. Chang SH, Shih CW, Lei MH. Pulmonalarterienstenose bei aggressiver mediastinalfibrose; diagnostik und 3D-darstellung mittels helikaler CT-untersuchung. *Aktuelle Radiol*. (1997) 7:197–9.

17. Lee CH, Park JS. Pulmonary artery stenosis and aneurysm with idiopathic mediastinal fibrosis. *Heart Lung Circ*. (2014) 23:e190–191. doi: 10.1016/j.hlc.2013.04.120

18. Leong DP, Dundon BK, Steele PM. Unilateral pulmonary vein stenosis secondary to idiopathic fibrosing mediastinitis. *Heart*. (2008) 94:776. doi: 10.1136/hrt.2007.124404

19. Mahnken AH, Breuer C, Haage P. Silicosis-induced pulmonary artery stenosis: demonstration by MR angiography and perfusion MRI. *Br J Radiol*. (2001) 74:859–61. doi: 10.1259/bjr.74.885.740859

20. Zhang R, Ma G, Xu X, Liang L. Percutaneous treatment for silicosis-induced pulmonary artery stenosis: a case report and review of the literature. *Medicine (Baltimore)*. (2018) 97:e9469. doi: 10.1097/MD.0000000000009469

21. Ojeifo O, Gilotra NA, Kemp CD, Leventhal A, Resar J, Zehr KJ, et al. Sarcoidosis, pulmonary hypertension, and acquired peripheral pulmonary artery stenosis. *Cathet Cardiovasc Diagn*. (1985) 11:69–74. doi: 10.1002/ccd.1810110110

22. Nelson WP, Lundberg GD, Dickerson RB. Pulmonary artery obstruction and cor pulmonale due to chronic fibrous mediastinitis. *Am J Med*. (1965) 38:279–85. doi: 10.1016/0002-9343(65)90182-8

23. Massumi A, Woods L, Mullins CE, Nasser WK, Hall RJ. Successful management of fibrosing mediastinitis with severe vascular compromise: report of two cases and literature review. *Respir Med Case Rep*. (2019) 29:100987. doi: 10.1016/j.rmcr.2019.100987

24. Papandreou L, Panagou P, Bouros D. Mediastinal fibrosis, and radiofrequency radiation exposure: is there an association? *Respiration*. (1992) 59:181–4. doi: 10.1159/000196054

25. Prieto LR, Schoenhagen P, Arruda MJ, Natale A, Worley SE. Pulmonary artery fibrous bands: report of a case with extensive lung infarction and superinfection with coccidioides immitis, Pseudomonas, and acid-fast bacilli. *Arch Pathol Lab Med*. (1999) 123:170–2. doi: 10.5858/1999-123-0170-PAFB

26. Neumann T, Kuniss M, Conradi G, Sperzel J, Berkowitsch A, Zaltsberg S, et al. Pulmonary artery stenosis in a patient with prior histoplasmosis and the discovery of complications. *J Cardiothorac Vasc Anesth*. (2020) 34:832–4. doi: 10.1053/j.jvca.2019.10.037

27. Doyle TP, Loyd JE, Robbins IM. Percutaneous pulmonary artery and vein stenting: a novel treatment for mediastinal fibrosis. *Am J Respir Crit Care Med*. (2001) 164:657–60. doi: 10.1164/ajrccm.164.4.2012132

28. Duan YC, Su HL, Wei R, Jiang KY, Wang AQ, Yang YH, et al. Pulmonary hypertension due to silicosis and right upper pulmonary artery occlusion with bronchial anthracofibrosis. *Respir Med Case Rep*. (2021) 34:101522. doi: 10.1016/j.rmcr.2021.101522

29. Ponamgi SP, DeSimone CV, Lenz CJ, Coylewright M, Asirvatham SJ, Holmes DR, et al. Fibrosing mediastinitis with pulmonary hypertension as a complication of pulmonary vein stenosis: a case report and review of the literature. *Medicine (Baltimore)*. (2018) 97:e9694. doi: 10.1097/MD.0000000000009694

30. Zhou X, Li YJ, Cao YS, Su HL, Duan YC, Su X, et al. Successful stenting of bilateral pulmonary veins stenosis secondary to idiopathic fibrosing mediastinitis. *JACC Cardiovasc Interv*. (2020) 13:1003–5. doi: 10.1016/j.jcin.2019.10.042

31. Welby JP, Fender EA, Peikert T, Holmes DR Jr, Bjarnason H, Knavel-Koepsel EM. Successful stenting of left pulmonary veins stenosis resulting from fibrosing mediastinitis. *Eur Heart J*. (2015) 36:2623. doi: 10.1093/eurheartj/ehu511

32. Beaconsfield T, Newman-Sanders A, Birch H, Glenville B, Al-Kutoubi A. Major pulmonary artery stenosis causing pulmonary hypertension in sarcoidosis. *Chest*. (1980) 78:888–91. doi: 10.1378/chest.78.6.888

33. Seckeler MD, Pineda JRET, Lotun K. Successful transcatheter recanalization of a chronically occluded left pulmonary artery due to fibrosing mediastinitis. *JACC Cardiovasc Interv*. (2021) 14:e215–216. doi: 10.1016/j.jcin.2021.04.004

34. Cohen AS, Beaconsfield T, al-Kutoubi A, Handler CE, Glenville BE. Mediastinal fibrosis of the pulmonary artery secondary to Tuberculosis. *AnnThorac Surg*. (2015) 100:e49–50. doi: 10.1016/j.athoracsur.2015.03.113

35. Cosio FG, Gobel FL, Harrington DP, Sako Y. Intraoperative and percutaneous stenting of congenital pulmonary artery and vein stenosis. *Circulation*. (1993) 88: II210–217.

36. Gustafson MR, Moulton MJ. Pulmonary venous dilatation in pulmonary veno-occlusive disease. *Am J Cardiol*. (1981) 48:585–9. doi: 10.1016/0002-9149(81)90092-8

37. Kolbe M, Helwig A, Habicht JM, Steinbrich W. Pulmonary artery stents: long-term follow-up. *Catheter Cardiovasc Interv*. (2010) 75:757–64. doi: 10.1002/ccd.22356

38. Lee CH, Park JS. Comparison of stent versus balloon angioplasty for pulmonary vein stenosis complicating pulmonary vein isolation. *J Cardiovasc Electrophysiol*. (2008) 19:673–8. doi: 10.1111/j.1540-8167.2008.01110.x

39. Leong DP, Dundon BK, Steele PM. Pulmonary vein stenting for the treatment of acquired severe pulmonary vein stenosis after pulmonary vein isolation: clinical implications after long-term follow-up of 4 years. *J Cardiovasc Electrophysiol*. (2009) 20:251–7. doi: 10.1111/j.1540-8167.2008.01316.x

40. Mangla A, Fisher J, Libby DM, Saddekni S. Percutaneous treatment for pulmonary hypertension caused by pulmonary artery stenosis due to anthracosis. *Int J Tuberc Lung Dis*. (2015) 19:747–8. doi: 10.5588/ijtld.14.0787

41. Nelson WP, Lundberg GD, Dickerson RB. Pulmonary stenting for the treatment of sarcoid induced pulmonary vascular stenosis. *Sarcoidosis Vasc Diffuse Lung Dis*. (2016) 33:281–7.

42. Papandreou L, Panagou P, Bouros D. Short-term efficacy and perioperative safety of catheter-based intervention for pulmonary vein stenosis caused by fibrosing mediastinitis. *Zhonghua Xin Xue Guan Bing Za Zhi*. (2022) 50:55–61. doi: 10.3760/cma.j.cn112148-20210507-00398

43. Perez MT, Alexis JB, Ferreira T, Garcia HP. Pulmonary hypertension due to fibrosing mediastinitis treated successfully with stenting of pulmonary vein stenoses. *Can J Cardiol*. (2015) 31:548.e5–7. doi: 10.1016/j.cjca.2014.12.025

44. Songster JC, Liu H, Brakke TR, Aron RA. Pulmonary hypertension complicating fibrosing mediastinitis. *Medicine (Baltimore)*. (2015) 94:e1800. doi: 10.1097/MD.0000000000001800

45. Ahn JH, Ahn JM, Lee SW, Choi SH, Oh SY, Lee SM, et al. Results of intravascular stent placement for fibrosing mediastinitis. *Congenit Heart Dis*. (2010) 5:124–33. doi: 10.1111/j.1747-0803.2010.00387.x

46. Condado JF, Babaliaros V, Henry TS, Kaebnick B, Kim D, Staton GW Jr. Treatment of pulmonary artery compression due to fibrous mediastinitis with endovascular stent placement. *Chest*. (2001) 119:966–8. doi: 10.1378/chest.119.3.966

47. Doucet KM, Labinaz M, Chandy G, Mielniczuk L, Stewart D, Contreras-Dominguez V, et al. Interventional therapy in sarcoidosis-associated pulmonary arterial stenosis and pulmonary hypertension. *Clin Respir J*. (2017) 11:906–14. doi: 10.1111/crj.12435

48. Ferguson ME, Cabalka AK, Cetta F, Hagler DJ. Percutaneous stenting of right pulmonary artery stenosis in fibrosing mediastinitis. *Catheter Cardiovasc Interv*. (2000) 49:321–4. doi: 10.1002/(SICI)1522-726X(200003)49:3<321::AID-CCD20>3.0.CO;2-5

49. Guerrero A, Hoffer EK, Hudson L, Schuler P, Karmy-Jones R. Catheter-based intervention for pulmonary vein stenosis due to fibrosing mediastinitis: the mayo clinic experience. *Int J Cardiol Heart Vascul*. (2015) 8:103–7. doi: 10.1016/j.ijcha.2015.06.005

50. Liu L, Xu J, Zhang Y, Fang L, Chai Y, Niu M, et al. Fibrosing mediastinitis presenting as pulmonary stenosis: stenting works. *Int J Cardiol*. (2007) 118:e85 8–6. doi: 10.1016/j.ijcard.2007.01.030

51. Kandzari DE, Warner JJ, O'Laughlin MP, Harrison JK. Cardiovascular collapse induced by position-dependent pulmonary vein occlusion in a patient with fibrosing mediastinitis. *Anesthesiology*. (2005) 103:661–3. doi: 10.1097/00000542-200509000-00032

52. Satpathy R, Aguila V, Mohiuddin SM, Khan IA. Pulmonary artery stenosis secondary to fibrosing mediastinitis: management with cutting balloon angioplasty and endovascular stenting. *Vasc Endovascular Surg*. (2011) 45:170–3. doi: 10.1177/1538574410393034

53. Shapiro BP, Sprung J, Scott K, Arendt K, Krowka MJ, Afessa B. Fibrosing mediastinitis: successful stenting of the pulmonary artery. *Can Respir J*. (2008) 15:41–4. doi: 10.1155/2008/835921

54. Smith JS, Kadiev S, Diaz P, Cheatham J. Endovascular treatment of bilateral pulmonary artery stenoses and superior vena Cava syndrome in a patient with advanced mediastinal fibrosis. *Tex Heart Inst J*. (2016) 43:249–57. doi: 10.14503/THIJ-15-5091

55. Thiessen R, Matzinger FR, Seely J, Aina R, Macleod P. Evaluation of outcomes following pulmonary artery stenting in fibrosing mediastinitis. *Cardiovasc Intervent Radiol*. (2021) 44:384–91. doi: 10.1007/s00270-020-02714-z

56. Valentin LI, Kuban JD, Ramanathan R, Whigham CJ. Refractory pleural effusion as a rare complication of pulmonary vascular stenosis induced by fibrosing mediastinitis: a case report and literature review. *J Int Med Res*. (2021) 49:3000605211010073. doi: 10.1177/03000605211010073

57. Yang S, Wang J, Li J, Huang K, Yang Y. Feasibility and efficacy of percutaneous pulmonary vein stenting for the treatment of patients with severe pulmonary vein stenosis due to fibrosing mediastinitis. *Zhonghua Xin Xue Guan Bing Za Zhi*. (2019) 47:814–81. doi: 10.3760/cma.j.issn.0253-3758.2019.10.008

frontiers | Frontiers in Cardiovascular Medicine

TYPE Case Report
PUBLISHED 30 May 2023
DOI 10.3389/fcvm.2023.1123385

OPEN ACCESS

EDITED BY
Pietro Enea Lazzerini,
University of Siena, Italy

REVIEWED BY
Devesh Rai,
Rochester General Hospital, United States
Kin Israel Notarte,
Johns Hopkins University, United States
Pietro Scicchitano,
ASLBari—Azienda Sanitaria Localedella provincia di Bari (ASL BA), Italy

*CORRESPONDENCE
Bin Wang
✉ mocw361@163.com
Rui Gao
✉ ruigao@xmu.edu.cn

RECEIVED 15 December 2022
ACCEPTED 27 April 2023
PUBLISHED 30 May 2023

CITATION
Ou W, Wang B, Zhang G, Ding L, Liu Z, Wu K, Sun G, Huang C, Li Z, Feng S and Gao R (2023) Acute myocardial infarction after inactivated COVID-19 vaccination: a case report and literature review.
Front. Cardiovasc. Med. 10:1123385.
doi: 10.3389/fcvm.2023.1123385

Acute myocardial infarction after inactivated COVID-19 vaccination: a case report and literature review

Weimei Ou[1], Bin Wang[1]*, Guoming Zhang[1], Licheng Ding[1], Zhixian Liu[1], Kaimin Wu[1], Guangfeng Sun[1], Chengmin Huang[1], Zhaokai Li[1], Shuyuan Feng[1] and Rui Gao[2]*

[1]Department of Emergency, Xiamen Cardiovascular Hospital of Xiamen University, School of Medicine, Xiamen University, Xiamen, China, [2]Institute of Cardiovascular Diseases, Xiamen Cardiovascular Hospital of Xiamen University, School of Medicine, Xiamen University, Xiamen, China

A number of vaccines have been developed and deployed globally to restrain the spreading of the coronavirus disease 2019 (COVID-19). The adverse effect following vaccination is an important consideration. Acute myocardial infarction (AMI) is a kind of rare adverse event after COVID-19 vaccination. Herein, we present a case of an 83-year-old male who suffered cold sweat ten minutes after the first inactivated COVID-19 vaccination and AMI one day later. The emergency coronary angiography showed coronary thrombosis and underlying stenosis in his coronary artery. Type II Kounis syndrome might be a potential mechanism, which is manifested as coronary thrombosis secondary to allergic reactions in patients with underlying asymptomatic coronary heart disease. We also summarize the reported AMI cases post COVID-19 vaccination, as well as overview and discuss the proposed mechanisms of AMI after COVID-19 vaccination, thus providing insights for clinicians to be aware of the possibility of AMI following COVID-19 vaccination and potential underlying mechanisms.

KEYWORDS

acute myocardial infarction (AMI), COVID-19 vaccination, kounis syndrome (KS), coronary heart disease (CHD), coronary thrombosis

1. Introduction

The coronavirus disease 2019 (COVID-19) has become a pandemic since March of 2020. At the time of writing, more than 640 million cases have been confirmed, including more than 6.6 million cases of death (1). A number of vaccines have been developed and deployed and shown to be the most effective strategy to restrain the spread of COVID-19 (2). Up to date, more than 13 billion doses of COVID-19 vaccines have been administered globally (1). However, many kinds of adverse events (AE) brought to people's attention after COVID-19 vaccination, even though the safety and efficacy have been tested (3–11), for example, acute myocardial infarction (AMI), myocarditis, pericarditis and so on (12–14). Importantly, it is reported that people showed individual differences in humoral immune response depending on many factors such as age, sex, serostatus, and underlying comorbidities (15, 16). Therefore, the AE cases could differ from each other as well. In general, most adverse reactions were mild, with the most common symptoms being injection-site pain, fatigue, headache, myalgia, and nausea (6, 9, 17–19). Even though the incidence of serious AE was low (3, 4, 18, 20, 21), genuine concerns and attentions should be raised on these rare serious AE.

Traditional inactivated whole-virus COVID-19 vaccine is safe and efficacious to prevent COVID-19 pandemic (9, 18). Generally, AE after vaccination are neither frequent nor

serious (9). However, rare AE such as acute myocardial infarction (AMI) are potentially life-threatening (22, 23). Herein, we present a case of an 83-year-old male who suffered allergic reactions developing to AMI ten minutes after the first inactivated COVID-19 vaccination in China. Coronary angiography (CAG) showed acute coronary thrombosis and underlying stenosis in the coronary artery. The potential mechanism of AMI after inactivated COVID-19 vaccination might be type II Kounis syndrome (KS), which was manifested as coronary thrombosis secondary to allergic reactions in patients with underlying asymptomatic coronary heart disease (CHD).

2. Case description

An 83-year-old man with a medical history of subtotal gastrectomy and cholecystectomy complained of cold sweat, dizziness, fatigue and transient loss of consciousness ten minutes after the first dose of inactivated COVID-19 vaccine (CoronaVac, 202106061Z, Sinovac Life Sciences, Beijing, China). He felt worse accompanied by chest tightness, diarrhea and a lowest blood pressure of 83/50 mmHg the following day, and was admitted to the emergency department (ED). The patient denied any history of CHD, hypertension, diabetes, renal dysfunction, asthma or allergic reaction. He also denied any cardiac or noncardiac symptoms before vaccination. The detailed medical history of the patient was showed in **Supplementary Table S1**.

Upon ED arrival, the physical examination showed the blood pressure was not very high with 98/66 mmHg, other vital signs were normal. Laboratory tests showed the markers of myocardial injury were elevated, with high sensitivity troponin-T level more than 2,000 (reference: 0-100) ng/L, myohemoglobin 291 (reference: 28–72) ng/ml, creatine kinase (CK) 2771.7 (reference: 50–310) U/L, CK-MB fraction 348.2 (reference: 0–19) U/L, D-dimer 1.09 (reference: 0–0.55) mg/L, and N-terminal pro-brain natriuretic peptide 1,770 (reference: 0–125) pg/ml. Infection indices of white blood cells [10.75 (reference: 3.5–9.5) $\times 10^9$/L], hypersensitive C-reactive protein [6.13 (reference: 0–3) mg/L] and procalcitonin [0.103 (reference: 0–0.05) ng/ml] were modestly increased. Other laboratory tests were within normal ranges.

On admission, the electrocardiogram (ECG) showed that ST segments were elevated in leads II, III and avF, with reciprocal depression in leads I and avL (**Figure 1A**). Transthoracic echocardiography revealed hypokinesia on the inferior and posterior walls, with a left ventricular ejection fraction of 54%. The CAG revealed 95% stenosis in the right coronary artery (RCA) with thrombotic shadow locally, 80% stenosis in the left anterior descending coronary artery, 70%–80% stenosis in the distal left circumflex coronary artery (d-LCX), and 80%–90% stenosis in the obtuse marginal branch (OM) (**Figures 2A,2C–E**).

Combined with the ECG result, RCA was considered as the culprit vessel. Therefore, thrombus aspiration was performed, and two drug-eluting stents (DES, Firebird 3.0 × 29 mm, Firebird 3.5 × 33 mm) were implanted into the RCA (**Figure 2B**). This was accompanied by oral drugs for secondary prevention (aspirin, ticagrelor, atorvastatin, metoprolol). Subsequently, the ECG showed pathological Q waves in the inferior leads with ST segment recovery (**Figure 1B**). Before discharge, a DES (Promus Element 2.25 × 20 mm) and a drug-coated balloon (Vesselin 3.0 × 16 mm) were implanted into the OM and d-LCX, respectively (**Figure 2F**). A week later, the abnormal cardiac injury markers were relieved. The patient was discharged from the hospital in good condition. Furthermore, at the 1-month and 6-month follow-up visits after discharge, he was doing well with no symptoms or abnormalities of cardiac markers. A schematic

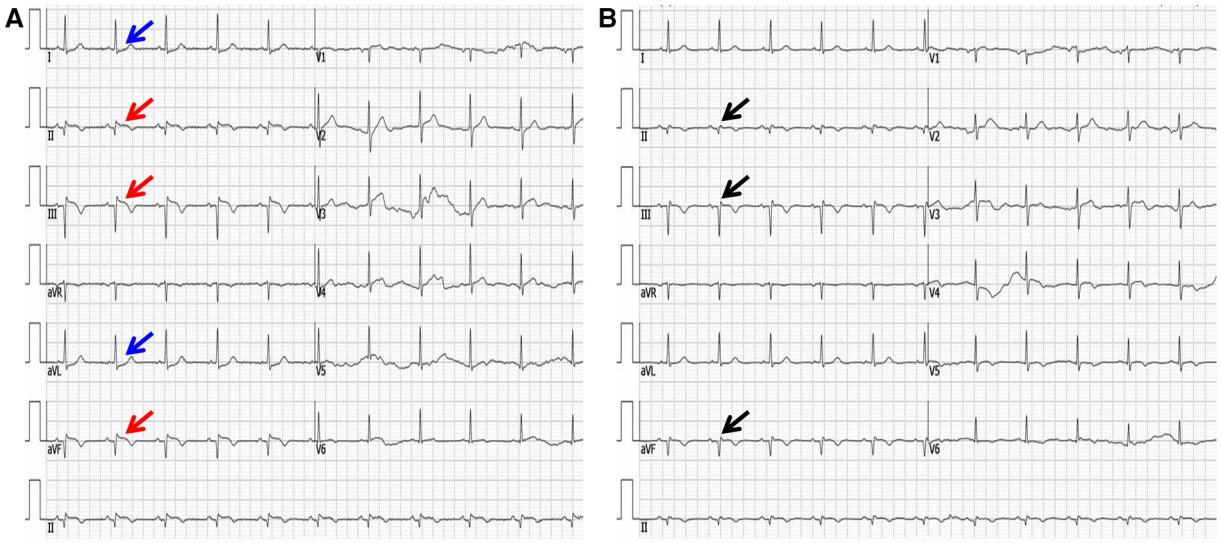

FIGURE 1
The electrocardiogram upon arrival (A) and one week later (B). (A) The red arrow shows ST segments were elevated in leads II, III and avF. The blue arrow shows ST segments were reciprocally depressed in leads I and avL. (B) The black arrow shows pathological Q waves in inferior leads, with ST segment recovery.

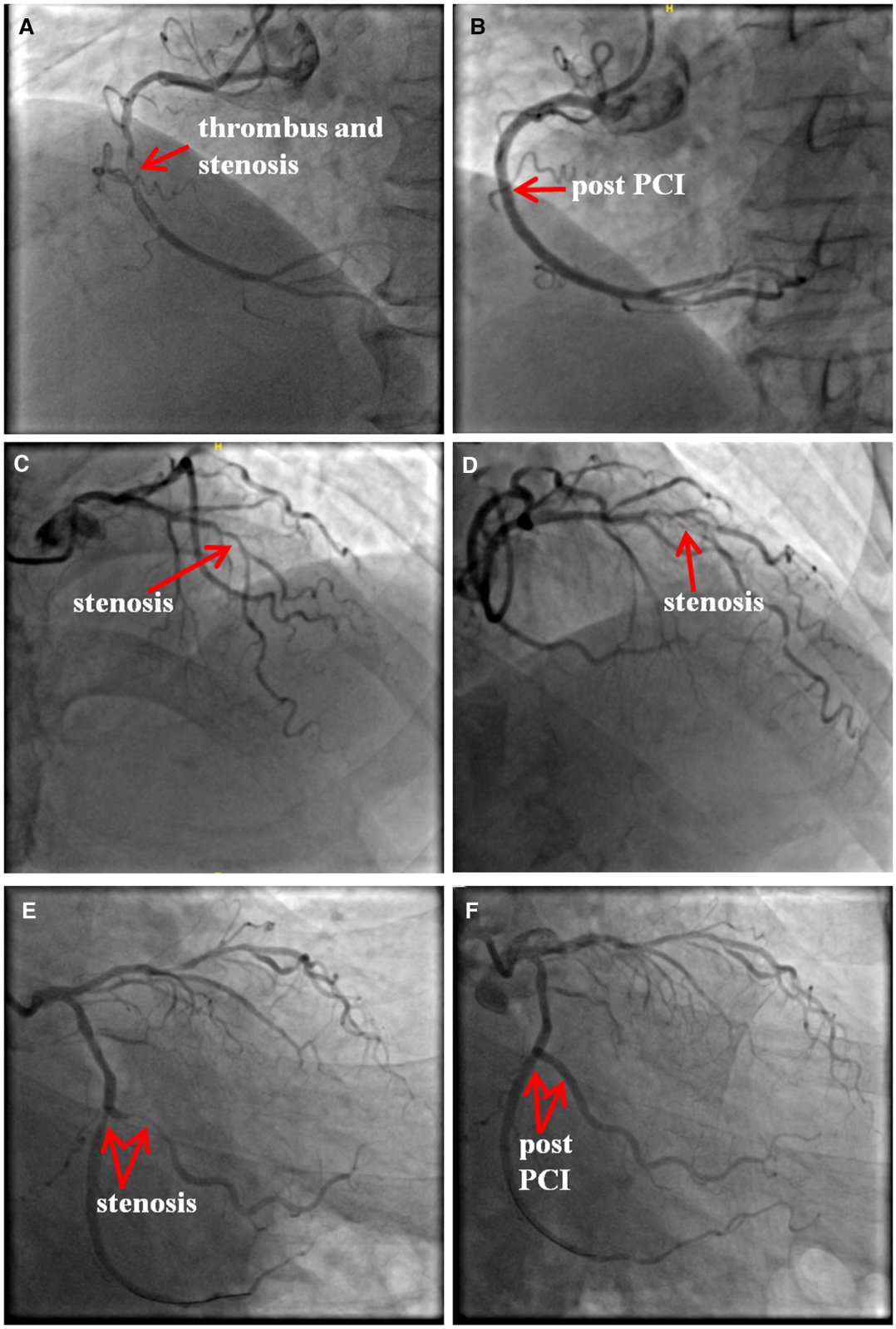

FIGURE 2
The results of coronary angiography. There was 95% stenosis in the right coronary artery (RCA) with a local thrombotic shadow (**A**), and two drug eluting stents (DES, Firebird 3.0 × 29 mm, Firebird 3.5 × 33 mm) were implanted into the RCA. (**B**) There was 80% stenosis in the left anterior descending coronary artery (**C**,**D**). There was 80%–90% stenosis in the obtuse marginal branch (OM) and 70%–80% stenosis in the distal LCX (d-LCX) (**E**), and a DES (Promus Element 2.25 × 20 mm) and a drug-coated balloon (Vesselin 3.0 × 16 mm) were implanted in the OM and d-LCX, respectively. (**F**) PCI, percutaneous coronary intervention.

diagram showing the timeline from vaccination to the onset of AMI up until patient discharge was showed in **Figure 3**.

3. Literature review and discussion

In this part, we will summarize the reported AMI cases, as well as overview and discuss the proposed mechanisms of AMI after COVID-19 vaccination. From the searching of literature databases, 21 literatures were found regarding AMI following COVID-19 vaccination. The summary is shown in **Supplementary Table S2**. Generally, there are 30 AMI cases following COVID-19 vaccination including our case. The cases reported located all over the world including the US, European countries and Asian countries. The vaccines administered in these cases varied from mRNA vaccine (16 cases; Pfizer-BioNTech and Moderna), adenoviral vector vaccine (10 cases; AstraZeneca), to inactivated virus vaccine (4 cases; Sinovac), suggesting AMI is not the specific AE from one kind of vaccine. The mean age of patients is 64, indicating the incidence of AMI following COVID-19 vaccination is more likely among old population, which agrees with the results in a systematic study published in 2021 (12). Most of the cases showed symptoms within 24 h (76.7%; 23 out of 30 cases) and chest discomfort is the most common seen symptom in AMI cases (66.7%; 20 out of 30 cases) that should be paid more attention after COVID-19 vaccination, consistent with the finding in the systematic review published recently (24).

So far, there are some proposed underlying mechanisms for AMI following COVID-19 vaccination. The most probable explanation is KS, which is the concurrent occurrence of acute coronary syndromes with allergic reactions. To date, four variants of the disease have been documented: (1) type I: coronary spasm in patients with (nearly) normal coronary arteries; (2) type II: coronary thrombosis in patients with underlying asymptomatic CHD; (3) type III: stent-related allergic coronary events, with IIIa (stent thrombosis) and IIIb (in-stent restenosis); and (4) type IV: anaphylaxis-mediated AMI in patients with coronary grafts (25–28). In our case, the patient denied any medical history of CHD, but we found not only acute coronary thrombosis but also underlying stenosis in his coronary arteries, suggesting he should have pre-existing asymptomatic CHD that was not realized by himself. Given his symptoms occurred only ten minutes after the vaccination with no other triggers identified, accordingly, our patient was speculated with type II KS after inactivated COVID-19 vaccination, which was similar to a previous report of type I KS in Turkey (29). In addition, vaccine-induced thrombotic thrombocytopenia (VITT) associated thrombosis could be another possibility for AMI post COVID-19 vaccination, but only ten minutes is not enough to develop VITT, therefore this potential is very rare (22). Moreover, there was also a possibility that the vaccination and AMI were just coincident, though it was scarce. Given possible life-threatening results and lack recognition of KS, more attention should be drawn to KS by clinicians post COVID-19 vaccination.

The pathophysiology of vaccine-induced allergic reactions could be derived from the following four kinds of mechanisms (30). (1) Reactions via the pathway of mast cell activation and degranulation as IgE/antigen through cross-linking of FcεRI on mast cells (31). This reaction typically occurs within minutes of exposure to the relevant allergen and always occurs within 4 h of exposure to the relevant allergen (32). This mechanism is confirmed by the specific IgEs detection and the increased levels of serum tryptase (30). (2) Non-IgE-mediated mast cell degranulation is another pathway that is performed via activation of the complement system, leading to the generation of anaphylatoxins C1q, C3a C4 and C5a. This complement pathway activation and positive biofeedback loops involving interleukin-5 (IL-5) and tryptase is also very common and should be considered (30, 33). (3) Life-threatening allergic reactions can be mediated via direct activation of the Mas-related G protein-

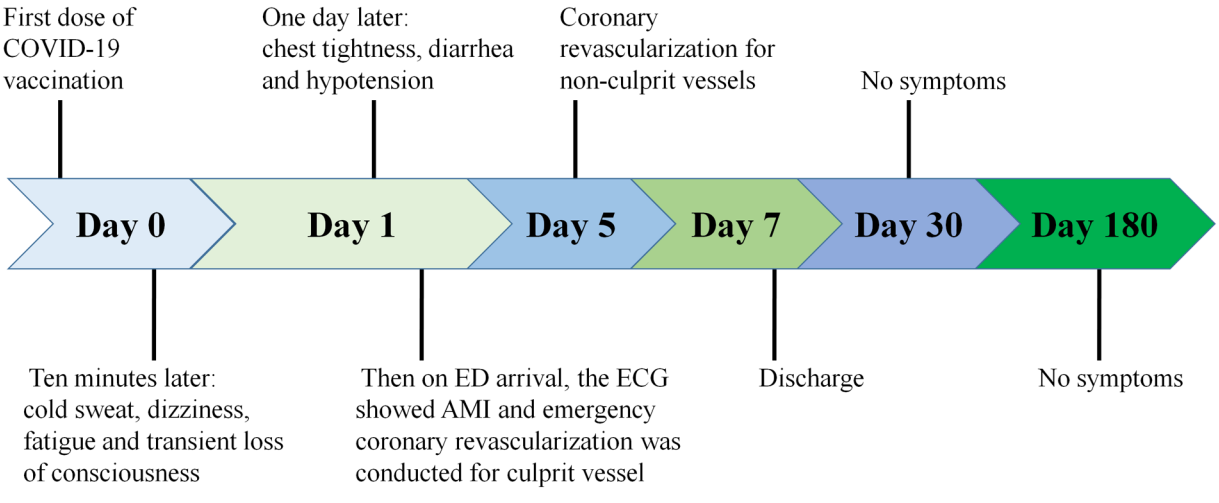

FIGURE 3
Schematic diagram showing the timeline from vaccination to the onset of AMI up until patient discharge.

coupled receptor X2 (MRGPRX2) that may activate mast cells via non-Fcϵ receptors. In this pathway, the specific IgEs may remain undetected, and tryptase levels may be normal even in serious KS (30). This might explain the conditions in cases reported by Baronti et al. (34) that even the tryptase testing is negative, allergic reactions cannot be ruled out. (4) Hypersensitivity delayed reaction generally begins 48 h after vaccination and peaks between 72 and 96 h (35), which is cell-mediated and antibody independent, derived from overstimulation of T cells and monocytes/macrophages and releases of cytokines that cause inflammation, cell death, and tissue damage (30). Vaccines containing anti-microbial agents and ingredients, such as thimerosal and aluminum, can be followed by delayed reactions (32). A schematic diagram regarding pathophysiologic mechanisms of KS was shown in **Figure 4**.

Allergic reactions to vaccines are rarely attributed to the active vaccine itself, rather than excipients which constitute inert substances added to vaccines and other drugs to improve stability, increase solubility, improve absorption, influence palatability, or create a distinctive appearance (30). The viral vector Covishield vaccine contains aluminum hydroxide, and excipients similar to AstraZeneca vaccines such as polysorbate 80 (PS80) and disodium edetate dihydrate (ethylenediaminetetraacetic acid). The Moderna vaccine contains polyethylene glycol which is also shown in Pfizer-BioNTech vaccine, and tromethamine (also known as trometamol). The Sinovac (Coronavac) vaccine contains disodium hydrogen phosphate, sodium dihydrogen phosphate monohydrate, and sodium chloride (36). These excipients are also found in other vaccines such as influenza vaccine, and in creams, ointments, lotions, other cosmetics, various dental materials, as well as anticancer drugs which could sensitize their users (36). This situation has been reported by Fialho et al. that one case of AMI patient after COVID-19 vaccination from AstraZeneca who had a medical history of acute coronary syndrome after influenza vaccine was diagnosed with type III KS (37). In this case, both vaccines (COVID-19 and influenza) contain a common excipient PS80 (37). Even though the skin tests with intravenous amiodarone, that contains PS80, were negative, which rule out the IgE-mediated PS80 reaction, but cannot exclude PS80 non-IgE mediated hypersensitivity reactions (37, 38).

Even though multiple AMI cases have been reported occurring within minutes to hours after COVID-19 vaccination, there is still no enough evidence to show the direct causal relationship between AMI and COVID-19 vaccination. Since AMI is a commonly occurring disease in old people, whether the cases recorded are due to COVID-19 vaccination or just coincidence need further studies to elucidate.

Preliminary clinical trials in the Food and Drug Administration briefing documents indicated that the incidence rate of AMI was 0.03% and 0.02% after receiving Moderna or Pfizer vaccines, respectively (39). Compared with the total number of vaccine doses given, the incidence of AMI is really very rare. But it is potentially life-threatening. Clinicians need to be aware of this situation that might present after the COVID-19 vaccination.

4. Conclusion

In recent two years, vaccines have been deployed to restrain the spreading of COVID-19. AMI is a kind of rare AE following COVID-19 vaccination. In this article, we are reporting an AMI case that showed symptoms only ten minutes after COVID-19 vaccination with no other triggers identified. KS could be a potential mechanism in our case. Moreover, we summarize the reported AMI cases, as well as overview and discuss the proposed mechanisms of AMI following COVID-19 vaccination, thus providing insights for clinicians to be aware of the

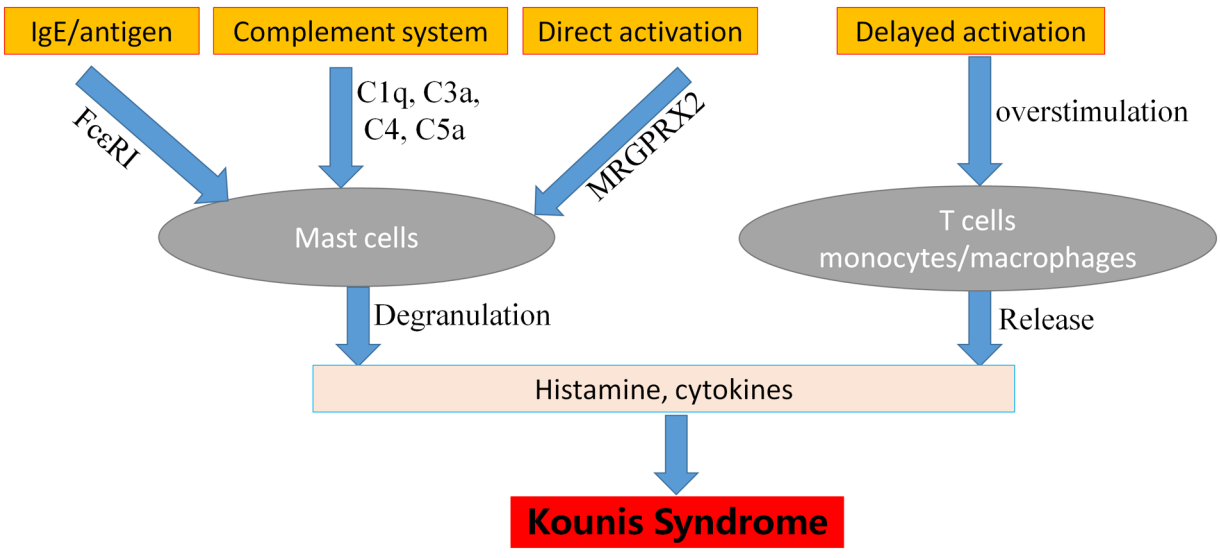

FIGURE 4
The mechanisms of Kounis syndrome pathophysiology. MRGPRX2: mas-related G protein-coupled receptor X2.

possibility of AMI following COVID-19 vaccination and potential underlying mechanisms.

Data availability statement

The original contributions presented in the study are included in the article/**Supplementary Material**, further inquiries can be directed to the corresponding author/s.

Ethics statement

The studies involving human participants were reviewed and approved by the Ethics Committee of Xiamen Cardiovascular Hospital of Xiamen University. The patients/participants provided their written informed consent to participate in this study. Written informed consent was obtained from the individual(s) for the publication of any potentially identifiable images or data included in this article.

Author contributions

WO: contributed to the study design and data acquisition. WO, BW, GZ, LD, ZL, KW, GS, CH, ZL, and SF: contributed to the clinical treatment of this case. WO, BW and RG: contributed to the drafting and critical revision of the manuscript. All authors contributed to the article and approved the submitted version.

Funding

This research was granted from the Medical Research Project of Xiamen Cardiovascular Hospital of Xiamen University (No. 2020-05) and a Startup Fund (Grant No. XZZX202103017) from Xiamen Cardiovascular Hospital of Xiamen University to RG.

Conflict of interest

The authors declare that the research was conducted in the absence of any commercial or financial relationships that could be construed as a potential conflict of interest.

Publisher's note

All claims expressed in this article are solely those of the authors and do not necessarily represent those of their affiliated organizations, or those of the publisher, the editors and the reviewers. Any product that may be evaluated in this article, or claim that may be made by its manufacturer, is not guaranteed or endorsed by the publisher.

Supplementary material

The Supplementary Material for this article can be found online at: https://www.frontiersin.org/articles/10.3389/fcvm.2023.1123385/full#supplementary-material.

References

1. Who (WHO Coronavirus (COVID-19) Dashboard). Available at: https://covid19.who.int/ (Assessed 06 Dec 2022).

2. Shiravi AA, Ardekani A, Sheikhbahaei E, Heshmat-Ghahdarijani K. Cardiovascular complications of SARS-CoV-2 vaccines: an overview. *Cardiol Ther*. (2022) 11:13–21. doi: 10.1007/s40119-021-00248-0

3. Polack FP, Thomas SJ, Kitchin N, Absalon J, Gurtman A, Lockhart S, et al. Safety and efficacy of the BNT162b2 mRNA COVID-19 vaccine. *N Engl J Med*. (2020) 383:2603–15. doi: 10.1056/NEJMoa2034577

4. Baden LR, El Sahly HM, Essink B, Kotloff K, Frey S, Novak R, et al. Efficacy and safety of the mRNA-1273 SARS-CoV-2 vaccine. *N Engl J Med*. (2021) 384:403–16. doi: 10.1056/NEJMoa2035389

5. Barda N, Dagan N, Ben-Shlomo Y, Kepten E, Waxman J, Ohana R, et al. Safety of the BNT162b2 mRNA COVID-19 vaccine in a nationwide setting. *N Engl J Med*. (2021) 385:1078–90. doi: 10.1056/NEJMoa2110475

6. Sadoff J, Gray G, Vandebosch A, Cardenas V, Shukarev G, Grinsztejn B, et al. Safety and efficacy of single-dose Ad26.COV2.S vaccine against COVID-19. *N Engl J Med*. (2021) 384:2187–201. doi: 10.1056/NEJMoa2101544

7. Soiza RL, Scicluna C, Thomson EC. Efficacy and safety of COVID-19 vaccines in older people. *Age Ageing*. (2021) 50:279–83. doi: 10.1093/ageing/afaa274

8. Voysey M, Clemens SAC, Madhi SA, Weckx LY, Folegatti PM, Aley PK, et al. Safety and efficacy of the ChAdOx1 nCoV-19 vaccine (AZD1222) against SARS-CoV-2: an interim analysis of four randomised controlled trials in Brazil, South Africa, and the UK. *Lancet*. (2021) 397:99–111. doi: 10.1016/S0140-6736(20)32661-1

9. Zhang Y, Zeng G, Pan H, Li C, Hu Y, Chu K, et al. Safety, tolerability, and immunogenicity of an inactivated SARS-CoV-2 vaccine in healthy adults aged 18–59 years: a randomised, double-blind, placebo-controlled, phase 1/2 clinical trial. *Lancet Infect Dis*. (2021) 21:181–92. doi: 10.1016/S1473-3099(20)30843-4

10. Moreira ED Jr., Kitchin N, Xu X, Dychter SS, Lockhart S, Gurtman A, et al. Safety and efficacy of a third dose of BNT162b2 COVID-19 vaccine. *N Engl J Med*. (2022) 386:1910–21. doi: 10.1056/NEJMoa2200674

11. Parmar K, Subramanyam S, Del Rio-Pertuz G, Sethi P, Argueta-Sosa E. Cardiac adverse events after vaccination-A systematic review. *Vaccines*. (2022) 10:700. doi: 10.3390/vaccines10050700

12. Aye YN, Mai AS, Zhang A, Lim OZ, Lin N, Ng CH, et al. Acute myocardial infarction and myocarditis following COVID-19 vaccination. *QJM*. (2021) 00:1–5. doi: 10.1093/qjmed/hcab252

13. Diaz GA, Parsons GT, Gering SK, Meier AR, Hutchinson IV, Robicsek A. Myocarditis and pericarditis after vaccination for COVID-19. *JAMA*. (2021) 326:1210–2. doi: 10.1001/jama.2021.13443

14. Abdel Moneim A, Radwan MA, Yousef AI. COVID-19 and cardiovascular disease: manifestations, pathophysiology, vaccination, and long-term implication. *Curr Med Res Opin*. (2022) 38:1071–9. doi: 10.1080/03007995.2022.2078081

15. Notarte KI, Guerrero-Arguero I, Velasco JV, Ver AT, Santos De Oliveira MH, Catahay JA, et al. Characterization of the significant decline in humoral immune response six months post-SARS-CoV-2 mRNA vaccination: a systematic review. *J Med Virol*. (2022a) 94:2939–61. doi: 10.1002/jmv.27688

16. Notarte KI, Ver AT, Velasco JV, Pastrana A, Catahay JA, Salvagno GL, et al. Effects of age, sex, serostatus, and underlying comorbidities on humoral response post-SARS-CoV-2 pfizer-BioNTech mRNA vaccination: a systematic review. *Crit Rev Clin Lab Sci*. (2022b) 59:373–90. doi: 10.1080/10408363.2022.2038539

17. Al Khames Aga QA, Alkhaffaf WH, Hatem TH, Nassir KF, Batineh Y, Dahham AT, et al. Safety of COVID-19 vaccines. *J Med Virol*. (2021) 93:6588–94. doi: 10.1002/jmv.27214

18. Tanriover MD, Doganay HL, Akova M, Guner HR, Azap A, Akhan S, et al. Efficacy and safety of an inactivated whole-virion SARS-CoV-2 vaccine

(CoronaVac): interim results of a double-blind, randomised, placebo-controlled, phase 3 trial in Turkey. *Lancet*. (2021) 398:213–22. doi: 10.1016/S0140-6736(21)01429-X

19. Huang Z, Su Y, Zhang T, Xia N. A review of the safety and efficacy of current COVID-19 vaccines. *Front Med*. (2022) 16:39–55. doi: 10.1007/s11684-021-0893-y

20. Beatty AL, Peyser ND, Butcher XE, Cocohoba JM, Lin F, Olgin JE, et al. Analysis of COVID-19 vaccine type and adverse effects following vaccination. *JAMA Netw Open*. (2021) 4:e2140364. doi: 10.1001/jamanetworkopen.2021.40364

21. Wu Q, Dudley MZ, Chen X, Bai X, Dong K, Zhuang T, et al. Evaluation of the safety profile of COVID-19 vaccines: a rapid review. *BMC Med*. (2021) 19:173. doi: 10.1186/s12916-021-02059-5

22. Hana D, Patel K, Roman S, Gattas B, Sofka S. Clinical cardiovascular adverse events reported post-COVID-19 vaccination: are they a real risk? *Curr Probl Cardiol*. (2022) 47:101077. doi: 10.1016/j.cpcardiol.2021.101077

23. Zafar U, Zafar H, Ahmed MS, Khattak M. Link between COVID-19 vaccines and myocardial infarction. *World J Clin Cases*. (2022) 10:10109–19. doi: 10.12998/wjcc.v10.i28.10109

24. Baqi DH, Kakamad FH, Mahmood ZH, Fattah FH, Ahmed SF, Hassan MN, et al. Myocardial infarction following COVID-19 vaccine administration; a systematic review. *Heliyon*. (2022) 8:e11385. doi: 10.1016/j.heliyon.2022.e11385

25. Kounis NG. Kounis syndrome (allergic angina and allergic myocardial infarction): a natural paradigm? *Int J Cardiol*. (2006) 110:7–14. doi: 10.1016/j.ijcard.2005.08.007

26. Dazy K, Walters D, Holland C, Baldwin J. Anaphylaxis mediated myocardial infarction in a coronary graft: a new variant of Kounis syndrome (a case report). *Int J Cardiol*. (2013) 168:e84–85. doi: 10.1016/j.ijcard.2013.07.044

27. Kounis NG. Kounis syndrome: an update on epidemiology, pathogenesis, diagnosis and therapeutic management. *Clin Chem Lab Med*. (2016) 54:1545–59. doi: 10.1515/cclm-2016-0010

28. Allam C, Saouma M, Chlawit R. Kounis syndrome must be considered in the differential diagnosis of myocardial infarction following COVID-19 vaccination. *QJM*. (2022) 00:1–2. doi: 10.1093/qjmed/hcac001

29. Ozdemir IH, Ozlek B, Ozen MB, Gunduz R, Bayturan O. Type 1 Kounis syndrome induced by inactivated SARS-COV-2 vaccine. *J Emerg Med*. (2021) 61:e71–6. doi: 10.1016/j.jemermed.2021.04.018

30. Kounis NG, Koniari I, De Gregorio C, Velissaris D, Petalas K, Brinia A, et al. Allergic reactions to current available COVID-19 vaccinations: pathophysiology, causality, and therapeutic considerations. *Vaccines*. (2021) 9:221. doi: 10.1093/qjmed/hcac001

31. Olivera A, Beaven MA, Metcalfe DD. Mast cells signal their importance in health and disease. *J Allergy Clin Immunol*. (2018) 142:381–93. doi: 10.1016/j.jaci.2018.01.034

32. Chung EH. Vaccine allergies. *Clin Exp Vaccine Res*. (2014) 3:50–7. doi: 10.7774/cevr.2014.3.1.50

33. Khan S. Mast cell tryptase level should be checked in all patients with suspected Kounis syndrome. *Eur Heart J*. (2020) 41:3018. doi: 10.1093/eurheartj/ehaa548

34. Baronti A, Gentile F, Manetti AC, Scatena A, Pellegrini S, Pucci A, et al. Myocardial infarction following COVID-19 vaccine administration: post hoc, ergo propter hoc? *Viruses*. (2022) 14:1644. doi: 10.3390/v14081644

35. Siegrist CA. Mechanisms underlying adverse reactions to vaccines. *J Comp Pathol*. (2007) 137(Suppl 1):S46–50. doi: 10.1016/j.jcpa.2007.04.012

36. Kounis NG, Koniari I, Mplani V, Kouni SN, Plotas P, Tsigkas G. Acute myocardial infarction within 24 hours after COVID-19 vaccination: is Kounis syndrome the culprit? *Am J Cardiol*. (2022a) 1:207. doi: 10.1016/j.amjcard.2021.09.032

37. Fialho I, Mateus C, Martins-Dos-Santos G, Pita J, Cabanelas N, Baptista SB, et al. Recurrent Kounis syndrome—a life-threatening event after COVID-19 vaccine administration. *J Cardiol Cases*. (2022) 25:400–3. doi: 10.1016/j.jccase.2022.01.014

38. Kounis NG, Mplani V, Koniari I, Kouni S, Plotas P, Tsigkas G, et al. Hypersensitivity coronary myocardial infarction (Kounis syndrome) and COVID-19 vaccines. *J Cardiol Cases*. (2022b) 26:242–3. doi: 10.1016/j.jccase.2022.05.001

39. Li YE, Wang S, Reiter RJ, Ren J. Clinical cardiovascular emergencies and the cellular basis of COVID-19 vaccination: from dream to reality? *Int J Infect Dis*. (2022) 124:1–10. doi: 10.1016/j.ijid.2022.08.026

Frontiers in Cardiovascular Medicine

Innovations and improvements in cardiovascular treatment and practice

Focuses on research that challenges the status quo of cardiovascular care, or facilitates the translation of advances into new therapies and diagnostic tools.

Discover the latest Research Topics

See more →

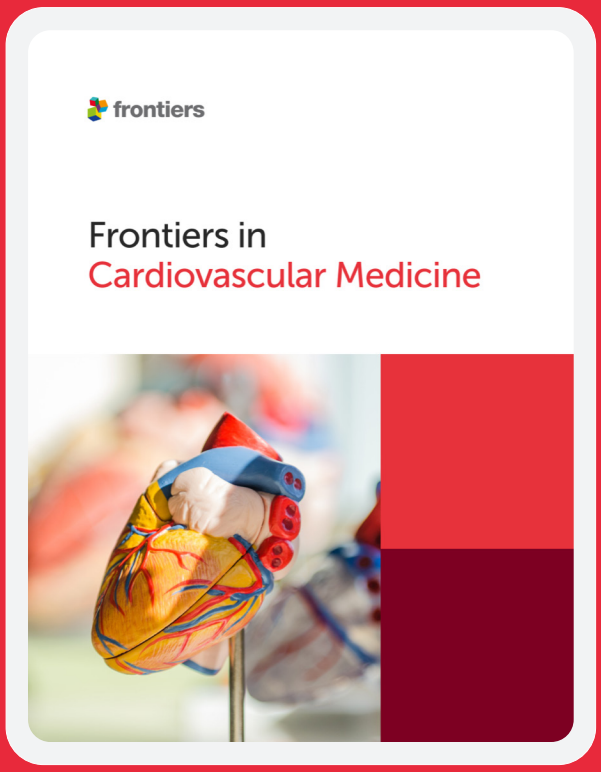

Frontiers

Avenue du Tribunal-Fédéral 34
1005 Lausanne, Switzerland
frontiersin.org

Contact us

+41 (0)21 510 17 00
frontiersin.org/about/contact